Metallurgy and Mechanics of Welding

Metallurgy and Mechanics of Welding

Processes and Industrial Applications

Edited by
Régis Blondeau

ISTE

WILEY

FSC
Mixed Sources
Product group from well-managed
forests and other controlled sources
Cert no. SGS-COC-2953
www.fsc.org
© 1996 Forest Stewardship Council

Table of Contents

**Chapter 3. Thermal, Metallurgical and Mechanical Phenomena in
the Heat Affected Zone**   89
Dominique KAPLAN and Guy MURRY

**Chapter 14. Standardization: Organization and Quality Control
in Welding** 473
Jean-Paul GOURMELON

Preface

Welding: The Permanent Bond
Between Two Solid Bodies

What a long story welding is! Seeing the light of day at the end of the 19th century in the mind of scientists, it passed quickly into the hands of technicians, first of all with the oxyacetylene technique, then with arc welding and resistance welding techniques. Other processes (we will not quote them all in this introduction) then followed and the 20th century ended with laser welding which had its origins in the 1980s.

However, it must be said that only since the 1950s has welding been the main means of assembly, as riveting was the most used method up to that point.

In fact, after abandoning this method to some extent, scientists renewed their involvement in the 1930s. In France, at the time, Albert Portevin set out *Les bases scientifiques de la soudure autogène* and a higher education teaching programme began in 1931 at L'Institut de soudure. In the 1930s welding was implicated in bridge failures, notably in Germany and Belgium, then during World War II came the failure of Liberty ships constructed in great numbers thanks to the technique of welding. Other later catastrophic failures affected pressure vessels. It is in this context that in 1948 L'Institut international de la soudure (IIS/IIW) was founded. It met the need for international collaboration, in particular with regard to safety and research, expressed by different national bodies and by the whole welding world, from scientists to users. Today in 2008, the IIS/IIW holds its 61st annual meeting: 16 commissions, with sub-commissions and study groups, cover the whole field of welding, from design to performance and safety, including teaching and research. This demonstrates the importance of this collaboration and the richness of its contribution.

Welding can be regarded, like the language of Aesop, as the best and worst of things. Indeed, it makes it possible to bond almost all materials, from metals to plastics, with continuity; however, this does not imply homogenity. The processes and hence possibilities are very numerous depending on the types of assemblies to be made, the properties required and evident economic constraints to be respected. At the same time welding can be regarded as the weak link of the majority of constructions as it is often called into question when problems arise. In the examples cited above (bridges, Liberty ships, pressure vessels) it is the welding that is called into question each time – often it must be added linked to a parent metal whose resistance to a sudden failure is insufficient.

The phenomena that occur during welding are both numerous and complex. In particular, the influence of extremely rapid thermal cycles and at high temperature on the physical, metallurgical and mechanical properties of welded materials always requires a better understanding.

In order to produce this work, the multiplicity of knowledge, scientific as well as technical, to be put in practice has led us to have recourse to a range of authors to share the task. The disadvantage is of course a certain disparity between the various chapters, as well as the risk of some repetitions. On the other hand, its richness is derived from this very fact as this work brings together the contributions of numerous French specialists well known in their specific field. It presents an entity as complete as possible on the knowledge available today on welding, without of course claiming to be exhaustive (for example, the welding of the plastics is outside its scope).

In a first part of 7 chapters, which deals with metallurgy and mechanics of welding, Chapters 1 and 2 present all the processes of welding, from the traditional processes with and without filler, with and without mechanical action, to the recent processes with high energy, electron beam and laser. Chapter 3 deals with the whole of the thermal, metallurgical and mechanical phenomena, which occur in the heat affected zone (HAZ) of the base material. Here the transformation phases with all the consequences they have on the structures and their properties are presented, as well as the phenomena of cracking, in particular cold cracking, which is a recurring theme of this work.

Chapter 4 is similar but deals with the question of molten metal in the weld, with other phenomena of cracking that are called into play.

The different types of filler products are then dealt with in Chapter 5 depending on the process used. The progress made in the manufacture of these products in order to improve the properties of the weld and resistance to cracking is explained.

Chapters 6 and 7 illustrate the problems of failure in service of welded constructions, the former dealing with resistance to fatigue, with solutions suggested both for materials and for the execution of the welds, the latter dealing with brittle failure, with, after setting out the methods of evaluation of the toughness and the evolution of the harmfulness of defects, proposals relating to the composition of the parent material, the quality of the filler metal and the importance of welding conditions.

The second part, Chapters 8 to 14, focuses on the applications of welding for various materials and in various industries.

First of all, Chapter 8 is devoted to the welding of thin sheets, both bare and coated, mainly used in the automotive market with the appropriate processes of welding. The importance of new steels with a very low percentage of carbon is underlined.

The subject of Chapter 9 is the welding of steel mechanical components in the automotive industry, with less traditional processes calling upon a minimum of molten metal.

The welding of steel structures is the subject of Chapter 10. The steels used and the techniques of welding with the precautions required in order to avoid defects are presented.

Chapter 11 concerns the welding of pressure vessels. It deals with examples of large components such as pressurized water reactors (PWRs) in the French nuclear industry and analyzes the various processes of welding and coatings used according to the parts of the vessel.

The majority of the preceding chapters refer to welding carbon and low-alloy steels, so Chapters 12 and 13 are devoted to other types of alloys. First of all, the welding of stainless steels is presented in detail, and for various families (martensitic, ferritic, austenitic and austeno-ferritic) with the concomitant problems of cracking and embrittlement, as well as the remedies and advice suggested according to the processes selected. Then, the welding of aluminum alloys is tackled with the various welding techniques used, the problems encountered and the rules to respect in order to obtain welds of good quality.

Chapter 14 is devoted to standardization developments in welding dealing with the general organization of quality and standards for non-destructive testing.

We extend our thanks to all those authors who have agreed to contribute to this work and especially those who work in the industry and who have been willing in their free time to contribute to this collection of the know-how and current research in the different fields of welding.

Régis BLONDEAU

Chapter 1

Traditional Welding Processes

1.1. Introduction

To avoid any misunderstandings, the definitions of the terms which appear in this text are those proposed in the document entitled "Terms and definitions used in welding and related techniques" published by the "Publications of Autogeneous Welding and the International Council of the French Language" [COL 96].

It has been specified in the preface to this book that welding makes it possible to reconstitute *metallic continuity* between the components to be assembled. This reconstitution involves the re-establishment of the interatomic metal bonding forces which requires at the same time a connection of the nodes of the crystal lattices and the absence of any foreign body likely to constitute a screen.

This chapter will successively cover the physical conditions necessary to create the metallic bond and the industrial processes which make it possible to establish this bond.

1.2. Conditions to create metallic bonding

Creating the metal bond consists, theoretically, of bringing the surfaces to be linked closer so that the surface atoms are at a distance of the order of the internodal distances of their own crystalline system.

Chapter written by Guy MURRY and Dominique KAPLAN.

This operation, which would assume at the beginning that surfaces are chemically clean and in a specular state of polish, is not practically feasible.

To mitigate this industrial impossibility, the surfaces to be joined will have to be activated with a view to eliminating the foreign bodies and elements likely to obstruct the creation of the bond.

1.2.1. *Activation of surfaces*

The most effective surface activation is fusion which can simultaneously ensure their cleaning. The metallic bond is created by solidification. Different procedures can be employed:

a) the two parts to be assembled undergo a surface fusion and thus contribute to the formation of a molten metal pool (possibly with the addition of a filler) which solidifies without mechanical action;

b) the two parts to be assembled undergo a surface fusion but an external mechanical action expels the molten metal and creates the assembly by placing the surfaces in contact at the solidus temperature;

c) the two parts to be assembled undergo a localized fusion and take part in the formation of a captive molten metal core which during its solidification is compacted by the action of an external effort of compression.

The activation of surfaces can also be obtained by heating without fusion. In general it is then supplemented by a mechanical action which enables, moreover, cleaning and improvement in contact of the surfaces to be assembled. It is possible to distinguish between:

a) the case where the heating and the cleaning of surfaces to be assembled are simultaneously carried out by mechanical friction (which implies the assembly of axisymmetric parts) and is followed, after stopping the latter, by a crushing ("forging") by axial compression; and

b) the case where the heating is carried out by external heating and the close contact is ensured by an effort perpendicular to the joint plane.

Finally, activation can result from a mechanical action without total heating of the parts to be assembled. This mechanical action causes a plasticization of the outer layer of each surface and generates a very localized heating which finally allows the establishment of the metallic bond. This process simultaneously requires a relative displacement of the surfaces to be assembled, parallel to the mating plane, coupled with a compressive force perpendicular to this same plane. It is necessary to carry

out a careful surface preparation and/or to make sure that relative displacements of the latter cause the rejection of the products which pollute them.

1.2.2. *Elimination of obstacles to bond creation*

Obstacles to the creation of the metallic bond can be of various kinds:

– geometrical surface irregularities,

– pollution of the surface (oxides, grease, moisture, etc.),

– chemical elements brought in by the surrounding air.

Surface irregularities are likely to disrupt the creation of metallic bonds in all the cases where there is not surface fusion of the parts to be assembled. It will then be necessary to carry out a surface preparation by mechanical means (grinding, machining, etc.).

All pollution of surfaces to be assembled will have to be eliminated by mechanical action (sanding, grinding) or by chemical means (solvents, scouring, drying, etc.).

It is necessary to neutralize the possible effects of chemical elements brought in by the surrounding air. Welding operations generally being carried out in atmospheric conditions, it is especially oxygen, nitrogen and hydrogen (carried in the air's humidity) which can be harmful.

Oxygen can react with the elements volatilized by the arc and in this way contribute to the creation of welding fumes. Furthermore, it can especially dissolve in the molten metal and, during solidification, contribute to the formation of:

– metallic oxides which constitute inclusions in solidified metal;

– porosities in the molten metal due to the drop in solubility which accompanies cooling and solidification. This formation of porosities can be aggravated by a reaction developing with an element contained in the metal and leading to the formation of a gas compound (for example, formation and release of CO during steel welding without protection against the atmosphere).

Protection against oxygen in the air can be ensured by the interposition of a neutral gas, a molten slag or by fixing in the form of oxides by the addition of oxygen hungry elements (silicon especially). In the vicinity of the molten metal, the surface of the parent metal raised to a high temperature can also react with oxygen and be covered with oxides, which is a further justification for using protective means, including at the back of the weld.

Nitrogen can dissolve in the molten metal and contribute to:

– either the formation of porosities in the molten metal due to the drop in solubility which accompanies cooling and solidification;

– or the formation of metal nitrides which, according to the conditions in which they appear, constitute inclusions or precipitates more or less hardening and weakening in nature;

– or for the part which remains in solid solution, a process of weakening by ageing.

Protection against nitrogen can be ensured by interposing a neutral gas or a molten slag.

Hydrogen dissolves in the molten metal and its concentration can reach high levels, even reaching saturation if precautions are not taken to limit its presence. Hydrogen, the solubility of which decreases when the temperature drops, can then contribute to the formation:

– of porosities during solidification;

– of cracks, in a solid state, when, oversaturated, it gathers in the form of gas molecules on the structural defects of a not very ductile metal.

Protection against hydrogen primarily consists of limiting its introduction into the molten metal by lowering the atomic or ionic hydrogen content of the plasma arc. To do this it is necessary to minimize the water content of the surrounding air (no welding in a damp atmosphere), to interpose a gas low in hydrogen between the surrounding air and the arc, to eliminate compounds supplying water (hydroxides, condensation, greases, basic non-dried coatings, fluxes, etc.) and other sources of hydrogen (cellulose or rutile coatings and grease).

1.2.3. *How can we classify the various welding processes?*

At this stage we are led to adopt a system of grading the welding processes according to the modes of action and means of protection against the atmosphere (see Table 1.1).

Activation	Complementary action	Protection
fusion	none	imperative
	compression	not essential
heating	compression	possible
friction	compression	none

Table 1.1. *Classing the welding processes according to modes of action and means of protection against the atmosphere*

Actually, the various welding processes are above all classified according to more practical criteria, which are:

– the energy source applied: flame, electric arc, plasma, Joule effect, spark, induction, friction, explosion, etc.;

– the means of protecting the hot metal: gas or slag.

1.3. Industrial welding processes

Industrial welding processes are set out here according to the criteria defined above, namely:

– processes utilizing the fusion without mechanical action;

– processes utilizing the fusion combined with mechanical action;

– processes utilizing heating without fusion but with a mechanical action;

– processes utilizing a mechanical action without heating.

A classification akin to industrial practices will be presented at the end of this chapter.

1.3.1. *Processes using local fusion of the parts without mechanical action*

For welding processes operating without voluntary mechanical action, the local fusion of the parts to be assembled can be described by distinguishing the mode of heating used and the means of protecting the molten metal against the chemical action of the surrounding air. Thus, it is possible to list:

– flame or gas welding;

– plasma welding;

– arc welding;

– vertical electroslag welding;

– aluminothermic welding.

It should be noted that, in all these processes, the molten metal weld pool is contained in a *crucible* formed by the shape of the parts to be assembled adjacent in the mating plane (sometimes the complete closure of the "crucible" is ensured by specific tools, e.g. slat, slides, mold). In this way a non-molten section of the parts, in the vicinity of the molten metal, is brought up to temperatures, according to its distance from the latter, between the temperature of the solidus of the metal and the initial temperature of the parts. The fraction of this volume (nearest to the molten metal), of which the structure and therefore the properties change because of this heating, is called the *heat affected zone* (HAZ).

1.3.1.1. *Flame welding*
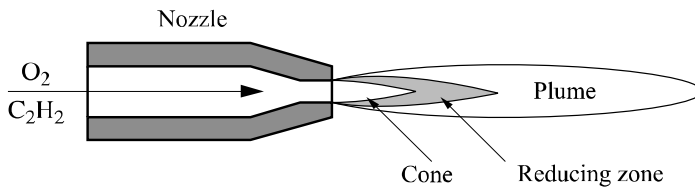
Figure 1.1. *Fusion of parent metals and filler metals obtained with a blowtorch*

The fusion of the parent metals and the filler is obtained by heating with a blowtorch (Figure 1.1) which enables us, by combustion of a gas (acetylene generally, hydrogen, propane) with a comburent (which is generally oxygen), to have an effective flame (of a fuel rating, with acetylene, about 100 to 300 W/cm^2 on a spot of heating [RYK 74], the diameter of which is about 5 to 10 cm).

This flame comprises two zones, each with a specific role:

– a cone at the immediate exit of the blowtorch nozzle whose surface constitutes the site of primary combustion (this, if acetylene is used, releases hydrogen and carbon monoxide). At the tip of the cone the temperature is very high (using acetylene, it exceeds 3,000°C) and the atmosphere is reducing;

– a plume where combustion is completed. According to the adjustment of the consumption ratio, namely the ratio r = volume of oxygen to volume of acetylene, this plume can be oxidizing, neutral or reducing (and thus carburizing for steels). In welding a neutral flame is used corresponding to $1 \leq r \leq 1.2$. The adjustment of blowtorch power is made by regulating the flow of acetylene which is governed by

the nozzle diameter. Four nozzle sizes exist which give acetylene flows ranging from 10 by 63 l/h to 1,000 by 4,000 l/h. The flow of oxygen is regulated accordingly. This choice of acetylene flow takes account of the metal being welded, its thickness, the type of joint and the position of welding.

It is possible to add a filler metal which is generally the same composition as the metal being welded and comes in the form of rods (from 1.6 to 5 mm in diameter).

Thus, the blowtorch, from the temperatures reached, allows the fusion of metals and, by its atmosphere, ensures the molten metal is protected against any chemical reaction with gases in the surrounding air.

However, with metals that are very sensitive to oxidation (aluminum, stainless steel, copper alloys) it is necessary to use a flux (spread out over the edges requiring welding or incorporated with the rod) to eliminate oxides formed on the surface.

1.3.1.2. *Plasma welding*
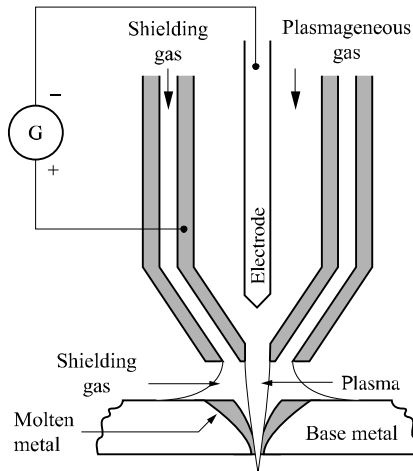
Figure 1.2. *Plasma non-transferred arc welding*

Fusion is carried out by heating using a plasma jet. This plasma is generated by the passage of a known plasma-producing gas (argon, with the possible addition of hydrogen or helium) in an electric arc created in the annular space formed between a coaxial nozzle and a refractory electrode (Figure 1.2). Generally, in DC, the refractory electrode is negative to avoid its destruction by the bombardment of electrons. The recombination in the jet of ionized species in the arc releases great energy and as a result generates a very significant rise in temperature which exceeds

10,000°C. The specific power can vary from 500 to 10,000 W/cm² on a heating spot [RYK 74] whose diameter varies from a few millimeters to a few centimeters). A peripheral tube ensures the distribution of an inert gas (generally argon or argon mixture + hydrogen) for the protection of the molten metal. This procedure, called a *non-transferred arc* or *blown arc*, is reserved for the assembly of relatively thin components.
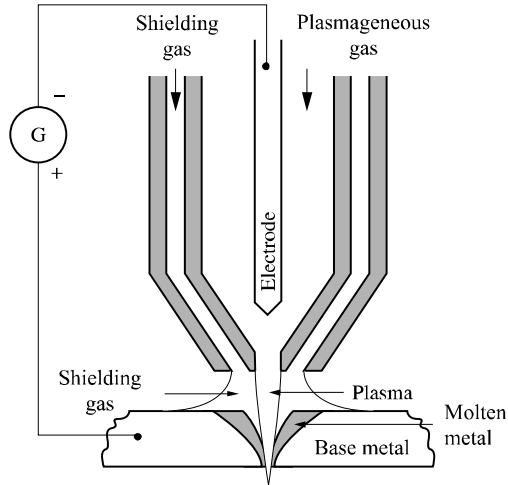
Figure 1.3. *Plasma transferred arc welding*

The transfer of heat and therefore thermal efficiency is improved by striking the arc between the refractory electrode and the parts to be assembled. The arc is then maintained by a pilot arc which is created between the nozzle and the refractory electrode (Figure 1.3). The name given is *plasma transferred arc welding*. It is the procedure most commonly used in welding. It makes the assembly of thicker products possible (albeit with a variable limit depending on the nature of the base metal, but in the order of a centimeter), often by using the keyhole procedure; the plasma jet crosses the joint by pushing the weld pool backwards where solidification occurs (the faces to be welded can thus be straight edged). In this way complete penetration is ensured and regularized. The use of a support at the back of the weld is generally not necessary because the molten zone is quite narrow (although this does not obviate the need for gas protection at the back). However, this process is not suitable for carrying out a filler pass. It is generally employed in flat welding and sometimes in horizontal/vertical welding. A filler can be introduced in the form of wire. To increase the rate of deposit, it can be beneficial to use the hot-wire technique. However, the filler can also be introduced in the form of powder into the shielding gas jet (thus around the plasma jet).

The synchronized generation of electric power pulses in the arc and in the plasma-producing gas flow makes it possible to weld in a vertical position. Such a procedure requires computerized control of all the parameters.

1.3.1.3. *Arc welding*

The contribution of heat used to form the molten weld pool is assured here by an electric arc operating in DC or AC. The specific power can vary here from 10^3 to 10^5 W/cm^2 on a heating spot [RYK 74] whose diameter varies from a few millimeters to a few centimeters.

It must be possible for the arc to be generated easily and then remain stable. To facilitate its generation (which will allow us to avoid resorting to a too high starting voltage compared to the arc's voltage in permanent mode) as well as to stabilize it, we have recourse to easily ionizable chemical elements which are introduced into the plasma arc. These elements can come from the fusible and volatile compounds included in the solid products which will form the slag or from gases applied to protect the molten metal. In addition, the power source must be adapted so that:

– its non-load voltage is high enough to allow arc generation,

– its normal operating voltage makes it possible to achieve arc lengths compatible with the technology employed,

– its voltage in the event of the arc's extinction is sufficient to allow the arc to be restored.

The choice of polarity, in either AC or DC, must take account of the different phenomena which occur at the cathode and the anode. Indeed, electron emission takes place at the cathode and all the more so if the cathode is heated to a high temperature. However, if its heating is partially due to the direct Joule effect and the bombardment by the positive ions, it is above all due to the contribution of heat coming from the Joule effect which occurs in the cathode's transition zone. This last point explains why the required current depends on the diameter of the cathode; the greater it is, the higher the current must be to maintain the cathode at a sufficient temperature.

Electrons bombard the anode and thus cause significant heating, increased further by the Joule effect in the anode's transition zone.

If the arc uses DC, the choice of polarity depends especially on the process and the metal being welded, given that the anodic zone is heated more than the cathodic zone. The AC current supply makes it possible to alternate the phenomena at the two ends of the arc.

When the filler comes from a consumable electrode, the transfer of this metal in the arc can be achieved in three different ways according to the electric mode of the arc. At high currents, the transfer takes place by pulverization, i.e. in the form of small droplets forcibly projected by the electric field towards the weld pool.

At moderate currents the transfer takes place in the form of large droplets which, with little force applied to them, follow irregular trajectories before falling in the molten metal or, possibly in the form of projections to one side – which is generally a sign of a bad adjustment of the welding parameters. At the lowest currents the transfer takes place by short-circuit. The magnetodynamic effect is insufficient (the current is too low) to detach the droplet from the surface of the electrode; the droplet grows bigger to the point that it comes into contact with the molten metal. The short-circuit then generates a current surge which detaches the droplet, which is incorporated in the molten metal.

The products that ensure the protection of the molten metal can, according to the process, be:

– fusible compounds which form a slag floating on top (and are likely to react chemically with it to refine its composition);

– often inert gases (argon, helium or mixtures sometimes with the addition of hydrogen) with, sometimes, the addition of carbon dioxide (whose decomposition in the arc will give protective carbon monoxide and oxygen which will be fixed by elements introduced with the filler products).

In this context, many processes have been developed that can be classified according to the conditions in which the arc is struck (between the two parts to be assembled or these components and an electrode) and that can also be distinguished according to the conditions in which the welding products are applied.
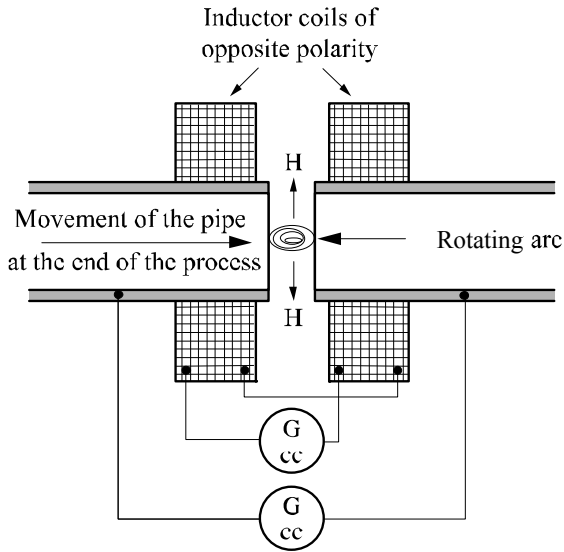
Figure 1.4. *Rotating arc welding on pipes*

a) The arc is struck between the two parts to be assembled

Arc welding with pressure created with a magnetic field

The arc is struck and moves between surfaces to be joined under the effect of a permanent magnetic field judiciously directed and controlled. After surface fusion, the parts to be joined are forced together (there is thus the formation of a seam). An alternative to this process is applied to tubular structures (Figure 1.4) using two coils which surround the tube and create two antagonistic magnetic fields. The resulting field is radial; it thus causes the rotation of the arc in the mating plane. This is rotating arc welding.

Arc welding of studs

The arc is formed between the end of the stud and the target zone of the support. After fusion of the stud end and creation of a molten pool on the surface of the support where the stud is to be fixed, the stud is plunged in the molten metal and maintained in position until solidification is complete. The power supply and stud displacement (contact, withdrawal for striking the arc, maintenance then lowering – Figure 1.5) are controlled automatically. The protection of the molten metal is generally ensured by the positioning of a refractory containment ring which ensures also the "molding" of the molten metal during its solidification. The power source

comes from DC or capacitor discharge; the current intensity of the arc is adjusted according to the diameter of the stud.

b) The arc is struck between a fusible electrode and the components to be assembled

Generally, this procedure allows, with each operation, the deposit of a certain quantity of molten metal, a quantity which varies with the type of process and energy brought into play. It can prove insufficient to form a sufficient seam section between thick components; it is then necessary to carry out several operations i.e. several passes. Such a situation often requires an edge preparation to be performed, a preparation which ensures proper weld creation (access for the electrode, type of assembly, position, penetration, possible prevention of deformations, etc.). These preparations have shapes and dimensions which vary especially according to the nature of the base metal and the process employed. The principal varieties are:

– straight edged (Figure 1.6a) for assemblies of limited thickness, possibly with spacing between the edges (distance increasing with the thickness). It may be necessary to carry out a pass on the reverse to ensure penetration but it is also possible to use a support at the back;
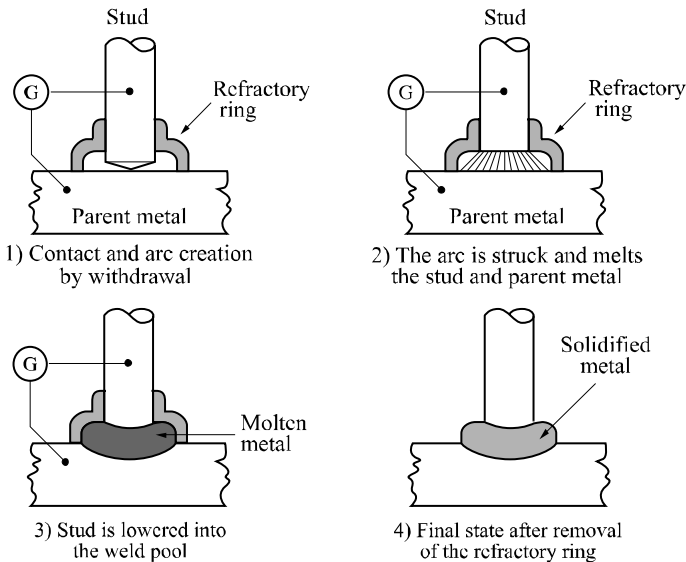
Figure 1.5. *Stud arc welding*

– V-shaped chamfer (Figure 1.6b) or Y-shaped (Figure 1.6c) with heel and possible edge spacing. This type of preparation is not employed for thick components because it gives rise to considerable distortion;

– X-shaped (Figure 1.6d) with heel and possibly edge spacing. This type of preparation requires access to both sides but limits distortion;

– asymmetric U-shaped (Figure 1.6e) or, better symmetric (Figure 1.6f) if there is access to both sides (with heel and possibly edge spacing). This preparation makes it possible to reduce the quantity of molten metal necessary.

Sometimes particular preparations such as half-V shaped, half-U shaped (known also as J), K-shaped, etc. are used.

The processes which will be described are known as "semi-automatic" if the electrode or the torch is handled by the welder and "automatic" if the latter is positioned and guided by automated devices.

a) Straight-edged   b) V-shaped   c) Y-shaped

d) X-shaped   e) asymmetric U-shaped   f) symmetric U-shaped
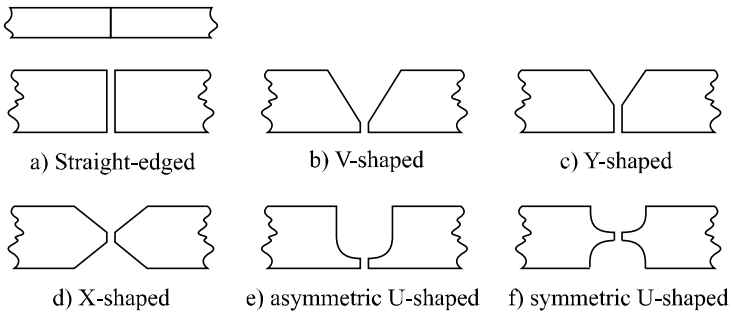
Figure 1.6. *Edge preparations*
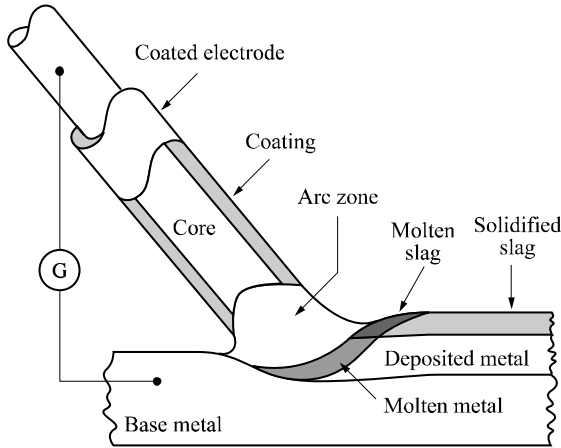
Figure 1.7. *Coated electrode arc welding*

Coated electrode arc welding

The electrode consists of a metallic core (whose diameter varies from 1 to 10 mm and whose length can be up to 450 mm) which serves as the electrical conductor and supplies the filler metal, as well as an adhesive coating made up of products which contribute to the formation of a protective slag and others that volatilize in the arc plasma to stabilize it and, possibly, of metal particles which help form the molten weld pool (Figure 1.7).

This coating can commonly be:

– cellulosic: this creates little slag but its combustion releases CO_2 and contributes to the enrichment of the molten metal caused by dissolved hydrogen;

– rutile: the basic component is titanium oxide; it contributes to the desulphurization of the molten metal; the binding agents used release hydrogen;

– basic (electrodes used in steel welding): the basic component is calcium carbonate; it releases little hydrogen but it is hygroscopic and so requires that the electrodes be correctly baked (300°C approximately) then protected (by maintaining them at around 100°C for example) before use.

Rutilo-basic mixed coatings (better desulfurization) or rutilo-cellulose (good penetration) are also proposed as well as coatings containing metal powders to increase the quantity of metal added (high-output electrodes) or to introduce alloying elements.

Core fusion slightly precedes that of the coating; it forms a crater which directs the transfer of the filler towards the molten metal. This transfer takes place in the form of large droplets (cellulosic or basic coatings) or by pulverization (rutile coatings).

In many cases, the arc can be DC in origin (the polarity is then selected according to the nature of the base metal, the coating and the welding position) but it is sometimes possible to use an AC current (in particular for steel welding). The intensity of the current is selected according to the diameter of the electrode; it is generally recommended by the manufacturer.
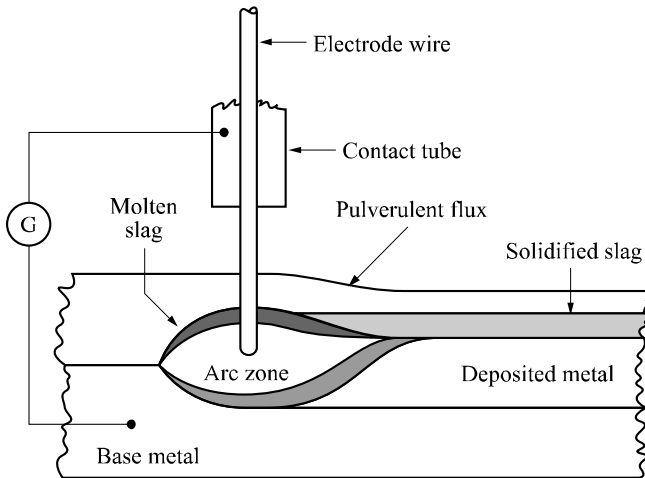
Figure 1.8. *Arc welding with powdered flux*

Welding is in practice possible in all positions, each one requiring particular adjustments and appropriate preparation.

Arc welding with powdered flux

The electrode is a solid wire (approximately 2 to 10 mm in diameter) whose supply is guaranteed by an automatic device through a torch equipped with a contact tube ensuring the power supply. Upstream of the torch (compared to the direction of the welding process) a nozzle in which the arc will be struck distributes the powdered flux, part of which will constitute the protective slag, whereas the rest, covering the weld area with a layer of non-molten flux which slows down cooling, will be recovered later on. The arc is not visible, so consequently this imposes a precise piloting of the torch displacement.

This process (Figure 1.8) makes it possible to weld with high currents and a high output. However, in general, dilution is significant, about 2/3 and it increases with the welding current.

The arc is struck using DC when the welding intensity does not exceed 1,000 A; the polarity can be direct (the wire is negative) if deep penetration is required or inverse (the wire is positive) if, on the contrary, a high welding speed and a reduction in dilution is desired. With elevated currents it is sometimes easier to use AC, which makes it possible to decrease the effects of magnetic arc blow.

The Joule effect along the length of wire electrode, between the contact tube and the arc, heats the filler metal (all the more depending on length and current) and facilitates its fusion, thus increasing the quantity of filler metal in the weld pool.

Fluxes used are mixtures of mineral compounds (generally silicon manganese or silico-alumino-calcic compounds) delivered in the form of calibrated pellets. The two principal manufacturing processes give them different properties:

– so-called molten fluxes are manufactured from minerals by fusion, molded and then crushed; they thus have a vitreous and/or crystallized structure and can be porous;

– so-called agglomerated fluxes are manufactured starting from natural mineral products agglomerated or sintered (with a binder). These fluxes can adsorb or absorb water and so it is necessary to take precautions to avoid any addition of hydrogen.

In general, the manufacturers of welding products combine flux and filler metal. Each combination often makes it possible to confer their own specific properties on the molten metal.

This welding process, due to the method of flux application, enables only flat welding (and possibly at an angle with a special support). It allows straight edged butt welding with edge spacing up to significant thicknesses (depending on the base metal) but to weld very thick components it requires a preparation which account for the possibility of making a pass(es) on the reverse side:

– no access: V-shaped preparation with heel, spacing and support at the back or tulip-shaped preparation or U-shaped with heel;

– access: X-shaped with heel and spacing or K-shaped preparation with heel.

Furthermore, welding can be accelerated by associating two (or more) welding heads each with its own power supply; the electrodes are generally placed in tandem at a distance of about 25 to 35 mm.
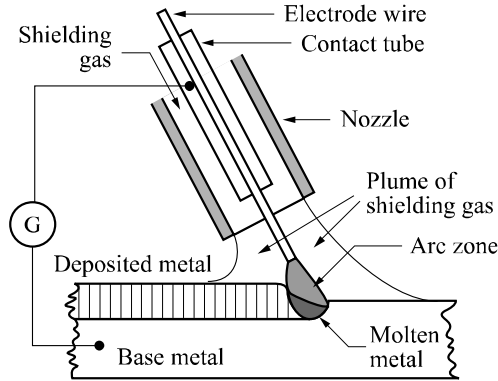
Figure 1.9. *MIG-MAG welding*

Gas shielded arc welding with a solid fusible wire

The electrode is a solid wire (from approximately 0.5 to 2.4 mm in diameter) whose supply is ensured by an automatic device through a torch equipped with a contact tube ensuring the connection to the power supply.

This torch comprises an annular gas delivery which will ensure the protection of the molten metal. This gas can be of two types (Figure 1.9). It can be inert and the process is then known as MIG (metal inert gas) welding. It can be argon (pure or mixed with helium) which ensures good arc stability and gives a good penetration, or helium mixed with argon; the proportion of argon must be high enough to preserve arc stability. It can be active and the process is then known as MAG (metal active gas) welding. In this case it contains oxygen and, more often, CO_2 mixed with neutral gases (argon mainly). The presence of oxygen (whether supplied or coming from the break up of CO_2) brings a certain number of advantages: the arc is more stable, the weld pool more fluid, the transfer by pulverization can be established over a broader range of power supply conditions, the chamfers are filled better and voids less likely. However, the risk of loss of elements transported in the arc leads to the introduction of elements likely to combine with oxygen into the wire electrode.

The power is generally supplied in DC and in inverse polarity (positive wire electrode) in order to increase the speed of wire fusion and to stabilize the mode of transfer, in the arc, of the molten metal. Two modes are mainly used:

– the transfer by axial pulverization for the welding of thick products but limited to butt and flat angle welding or gutter welding;

– the transfer by short-circuit which involves little energy and allows welding of thin products and all types of *in situ* welding.

Certain modern equipment makes it possible to superimpose pulses over the basic current in order to cause the detachment of the drops at fixed frequency and thus to stabilize their size. It then becomes possible to control their transfer and to regulate their flow whatever the welding current. The term used is *pulsed welding*.

Assemblies are made with all the preparation types already evoked but taking account of the need to allow sufficient access for the torch. This access can be facilitated by lengthening the wire electrode between the contact tube and the arc, with a resultant increase in the quantity of metal deposited in consequence of the heating by Joule effect in this length of wire and, generally, reduction in penetration. Welding can be carried out in all positions after adaptation of operational parameters.
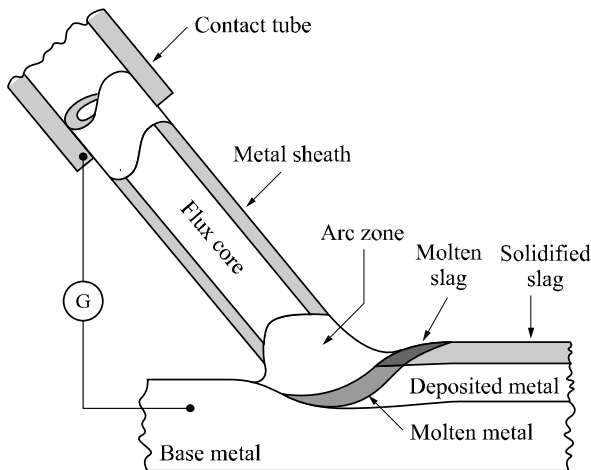
Figure 1.10. *Cored wire arc welding*

Cored wire arc welding

This process (Figure 1.10) is derived from gas shielded solid wire arc welding by a simple replacement of the solid wire with a flux cored wire (diameter from 1 to 4 mm). A cored wire consists of a tubular metal envelope filled with a powder (flux) whose composition and role are comparable with those of the coating on a coated electrode. According to the manufacturing process of cored wire, this can be closed (by drawing of a hollow cylindrical wire filled with flux) or formed by pleating or crimping and thus more or less sealed (but it can again comprise two parallel fillings containing flux and a metal filler powder). As the fluxes are hygroscopic and the metal sheath more or less sealed, it is necessary to take the same precautions for use as for coated electrodes. However, cored wires without slag (and thus containing

metal powders) enable us, with an effective gas protection, to appreciably increase the welding speed and the quantity of metal added.

As in MIG or MAG welding, the supply of the wire is guaranteed by an automatic device through a torch equipped with a contact tube ensuring the power connection. This torch makes an annular gas supply possible, which will ensure protection of the molten metal. This gas is generally reactive (CO_2, possibly mixed with argon).

The filled wire being more rigid than solid wire makes it possible to further increase the length of the wire electrode between the contact tube and the arc and thus to facilitate access (it is necessary to avoid over lengthening this distance so as not to separate the molten metal too much from the shielding gas).

Assemblies are made with all the types of preparation already evoked by taking account of the improved accessibility given by the increased length of the wire electrode between the contact tube and the arc. This makes it possible to reduce the chamfer openings. In addition, the good penetration makes it possible to increase the height of the heels and to decrease the spacing between surfaces to be assembled. Welding is generally carried out on the horizontal and sometimes in other positions, in which case, a small diameter cored wire is used.

Cored wires are also offered for welding without a shielding gas. Protection is then assured by both the slag (of which the limited quantity is not sufficient to ensure total protection) and by a dense atmosphere generated by specific products introduced into the flux. In addition, the metal sheath of the filled wire contains elements likely to decrease the harmful effects of an incomplete protection (deoxidizers and denitrifying agents). Finally the welding parameters are adjusted to reduce the length of the arc. These cored wires make it possible to decrease the size of the welding torch, to facilitate access and thus limit the preparation required.
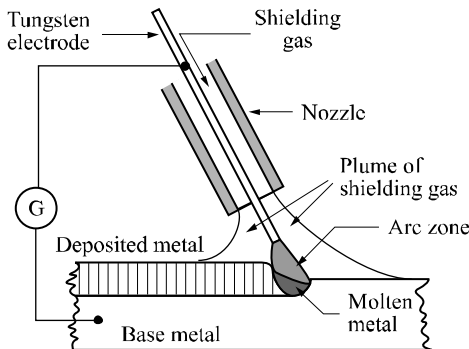
Figure 1.11. *TIG (tungsten inert gas) welding*

c) The arc is struck between a refractory electrode and the components to be assembled

The non-consumable electrode consists of a tungsten tip (Figure 1.11) held in a torch equipped with an annular gas delivery which will ensure the protection of molten metal. This gas is neutral: argon (sometimes with the addition of hydrogen – up to approximately 30%) or helium. Argon gives good arc stability but helium ensures better thermal efficiency and thus deeper penetration. These considerations mean that argon-helium mixtures (about 80% Ar and 20% He) are often used. This process is most commonly called *TIG* (tungsten inert gas) *welding*. It can be necessary, depending on the base metal, to set up a gas protection on the reverse side using a gas which can be either identical or different from that supplying the torch (nitrogen-hydrogen).

The electrode (0.5 to 10 mm in diameter) can be pure tungsten or tungsten with an addition of zirconium oxide (0.3-0.5%) or thorium (1-2%). These additions make it possible to increase the electrode emission capacity and thus to improve arc stability and help arc initiation. They also increase the electrode performance and thus the acceptable maximum current. The shape of the electrode point is a significant parameter of TIG welding. The electrode is often pointed in DC mode, and hemispherical in AC.

The power supply is generally DC with direct polarity (negative electrode) so as not to subject the electrode to electron bombardment. In this way the energy impact is concentrated on the parts to be assembled and at the same time a narrow bead and good penetration are achieved. The arc can also be established by AC (with a suitable power source) when an electronic bombardment is desired to clean the parts to be assembled. Arc initiation is often assisted using a pilot arc.

A filler can be introduced directly into the molten metal pool either in the form of rods or in the form of wire using a mechanized reel, allowing, if necessary, the pre-heating of the wire to improve the deposit rate.

Assemblies are produced using all the preparation types already evoked above taking account on the one hand of the limitation of the volume of molten metal and, on the other hand, of the need for taking particular care (cleanliness, dimensional accuracy especially with regard to the spacing of the parts – it can be useful to set up a support on the reverse side). Welding can be carried out in all positions after adaptation of the operational parameters.

An easier use of the TIG process and an increase in penetration can be obtained by applying a fine layer of a reactive flux to the surface of the edges to be assembled.

The composition of this flux (often formed of oxides and/or halides) must be selected according to the nature of the base metal.
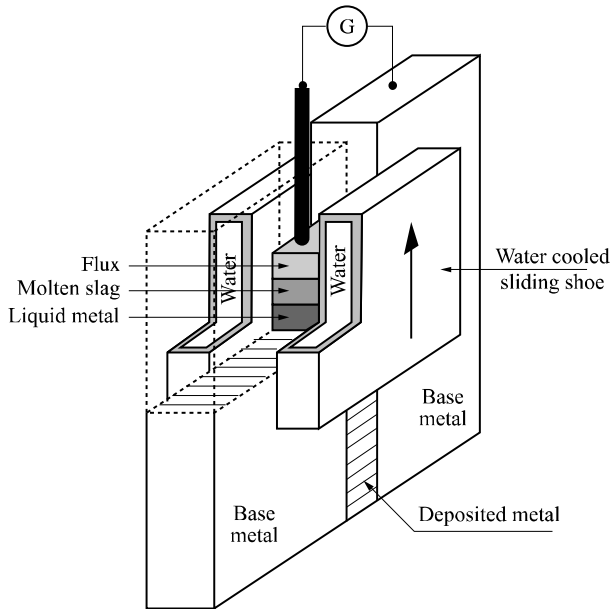
Figure 1.12. *Vertical electroslag welding*

Vertical electroslag welding

This process consists of forming a molten metal bath in a vertical parallelepipedal mold formed by the two sections to be assembled and two water-cooled copper shoes applied to the surface of the two parts (Figure 1.12). The continuous supply of molten metal due to the filler fusion (consumable wire electrode and possibly fusible wire guide) and the progressive solidification of the molten metal little by little consolidate the two parts. Above the molten weld pool, a bath of slag (thickness 40 to 60 mm) ensures its protection. The permanent heating is due to the Joule effect which develops partly in the electrode but especially in this molten mineral pool. Welding progresses vertically upwards. It begins with the striking of an arc between the wire electrode and an appendage which closes the bottom of the mold and on which a welding flux is deposited (which will form the slag).

When the volume of molten metal is sufficient, the quantity of flux necessary to constitute the slag layer is introduced; the arc then ceases. It is generally preferable to set up, in the edge prolongation to be assembled, two blocks of the same

composition as the base metal and of the same thickness. The weld's end point will be after the molten metal has reached the level of these blocks so that the shrinkage at the end of solidification does not affect the weld *per se* (any surplus deposit thus created will be removed later on). According to the dimensions of the parts to be assembled, the side shoes can be moved upwards to follow the progression of welding.

The heat affected zone is wide, because of the very significant heat generation. According to the thickness of the parts to be assembled several wire electrodes can be used simultaneously. To carry out welds of considerable height, a fusible wire guide plunged in the slag and melting simultaneously the wire electrode(s) can be employed; this fusible wire guide contributes to the molten metal weld pool. The term then employed is *vertical electroslag welding with fusible wire guide*. The procedure generally makes use of AC.

This process allows butt welding and welding at an angle (by using adapted shoes) of work pieces whose thickness is generally not less than 40 mm.

Aluminothermic welding

In this process the welding is carried out by running a metal in fusion (filler) into a mold built around the two faces of the parts to be assembled, placed face to face, at a specified distance. These two faces are often pre-heated with a flame via holes provided in the mold. The molten metal is created on the spot by aluminothermy, i.e. exothermic reaction between oxides (of the metal filler) and powdered aluminum. This operation is carried out in a crucible placed at the top of the mold. As the molten filler is run in, the surface of the parts to be assembled melts, preceding solidification of the assembly. The protection of the molten metal is ensured by the slag which is formed during the aluminothermic reaction. Afterwards, it is necessary to remove the mold and grind the assembled parts, so as to eliminate any excess deposits.

1.3.2. *Processes using local fusion of components with mechanical action*

The contribution of heat used to form the molten weld pool is assured here by the Joule effect of a high intensity alternating current which crosses the mating plane. It is the contact resistance between the two surfaces of the parts to be assembled which makes it possible to concentrate fusion in this plane.

Several processes have been developed that we can classify according to the fate reserved for the molten metal; containment or expulsion. All require rather heavy and specific equipment.

1.3.2.1. *Resistance welding with containment of the molten metal*

This process combines the Joule effect and a mechanical pressure applied to the outside of the assembly, perpendicular to it and right where the molten metal zone is. This force has the aim of ensuring a good electrical contact between the parts to be assembled, thereby confining the molten metal in the zone where it is formed and applying pressure to it after its solidification in order to improve its compactness by avoiding shrinkage (an operation known as spot forging). Generally the electrodes carrying the current apply this effort. These considerations show that they are overlapping assemblies of products of limited thickness. The containment of the molten metal within the joint avoids any contact with the air; the problem of its protection thus does not arise.

The effectiveness of this process is related to the localization of the zone heated by the Joule effect, which depends on the electric contact resistance between the parts; precautions must be taken so that, on the one hand, other resistances in series in the electric circuit are much lower and that, on the other hand, there is no possibility of the welding current being diverted to one or more parallel circuits.

The piloting of the welding current as well as that of the compression force are handled by automatisms which can:

– apply pressure before the passage of the current, to bring the two components into close contact and to ensure the electrical contact,

– adjust the current intensity and limit its duration (in general, of a few periods to a few tens of periods i.e. durations which are calculated in tenths of a second),

– adjust the pressure during the passage of the current to prevent the surfaces separating (due to dilation) and the consequent dispersion of the molten metal,

– maintain or increase the effort to ensure the compactness of the volume of molten metal,

– if required, run a reduced current as a post-heating.

The electrodes are copper-based alloys. The addition of alloying elements (Cr, Zr, W, Cd, Co, Be, etc.) confers the necessary mechanical performance without overly affecting their electric conductivity and thermal conductivity. Their contact surface to be welded must be clean and uniform in shape.
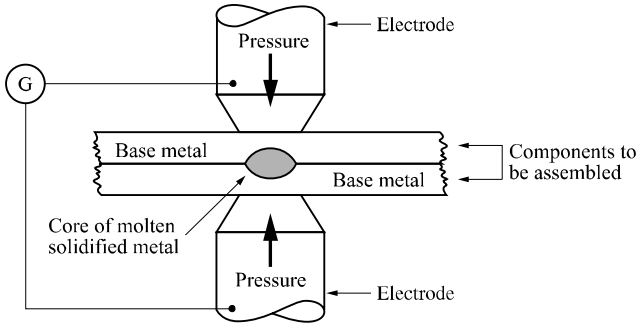
Figure 1.13. *Resistance spot welding*

In this way resistance spot welding, projection and roller seam welding can be carried out.

Resistance spot welding

In this process current supply and load application are carried out by cylindrical electrodes with tips in the shape of a truncated cone cooled by internal water circulation. Their contact surface is generally flat or slightly convex. They are installed on fixed machines or mobile tools; it is always desirable that the step-down current transformer is placed as close as possible to the welding zone.

The volume of molten metal has an ovoid form and is called a *spot weld*. The welding is discontinuous and a seal cannot be guaranteed. The final load application generally causes an indentation on the two faces of the joint; it is possible to avoid on one of the two faces by replacing the electrode with a copper plate through which the welding current passes.
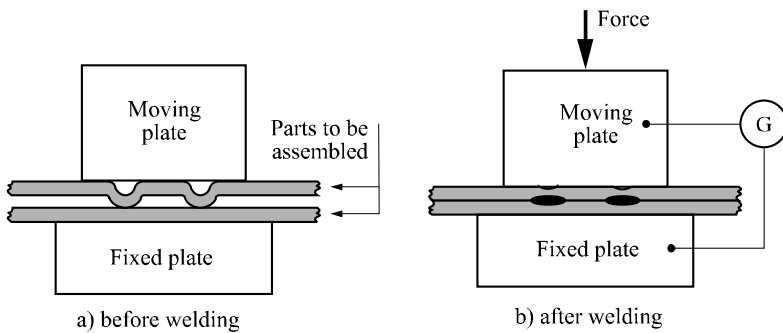
Figure 1.14. *Projection welding*

It is possible, in certain cases, to carry out two spot welds simultaneously by coupling two transformers (double spot in series with push-pull assembly), or with only one transformer (provided that it is possible to control the currents).

Resistance projection welding

In this welding process (Figure 1.14), the passage of the current is localized by raised areas called *projections* created on one or both of the assembly surfaces. These bosses are stamped on thin flat sheets and machined in other cases. The supply of the current and the load application are applied, generally, using plates; during the heating and fusion the bosses collapse and the mobile plate must react very quickly to ensure the close contact of the parts to be assembled. If the power supply is powerful, it is possible and economic to weld several bosses simultaneously. The wear of the plates and deformation of the components are minimal. The geometry of the projections must be precisely controlled.

Roller resistance welding

In roller resistance welding (Figure 1.15), the electrodes are replaced by copper or copper alloy discs called *rollers*. These rollers are driven to ensure the progression of the components. Of course, they carry the electric current and apply the necessary load.

The electric current, in general, is modulated as in spot welding but in a repetitive way and the welding consists of successive spots. It can be:

– discontinuous if the successive spots do not overlap. It is possible to stop the roller rotation at each spot and to carry out spot compression, and the result is identical to that of spot welding. It is also possible to work uninterrupted but in this case without forging (the effort applied remains constant),

– continuous if the various points overlap, i.e. if the formation of each point involves the partial remelting of the preceding spot. The welding then forms a perfect seal.

It is possible, in roller welding, to carry out the seam welding of thin sheets using the force applied during welding; the extra thickness is then eradicated. It is necessary, to achieve this, that the overlap does not exceed one and a half times the thickness and that the sheets to be assembled are gripped very tightly.
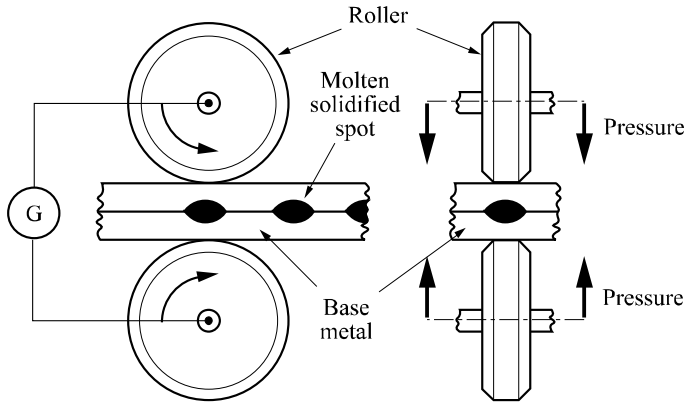
Figure 1.15. *Roller resistance welding*

1.3.2.2. *Resistance welding with expulsion of the molten metal*

These processes combine the Joule effect with applied mechanical pressure, after heating, from outside of the assembly and perpendicular to it, over all its surface. This force has the aim of creating the bond by keeping in close contact the surfaces heated to their solidus temperature. A weld metal bulge is formed at the ends of the assembly, which must then be eliminated. As the heated zone is confined, the problem of its protection is not relevant. Within this framework two rather different processes are employed.

Upset resistance butt welding

The effort is applied in two stages: first of all for the cold joining of the parts in order to allow the passage of the current through the surfaces to be assembled, then, after passage of the current, to ensure the weld bond; an excess, or weld bead, is formed which must be eliminated. The Joule effect is limited to the contact zone between the two parts and the heating must bring them up to the forging temperature.

This process is a large-scale consumer of energy and requires careful preparation of the faces to be assembled (which must be parallel and perpendicular to the effort applied). Therefore, flash welding is sometimes preferred.

An alternative used for the longitudinal closure welding of cold formed sections utilizes high frequency (HF) induction heating. The HF current is applied by two contacts rubbing on the weld edges, above the intended weld, where they are still separate.

Due to the skin effect, the current works its way along the edges to the contact point, where it generates heat (eventually to the point of fusion) and allows the bond to be formed with the pressure of two rollers. This process can be implemented each time it is possible to create an induced current which crosses the mating plane.

Flash welding

The parts are brought closer only after the current is supplied so that the current is first of all only transmitted by contact points created by the imperfections of the opposing surfaces; at these points the current density is very high. From the beginning of fusion the liquid part is expelled in the form of small incandescent particles; this is the *flash*. Gradually this flashing takes over the whole mating surface. Once this result is achieved the contact pressure is increased to drive out the molten metal and the impurities which it contains and to ensure the connection; the current is simultaneously shut off. An excess weld bead is formed in this last phase; it will have to be eliminated. A pre-heating of large section parts limits the electric output and the force required. It also decreases the loss of matter during flashing but increases the volume of the bead and the duration of the operation.

This process does not require a careful preparation of the faces to be assembled; flashing alone is sufficient. In general, it is not necessary to protect the molten zone from oxidation in as much as the force is applied straight after the flashing.

This process allows end to end welding of variously shaped components and sections (from just a few mm² to more than 1,000 cm²).

1.3.3. *Processes using heating without fusion but with mechanical action*

Heating can be achieved from an external source (resistance or induction) or by mechanical action (friction). The applied forces must be carefully controlled. These processes thus require very specific equipment.

Diffusion welding

Diffusion welding is a process of solid state coalescence in which the parts to be assembled, put in contact under suitable pressure, are brought up to and maintained at a sufficiently high temperature (but very slightly lower than the melting point) to allow atom diffusion through the mating plane. This, helped by localized plastic deformations, can ensure metal continuity. The pressure can be:

– perpendicular to the mating plane: it is then often recommended that to avoid macroscopic deformation, it does not exceed the limits of elasticity of the metal at the diffusion temperature,

– isostatic: the pressure is in this case not limited and the resorption of porosities is greatly improved.

The surfaces to be assembled must have undergone a careful preparation by fine polishing (to ensure the closest contact possible) and cleaning (to eliminate any pollution likely to obstruct the diffusion). It is possible to insert one or more non-fusible leaves (strip iron or deposit) between them.

Precautions must be taken to avoid any hot reaction of these surfaces with the atmosphere (vacuum welding or in a neutral atmosphere). For a given preparation, the quality of the assembly depends on the pressure, the temperature and the duration of maintenance at temperature.

It has been shown [LEF 92] that fast localized heating by induction under a judiciously modulated axial load (so as to be at any temperature equal to the corresponding limit of elasticity) makes it possible to achieve an assembly following a maintenance at a temperature whose duration varies, depending on its level, between 1 and 60 seconds. The heating conditions make it possible, in addition, to carry out a heat treatment within the framework of the thermal welding cycle. This procedure is applicable to many metals.

Friction welding

Friction welding is a process of butt welding under pressure which involves a rotation of the parts against each other (maximum circumferential speed of about 150 m/min) and the application of an axial load in order to generate, by friction, heat at the interface (only one part is put in rotation; it must be circular and its diameter, if solid, can vary from a few mm to 150 mm approximately). When the required temperature is reached, rotation is stopped and the axial load is simultaneously increased to ensure welding by forging.

The rotating part is turned by a servo motor or a flywheel. In the first case movement stops due to disengaging and braking, in the second the stop follows the exhaustion of the flywheel's kinetic energy (which was spun before the operation at a sufficient speed to ensure the required heating).

The joint does not contain molten metal and this fact has two principal consequences:

– the joint has good mechanical properties;

– it is possible to weld different metals (iron and aluminum for example).

An excess bead is formed at the periphery of the joint; it must be eliminated. The cleaning of the surfaces to be assembled is ensured by friction; this process thus

requires neither careful preparation of the surfaces nor their protection in the course of the welding operation.

If none of the two parts to be assembled can be rotated, it is possible to intercalate an adapter which can be rotated.

A process which can be compared to friction welding is currently proposed under the name *friction stir welding*. It employs a non-consumable rotary tool, of suitable shape, which penetrates the mating plane; friction causes significant heating which lowers the elastic limit of the base metal. A significant plasticization develops and the tool movement (at a speed which would be approximately that used in arc welding) causes a flow of matter running from the front to the back of the tool, where it ensures the bond between the two parts to be assembled. The properties of such an assembly are interesting.

Forge welding

In this process the parts to be assembled are heated to a sufficient temperature then hammered to cause the connection by plastic deformation at the interface. Between the two faces to be assembled, it is necessary to employ a cleaning product (equivalent to a flux) which ensures the elimination of oxides by ejection during hammering.

1.3.4. *Processes using mechanical action without heating*

Ultrasonic welding

This is a process of lap welding under contact pressure, during which ultrasonic vibrations (20 to 100 kHz) are briefly applied so that the two faces to be assembled are set into motion against each other. A negligible volume of metal, on both sides of the mating plane, is thus raised (by friction) to the recrystallization temperature and ensures the bond as a result.

The ultrasonic energy required is that much greater the thicker (generally not exceeding 2 mm) and harder the components are. It is possible to weld different metals.

Explosive welding

This welding process is used to produce assemblies by covering or cladding. The covering or cladding metal is violently projected against the base metal by the progressive detonation of an explosive layer distributed on its outside face. The shock wave, as it spreads, causes the ejection, in front of the contact zone, of a jet of metal which perfectly cleans the faces to be assembled and enables the creation of

the bond. However, for this to occur, it is necessary that, before welding, a gap is established between the two faces which have been chemically cleaned beforehand. Their surface (from a few cm² to several m²) can be flat, cylindrical – tubes – or crooked. It is possible to assemble different metals.

1.4. Bibliography

[COL 96] COLLECTIF, *Termes et définitions utilisés en soudage et techniques connexes*, Publications de la Soudure Autogène, 1996.

[LEF 92] LEFRANCOIS P., KERGOAT M., CRIQUI B., HOURCADE M., "L'assemblage de l'acier en quelques secondes grâce au soudage-diffusion-dynamique à l'état solide: cas du 27CD4 soudé à 1050°C", *Mémoires scientifiques de la Revue de Métallurgie*, January 1992.

[RYK 74] RYKALINE N.N., "Les sources d'énergie utilisées en soudagé", *Soudage et techniques connexes*, December 1974.

Chapter 2

High Density Energy Beam Welding Processes: Electron Beam and Laser Beam

Welding processes using high density energy beams result from the application, in the second half of the 20th century, of work conducted by physicists in the fields of x-rays and vacuum techniques for the process of electron beam welding and optronics for laser beam welding. The possibility of concentrating these beams on points having a very small surface area led engineers to use this property to melt materials to achieve welds or cuts.

Compared to traditional arc welding processes, these two processes are characterized by a very high energy density at the impact point on the work piece. Rykaline [RYK 74] gave a representation comparing for several processes the heat flows at the center of the heat sources and the diameters of these sources. We can observe that the energy density measured at the focal point of a laser beam or an electron beam is 10,000 times higher than that reached in an oxy-fuel flame (see Figure 2.1).

2.1. Welding properties using high density energy beams

These result from the dimension of the focal points (lower than a millimeter in general) used at the level of the parts to be welded. These properties are as follows:

– single pass welding;

Chapter written by Abdelkrim CHEHAÏBOU and Jean-Claude GOUSSAIN.

– welding without filler material when there is no gap between the parts to be joined;

– welding of thin parts (tenths of millimeters) by heat conduction;

– welding of very thick parts (tenths of millimeters) by the formation of a vapor capillary. In this last case, two modes of welding are observed:

- complete penetration weld using a keyhole when the electron or photon beam passes through the whole thickness of the workpiece (see Figure 2.2),

- partial penetration weld when the beam only melts part of the thickness of the workpiece (see Figure 2.2);

– very narrow welds (molten zone and heat affected zone) because of the very high energy density;

– welds inducing very low distortion, which makes these two processes a precision mechanical solution, since it thus becomes possible to weld machined parts or parts not requiring deformation correction after welding. Figure 2.3 illustrates the deformation (transverse and longitudinal shrinkage) obtained during the welding of a 15 mm thick sheet of martensitic steel by GTAW, plasma arc, GMAW and electron beam;

– welds with gas protection (laser) or under vacuum (electron beam), which ensures a good protection against the oxidation of the molten zones and heat affected zones and makes it possible to weld materials sensitive to this phenomenon such as titanium and zirconium.
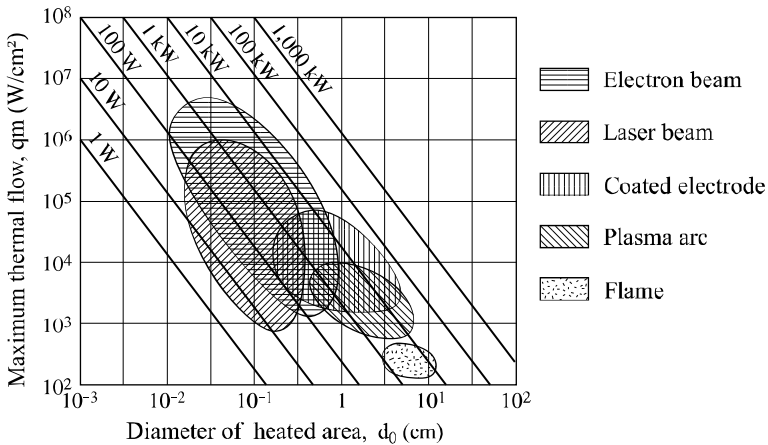
Figure 2.1. *Rykaline's diagram*
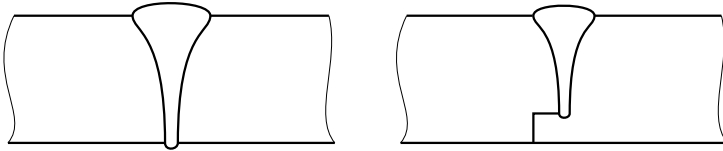
Figure 2.2. *Complete penetration and partial penetration welds*
(Institut de Soudure document)
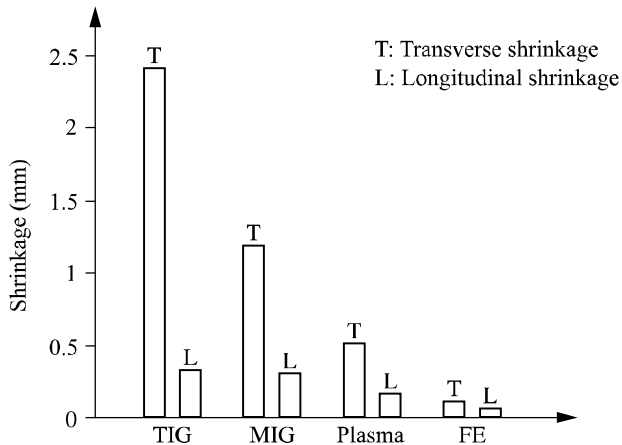
Figure 2.3. *Comparison of the transverse and longitudinal shrinkage of a butt welded martensitic stainless steel assembly (Institut de Soudure document)*

2.2. Laser beam welding

2.2.1. *History*

Einstein surely did not suspect the technological revolution to which his stimulated emission theory, established in 1917, would give rise. The technological adventure could only really start in 1954 when Professor Townes and his team developed the first stimulated emission amplifier and oscillator, which they baptized "MASER" (*Microwave Amplifier by Stimulated Emission of Radiation*). This discovery was followed by many others. In 1958, Schawlow and Townes demonstrated the theoretical possibility of producing coherent light by stimulated emission of radiation. The first laser source was a ruby laser produced by Maiman in 1960. It was very quickly followed by the development of the first gas laser by Javan (helium-neon laser). Many mediums were then studied and used for the

manufacture of lasers: doped crystals, semiconductors, ionized gases, molecular gases, liquids, dyes.

Laser is currently experiencing an extraordinary development. It is used in many spheres of activity.

2.2.2. *Principle*

Laser is an acronym formed by the initial letters of *Light Amplification by Stimulated Emission of Radiation*.

An atom can pass from a fundamental state E_1 to excited state E_2 by the absorption of a certain energy quantity ($h\upsilon$). This energy contribution can be mechanical or kinetic in origin. This atom will revert to its fundamental state by the restitution of this energy quantity, it is "the spontaneous emission" expressed by the following relation:

$$h\upsilon = E_2 - E_1$$

where h is Planck's constant and υ the emerging photon frequency.

These randomly emitted photons produce a light known as "incoherent". There is no relationship of phase, direction and polarization between all these photons.

If an incident photon causes a return to the fundamental state of the excited atom, there is "stimulated emission". The two emerging photons are in phase, they have the same direction and same polarization as the incident photon: there is light amplification by stimulated emission of radiation.

The excitation of the medium is called "pumping". It allows the population inversion between excited and non-excited atoms. Pumping requires an external energy source which can be assured by electrical discharge or radio frequency in the case of gas lasers, and by lamps or laser diodes in the case of solid lasers.

A laser source must thus be made up of three principal elements:

– an active medium made up of particles (atoms, ions, molecules),

– an energy source to carry out the pumping of the medium and thus to obtain the population inversion,

– a resonator cavity made up of two mirrors ensuring photon oscillation. If one of the mirrors is partially reflective, it will allow some of the photons to escape which will constitute the coherent light beam.

The laser beam thus obtained will have certain characteristics of divergence, polarization and energy distribution which will define the quality of the laser beam.

2.2.3. *Various laser types*

2.2.3.1. *CO_2 laser sources*

Gas laser sources are most commonly used for working on materials. The active medium consists of a gas mixture containing helium (50%), nitrogen (40%) and CO_2 (10%). Pumping is carried out by electrical discharge or more often by radio frequency. The excited nitrogen molecules transfer their excitation to the molecules of CO_2. The radiation wavelength of 10.6 µm thus obtained does not allow the transport of the beam by optical fiber. Only transport by mirrors, a less flexible system, is possible. In spite of the possibility of pulsing the beam, welding mainly uses CO_2 in a continuous mode of operation. The electrical efficiency of such laser sources is lower than 10%.

The search for increasingly powerful laser sources with a better beam quality and better efficiency have led to the development of various technologies. Those differ in the direction of gas circulation, the type of excitation and the shape of the cavity. We can distinguish five.

Sealed laser sources

These consist of a discharge tube containing the gas mixture. They are limited in power (≤600 W) but deliver a very good quality beam. In the field of metallic materials, they are particularly well adapted to engraving and cutting thin sheets. However, their good beam quality also enables them to be used for the welding of thin strip iron. Advantages of such sources rest in their low cost and the possibility of installing them on mechanized systems.

Slow axial flow laser sources

These are the first CO_2 laser sources to have been developed. The gas circulates slowly in the tubes in the axis of the laser beam (10 m/s). The excitation of gas is ensured by electrical discharge. These laser sources produce a very good quality beam but their power per unit of volume is limited to 0.5 W/cm^3.

The maximum power of these laser sources is low (≤1,000 W). They can be used for cutting and welding thin materials.

Fast axial flow laser sources

The gas moves at high speed in the beam's axis (≥200 m/s) using pumps or turbines in the cavity made of glass tubes. The excited gas is then cooled by heat

exchangers and progressively regenerated. The excitation can be obtained by electrical discharge but the most recent sources use radio frequency. This mode of excitation has several advantages:

– more homogenous excitation,

– the electrodes placed externally suffer less and their maintenance does not require the opening of the cavity,

– greater flexibility in use.

The power obtained per unit of gas volume can reach 2 to 3 W/cm^3 for an excitation by electrical discharge and from 8 to 10 W/cm^3 for excitation by radio frequency. Increasingly compact laser sources are obtained by reducing the cavity shape. Sources of 20 kW are proposed in today's industrial market.

These are the laser sources most commonly used today. They equip cutting and welding machines.

Transverse flow laser sources

 The gas flow moves transversely across the axis of the laser beam thanks to one or more turbines. They do not use glass tubes. The cavity consists of a sealed metal chamber. The power per unit of gas volume is about 2 to 3 W/cm^3. The maximum power reached is high (up to 45 kW). The laser beam obtained is of lower quality than for a fast axial flow laser. Such beams are mainly used for welding or surface treatments.

So called SLAB laser sources

The parallelepipedic cavity generates a rectangular beam configuration. The beam then passes into a spatial filter which makes it circular. The gas moves slowly in the cavity. The excitation of gas is carried out by radio frequency. The power available lies between 100 W and 6 kW. This technology makes it possible to obtain compact sources of a higher efficiency. Gas consumption is low and the beam obtained is of very good quality (close to Gaussian beam TEM_{00}).

2.2.3.2. *Neodymium YAG laser sources*

It is a solid-state laser whose active medium is yttrium aluminum garnet monocrystal doped with neodymium ions (Nd^{3+}). The wavelength of this laser, 1.06 μm, enables it to be transported by optical fiber. This low volume monocrystal (for example, a bar 150 mm in length and 9.52 mm diameter) is placed in a reflective cavity. The excitation of the medium is ensured by xenon lamps or laser diodes. The electrical efficiency of the laser depends on the pumping system, 1-3%

for a lamp pumped system and in the order of 10% for laser diodes. The cooling of the system is ensured by water circulation in the cavity.

Two modes of Nd:YAG laser operation should be noted: pulsed and continuous.

Pulsed YAG laser sources

Pulsed YAG laser sources generally consist of a pumping module that delivers an average power ranging between 300 and 500 W. These YAG lasers can reach up to 2 kW on average by adding, in series, additional amplifying modules to this pumping module. The pulsed operation mode is ensured by flash lamps which produce with each impulse an optical response of a defined frequency and pulse length. The mode of operation for these lasers is schematized in Figure 2.4.
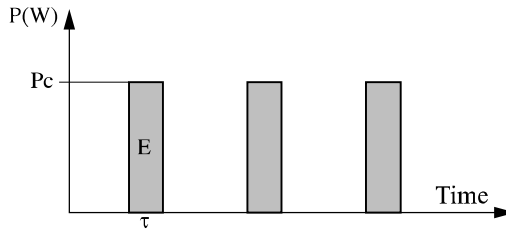
Figure 2.4. *Pulsed YAG laser mode*

The characteristics of a pulsed YAG laser are related to its peak power, which can reach 50 kW. The relations between the various laser parameters are as follows:

– peak power: $Pc = \dfrac{E}{\tau}(W)$;

– average power: $Pm = E \times F(W)$;

– pulse duration: $\tau(ms)$;

– pulse energy: $E(J)$;

– pulse frequency: $F(Hz)$.

High peak powers are reserved for drilling or cutting operations. For welding, the peak power must be limited and depends on the material and the thickness to be welded. They should not exceed 4 kW. The use of a high peak power will cause material spattering. For this reason, the average power of the sources intended for welding should be limited to 500 W. Sources of greater power will be used only for high pulse frequencies. The penetration depth will in any event be limited to 1.5 mm for a quality steel weld.

Continuous YAG laser sources

These were developed after pulsed YAG laser sources. The excitation of the medium is ensured by continuously lit xenon lamps. The average powers reached are higher than in the case of the pulsed YAG laser sources: 4 to 5 kW. The essential difference between the pulsed mode and the continuous mode lies in the peak power. In the case of the continuous mode, the peak power is equal to the average power.
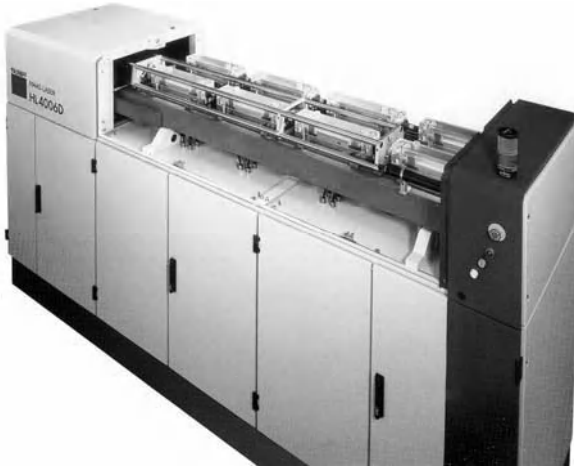
Figure 2.5. *Pumping chambers of a continuous lamp pumped rod YAG laser (4kW average beam power) (Trumpf document)*

The current developments are mainly directed towards increasing the power of these sources and of the pumping system (see Figure 2.5). The power increase is obtained by the increase in the number of pumping chambers (resonators and amplifiers). In the case of a conventional laser source with cylindrical bars and lamp-pumping, the maximum number of pumping chambers currently put in series is eight. This limitation is mainly due to beam degradation. The beam quality of industrial continuous YAG lasers around 25 mm.mrad enables a laser beam of more than 4 kW to be carried in a 0.6 mm diameter optical fiber.

The development of diode-pumped rod Nd:YAG laser sources in the year 2000 has offered scope for progress (see Figure 2.6). The system of pumping by laser diodes allows a better efficiency ($\geq$10%) and a clear improvement in beam quality (15 mm.mrad).
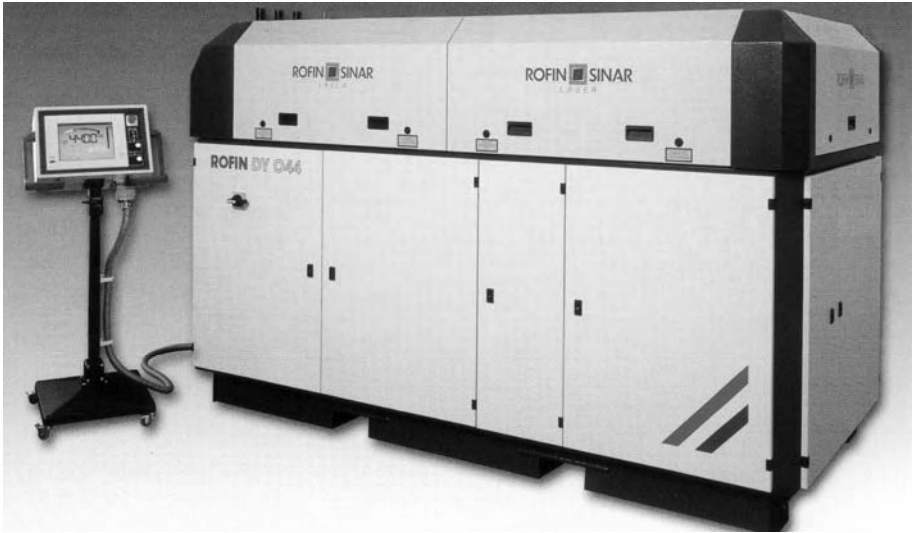
Figure 2.6. *4.4kW YAG laser source using laser diode-pumped rods (Rofin Baasel document)*

The development of diode-pumped rod laser sources were a stage in the technological development of YAG laser sources but they have not been used industrially. They have encountered considerable technical problems linked to the reliability of the diode laser sources used for pumping. Today they have been replaced by new types of laser sources, diode-pumped disk laser sources and fiber laser sources.

Disk laser sources

For diode-pumped disk laser sources, the active medium consists of small sized YAG disks (see Figure 2.7). Laser sources up to 8 kW power beam are available for industry today, with a very high beam quality (0.8 mm.mrad) and high degree of efficiency. As opposed to the rod systems, the disk laser has no thermal lensing. This means that the beam quality is constant across the entire power range. Further developments of more powerful laser sources are expected in the near future (16 kW). The exceptional beam quality obtained using these laser sources allows the transport of up to 8 kW beam power in a 0.2 mm diameter optical fiber.
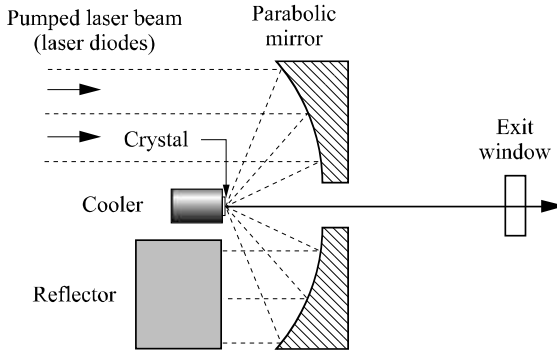
Figure 2.7. *Resonator diagram of a laser diode pumped disk source (Trumpf document)*

Fiber laser sources

This new laser source has recently been developed for industrial applications. It was initially developed for the telecommunications industry in the early 1990s. Its active gain medium is an optical fiber doped with a rare element like Ytterbium. This type of laser source can produce a very high power output (over 20 kW) with a very good beam quality. The efficiency attained is around 25%.

2.2.3.3. *Semiconductor laser sources (or laser diodes)*

The stacking of a multitude of semiconductors makes it possible to obtain laser diode systems from a few tens of watts to several kilowatts. The wavelengths available are 0.808 and 0.940 μm. The multiple beams emerging from these stacks are treated by sophisticated optical systems in order to be combined. The poor quality of beam produced is not conducive to optimal beam focalization. The rectangular and large-sized focal point generates power densities on the workpiece lower than 10^5 W/cm², which is insufficient for keyhole welding.

These characteristics make it an excellent tool for the welding of synthetic materials, brazing, surface treatment or conduction welding. The particular advantage of this technology lies in its high energy efficiency (>25%), the compactness of the sources, the low operating costs (absence of lamps or lasing gas) and the low wavelengths (better absorption by metallic materials and possible transport by optical fiber). The development of optical systems allowing for a better focusing of the laser beam is keenly awaited and will revolutionize the use of these laser sources.
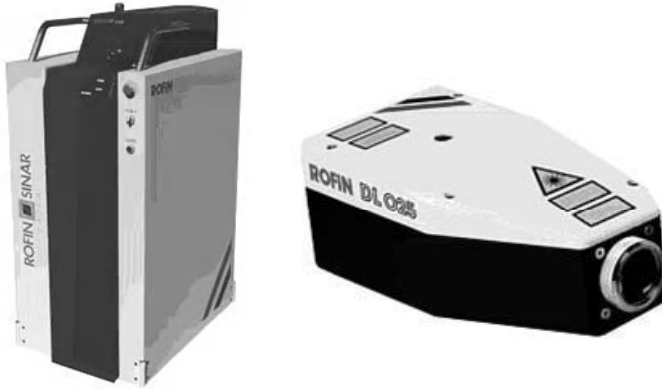
Figure 2.8. *Diode laser source (Rofin Baasel document)*

2.2.4. *Laser systems*

2.2.4.1. *Laser beam transport*

The beam emitted by a laser source must be transported to the component to be welded with minimal losses. The transport and focusing systems used depend on the laser beam's wavelength. Nd:YAG laser beams can be transported by optical fiber whereas the CO_2 laser can only be transported by mirrors. In this case, the optical pathway must be confined and pressurized in order to avoid the mirror deterioration and the possible degradation of beam quality.
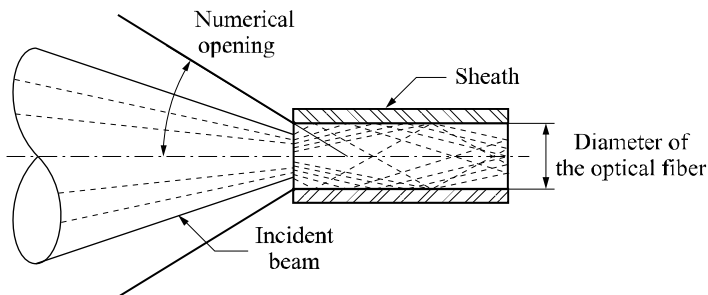
Figure 2.9. *Insertion of a laser beam in an optical fiber; from [HAV 96]*

The optical fiber must be as small in diameter as possible. The beam quality is then essential. Pulsed YAG laser beams averaging from 400 to 500 W in power can be inserted into a fiber 400 μm in diameter, continuous YAG lasers pumped by 4 kW lamps use optical fibers 600 μm in diameter and disk laser sources pumped by laser

diodes benefit from a reduction in the optical fiber diameter (an 8 kW beam using a 200 μm diameter optical fiber). The power losses are limited to less than 10% per optical fiber.

The mirrors most commonly used for CO_2 laser beam transport can be made out of bare copper, gilded copper or covered in molybdenum. Gilded copper is valued for its very low absorption properties but it is fragile and expensive. Bare copper also has low absorbance and is comparatively inexpensive, but tends to oxidize. Molybdenum covered copper is extremely resistant but its reflective properties are lower than the others. There is no precise rule for the choice of mirrors. It is however advisable to avoid using bare or gilded copper for focusing heads subjected to projections and welding fumes. The pressurized optical transport can consist of bare copper mirrors (less expensive), of gilded copper mirrors (good reflectivity) or of molybdenum covered mirrors (more resistant but more absorbent).

2.2.4.2. *Focusing*

The laser beam must be focused on the workpiece in order to obtain the power density necessary to weld. YAG laser beams are generally focused using glass lenses. CO_2 laser beams whose power is lower than or equal to 3 kW can be focused using selenium-zinc lenses or mirrors. Higher powered CO_2 laser beams are generally focused using mirrors alone. These can be bare or gilded copper, molybdenum covered copper or solid molybdenum. Gilded copper is generally avoided for the construction of optical focusing heads because of its fragility.

The dimensions of the focused beam depend on the beam wavelength, its quality and the focusing system used. The diameter of the focal point is related to these parameters by the following equation:

$$d = M^2(4\lambda f / \pi D)$$

with:

- d: diameter of the focal point,

- M^2: factor of beam quality,

- λ: wavelength,

- F: focusing distance of the optical system,

- D: diameter of the beam before focusing.
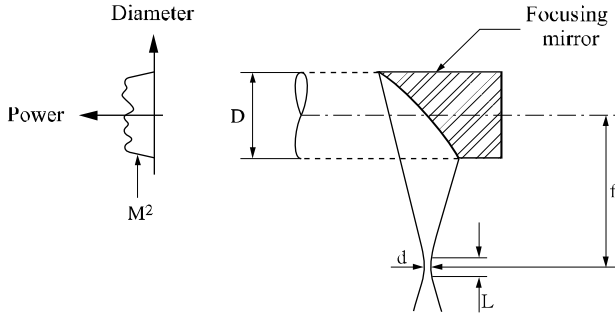
Figure 2.10. *Laser beam focalization; from [HAV 96]*

In the case of YAG lasers, the focal point diameter depends primarily on the optical fiber diameter, and on the collimation and focusing system (see Figure 2.11), which explains the importance of minimizing the optical fiber diameter:

$$d = \left(\frac{f}{f_c} \right) d_c.$$
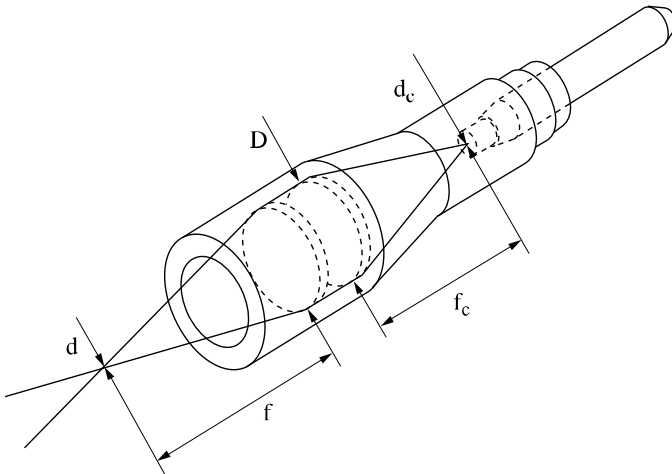
Figure 2.11. *YAG laser beam focalization; from [HAV 96]*

Another important dimensional specification of the focal point is the field depth *L*. It is defined as being the zone in which the diameter of the beam increases no more than 5%. It can be expressed in the following way:

$$L \cong \frac{d2}{2\lambda M^2} \cdot$$

While remaining within this tolerance of ±5% of the focal point diameter, the variation in the resulting power density does not exceed 10%. We will see hereafter the importance of this criterion for the welding process.

2.2.4.3. *Beam and workpiece displacement system*

There exist various mechanized beam and/or workpiece displacement systems. These systems are conceived according to the type of laser source used, the dimension of the parts to be welded and economic considerations. Contrary to the market of laser beam cutting, welding machines are often dedicated to an application. In order to reduce the costs, the manufacturers propose more and more machines by catalog or machines made up of standardized sub-assemblies.
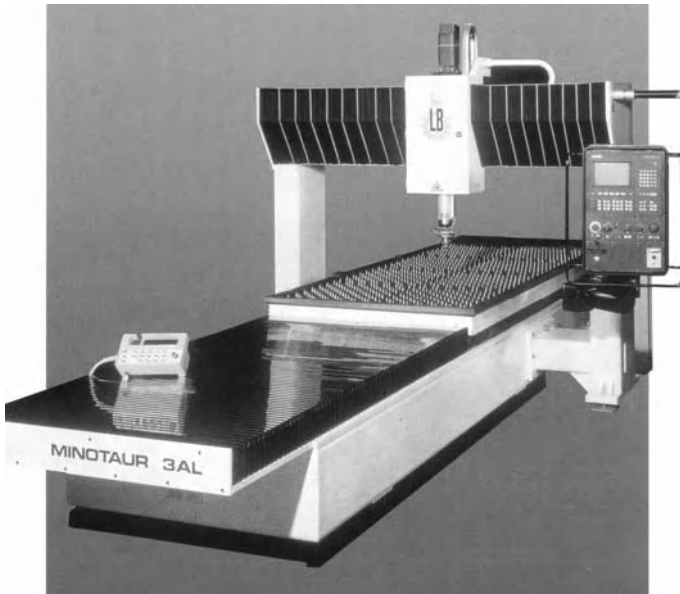
Figure 2.12. *Mixed three axis system (Balliu document)*

For the simplest components, machines with fixed optics are used. The components are moved under the focused beam. Only the focusing optics are moved vertically to adjust the position of the focal point or to allow the loading and the unloading of the part. For this type of simple application, the optical pathway does not justify the use of optical fibers.

For more complex trajectories, we may have to use robotized systems with several axes of motion. There are two types: Cartesian robots or polyarticulated robots. Cartesian robots are mainly used for the mirror displacement in the case of CO_2 lasers. They can incorporate up to five axes of motion. These precision mechanical systems, are expensive and require a rigorous optical pathway design (see Figures 2.12 and 2.13).
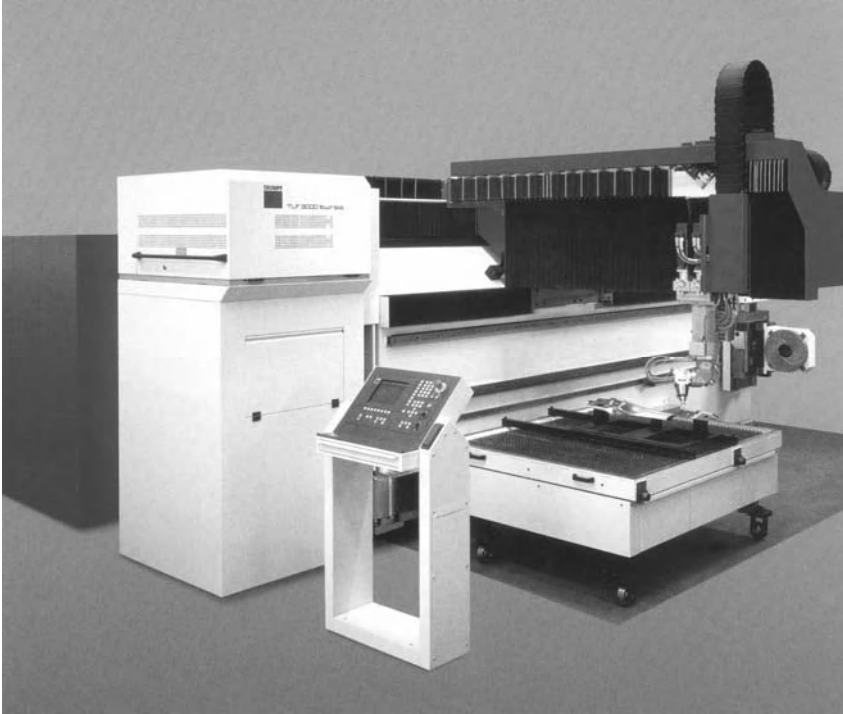
Figure 2.13. *Five axis system with mobile optics (Trumpf document)*

The development of high power continuous YAG laser sources and of beam transport by optical fibers has increased the use of polymorphic robots for welding operations. Their unquestionable advantage is the very competitive installation cost compared to the five axis Cartesian systems. The applications are currently mainly for the welding of automotive bodyshells (see Figure 2.14).

These robots offer less positional precision than gantry robots, but this disadvantage can be compensated by the use of real-time trajectory monitoring systems.
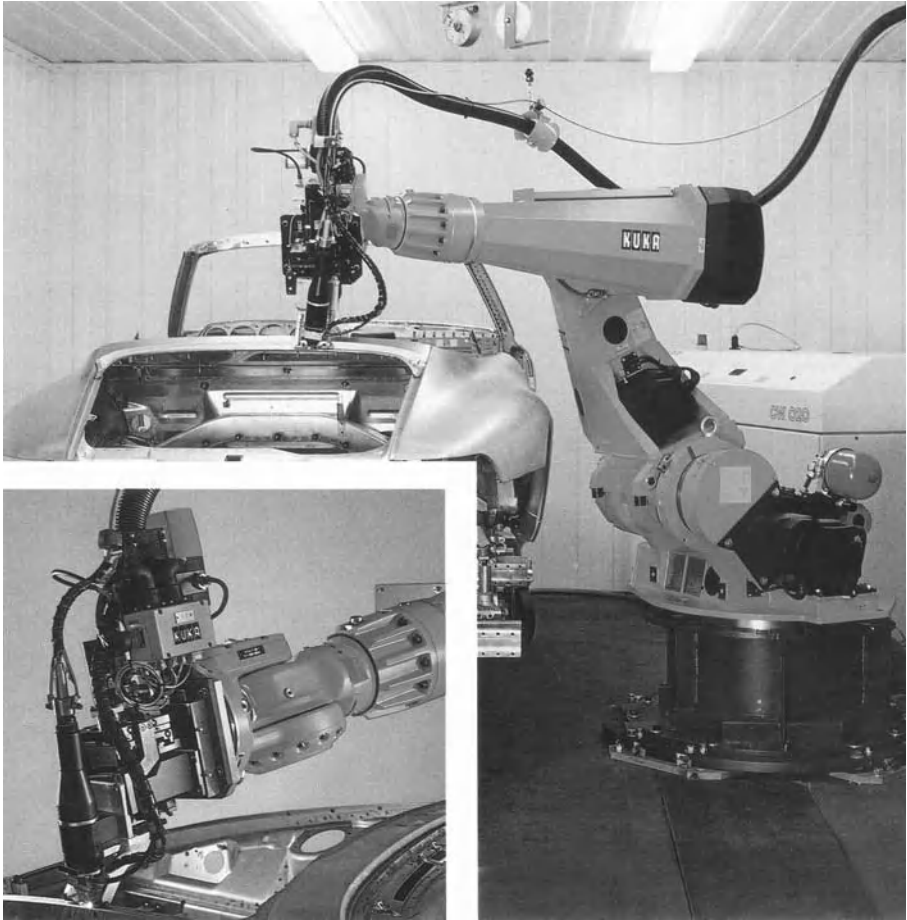
Figure 2.14. *Six axis robot equipped with optical fibers for a YAG laser (Kuka document)*

These robots can be equipped with a remote welding system (see Figure 2.15). This technology makes welding possible at a considerable distance from the workpiece. This remote process uses the latest high quality laser sources (disk laser and fiber laser sources).

2.2.4.4. *Peripheral systems*

Peripheral systems are the devices that monitor the correct functioning of the laser system (power measurement, beam analysis, etc.), to supervise the welds being made (infrared thermography, plasma analysis) and facilitate robot operation (joint monitoring systems).

Figure 2.15. *Six axis robot equipped with a remote laser welding system (Trumpf document)*

Power measurement

Laser sources are equipped with an internal system of power measurement. It gives an indication of the beam power emitted by the source. This power value does not take account of possible losses along the optical pathway. External measurement systems are available to measure the beam power at the component site. These systems do not allow the power measurement during welding, so they will be complementary to internal measurement systems, which can give an indication during the welding process.

Beam analysis

In the case of laser beam welding, the focused beam constitutes the welding tool, hence the importance of understanding its characteristics perfectly. Empirical methods allow an evaluation of the position and diameter of the focusing zone. The difficulty in using these methods increases with the power of the laser beam.

Devices have been developed in order to determine laser beam characteristics in a precise way. The operating principle of these devices is based on taking away of part of the beam and analyzing it using photodiodes. On average, beams up to 20 kW with power densities 10^7 W/cm² can thus be analyzed.

Weld monitoring

One of the principal advantages of laser beam welding is its high speed. This advantage can quickly become a disadvantage if a defective weld is not detected in time. This can lead to the rejection of a great quantity of parts. It is thus necessary to monitor the welds on the production line in order to detect the defects as soon as possible. Several methods are employed.

Infrared thermography – an infrared camera scans the back of the weld bead, very close to the weld pool. The anomalies noted in the temperature isotherms make it possible to highlight the formation of a welding defect. This control technique indicates the presence of an anomaly but does not give information about the quality of the weld. It can be used in addition to other monitoring techniques. This technique, which is difficult to control, is not very well suited for production line monitoring.

Plasma analysis – this method consists of analyzing the emission of plasma and the weld pool. The sampling of data is carried out at the level of the laser/material interface by optical fibers or optical components located in the optical pathway. The sensors used are photodiodes whose fields of sensitivity can be located in the ultra-violet (emission of plasma), the visible range or infrared (emission of the weld pool). An analysis of the signal makes it possible to correlate the events detected with the appearance of weld defects. These devices make it possible to detect in real-time the formation of defects and to set off an alarm at a predetermined level. Control by closed loop is at the development stage.

Seam tracking system

Seam tracking, initially developed for conventional welding, has been adapted to laser welding. The laser triangulation technique makes it possible to carry out detection of the joint position in a reliable way for an environment where normal vision is disturbed (fumes, projections, highly emissive plasma). The majority of systems use the projection of a laser line which is compared with a computerized model [BOI 98]. Visualization by CCD camera is nowadays offered as a competitive alternative to laser triangulation.

2.2.5. *Implementation of laser beam welding*

Laser/material interaction

The laser beam is focused on the surface of the part so as to obtain a power density in the range of 5.10^5 and 5.10^6 W/cm². Figure 2.16 shows that a power density threshold exists for the creation of a vapor capillary or *keyhole*.
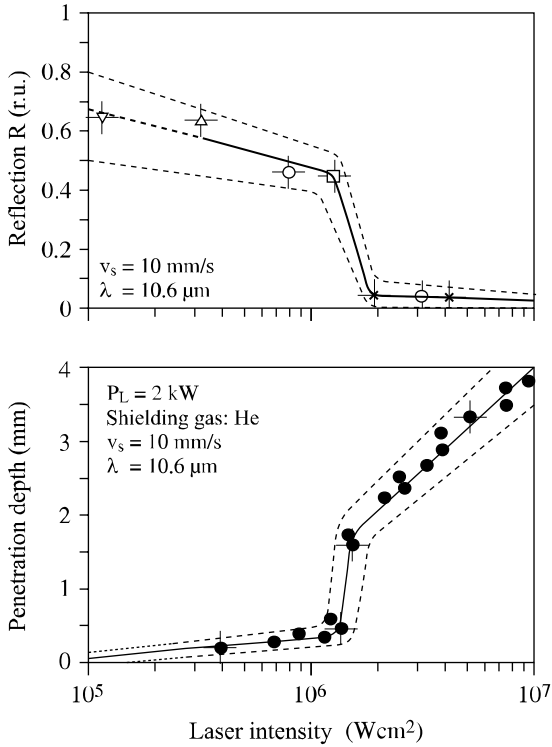
Figure 2.16. *Penetration depth and absorption coefficient in relation to laser beam intensity; from [HER 86]*

The threshold of the power density is a function of the following factors:

– the nature of the material to be welded,

– the laser beam wavelength,

– the shielding gas,

– the workpiece surface quality.

The nature of the material plays a big role in the creation of the vapor capillary. Materials such as silver, gold, copper alloys and aluminum alloys are not easily weldable by laser beam because of their low absorption coefficients.

Figure 2.17 shows that, because of their wavelengths, YAG laser beams and laser diode beams are absorbed better by metallic materials than a CO_2 laser. We will see that the wavelength can be a selection criterion for the welding of materials with a low absorption coefficient.
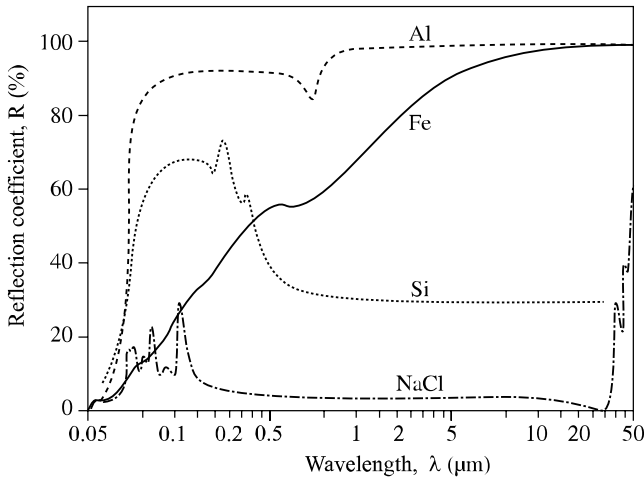
Figure 2.17. *Beam absorption in relation to wavelength; from [ROE 86]*

The low absorption coefficient of a material can be compensated by a high power density. This high power density can be obtained by the use of a good quality laser beam, the choice of short focal length optics, the increase in laser power or, in the case of a YAG laser, the use of a small diameter optical fiber.

The choice of assistant gas is also paramount. A good control of the gas supply and an appropriate choice in its composition have an important impact on the welding process and weld quality.

Shielding gas

The majority of the fusion welding processes (except the electron beam) require a shielding gas at the weld surface and if necessary at the back of the weld bead. In certain cases, a shielding gas covering can be used.

We can distinguish three zones to be protected: the weld pool, the surface of the weld just after solidification while still sufficiently hot to oxidize, and the root of the weld bead. For the protection of the weld pool and vapor capillary, we can use:

– a coaxial nozzle,

– a lateral nozzle,

– a plasma blowing system.

The coaxial and lateral nozzles transport gas at atmospheric pressure and at a low flow (15 to 30 l/min according to the power of the laser beam). They allow a good protection of the weld bead without disturbing the weld pool. The coaxial nozzle has the advantage of being usable for welding in all directions, which is not the case of the lateral nozzle.

The use of a plasma jet is used in some particular cases. This consists of using a small diameter tube ($\leq$6 mm) tilted at an angle ranging between 35 and 45° in relation to the surface of part with a high gas output. The gas jet, directed a few millimeters above the surface of the part, blows the gas plasma. This system is little used, because it does not allow a good gas protection and tends to disturb the weld pool.

The principal assistant gases used are the inert gases helium and argon or the active gas, that is, nitrogen. In the case of laser beam welding, gas protection does not only have the role of protecting the weld pool from contamination, it also takes part in the interaction between laser and material. The choice of gas thus depends on many factors:

– ionizing potential of gases,

– laser beam wavelength,

– nature of the material to be welded.

Gases subjected to a high density of power ionize more or less easily. Helium whose ionizing potential is high (24.46 eV) creates a not very intense and rather permeable plasma regardless of the laser beam's wavelength. It can be used up to powers of 45 kW without particular problems. Argon and nitrogen, whose potential for ionization are lower (Ar: 15.68 eV and N_2: 15.51 eV), create an intense plasma which hinders the interaction of beam and material. In the case of the CO_2 laser beam, the use of these gases will be limited to powers $\leq$5 kW. From the perspective of welding performance, helium ensures the deepest weld penetration compared to nitrogen and argon and the narrowest weld beads. The addition of helium to argon makes it possible to limit the harmful influence of argon generated plasma. Commercial mixtures (helium/argon) are offered, especially for welding by laser beam. These mixtures can be used for powers up to 10 kW.

In the case of the Nd:YAG laser, the choice of gas is not so important. The first data collected indicates that the use of argon or nitrogen with a Nd:YAG laser or fiber laser is possible with powers up to 10 kW.

Argon and helium, being inert, can be used whatever the nature of the material to be welded, which is not the case with nitrogen. The latter can cause metallurgical transformations in the materials to be welded. It is not to be used for welding zirconium and titanium alloys, as it will form titanium nitrides and zirconium nitrides which will weaken the assemblies. Nitrogen can also cause an increase in the sensitivity to hot cracking of austenitic stainless steels because of its gammagene effect (it leads to the formation of austenite as well as primary austenite solidification). For these materials, its use will be subject to procedures that prevent hot cracking. However, because it is soluble in stainless steels, nitrogen could be used with some advantage to avoid the formation of porosities in the molten zone [BAR 98]. Its use for welding non-alloyed and slightly alloyed steels does not pose a particular problem if a high quality of welding is not required.

2.3. Electron beam welding

2.3.1. *History [FRI 98]*

The earliest applications of the electron beam result from the work completed by K.-H. Steigerwald in Germany and by J.A. Stohr at the CEA (Atomic Energy Commission) in France. For the latter, this work was justified for the welding of combustible material casings made of zirconium alloy, a material very sensitive to oxidation and for which there did not exist, at that time, a suitable welding process. The production of an electron beam required vacuum conditions which naturally gave protection against oxidation. Thus, welding was made possible and the first EB welds were obtained using a focused electron beam produced by a Guinier cathode system. A patent was thus declared in 1956 and licenses granted to companies for the construction of machines, which appeared on the market in 1960.

The first machines had low power electron beam guns (a few kilowatts), which limited the thicknesses that could be welded to approximately ten millimeters. Very quickly, the gun power that could be increased (30 kW in 1970), which made it possible to consider the welding of very thick parts (40 to 50 mm) encountered in boiler manufacturing or heavy engineering.

During the 1980s, new applications were sought, with more than 1,000 machines being built in Western Europe between 1980 and the end of the 20th century.

2.3.2. *Principle*

The process of EB welding uses the energy dissipated by electrons at the moment they strike the part to be welded.

The electronic beam

The electron is a particle characterized by its mass $m = 9.1 \times 10^{-31}$ kg and its negative electric charge $e = 1.6 \times 10^{-19}$ Coulomb. When this electron is placed in a space where an electric field E and a voltage V exists, it is subjected to a force $F = eE$. Under the action of this force, the electron moves with a speed v and will acquire, by ignoring the relativity effect, kinetic energy:

$$E_c = \frac{1}{2} mv^2 = eV$$

If we consider n/t electrons emitted per unit of time, the power transported by the electron beam will be:

$$W = \frac{1}{2} \times \frac{n}{t} \times mv^2 = \frac{ne}{t} \times V = I \times V$$

with:

– V: acceleration voltage of the electrons,

– I: intensity of the beam.

Specific power

This is defined as the ratio between the power transported by the beam and the impact area of the beam on the parts to be welded. In welding, this specific power is a few tens of kW/mm^{-2}.

In fact, all the power is not transformed at the point of impact because of losses in the electron trajectory between the emission point and the point of impact on the part.

The first losses are due to collisions with the atmospheric molecules; they are all the more significant the higher the air pressure is.

The second losses are less important in quantity; they are due to re-emission phenomena, the most important of which is x-ray emission. The energy quantity thus dissipated is low (~ 1%) but the consequences are important from the perspective of safety.

2.3.3. *Equipment*

Three welding techniques appear according to the pressure value P close to the workpiece:

– $P > 10^{-5}$ mbar: secondary vacuum welding,

– $P \sim 10^{-2}$ mbar: primary vacuum welding,

– $P \sim 1,000$ mbar: welding without vacuum.

The equipment used is obviously different but they all include:

– an electron beam gun with its viewing system,

– a welding chamber containing the parts to be welded and sometimes the electron gun. This enclosure also contains the displacement systems for the parts and the gun,

– a pumping unit to obtain a reduced pressure into the gun and the chamber,

– a power supply and numerically controlled command and control circuits.

The electron gun

Figure 2.18 illustrates the principles of a triode electron gun, which include:

– a cathode made of a very emissive material: tungsten, tantalum or lanthium hexaboride. This cathode is heated in vacuum conditions, either directly by an electric current (direct heated electron gun), or indirectly by a primary electron beam resulting from a heated filament (indirect heated electron gun);

– a non-magnetic *Wehnelt* surrounding the cathode and acting, on the one hand, on the shape of the equipotential surfaces and thus on the shape of the beam (the electrons move perpendicularly to these surfaces) and, on the other hand, on the electron acceleration where this plays the part of a grid in a triode;

Cathode heating current

Direct heated
cathode (filament)

+ Polarizing voltage of the Wehnelt
−

+ Electron acceleration voltage

Anode

Electric field

Focusing coils

Deflection coils

Magnetic field

Workpiece
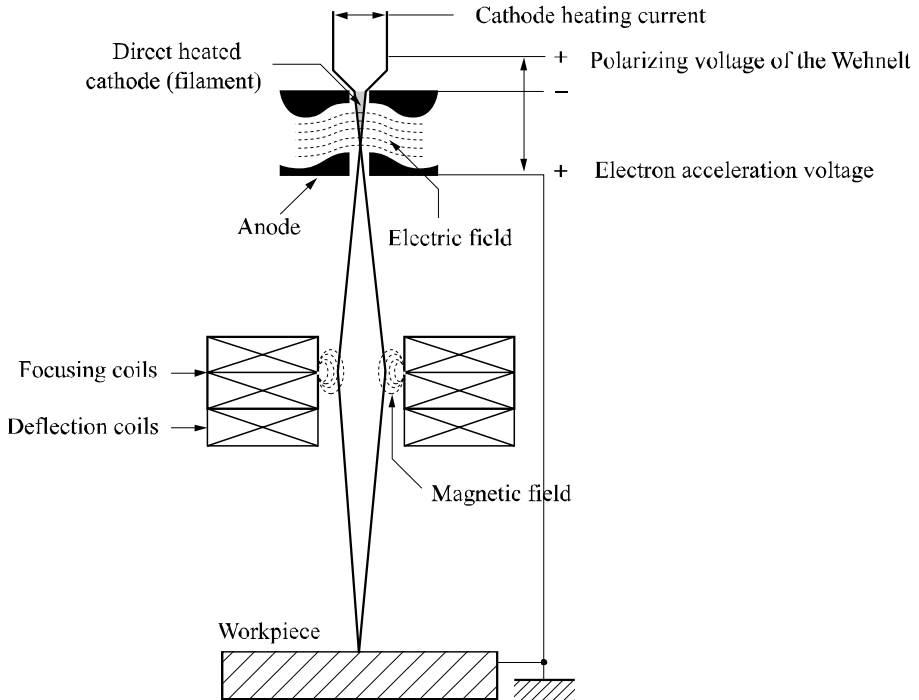
Figure 2.18. *Principle of a triode electron gun (Institut de Soudage document)*

− a copper anode carrying a positive charge compared to the *Wehnelt* creating the electric field to accelerate the electrons. This anode is bored in its center with a channel which allows the electron beam to pass through. This converges immediately at the exit of the anode then diverges under the effect of mutually repulsive electrons as they move apart;

− a magnetic focusing coil with windings in the same axis of symmetry as the gun. It reconcentrates the divergent beam and concentrates it on a small point (about a millimeter in diameter);

− a set of magnetic deflection coils enabling the beam to move in relation to its axis (side sweepings, circular movement, etc.);

− a system for accurately positioning the beam on the joint by an optical viewing system or a television camera system.

According to the electrode geometry and in particular of those of the anode and Wehnelt, the maximum current available *I* will be determined according to the acceleration voltage *V* by a characteristic of the gun called perveance p and expressed as:

$$I = p \times V^{3/2}$$

The gun powers vary according to the thicknesses which need to be welded. They range from 5 to 100 kW but most of the installations are equipped with guns that have a power ranging between 10 and 30 kW. With regard to the acceleration voltages, here those lie between 45 kV and 150 or even 300 kV, depending on the technologies chosen by the manufacturers and the power required from the gun.

The welding enclosure and displacement mechanisms

The enclosure (vacuum chamber) contains the parts to be welded with their tools and their workpiece displacement. It can also contain the electron gun with its displacement system with one or more axes. Generally, this enclosure must be of a low volume compatible with that of the parts to be welded, but it should be understood that too large a volume involves a longer pumping time, which has a detrimental effect on the equipment productivity.

Figure 2.19. *6 kW EBW machine; dimensions*
0.6 m ×0.6 m ×0.9 m (Techméta document)

In addition, these enclosures must be designed to resist atmospheric pressure without any deformation and their internal sides walls must be clean in order to limit the effects of gas adsorption and thus reduce the pumping time.

The enclosure volumes used industrially vary between 0.5 m^3 and more than 1,000 m^3 (see Figures 2.19 and 2.20).
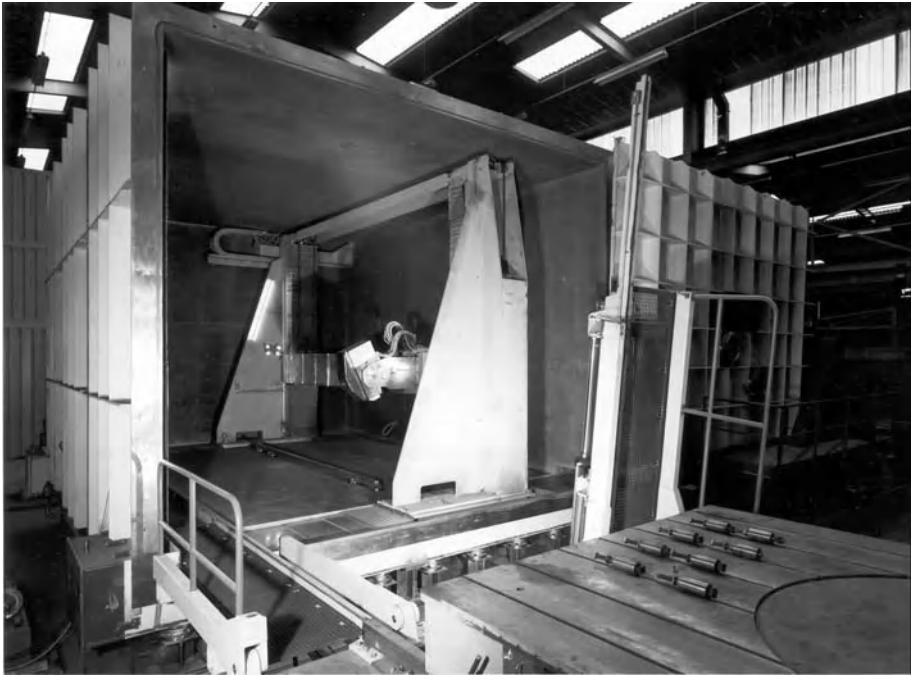
Figure 2.20. *50 kW EBW machine with internal gun; dimensions 8 m $\times$ 5 m $\times$ 5 m (Techméta document)*

In order to avoid building large-scale enclosures, it is desirable to create the vacuum locally, where the weld is to be made. This solution was adopted between 1970 and 1980 for various applications, including the welding of connecting pipes on boilers or tubes on tubular exchanger plates. Although tempting *a priori*, this solution has effectively been abandoned, because equipment with localized vacuum chambers was very expensive due to its application to only one type of part, and it did not offer great flexibility in use.

The systems for positioning and moving the parts are tables with one or two axes or turning gears for the welding of rotating parts. These mechanical axes are controlled numerically.

Vacuum creation systems

For the machines in primary vacuum, the pumping unit consists of standard mechanical pumps (rotary vane pumps or Roots booster pumps).

For those working in secondary vacuum, one or more oil diffusion pumps or turbomolecular pumps are added.

The pumping unit's delivery is a function of the enclosure volume to be pumped, the pumping time and degasification related to the nature and the thickness of material being welded. This last criterion is particularly important when welding very thick parts. This pumping delivery can reach levels from 2,000 to 5,000 $m^3.h^{-1}$ for mechanical pumps and from 10,000 to 20,000 $l.s^{-1}$ for oil or turbomolecular pumps.

Non-vacuum machines or under reduced pressure [POW 00]

The first industrial non-vacuum EB welding machine was used in the USA automotive industry towards the end of the 1960s. The essential characteristic of this type of equipment lies in the absence of a vacuum chamber, which is very important for mass production, e.g. automotive components like transmission components, torque converters and exhaust systems. Counterbalancing this advantage is the disadvantage of having to use a very high acceleration voltage (150 kV) in order to obtain a sufficiently powerful beam on the work piece, in spite of passing through a gaseous atmosphere of only a few millimeters. This high voltage generates strong X-ray emissions and it is thus necessary, in order to protect the operators working on the machine, to create an enclosure ensuring containment of this radiation.

Unlike in the USA, this type of process was little used in Europe. However, since 1990, significant developments have led to new equipment which functions at atmospheric pressure or under reduced pressure (<1 mbar). There is thus a renewed interest in this technology in two fields: thin sheet welding for the automotive industry (welding of aluminum panels) and welding of thick parts such as pipes for gas pipelines and containers for storage of radioactive elements.

Implementation of EB welding

Achieving a good quality weld requires the following parameters to be monitored:

– the power transported by the beam: it is the product of the electron acceleration voltage and the beam intensity. The power will be selected according to the thickness of the parts to weld, the nature of material and its physical properties (for the same thickness, we need more power to weld copper than steel) and welding speed;

– the welding speed: this should not only be selected according to gun power but it must be determined by the metallurgical weldability of material, i.e. its ability to form a defect-free weld (with no cracks for example);

– the pressure in the enclosure: this parameter is linked to the equipment, which is designed to work either in primary vacuum or in secondary vacuum. Some machines are able to work either in primary vacuum or in secondary vacuum; in this case, the choice of the pressure will be dependent on the material to be welded and its reactivity with oxygen (zirconium alloys for example);

– focus current: this very important parameter because it determines the specific power and thus has an important effect on the geometry of the molten zone. This parameter varies according to the nature of material to be welded and its thickness. It is thus related to the acceleration voltage and the welding intensity;

– beam deflection makes it possible, by movements imparted to the beam, to carry out welds by limiting the movement of the component. It is possible for example to perform a small diameter circular weld without any movement of the workpiece or of the gun while making the beam describe a cone having for its axis that of the workpiece;

– beam vibration: depending on the signal imparted to the deflection coils, it is possible to impart sweeping movements to the beam, (transverse or parallel to the welding seam and circular or elliptic in shape). Two parameters, amplitude and frequency, are added to the signal, which have a bearing on the width of sweeping and the stirring of molten metal. This beam vibration is used at an operational level to widen the molten zone and thus to tolerate a gap between the components, to improve the quality of the weld pool when welding in position. From a metallurgical perspective, it can help reduce hot cracking observed with certain materials (nickel alloys for example) and aid degassing of the weld pool, thus limiting porosities;

– the welding position: a flat welding position (beam axis is vertical) is used for welding thicknesses from 15 to 20 mm with a complete penetration mode. This limitation is due to the loss of balance between the surface tension forces which maintain the molten metal on the edges of the capillary and gravitational force. In partial penetration mode, the maximum weldable thickness in flat position is about 130 mm for steels. Beyond these limits, it is necessary to use the horizontal/vertical welding position (beam axis is horizontal). In this case the thicknesses are dependent on the electron gun's power. Vertical upwards welding and vertical downwards welding can also be used on steel thicknesses from 60 to 80 mm. For the overhead welding position, the maximum thickness is the same as that of the flat welding position.

2.3.4. *Design and preparation of the parts*

In general, welding is carried out without filler, on straight joined edges. Figure 2.21 illustrates some frequently used preparations.
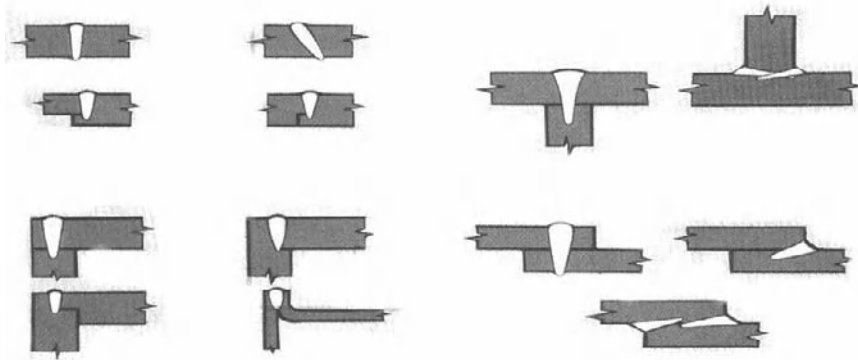
Figure 2.21. *Examples of joint preparation (Institut de Soudure document)*

These few examples show that, to profit from all the advantages offered by these processes, the choice of process will have to be made in the research department. The absence of a gap is sometimes difficult to achieve. Some gap between components can be tolerated; its value will vary with the thickness of the parts to be welded but, for thicknesses lower than 15 mm, this gap is approximately 10% of the thickness. Above this, it is necessary to use a filler in order to avoid overly thin areas. This is frequently carried out by laser beam; in EB welding, implementation is more delicate.

Because of component machining, a thorough degreasing prior to welding and an elimination of oxides present close to the joint are required to obtain a quality weld.

In EB welding, special attention must be paid to the remanent magnetism of components because of the risk of electron beam deviation and consequently of a welding defect like lack of fusion. This magnetism will thus have to be monitored before welding and the parts can possibly undergo a demagnetization operation. It is however necessary to realize that this is a delicate operation and does not always lead to the anticipated result.

In order to ensure a precise positioning of the photon or electron beam in relation to the joint, positioning and fastening assemblies are often required. These must be precise and made of non-magnetic materials in the case of EBW.

2.4. Metallurgy of high density energy beam welding

The principal features of high density energy density beam welding processes compared to conventional welding processes (arc welding) are:

– the absence of filler wire in most cases,

– high welding speeds which involve higher solidification and cooling rates,

– a narrow molten zone and heat affected zone,

– low heating and a limited deformation of the parts,

– no direct contact between the energy source and the component.

These features involve characteristics related to the behavior of the materials to be welded. In order to study these characteristics, it is advisable to distinguish, on the one hand, pulsed welding modes such as pulsed YAG laser beam welding and, on the other hand, continuous welding such EBW, CO_2 laser and continuous YAG laser processes. The thermal cycles obtained during pulsed welding are shorter than those obtained in continuous mode.

In order to present the weldability problems of various metallic materials in a coherent way, we will distinguish [MUR 94]:

– operative weldability: this relates to problems encountered at the time of welding, when the behavior of the metal or alloy to be welded prevents the weld being completed;

– metallurgical weldability: during the welding process, one of the zones which constitute it (molten zone, bond area, or HAZ) can be altered because of the operation itself, to the point of questioning the performance of the assembly under the operating conditions envisaged.

Operative and metallurgical weldabilities will be presented for the main metal alloys (steels, aluminum alloys, nickel alloys, titanium alloys, zirconium alloys and copper alloys).

2.4.1. *Steels*

2.4.1.1. *Operative weldability*

Steels generally offer a good operative weldability. In addition to the advantage linked to the absence of a vacuum enclosure, the laser welding processes offer, compared to EB welding, the advantage of being insensitive to beam deviations, remanent magnetism in the case of ferritic steels or, in the case of heterogenous

assemblies, the Peltier effect. Stainless steels must however be welded with gas protection, catered for by using a gas carriage.

2.4.1.2. *Metallurgical weldability*

Non-alloyed or low-alloyed steels

With regard to metallurgical weldability, apart from certain features of the high density energy beam processes evoked before (no contact with the parts, absence of hydrogen, lower shrinkage stresses), these welding processes significantly limit the cold cracking phenomenon.
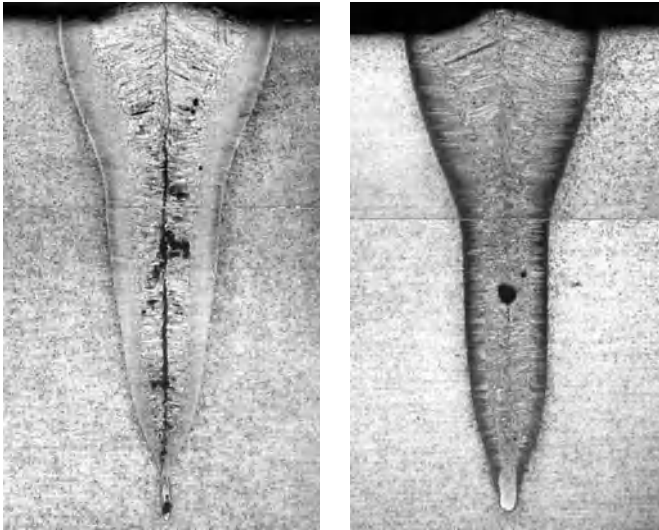
Figure 2.22. *Illustrations of CO_2 laser welds in 25 CrMo4V steel (from [COL 97]).*
25CrMo4V: 0.005% of sulfur, 0.015% of phosphorus (no cracking)
25CrMo4V 4: 0.031% of sulfur, 0.016% of phosphorus (cracking)

On the other hand, work completed at the Institut de Soudure [COL 97] highlighted an increase in hot cracking due to the combined effects of the high welding speed and presence of residual elements, sulfur and phosphorus in particular (see Figure 2.22).

The ranges of chemical composition recommended by the current standards do not take account of the specificities of the high density energy beam welding processes. A restriction in residual elements (sulfur, phosphorus) is essential in order to limit the risks of hot cracking.

Austenitic stainless steels

Many prediction diagrams depicting the metallurgical structure of as-welded alloys have been established and modified as welding processes have evolved. *Inter alia*, the Schaeffler diagrams [SCH 49], Delong team diagrams [DEL 56] or Suutala diagram [SUU 79] established for conventional welding processes are no longer applicable for welding processes involving rapid cooling. For this reason, a study carried out by the Institut de Soudure [CHE 93] looked at the influence of thermal conditions and steel composition on the liability of stainless steels to hot cracking when welded by a laser beam. It was shown that these hot cracking phenomena are not very important during continuous welding mode but become highly significant during pulsed welding.
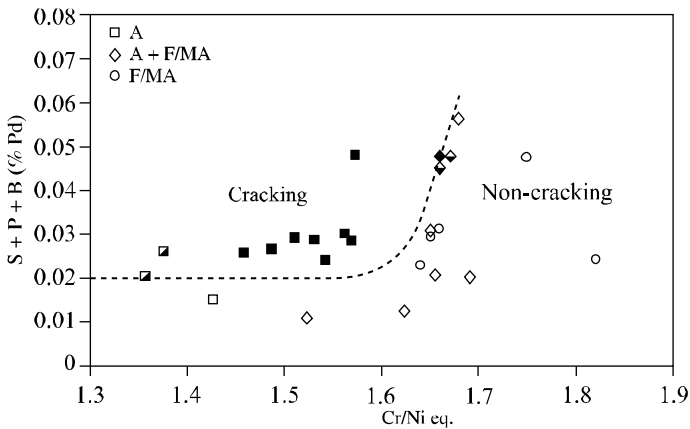
Figure 2.23. *Prediction diagram of hot cracking during pulsed YAG laser beam welding of austenitic stainless steels; from [CHE 93]*

A new prediction diagram for hot cracking dependent on the sulfur, phosphorus and boron content of the alloy's chemical composition in terms of equivalent Cr/Ni, and of the primary solidification mode (austenitic or ferritic) has been established for the pulsed YAG laser and CO_2 laser beam processes (see Figure 2.23).

$$\frac{Cr}{Ni}\,eq. = \frac{Cr + 1.37Mo + 1.5Si + 2Nb + 3Ti}{Ni + 0.31Mn + 22C + 14.2N + Cu}$$

This diagram presents three distinct fields: two non-cracking domains and a cracking domain. The alloys, of which the Cr/Ni equivalent is higher than 1.7, are not very sensitive to hot cracking up to a high impurity content. They result from a ferritic solidification mode followed by a solid state austenitic transformation. The

second non-cracking domain corresponds to alloys whose Cr/Ni equivalent is lower than 1.58 but whose impurity content is low (S + P + B ≤200 ppm). The cracking domain is defined by a Cr/Ni equivalent lower than 1.58 and an impurity content of (S + P + B) >200 ppm. Alloys whose Cr/Ni equivalent is between 1.58 and 1.70 are in a transitory zone where hot cracking depends on impurity content.
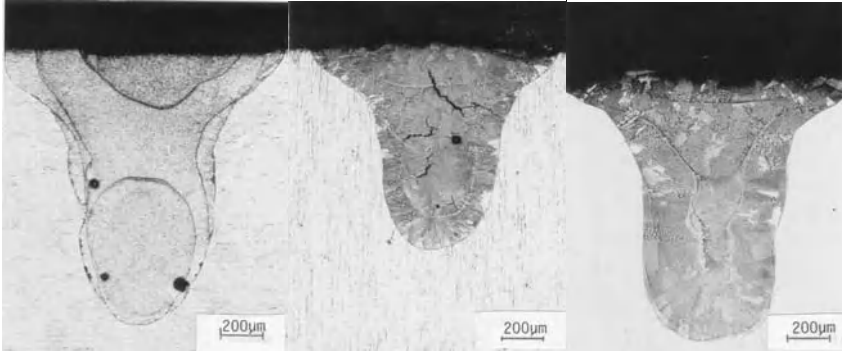
Figure 2.24. *Austenitic stainless steel pulsed YAG laser bead on plates; from [CHE 93a]. X2CrNi18-09 Cr/Ni eq. = 1.75% (S + P + B) = 0.0475% (figure on left) X2CrNiMo17-12-2 Cr/Ni eq. = 1.57% (S + P + B) =0.0481% (middle) X2CrNiMo17-12-2 Cr/Ni eq. = 1.523% (S + P + B) =0.0106% (figure on right)*

This work showed that external factors, such as the use of nitrogen (gammagene) as a shielding gas, can contribute significantly to the formation of cracks (see Figure 2.25).

Ferritic stainless steels

The main issues encountered during the welding of ferritic stainless steels are grain enlargement and nitride and chromium carbide precipitation which can cause intergranular corrosion. These phenomena are particularly prevalent during the use of welding processes using high linear energy. The high density energy beam welding processes, with low heating and high cooling rate, limit these phenomena and improve the welded joint's mechanical strength in a significant way.
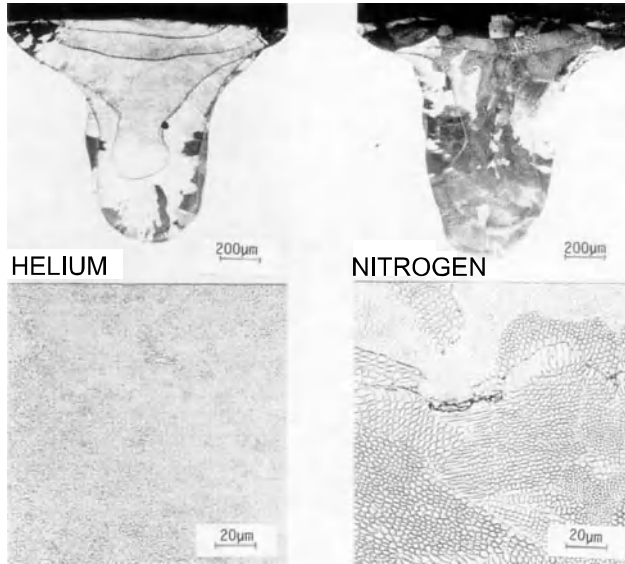
Figure 2.25. *Comparison of beads on plates carried out with various shielding gases (from [CHE 93]). Bead on plate with helium (figure on left). Bead on plate with nitrogen (figure on right)*

Martensitic stainless steels

Martensitic stainless steels can be sensitive to the cold cracking phenomenon. The factors which give rise to cold cracking are:

– high percentage of carbon (>0.3%),

– stresses caused by the welding process or unsuitable joint design,

– high cooling rates,

– the presence of hydrogen in solution.
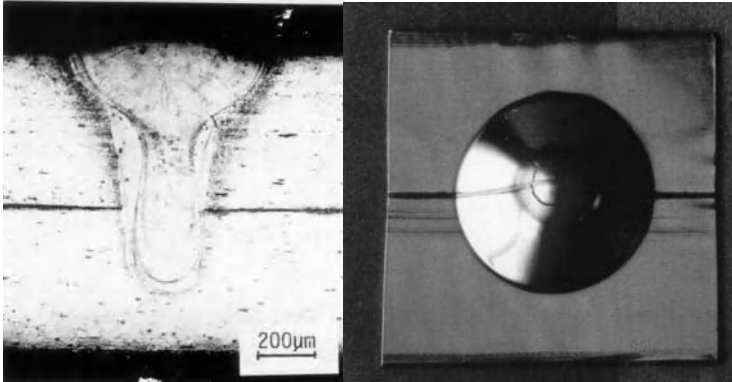
Figure 2.26. *CO_2 laser beam lap weld of X2CrMoTi 18-2 ferritic stainless steel*
(Institut de Soudure document)

Various arrangements make it possible to limit or avoid the cold cracking of these steels:

– the use of an austenitic filler wire,

– pre-heating and post-heating,

– avoidance of hydrogen introduction.

The high density energy beam welding processes have great advantages compared with conventional processes. Having no contact with the part to be welded, they limit hydrogen contamination, and with the molten zone being very narrow, the stresses caused by shrinkage during solidification are significantly reduced. Certain steels considered unweldable by arc processes have been welded without filler wire and pre-heating.

Precipitation hardening martensitic stainless steels lose their mechanical properties after welding if they are welded in an age hardened state. It is appropriate, if the design of the parts allows it, to weld in a hyperquenched state and to carry out the ageing treatment after welding.

Austenoferritic stainless steels (duplex or super-duplex)

These steels owe their good mechanical characteristics and their good corrosion resistance to their microstructure made up of 50% of austenite and 50% of ferrite. The high cooling rate induced by welding causes an imbalance between ferrite and austenite. The high cooling rate generated by the high density energy beam welding processes involve the formation of an almost entirely ferritic structure in the molten zone. The reduction in welding speeds and/or the introduction of nitrogen as a

shielding gas increases the austenite content. Unfortunately, these techniques do not suffice to obtain a duplex structure (see Figure 2.27). The high density energy beam processes will be usable only whenever the corrosion requirements are not at maximum.
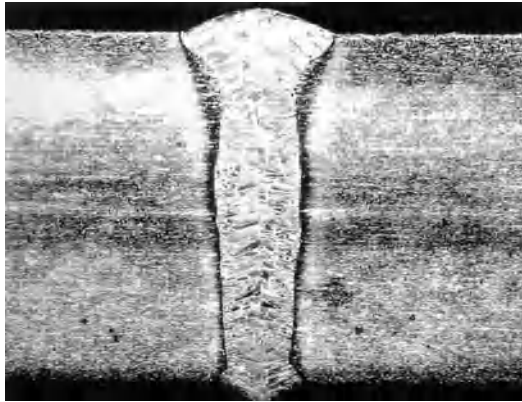
Figure 2.27. *CO₂ laser butt welded joint of 3 mm thick austenoferritic stainless steel; X2CrNiMoN22-5-3 (Institut de Soudure document)*

2.4.2. *Aluminum alloys*

Operative weldability

The main issues of operative weldability for aluminum alloys relate to the presence of the refractory oxide layer and their high conductivity. The oxide layer requires the surface cleaning of the parts before welding, whatever the welding process used. The laser welding of aluminum alloys is made more difficult because of their low absorption coefficient. In this case, a YAG laser has a slight advantage compared to the CO_2 laser because of its lower wavelength, which allows a better radiation absorption.

Electron beam welding has advantages for the welding of these alloys because it does not have the absorption problem of laser beams, while the weldable thicknesses are high (see Figure 2.28) and the weld beads are narrow. The thermal welding cycle is sufficiently short, which limits the problems caused by aluminum's high thermal conductivity.
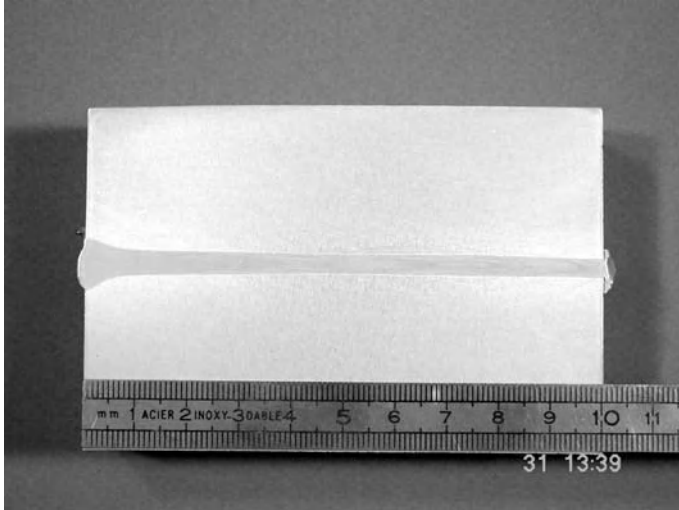
Figure 2.28. *Electron beam weld of aluminum alloy 5754*
(Institut de Soudure document)

Metallurgical weldability

In a similar way to austenitic stainless steels, aluminum alloys react differently to the pulsed or continuous welding mode.

The solidification speed obtained during pulsed YAG laser beam welding causes the systematic appearance of hot cracking. Only pure aluminum and the 4000 series aluminum (Al, Si) can be welded without hot cracking. The 5000 (Al, Mg) and 6000 (Al, Mg, Si) series aluminum alloys can be welded either in a heterogenous assembly with the 4047 aluminum alloy (or 4043) or by using this alloy as filler wire.

Continuous mode welding processes cause fewer hot cracking problems. They make it possible to weld 3000, 4000, 5000 and 6000 series aluminum alloys under good conditions. The 6000 series can however present hot cracking phenomena for high welding speeds. For laser welding, the use of 4047 (or 4043) filler wire can avoid this hot cracking phenomenon. However, this can give rise to a liquation phenomenon.
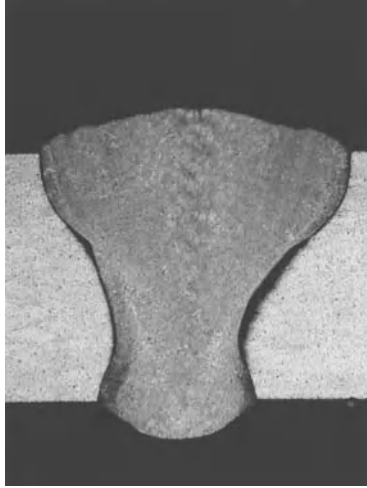
Figure 2.29. *CO$_2$ laser beam weld of 5 mm thick
aluminum alloy 6013; from [CHE 98]*

In the case of 2000 series aluminum alloys, only alloy 2219 is truly weldable. Aluminum alloy 2024 can be welded with caution at a low welding speed.
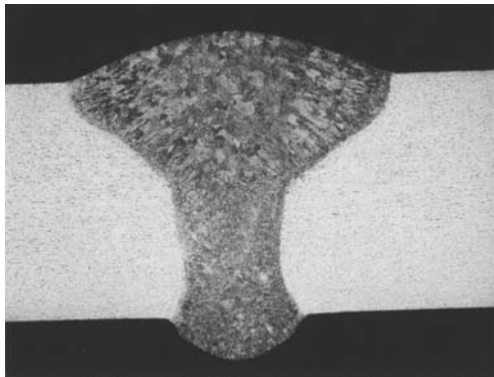
Figure 2.30. *CO$_2$ laser beam weld of 5 mm thick
aluminum alloy 2219; from [CHE 98]*

The 7000 series alloys must be welded with precaution, because they have a strong tendency to hot cracking. Aluminum alloy 7020 can be welded by electron beam (see Figure 2.31). It is advisable in this case to take account of the restraint effects caused by the design of parts.

Figure 2.31. *2 mm penetration depth in a aluminum alloy 7020 welded by electron beam (Institut de Soudure document)*

2.4.3. *Nickel-based alloys*

Operative weldability

Like stainless steels, nickel-based alloys do not pose any particular operative weldability problem. It is however necessary in the case of laser welding to provide an adequate shielding gas using a gas carriage.

Metallurgical weldability

Nickel-based alloys can be classified into two big groups:

– non-heat-treated alloys: these offer good corrosion resistance. Such alloys offer, in general, good weldability;

– precipitation hardening alloys: these are used for their good mechanical properties at high temperature. They are sensitive to hot cracking. A post-weld heat treatment is often necessary (see Figure 2.32).
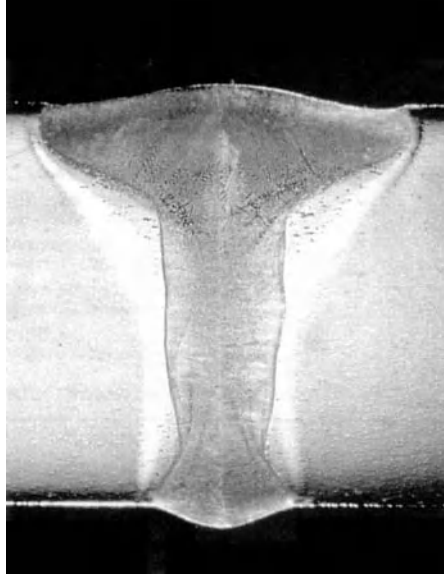
Figure 2.32. *CO₂ laser beam weld of 6 mm thick Inconel 718
(Institut de Soudure document)*
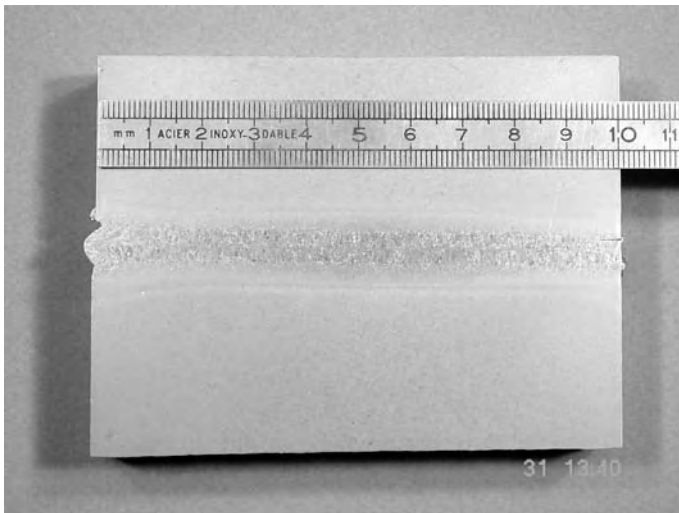
Figure 2.33. *Electron beam weld of 100 mm thick titanium alloy TA5E
(Institut de Soudure document)*

2.4.4. *Titanium-based alloys*

Operative weldability

Titanium alloys respond well to laser beam or electron beam welding. They have a good fluidity which helps the formation of an aesthetic weld bead. The use of excessive energy densities will cause surface defects like undercuts (see Figure 2.33).
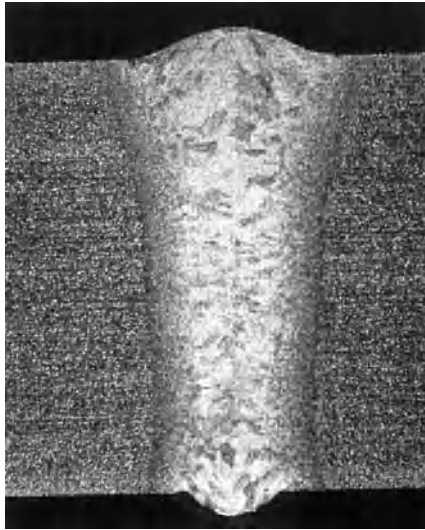
Figure 2.34. *CO_2 laser beam weld of 6 mm thick alloy TA6V*
(Institut de Soudure document)

They have, however, a great sensitivity to oxygen and nitrogen. An effective gas shield is required during welding. Contamination by oxygen and nitrogen entails particle formation, which increases mechanical resistance to the detriment of toughness and thus will weaken the structure. For this reason the vacuum electron beam is an excellent alternative.

Metallurgical weldability

Certain alloys are sensitive to grain enlargement during welding. As for ferritic stainless steels, high density energy beam processes significantly limit this phenomenon. The weld beads obtained by laser or electron beams have a better ductility than those obtained by arc welding. The alloys usually employed are not very sensitive to hot cracking.

2.4.5. *Zirconium-based alloys*

Operative weldability

The behavior of zirconium alloys is similar to titanium-based alloys. They can be easily contaminated by ambient air. Oxidation starts at 400 to 500°C. Surface and back gas shielding must be guaranteed. The electron beam is the favored process for these alloys. A pulsed YAG laser beam can be used because of the limited heating effect.
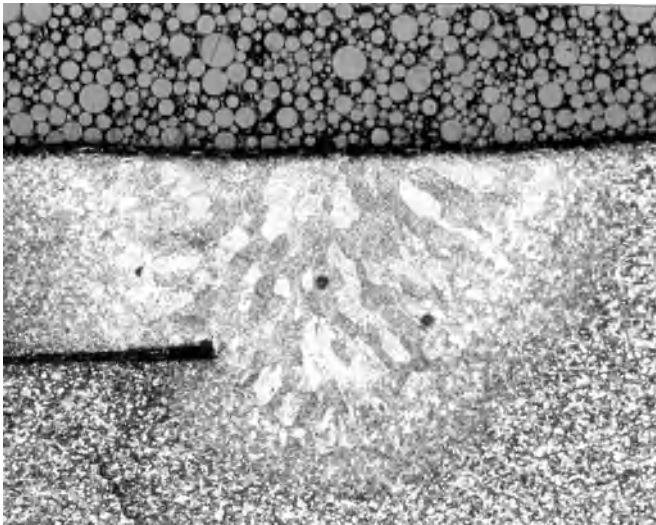
Figure 2.35. *Pulsed YAG laser weld of 1 mm thick zirconium alloy Zy4 (Institut de Soudure document)*

Metallurgical weldability

Certain alloys are commonly used because of their good metallurgical weldability. This is the case for Zircaloy in the manufacture of casings for the nuclear industry. Zirconium alloys are sensitive to grain enlargement, hence the value in using high density energy processes.

2.4.6. *Copper-based alloys*

Operative weldability

The great reflectivity and high thermal conductivity of copper alloys are major disadvantages for laser beam welding. It acts just as a mirror. The pulsed YAG laser

beam, thanks to its high density of energy, can sometimes be used for welding very thin parts. On the other hand, the electron beam presents many advantages. It makes it possible to weld thick sections without pre-heating. The weld beads obtained are narrow.
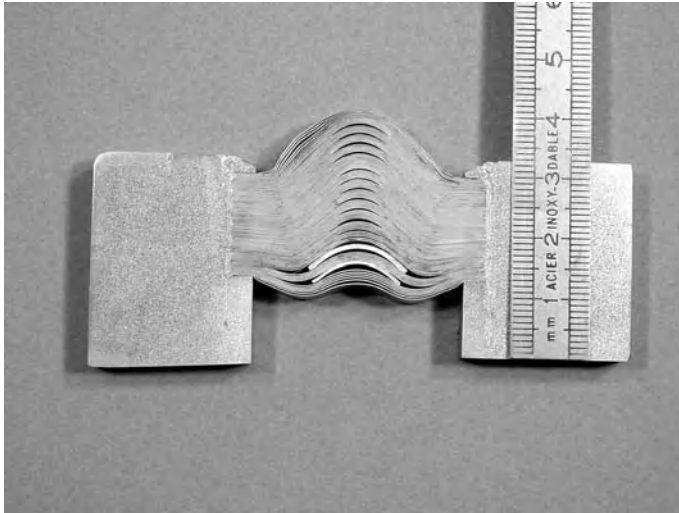
Figure 2.36. *Electron beam welding of a copper part (Institut de Soudure document)*

Metallurgical weldability

Pure copper exists in different levels of purity:

– Cu-a_1: 99.90% pure, contains up to 0.1% of oxygen,

– Cu-b: 99.90% deoxidized with phosphorus,

– Cu-c_1: 99.94% pure,

– Cu-c_2: 99.96% pure.

Copper must be welded in deoxidized types Cu-c_1 or Cu-c_2. Whatever the origin of the oxide, when it occurs as intergranular precipitates, it weakens the weld and its surroundings. It can also cause the formation of porosities.

The main copper alloys have a good metallurgical electron beam weldability. A hot cracking phenomenon is possible for certain alloys such as cupro-aluminums, cupro-berylliums and certain brasses. It is absolutely essential to avoid the presence of lead (alloys with improved workability) which increases the tendency to hot cracking.

2.5. Mechanical properties of welded joints

High density energy beam welds have specific characteristics such as single pass welding, a narrow molten zone and the absence of filler wire. These characteristics will have an influence on the traditional mechanical properties.

With regard to the tensile test, the transverse rupture of tensile specimens generally occurs in the base metal. Only austenitic steels present a rupture close to the fusion line but at a breaking load very close to that of the base material. For materials with structural hardening, the rupture occurs in the molten zone. The tensile tests in the longitudinal direction are not carried out because of the difficulty in taking a test piece due to the narrowness of the molten zone.
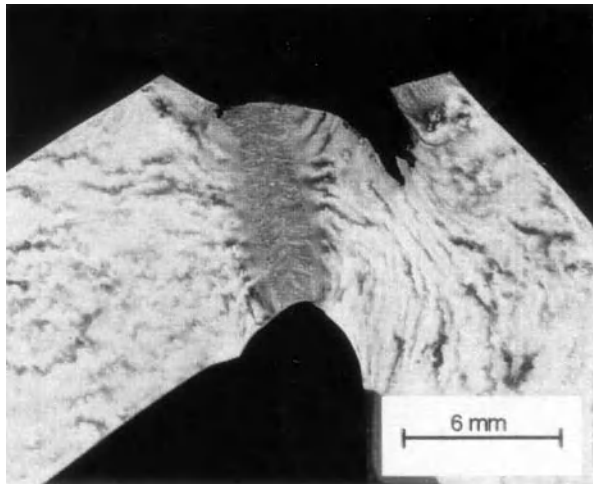
Figure 2.37. *CO_2 laser beam weld of 12 mm thick non-alloyed steel*
(Institut de Soudure document)

Bend tests lead to good results. It should however be noted that in welds carried out on alloyed steels, the hardness difference observed in the weld area causes a deformation during the transverse bending test on either side of the molten zone. Longitudinal bend testing is thus more useful since it forces all the zones to deform in the same manner.

For the impact test, a crack deviation and the absence of rupture is often observed in the test sample.

This then raises the problem of the test's validity. Palliative solutions have been developed to try to evaluate the strength of these welds. Currently there is no

universal agreement, and further work is necessary to find a new test that is easy to carry out, inexpensive and gives valid results.

The hardness test, which shows the various joint structures, are characterized by a lower value in the molten zone than in the heat affected zones (HAZ). This can be explained by a different cooling rate and the loss of quenching elements from the molten zone, such as manganese in steels. In arc welding processes, the hardness test is often associated with cold cracking and the threshold criterion of maximum hardness of 350 Vickers. For the laser and EB processes, this threshold is exceeded in the majority of cases. However, as the welding is performed in the absence of hydrogen since it is in a vacuum or under gas protection, the risk of cold cracking is almost zero, except for highly alloyed tempered steels or those with high levels of carbon.

Fatigue resistance,is in general satisfactory, due to the presence of compressive stresses on the bead surfaces.

2.6. The quality of the assemblies

The quality of a weld is measured with respect to its conformity to specifications imposed on the final assembly. It can be a question of its mechanical performance, water/air-tightness, or resistance to corrosion. Quality is tested overall using tests on the complete assembly or on the test specimens produced under the same operating conditions, and/or by observing this assembly in a very precise way, using both non-destructive and destructive tests.

In the following section, we will present a non-exhaustive list of the possible defects in HEDB welds, the control methods most commonly used and the principal standards in operation.

2.6.1. *Weld defects*

Standard NF EN 26520 is a "classification of the defects in the fusion welds of metals with explanatory comments" and makes it possible to enumerate and classify the defects according to their geometry, their position in the weld and their origin. HEDB processes, due to their particular features, give rise to the appearance of special defects.

Cracks

Hot cracks are most frequently encountered because of high solidification speeds and, in most cases, the absence of filler wire addition. They are emerging or

non-emerging and small in size. They are called *hot cracks* when they appear at the end of solidification on a molten pool. There are interdendritic or intergranular cracks, related to segregation phenomenon. The pulsed YAG laser beam welding process has a tendency to produce such defects in austenitic stainless steels, aluminum alloys and some nickel base alloys.

The cracks are known as *cold cracks* when they appear towards the end of cooling, at around 150°C or less. These cracks are found in the molten zone or the heat affected zone. They are related to martensitic quench hardening, hydrogen embrittlement and internal stresses. Non-alloyed or low alloyed steels are sensitive to cold cracking according to their percentage of carbon and alloying elements. Various formulae have been proposed to define a weldability limit for these steels. Such formulae, established for conventional welding processes, only account for the composition of steels in terms of carbon equivalence but disregard the cooling speed. These formulae are not applicable in the case of HEDB processes because of its high cooling speed, and also the fact that they do not introduce hydrogen and that shrinkage stresses are limited. These cracks, encountered less frequently than hot cracks, are quite small.

Cavities

These are voluminal defects. They include shrinkage due to the shrinking of metal during solidification and often appear halfway down in the middle of the molten zone or in the craters at the weld end. Crater shrinkages are often accompanied by microscopic hot cracks. They are often observed in a widening of the molten zone or *bulge* related to poorly focused laser or electron beam. They are more often found in very thick components and when high levels of impurities, sulfur and phosphorus, are found in the alloy. They are aligned with the axis of the molten zone.

Cavities also include the pores formed by gas trapped during solidification. They appear in the form of isolated pores or distributed along the weld zone. They are frequent in partial penetration welds. They occur more frequently when welding thick components and in cases of poor cleaning (aluminum alloys, titanium alloy). In laser and EB weld beads, their size can vary from a few tenths of a millimeter to a maximum of two millimeters, a result of the molten zone's narrowness. They are located mostly half way down or at the weld root.

Lack of fusion or penetration

The lack of fusion is a lack of connection between the base metal and the weld zone. It is a flat defect. It can be related to a discrepancy between the beam and the weld seam. In the case of a heterogenous assembly, it is due to a significant

difference in conductibility between materials. It is not easily detectable by non-destructive tests.

Lack of penetration is a lack of fusion between the edges to be welded. It is located at the weld root. It is often caused by insufficient beam power or a degradation in beam focus.

Shape defects

We can distinguish the following defects:

– undercuts: in the case of arc welding processes, these are due to a very localized lack of metal. They form an acute line on the surface at the front or on the reverse sides at the weld zone and base metal limits. In HEDB processes, undercuts are often due to a hollowing out of the weld bead on both sides of the molten zone. They are produced by an excessive power density or excessive welding speed. They are often encountered during the welding of titanium alloys;

– insufficient thickness: this is caused by a collapse of the molten metal in the weld zone. There can be various causes:

- a lack of material due to an excessive gap between the parts to be welded,

- when welding very thick parts in flat position (the limits are: 20 mm for EB welding, 15 mm for laser beam welding),

- an excessive power density;

– misalignments: these are due to a shift in position between the two parts to be welded. This shift can lead to lack of weld root fusion.

Projections (splatters)

Metal splatter during welding can be adherent or not. It can be caused by excessive power density, the presence of organic materials on the surface of the part or in the seam, or an inadequate gas protection. The welding of nitrided or carbo-nitrided steels can cause these projections.

2.6.2. *Weld inspection methods*

For HEDB welds, non-destructive tests make the detection of small defects possible. The welding speed requires the use of fast and inexpensive control test procedures. Controls can be carried out off-line (visual, radiography, ultrasound, magnetoscopy, Foucault current, etc.) or on-line (plasma analysis, infrared thermography, visually using a camera, etc.). In mass production, off-line control cannot be applied to all components, so on-line testing is preferred. Very often, an

on-line control is accompanied by sampling. In this case, a destructive test will be applied to a selection of parts.

Destructive tests (clamped side stamping tests, metallography, etc.) are long and expensive. However, they make it possible to detect certain welding defects (cracks, lack of penetration or bond) and do not prejudge the total quality of the assembly.

2.6.3. *Standardization and qualification of the welding operating mode*

EB welding has been the object of thorough standardization. Laser beam welding, a more recent process, is still in the process of standardization. The main welding standards are common today with ranges of different thicknesses for the two processes. The principal welding standards in force are as follows:

– EN ISO 13.919-1: Welding – Joints welded by laser beam and electron beam – Guide to the quality levels of defects – Part 1: Steel;

– EN ISO 13.919-2: Welding – Joints welded by laser beam and electron beam – Guide to the quality levels of defects – Part 2: Aluminum alloys;

– EN ISO 15.609-3: Description of welding procedures by electron beam;

– EN ISO 15.609-4: Description of welding procedures by laser beam;

– EN ISO 15.614-11: Welding procedure test for electron beam and laser beam.

2.7. Economic aspects

The main obstacle to the large scale development of HEDB processes is the operational and capital cost of this equipment. The investor must be certain of the technical advantage of the process but more especially its economic benefit. It is difficult to speak about costs for rapidly evolving processes. We will limit ourselves to touching on laser components and their operational and capital costs in order to give the reader the principal elements of any calculation [SAY 99].

2.7.1. *Cost of an electron beam machine*

The cost of a machine will vary according to the following factors:

– technology selected: vacuum or non-vacuum,

– electron acceleration voltage,

– gun power,

– enclosure volume,

– displacement systems of the parts and the gun.

It is difficult in these circumstances to estimate a price. To give some idea however, a machine equipped with a 30 kW gun and with a 1 m^3 enclosure pumped in secondary vacuum will cost about €600,000.

With regard to operating costs, the consumable costs are primarily electricity, cathodes and filaments whose lifespans vary according to use but can reach several dozen hours. The principal operating costs lie in maintaining the cleanliness of the enclosure and the gun, which has a very significant impact on the equipment productivity (a clean enclosure leads to reduced pumping times) and on the weld quality (a clean gun cuts the risk of beam interruption owing to lack of insulation).

2.7.2. *Cost of a laser beam machine*

The hourly use rate of a laser system is mainly made up of paying off the capital cost, consumables, and the expenses of maintenance and labor. The most significant part of the total hourly rate is paying off the capital investment.

Depreciation

Companies tend to envisage increasingly shorter depreciation periods (less than 3 years). In the overall investment costs, it is necessary to take account of the laser source, the robot, the peripheral systems, the tools, the installation and integration expenses of the system.

Consumables

These depend on the laser system chosen.

The CO$_2$ laser system

The "lasing" gas: consumption depends on the source type and the laser power. For lasers with fast axial flow, the gas outputs are low, about 30 l/hr for helium. Laser sources known as SLAB offer the lowest gas consumption.

Shielding gas: the gas flow rates are about 15 to 30 l/min. The most expensive gas is helium; it is also the most frequently used because of its high ionization potential.

Electricity: CO$_2$ lasers have an electrical efficiency output of about 5 to 10%. The cost depends on the power used. It is important to take into account the consumption of the complete installation, cooler included.

Maintenance: this is estimated to be 5% of the annual capital investment.

Optics: the cost of optics can increase significantly if the optical path is badly designed. It depends on the number of mirrors in the optical path, the type of mirrors and the protective systems used in the focusing head. It also depends on the procedure (clean parts, presence of oxides or oil) and on the operating environment.

YAG laser system

Lamps: the cost depends on the number of lamps employed and their lifespan. Lamps in continuous YAG lasers have an average lifespan of 1,000 hrs. The lifespan of the lamps depends on their use and can reach 2,000 hrs.

For a pulsed YAG laser, the lifespan is given as a number of pulses. This can reach several million pulses.

Shielding gas: argon is more easily usable than in the case of the CO_2 laser. The gas flow rates are comparable.

Electricity: a YAG lamp pumped laser has a lower electrical output efficiency than a CO_2 laser, about 1 to 3%. A YAG laser diode-pumped laser offers a much better output of about 10%. Electricity consumption depends of course on the power of the laser.

Fiber-optics: these should not deteriorate in normal use. It is however necessary to envisage their eventual replacement or repair.

Focusing optics: these are very seldom replaced because of their glass protection. They are less expensive than lenses made of zinc selenium or mirrors.

Protective glass: it is necessary to envisage the regular replacement of protective glass, at a frequency which will depend on the application.

Currently the choice of a laser system is made at four levels:

1) choice of pulsed or continuous mode: this choice is determined by the type of application (material to be welded, thickness, distortion, etc) and by the production speed required;

2) choice of the laser type (YAG or CO_2): flexibility (fiber or mirrors), thickness to be welded (powers available), materials (wavelength);

3) YAG laser pumped by lamps or pumped by diode: this issue is often raised because of the recent development of diode-pumped YAG lasers. The advantage of this laser is uncertainly its high quality beam. It is however necessary to make the comparison between the operating costs of both systems. A diode-pumped YAG

laser does not require a change of lamps and its electrical output efficiency is higher. However, the high cost of laser diodes makes its capital cost much higher than that of a conventional YAG laser, which considerably increases its utilization cost. A reduction in the cost of laser diodes is expected, and this should reverse the trend;

4) choices of the mechanized system: the choice of a polyarticulated robot or a Cartesian robot will depend on the application and the choice of the laser type (YAG or CO_2). It should be noted that the capital cost of a Cartesian robot is definitely higher than that of a polyarticulated robot.

2.8. Safety [HEE 00]

The use of lasers in industry is recent and the technology is evolving quickly, which explains the regulatory weaknesses both in Europe and in France. The principal reference text is standard NF EN 60.825-1 "Safety of laser equipment – Part 1: Equipment classification, requirements and user guide". Other specific standards cover particular questions such as: standard NF EN 12.626 December 1997 "Safety of machines. Laser machines. Safety regulations" and standards NF EN 207 "Laser safety glasses" and NF EN 208 "Safety glasses for laser adjustment", December 1998.

The principal risks when using a laser are to the eye. They derive from the physical characteristics of the laser. Certain radiations, according to their wavelengths, are transmitted to the retina and are focused by the crystalline lens. The power density received can be 5.10^6 times higher on the retina than on the cornea. The retina is particularly vulnerable to radiation from the visible or near-infrared spectrum (0.4 to 1.4 µm). If the density of energy received by the retina is excessive, it can cause an irreversible lesion. Standard NF EN 60.825 classes various lasers according to their risk.

For EB welding machines, apart from the risks related to the presence of high voltages, which is controlled via the safety measures taken by the manufacturer, the principal risk is that of the production of x-rays, as previously mentioned. There again, the precautions taken by the manufacturer should be sufficient and are the subject of special attention at the time of delivery of the machine. It is thus incumbent on the user not to modify the equipment, particularly the enclosure without checking that the biological shields are properly in place.

2.9. Examples of industrial applications

2.9.1. *Electron beam welding*

The industrial applications of EB welding are now well-known and encompass all the industrial sectors, from the automotive (transmission components) and aeronautical (manufacture of jet engines) to the manufacture of diverse parts or sensors (Figures 2.38-2.40).

Figure 2.38. *Copper electrical connection (Techméta document)*
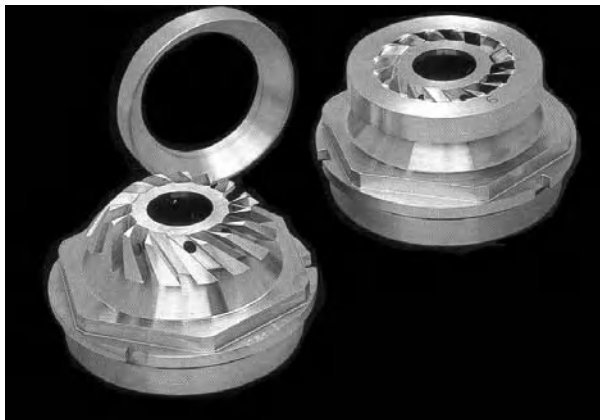
Figure 2.39. *Stainless steel turbine*

2.9.2. *Laser beam welding*

We can list, in the following table, some well-known industrial applications.

Application	Industry	Type of laser	Materials	Thickness
Welding of blanks	Automotive	CO_2	Non-alloyed steels coated or not	0.7 to 2 mm
Bodyshells	Automotive	Continuous YAG	Coated non-alloyed steels	1.2 mm
Gear box pinions	Automotive	CO_2	Non-alloyed steels	2 to 5 mm
Tubular radiators	Equipment	Pulsed YAG	Non-alloyed steels	1 mm
Pipings	Aeronautic	CO_2	Titanium alloy	1 mm
Stiffeners	Aeronautic	Continuous YAG or CO_2	Aluminum alloy	1 to 4 mm
Plate heat exchanger	Food	CO_2	Stainless steels	1 to 2 mm
Casing closures	Electronics	Pulsed YAG	Aluminum, titanium, nickel alloys	1 mm
Oil filters	Automotive	Continuous YAG	Aluminum alloy	1 mm
Cardiac pacemaker	Medicine	Pulsed YAG	Titanium alloys	0.5 mm
Pipes	Iron and steel industry	CO_2	Non-alloyed or slightly alloyed	5 to 16 mm
Power-assisted steering	Automotive	Continuous YAG	Non-alloyed steels	2 mm
Airbag initiators	Automotive	Pulsed YAG, continuous YAG or CO_2	Aluminum alloy, stainless steels	0.5 mm

2.10. Development prospects

The two processes are often presented in opposition. This does not appear realistic, each process having specific advantages which will make it better adapted to a particular industrial application.

Figure 2.40. *Superconducting niobium cavity (Techméta document)*
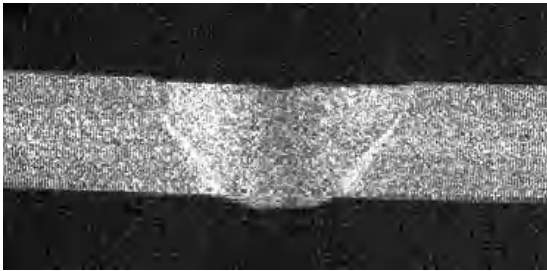
Figure 2.41. *Automobile blank welding in aluminum alloy, 1.25 mm thick, power used 7.5 kW, welding speed 18 m.min^{-1} (igm Steigerwald Strahltechnik document)*

Electron beam welding reached its zenith in the 1970s. The application fields were the nuclear, aeronautical and automotive industries. Its principal handicap is the vacuum enclosure. However, a renewed interest is currently noted with the development of new non-vacuum welding machines dedicated to automotive applications (see Figure 2.41).

It should however be noted that, for several years, the appearance of sufficiently powerful laser sources has led, for certain applications, to the replacement of EB welding by laser welding because of an increased productivity related to the absence of pumping. The main instigator of developments in laser welding processes has been the automotive industry. After the welding of mechanical components (gear box pinions), the welding of thin sheet was developed. Steelmakers started by

offering tailored welded blanks and today manufacturers invest in the spot welding of bodyshells on a continuous production line.

Electron beam welding machines are no longer the focus of significant developments, whereas laser systems are evolving rapidly. Laser CO_2 sources are more compact, and the beams are of higher quality. A significant effort is being made to reduce consumables. The most significant developments relate to YAG laser sources and diode lasers.

The power of continuous Nd-YAG laser sources with cylindrical rods is technically limited to 5 kW, to obtain a beam quality compatible with transport by fiber-optics. The advent of laser diode pumped systems makes it possible to increase the power with equivalent beam quality. The ongoing developments in continuous YAG disk lasers will bring further improvements in beam quality and thus an increase in the power of these sources.

Lasers using laser diodes also offer great promise, because of their high output and their low wavelength. Their use in welding is related to the improvement in the beam focus.

Amidst development projects, peripheral systems are not to be ignored. These relate to joint monitoring systems and on-line test systems.

To improve the productivity of the laser welding process, efforts to combine a laser beam with an electric arc are underway. This new welding process is called *hybrid laser welding*. The advantages of this process are numerous:

– increase in acceptable gap between parts,

– increase in welding speeds at equivalent laser power,

– improvement of the laser/material interaction (aluminum alloys),

– improvement of the metallurgy of welding by a reduction in the solidification speed, cooling rate and by the filler wire addition (reduction in the sensitivity to hot cracking).

This process is promising. It should extend the range of laser applications.

2.11. Bibliography

[BAR 98] BAROUILLET C., CHEHAÏBOU A., "Soudage par faisceau laser CO_2 d'un acier inoxydable martensitique à durcissement direct – Influence de l'azote comme gaz de protection", 6th *CISFFEL*, vol. 1, 1998.

[BOI 98] BOILLOT J.P., "La vision laser à haute vitesse, un atout indispensable pour…", 6th CISFFEL, vol. 1, 1998.

[CHE 93] CHEHAÏBOU A., GOUSSAIN J.-C., BAROUILLET C., "Etude de la sensibilité à la fissuration à chaud des aciers inoxydables austénitiques soudé par faisceau laser", 5th CISFFEL, vol. 1, 1993.

[CHE 98] CHEHAÏBOU A., GOUSSAIN J.-C., KNISPEL D., "Soudage par faisceau laser CO_2 de différentes nuances d'alliages d'aluminum", 6th CISFFEL, vol. 1, 1998.

[COL 97] COLLECTIF, Etude du soudage par faisceau laser des aciers de mécanicien dans le cas d'un emboîtement – Investigation pour cerner la limite des nuances soudables, Rapport Institut de soudure no. 31729 (study financed by Cetim), November 1997.

[DEL 56] DELONG W., OSTROM G., SZUMACHOWSXI E., "Measurement and calculation of ferrite in stainless steel weld metal", Welding Journal, vol. 35, no. 11, 1956.

[FRI 98] FRITZ D., LAZARENKO O.K., IRIÉ H., ABE N., OHMINE M., "Forty years of electron beam welding and material processing", 6th CISFFEL, vol. 1, 1998

[HAV 96] HAVRILLA D., Laser welding design and process fundamentals and troubleshooting guideline, Document Rofin Sinar, May 1990, revised 19 April 1996.

[HEE 00] HEE G., MEREAU P., DORNIER G., Les lasers, Document INRS ED 5009, 2000.

[HER 86] HERZIGER G., "The influence of laser-induced plasma on laser materials processing", in David Belforte and Morris Levitt (eds.), The Industrial Laser Handbook, Penwell, 1986.

[MAI 84] MAILLET H., Le Laser – Principes et Techniques d'Application, Lavoisier, 1984.

[MUR 94] MURRY G., "Soudage et soudabilité métallurgique des métaux", Techniques de l'ingénieur, M 715, 1994.

[POW 00] POWERS D., SCHUBERT G., "Electron beam welding: the useful tool for the automotive industry", Welding Journal, p. 35-38, February 2000.

[ROE 86] ROESSLER D.M., "An introduction to the laser processing of materials", in David Belforte and Morris Levitt (eds.), The Industrial Laser Handbook, Penwell, 1986.

[RYK 74] RYKALINE N. N., Les sources d'énergie utilisées en soudage, Assemblée annuelle de l'Institut international de la soudure, Doc. IIS/IIW-465-74, Budapest, 1974.

[SAY 99] SAYEGH G., "Eléments à considérer dans l'évaluation économique d'un investissement laser", LaserAP3, Sarlat, 1999.

[SCH 49] SCHAEFFLER A.L., "Constitution diagram for stainless steel weld metal", Metal Progress, vol. 56, no. 11, p. 680, 1949.

[SUU 79] SUUTALA N., KUJANPAA V., TALAKO T., MOISO T., "Correlation between solidification cracking and microstructure in austenitic-ferritic stainless steel welds", Welding Research Int., vol. 2, p. 55, 1979.

Chapter 3

Thermal, Metallurgical and Mechanical Phenomena in the Heat Affected Zone

As a general rule, welding operations modify the metallurgical structures and the local properties of the assembled parts deeply. In certain extreme cases, they can be at the origin of defects such as cracks, porosities or local embrittlement. Consequently, it is important to thoroughly understand the influence of various factors such as the thermal welding cycles and the chemical composition of the parts to be assembled.

In this chapter, we will successively examine:

– particular thermal phenomena associated with the operations of welding;

– the microstructural modifications and principal metallurgical consequences associated with these thermal phenomena;

– the modifications of the mechanical properties in the zone adjacent to the molten metal, i.e. in the *heat affected zone* (HAZ).

3.1. Thermal aspects related to welding

In spite of their great diversity, the welding processes have localized heat concentration as a common characteristic.

Chapter written by Dominique KAPLAN and Guy MURRY.

A welding operation can thus be described as a short passage of a small amount of matter at a very high temperature followed by a cooling, primarily by conduction in the adjacent parts: cooler adjacent metal, clamping tools, electrodes (in the case of spot welding). The thermal cycle at any point close to the welded zone thus represents the heat dissipation associated with the welding, and thus depends on variables related to the process (quantity of effective heat applied), on the material (thermal conductivity) and the configuration of the assembly. This localized heating can be carried out without displacement of the heat source (in the case of resistance or aluminothermic welding) or by displacement of the source relative to the part (in general arc and laser welding).

In the second case, if a constant rate of travel is considered, the thermal characteristics of a *quasi-stationary* mode, where the temperature redistribution around the source adopts a stable form in relation to time, can be determined.

A resolution of the simplified heat equation was proposed by Rosenthal [ROS 46] as early as 1935, followed up by Rykaline [RYK 61], Clyde and Adams [CLY 58]. The principal points are the following: if one imagines a specific heat source q moving at a constant speed along an axis x, the differential heat equation is written, in a series of coordinates (x,y,z) (see Figure 3.1):

$$\alpha\left(\frac{\partial^2\theta}{\partial x^2} + \frac{\partial^2\theta}{\partial y^2} + \frac{\partial^2\theta}{\partial z^2}\right) = \frac{\partial\theta}{\partial t} \qquad\qquad [3.1]$$

with:

- θ: temperature;

- t: time;

- α: thermal diffusivity (m^2 s^{-1}) of material $= \lambda/pC$, with:

  - λ: thermal conductibility (J m$^{-1\circ}$K^{-1}s^{-1}),

  - ρC: voluminal calorific capacity (J m$^{-3\circ}$K^{-1}).

A system of mobile coordinates can be defined related to the source by posing: ξ = x - vt.

In stationary mode ($\frac{\partial\theta}{\partial t}$ = 0), the preceding equation then becomes:

$$\alpha\left(\frac{\partial^2\theta}{\partial\xi^2}+\frac{\partial^2\theta}{\partial y^2}+\frac{\partial^2\theta}{\partial z^2}\right)=-v\left(\frac{\partial\theta}{\partial\xi}\right) \qquad [3.2]$$
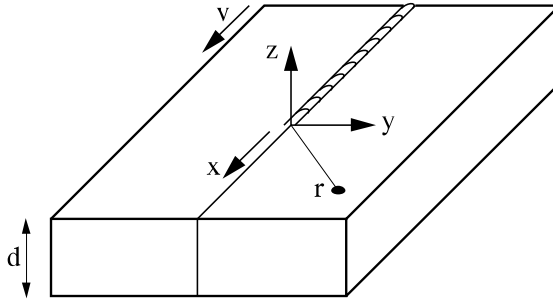
Figure 3.1. *Definition of the system of co-ordinates where a heat source moves at a constant speed v*

a)   b)
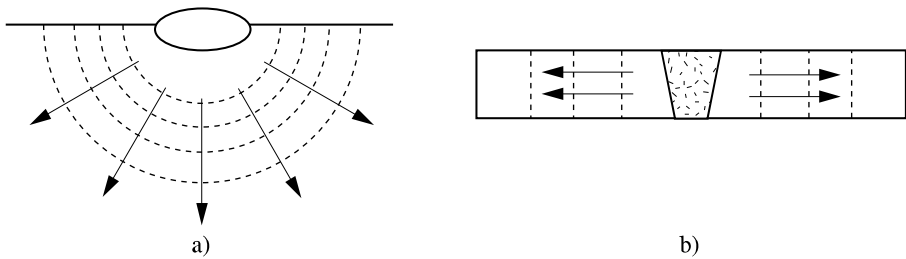
Figure 3.2. *Diagrammatic flow of heat in the case of welding "thick" (a) or "thin" products (b)*

Equation [3.2] can be solved by considering two distinct situations (see Figure 3.2).

In the case of welding "thick"[1] products, the dissipation of heat occurs primarily radially compared to the source. At any point, the change in temperature according to time and the distance is expressed:

$$\theta=\theta_0+\frac{q/v}{2\pi\lambda t}\,e^{-\frac{r^2}{4\alpha t}} \qquad [3.3]$$

---

1 The notions of *thin* or *thick* products will be quantified more precisely later.

with:

   – r: outdistance point considered compared to the source of heat

$$(r = \sqrt{(\xi^2 + y^2 + z^2)});$$

   – q: calorific contribution (J);

   – v: rate of travel of source (m/s). The q/v term indicates linear energy or the quantity of heat introduced per unit of length of the welded joint;

   – θ_0: initial temperature.

   In the case of welding thin products, the heat dissipation is negligible in depth. The isotherms are thus perpendicular to the surface of the parts. A simplified solution of equation [3.2] is written:

$$\theta = \theta_0 + \frac{q/v}{d(4\pi\lambda\rho Ct)^{1/2}} \, e^{-\frac{r^2}{4ct}} \qquad\qquad [3.4]$$

where d indicates the thickness of the welded parts.

   Portevin and Séférian [POR 34] put forward a pictorial image, a *thermal solid*, to represent welding temperatures in spatial terms, expressed in equations such as [3.3] or [3.4]. Figure 3.3 presents the example of such a diagrammatic representation, axis Ox indicating the welding direction (x indicating distance as well as time), axis Oy the distance to the axis of the welded joint, and the axis Oz the temperature.

   With a given distance from the axis (y_1 fixed), the thermal cycle $\theta(t)$ is described by the intersection of the thermal solid with the plane parallel to (xOz) in y_1. In the same way, at a given temperature θ_1, the form of the isotherm is described by the intersection of the thermal solid with a plane parallel to (xOy) in θ_1. It is precisely by using this last representation that the differences in temperature distribution during welding of thin or thick products can be appreciated (see Figure 3.4). It will thus be observed that the network of isotherms is much denser upstream of the passage of the heat source, which translates to the fact that the rise in temperature (heating phase) is faster than the descent (cooling phase).
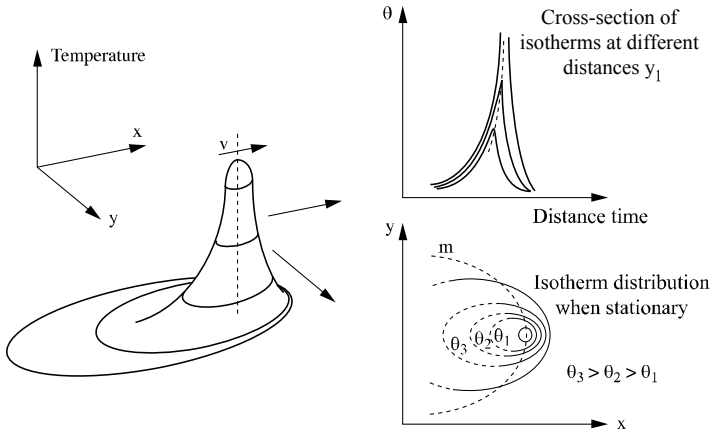
Figure 3.3. *3D representation of welding temperature distribution in the case of a mobile source; from [EAS 83]*

Because of the finite speed of heat propagation, all the fibers parallel with the welding axis do not simultaneously reach their maximum temperature. The plot of points corresponding to this maximum is the curve (*m*). Compared to the direction of displacement of the source of heat, all the points upstream of this curve are in the heating phase, and behind, in the cooling phase. The cooling and heating rates are correspondingly greater as the linear energy (q/v) is weaker or the products are thicker and the conductibility greater.

In the case of welding of thin products, the temperature distribution is more spread out in the longitudinal and transverse direction than in the case of thick materials. The difference derives from the possibility, in this last case, of heat dissipation throughout its depth.

Compared to materials with lower conductibility (e.g. austenitic stainless steel, $\lambda \cong 0.02$ Wmm^{-1}°C^{-1}), the welding of material such as aluminum ($\lambda \cong 0.23$ Wmm^{-1}°C^{-1}) leads to a widened isothermic distribution, albeit less extended in the longitudinal direction of the source displacement.
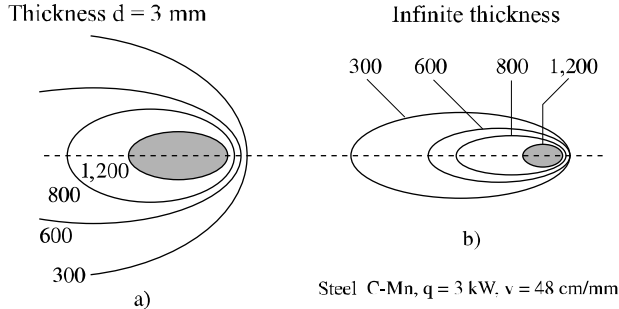
Figure 3.4. *Example of temperature distribution during the welding of (a) thin or (b) thick sheet steel assembled under identical conditions; from [EAS 85]*

At this stage, we must keep in mind that the analytical calculations presented rest on many assumptions (specific heat source, thermal properties independent of temperature, ignoring latent heat due to phase transformations and heat losses by convection or radiation, etc.). Although new digital methods (see for example [GRO 94, KOV 86, WEI 95, ZAC 93]) allow for a more complete consideration of parameters, experience shows that this simplified approach makes it possible to solve the great majority of problems with satisfactory precision.
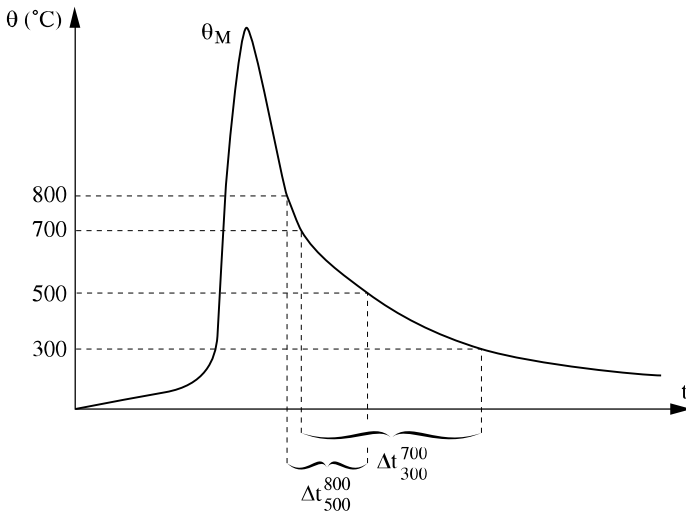
Figure 3.5. *Diagrammatic representation of the thermal cycle in HAZ. Definition of the parameters θ_M, Δt_{300}^{700}, Δt_{500}^{800}*

We will now reconsider the thermal cycle θ *(t)* applicable at any point of the HAZ. Whatever the type of welding process (fixed source or mobile), it typically comprises (see Figure 3.5):

– a very fast heating phase, of which the mean velocity is typically from some 10^2°C/s (arc welding), rising to 10^4°C/s for the HDE processes such as laser welding [DEV 89];

– a passage at a maximum temperature θ_M. In general, the duration at this temperature is very short, and is all the more reduced the higher θ_M is;

– a more or less fast cooling phase. To simplify matters, we generally characterize the intensity of this cooling by time passing between two given temperatures:

- either between 800 and 500°C, the cooling parameter is then Δt_{500}^{800} ,

- or between 700 and 300°C (Δt_{300}^{700}). The relationship between this parameter and the previous one generally lies between 2 and 4.

The choice of these two criteria was guided in particular by the fact that the majority of metallurgical transformations occur in these two temperature ranges in the case of carbon-manganese steels.

Experience actually shows that the final metallurgical structure at any point of the HAZ depends almost entirely on the maximum temperature θ_M reached at this point, and on the cooling parameter as defined by Δt_{500}^{800} . Certain thermal aspects concerning these two parameters will now be more fully developed.

3.1.1. *Maximum temperature attained in the HAZ*

It was seen that expressions like [3.3] and [3.4] described the temperature change according to time in the respective cases of welding thick or thin products. The maximum temperature is reached at a time t_M such that:

$$\left(\frac{\partial \theta}{\partial t}\right)_{t_M} = 0.$$

Moreover, in order to avoid the singularity ($\theta_M \rightarrow \infty$) when ($r \rightarrow 0$), the limiting condition is imposed: $\theta_M = \theta_f$, melting point, when $r = R$, radius of the molten metal deposit.

We are then led to the following expressions:

– maximum temperature attained in the case of thick sheet welding (two-dimensional flow of heat in a section perpendicular to the welding direction):

$$\frac{1}{\theta_M - \theta_0} = \frac{\pi e \rho C (r^2 - R^2)}{2\,q/v} + \frac{1}{\theta_f - \theta_0} \tag{3.5}$$

– maximum temperature attained in the case of thin sheet welding (unidimensional flow of heat in a section perpendicular to the welding direction):

$$\frac{1}{\theta_M - \theta_0} = \frac{\sqrt{2\pi e}\,\rho C d r}{q/v} + \frac{1}{\theta_f - \theta_0} \tag{3.6}$$
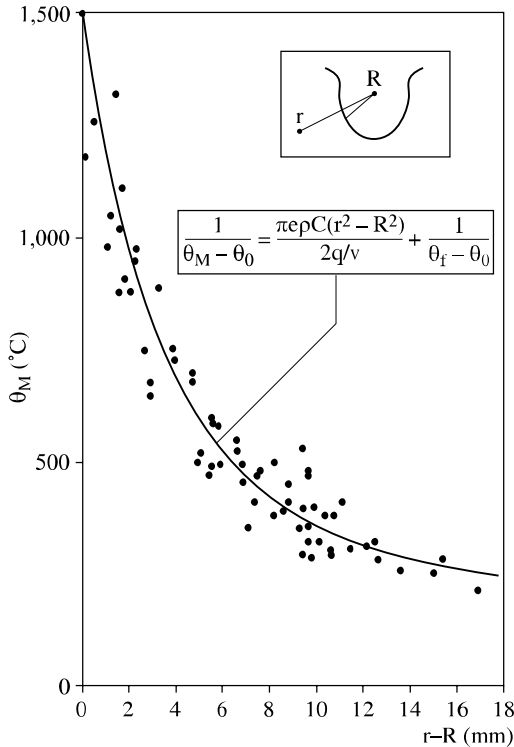
Figure 3.6. *Evolution of peak temperature according to the distance to the fusion line. Comparison of the analytically calculated temperatures and those recorded in experiments (submerged arc welding); from [DEV 87]*

Thus, the maximum temperature in the HAZ varies in approximately inverse proportion to the distance r to the fusion line (i.e. in thin materials) or to its square (i.e. thick materials). In the case of plates, the maximum temperature reached does not depend on the product thickness.

In spite of their simplicity, these expressions generally give a good account of the maximum temperature evolution in the HAZ, as Figure 3.6 testifies. This presents a comparison of experimental data recorded by thermocouples of thermal cycles in the HAZ, with the results of an analytical calculation (welding of thick products in the case presented here).

3.1.2. *Cooling parameter in the HAZ*

With the maximum temperature, the cooling speed, quantified by the parameter Δt_{500}^{800}, is the most significant determining factor for the metallurgical structure of the HAZ. Expressions [3.3] and [3.4] make it possible to calculate:

– the cooling parameter associated with thin sheet welding:

$$\Delta t_{500}^{800} = \frac{(q/vd)^2}{4\pi\lambda\rho C}\left[\frac{1}{(500-\theta_0)^2} - \frac{1}{(800-\theta_0)^2}\right] \qquad [3.7]$$

(temperatures expressed in °C);

– the cooling parameter associated with thick sheet welding:

$$\Delta t_{500}^{800} = \frac{q/v}{2\pi\lambda}\left[\frac{1}{(500-\theta_0)} - \frac{1}{(800-\theta_0)}\right]. \qquad [3.8]$$

Readings of thermal cycles taken for welded joints [DEF 75, MUR 67] show that the cooling parameter varies very little within the same welded joint. In this way, it can be said that the various zones of a welded deposit can be characterized by a single cooling parameter value Δt_{500}^{800} (or Δt_{300}^{700}). The continuing evolution of the microstructure thus depends only on that of the maximum temperature reached locally, all the points undergoing a practically identical cooling rate.

It now remains to link the cooling parameter to the welding conditions in a more precise way: if welded joints are produced, starting from products of various thicknesses while varying the linear energy of welding, the variation of the cooling parameter associated with these conditions is presented in Figure 3.7.
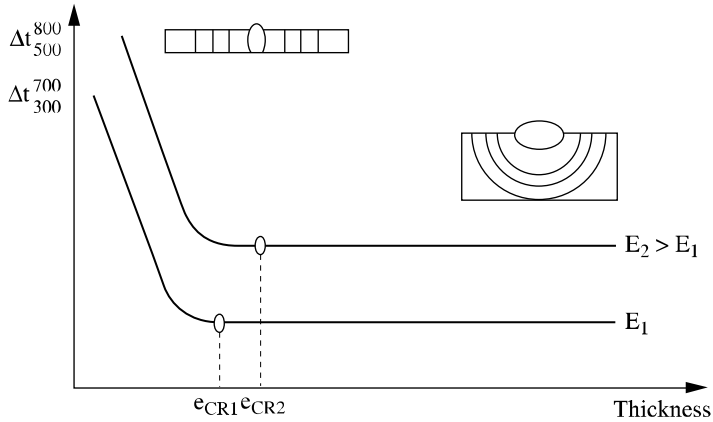
Figure 3.7. *Influence of the thickness and linear welding energy on the cooling parameters*

Beyond a certain thickness, the cooling parameter does not vary. This critical thickness, called the *thickness limit*, is correspondingly higher the greater the welding energy is. From the point of view of welding, a product will thus be regarded as "thick" for a given energy of welding, if its thickness is higher than the thickness limit.

In reality, this concept of thickness limit represents the modification of the nature of heat dissipation in the welded joint: below the limit, the flow of heat is two-dimensional, with normal isotherms compared to the plane of the product. Beyond this, the flow is three-dimensional and the isotherms take on a cylindrical form. There exists a zone of transition between these two modes, where the isothermal form is affected by radiation to the lower part of the component.

In practice, it is important to define the welding linear energy (term q/v in the preceding expressions) encountered in this phenomenon. This is the product:

– of linear electrical energy E_e, defined from the welding parameters: for example, in arc welding, carried out with a voltage U and current intensity I, the expression can be written: $E_e = \dfrac{UI}{v}$, E being frequently expressed in kJ/cm;

– of a thermal efficiency coefficient η_P, intrinsic to the welding process used, which characterizes the relationship between the energy actually transferred to the part and electrical energy. Table 3.1 indicates generally accepted values.

Welding process	Thermal efficiency η_p
Submerged arc welding	0.9 to 1
Welding with coated electrode	0.7 to 0.85
MIG welding	0.7 to 0.85
TIG welding	0.2 to 0.8
Electron beam welding	0.8 to 0.95
Laser	0.4 to 0.7

Table 3.1. *Thermal efficiency coefficient of various welding processes; from [CHR 65, CON 87, DEV 85, GRO 94, ION 97, NIL 75]*

It will be noted that TIG welding's efficiency is generally low and varies with many factors: intensity, DC or AC, shielding gas, etc. In the same way, the efficiency of laser welding is very variable according to the reflectivity of the part: low for copper or polished aluminum parts, the efficiency (and thus the beam penetration) can be increased by depositing a fine layer of graphite or zinc phosphate.

The linear welding energy is also the product of a coefficient η_G related to the geometry of the deposit and assembly. By definition, a flat deposit (heat diffusion at an angle of 180°) will be expressed as: $\eta_G = 1$. A T-shaped assembly (diffusion of heat at 270°) will be characterized by the coefficient $\eta_G = \dfrac{180}{270} = \dfrac{2}{3}$. This approach can be generalized for more complex examples (preparation of X-shaped, V-shaped chamfers, etc.).

The effective linear welding energy is then written: $E = \eta_P \times \eta_G \, \dfrac{UI}{v}$.

This value, as well as the thickness of the welded products, makes it possible to define the thermal welding mode: in a remarkable study [BER 72] based on a theoretical and experimental approach, G. Bernard could specify the field of thick and thin products with respect to welding heat dissipation.
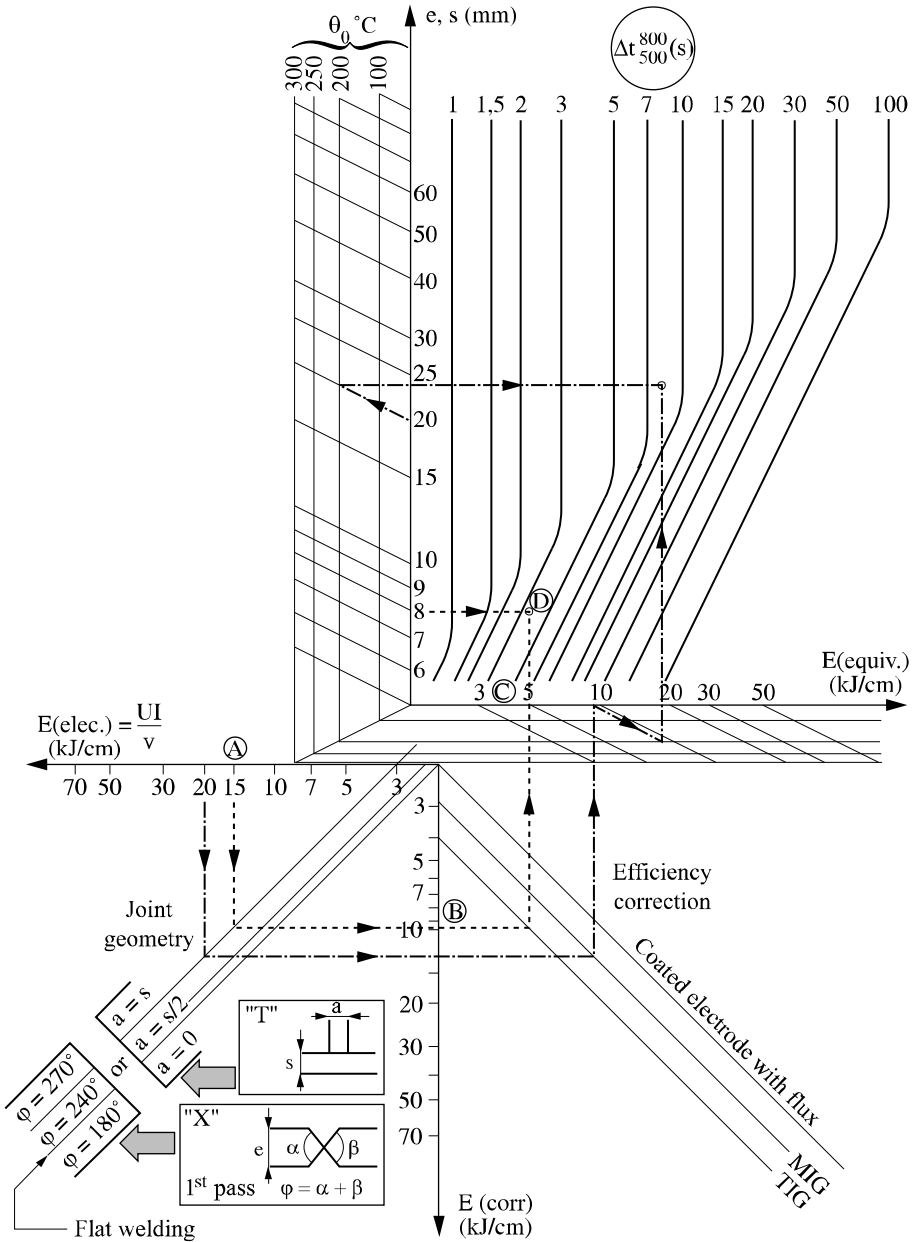
Figure 3.8. *Graph determining the cooling parameter* Δt_{500}^{800}
according to the welding conditions; from [ATS 80]

In the absence of pre-heating ($\theta_0 = 20°C$), a part will be regarded as thick based on the criterion Δt_{500}^{800} if its thickness d (mm) is such that:

$$d > 4.5 \sqrt{E}$$

E being expressed in kJ/cm. In the case of the criterion Δt_{300}^{700}, this condition would be written:

$$d > 6.35 \sqrt{E}$$

From such criteria, it is then possible to calculate the Δt parameter values according to expression [3.7] or [3.8].

To enable rapid estimations, IRSID [ATS 80] developed a forecast graph of the value of Δt_{500}^{800} starting from the various parameters in the case of arc welding (see Figure 3.8). Thus, as an example, we can consider a TIG welded joint with an energy $\dfrac{UI}{v}$ of 15 kJ/cm on a T-shaped assembly. Starting with electrical energy (point A), corrections related to the geometry of the assembly (point B) and to the efficiency of the process lead to an effective energy E (point C) of 5 kJ/cm. Under these conditions, the welding of 8 mm thick materials will lead to a value of Δt_{500}^{800} of 4 seconds (D).

Another example (MIG welding at 20 kJ/cm) shows how it is possible to take account of the pre-heated temperature θ_0 (here 200°C) by a correction of the thickness and effective energy.

As an indication, Table 3.2 gathers some typical values of cooling speeds observed for various welding processes, in the range of thicknesses used in these processes.

Welding process	resistance (spot, roller…)	TIG, ERW, plasma	LASER	Flash	Coated electrode	MIG, MAG	Submerged arc	Electroslag Electrogas
Δt_{500}^{800}	< 1 s	< 3 s	< 5 s	1-10 s	2-15 s	4-30 s	5-50 s	100-250

Table 3.2. *Typical cooling speed values* Δt_{500}^{800}
of various welding processes

3.2. Microstructural modifications in the HAZ: metallurgical consequences of the thermal cycles of welding

3.2.1. *Transformations in the HAZ during heating*

In a strict sense, the rapidity of the welding thermal cycles does not make it possible to use the balance diagrams to forecast the true nature of the various phases in the vicinity of the line of fusion. However, following the example of Easterling [EAS 83], this type of diagram is a suitable starting point to interpret the microstructural modifications qualitatively. To serve as an example, structural steels, which are the most widely used in welding applications, will be considered by examining the diagram (Fe-C) in parallel with the maximum temperatures reached in a welded joint (see Figure 3.9).
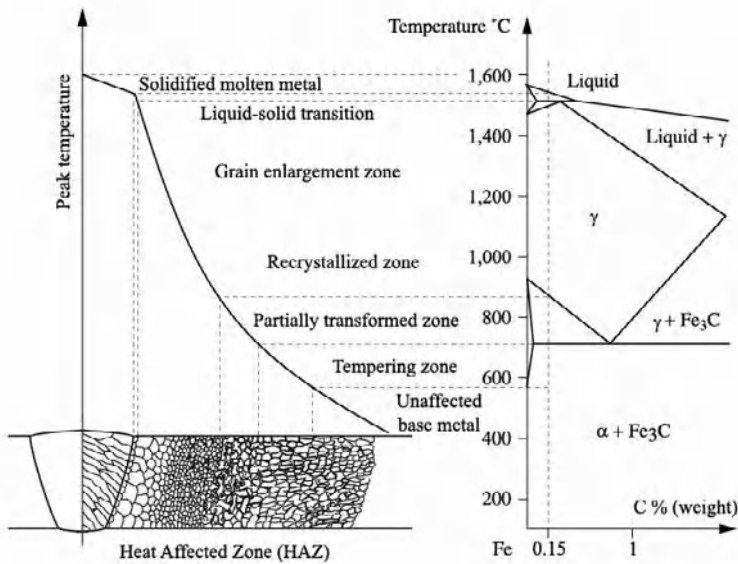
Figure 3.9. *Presentation of the various constituent parts of a welded joint; from [EAS 83]*

Let us consider for example the case of welding a 0.15% steel. As we approach the molten zone, the following zonal situations are to be found.

The base metal has not undergone a transformation phase in the heating, i.e. it has been heated to a temperature lower than the transformation point A_1 (727°C). On balance, it is thus a microstructure made up of ferrite α (solid solution carbon

insertion in iron, of a centered cubic structure) and of iron carbides Fe_3C (or cementite) or more precisely of pearlite, a lamellar aggregate of ferrite and cementite.

We have a subcritical zone, where a phase shift has not yet occurred. However, when the temperature reached is sufficiently high (for example $\theta > 600°C$), certain phenomena such as tempering, the spheroidizing of the cementite *lamellae*, the recrystallization in the case of welding of strain hardened products, ageing, etc., can possibly occur [GRA 95].

We also have a partial transformation zone (or intercritical zone), between A_1 and A_3 ($\approx 830°C$ for the composition considered). In this field ferrite coexists with a newly formed phase, austenite γ, a solid insertion solution of cubic centered face structure. It is starting from this zone ($\theta > A_1$) that the heat affected zone begins.

From temperature A_3 up to approximately 1,495°C, the transformation into austenite is total. The new structure thus replaces and erases any trace of the former ferritic structure. It is within this zone that an austenitic grain enlargement occurs: this is of a very small size at temperatures slightly higher than A_3, and can reach a few hundred microns for the highest temperatures. In this case, the term employed is *coarse grain zone* (for example, when the austenitic grain size exceeds a few tens of microns) and in general it is this zone which is the most likely to cause certain metallurgical problems, as will be seen later.

We have another zone partially in the liquid state, where a solid ferritic phase (δ) and a liquid phase coexist. Very small in size (and thus difficult to observe micrographically), this zone constitutes the connection between the base metal and the molten metal. On the balance diagram, this corresponds to the temperature interval between the beginning and the end of fusion (*solidus-liquidus interval*).

Certain phenomena (local decarburization by enrichment of the liquid in the solute, intergranular liquation by eutectic formation at low melting point in the case of impurities, etc. [GRA 95, HAL 84]) can intervene in this bond zone.

Finally, the molten metal often has a composition different from that of the base metal, because of the volatilization of certain elements, reactions with the surrounding medium, or of enrichment by external elements (filler material). The first molten metal nuclei are solidified by epitaxy (crystallographic coherence) on the grains of the HAZ.

At this stage, it is necessary to note the following points:

– the transformations and temperature ranges evoked above correspond to a state of balance. In reality, the brevity of the thermal cycles means that phase

transformations and structural homogenity intervene at temperatures sometimes considerably higher than these balanced temperatures;

– the particular case considered here (alloy Fe-0.15% C) presents a situation where phase shifts occur during heating. In the case of other materials (for example: aluminum alloys, copper, ferritic stainless steels, etc.), the thermal welding cycle intervenes in a single-phase area. A grain enlargement will then be found throughout the cycle, without possibility of refinement by phase shift;

– starting from expression [3.5] or [3.6] and the knowledge of the phase transformation temperatures, it is possible to predict the HAZ width in various conditions of welding. The calculations, confirmed by observations of welded joints, show that this can vary from a few hundreds of microns (for example: low power densities in laser welding [ION 97] and resistance welding [CHA 74]) to 15 mm in electroslag welding [DEB 82, HAR 80].

In addition to these microstructural modifications, welding operations have a marked influence on the precipitates possibly present in the base metal. Indeed, it is known that modern steels draw their mechanical properties (resistance, ductility, toughness) from an optimized combination of hardening, by the nature of the microstructure, the grain and precipitation refinement. This balance is significantly modified by the thermal welding cycles.

Generally, the dissolution of various particles (carbides, nitrides, sulfides, oxides) can be quantified, starting from the variation of their solubility product with the temperature, described in this form (case of diluted solutions) [RIS 74]:

$M_aN_b \Longleftrightarrow aM + bN$, a and b defining the stoichiometry of the initial compounds:

$$\log [\%M]^{\,a} [\%N]^{\,b} = -\frac{\Delta G_o}{RT} = A - \frac{B}{T}$$

ΔG_0 indicates the free energy of the reaction, T the absolute temperature, R the constant of perfect gases (1,987 cal. K^{-1} mol^{-1}). Table 3.3 and Figure 3.10 present the solubility product of some compounds, from which the temperature at which they are totally soluble can be calculated.

Type of precipitate	$A - \dfrac{B}{T}$
NbN	$4.04 - 10230/T$
VN	$3.02 - 7840/T$
AlN	$1.79 - 7184/T$
TiN	$4.35 - 14890/T$
TiC	$5.33 - 10475/T$
NbC	$2.26 - 6770/T$
MnS	$2.93 - 9020/T$
Al_2O_3	$20.43 - 125986/T$
SiO_2	$5.10 - 44801/T$
MnO	$-5.71 - 24262/T$
Ti_2O_3	$16.18 - 104180/T$

Table 3.3. *Expression of the solubility product of various compounds in austenite; concentrations in % by weight, T in °K*

The higher the temperature reached locally in the HAZ, the greater the likelihood of precipitates decomposing. In decreasing order, the stability of these compounds is as follows: oxides, nitrides, sulfides, carbides.

For common compositions of structural steels, decomposition of carbides in the HAZ will be observed around 1,100-1,150°C (VC, TiC) [HRI 95], nitrides around 1,150 to 1,300°C, sulfides being generally dissociated around 1,100 to 1,200°C. Taking into account their very strong stability, oxide inclusions resulting from the steel making in the liquid state (alumina, silicates, etc.) are not affected by the welding cycle. Being very few, and relatively large in size (for example: several tenths to a few microns), these oxides generally do not play a role at the time of the heating phase in the HAZ. It is not the same for nitrides or carbo-nitrides. Indeed, it is known that these numerous, fine and dispersed particles slow down the growth of austenitic grain since the joint displacement this achieves is accompanied by a local increase in enthalpy.
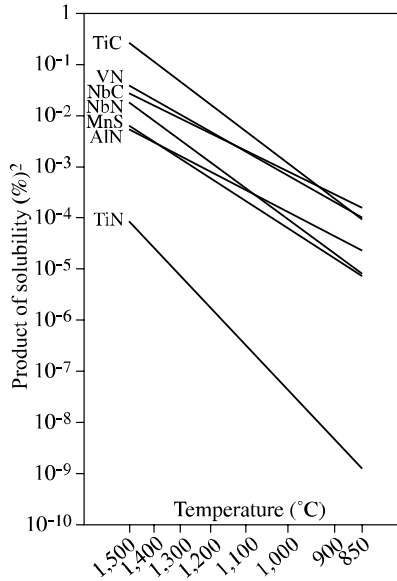
Figure 3.10. *Solubility products of various compounds in austenite*

Maximum size of grains d_{max}, in the presence of a population of precipitates of size r and whose voluminal fraction is V_F, can be expressed by the Zener relation [ZEN 48]: $d_{max} = \dfrac{4r}{3V_f}$.

In general, an increased austenitic grain size in the HAZ leads thereafter to a coarser ferritic structure. To limit this phenomenon, it is possible to show that low additions of titanium (an element which forms, as was seen previously, very stable nitrides at high temperature) slow down the growth of the austenitic grain effectively (see Figure 3.11). It should however be stressed that this result is obtained only if these nitrides are relatively fine (a few tens of nanometers), i.e. primarily if they are formed after solidification during steelmaking and not in the form of coarser precipitates (micrometric particles, formed in the molten metal).
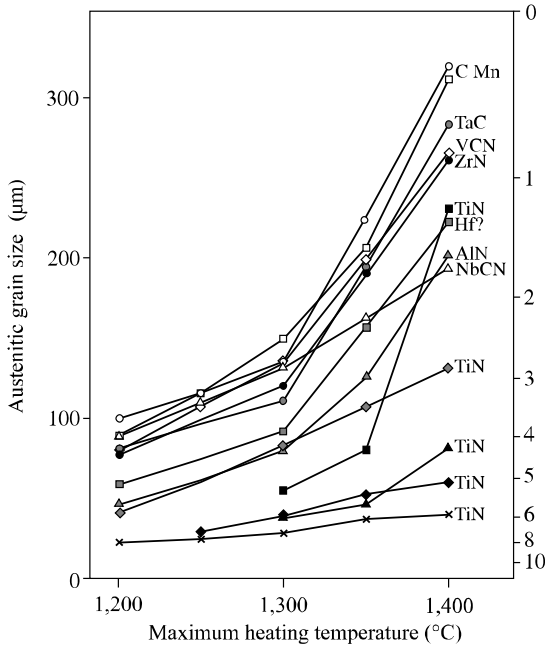
Figure 3.11. *Influence of maximum temperature on the austenitic grain size in HAZ of steels containing various types of precipitates; from [KAN 76]*

3.2.2. *Transformations in the HAZ during cooling*

In the case of structural steels, the microstructures observed in the HAZ of welded joints correspond to transformed products of austenite. It is in fact difficult to study these metallurgical transformations starting from traditional CCT diagrams (continuous cooling transformation). Indeed, these are generally established starting from austenitic treatments at a relatively low temperature (900-950°C) and for long durations, i.e. a situation exactly opposite to that encountered in the HAZ. In order to consider more representative conditions, the metallurgical phenomena starting from thermal heating and cooling cycles very close to those met in welding are studied. These tests are generally carried out on specific thermal simulators (Gleeble and Smitweld simulators, etc.). For a given material (see Figure 3.12) and austenitization conditions (temperature generally higher than 1,200°C, so as to simulate the HAZ with coarse grains), the transformations of the austenite according to the cooling speed using the CCT diagram in welding conditions or more simply of the evolution of hardening the final microstructure with temperature can be gathered.
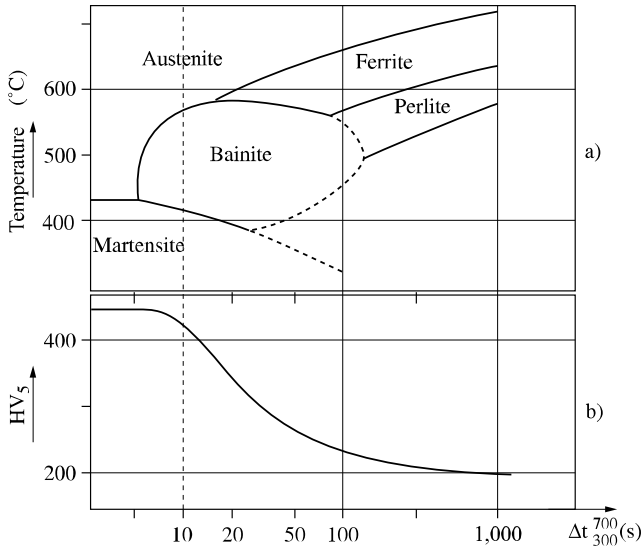
Figure 3.12. *(a) Example of CCT diagram in welding conditions (θ_M = 1,300°C);
(b) corresponding graph (hardness-criterion of cooling Δt).
Steel C = 0.18%, Mn = 1.4%, Si = 0.4%*

According to the cooling speed, various types of microstructures are liable to be formed.

For very high speeds (lower than the critical quenching rate V_{CM}, which corresponds to a plateau on the hardness-criterion cooling graph or *HV-Δt*), martensite appears. Having a tetragonal crystallographic structure, this supersaturated solid solution of carbon in iron is formed by a shearing mechanism without atomic diffusion. Identical in composition to that of the mother austenite, martensite has a hardness HV_M which depends virtually only on the percentage of carbon in the steel alone, according to the expression: HV_M=283+930(%C) [IRS 77][2].

At intermediate speeds, bainitic structures appear. Formed starting from metastable austenite at temperatures too low for the carbon to be able to diffuse at the grain boundaries, the bainite is characterized by the very fast growth of ferrite needles by shearing and a precipitation of carbides. Without returning to the complex debate relating to the description of bainitic structures (see for example [BHA 97, HEH 72, HON 95, OHM 74]), we will simply recall that faster cooling

---

2 Other similar expressions have been proposed: HV_M = 293+812(%C) (Satoh), 305+802(%C) (Duren) or HV_M= 294+884[%C(1-0.3 (%C))²] (Yurioka), etc.

speeds lead to the formation of the harder lower bainite structures (carbide precipitation in the shape of thin platelets within the ferrite laths), whereas slower speeds are associated with higher bainite formation (carbides rejected from the ferrite lath joints, sometimes in the form of quasi-continuous cementite *lamellae* [CON 92]). In this last case, the local carbon content can be such that the formation of compounds between the laths occurs where martensite and austenite coexist (M-A compounds), the latter being stabilized because the transformation temperature Ms is lowered below room temperature [AND 65].

Slower cooling speeds in welding correspond to the precipitation of proeutectoïd ferrite at the old austenitic grain boundaries and the evolution towards a ferrito-perlitic structure. It is also in this range of cooling speeds that some compounds (vanadium and niobium nitrides or carbo-nitrides, etc.), dissolved at the time of the heating phase, can re-precipitate in a more or less complete form.

Various more or less complex formulae have been proposed in order to describe the evolution of HV_{max} hardness in the large grained HAZ of C-Mn steels according to their composition and the speed of cooling. We can for example quote that of Yurioka [YUR 87], applicable to steels of less than 0.3%C, 5%Ni, 1%Cr without B (Δt_{500}^{800} expressed in s, content in %):

$$HV_{max} = 206 + 442\ C + (402\ CE_I - 90\ CE_{II} + 80)\ \text{arctan}\ (x) + 99\ CE_{II}$$

with:

$$CE_I = C + \frac{Mo}{4} + \frac{Mn}{6} + \frac{Cr}{8} + \frac{Ni}{12} + \frac{Cu}{15} + \frac{Si}{24}$$

$$CE_{II} = C + \frac{Mo}{2.5} + \frac{Nb}{3} + \frac{Mn + Cr + V}{5} + \frac{Cu}{10} + \frac{Ni}{18} + \frac{Si}{24}$$

$$x = \frac{\Delta t_{500}^{800} - 2.3 CE_I - 1.35 CE_{III} + 0.882}{1.15 CE_I - 0.673 CE_{III} - 0.601}$$

$$CE_{III} = \frac{C + \frac{Mn}{3.6} + \frac{Mo}{4} + \frac{Cr}{5} + \frac{Ni}{9} + \frac{Cu}{20}}{}$$

These expressions reveal the concept of *carbon equivalent* (CE, a function of the level of C, M, Mo, etc.), which will be subject of further discussion in connection with cold cracking. At this stage, it must be retained that it is a factor quantifying the

capacity for hardening. At a given cooling speed, limiting hardness amounts to limiting the percentage of carbon equivalent.

As has been previously stressed, the microstructure formed at any point of the HAZ depends on the temperature reached locally. Figure 3.13 illustrates, in the case of a 32C1 steel, the influence of the temperature on the transformation of austenite. If cooling is sufficiently fast (for example, $\Delta t_{300}^{700} <1$ s), all the zones where the temperature exceeds 1,000°C are martensitic. In the case of a slower cooling (for example, $\Delta t_{300}^{700} \cong 5$ s), the part of the HAZ heated to around 1,000°C has a bainitic structure, whereas the coarse grained part of the HAZ (1,100 to 1,200°C) is martensitic. This microstructural difference explains why the majority of the metallurgical problems (toughness, sensitivity to cracking in the presence of hydrogen) occur primarily in the coarse grained part of the HAZ, heated to a higher temperature.
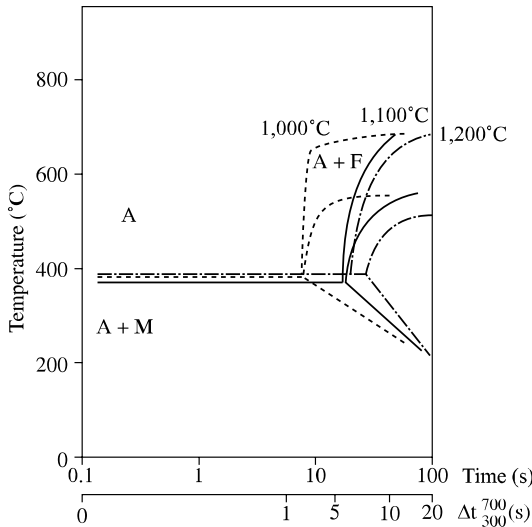
Figure 3.13. *Influence of maximum temperature in the HAZ on a CCT diagram in the welding of a steel 0.3% C, 0.8% Mn, 0.2% Si, 0.3% Cr*

3.2.3. *Case of multipass welding*

Beyond a certain thickness, the product assembly generally involves a number of successive deposits (welding involving several passes, or *multipass*). Except in the last deposit, all the points of the HAZ undergo, during this operation, a complex succession of reheating cycles [DEV 87]. In reality, if a point is located in the HAZ

in the immediate vicinity of given pass N, the progressive distance of the deposits means that their metallurgical influence quickly becomes negligible (maximum temperature lower than 500°C) beyond pass $N + 2$. Moreover, it is understood that austenitization at very high temperature erases the metallurgical influence of the preceding cycles at lower temperature; therefore, the metallurgically effective thermal history in a multipass HAZ can be summarized with some characteristic combinations, comprising at most three thermal peaks. Thus, the three following zones can be distinguished (see Figure 3.14).
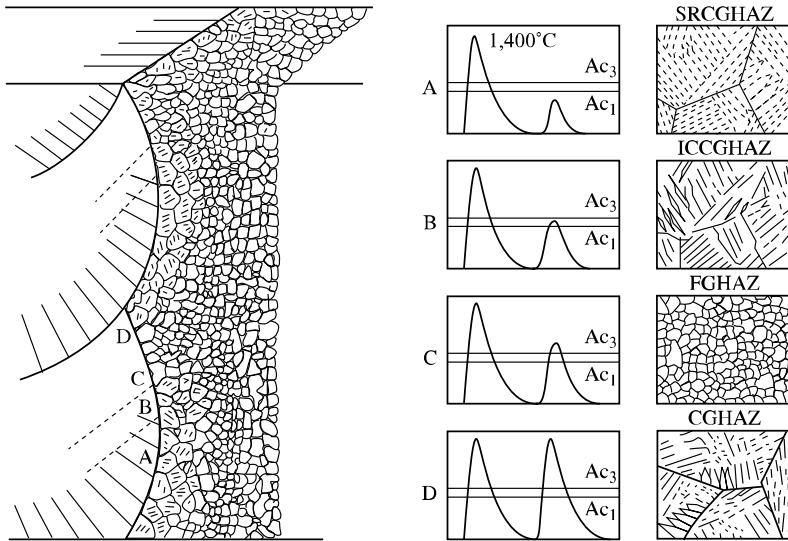
Figure 3.14. *Diagrammatic illustration of the thermal cycles and the microstructures encountered in multipass welding; from [MAT 94]*

A zone with coarse grains is unaffected by the subsequent passes, because it is heated to a temperature lower than A_{c1} (zone A in the figure, or SRCGHAZ: *subcritically reheated coarse grain heat affected zone*). In general, the microstructure and the mechanical properties of this zone are relatively close to those of a zone with coarse grains in a rough state (CGHAZ, zone D).

A zone with coarse grains heated in the intercritical field, between A_{c1} and A_{c3} (ICCGHAZ: *intercritical reheated coarse grain heat affected zone*, zone B). The transformation $(\gamma \rightarrow \alpha)$ occurs in particular in the zones of easy diffusion, such as the former austenitic grain boundaries, the zones richest in carbon (carbides, M-A compounds) or the segregated zones. The austenite which is formed locally is increasingly carbon enriched the lower the temperature is. With cooling, the

austenitic sites can be transformed into martensite or to austenite (M-A compounds) according to a mechanism described in the preceding section. As many studies have highlighted the poor character of these compounds with respect to toughness [IKA 80, LAM 99, MAT 94], it is generally considered that the zone heated in the intercritical field is, with the coarse grained zone, the zone of least toughness in multipass welded joints. However, the brittleness of this zone all but disappears with a reheating to a sufficient tempering temperature (for example: 350-400°C) related to the deposit of a subsequent welding pass or a stress relieving heat treatment.

When structural steels must provide guarantees of toughness in multipass welded joints, manufacturers and steelmakers particularly endeavor to minimize the proportion of local brittle zones (LBZ, coarse grain or intercritical zones [HRI 95, TOY 86]) in the vicinity of the molten metal by controling the conditions of welding and the chemical composition.

Finally, a zone with fine grains (FGHAZ, *fine grain heat affected zone*) is encountered, associated with a temperature peak slightly higher than A_{c3}. The very fine microstructures associated with this type of treatment correspond to structures resulting from normalization treatments and present excellent mechanical properties. A wise choice of welding conditions, so as to maximize this zone with fine grains and to favor the transformation of M-A compounds, makes it possible to guarantee good toughness properties of multipass joints [IKE 95, KAW nd, KOS 81, LIN 89].

To conclude, it should be noted that certain software, based on a thermal and metallurgical modeling, have been developed in order to forecast the risk of brittle zones appearing in multipass HAZs and their effects on mechanical properties [DEV 91, KAP 98, REE 94].

3.2.4. *Cold cracking*

The concept of *weldability* has often been confused with and reduced to sensitivity to cold cracking, which gives some indication of the importance of this phenomenon.

During arc welding, the molten metal is likely to dissolve hydrogen derived from the decomposition of water present (ambient air, moisture, etc.), or from that of hydrogenated matter (greases, etc.) and possibly from hydrogen in the welding gas; the dissolved quantity can be high. Results published by Granjon [GRA 95] show that, during structural steel welding, the quantity of diffusible hydrogen present in 100 grams of molten metal can reach, on average:

– 15 cm^3 in welding with electrodes with a rutile coating,

– 9 cm^3 in welding with powdered flux,

– 7 cm^3 in welding with electrodes with a basic coating,

– 4 cm^3 in MIG welding.

During solidification, cooling and any possible allotropic transformations, the solubility of hydrogen decreases appreciably. This fact could be responsible for the formation of porosities during solidification and will generate thereafter a diffusion of gas towards the atmosphere and, if this is insufficient (fast cooling), a supersaturation of the solid metal with *in situ* formation of H$_2$ molecules. The gas thus produced gathers in the spaces caused by structural defects and decohesions between metal and inclusions. In these places, the gas pressure rises with the diffusion of hydrogen and can reach elevated levels, which generates considerable localized stresses likely to combine with shrinkage stresses. If the structural state of the metal is not sufficiently strong under these conditions, a crack is likely to develop.

This precise situation is encountered during the welding of structural steels likely to undergo a $(\gamma \Leftrightarrow \alpha)$ transformation; it leads to *cold cracking*.

Indeed, in a joint:

– the transformation in molten metal (when it is susceptible to a $(\gamma \rightarrow \alpha)$ transformation, which is generally the case) starts before that of the HAZ because, if it cools like the latter, it is lower in carbon and its Ms point is higher. Any hydrogen contained is thus released, partially towards the atmosphere and partially towards the HAZ (as long as the latter is in an austenitic state);

– the $(\gamma \rightarrow \alpha)$ transformation in the HAZ, by the effect of heat gradients and the differences in hardenability caused by the enlargement of the austenite grains, progresses from the coolest parts (close to the base metal) towards the limit of the molten metal.

Consequently, hydrogen is trapped in the most overheated part of the HAZ, whereas its solubility decreases as a result of cooling and especially from the passage to the α state. If this part is transformed into martensite (not very plastic, even brittle), it can fissure under the action of stresses caused by the localized hydrogen pressures and the shrinkage stresses. Thus, cold cracking will occur.

To assess the risks of cold cracking, it is necessary to carry out tests for cracking under the welding conditions considered. If it is easy to reproduce thermal cycles and the hydrogen loading (it is sufficient to apply identical welding conditions), it is on the other hand very difficult to reconstitute the pattern of shrinkage stresses. For this the tests employed will be conventional. The most common and most significant

is the implant test defined by French standards NF A 89-100 and NF A 03-185 and by the recommended procedure IIS/IIW-447-73. A notched cylindrical test-piece is implanted in a thick plate. The test weld is carried out under the selected conditions then, upon the solidification of the molten metal, the implant is subjected to traction (see Figure 3.15).
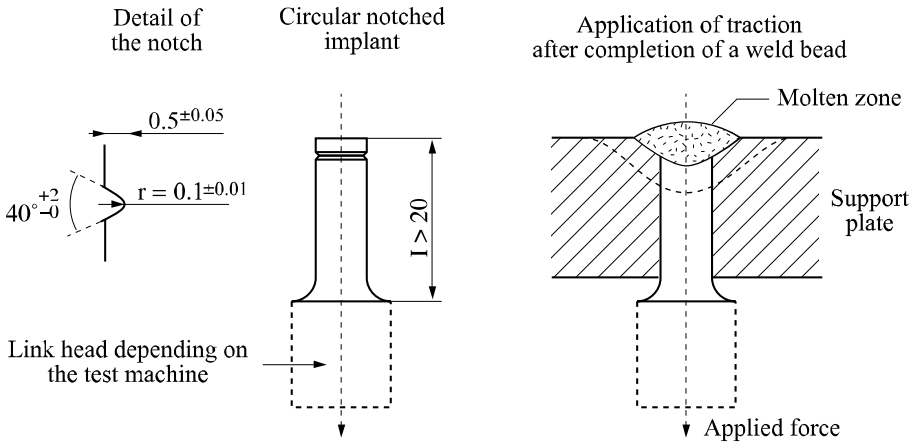
Figure 3.15. *a) Example of implant with a circular notch; b) implant subjected to traction after deposit of a weld bead*

Micrographic sections taken after cooling and waiting time allow the detection of possible cracks. While simultaneously varying the welding conditions (energy and thickness of the support plate) and the load applied to the implant, we have the necessary information to plot a *cracking curve* which distinguishes, within the *tensile effort/cooling parameter* coordinates, the fields where cracking occurs and where it is avoided (see Figure 3.16). Such a curve is characterized by the steel, the welding process and the hydrogen content under consideration. This procedure has made it possible to qualify the metallurgical weldability of many steels with respect to the risk of cold cracking and to define minimal energies to employ when welding them without risk. It should however be noted that the influence of hydrogen content is foremost; it is often enough to lower this to make cold cracking disappear, as shown in Figure 3.17 for a simple C-Mn steel. It is then this factor that the welder will have to consider as a priority.
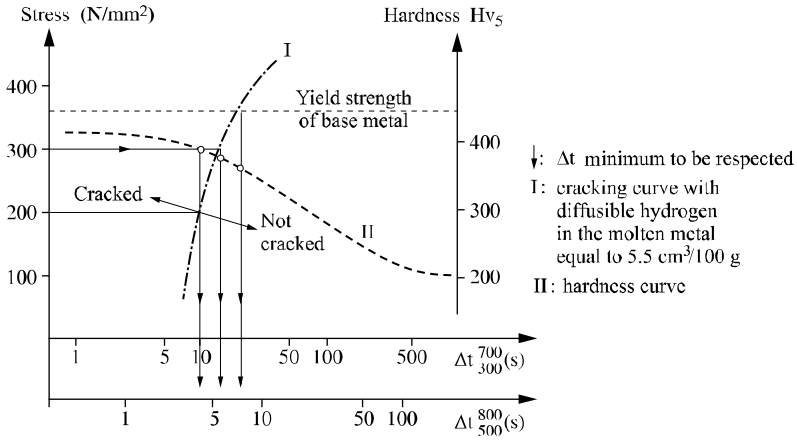
Figure 3.16. *Example of a cracking curve determined from the implant test*

However, if lowering the hydrogen content is impossible or insufficient, the welder can still intervene by carrying out a careful pre-heating and possibly a post-heating. These two operations (which we should not regard as being heat treatments) consist of modifying the thermal evolution of a weld by heating up the parts which constitute the assembly at a higher temperature than room temperature (this is pre-heating) and possibly by maintaining this heat, after welding, for a given time (this is post-heating).
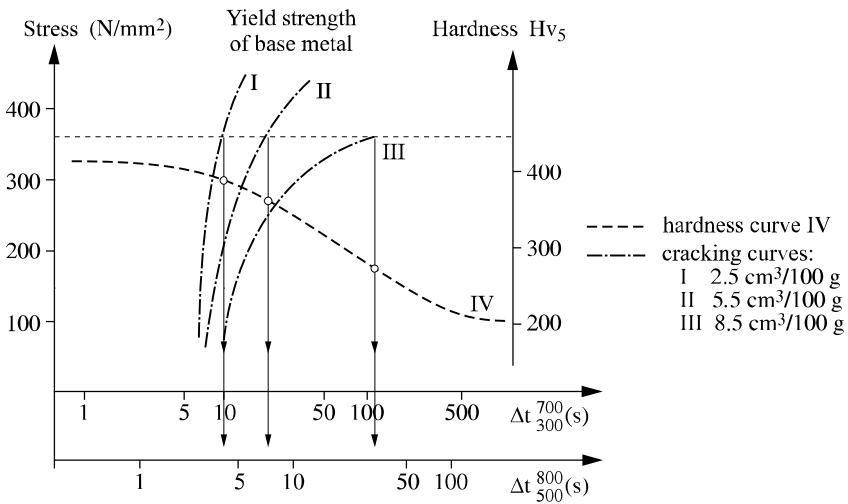
Figure 3.17. *Influence of hydrogen content on cold cracking*

These procedures:

– slow down the joint cooling which is applied with a cooling medium – the base metal – no longer at room temperature but maintained at the temperature of pre-heating. If the base metal is not too hardenable, this slowing down modifies the ($\gamma \rightarrow \alpha$) transformation by allowing a certain proportion of bainite to form before the martensitic transformation; the metal of the HAZ is less hardened and thus less hard but especially less brittle. In addition, starting from the pre-heating temperature just as starting from the temperature of post-heating, the final cooling is very slow since it corresponds to all of the pre-heated and possibly post-heated area. The end of the martensitic transformation thus occurs very slowly in the presence of a hydrogen quantity which gradually decreases since it diffuses into the atmosphere, outside the joint. The relatively long duration of post-heating and between the latter and the ambient temperature constitute a tempering operation to which the already formed martensite is subjected, causing a further decrease in its brittleness;

– increase the HAZ depth and decrease the temperature gradients. The dilation gradients are in this way decreased and, consequently, the possibilities of shrinkage and thus significant stresses are reduced.

All these effects have the same beneficial result; they decrease or eliminate the risk of cold cracking.

To assess *a priori* the risk of cold cracking, on a practical level, a particular parameter called *carbon equivalent* (C_{eq}) has been used on a regular basis, calculated on the chemical composition of the parent metal. Many formulae have been proposed, the best known being that employed since 1940 by the International Institute of Welding [DEA 40]:

$$C_{eq} \ (\%) = C\% + Mn\%/6 + (Cr\% + Mo\%+V\%)/5 + (Cu\% + Ni\%)/15$$

With a constant C_{eq}, metallurgical weldability would be constant and the lower the C_{eq}, the lower the risk of cold cracking. Such a method of assessing this risk does not appear very satisfactory, indeed:

– C_{eq} does not take into account the hydrogen content of the molten metal, the importance of which has just been discussed (certain formulae have been proposed which remedy this oversight);

– C_{eq} does not take into account the cooling conditions, which are a determining factor concerning the proportion of martensite formed;

– C_{eq} regrettably confuses the capacity for hardening (and thus the risking of martensite brittleness) which depends on the percentage of carbon and secondly

hardenability (and thus the risk of martensite formation) which depends on the content of alloying elements.

C_{eq} can therefore only be used to make comparisons within very limited fields.

Currently, some NF EN standards define limiting values for this C_{eq}. As an example, and to highlight the improvements in weldability achieved thanks to the developments in iron and steel processes, the maximum guaranteed value can be cited for steels meeting standard NF EN 10113 and delivered in a normalized state or after thermomechanical treatment in the form of flat products with a thickness ranging between 16 and 40 mm.

Lastly, it is important to stress that the development of many iron and steel products during the last few decades has been guided mainly by the desire to decrease the sensitivity to cold cracking. Consequently, the concept of metallurgical weldability has played a crucial role in the evolution of structural steel composition.

C_{eq} maximum (%) of steels according to NF EN 10113 (16 < thickness mm ≤40)			
Part 2 after normalization		Part 3 after thermomechanical rolling	
S275N	Ceq <= 0.40%	S275M	Ceq <= 0.34%
S355N	Ceq <= 0.43%	S355M	Ceq <= 0.39%
S420N	Ceq <= 0.48%	S420M	Ceq <= 0.43%

3.2.5. *Lamellar tearing*

It will be noted later that welding leads to the formation of stresses and significant deformations. A possible consequence of this phenomenon is lamellar tearing, which corresponds to a particular type of crack developing parallel to the bond zone of the welded joints and perpendicular to the grain of flat-rolled products (see Figure 3.18). Its appearance corresponds to an insufficient ductility of the welded material in the direction of its thickness, caused by the presence of inclusions aligned in the direction of rolling.
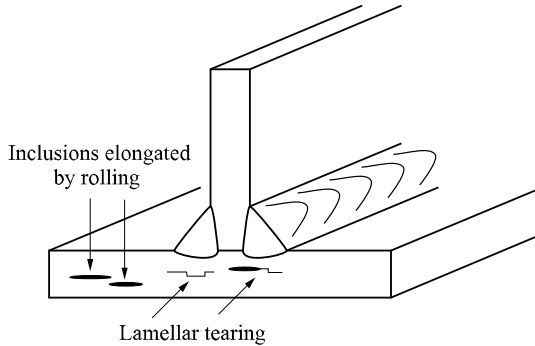
Figure 3.18. *Cracking due to lamellar tearing*

Examination of the ruptures primarily reveals a characteristic step-like break corresponding to decohesion between the inclusions (essentially sulfides) lengthened by rolling and the matrix. This type of cracking can be avoided:

– by the joint design, avoiding procedures which lead to high levels of stress in the short transverse direction as much as possible (geometry, preliminary buttering, limitation of the elastic limit for the molten metal, etc.);

– by the choice of the metallurgical quality of the steel, which must have a sufficient ductility in its thickness. This characteristic is checked on cylindrical tensile test-specimens taken in this direction, and on which striction (Z%) is measured after rupture. So we talk about "Z… steels" in connection with products with guaranteed properties in their thickness, which are obtained by limitating the inclusion content (in particular expressed by the sulfur behavior) and/or controling the morphology of these inclusions (treatment in production by addition of calcium, rare earths (cerium, etc.) [OLE 81], etc.).

3.3. Influence of the thermal cycles on the mechanical properties of the HAZ

Important modifications in microstructures caused by welding are naturally accompanied by significant changes in the mechanical properties compared to the base metal. These will be examined with regard to localized tensile, hardness or toughness properties.

3.3.1. *Modifications of the mechanical properties of hardness or traction in the HAZ*

The modifications of mechanical properties in the HAZ (mechanical resistance, or more simply hardness [GRU 81]) must obviously be understood in comparison with the base metal, whose properties can result from various combinations (thermomechanical composition/treatments). Thus, it is possible to enumerate among the big groupings of structural steels, for example the C-Mn steels of ferrito-pearlitic structure obtained by normalization treatments, high strength steels (HSLA) combining refinement of the ferritic grain and fine hardening precipitation, steels with high or very high strength (ferrito-bainitic, or bainitic with very low carbon (ULCB)), dual-phase steels (ferrite-martensite), quenched and tempered steels, etc.

In general, the thermal cycles associated with the coarse grain zone lead to a localized increase in hardness compared to that of the base metal, particularly in the case of a fast cooling after welding. The purpose of this mechanical heterogenity is often to displace the rupture site towards the base metal in the case of smooth tensile or bending tests across the welded joints. In the case of mechanical tests comprising a notch located in the HAZ, the presence of the less hard adjoining base metal contributes to the development of a plastic zone and to a rise in apparent toughness [DEV 86a]. In certain extreme cases (very large difference in hardness between the welded zone and the base metal, very narrow welded zone, as in the case of welds by laser or electron beam), a marked deviation of the rupture can be noted towards the least hard zones [DEV 86b, GOL 76].

More generally, this illustrates the possible difference between intrinsic mechanical behavior in a given zone and that obtained in the presence of the adjoining zones with different behavior patterns, possibly in the presence of a mechanical defect. The whole of these rather complex questions, the interaction of the mechanical properties in the various parts of the welded joints, is known as the *matching* of welded joints (see for example [LON 94, TOY 92]).

In certain cases (base metal with high yield strength obtained by thorough thermomechanical treatment), the thermal cycles can involve the formation of softened zones compared to the base metal. Softening appears at a temperature corresponding to A_{c1} or A_{c3} [DEV 83, ITO 00] and increases the higher the energy is (for example: aluminothermic welding of rails). Very often, the triaxiality of the stresses and the localized consolidation make it possible to avoid an excessive concentration of deformations within the softened zone. It is advisable to limit the amplitude of softening (difference in hardness between the base metal and the HAZ) as well as the width of the softened zone [DEV 84], so as to avoid rupture or a premature wear by concentration of the deformation in this zone. Finally, it should be noted that the presence of this softened zone can sometimes be associated with a

cracking due to localized hydrogen (*stress oriented hydrogen induced cracking*, or SOHIC) [TAK 95].

3.3.2. Toughness properties of the HAZ

The mechanical properties in the HAZ are the subject to increasingly severe demands from users and of construction codes, with the aim of guaranteeing the viability of the welded joints with respect to brittle fracture. The toughness of the HAZ can clearly be assessed by direct removal of notched samples from within welded joints. However, this method presents many difficulties (delicate positioning of the notch within very narrow zones with high microstructural gradients, residual stresses, etc.) which leads in practice to an excessive spread in the toughness results. This is why the tenacity of these zones is often assessed on the basis of experimental on test-samples that have undergone simulated thermal treatments representative of those encountered in the HAZ.

On the basis of such simulation tests, Figure 3.19 presents the influence of the cooling speed in the coarse grain HAZ on the transition temperature to the level 28 Joules of impact strength. In parallel, it includes the corresponding evolution of hardness in the HAZ.
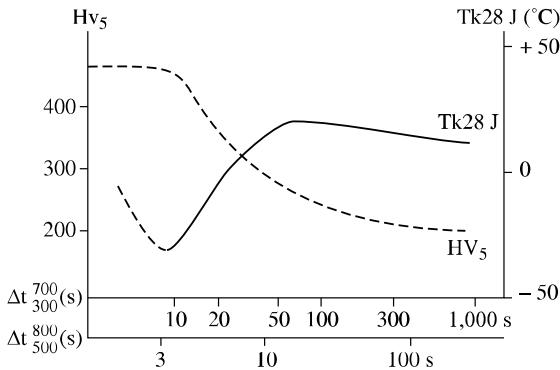
Figure 3.19. *Influence of the cooling speed on impact strength and hardness in the coarse grain HAZ; steel C = 0.18%, Mn =1.4%, Si = 0.4%; from [BER 75]*

Looking at the fastest cooling speeds, three successive phases will be noted.

An optimal toughness in the HAZ corresponding to the end of the martensite area. The martensites obtained in welding are frequently self-tempered laths, characterized by the presence of carbide sticks aligned according to the direction <111> of the slats. Indeed, in steels with a low percentage of carbon, the temperature

of the end of martensitic transformation M_F is so high that it allows a certain tempering of martensite even during the welding cycle. The presence of lower bainite in these predominately martensitic HAZs is rather frequent. The toughness of the HAZ structures obtained from these fast cooling speeds is thus similar to that of tempered martensites and the mixed martensite-bainite structures obtained by traditional heat treatments [HEI 75, OHM 74].

An abrupt drop in toughness is then observed when the cooling speed decreases. This is related to the evolution of lower bainite towards the higher bainite, whose slat sizes or bainitic *packages* offer less cleavage resistance.

For the slowest cooling speeds (ferrite-carbide structures), a stabilization of toughness is finally observed, possibly after a slight fall in the temperature of transition. As already seen (see section 3.2.2), this cooling speed field corresponds to ferrite extension and certain authors [OTT 80] put forward a connection between the degradation of toughness and the thickness of the ferrite proeutectoïd joints appearing at the old austenitic grain boundaries.

At this stage, it should be noted that simultaneous requirements concerning toughness and resistance to cracking can sometimes appear contradictory: indeed, the guarantee of a minimum toughness can be dependent on the limitation of the cooling parameter (for example: $\Delta t_{500}^{800} < \Delta t_{1\ crit.}$). On the other hand, the desire to avoid cold cracking can result in the requirement for a minimum cooling speed, in order to avoid too strong a martensitic proportion (generally 80%), that is to say: $\Delta t_{500}^{800} > \Delta t_{2\ crit.}$. It can thus be seen that the simultaneous respect of these two criteria can lead to the concept of *a metallurgical weldability field* between the values $\Delta t_{1\ crit}$ and $\Delta t_{2\ crit}$.

The influence of various elements present in C-Mn and micro-alloyed steels on toughness in the coarse grain HAZ can be schematized as follows.
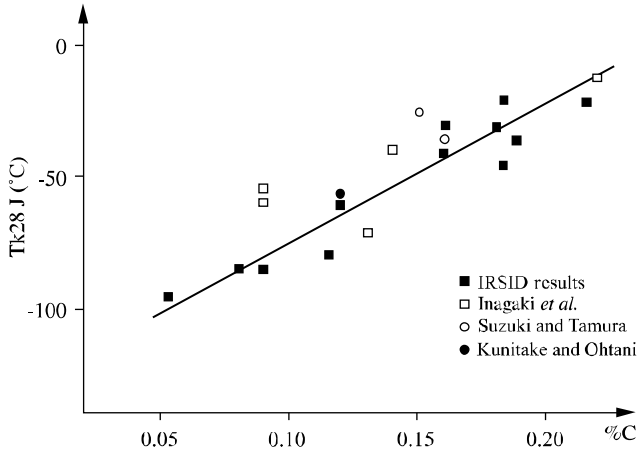
Figure 3.20. *Influence of the percentage of carbon on the transition temperature TK28J in the HAZ structure (martensite + lower bainite); from [DEV 88]*

Carbon decreases the toughness of the HAZs equally in the case of fast and slow cooling speeds. Figure 3.20 thus shows the unfavorable influence of carbon on the transition temperature of impact strength for HAZs of optimal microstructure (martensite-bainite), therefore cooled relatively quickly.

In the case of the slowest coolings (for example, when $\Delta t_{500}^{800} >100$ s), carbon and nitrogen (the latter having an even more marked influence) have a detrimental influence on toughness [DEV 88]. Nitrogen's detrimental effect exists both in as-welded and stress relieved states.

It is also interesting to limit silicon a certain extent, an element which leads to the formation of M-A compounds decreasing the toughness of the coarse grain HAZ and the reheated HAZ in the intercritical field [TAI 95].

Within certain limits (P $< 20 \times 10^3$%), phosphorus seems to have rather little influence on the HAZ toughness in the case of high energy welding, but has a significantly detrimental effect in the case of welding at low energy levels, in particular after stress relief [GRO 86].

As has been observed previously, controlled additions of titanium slow down the growth of the austenitic grain. This beneficial action on toughness is also reinforced by the fixing of part of the free nitrogen. If moreover the aim is to avoid coarse nitride precipitation in the liquid state, the titanium and nitrogen content must be such that the product of their activity remains lower than the product of solubility in

the liquid state. Various pieces of research have shown that effective additions of titanium must be carried out in steels with a low nitrogen content ($<5 \times 10^{-3}$%) and must be themselves fairly low (Ti $\approx 10 \times 10^{-3}$%) [BAK 97, DEV 88, YAO 90].

Recently developed steels, comprising complex titanium oxides, also show very good toughness properties in the HAZ. In this case, these thermally very stable oxides can be used as sites of ferritic germination with cooling in the HAZ, even at high temperature (1,400°C, for example), and involve the formation of a fine, disorientated acicular ferrite structure.

Boron is a very effective element with which to increase hardenability and to limit the formation of proeutectoïd ferrite or Widmanstätten ferrite. It is however advisable to limit the B content to 10-15 ppm to avoid an embrittlement by precipitation of boro-carbides or the formation of M-A compounds [RAM 86].

The gammagene property of nickel significantly lowers the transformation temperatures in cooling and refines the grain size. From a content of 0.3 to 0.5%, it improves toughness in the HAZ as well as in the base metal.

In the case of slow cooling (for example when $\Delta t_{500}^{800} > 100$ s) or at the time of a later tempering, the dispersoid elements such as niobium and vanadium can reprecipitate and lead to a certain embrittlement. For a given grade of steel, it should however be noted that this possibly unfavorable influence is largely compensated by the fact that the presence of these elements is generally associated with a significant reduction in the percentage of carbon.

3.3.3. *Residual stresses associated with welding*

The origin of residual welding stresses is related on the localization of the heat source and the variations of the mechanical properties of materials according to the temperature. Two sources of residual stresses can be distinguished:

– residual stresses, purely thermal in origin, result from the following fact: subjected to a rise in temperature $\Delta\theta$, an element of the heated central zone should dilate to the degree $\varepsilon = \alpha \, \Delta\theta$, α indicating the linear dilation coefficient of the material. Actually, this expansion is very limited since the neighboring cold parts play a restraining role. The element is thus subjected to a compression from them. The flow limit being very weak at high temperature, all the deformations that appear correspond to plastic deformations. With cooling, the situation is reversed: the heated central zone cannot retract freely, and is put under pressure by the neighboring zones. After cooling, the heated zones (molten metal and HAZ) will be subjected to residual tensile stresses, the neighboring zones being, for reasons of

balance, in compression. In the molten metal, the stresses thus created can be very high, in the order of material yield strength at room temperature. Figure 3.21 presents a typical example of longitudinal distribution or transverse stresses (compared to the direction of welding) within a welded joint;

– residual stresses associated with allotropic transformations on cooling: in the case of construction steels, the transformation of austenite is always accompanied by a more or less marked expansion. If this occurs at relatively low temperature (temperable materials, fast cooling, etc.), the associated deformation will no longer be plastic, but elastic. The expansion, opposed by the neighboring zones, results in the formation of residual compressive stresses.

Superimposed on the thermal stresses, these can decrease the level of tensile stresses, and even lead to compression stresses in the HAZ [MAS 80].
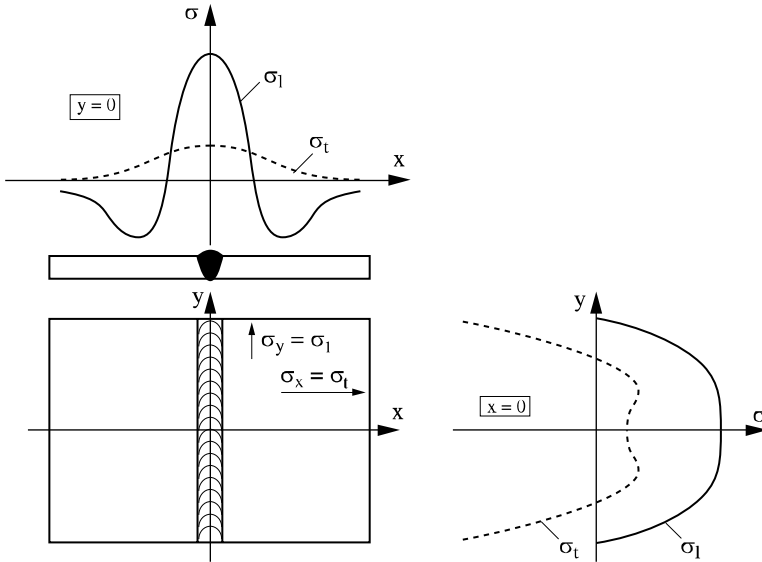
Figure 3.21. *Typical example of longitudinal distribution and transverse residual stresses within a welded joint, from [MAC 77]*

The residual stresses resulting from welding are superimposed on the in-service stresses, and for this reason play a role in various phenomena or properties: cold cracking, fatigue strength, rupture, stress corrosion, etc.

3.3.4. *Influence of residual stress relieving heat treatments in the HAZ*

In certain cases, the residual stresses of welding can seriously reduce the service performance of assemblies, and it is necessary to lower their level by stress relieving treatment. The principle aspect of this operation consists of transforming the residual elastic stresses into plastic deformations. In general, this is carried out by a post-welding heat treatment at a temperature such that the elastic limit of material is sufficiently reduced to obtain this transformation. This type of treatment thus comprises:

– a slow heating to a temperature where relief is sufficiently significant;

– a maintenance at this temperature (for example: to around 530 to 630°C for C-Mn and micro-alloyed steels and, 670 to 710°C for Cr-Mo steels, etc.);

– a sufficiently slow cooling so as not to introduce new residual stresses.

We will restrict ourselves here to pointing out some general metallurgical consequences of this type of treatment, by recalling that the precise choice of conditions depends on many factors (type of material, thickness, and of course any regulations in place [BER 78]).

In general, the tempering associated with the relief treatment has a beneficial effect on quenched microstructures, although this is less favorable when the initial structures in the HAZ are ferrite-carbide. A favorable effect caused by the restoration of possible strain hardened-aged zones during welding, or after cold working should also be noted.

As has been seen, the precipitation of micro-alloying elements (Nb, V) is generally incomplete during coolings in the HAZ. The complementary precipitation which can occur during the stress relieving heat treatment will generally have a detrimental influence on toughness. Thus, the metallurgical effect of the treatment will often result from a conflict between a mechanism of matrix softening (favorable) and a more or less significant precipitation (unfavorable).

The tempering treatment can sometimes have a post-heating role, allowing the diffusion of hydrogen out of the welded joints, lowering the levels of hardness, and thus reducing the risk of cold cracking (see section 3.2.4).

In the case of low alloyed steels, the additions of Mn, Cr, Ni can lead to a certain deterioration of tenacity for a stress relief treatment followed by a slow cooling, contrary to the additions of Mo [BLO 80]. This phenomenon is more accentuated the coarser the grain involved and the greater the temper. To avoid the problems of reversible temper brittleness [BLO 88], it is important to limit the impurity content,

which can be achieved by, for example, using the Bruscato parameter: $\overline{X} = (10P + 4Sn + 5Sb + As)/100$, lower than a value of 10 for demanding specifications [BER 97].

In certain cases (low alloy steels, alloys containing nickel, etc.), it is observed that stress relief heat treatments lead to an intergranular cracking in the HAZ, known as *reheat cracking* [DHO 87, DHO 92].

This phenomenon occurs in the presence of significant residual stresses, accentuated particularly by localized stresses caused by the geometry, in coarse grain zones weakened by intergranular precipitations (AlN, Mo, Nb, V carbides) and segregated impurities (S, P, As, Sn, Sb, etc.) within these same joints. The appearance of such cracks is generally interpreted from a precipitation hardening of the grain interior during the post-welding treatment, which limits all stress relief or plastic deformation within the grains, by concentrating them on the less resistant grain boundaries. The prevention of reheat cracking thus involves the adoption of less sensitive materials, but also by use of suitable welding conditions: low resistance molten metal, *buttering*, increased contribution of heat and/or pre-heating, use of the *temper bead* method, i.e. narrow passes to achieve a refinement of the preceding ones, etc.

3.4. Bibliography

[AND 65] ANDREWS K.W., "Empirical formulae for the calculation of transformation temperature", *Journal of the Iron and Steel Institute*, no. 7, July 1965.

[ATS 80] ATS/OTUA, "Conseils pour le soudage des aciers de construction métallique et chaudronnée à limite d'élasticité garantie ≤ 420 N/mm²", *Cahiers de l'ATS/OTUA*, 1980.

[BAK 97] BAKER T.N., *Titanium Technology in Microalloyed Steels*, Institute of Materials Publications, 1997.

[BER 72] BERNARD G., PRUDHOMME M., "Compléments à l'étude des phénomènes thermiques dans les joints soudés", *Revue de Métallurgie*, July-August 1972.

[BER 75] BERNARD G., "A view-point on the weldability of C-Mn and microalloyed structural steels", *Microalloying Symposium 75*, Washington, October 1975.

[BER 78] BERNARD G., Opportunité des traitements thermiques de relaxation dans les constructions soudées, Doc. IIS/IIW no. X.913-78, 1978.

[BER 97] BERANGER G., HENRY G., LABBE G., SOULIGNAC P., *Les aciers spéciaux*, Lavoisier, 1997.

[BHA 92] BHADESHIA H.K.D.H., *Bainite in Steels*, Institute of Materials, 1992.

[BLO 80] BLONDEAU R., "Les aciers faiblement alliés soudables, influences des éléments d'addition", *Soudage et Techniques Connexes*, January-February 1980.

[BLO 88] BLONDEAU R., "La fragilité de revenu réversible, facteurs et remèdes", *Traitement thermique*, 220, 1988.

[CHA 74] CHANDEL R.S., GARBER S., "Mechanical and metallurgical aspects of spot-welded joints in heat-treated low-carbon mild steel sheet", *Metals Technology*, September 1974.

[CHR 65] CHRISTENSEN N., DAVIES V. DE L., GJERMUNDSEN K., "Distribution of temperatures in arc welding", *British Welding Journal*, February 1965.

[CLY 58] CLYDE M., ADAMS C.M., "Cooling rates and peak temperatures in fusion welding", *Welding Research Supplement*, May 1958.

[CON 87] CONNOR L.P., *Welding Handbook,* volume 1, American Welding Society, 1987.

[CON 92] CONSTANT A., HENRY G., CHARBONNIER J.C., *Principes de base des traitements thermomécaniques et thermochimiques des acier*s, PYC Edition, 1992.

[DEA 40] DEARDEN J., O'NEILL, "A guide to the selection and welding of low alloy structural steels", *Trans. Int. Welding*, 1940.

[DEB 82] DEBROY T., SZEKELY J., EAGAR T.W., "Temperatures profiles, the size of the Heat-Affected Zone and dilution in electroslag welding", *Materials Science and Engineering*, no. 56, 1982.

[DEF 75] DEFOURNY J., BRAGARD A., "Caractérisation des cycles de température en soudage bout à bout à l'arc submergé de tôles d'aciers au moyen de deux grandeurs du champ thermique", *Revue Belge de la Soudure*, no. 3, Lastijdschrift, 1975.

[DEV 83] DEVILLERS L., KAPLAN D., MOUSSY F., Soudabilité des aciers trempés et revenus obtenus par trempe directe, Final research report, CECA no. 7210 KA/308, 1983.

[DEV 84] DEVILLERS L., KAPLAN D., MOUSSY F., Prévision et comportement de la zone adoucie des aciers trempés-revenus, IRSID Report no. RE 1137, September 1984.

[DEV 85] DEVILLERS L., KAPLAN D., Propriétés d'emploi d'assemblages obtenus par faisceau d'électrons des tôles de forte épaisseur en acier de construction, Final research report CECA no. 7210 KA/310, IRSID Report RE 1252, December 1985.

[DEV 86a] DEVILLERS L., KAPLAN D., MAAS E., "Aspects mécaniques de l'évaluation de la ténacité d'éprouvettes métallurgiquement hétérogènes", *Revue de Métallurgie,* CIT, April 1986.

[DEV 86b] DEVILLERS L., KAPLAN D., Interpretation of deviated fracture of electron beam steel welds in notch bending tests, IRSID Report no. RE 1319, 1986.

[DEV 87] DEVILLERS L., KAPLAN D., JANSEN J.P., "Simulation thermique des zones affectées par la chaleur en soudage multipasse des aciers de construction", *Soudage et Techniques connexes*, March-April 1987.

[DEV 88] DEVILLERS L., KAPLAN D., JANSEN J.P., "Aspects thermiques et métallurgiques de la ténacité des ZAC", *Revue de Métallurgie,* CIT, March 1988.

[DEV 89] DEVILLERS L., KAPLAN D., Aspects métallurgiques de l'assemblage des tôles de faible épaisseur par LASER CO_2, Final research report CECA no. 7210 KA/314, IRSID Report RCA 89333, October 1989.

[DEV 91] DEVILLERS L., KAPLAN D., TESTARD P., An approach for predicting microstrucrures and toughness properties in HAZ of multipass welds, IRSID Report 91316, March 1991.

[DHO 87] DHOOGE A., VINCKIER A., "Reheat cracking – a review of recent studies", *Int. J. Pres. Ves. and Piping*, 27, 1987.

[DHO 92] DHOOGE A., VINCKIER A., "La fissuration au réchauffage- revue des études récentes (1984-1990)", *Le Soudage dans le Monde*, vol. 30, no. 3-4, 1992.

[EAS 83] EASTERLING K., *Introduction to the Physical Metallurgy of Welding*, Butterworths, 1983.

[GOL 76] GOLDAK J., BIBBY M., "The toughness of EB welds in HSLA steels", *Welding of HSLA Structural Steels Conference,* Rome, ASME Publications, 1976.

[GRA 95] GRANJON H., *Bases métallurgiques du soudage,* Publications du soudage et ses applications, 2nd edition, 1995.

[GRO 86] GRONG O., AKSELSEN O.M., "HAZ toughness of microalloyed steels for offshore", *Metal Construction*, September 1986.

[GRO 94] GRONG O., *Metallurgical Modelling of Welding*, Institute of Materials, 1994.

[GRU 81] GRUMBACH M., *Les essais de dureté*, Collection IRSID-OTUA, 1981.

[HAL 84] HALE G.E., NUTTING J., "Overheating of low-alloy steels", *International Metals Review*, vol. 29, no. 4, 1984.

[HEH 72] HEHEMANN R.F., KINSMAN K.R., AARONSON H.I., "A debate on the bainite reaction", *Metallurgical Transactions*, vol. 3, May 1972.

[HEI 75] HEISER F.A., DE FRIES R.S., "Temper embrittlement in steel for thick wall gun tubes", *Journal of Metals*, January 1975.

[HON 95] HONEYCOMBE R.W.K., BHADESHIA H.K.D.H., *Steels, Microstructure and Properties*, Edward Arnold, 1995.

[HRI 95] HRIVNAK I., "Weldability of modern steel materials", *ISIJ International*, vol. 35, 1995.

[IKA 80] IKAWA H., OSHIGE H., TANOUE T., Effect of M-A constituent on HAZ toughness on a high strength steel, Document IIS-IIW, no. IX-1156-80, 1980.

[IKE 95] IKEUCHI K., LIAO J., TANABE H., MATSUDA F., "Effect of temper-bead thermal cycle on toughness of weld ICCGHAZ of low alloy steel SQV-2A", *ISIJ International*, vol. 35, 1995.

[INO 98] INOUE K., *ISIJ International*, vol. 38, no. 9, 1998.

[ION 97] ION J.C., "Modelling of LASER welding of Carbon-Manganese steels", in H.C. Cerjak (ed.), *Mathematical Modelling of Weld Phenomena 3*, Institute of Materials, 1997.

[IRS 77] IRSID, "Courbes dureté-paramètre de refroidissement en conditions de soudage", collection established at the IRSID, 1977.

[ITO 00] Ito R., Shiga C., Kawaguchi Y., Hayashi T., Shinohara H., Torizuka S., Microstructural analysis of softening region on weld HAZ of ultra-fine grained steels, Document Institut International de la Soudure no. IX-1968-00, 2000.

[KAN 76] Kanazawa S., "Improvement of weld fusion zone toughness by fine TiN", *Transactions ISIJ*, vol. 16, 1976.

[KAP 98] Kaplan D., Sturel T., "Couplage d'un modèle métallurgique de soudage et de critères locaux de rupture pour prévoir la ténacité des joints soudés multipasses", *9èmes Journées AFIAP*, Paris, October 1998.

[KAW nd] Kawabata F., Amano K., Toyoda M., Minami F., Tempering effect by succeeding weld passes on multi-layered HAZ toughness, doc. Kawasaki Steel, no date.

[KOS 81] Koso M., Miura M., Ohmori Y., "Microstructure and toughness of weld HAZ in 785 MNm^{-2} steel", *Metals Technology*, December 1981.

[KOU 86] Kou S., Wang Y.H., "Computer simulation of convection in moving arc weld pools", *Met. Trans. A*, vol. 17A, December 1986.

[LAM 99] Lambert A., Drillet J., Gourgues A.F., Sturel T., Pineau A., Microstructure of M-A constituent in HAZs of HSLA steel welds in relation with toughness properties, IRSID report, no. 99 21, 1999.

[LIN 89] Lin Y., Abken M.G., Bowker J.T., "Mechanical and microstructural analysis of multi-pass welded HAZ", *Proceedings of Recent Trends in Welding Science and Technology*, ASM International, Gatlinburg, 1989.

[LON 94] Longaygue X., Kaplan D., Maurickx T., "Etude paramétrique de l'influence des facteurs d'hétérogénéité mécanique sur le comportement en service des assemblages soudés", *Revue de Métallurgie*, CIT, June 1994.

[MAK 77] Macherauch E., Wohlfahrt H., "Different sources of residual stress as a result of welding", in *Residual Stresses in Welded Construction and their Effects,* The Welding Institute Publications, London, 1977.

[MAR 80] Marquet F., Defourny J., Marique C., Mathy H., Bragard A., Recherches sur les connaissances de base en vue d'améliorer le soudage des aciers sous haut apport calorifique, Rapport final de recherche CECA no. 7210 LA/303, 1980.

[MAS 80] Masubuchi K., *Analysis of Welded Structures,* Pergamon Press, 1980.

[MAT 94] Matsuda F., Fukada Y., Okada H., Shiga C., Ikeuchi K., Horii Y., Shiwaku T., Suzuki S., Review of Mechanical and Metallurgical Investigations of M-A constituent in Japan, Doc. IIS-IIW no. IX-1782-94, 1994.

[MIE 92] Miettinen J., "Mathematical simulation of interdendritic solidification of low-alloyed and stainless steels", *Acta Polytechnica Scandinavica*, Chemical Technology and Metallurgy Series, no. 207, 1992.

[MUR 67] Murry G., Prudhomme M., Constant A., "Etude des transformations dans la zone thermiquement affectée lors du soudage et son intérêt pour l'estimation de la dureté sous cordon", *Revue de Métallurgie*, 64, no. 6, June 1967.

[NIL 75] NILES R.W., JACKSON C.E., "Weld thermal efficiency of the GTAW process", *Welding Journal, Welding Research Supplement*, January 1975.

[OHM 74] OHMORI Y., OHTANI H., KUNITAKE T., "Tempering of the bainite/martensite duplex structure in a low-carbon low-alloy steel", *Met. Sci.*, vol. 8, 1974.

[OKA 92] OKAGUCHI S., *ISIJ International*, vol. 32, no. 3, 1992.

[OLE 81] OLETTE M., GATELLIER C., "Action d'une addition de calcium, de magnésium ou des éléments des terres rares sur la propreté inclusionnaire des aciers", *Revue de Métallurgie,* CIT, December 1981.

[OTT 80] OTTERBERG R., SANDSTRÖM R., SANDBERG A., "Influence of Widmanstätten ferrite on mechanical properties of microalloyed steels", *Metals Technology*, October 1980.

[POR 34] PORTEVIN A., SEFERIAN D., *XIe Congrès de l'Acétylène et de la Soudure Autogène*, Rome, vol.3, 1934.

[RAM 86] RAMBERG M., AKSELSEN O.M., GRONG O., "Embrittlement phenomena in the intercritical HAZ of boron-containing steels", *Advances in Welding Science and Technology,* Publications de l'ASM, Gatlinburg, 1986.

[REE 94] REED R.C., BHADESHIA H.K.D.H., "A simple model for multipass steel welds", *Acta Metall. Mater.*, vol. 42, no. 11, 1994.

[RIS 74] RIST A., ANCEY-MORET M.F., GATTELLIER C., RIBOUD P.V., "Equilibres thermodynamiques dans l'élaboration de la fonte et de l'acier", *Techniques de l'Ingénieur*, M 1733, 1974.

[ROS 46] ROSENTHAL D., "The theory of moving sources of heat and its applications to metals treatments", *Transactions ASME*, vol. 68, 849, 1946.

[RYK 61] RYKALINE N.N., "Calcul des processus thermiques de soudage", *Soudage et techniques connexes*, no. 1-2, 1961.

[TAI 95] TAILLARD R., VERRIER P., MAURICKX T., FOCT J., "Effect of silicon on CGHAZ toughness and microstructure of microalloyed steels", *Met. Trans. A*, vol. 26, February 1995.

[TAK 95] TAKAHASHI A., OGAWA H., "Influence of softened heat-affected zone on stress oriented hydrogen induced cracking of a high strength line pipe steel", *ISIJ International*, vol. 35, 1995.

[TOY 86] TOYODA M., Fracture toughness evaluation of steel welds (Review), Osaka University Document, July 1986.

[TOY 92] TOYODA M. (ed.), *Proceedings of the Workshop Mismatching and its Control*, Osaka University, Tokyo, July 1992.

[WEI 95] WEISS D., SCHMIDT J., FRANZ U., "A model of temperature distribution and weld pool deformation during arc welding", *Mathematical Modelling of Weld Phenomena 2*, Institute of Materials, 1995.

[YAO 90] YAO S., KOÇAK M., Influence of titanium on HAZ microstucture and toughness of offshore steel welds: literature review – part 1, Report GKSS, no. 90/E/39, 1990.

[YUR 87] YURIOKA N., OKUMURA M., KASUYA T., COTTON H.J.U., "Prediction of HAZ hardness of transformable steels", *Metal Construction*, April 1987.

[ZAC 93] ZACHARIA T., DAVID S.A., "Heat and fluid flow in welding", *Mathematical Modelling of Weld Phenomena*, Institute of Materials, 1993.

[ZEN 48] ZENER C., *Transactions ASME,* no. 45, 1948.

Chapter 4

Molten Metal

4.1. Metallurgical reminders

Broadly speaking, the mechanical characteristics of a steel result from its structure and its chemical composition. For a given structure, the chemical composition influences the mechanical properties due to the effect of the elements in solid solution.
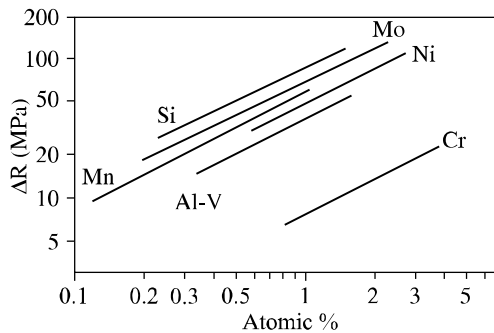
Figure 4.1. *Increase in the tensile strength of iron due to the effect of various elements in solid solution; from [GAR 75]*

Figure 4.1 shows that this effect is modest since an atomic addition of 1% of chromium or molybdenum modify the fracture strength of the ferrite by only 6 or 70 Mpa respectively.

Chapter written by Christian BONNET.

As for the structure of steel, it depends on the heat treatment but also on the chemical composition which determines its hardenability. Thus, two steels of different chemical composition will not lead to the same structure for the same heat treatment and will thus have different mechanical properties.
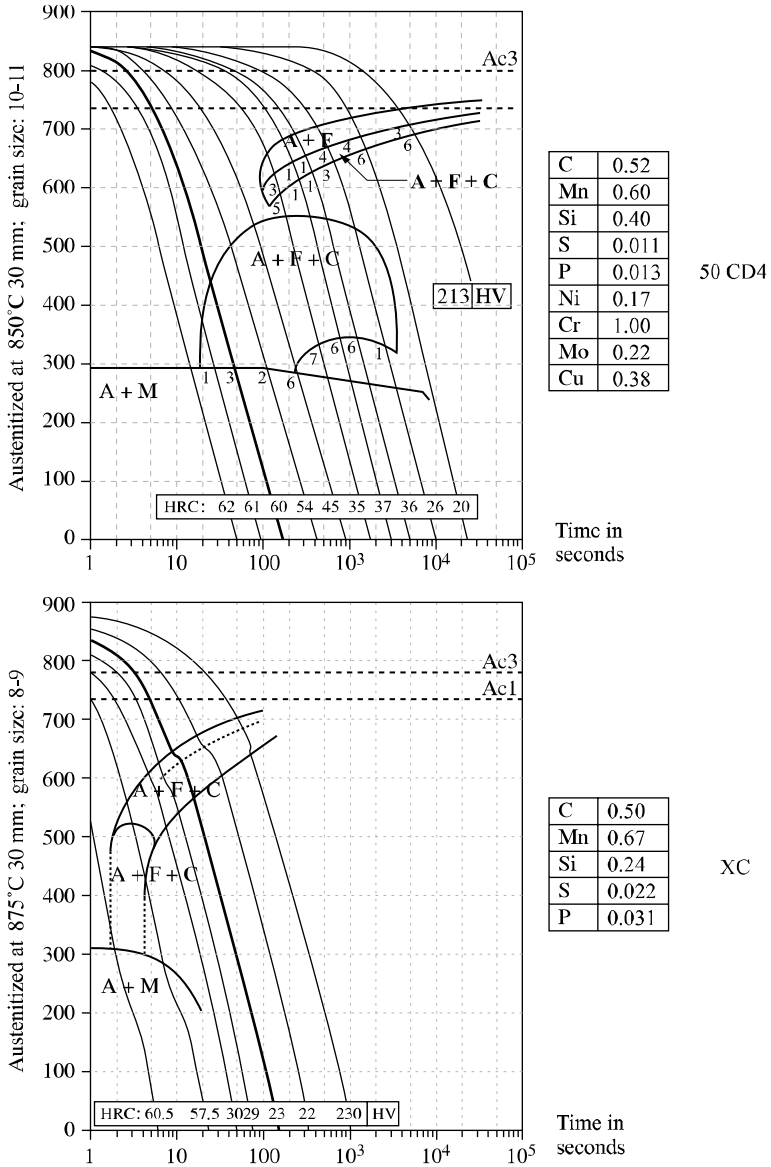
Figure 4.2. *Continuous cooling transformation (CCT) diagrams; from [COL 74]*

The CCT diagrams of steels XC48 and 50CD4 show very clearly that the structural influence is infinitely higher than the effect of the solid solution of alloying elements. Indeed, the two steels with similar carbon percentage have similar hardnesses when they are in the same structural state (hardness: 210/220 Hv in the ferrite + pearlite state; 60/62 HRc in a martensitic state) but have extremely different characteristics when they are subjected to the same heat treatment. Thus, for the cooling speed highlighted in Figure 4.2, steel 50CD4 has a primarily martensitic structure which confers a hardness of 60 HRc, while steel XC48 has a ferrite + pearlite structure whose hardness is only 23 HRc.

These metallurgical principles are very broad and thus also apply to the welding metallurgy. Thus, we will have to examine any welding operation from a thermal as well as a chemical point of view.

4.2. Molten metal

4.2.1. *Thermal aspect*

The thermal aspect has already been covered in Chapter 3. The approach used then applies to any point in the molten metal and it is thus possible to determine with the cooling conditions of each pass of an assembly with sufficient precision, provided that the welding energy, the type of joint, the process, the thickness/es concerned, the pre-heating temperature and/or the inter-pass temperature are known.
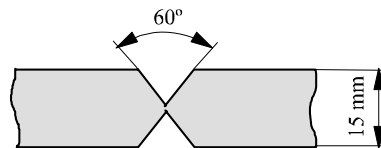
Figure 4.3. *Bypass submerged arc weld*

The effect of variations in the operating conditions on the thermal cycle is generally underestimated by the majority of the welders. By means of the IRSID graph for example (see Figure 3.8), it can be seen that minor modifications of the electric parameters or temperature between passes can significantly modify the thermal welding cycle and, consequently, the mechanical properties of the welded joint (see Table 4.1).

Such variations can be employed by a welder to improve wetting or to save time during the execution of a small-size homologation sample which will lead to a much

higher temperature between passes than will be the case in real construction conditions.

Influence of welding energy			
1st pass	**Example 1**	**Variation**	**Example 2**
Welding parameters	600 A; 28 V; 50 cm/min		660 A; 30 V; 40 cm/min
Welding energy	20.16 kJ/cm	**47.3%**	29.7 kJ/cm
Δ*t* 800/500	**11 s**	**263%**	**40 s**

Influence of temperature between passes			
2nd pass	**Example 3**	**Variation**	**Example 4**
Welding parameters	600 A; 28 V; 50 cm/min		600 A; 28 V; 50 cm/min
Temperature	20°C	**130°C**	150°C
Welding energy	20.16 kJ/cm	**-**	20.16 kJ/cm
Δ*t* 800/500	**11 s**	**82%**	**20 s**

Table 4.1. *Evaluation of the thermal cycle based on the IRSID graph; from [COL 77]*

4.2.2. *Chemical aspect*

Constitution of the molten metal

The chemical composition of molten metal results from the metal mixture added by the welding product and the base metal. The proportion of base metal in a weld bead is characterized by the dilution ratio (see Figure 4.4).

$$Dilution\ ratio = \frac{Surface\,(B)}{Surface\,(A+B)}$$
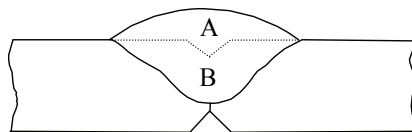
Figure 4.4. *Influence of the base metal on the composition of the molten metal*

According to the process, the type of joint and the welding procedure, the proportion of base metal is more or less important and in the case of a multipass joint, it varies from one pass to another. However, the products of welding are balanced chemically so that their deposits "outside dilution" acquire the necessary mechanical properties under the cooling conditions corresponding to the most traditional thermal welding cycles. It should be understood that each time a welding material undergoes cooling transformation phases, the analysis of the metal added by the welding product which makes it possible to obtain the same mechanical properties is different from that of the base metal, because the cooling conditions during the manufacture of the latter are very different from those which are associated with welding. Thus, by dilution effect, the molten metal has an intermediate analysis between that of the added metal and that of the base metal and this analysis can vary from one pass to another in multipass welding. This is why the majority of the operating mode procedures require a check on the properties at various levels in the welded joint and, in particular, in the root zone where the dilution ration is the highest and consequently where the lowest impact strength values will often be found. In spite of these qualifications, the manufacturers are not spared unpleasant surprises while checking the properties of the assemblies during production if they have recourse to materials of various sources. This results from the fact that the qualification of the operating procedure takes the standardized designation of the base metal into account and that in the majority of cases, this is based on the product's mechanical properties. Thus, according to the different manufacturing techniques available to them, the various steelmakers will use significantly variable analyzes to comply to the same standardized designation as the analyzes of three steels used indifferently by the same manufacturer show (see Table 4.2). If they are welded with the same filler product, these steels, although conforming to the required standard, will lead to very different analyses and mechanical properties of the molten metal in the zones where there is a high dilution rate.

%	C	Si	Mn	P	S	Cu	Ni
NF EN 10028: P295GH	0.08 0.20	<0.4	0.9 1.5	<0.030	<0.025	<0.30	<0.30
Steel 1	0.20	0.23	1.02	0.014	0.008	-	-
Steel 2	0.13	0.28	0.99	0.013	0.010	0.29	-
Steel 3	0.12	0.40	1.34	0.018	0.008	0.24	0.12

Table 4.2. *Examples of analytical variations in steels complying to the same standardized designation*

Analytical characteristics of the deposited metal

The deposited metal comes from the fusion of the filler product in the atmosphere of the arc. The welding processes with a refractory electrode (TIG, plasma) generally takes place in an inert atmosphere to avoid rapid deterioration of the tungsten electrode. When these processes are employed, the analysis of the deposited metal is then very close to that of the filler; it differs only in the volatilization of various elements present, which are a function of their respective vapor tensions. Thus, a slight reduction will be noted in the manganese content in the deposited metal compared to the filler.

On the other hand, for all the other processes the arc atmosphere is deliberately more or less oxidizing because a light oxidation of the base metal's surface aids electron emission and, thus the stability of the arc. This being the case, oxido-reduction reactions occur, mainly in the metal drops which transfer in the arc, so that the analysis of the deposited metal deviates notably from that of the filler. It is easy to take these chemical exchanges into account at the time the welding product is formulated, so as to adjust the alloying elements to obtain the content desired in the added metal but one will never be able, with these processes, to lower the oxygen content of the deposited metal to the level of that of the base metal (see Table 4.3). Oxygen being practically insoluble in the majority of metals, it will be found in the form of inclusions finely dispersed in the weld. In the case of steels, we will see later that under certain conditions these inclusions can play a key role at the time of the austenite transformation of the molten metal.

		Molten metal			
	Steel	TIG/Plasma	MAG		SMAW/ SAW
			Solid wire	Filled wire	
O ppm	15-40	20-60	250-550	300-1,100	280-1,100

Table 4.3. *Ranges of oxygen content variations in steel welds according to the processes and the types of welding products*

In welding with a coated electrode (SMAW), there is another element whose content in the molten metal cannot be kept as low as we could wish: nitrogen. Indeed, although coatings of the coated electrodes always contain components which break up during fusion and generate at the level of arc gases in order to protect the metal droplets from the ambient air, the protection thus obtained is never perfect and we cannot avoid a certain amount of contamination. Because the process is manual, it is clear that the extent of this contamination depends on dexterity on the welder but, whatever it is, it is very difficult to have less than 100 ppm of nitrogen in the deposited metal, particularly in all-positional welding.

4.2.3. *Microstructures in ferritic steel welds: relationship with impact strength characteristics*

As in the HAZ, the mechanical properties of the molten metal depend on its structure and its chemical composition.

If it is easy to define a chemical analysis of the molten metal so as to make it compatible with the tensile properties of the base metal, it is not so simple from the perspective of toughness. Consequently, we will limit our comments here to the issue of impact strength, because this simple and inexpensive test is systematically employed in welding.

In a multipass joint, two types of zone can always be distinguished (see Figure 4.5): the first has preserved an as-solidified structure while the second has been "reaustentitized" during the execution of successive passes. The microstructural components of these various zones are in general very different. Except in the case of a strongly alloyed weld, the reaustenitized areas have a ferritic structure with a small proportion of pearlite because the percentage of carbon in welding products is always very low.

The toughness of this ferritic structure with equiaxial grains depends, as always in metallurgy, on the fineness of the grains. It is thus a function of the thermal welding cycle, which dictates the time spent in the austenitic state and the cooling speed and so the transformation temperature of the austenite. It also depends on the presence of elements such as titanium, niobium, vanadium, aluminum or boron, which limit grain enlargement at the reaustenitization phase. At all events, this reheated structure is generally not at the origin of problems of impact strength in welded joints.

On the other hand, the *as-solidified zones* can have very different structures from one joint to another and, therefore, considerable variations in terms of their impact strength characteristics, as illustrated in Figure 4.6.

The proportion of the *as-solidified and reheated zones* depends on the process and the welding conditions. In the case of TIG multipass welds or when using small diameter coated electrodes, a narrow bead width effectively ensures that the whole of the molten metal has a reheated structure. On the other hand, in submerged arc welds, the as-solidified zones never represent less than 50% of the molten metal and can even reach 90% in the case of double sided bypass welds.
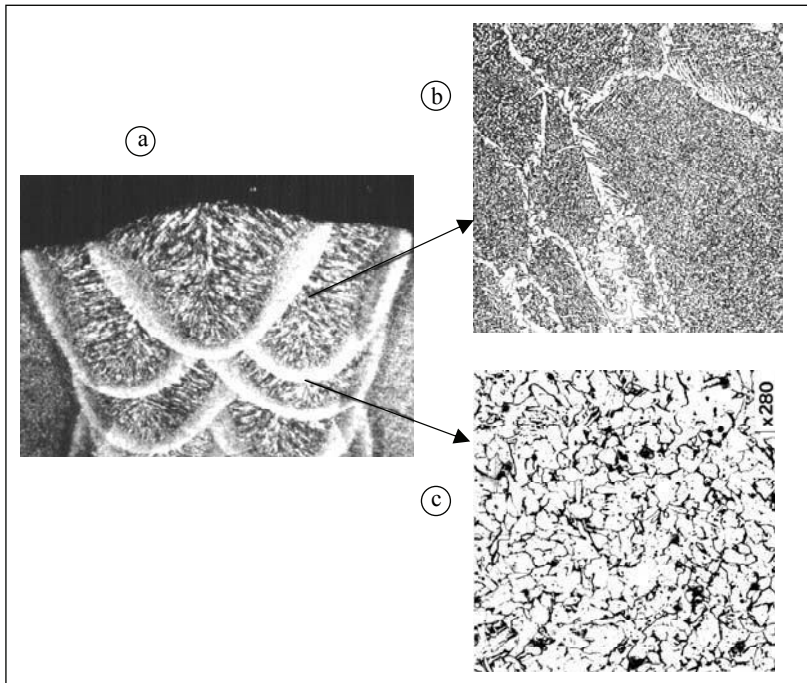
Figure 4.5. *Submerged arc welding: a) macrographic aspect; b) microstructure of the as-solidified zones; c) microstructure of the reheated zones*

The proportion but especially the position of these two types of structure at the notch bottom of the impact test specimens will affect the result. Indeed, the fracture energy measured during this test is the sum of energy necessary to initiate a crack at the notch bottom and the energy necessary for it to progress and lead to the creation of two surfaces. The crack will be initiated under the pendulum impact as soon as the critical initiation stress which is specific to each microstructure is reached in one or other of them. Thus, the stress which develops at the notch bottom under the pendulum impact decreases from its center towards the sides. This is why, in a perfectly homogenous material, the rupture is always initiated in the notch center, while in a heterogenous material, initiation could be offset laterally if the microstructure located at the notch center has a critical cracking stress higher than that of an adjacent structure. Thus, when the most fragile structure is offset compared to the notch center, the *initiation* component of the rupture energy measured during the impact test is much higher than when this same structure is located at the center. As for the propagation energy, it can be readily conceived that it is a function of each microstructures' size and their intrinsic characteristics.

A	% x 1000	B
64	C	67
1510	Mn	1500
370	Si	370
17	S	16
18	P	18
52	Ni	53
65	Cr	67
4	Mo	4
71	Cu	75
4	Ti	8
12	Al	10
1	Nb	1
9	V	11
72	O	75
17	N	17
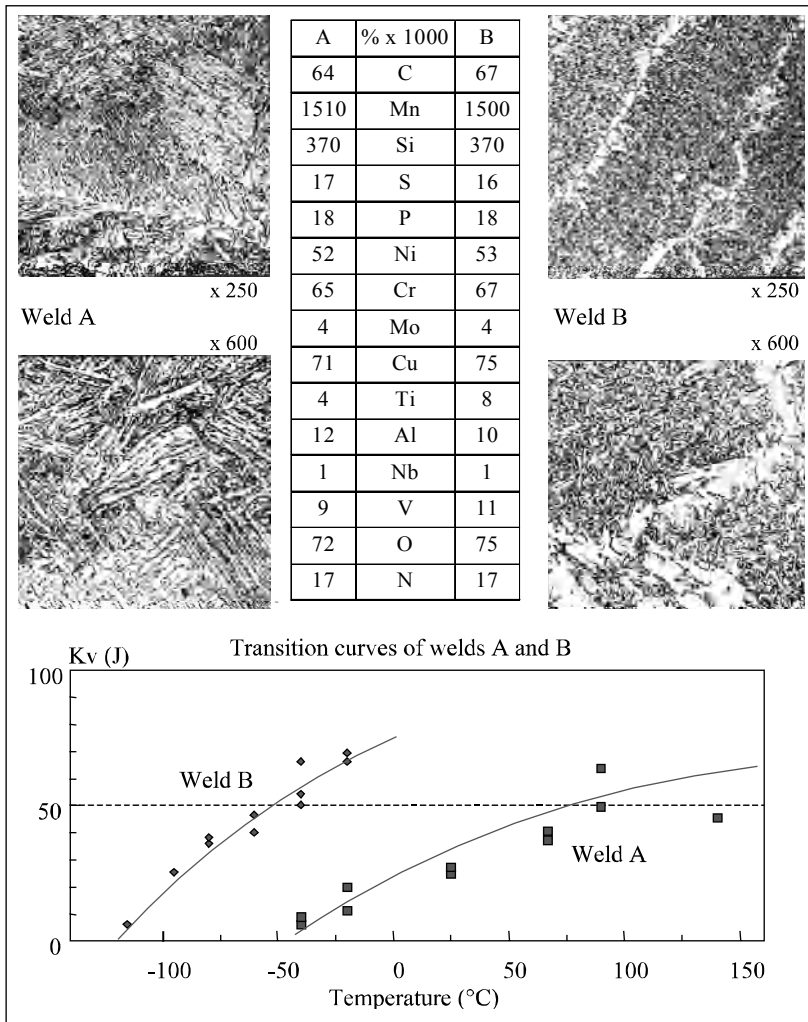
Figure 4.6. *Influence of microstructure on impact strength*

The principal microconstituents likely to exist in the as-solidified zones are represented in Figure 4.7.

In the IIS/IIW-999-88 document, the International Institute of Welding proposes a finer analysis and distinguishes more constituents, however, this is not the important point. Indeed, all metallurgists know that toughness is improved by refining the structure.

Under these conditions, it is clear, looking at the micrographies in Figure 4.7, that the as-solidified zones which lead to the best impact strength characteristics will be primarily made of acicular ferrite.

This microconstituent, which never appears in steels, exists in the molten metal only in the presence of certain inclusions which allow the intragranular germination of the ferrite at the time of the transformation of austenite [ABS 78, COC 78]. It is known that the existence of these inclusions depends on the oxygen content of the deposited metal but, so that there is intragranular ferrite germination, it seems necessary that these complex inclusions, which result from oxido-reduction reactions in fused metal and which are trapped during solidification, have locally on their surface Ti oxide TiO [STL 93] or a MnTi oxide, $MnTi_2O_4$ [BLA 99]. It should be understood then that titanium plays a fundamental role [CHA 83, EVA 97] and besides it is its variation (0.004 to 0.008%) which explains the difference between the structures and the impact strength values of the welds A and B in Figure 4.6. However, it is not enough to have a minimum of titanium so that it is found in one or other of the desired forms on the inclusion surface. What is more, it is necessary that the reaction kinetics which lead to the formation of inclusions allow this result. Thus, in addition to the oxygen content, the nature and the quantity of all of the deoxidizing elements present in the molten metal will play a part, whether they come from the wire or the base metal [BUR 88, DEV 83].

A: Proeutectoïd ferrite
B: Lamellar constituent
C: Acicular ferrite
D: Granular bainite
E: Sub-pearlitic constituent
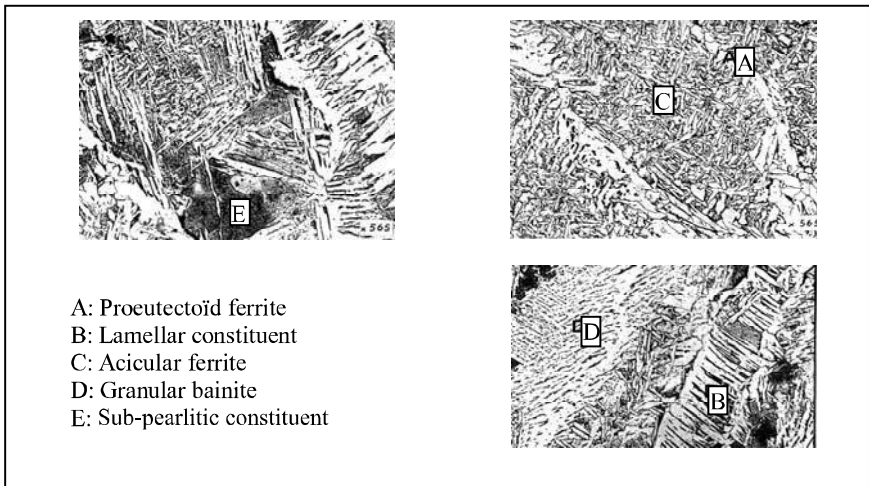
Figure 4.7. *Principal microconstituents of the solidified molten metal in its as-solidified state*

The complexity of these phenomena means that even today it is impossible to predict the presence of the germs necessary to the formation of acicular ferrite with a simple reading of a chemical molten metal analysis. Only a metallographical examination enables us to definitely determine the presence of this component.

These particular inclusions are necessary to achieve a structure rich in acicular ferrite and as a result a good toughness in all the welding zones (including the as-solidified zones). However, this condition is not sufficient because the proportion of acicular ferrite depends on the thermal welding cycle and the chemical composition of the molten metal which determines its hardenability.

Influence of cooling speed

In metallurgy, CCT diagrams make it possible to obtain a precise idea of the structure and hardness of a steel according to the cooling speed after austenitization. These diagrams are specific to each steel and each austenitization condition (austenitic grain size).

In welding, such diagrams do not exist and will undoubtedly never exist because the variations in cooling speed in the field of austenite transformation ($\Delta\tau$ 800/500 or $\Delta\tau$ 700/300) are always accompanied by a variation in the conditions of austenitization, but there is no correlation between these two factors: the increase in the welding energy, the pre-heating temperature, thickness of the parts to be assembled or the implementation of different welding processes do not have similar consequences on the upper (austenitic field) and lower parts (field of transformation) of the thermal cycle [BON 80].

In any event, if the necessary inclusions are present, it has been clearly shown [ANT 81] that an increase in the cooling speed leads, initially at least, to an increase in the proportion of acicular ferrite and is accompanied by an improvement in toughness (see Figure 4.8). Secondly, additional hardened structures (lower bainite and/or martensite) can be found if the hardenability of the molten metal is high.

Influence of alloying elements

The addition of alloying elements to a steel increases its hardenability by delaying transformations which proceed by germination and growth, and lowering the temperature at which martensitic transformation (Ms) begins. If the CCT diagram is considered, the principal effect of this additions is to shift the curves of the diagram towards the right.
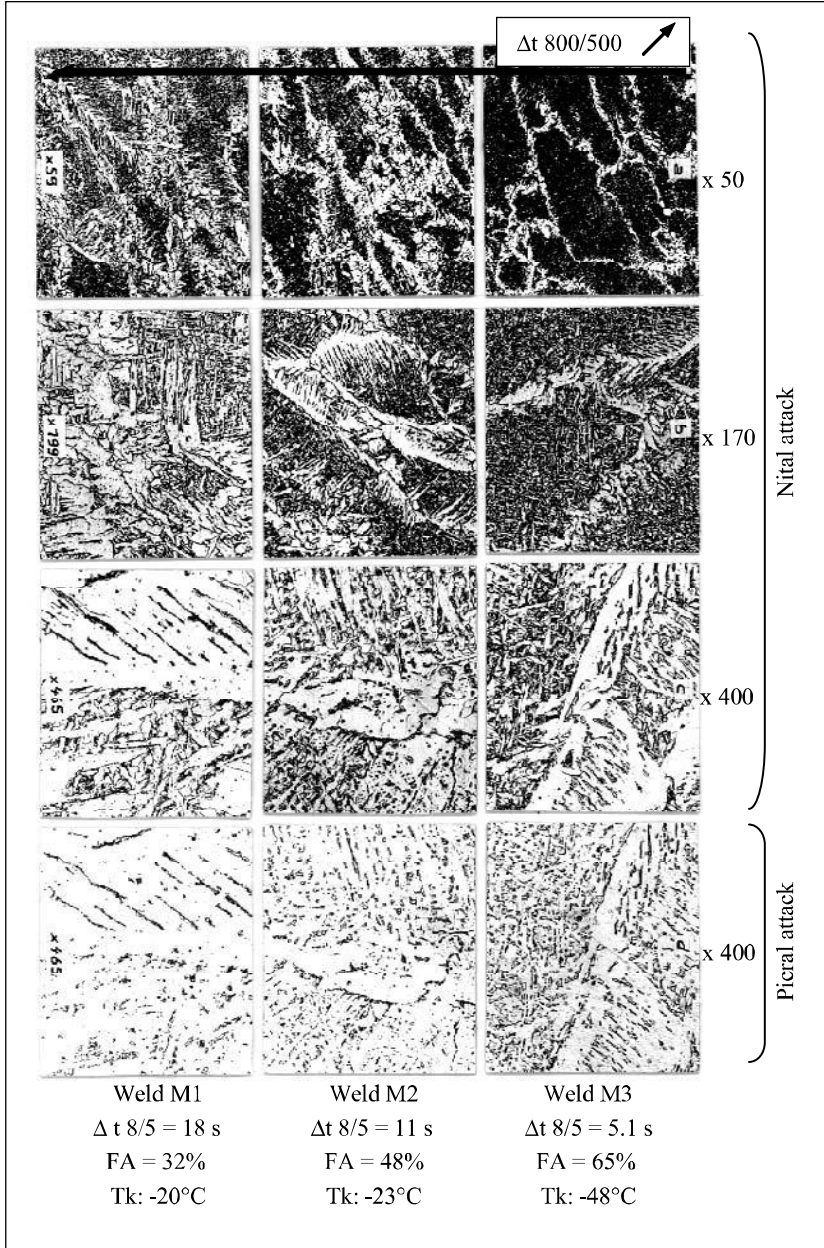
Figure 4.8. *Influence of the thermal cycle on the structure and the temperature transition – analysis of the molten metal: 0.066% C; 0.94% Mn; 0.62% Si; from [BON 80]*

It is much the same for molten metal, except that the slowing of transformations by the addition of alloying elements seems to favor the "traditional" transformations more than acicular ferrite formation. That is easily explained when we consider that, for a field in which austenite is transformed into acicular ferrite to exist, specific inclusions must be present which play the part of pre-existing germs. Then, the addition of alloying elements can have an effect on the germination speed of acicular ferrite but only on its growth.

Thus, at a constant cooling speed, the addition of alloying elements causes an evolution in the microstructure similar to that which the increase in cooling speed causes at a constant chemical composition: initially at least, the proportion of acicular ferrite increases because the transformations which preceded its formation are considerably slowed down; then, the acicular ferrite grains are refined then, finally, these are gradually replaced by an increasing proportion of martensite and/or lower bainite.
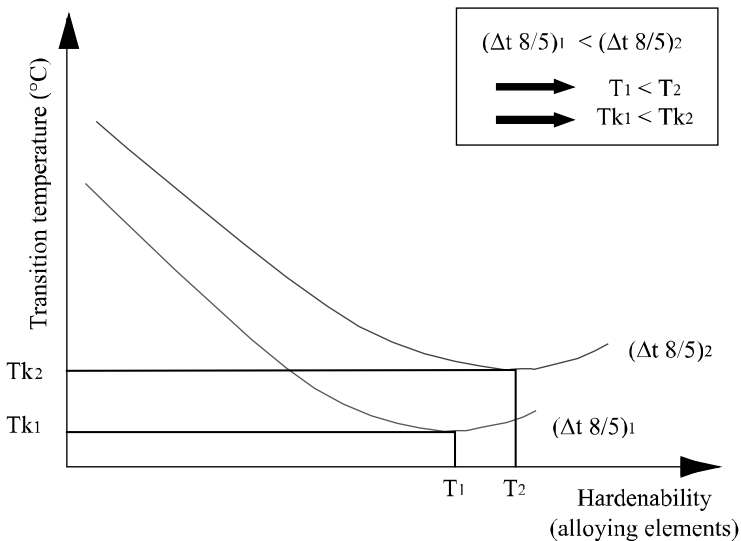
Figure 4.9. *Influence of alloying elements and cooling rate on the transition temperature of the molten metal*

However, from the perspective of mechanical properties, the increase in the cooling speed and the addition of alloying elements are not completely equivalent. Indeed, in the same microstructure, the presence of a greater quantity of alloying elements causes, through a solid solution effect, an increase in rupture strength, yield strength and hardness but also a reduction in impact strength values.

It is then possible to summarize the effect of the cooling speed and chemical composition on the impact strength characteristics in the following way (see Figure 4.9):

– when the content of an alloying element is low (low hardenability), we obtain a very coarse as-solidified structure primarily made up of proeutectoid ferrite and a lamellar component. Toughness is then badly effected whatever the cooling speed (high transition temperature);

– when the alloying content (Mn, Mo, etc.) is increased and if favorable inclusions are present, the acicular ferrite proportion increases, its grains become increasingly fine and toughness improves considerably;

– if the content of alloying elements is increased further beyond T1 for $(\Delta t\ 8/5)_1$ or T2 for $(\Delta t\ 8/5)_2$, a deterioration in the values of impact strength is observed because the negative effect of hardening through the solid solution effect related to the increase in the alloying elements becomes higher than the positive effect resulting from the increase in the quantity and fineness of the acicular ferrite;

– comparison of the two curves in Figure 4.9 shows conclusively that an increase in the cooling rate $(\Delta t\ 8/5)_1$ compared to $(\Delta t\ 8/5)_2$ always improves the impact strength.

In the absence of inclusions essential to the formation of acicular ferrite, granular bainite is first seen to appear then lower bainite. These structural variations are also accompanied by a certain improvement in impact strength values but they remain significantly lower than those obtained in the presence of acicular ferrite.

Influence of oxygen content

In ferritic steel welds, a minimum oxygen content is necessary so that the transformation of austenite into acicular ferrite can exist. This minimum content depends on the other deoxidizers present and increases particularly with the aluminum content. It is about 250 ppm when the aluminum content is lower than 0.015%; it can reach 350 to 400 ppm for an aluminum content of about 0.035 to 0.040%.

It is because this minimum is not reached that poor impact strengths are obtained at low temperature in ferritic steel welding carried out by means of high energy density processes such as plasma, electron beam and laser.

The oxygen content also gives a certain indication of the inclusion rate and this rate has a direct incidence on the ductile rupture energy: all things being equal otherwise, an increase in the inclusion rate generates a reduction in the ductile rupture energy (see Figure 4.10).

There thus exists an optimum oxygen parameter for ferritic steel welds when the required tensile characteristics are accessible to an acicular ferrite structure (<650 or 700 MPa) because the best tensile/toughness compromise will be obtained. Beyond this, structures of lower bainite or martensite will have to be resorted to and a maximum reduction in oxygen content sought so as to minimize the inclusion rate. Obviously this is also the case for austenitic stainless steel welds or, more generally, of face centered cubic materials which do not present a ductile/brittle transition.
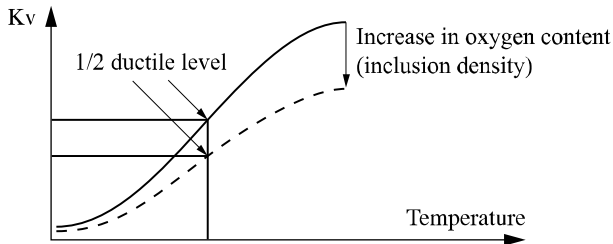
Figure 4.10. *Influence of oxygen content on the Charpy-V transition curve*

Influence of nitrogen, niobium and vanadium

In ferritic steels, nitrogen can be associated with three metallurgical phenomena:

– solid solution effect: the nitrogen atoms in an interstitial position in the cubic centered iron lattice generate large distortions of the crystal lattice that cause an increase in the tensile and hardness characteristics, associated with a reduction in toughness. It is to these free nitrogen atoms that the most harmful effect is generally attributed;

– precipitation hardening: this hardening results from a coherent precipitation of nitrides or carbo-nitrides of elements with a strong affinity for nitrogen (in particular niobium and vanadium). This precipitation primarily occurs in the temperature range 400-650°C;

– ageing: this stems from the diffusion of nitrogen atoms in the interstitial solid solution towards the crystalline defects that strongly limits the possibilities of dislocation displacements.

An increase in the elasticity limit is then observed, while impact strength drops. This phenomenon really appears only at low temperatures (ambient/250°C).

In the welding of these steels, the increase in nitrogen content is observed to have a negative effect on impact strength in all the zones of multipass weldings, that is to say not only in the last pass, which has an as-solidified structure rich in acicular ferrite, but also in the reaustenitized zones which have an equiaxed ferritic structure

with fine grains and the zones with an as-solidified structure but reheated to a value lower than Ac1 during the execution of subsequent passes [BON 86]. In these last zones, the increase in transition temperature with the nitrogen content is more marked when the welding contains a small quantity of niobium and, more still when it contains vanadium.

Niobium and vanadium are very seldom added voluntarily in welding products but they are necessary for TMCP (*Thermal-Mechanical Controlled Processing*) steel manufacturing, and are also found in certain quenched-tempered steels. Via a dilution effect, some will be found in molten metal and particularly in the root passes, where they will cause a reduction in impact strength values, which are increasingly significant the higher the nitrogen content. This embrittlement will be even more marked if the assembly has to undergo a post-welding relief treatment, because it will allow niobium carbo-nitrides and vanadium nitrides to precipitate more completely.

The titanium/boron effect

This effect results from the presence of a very small quantity of boron (typically 20 to 60 ppm) that considerably delays the appearance of proeutectoid ferrite in the austenitic grain boundaries during the cooling of the weld bead. Thus, the austenite transformation can occur primarily by intragranular acicular ferrite germination on the inclusions, provided that these have the necessary characteristics and are thus present on titanium oxide surface zones. When the whole chemical analysis of the molten metal is well balanced in terms of manganese, and possibly nickel, so that its hardenability is optimal for the thermal cycle undergone by the weld, the proeutectoid ferrite network is reduced to a fine edging, the remainder of austenite being transformed into acicular ferrite. What is more, if it is possible to resort to an addition of molybdenum, which is the case when a yield strength higher than 550 or 600 Mpa is sought, a synergic boron-molybdenum effect is thus obtained which makes it possible to remove the proeutectoid ferrite network completely and to obtain a structure only made up of acicular ferrite whose toughness properties are remarkable. Lastly, it should be noted that the action of titanium and boron is not limited to the increase in the proportion of acicular ferrite, in the zones with a rough solidification structure, it also causes a refinement of the ferrite grains in the reaustenitized zones (see Figure 4.11).

Our recourse to the titanium-boron effect thus makes it possible to achieve a notable improvement of impact strength values in all the weld zones and a better homogeneity of the properties in these various zones. However, these positive results are obtained only if the nitrogen content is low and perfectly controlled. This is why this effect was originally implemented in the filler products for the manufacture of large tubes by bypass multielectrode sub-merged arc welding. It was then used in filled rutile wire and gave this product a privileged position as it

conformed to the strictest metallurgical specifications. On the other hand, it is not used in coated electrodes because this process does not allow a sufficient control of the nitrogen content in the added metal.

4.3. Principal welding defects

We will not deal with defects of a purely operational origin such as grooves, lack of penetration, sticking, etc. here; we will rather consider only internal defects, that is to say, hot cracks, cold cracks, reheating cracks and porosities.

We will endeavor to clarify the criteria which make it possible to identify these phenomena and to show the mechanisms of their formation in order to deduce the precautions we must take to avoid them or the remedies to be applied when the problems appear.

4.3.1. *Hot cracking*

Under this term, we include solidification cracks, liquation cracks and cracks resulting from a lack of ductility at high temperature.

Solidification cracks

These appear at the end of solidification. They can be internal or emerge on the surface but they are always localized in interdendritic spaces and thus follow the directions of solidification. Thus, they are perpendicular to the isotherms at any point. As they are formed at high temperature, they are oxidized in contact with the air when they emerge on the surface. Lastly, they are always broad because of contractions in the surrounding metal during cooling.

The factors that influence hotcracking are partly dependent on the analysis of the molten metal and partly on the welding procedure (see Table 4.4).
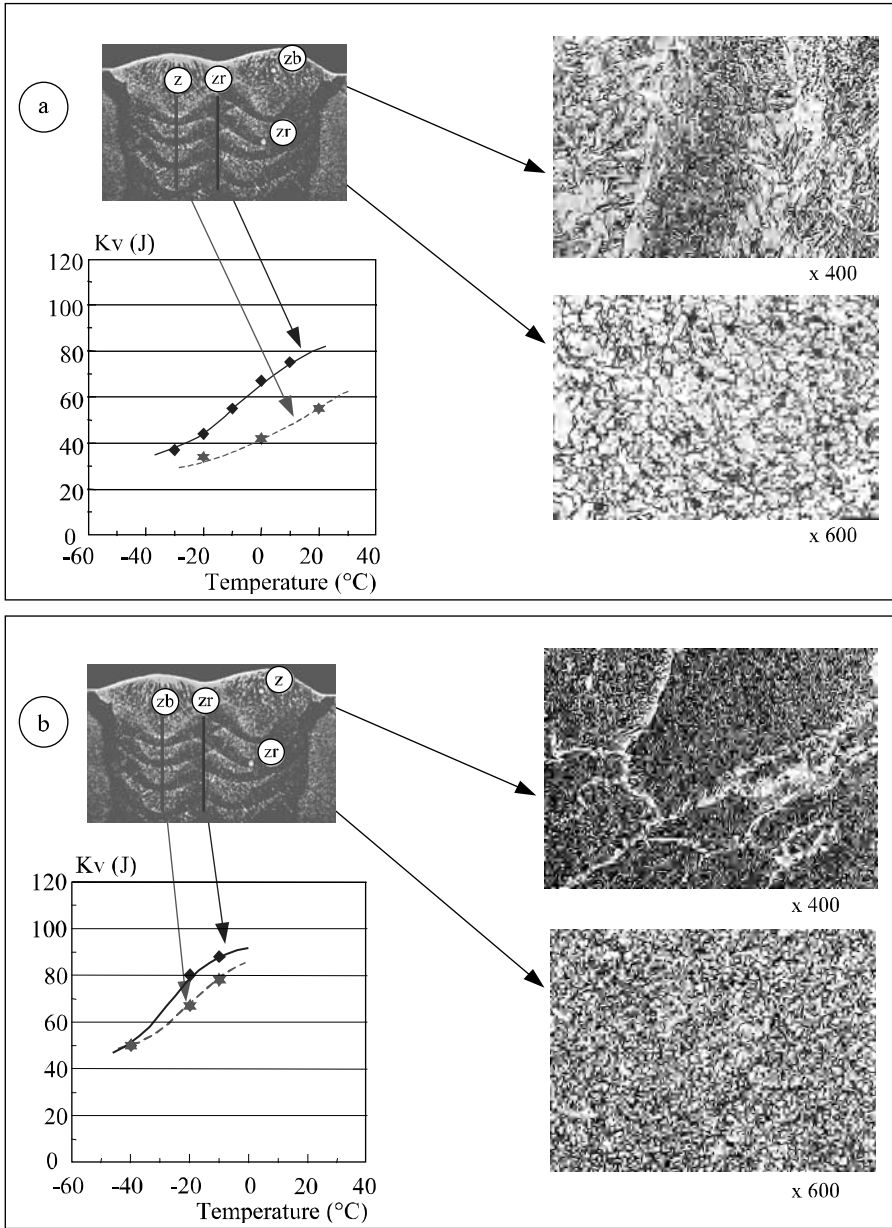
Figure 4.11. *a) Rutile filled wire without Ti-B effect; b) same formula with addition of boron. Impact test notches positioned in the pass axis (zb) and in the mold axis (zr)*
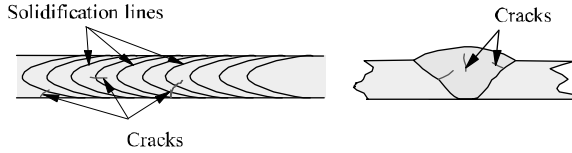
Figure 4.12. *Localization of solidification cracks*

A long solidification period and the presence of constituents with a low melting point mean that the solid and liquid phases will coexist over a vast temperature range. During cooling in this field, the liquid is transformed into a solid while contracting (volume variation in solidification) while the solid already formed contracts according to its own dilation coefficient. It can be understood that the longer the solidification time, the greater the risks of insufficient material at the end of solidification and of a crack appearing in the zones which solidify last, i.e. in the interdendritic spaces.

Factors related to material	Factors related to the operational process and the welding process
Lengthy solidification	Certain weld bead shapes (concave surface, width/depth ratio <0.7)
Constituents with a low melting point	High speed of welding
Base metal with high elastic limit	Rigorous clamping

Table 4.4. *Factors leading to cracking on solidification*

The influence of the base metal's yield strength and the clamping of the parts to be assembled are of a different nature. When the molten zone cools, it contracts so that stresses will develop if the shrinkage cannot freely take place. These shrinkage stresses will apply to the molten metal in the course of cooling, forcing it to distort, which it will be able to endure or not as the case may be. The greater the internal or external clamping thus limiting the deformations of the assembly, the greater these stresses will be.

Although often underestimated, the shape of the weld beads and the welding speed have a major influence. The zone which solidifies last concentrates the impurities because of their rejection in the liquid phase during solidification. This makes it chemically more sensitive to the risk of cracking and, when the weld has a concave surface, this zone is also smaller in its cross-section. Thus, shrinkage stresses are more likely to generate cracking than when the surface is convex (see Figure 4.13). In the same way, when a bead penetrates deeply (low

width/penetration ratio), its edges are parallel so that the final stage of solidification affects its entire height (central column); on the other hand, when the form is triangular, solidification finishes on the bead surface, which reduces the risks of cracking. Lastly, a reduction in the welding speed, and thus the solidification speed, makes it easier for the remaining liquid to fill the gaps created between the interdendritic spaces by the reduction in volume related to the liquid to solid phase; thus, the risk of cracks appearing are reduced.
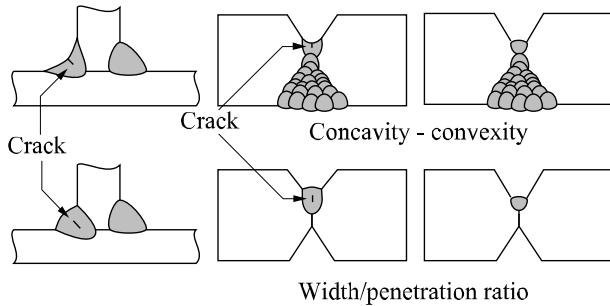
Figure 4.13. *Influence of the shape of weld beads on solidification cracking*

These considerations are general and thus apply to all types of materials, but to state that a lengthy solidification period or the presence of constituents with a low melting point worsens the risk of cracking is not in practice of any great use for the welding engineer who must use materials of whose characteristics he is often unaware. It is more in his interest to take account of these risks by using the material's chemical analysis.

In the case of mild and low alloyed steels, Bailey [BAI 78] deduced from a factorial experiment the parameter UCS (*Units of Crack Susceptibility*) which characterizes susceptibility to the formation of cracks at solidification in submerged arc welding analyzing the molten metal:

$$UCS = 230C* + 190S + 75P + 45\ Nb - 12.3Si - 5.4Mn - 1$$

with C* = 0.08 if C < 0.08% and C* = C if C > 0.08%.

He indicated its validity for the following values: C<0.23%; S 0.010-0.050%; P 0.010-0.045%; Si 0.15-0.65%; Mn 0.45-1.6%; Nb<0.07%; Ni <1%; Cr <0.5%; Mo <0.4%; V <0.07%; Cu <0.3%; Ti <0.02%; Al <0.03%; B <0.002%; Pb <0.01%; Co <0.03%. Later [BAI 94], he specified that an increase in chromium, molybdenum or vanadium beyond these values reduces the risk of cracking at solidification, while an increase in nickel and boron have a negative effect. However, he also stated that the

harmful influence of boron was demonstrated only for values higher than 0.01%. In this same document, the author considered that the risk of cracking is negligible when the UCS parameter is lower than 10 and very large when it is higher than 30, value 20 corresponding to the threshold of appearance of cracks during the execution of fillet welds in the first publication.

From this formula, it is seen that carbon does not have an effect up to 0.08% but proves to be the most harmful element beyond this value, i.e. from the moment when solidification involves the peritectic reaction. That is broadly explained by the fact that the solubility of sulfur and phosphorus are much lower in austenite than in ferrite, so that the appearance of the peritectic reaction results in an increase in the segregation of these elements, thereby promoting the formation of interdendritic films with a low melting point and thus the risk of cracking.

The element coefficients which play a part in this UCS parameter are relative to submerged arc welds. They cannot be generally applied to other processes, in particular because other factors which have an influence on cracking (bead geometry, welding speed) differ enormously from one welding process to another. Nevertheless, the chemical elements with negative or positive effects remain the same. Faced with a problem of solidification cracking in a C-Mn or low alloyed steel weld, it will always be beneficial to reduce the content of elements C, S, P and Nb and to an increase in Mn and S in the molten metal. A wise choice of the filler product can contribute to increase Mn and Si but will not have an effect on the harmful elements because these elements do not vary significantly in welding products. In practice, if their concentration is at an unacceptable level in the molten metal, this is because they come from the dilution of the base metal. A procedure will then have to be implemented which makes it possible to minimize dilution and will, in extreme cases, involve preliminary buttering of the faces to be joined.

In the case of austenitic stainless steels, the risk of solidification cracking is closely related to the phases involved at this time. Indeed, depending on their chemical composition, austenitic stainless steel welds can solidify completely in austenite or primary austenite then ferrite, or in primary ferrite then austenite or, finally, completely in ferrite.

However, we have already seen that the solubility of impurities such as sulfur and phosphorus was much greater in ferrite than in austenite and that the segregation of these elements could lead to interdendritic film formation at a low melting point. If the results of the many studies relating to the cracking sensitivity of austenitic stainless steels are classified according to the mode of solidification [KOT 93], an increasing resistance is observed passing from the purely austenitic mode to the primary austenite mode, then to the completely ferritic mode and finally to the primary ferrite mode. The large resistance of the primary ferrite mode compared to

the completely ferritic mode probably resulting from the fact that the mixed solidification ferrite + austenite generates a greater length of interfaces and thus minimizes the segregations.

Many diagrams exist for predicting the structure of the deposited metal added according to the content of alpha gene elements (chromium equivalent) and gamma gene elements (nickel equivalent), the first and best known of them being that established by Schaeffler more than 50 years ago [SCH 49]. However, the majority of these diagrams indicate the structure of the as welded metal after cooling to room temperature and this structure can be very different from that which existed at the time of solidification because, during cooling, the ferrite generally regresses into austenite. Suutala [SUU 83] proposed a diagram to forecast the solidification mode, in which he distinguishes the fields of solidification in primary austenite and primary ferrite. However, in our opinion, the most informative and best adapted diagram to modern day steels is WRC 92 (see Figure 4.14) because it marks out the zones corresponding to the four solidification modes and also gives, expressed in terms of *Ferrite Number*, the ferrite content after cooling.

From this diagram it is thus possible to evaluate the cracking sensitivity of a weld according to the position of the point being analyzed in the fields A, AF, FA or F; this analysis can be the result of a measurement or an evaluation starting from the analysis of the base metal, the deposited metal and the estimated dilution rate. The risk can also be evaluated by measuring the ferrite number of a standard weld representative of the proposed joints with an apparatus such as the feritscope MP30 since it can be seen in this diagram that a ferrite number higher than 4 corresponds in the majority of cases to welds solidifying in the FA field (most resistant) or F. If the representative point is in a zone at risk (A or AF, or FN <4), it will be found to be very beneficial, unless the specifications prohibit it, to modify the choice of filler product or the welding procedure (dilution rate) so as to fall inside the fields FA or F. Lastly, for the cases where that proves to be impossible, it will be absolutely essential to pay attention to the shape of the bead, to minimize clamping and to use a low welding speed as we indicated before.
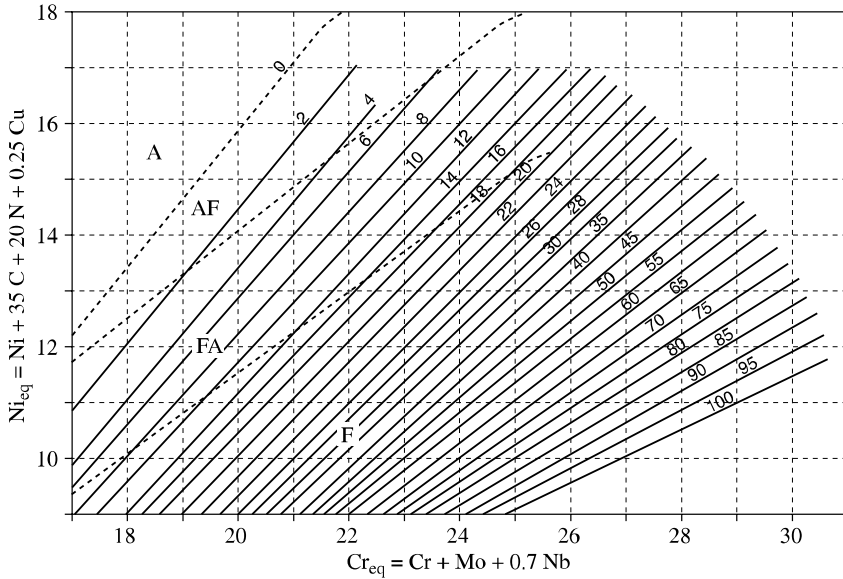
Figure 4.14. *WRC 92 diagram; from [KOT 92]*

Liquation cracks

Liquation cracks occur mainly in the base metal's HAZ, in the vicinity of the bond zone. They can also occur in the molten metal during thermal reactivation by a later pass, but in this case are generally prolonged in the form of solidification cracks in the pass currently being made. They are localized in the part of the HAZ brought up to temperatures that conform to the material's solidification interval, a period which will be longer, the greater the content of the material's microsegregations of elements which support the formation of constituents at low melting point. Under the shrinkage effect associated with cooling, these partial fusion zones will be all the more likely to experience cracks the deeper they extend inside the HAZ. It is this type of mechanism which is frequently encountered during the welding of molded products; it is very close to the formation mechanism of solidification cracks in the molten metal.

Another cause of the appearance of liquation cracks can be the formation of a eutectic around a phase of the dissolution process in the matrix.

This can occur when a thermodynamic phase, stable at room temperature, is unstable at high temperature and its return into solution could not be complete or its chemical homogenity reached because of the speed of the thermal welding cycles in regard to the kinetics of dissolution and diffusion. In this case, a liquid phase will

appear inside the HAZ and will penetrate the surrounding grain boundaries, entailing their liquation and their cracking upon cooling because of shrinkage.

The sensitivity of any material to liquation cracking can be evaluated by means of hot tensile tests conducted via a simulation of a thermal welding cycle during the heating phase and the cooling phase (see Figure 4.15). This test makes it possible to determine the difference between the temperature at which the reduction in the rupture area becomes zero after heating and the temperature at which a certain capacity for deformation is restored on cooling. The greater the difference, the more susceptible the material is.
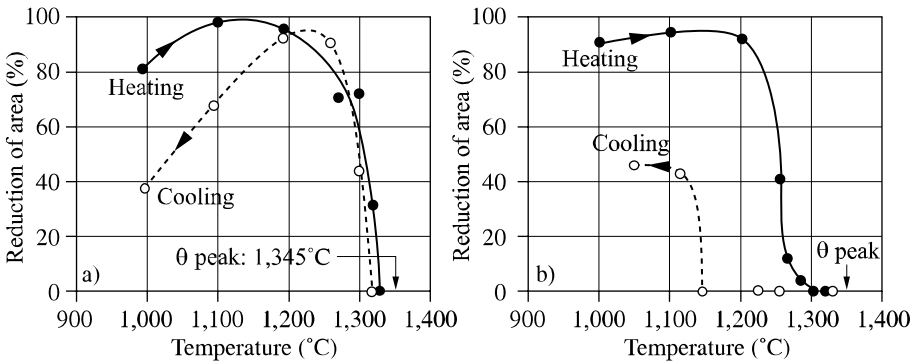
Figure 4.15. *Hot ductility of the Cabot 214 alloy containing (a) 2 ppm of boron, or (b) 30 ppm; from [CIE 93]*

This sensitivity to liquation cracking by is thus an intrinsic characteristic of the material; it depends on all of the chemical elements present, their distribution and the microstructure, i.e. that the welding process has little influence on the result unless using a filler product whose melting point is significantly lower than that of the base metal (braze welding).

Cracks due to lack of hot ductility (ductility dip cracking)

During cooling from the liquid state, many industrial alloys enjoy a temperature range in which the liability for deformation is notably lower than for the temperatures either side. The cooling curve in Figure 4.15a makes it possible to predict such behavior.

This decline in ductility, which is more marked the lower the deformation speed, is in the vicinity of the alloy's recrystallization temperature. It can be at the origin of intergranular cracks both in the HAZ as well as in the molten metal, due to shrinkage caused by the weld cooling [HEM 69] but this type of cracking is seldom

evoked in the case of ferritic steels. In these steels, however, certain authors [LIM 96] consider that these intergranular cracks can be prolonged, after complete cooling, by transgranular cracks induced by hydrogen, and would be at the origin of herringbone cracks (see following section).

On this subject, the bibliography is more descriptive than explanatory; nevertheless, it seems that there still, sulfur accentuates the phenomenon.

4.3.2. *Cold cracking*

These cracks appear at low temperatures (lower than 200°C). Thus, they are fine and do not have an oxidized surface. They do not have a particular orientation compared to the microstructure. They generally develop in the HAZ but can sometimes occur in the molten metal when it has a very high elastic limit. They derive from the stress field, which explains why they occur in the concentration zones which constitute the surface defects (poor wetting, grooves) or discontinuities related to the assembly design (partial penetration for example).
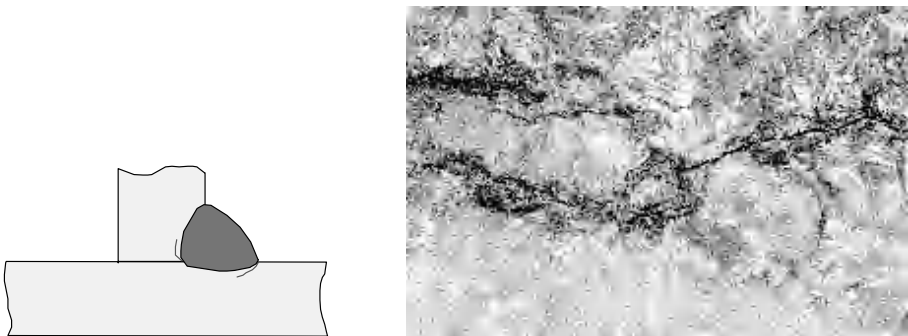
Figure 4.16. *Example of cold cracking*

These cracks require the combination of three factors to occur:

– a not very ductile structure (martensite),

– stresses,

– hydrogen.

The respective influence of these three factors is perfectly highlighted by means of implant tests. To carry out these tests, cylinders of the material under consideration are taken. A notch of well defined geometry is machined close to one of the ends. The bar is placed in a support plate (see Figure 4.17) then a weld bead is

made so that the notch of the bar is located in the HAZ of the weld bead. During cooling, a load is applied to the other end of the bar and is maintained for several days. The specimen is then cut open in order to determine whether cracks have developed at the notch extremity.

The test is repeated by applying various loads in order to evaluate the minimal cracking load of the structure in the notch bottom. It is also repeated by modifying the welding conditions, which makes it possible to highlight the influence of Δt 800/500 and to plot the cracking curve as it appears in Figure 4.16. In parallel the hardness curve under the bead is plotted according to the same Δt 800/500 parameter, the hardening evolution in fact representing the structural evolution.
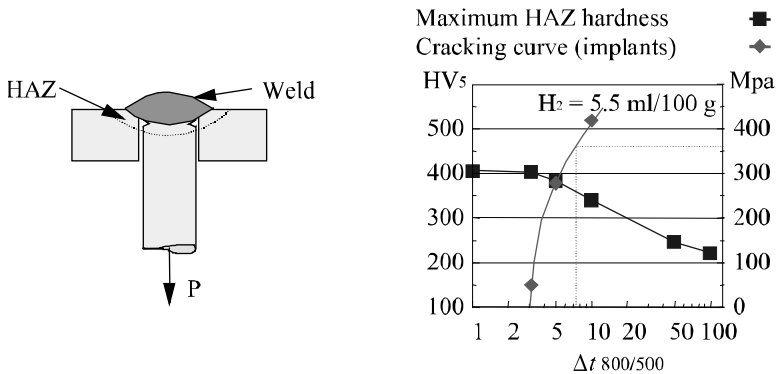
Figure 4.17. *Implant test*

We thus see in Figure 4.17 that for low Δt 800/500 parameters which are associated with a martensitic structure (peak of the hardness curve), the cracking stress is very low but, as soon as the structure is no longer 100% martensitic, the cracking stress increases significantly. The steel considered in this example being of type E36, it can moreover be seen that in this figure there will be no risk of cracking if Δt 800/500 is higher than 7 or 8 seconds, since then the coarse grain zone is able to support a stress higher than the elastic limit of the base metal without fissuring, which cannot occur because that would generate the deformation of the base metal and its stress relaxation.

All steels have a behavior similar to that in Figure 4.17 where the relation between cracking stress and structure is clearly seen.

The tests corresponding to this figure were carried out using a welding product whose diffusible hydrogen content was of 5.5 ml per 100 g of metal deposited. The

same tests can be reproduced with other hydrogen contents in order to evaluate the influence of this third factor.

In Figure 4.18 we see that when diffusible hydrogen content increases, cracking stress significantly decreases whatever the Δt 800/500 considered. Thus, hydrogen seems a fundamental determinant of cold cracking. However, even when hydrogen is in a reduced quantity, a low stress is enough to cause cracking if the structure is completely martensitic. Thus, wherever possible, it will be necessary to choose welding conditions (welding energy, pre-heating) which avoid the formation of a 100% martensitic structure in the HAZ.
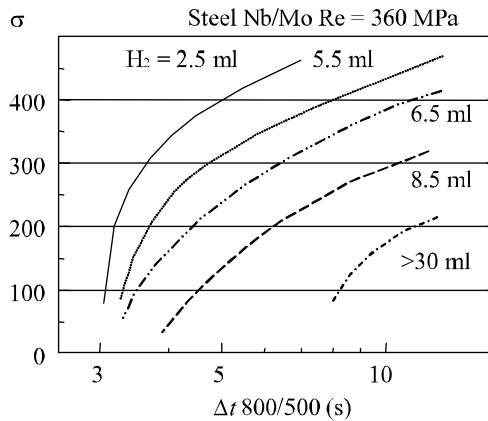
Figure 4.18. *Influence of diffusible hydrogen content on the cracking curve; from [COL 77]*

However, this is not possible with all steels. Indeed, some, like martensitic stainless steels for example, have a hardenability such that to avoid the martensitic transformation, cooling should last several days. To weld such steels it is imperative to ensure that hydrogen has been expelled before letting the assembly cool in the temperature range, otherwise cracking may appear (under 200°C). This is the aim of post-heating.

The crack curves in the preceding figures relate to the HAZ but the influence of hydrogen, the stress and the structure which these figures illustrate turns out to be identical when tests are carried out by taking extracts from the deposited metal [DEB 92].

As we indicated previously, cold cracking can occur in molten metal when steels of high elasticity limits are welded. Generally, it is in this case transverse across the

bead but can also be longitudinal when a discontinuity exists under the bead root (partial penetration) or take the appearance of a herringbone crack (microscopic cracks angled at 45° to the welding direction) in welds with intermediate tensile characteristics [MOT 82]. This transfer of cold cracking localization away from the HAZ towards the molten metal is increasingly likely the higher the elastic limit of the deposited metal, given that welds are made with steels of modern design whose carbon content is low. Thus, during the welding of these steels, it is no longer the analysis of the base metal which dictates the pre-heating temperature required to avoid cracking in the HAZ, but the analysis of the molten metal in order to avoid bead cracking.

An interesting means of reducing the risk of cold cracking and consequently pre-heating temperature during the welding of these steels consists of using a filler for the execution of the root passes for "X" or "K" shaped assemblies, the remainder of the joint being filled with a filler product akin to the mechanical characteristics of the base metal. By doing this, it has been shown that the pre-heating temperature can be reduced by 50 to 100°C, a reduction of 50°C when compared to the use of a single product, and this of course without affecting the overall tensile characteristics of the joint [VUI 94]. In many cases, this amounts to eliminating the need for pre-heating, which, in addition to presenting a direct and immediate economic advantage for the manufacturer, considerably improves working conditions for welders and generally results in a reduced rate of operational defects, and therefore of repairs. Curiously, this practice is still not very widespread today.

The actions required to avoid cold cracking are thus derived from all the above considerations, and are recapitulated in Table 4.5.

4.3.3. *Reheat cracking*

Reheat cracking, intergranular in nature, occurs primarily in the coarse grain HAZ and occasionally in the molten metal. It begins during the post welding heat treatment or in service at high temperature [DHO 92]. It relates to low alloyed steels containing carbide-forming elements (Cr, Mo, V) but also certain austenitic stainless steels such as steel AISI 347, as well as precipitation hardening nickel alloys (Inconel 800H for example).

1) Minimize the quantity of hydrogen introduced into the weld pool	
– Cleanliness of the joint	Moisture, oil, grease, etc.
– Choice of welding products	Low diffusible hydrogen.
– Heating and conservation of the products (except if cases of airtight stocking)	According to supplier recommendations.
2) Wherever possible, use a filler product with very low elastic limit and very low hydrogen content for the execution of the first pass and the secondary pass of thick assemblies	
3) Control the welding conditions to avoid the formation of a martensitic structure	
– Welding energy – Pre-heating – Temperature between passes	To choose starting from the under bead hardness curves according to Δt 800/500 and the IRSID graph for example [COL 77]
4) Envisage a post-heating to evacuate hydrogen before cooling (case of steels having a great hardenability), always associate with a pre-heating to avoid cooling lower than the critical temperature before post-heating is effective	
5) Minimize the internal or external stresses	
– Welding procedure – Clamping	

Table 4.5. *Actions to take to avoid cold cracking*

Such cracking derives from the relieving of strong residual stresses resulting from manufacture when the deformations which accompany it are concentrated at the level of the grain boundaries. This is the case for the coarse grain HAZ of precipitation hardened materials because, during welding, the carbides which harden these alloys are put back in solution in the zones taken to a very high temperature in the vicinity of the bond zone and remain during cooling because of the speed of the welding thermal cycles.

During a later reheating, in service or during the post welding heat treatment, the carbides will precipitate inside the grains on the dislocations created by strain hardening that results from thermal cycles. This will reinforce the matrix considerably, so that the creep deformations associated with stress relief will locate themselves on the level of the grain boundaries which cannot support them.

This type of crack thus relates primarily to thick assemblies of materials designed to resist creep, the thickness inducing a high level of residual stresses. However, the risk is not only related to the nominal analysis of material, it is also a function of the impurity content (S, P, As, Sb) and residuals (Cu, Sn), because these elements segregate to the level of the grain boundaries and weaken them.

Various methods are used to evaluate susceptibility to reheat cracking [DHO 98, TAM 95], but our preference is to reduce the area measurement during hot tensile isothermal tests of specimens in which, by thermal simulation, the structure of the coarse grain zone has previously been reproduced. Indeed, it is considered that the risk is very low when no reduction of area value lower than 20% is recorded regardless of the test temperature; on the other hand, it is very high when the striction becomes lower than 10%.

In practice, to minimize risks when a susceptible material must be used, it is of great importance to:

– design the joints to reduce clamping as far as possible,

– choose a welding product that has the lowest hot tensile characteristics compatible with the application,

– use a low energy welding process in order to limit the pass volume and to thus reduce the dimension of the coarse grain HAZ,

– distribute the passes to reaustenitize the coarse grain zones created by the preceding passes and thus decrease the grain size,

– envisage welding sequences to minimize residual stresses,

– ensure a good wetting of the finishing passes and the absence of grooves so as to avoid stress concentrations.

In addition, the handling of the post-welding heat treatment can have a capital incidence on reheat cracking since it has been shown in the laboratory and production, that the cracking of a CrMoV steel which has a low ductility in the interval 550-650°C can be avoided by carrying out a stage at a temperature of about 450°C then very quickly crossing the field of low ductility in order to reach the treatment temperature [PIL 86].

4.3.4. *Porosities*

We will distinguish four mechanisms likely to engender porosities in molten metal:

– the instability of the gas capillary for weldings carried out by means of HDE processes,

– an excessive gas pressure under the bead root,

– a dissolved gas content in molten metal higher than the solubility limit in solid metal at the solidification temperature,

– a chemical reaction within the weld pool giving rise to a gas.

The HDE processes involves *keyhole* work. This implies that the weld pool is maintained in balance thanks to the gas vapor pressure which is exerted on the capillary walls created by the volatilization of metal under the influence of a very high density plasma arc, laser beam or electron beam. When the operating conditions allow us to maintain a perfectly stable state of balance, the liquid wall located at the back of the capillary can collapse in a more or less periodic way and enclose part of the metal vapors which maintained it, thus forming porosities. These hydrodynamic porosities could generally be avoided by modifying the power density distribution of the incidental beam (point of focusing, vibration, etc.) and by reducing the welding speed.
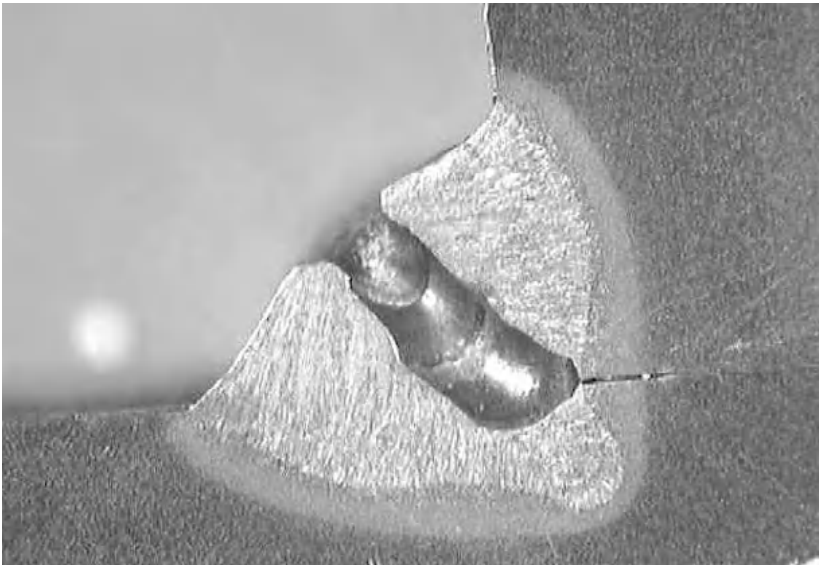
Figure 4.19. *Pre-painted sheet fillet weld – porosity resulting from paint decomposition under the bead*

When porosities result from excessive gas pressure under the bead root, they take a lengthened form and maintain a connection with the zone at the origin of this excessive pressure.

The pressure can result from the heating of air imprisoned under the bead; this is typically the case for butt welds with a preparation by joggling when the penetration is insufficient. It can also derive from a gas release that results from the decomposition or volatilization of product coating sheets, as is the case during fillet welding of pre-painted sheets (see Figure 4.19) or lap welding with galvanized

sheets. Lastly, its origin may be a degasification of the faces to be assembled; it is, for example, the nitrogen released from the plasma air cut faces which explains many porosities which are formed in the first pass of a butt welded assembly when there is no lower edge spacing of the joint (see Figure 4.20).
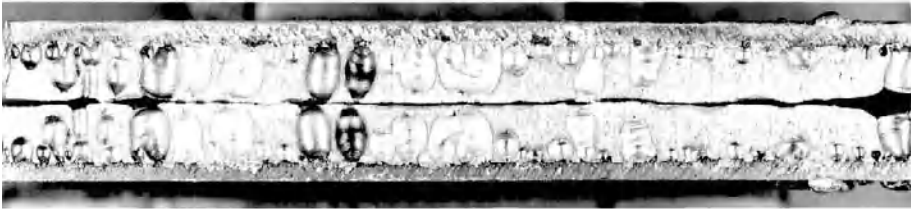
Figure 4.20. *Texture test after the first pass of a submerged arc butt welded joint of as-cut sheets cut by the plasma air process*

The sudden reduction in the solubility of a gaseous element at the time of the passage from the liquid state to a solid state is the leading cause of porosities in the weld beads because this variation is common to all materials (see Figure 4.21). Indeed, when the dissolved gas concentration in molten metal is higher than the solubility limit in solid metal at the solidification temperature, there is a rejection of gas to the solid-liquid interface. This causes the liquid to experience a local increase in the dissolved gas content and, when this becomes higher than the solubility limit in the liquid, a gas bubble is formed.

In welding, the weld pool can be contaminated by atmospheric nitrogen and oxygen if protection is not assured, or by hydrogen coming from welding products that have absorbed moisture, by water vapor which condenses on the surface of a cold sheet, an escape in the coolant circuit of the torch, or the decomposition of oil or grease present at the surface of a badly prepared joint. Oxygen is generally not at the origin of porosities because it reacts with the majority of materials to form oxides. In ferritic steels and nickel alloys not containing nitride forming elements (Ti, Al, Nb), it is in general the nitrogen which is at the origin of porosities, while it is hydrogen in aluminum alloys but also in austenitic stainless steels, although they are more resistant than light alloys.
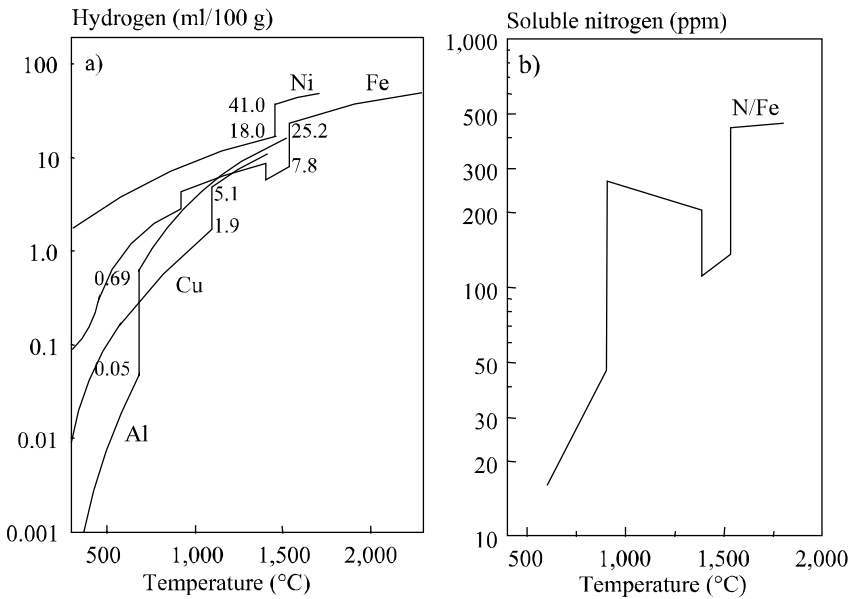
Figure 4.21. *Evolution of solubility with temperature: a) hydrogen in various pure metals [LAN 99]; b) nitrogen in pure iron [KOU 87]*

A chemical reaction giving rise to a gas within the weld pool constitutes the last cause of porosities which we will deal with here. Formation of carbon monoxide was at the origin of porosities which were inevitably formed during TIG welding of rimmed steels unless a filler very rich in deoxidizers was used. However, even if we no longer encounter this kind of steel, the CO release in molten metal can still occur when the residual oxygen of steel is present in the form of silicates, because at very high temperature (>1,600°C) they can be reduced by the carbon of the steel. This reaction is particularly intense during electron beam welding because the surrounding vacuum moves thermodynamic balances. It also favors this reduction to the extent that it becomes impossible to obtain a sound weld, unless the steel contains residual aluminum (approximately 0.02%), aluminates being more stable than carbon monoxide at the temperature of the weld pool (see Figure 4.22). Steam formation in the weld pool can also be at the origin of porosities. This will occur in the presence of hydrogen with materials for which the enthalpy of oxide formation is lower in absolute value than that of steam at the temperature of the weld pool. This is the case for copper, particularly when it is not deoxidized; it is also the case for pure nickel, Monel metal and even certain nickel-chromium-iron alloys [LAN 99]. There is only one remedy: use filler products which contain powerful deoxidizers such as titanium and aluminum to avoid this reaction.
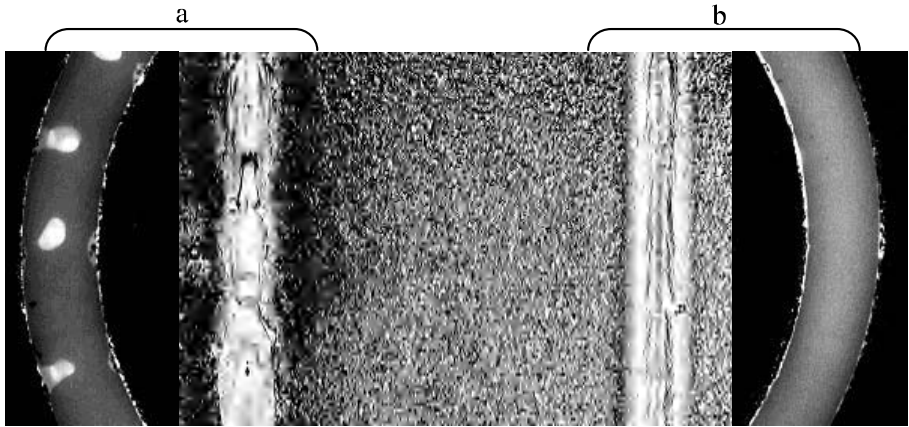
Figure 4.22. *Surface aspect and X-ray on a section of EB welds of XC 38 (Al = 0.002%): a) without insertion; b) with insertion in the mating plane of an aluminum foil 0.02 mm thick*

4.4. Bibliography

[ABS 78] ABSON, DOLBY R.E., HART P.H.M., "The role of non-metallic inclusions in ferrite nucleations in carbon steel weld metal", *Proceedings of Trends in Steels and Consumables for Welding*, The Welding Institute, Paper no. 25, London, 14-16 November. 1978.

[ANT 81] ANTUNES M., BONNET C., "Application d'un essai de trempabilité à la recherche des facteurs ayant une influence sur la formation de la ferrite aciculaire", *Journées d'information Métallurgie de la Zone Fondue*, Société Française de Métallurgie/Société des Ingénieurs Soudeurs – Section sud-est, Conférence no. 9, Publication de la Soudure Autogène, 1981.

[BAI 78] BAILEY N., JONES S.B., "The solidification cracking of ferritic steel during submerged arc welding", *Welding Journal*, p. 217s-231s, August 1978.

[BAI 94] BAILEY N., *Weldability of Ferritic Steels*, Abington Publishing, 1994.

[BLA 99] BLAIS C., L'ESPÉRANCE G., EVANS G.M., "Characterisation of inclusions found in C–Mn steel welds containing titanium", *Science and Technology of Welding and Joining*, vol. 4, no. 3, p. 143-150, 1999.

[BON 80] BONNET C., "Relation Structure – Résilience dans les soudures d'aciers doux et faiblement alliés brutes de solidification", *Soudage et Techniques Connexes*, p. 3, July-August 1980.

[BON 86] BONNET C., GASPARD-ANGELI A., "Influence de la teneur en azote sur la résilience des soudures d'aciers C-Mn", *Soudage et Techniques Connexes*, p. 3, May-June 1986.

[BUR 88] BURKHARDT J., LAU T., NORTH T.H., L'ESPÉRANCE C., "Effect of aluminum on the Ti-O-B-N balance in submerged arc welding", *Welding Journal*, p. 25-30, August 1988.

[CHA 83] CHARPENTIER J.P., BONNET C., "Effect of deoxidation residues in wire and of some particular oxides in CS fused fluxes on the microstructure of submerged-arc weld metal", in *Proceedings of the Effects of Residual, Impurity and Micro-alloying Elements on Weldability and Weld Properties*, The Welding Institute, Paper no. 8, London, 15-17 November 1983.

[CIE 93] CIESLIAK M.J., "Cracking phenomena associated with welding", *ASM Handbook*, vol. 6, p. 88-96, 1993.

[COC 78] COCHRANE R.C., KIRKWOOD P.R., "The effect of oxygen on weld metal microstructure", *Proceedings of Trends in Steels and Consumables for Welding*, The Welding Institute, p. 103, London, 14-16 November 1978.

[COL 74] COLLECTIF, Courbes de transformation des aciers de fabrication française, edited by the CPS, 1974.

[COL 77] COLLECTIF, Courbes Dureté/Paramètre de refroidissement en conditions de soudage, collection established at the IRSID, 1977.

[DEB 92] DEBIEZ S., GAILLARD L., MALTRUD F., Etude de la soudabilité d'un acier de nuance E690 T+R de Sollac avec des produits d'apport à bas et très bas hydrogène, Rapport Institut de Soudure no. 28406, 1992.

[DEV 83] DEVILLERS L., KAPLAN D., MARANDET B., RIBES A., RIBOUD P.V., "The effect of low level of some elements on the toughness of submerged-arc welded CMn steel welds", *Proceedings of the Effects of Residual, Impurity and Micro-Alloying Elements on Weldability and Weld Properties*, The Welding Institute, London, 15-17 November 1983.

[DHO 92] DHOOGE A., VINCKIER A., "La fissuration au réchauffage – revue des études récentes (1984-1990)", *Le Soudage dans le Monde*, vol. 30, no. 3-4, p. 45-71, 1992.

[DHO 98] DHOOGE A., "Survey on reheat cracking in austenitic stainless steels and Ni base alloys", *Welding in the World*, 41, p. 206-219, 1998.

[EVA 97] EVANS G.M., BAILEY N., *Metallurgy of Basic Weld Metal*, Abington Publishing, 1997.

[GAR 75] GARLAND J.G., KIRKWOOD P.R., "Towards improved submerged arc weld metal toughness", *Metal Construction*, p. 275-283, May 1975, p. 320-330, June 1975.

[HEM 69] HEMSWORTH B., BONIZEWSKI T., EATON N.F., "Classification and definition of high temperature welding cracks in alloys", *Metal Construction and British Welding Journal*, p. 5-16, February 1969.

[KOT 92] KOTECKI D.J., SIEVERT T.A., "WRC-1992 constitution diagram for stainless steel weld metals: a modification of the WRC-1988 diagram", *Welding Journal*, p. 171s-178s, May 1992.

[KOT 93] KOTECKI D.J., "Welding of stainless steel", *ASM Handbook*, vol. 6, p. 677-707, 1993.

[KOU 87] KOU S., *Welding Metallurgy*, John Wiley & Sons Inc., 1987.

[LAN 99] LANCASTER J.F., *Metallurgy of Welding*, Abington Publishing, 1999.

[LIM 96] LIMU H., HANNERZ N.E., "Influence of vanadium and niobium on weld solid state cracking", *Int. J. for the Joining of Materials*, vol. 8, no. 4, p. 134-144, 1996.

[MOT 82] MOTA J.M.F., APPS R.L., "Chevron cracking – a new form of hydrogen cracking in steel weld metals", *Welding Journal*, p. 222, July 1982.

[PIL 86] PILARCZYK J., DEBSKI E., "Reheat cracking in low alloy steel weldments and welded structures", *Proceedings of 3rd International Conference Joining of Metals (JOM-3)*, Helsinki, Finland, December 1986.

[SCH 49] SCHAEFFLER A.L., "Constitution diagram for stainless steel weld metal", *Metal Progress*, 56, S 680, 1949.

[STL 93] ST LAURENT S., Etude de l'influence du Bore, de Titane et de l'Azote sur les propriétés de la zone fondue de dépôts soudés d'aciers microalliés, Thesis, University of Montreal, Ecole Polytechnique, July 1993.

[SUU 83] SUUTALA N., "Effect of solidification conditions on the solidification mode in austenitic stainless steels", *Metall. Trans.*, 14A, p. 191-197, 1983.

[TAM 95] TAMAKI K., SUZUKI J., IMAI I., HORII Y., KUMAGAI T., "Effects of impurities and alloying elements on reheat cracking sensitivity of 720 N/mm^2 class high-strength steel", *Welding International*, vol. 9, no. 12, p. 960-966, 1995.

[VUI 94] VUIK J., VAN WORTEL J.C., VAN SEVENHOVEN C., "Application of very low yield strength consumables in the root pass of weldments to avoid preheating", *Welding in the World*, vol. 33, no. 5, p. 362-369, 1994.

Chapter 5

Welding Products

5.1. Coated electrodes

5.1.1. *Constitution of coatings: consequences*

The classification standards of welding products distinguish several types of coated electrodes according to the kind of coating.

An electrode coating is always composed of many constituents which provide various functions:

– mineral products which act on fusion characteristics, contribute to the protection from the surrounding atmosphere of the drops and the weld pool by breaking up into a gaseous emission under the influence of the arc heat and constituting a slag whose physico-chemical characteristics have a major influence on the operational characteristics of the electrode;

– metal products which by being combined with metal resulting from the fusion of the electrode core, make it possible to adjust the analysis of the weld metal so as to obtain properties equivalent to those of the steel used in the welded joint;

– organic materials added in small quantity in basic coatings as an extrusion agent and which will be destroyed during high temperature heating of these electrodes. They are present in much larger quantities in electrodes baked at low temperature (cellulose, rutiles, etc.) because the decomposition of these products in the arc causes a release of hydrogen which confers operational characteristics on them which prove valuable in many applications;

Chapter written by Christian BONNET.

– binders which make it possible to obtain a solid coating which adheres to the metal core. There are in general simple or complex silicates of sodium, potassium or lithium, which in addition to their adherence function act on the arc characteristics because of the low ionization potential of the alkaline elements.

In industry, basic and rutile electrodes are the most commonly used. Table 5.1 makes it possible to compare on the one hand the constituents and the baking conditions and, on the other hand, the consequences which result from this both for operational properties and chemical analysis of the deposited metal.

Type of electrode		Rutile	Basic
Principal components	Non-metallic	TiO_2, Al_2O_3, SiO_2, Carbonates, cellulose, etc. Silicates, extrusion additives	CaF_2, MgO, Carbonates, etc. Silicates, extrusion additives
	Metallic	Alloying elements Deoxidizers	Alloying elements Deoxidizers
Stoving temperature		Low (<160°C)	High (350/480°C)
Consequences	Operational	Soft fusion, stable arc, Transfer in fine drops, no or few short-circuits, Easy restarting, Slag with high melting point favoring wetting	Irregular fusion, unstable arc, aggressive, Transfer in large drops with short-circuits, Difficult restarting, Slag with low melting point, tendency to undercut
	Analytical	O: 600 to 1,000 ppm Ti: 300 to 800 ppm Nb: 100 to 300 ppm V: 50 to 250 ppm H_2Diff: >15 ml/100 g DM	O: 200 to 500 ppm Ti, Nb, V: adjustable to the desired values H2Diff: <5 ml/100 g DM

Table 5.1. *Principal constituents and characteristics of rutile and basic electrodes*

Thus, it appears that *rutile* type electrodes present the best properties in use: a very good arc stability, transfer of metal in fine drops which generally results in a low level of spatters and lower fume emission than the basic electrodes, a very good bead wetting and a very easy restart from cold.

However, by its nature, this slag has an influence on the content of residual elements in the deposited metal, elements which are in general not desirable from the perspective of optimizing mechanical properties.

The oxygen content of the deposited metal can vary according to the nature and the quantity of the deoxidizing elements present in the coating, nevertheless, it cannot be lowered to the level which can be reached with a basic electrode. This results in a more significant inclusion content and consequently in a lower ductile fracture energy during impact tests.

The titanium content of the deposited metal cannot be adjusted, as we would wish, in order to optimize the mechanical properties. Indeed, the slag being mainly composed of rutile elements (titanium oxide TiO_2), some titanium is inevitably transferred to the deposited metal in variable quantities according to the oxido-reduction reactions and the metal-slag exchanges which occur in the arc and at the interface with the weld pool. These reactions depend on all the chemical elements present, which must be balanced according to the various mechanical characteristics that the weld must meet (tensile strength, yield strength) and depending on the type of steel that we have to weld.

The niobium and vanadium content of the deposited metal cannot be lowered beyond a certain point because these elements exist as impurities in the natural rutiles used in the manufacture of welding products. The use of synthetic rutiles, which are therefore very pure, is possible but not common because its cost is significantly higher than that of the natural rutiles.

The diffusible hydrogen content of welds created with rutile electrodes is always very high. This results from the presence of organic materials added to facilitate extrusion and to improve the arc's characteristics. However, it is also a result of low baking temperatures which makes it possible to eliminate only a small proportion of the water incorporated with the silicate and it does not break up the extrusion agents.

Thus, rutile electrodes are valued for their user-friendliness and the creation of a weld bead, whereas basic electrodes are essential when the joints to be made must satisfy severe metallurgical quality standards.

A basic electrode must satisfy the required mechanical properties of the steels which it is intended to weld (tensile, impact strength, CTOD, creep, etc.). Many analytical combinations make it possible to obtain the tensile characteristics sought in the deposited metal, but the solutions that satisfy both the tensile and toughness characteristics are much more limited. This is increasingly true the higher the tensile properties. In addition, the chemical balance retained for an electrode must be the most robust possible, i.e. it must satisfy the various requirements in spite of the

variations inherent in any industrial production, and that, in a broad field of welding conditions (thermal cycles). Lastly, a basic electrode must be designed so that the diffusible hydrogen content in the deposited metal is as low as possible in order to avoid any risk of cold cracking, while minimizing or even precluding pre-heating and post-heating.

5.1.2. *Basic electrodes and diffusible hydrogen*

The determination of the diffusible hydrogen content of welding products is problematic because, due to its small size, the hydrogen atom diffuses easily and escapes from steel even at room temperature, so that it is impossible to know the exact quantity of hydrogen introduced during welding. Faced with this difficulty but also the need to classify welding products according to their cold cracking susceptibility, the determination of the diffusible hydrogen content is the subject of strict guidelines which very precisely describe the methodology to be used. This methodology must be respected scrupulously if extreme variations in results (as much as double) are not to be recorded (ISO 3690 or AWS 4.3-1993).
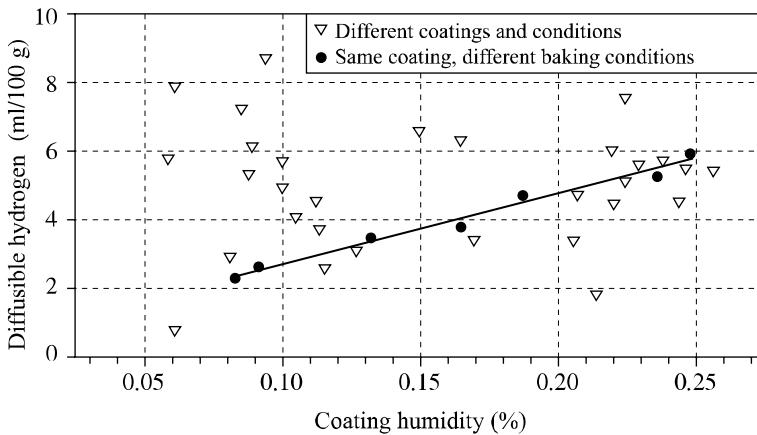
Figure 5.1. *Diffusible hydrogen/coating humidity ratio for electrodes of type AWS 7018*

The diffusible hydrogen content is generally expressed in milliliters per 100 grams of deposited metal (ml/100 g DM). It is naturally a function of the moisture contained in the welding product, but Figure 5.1 clearly shows that there is no general relation between these two measurements and we see in Figure 5.2 that even while being limited to a particular electrode coating, two different relations exist

according to whether the variation of moisture results from a modification of the baking conditions or from moisture pick-up.
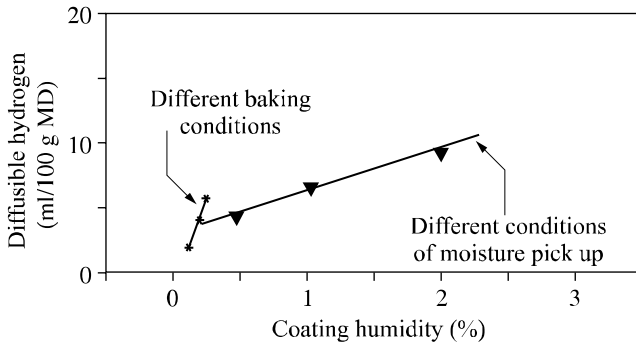
Figure 5.2. *Diffusible hydrogen/coating humidity ratio for an electrode type AWS 7018*

In fact, the complexity of the relations connecting diffusible hydrogen and the coating humidity derives from the fact that water exists in various forms: the water known as *free* which corresponds to the first water state taken up during an exposure to a damp atmosphere, and the water called *water of crystallization*, which is chemically bound to the various electrode constituents. If the temperature of the coating is raised, free water escapes as soon as it exceeds 100°C, while water of crystallization is released only at much higher temperatures which depend on the type of bond, and therefore the material from it is derived. Thus it can be seen that for the same quantity of water in the electrode coating, the higher the extraction temperature of this water, the more it will be released near the arc in the course of welding and the greater the transfer of hydrogen in the weld pool. Thus, when the electrode baking temperature is lowered during the manufacture of a basic electrode, a decreasing quantity of water of crystallization is eliminated from the coating material. This small variation of residual water from the baking results in an increase in the diffusible hydrogen content, much greater than a similar variation of water content in the coating when it results from moisture pick-up (see Figure 5.2). As a corollary, it is clear that to impose a maximum moisture content in the purchase specifications of electrodes (or flux for submerged arc welding) with the aim of obviating the risk of cold cracking has no practical logic, since no universal relation connecting moisture to diffusible hydrogen exists. On the other hand, using the humidity measurement, which is much simpler and more rapid than the measurement of diffusible hydrogen, to verify the manufacturing consistency of a given electrode at the end of the baking process is a practice that is viable and accepted. This is acceptable because, for each electrode, a single relation exists between the residual baking humidity and diffusible hydrogen.

Today, the majority of welding product manufacturers have a range of basic electrodes with very low levels of diffusible hydrogen. The best of these guarantees a level lower than 3 ml/100 g of deposited metal with rods from a newly opened package. Such a result can be achieved only by a rigorous selection of raw materials, a high baking temperature and airtight packaging, so as to avoid moisture pick-up during product storage [LED 92]. In general, these electrodes are also characterized by a low moisture pick-up when they are exposed to a humid atmosphere.
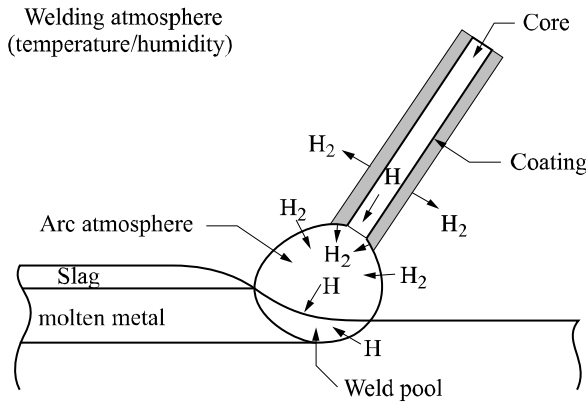
Figure 5.3. *Origins of diffusible hydrogen in the molten metal*

However, the diffusible hydrogen content of the deposited metal is not only a function of the hydrogen brought in one form or another by the welding product. In the case of coated electrodes, the gas flow resulting from the decomposition of the coating's constituents is not sufficient to prevent an exchange with the surrounding atmosphere (see Figure 5.3). Thus, the partial hydrogen pressure at the arc level and, consequently, diffusible hydrogen in the deposited metal increase in concert with the absolute humidity content of the surrounding atmosphere (see Figure 5.4).
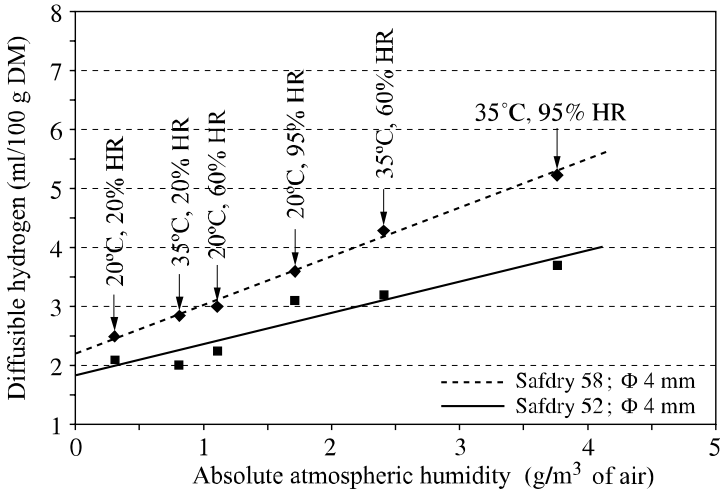
Figure 5.4. *Influence of atmospheric water content on diffusible hydrogen in the deposited metal (SAF data)*

Dickehut and Ruge proposed a diagram which makes it possible to know the diffusible hydrogen content under any temperature and pressure conditions, provided that we know the result under any single condition. This graph is not universal because atmospheric exchanges are necessarily dependent on the protection given to the electrode (crater depth, volume of released gas, etc.). Nevertheless, the experiment shows that as a first approximation it encompasses the behavior of the majority of low hydrogen electrodes of type AWS 7018 currently marketed.

5.2. Fluxes for submerged arc welding

5.2.1. *Fused fluxes and granular fluxes: advantages and disadvantages*

Fluxes for submerged arc welding can be produced by fusion or granulation.

Fused fluxes are manufactured from coarse raw materials which are mixed before being introduced into an electric furnace. They are then brought up to a temperature of about 1,600°C which makes it possible to obtain a chemically homogenous liquid product. This product is then cast on a plate, strongly cooled in order to confer a glassy structure after solidification and cooling to room temperature, thus preserving a perfect chemical homogenity.

This glass is then crushed and sieved so as to obtain the desired granulometric distribution. In an alternative manufacturing process, the liquid product is atomized in a water jet instead of being cast on a plate, which obviates the crushing operation.

The manufacture of granular fluxes begins with a dry mixture, formed from raw materials which in this case have a very fine granulometry (in general lower than 300 microns). After homogenization of the dry mixture, mixing is carried out by adding a simple or mixed silicate of sodium, potassium or lithium. Granulation, i.e. the agglomeration of small particles taken from various raw materials, can then take place thanks to the silicate binder. This is followed by a pre-drying stage often using a fluidized bed, then by baking at a temperature of about 500°C if the manufactured flux contains carbonates or at higher temperature (800°C approximately) even if it does not contain any.

Fused fluxes and granular fluxes each have their advantages and disadvantages.

Each grain of a fused flux is chemically identical to the others, unlike those of a granulated flux whose particles are not chemically homogenous. Thus, it is possible to manufacture fused fluxes in which a particular element must be present in very small quantity, without risking segregation formulae (boron for example). This is particularly critical for a granular flux.

The manufacture of fused fluxes does not require the use of binder. This brings two advantages and one disadvantage compared to granular fluxes:

– the moisture pick-up of fused fluxes is practically negligible, since water is only adsorbed on the grain surface. That of a granular flux is on the contrary much greater because the binder reacts with atmospheric humidity [GAS 86];

– the fused flux grains are more solid than those of granular fluxes which makes them more suitable for recycling;

– however, the binders used in the manufacture of granular fluxes generally create better arc stability than fused fluxes.

Fused fluxes, unlike granular fluxes, cannot contain either ferro-alloys or deoxidizers because these would be oxidized during production in the liquid state. This enables the slag to be reground after welding and reused, mixed with new flux – a practice that can be economically beneficial for certain large industries whose flux consumption is high (manufacture of tubes for example) [GAS 86]. On the other hand, it precludes analytic adjustments and control of the oxygen content of the deposited metal something which can be achieved with a granular flux by the addition of deoxidizing elements.

Today, granular fluxes are most commonly used in Europe and the USA, whereas fused fluxes are still very popular in Japan and Russia.

5.2.2. *Roles of flux: metallurgical aspects*

Submerged arc welding involves the use of a solid or cored wire and a flux, the arc striking into the flux from the end of the wire to the parts to be assembled. The flux must perform two fundamental functions: it must provide good arc stability and it must protect the weld pool and the metal drops from atmospheric nitrogen and oxygen contamination during their transfer in the arc. Flux also has an important effect on the shape of the weld bead (wetting and penetration). This is because it alters the power distribution in the arc as well as the physical characteristics of the slag, which result from its fusion and the oxido-reduction reactions occurring during welding. This is why, depending on its formulation, a flux can be more or less well adapted to fillet welding, high speed welding or multielectrode welding. Yet, from a strictly metallurgical perspective, the fundamental characteristics of a flux derives from the fact it governs the oxygen and diffusible hydrogen contents of the deposited metal for a given wire.

All contemporary manufacturers of welding products still use the empirical formula initially put forward by Tuliani to classify submerged arc welding fluxes [TUL 69]. This formula makes it possible to calculate a *basicity index* by distinguishing the flux constituents according to their basic character; acid, amphoteric or neutral:

$$BI = \frac{[CaO]+[MgO]+[BaO]+[SrO]+[Li_2O]+[Na_2O]+[K_2O]+[CaF_2]+\frac{1}{2}([FeO]+[MnO])}{[SiO_2]+\frac{1}{2}([Al_2O_3]+[TiO_2]+[ZrO_2])}$$

with [AxBy] = percentage by weight of flux constituent AxBy.

Tuliani, and others after him, showed that the oxygen content of the deposited metal decreases when the basicity index increases up to 1.5, then stabilizes around 280 to 300 ppm (see Figure 5.5). The net result is that it is pointless to resort to a flux with a significantly higher basicity index when seeking to optimize the characteristics of the deposited metal.
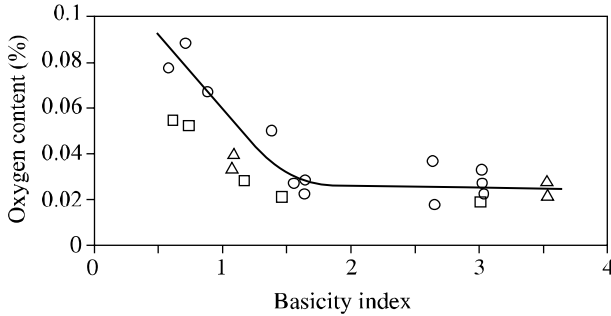
Figure 5.5. *Relation between the oxygen content of the deposited metal and the basicity of the flux; from [EAG 78]*
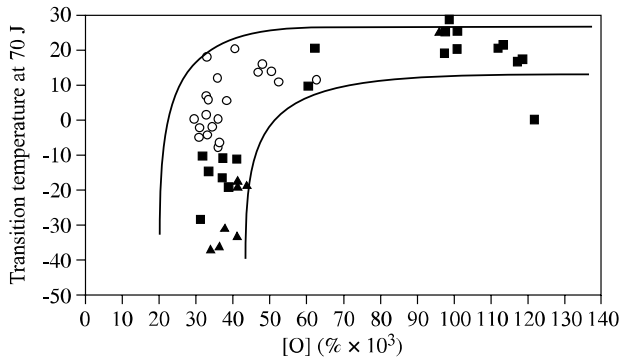
Figure 5.6. *Relation between the transition temperature at 70 J and the oxygen content of submerged arc welds; from [TAY 75]*

What is more, if the temperature change corresponding to a certain value of rupture energy (70 J in Figure 5.6) measured during impact tests on a great number of welds according to their oxygen contents, it appears that above 400 to 450 ppm of oxygen this temperature is always high. Conversely, at lower values a very great disparity in the results appears. This confirms the fact that oxygen content, an imperfect indicator of the inclusion rate, governs the ductile energy of rupture, which, for high rates, comes very close to the value selected here to characterize the transition. On the other hand, the very great scattering observed in Figure 5.6 for oxygen contents lower than 400-450 ppm shows that this factor is not determining because it is in fact the microstructure which governs the ductile/fragile transition.

The second property of a flux, fundamental on the metallurgical level, lies in the hydrogen content of the deposited metal which it controls. With regard to granular fluxes, what was stated previously for coated electrodes applies:

– there is no universal relation between flux humidity and diffusible hydrogen;

– for a given flux, two different relations exist between humidity and hydrogen depending on whether the moisture variation results from a variation in residual humidity after baking or from moisture pick-up;

– to achieve low hydrogen levels requires a selection of raw materials containing little water of crystallization and releasing this water at the lowest possible temperature;

– the use of mixed binders i.e. sodium, potassium, lithium makes it possible to minimize moisture pick-up;

– a rise in flux baking temperature makes it possible to lower the diffusible hydrogen content of the deposited metal.

However, we should not lose sight of the fact that a flux must satisfy requirements for operational weldability which often prove incompatible with the search for a very low hydrogen level. To preclude this difficulty, certain basic fluxes are not baked at very high temperature, they then contain carbonates which while breaking up in the vicinity of the arc make it possible to lower the partial hydrogen pressure in the gas cavity and thus reduce the transfer of hydrogen into the molten metal.

In the case of fused fluxes, the factors which influence the diffusible hydrogen content are fewer than with granular fluxes but even for a given flux formula, it is not possible to make the least correlation with the moisture content. This is owing to the fact that humidity measurements are conventionally taken at 950 or 1,000°C, whereas the preparation of fused fluxes involves taking the flux in its liquid state up to 1,500 or 1,600°C. The moisture measurement, such as it is practiced, cannot thus reveal water content still present in the flux because it is released only at a higher higher temperature than the manufacturing temperature of fused fluxes. In fact, for each flux formulation, a strict correlation between its manufacturing temperature and the content of diffusible hydrogen in the deposited metal is observed (see Figure 5.7).

A low diffusible hydrogen content is thus not necessarily associated with fused fluxes; conversely, the exposure of the flux to a humid atmosphere is of little consequence, which minimizes the precautions to be taken before its use (storage conditions or heating conditions, etc.).
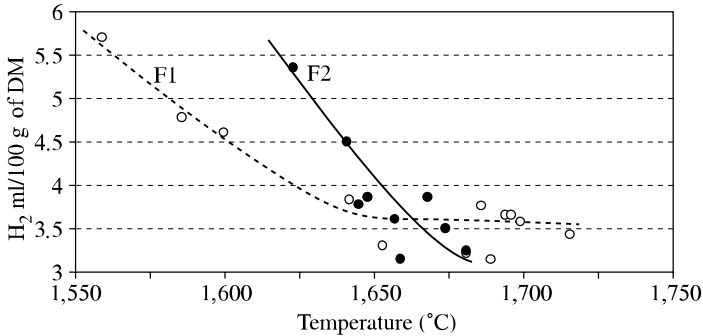
Figure 5.7. *Influence of manufacturing temperature on the diffusible hydrogen content of the metal deposited by two calcium-silicate fused fluxes*
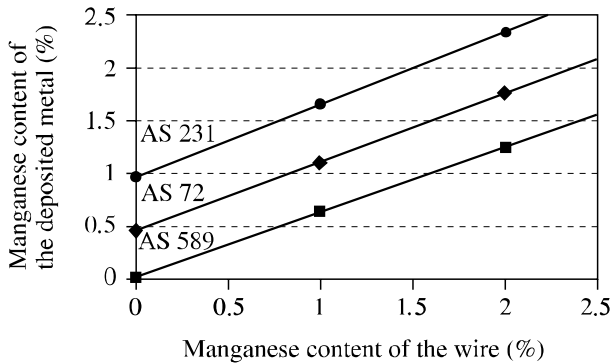
Figure 5.8. *Manganese transfer of granular fluxes AS 231 and AS 589 and fused flux AS 72 (SAF data)*

A final characteristic to take into account for fused as well as granular fluxes relates to the transfer of alloy elements in the arc. Indeed, the flux determines the arc atmosphere and thus the chemical exchanges which occur there: the analysis of the deposited metal is never the analysis of the wire used. Generally, we observe an enrichment in silicon while the manganese content can be above or below that of the wire depending on the flux used (see Figure 5.8). This does not constitute a quality standard but these chemical transfer characteristics, given by the supplier, must be taken into account before choosing the wire appropriate for the flux, or dictated by the properties sought for the weld.

5.3. Welding gases

5.3.1. *Welding processes under a gas flux with an infusible electrode*

TIG (*tungsten inert gas*) and plasma processes both use a tungsten electrode as a cathode. Since tungsten is a very oxidable material and, what is more, tungsten oxide sublimates at low temperature, the shielding gas for TIG and the plasmagenous gas for plasma welding can contain neither oxygen nor CO_2. In addition, the nitrogen content must be maintained below 2% so as not to adversely affect the electrode's lifespan, even when from a metallurgical perspective it is advantageous to have more (in the case of welding of duplex stainless steels for example).

Thus, leaving aside the rare and extremely expensive gases such as neon, xenon and krypton, the only gases usable in the mixtures associated with these processes are argon, helium, hydrogen and nitrogen, within the limit indicated before.

Argon and helium are neutral gases and can thus be used whatever materials are to be welded, but their respective physical characteristics confer on them specific effects when welding:

– argon has a much lower ionization potential than helium (15.7 and 24.5 eV respectively) and a much higher electric conductivity (see Figure 5.9). The result is that it is much easier to start an arc and to stabilize it under argon than under helium but also that an arc of given length is, for the same current, more powerful under helium than under argon (higher voltage);

– the thermal conductivity of helium is much greater than that of argon. Thus, with the same current, an arc under helium is more opened out than under argon, and leads to a lower heat gradient at the level of the parts to be assembled, promoting bead wetting.

Hydrogen is a diatomic gas at room temperature. When the temperature rises, it passes initially into an atomic state then to an ionized state, which explains the two thermal conductivity peaks of Figure 5.9, whereas the other gases show only the ionization peak. This characteristic has very important consequences for arc welding:

– the hydrogen molecule of the shielding gas absorbs energy by disintegrating around the periphery of the arc column, which lowers the temperature locally and causes arc constriction;

– the atomic hydrogen present in the arc will recombine while releasing some energy in the "cool" zones, i.e. at the level of the weld pool, etc.
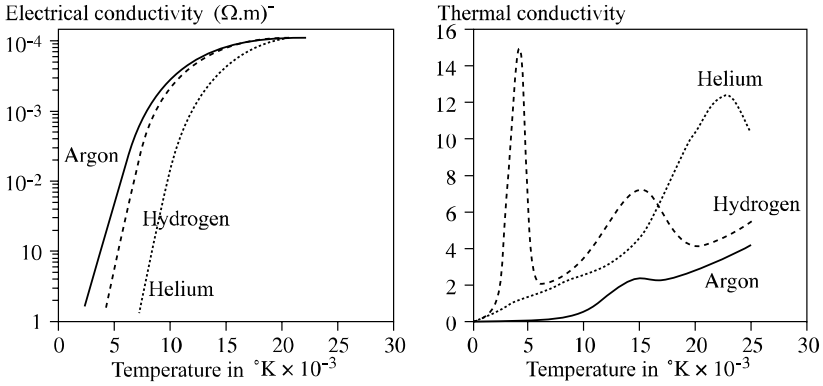
Figure 5.9. *Electric and thermal conductivities of various gases depending on the temperature; from [BOU 83]*

The arc constriction increases the power density and consequently the penetration, as the recombination of the hydrogen atoms at the site of the weld pool thus improves the transfer of energy and thus the efficiency of the welding process (see Figure 5.10). As a corollary, for a given electric output and thickness, the combination of these two effects makes it possible to significantly increase the welding speeds in the TIG or plasma process by using an argon-hydrogen mixture rather than pure argon or argon-helium.
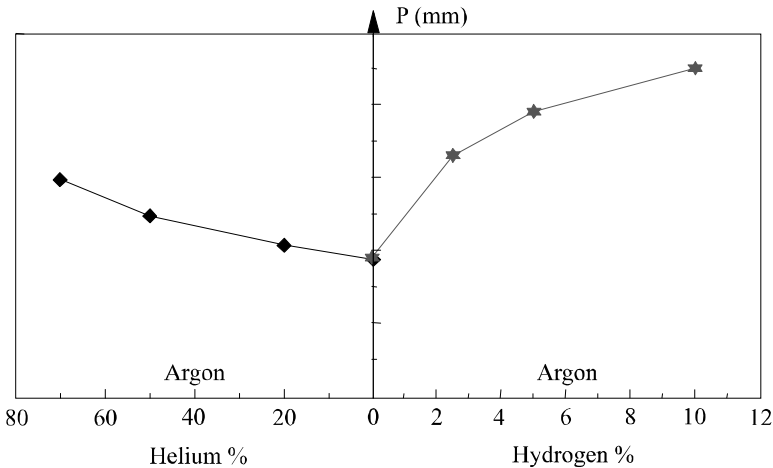
Figure 5.10. *Influence of the shielding gas on penetration in TIG welding (316L steel: I = 200 A; distance of electrode to part = 2 mm; welding speed 20 cm/min*

Thus, the basic gas in TIG or plasma welding is argon, but each time that it is possible, i.e. in the absence of adverse metallurgical effects, it will be beneficial to favor the use of argon-hydrogen mixtures. This is because they allow an increase in welding speed or pass thickness which, in both cases, leads to a significant improvement in productivity. The use of the ternary mixture Ar-He-H$_2$ can further raise welding speed, with helium aiding the bead wetting.

Metallurgical incompatibility can result from the formation of porosities in the weld bead with alloys presenting an important variation in the solubility of hydrogen on solidification like aluminum alloys for example. It can also derive from the risk of cold cracking with ferritic steels when they are sufficiently "hardenable" to develop a non-ductile structure in the HAZ or the molten metal. This last risk must however be carefully calculated because the diffusible hydrogen content carried into the molten metal of course depends on the hydrogen content of the gas mixture used, but remains lower than 5 ml/100 g for a hydrogen content of 3% in argon. On the other hand we can, without disadvantage, use mixtures containing up to 5% of hydrogen to weld austenitic stainless steels or nickel alloys.

When a filler wire is used in TIG or plasma welding, it is introduced in front of the arc, just above the liquid bath. It is then molten at the periphery of the arc and the drops are incorporated one by one in the weld pool without being exposed to the very high temperatures reached in the center of the arc column. Consequently, there are few analytical differences between the deposited metal and the filler wire, the only notable variation relating to the loss of nitrogen during the welding of duplex and superduplex steels. The use of a welding gas containing nitrogen makes it possible to adjust the content in the deposited metal and to thus improve the corrosion resistance of the weld bead (see Figure 5.11).
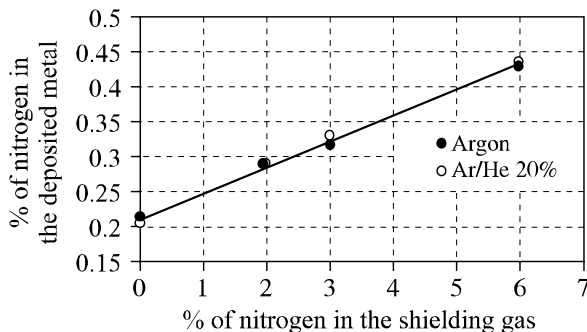
Figure 5.11. *Nitrogen content of the deposited metal as a function of the nitrogen content of the shielding gas (TIG welding); superduplex wire; nitrogen in the wire: 0.25%*

5.3.2. *Welding processes under a gas flux with a fusible electrode*

The gas mixtures used in welding with fusible wire (GMAW) have an influence on arc stability, the mode of metal transfer from the wire to the weld pool and the bead shape. They also determine the chemical exchanges in the arc and consequently the analysis of the deposited metal with a given wire.

Operational aspects

Arc stability is dependent on the more or less easy extraction of electrons from the cathode in order to maintain the arc. However, in MIG/MAG welding, it is actually the parts to be assembled which form the cathode. This is why, each time it is metallurgically acceptable, oxidizing gas mixtures are used, so as to form a fine oxide coating just in front of the arc which aids thermo-electronic emission [JON 95].

The metal transfer can take various forms depending on the parameters used:

– with low welding currents, i.e. for low wire feed speeds, the metal transfer from the wire to the weld pool is performed by *short-circuit* (*short arc* mode). The arc periods are interrupted with periods during which the drop which was formed at the end of the wire comes into contact with the weld pool. During this phase, the arc dies out and the current greatly increases which, via electromagnetic forces, initially causes a striction of the molten metal at the upper part of the drop, then its detachment. The arc can then be restored and the process started again;

– with high currents (high wire feed speeds), the metal transfer takes place by *axial pulverization* (*spray arc*). The end of the wire takes the shape of a cone from the point of which fine droplets are ejected in the wire axis, which are then transfered towards the weld pool. The higher the current, the finer the droplets and the greater their speed;

– with intermediate currents, the transfer is known as *globular*. The drops which are formed at the end of the wire grow bigger until reaching a diameter significantly higher than that of the wire and are detached in an erratic way before the short-circuit occurs. This mode, which is relatively unstable, is the origin of much spattering.

The welding current is thus a determining factor of the mode of transfer. Nevertheless, for a current compatible with transfer by short-circuit or by axial pulverization, it is possible to obtain a globular transfer by adjusting the voltage (very high voltage with low currents or very low voltage with high currents).

Generally, the various transfer fields can be represented in a diagram U = f (I), as in Figure 5.12.
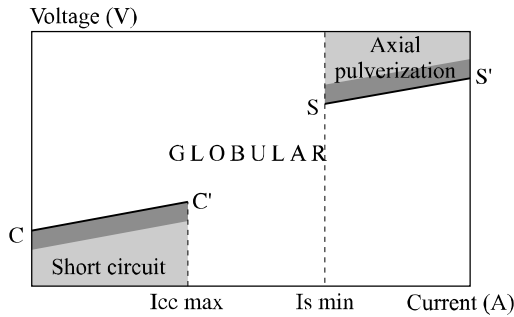
Figure 5.12. *Modes of metal transfer according to MIG/MAG welding parameters*

In this figure, the points to be noted are the following:

– the current Icc max, which corresponds to the maximum at which a transfer by short-circuit is possible;

– the right segment CC' which delimits the maximum voltage value permitting this type of transfer; in practice, welders regulate the voltage to a value slightly lower than this maximum (see shaded zone);

– the current Is min., which corresponds to the minimum at which transfer by axial pulverization can be achieved;

– the segment SS' indicates the minimum voltage at which a transfer by axial pulverization is observed, welders generally working with a slightly higher value;

– the precise limits of these transfer fields in the diagram U = f (I) are characteristic of a given wire/gas combination. They change with the nature of the shielding gas but also with the wire diameter used: any addition of CO_2 and/or oxygen in the argon increases the size of the globular field by decreasing Icc and by increasing Is (see Figure 5.13) so that it is no longer possible to obtain a metal transfer by axial pulverization as soon as the CO_2 content exceeds 50% in the argon.

In addition, an increase in wire diameter causes an increase in current Is, Icc remaining practically unchanged (see Figure 5.14).
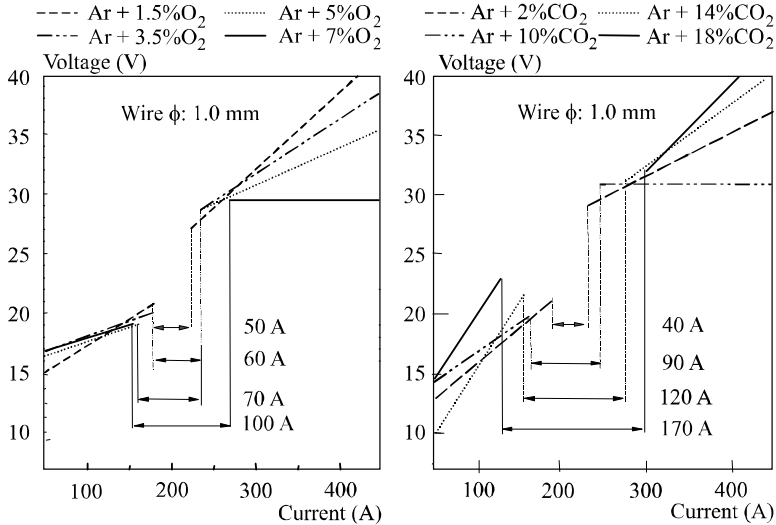
Figure 5.13. *Influence of O_2 and CO_2 content in argon on the size of the globular field in MAG welding (wire ER 70S3; ϕ 1 mm; distance of contact tube to part, 15 mm)*
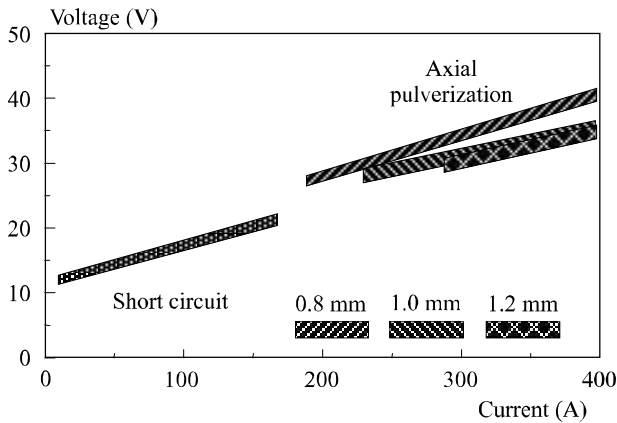
Figure 5.14. *Influence of wire diameter on the transfer fields in MAG welding (wire ER 70S3; gas: Ar + 3% CO_2+ 1% O_2; distance contact tube and contact/part, 15 mm)*

In addition to these three basic fields, a mode exists at very high currents when welds are made with a large gap from the contact tube to the part (>25 mm), where the transfer is rotary (*rotating jet transfer* or *rotating spray*) [LES 58, USC 93]. Beyond a certain value of welding current, the cone which is formed at the end of

the wire electrode becomes sufficiently long and malleable to curve in on itself and rotate under the electromagnetic forces. The curve is more pronounced the higher the current is and can even reach 90°, so that the molten metal drops which are ejected according to the direction of the cone end then give rise to many spatters. This is undoubtedly the reason why this type of transfer has long been regarded as undesirable; nevertheless, as long as the curve remains slight, it can lead to an improvement in bead wetting and compactness because it is strongly dependent on the shape of the penetration.

The shape of the penetration is directly related to the mode of metal transfer. In short-circuit or globular mode, a lenticular penetration is observed which is explained simply from the laws of heat propagation from the surface. On the other hand, when the transfer is carried out by axial pulverization, the penetration becomes pointed. This is because the drops which are propelled at high speed in the wire axis cause a depression of the liquid bath at their impact point and impart a movement to it, which transfers heat towards the bead bottom. In this part of the bead, shaped like a glove finger, the solidification speed is much higher than in the remainder of the bead and when this is very deep, i.e. that at high welding currents, we often observe a lack of compactnesses such as blisters and shrinkage cavities are observed (see Figure 5.15). On the other hand, the rotating transfer mode generally leads to sound beads in spite of the very high currents employed, because the impact of the drops in the weld pool changes place permanently, so that round or even flat penetration is found, which does not imply high solidification speeds.
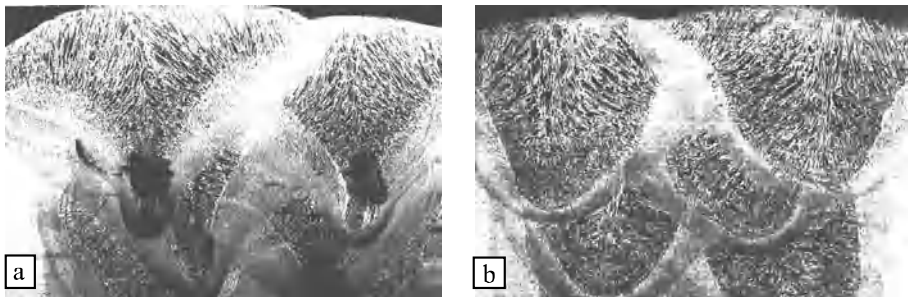
Figure 5.15. *Morphology and compactness of beads created at high currents according to the mode of metal transfer: a) transfer by axial pulverization; b) rotating transfer*

The various fields which we have just described correspond to natural evolutions in the metal transfer modes according to the current density in the wire electrode, the arc length (voltage) and its atmosphere; provided a simple voltage generator is used for welding. This causes some problems for the welder because these natural transfer modes are closely related to the energy employed which, in practice, cannot

be selected independently of the welding position and the type of joint envisaged. Thus, a current corresponding to the axial pulverization mode cannot be employed to weld in vertical or overhead positions because the weld pool would be too bulky and would collapse. Thus, we must weld in the globular mode and accept the erratic transfer and the associated spatters, unless we reduce productivity considerably by lowering the current and welding in the short arc mode. To mitigate these disadvantages, and to a certain extent to dissociate the metal transfer mode from the current and the welding voltage, certain generators employ electronics which constantly control the current in a very fast and precise way, so that the transfer of the drops can be regulated and controlled even for average values of the welding current and voltage which would naturally incline us to the globular mode. This is called the pulsed mode. For each average current and thus wire feed speed, this mode is characterized by a base current and time value, a peak current and time value as well as the ascending and descending slopes. The peak current must be higher than the minimum current allowing axial pulverization (Is in Figure 5.12), the other parameters being programmed so that only one metal drop transfers from the wire towards the weld pool in each cycle. This leads to a perfectly stable mode, free from spatters – provided of course that programming the various pulsed mode parameters is well adapted to the wire/gas combination. Recall that each wire/gas combination has "natural" transfer characteristics which are intrinsic to it.

Generally, the same generators which are equipped with fast control electronics are also able to preserve the short-circuit transfer mode for average current values higher than Icc in Figure 5.12. This is particularly advantageous when we want to weld at high speed, because it is possible to utilize a linear energy adapted to the travel speed while preserving a very short arc, which is thus less likely to stall than the "natural" or pulsed arc corresponding to the same average current.

Chemical aspects

The analysis of a deposited metal is never identical to the analysis of a wire electrode in welding under a gas flow with a fusible wire, because during their transfer in the arc, the metal drops on the surface reach boiling point. Thus, the more volatile elements are vaporized more intensely than the others, which explains why they are found in great quantities in welding fumes but are less prevalent in the deposited metal than in the filler wire. Typically this is true of manganese in steels, magnesium in 5000 series alloys or zinc in brasses.

In addition to this *fractional distillation* and independent of the welding atmosphere, chemical reactions occur, especially at the level of the drops, when the shielding gas has some capacity for oxidation. The greater this oxidation capacity, the greater the analytical variations between the deposited metal and the wire, and the more oxidable elements (Si, Mn, Al, Ti, etc.) occur as slag on the surface of the

beads (see Figure 5.16). At the same time, the oxygen content of the deposited metal and the inclusion rate increase.

Conventionally, the International Institute of Welding considers that the oxidation power of a shielding gas is equal to the sum of its oxygen content and half of its CO_2 content (Doc. IIS XII-543-77). The two graphs in Figure 5.16 show that this approach is very approximate since the losses of manganese and silicon are much greater than the IIS suggest with its comparison of argon-oxygen mixtures and argon-CO_2 mixtures. In addition, depending on the percentage of carbon in the wire and of CO_2 in the shielding gas, there will be a carburizing or decarburizing effect in addition to its oxidizing effect. Thus, an argon mixture + 18% CO_2 will be carburizing if the percentage of carbon in the wire is lower than 0.07% and decarburizing above that value; for the same reason, we should not have more than 1.5% of CO_2 in the shielding gas if we hope to preserve the low carbon characteristic (<0.03%) of an austenitic stainless steel weld (Figure 5.17).
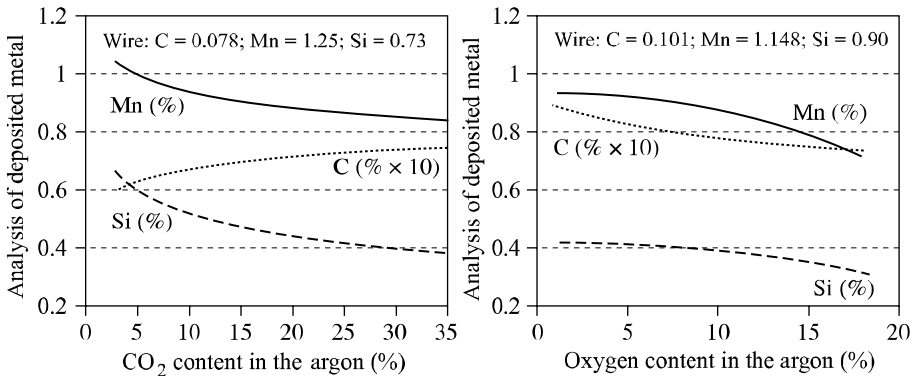
Figure 5.16. *Chemical transfers according to the CO_2 and oxygen content in the shielding gas*
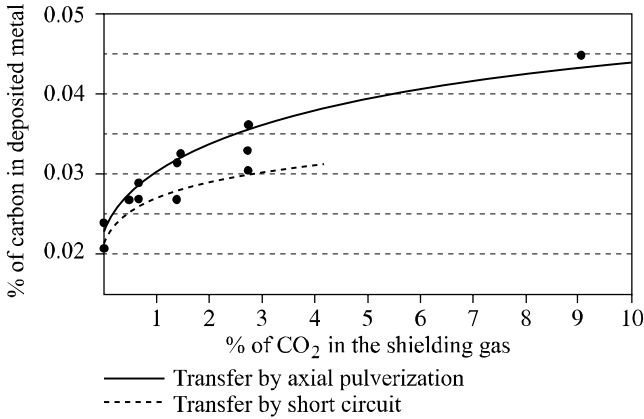
Figure 5.17. *Influence of CO_2 content in the shielding gas on the percentage of carbon in the deposited metal depending on the transfer mode (ER308LSi wire with C=0.18%)*
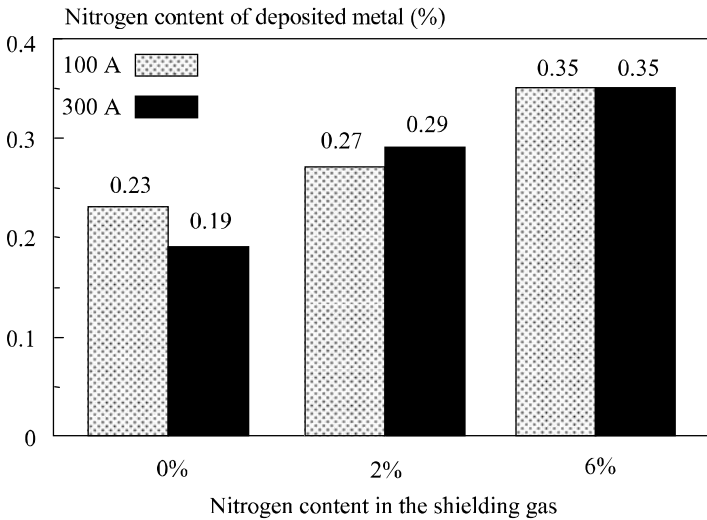
Figure 5.18. *Influence of nitrogen content of the shielding gas on the nitrogen content in the deposited metal (MIG welding); superduplex wire (N = 0.24%); two transfer modes*

Thus, for GMA welding as for welding with a solid flux, the chemical characteristics of welds are not only related to the wire used but to the wire/flux combination. However, a difference exists. Whereas, depending on the solid flux used, the deposit can be more or less rich in alloying elements than the filler wire, it

is generally less rich in welding with a gaseous flux except for carbon, as we have seen previously, and nitrogen, a certain quantity of which can be transferred into the deposited metal when nitrogen is present in the shielding gas (Figure 5.18).

5.4. Cored wires

5.4.1. *Manufacturing processes*

The cored wires marketed today are mainly manufactured according to one or other of the two processes presented in Figure 5.19.

To manufacture a wire according to Chemetron technology, we start from cold rolled strip iron small in size (about 13 × 1 mm) which is formed initially into a U. A homogenous mixture of the various constituent raw materials is then placed inside and shaped in an O, which is then drawn out to the required diameter. Annealing at low temperature is finally carried out so as to destroy the residual soap still present on the wire and to slightly oxidize its surface in order to confer a sufficient resistance to atmospheric corrosion.
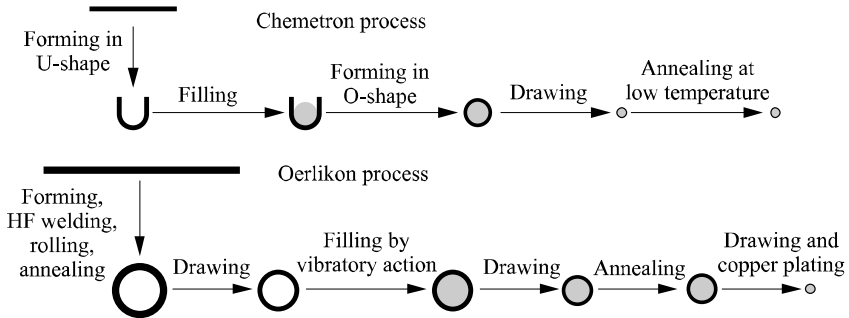
Figure 5.19. *Cored wire manufacturing processes*

The Oerlikon technology is more complex. It begins with the manufacture of a tube approximately 16 mm in diameter starting from hot rolled strip iron slightly more than 2 mm thick welded at high frequency then rolled to a diameter of about 13 mm. Softening is carried out by annealing, then the tube is drawn out to the filling diameter, which varies according to the manufacturing specifications.

Filling then takes place, the powder rising by vibration in tube sections of approximately 500 kg installed on a vibrating table. The filled tube is then drawn out into an intermediate diameter, at which stage it has to undergo recrystallization heat treatment before being drawn its final diameter, where it will be copper plated.

Thus, Oerlikon technology makes it possible to produce sealed filled coppered wires which resemble solid wires and are used as such. These cored wires are completely impervious to moisture pick-up and typically have diffusible hydrogen levels of about 2 to 3 ml/100 g of deposited metal. This is because chemical reactions occur inside the tube during the recrystallization annealing, releasing hydrogen, which escapes through the tubular sheath. However, this process implies a preliminary powder granulation by means of a silicate in order to avoid segregations at the time of the vibratory filling operation. Moreover, these granulated powders must be able to support the high temperatures associated with the recrystallization treatment applied to the tube without undesirable changes.

Such constraints do not exist with the Chemetron process. It is by no means necessary to granulate the powders or introduce a silicate which might have undesirable side-effects during welding, or even take into account a possible constituent decomposition during the heat treatment, which in this case is carried out at low temperature. Moreover, this technology makes it possible to produce wire with a higher filling rate (ratio of the powder weight to the wire weight) and as a result to obtain a greater deposition rate for a given welding current. On the other hand, as the Chemetron wires, are not welded, they are more or less liable to humidity pick-up depending on their content and so require more precautions during storage and use.

5.4.2. *Types of cored wires*

Both technologies make it possible to manufacture all varieties of cored wire designed to be used with a shielding gas, cored wires without gas only being produced today by means of the Chemetron technology.

Depending on the nature of the filling powders, three types of cored wires with shielding gas are to be found: rutile cored wires, basic cored wires and metal powder cored wires. Table 5.2 displays the principal components of these various types of cored wire, as well as the operational and metallurgical consequences which result from them. When it is compared to Table 5.1, relative to coated electrodes, we see great similarities between cored wires and electrodes of the same type, but also some important differences from the perspective of non-metallic components and the operational and metallurgical consequences.

Type of wire		Rutile	Basic	Metallic
Principal components	**Non-metal**	TiO_2, Al_2O_3, SiO_2, Ionizing elements	CaF_2, MgO, Carbonates, etc. Ionizing elements	<1% Ionizing elements
	Metal	Alloying elements Deoxidizers	Alloying elements Deoxidizers	Alloying elements Deoxidizers
Consequences	**Operational**	Soft fusion, Stable arc, Great transfer field by axial pulverization, Very good wetting, Easy welding out of position.	Crackling arc, Globular transfer, Spatters, Difficult welding out of position.	Stable arc, Transfer by axial pulverization with high current.
	Analytical	O: 450 to 1,000 ppm Ti: 300 to 800 ppm Nb: 100 to 300 ppm V: 50 to 250 ppm H_2Diff: 2 to 15 ml/100 g DM	O: 300 to 500 ppm Ti, Nb, V: adjustable to the desired values, H_2Diff: <5 ml/100 g DM	O: 500 to 1,000 ppm Ti, Nb, V: adjustable to the desired values H_2Diff: 2 to 8 ml/100 g DM

Table 5.2. *Principal constituents and characteristics of cored wires with shielding gas*

In wires manufactured by Chemetron technology, we always add ionizing elements in order to help arc stability; it is not essential in the Oerlikon process, this role being played by the silicate used for the granulation of filling powders.

Unlike coated electrodes, cored wires with shielding gas do not systematically contain carbonates because, in this case, it is the shielding gas which prevents the contamination of the drops and the weld pool by atmospheric nitrogen and oxygen.

Rutile wires never contain organic elements such as cellulose or extrusion agents in the electrodes. Thus, for cored wire, the rutile or basic character has no impact on the diffusible hydrogen of the deposited metal.

More powerful deoxidizers, or deoxidizers added in greater quantity than in rutile electrodes, can be used in wires. This makes it possible to have formulae

which associate good operational properties with oxygen contents of the deposited metal around 450 ppm, i.e. not very different from the basic products.

The current density is much greater when welding with cored wire than with coated electrodes (120 to 300 A for a wire 1.2 mm in diameter, compared to 80 to 120 A for an electrode with a diameter of 3.2 mm). This makes it possible to attain the axial pulverization mode of metal transfer with rutile wires and metal powder cored wires,. This mode leads to a very stable arc and the virtual absence of spatter.

Combining of the axial pulverization mode with the physical characteristics of certain rutile slags (melting point, viscosity and surface tension) imparts a much higher productivity to these wires than all the others wires, cored or solid, during out of position welding (+ 50% in vertical up welding for example); such a variation does not exist between rutile and basic electrodes.

If we consider the metallurgical potential of these various types of wire, the basic wires are the best, followed by metallic powder cored wires then rutile wires; on the other hand, precisely the opposite classification is reached on the basis of their operational quality with a very great advantage for rutile wires when it is a question of welding in all positions. This is why for about 15 years, developments have been primarily related to the improvement of metallurgical qualities in rutile wires by refining the microstructure of the weld metal employing the titanium/boron effect. These efforts have met with success, so that today basic wires are effectively used only for welding steels with a very high yield strength (≥690 MPa). The remainder of the market is divided between metal powder cored wires, valued in flat welding because they offer better performance than the other wires (absence of slag), and rutile wires when it is necessary to weld in all positions.

5.4.3. *The titanium/boron effect in relation to rutile cored wires*

This effect results from the presence of a very small quantity of boron (typically 20 to 60 ppm), which considerably delays the nucleation of proeutectoid ferrite at the austenitic grain boundaries while the weld bead cools. Thus, the transformation of austenite can occur primarily by intragranular acicular ferrite germination on inclusions, provided that these have the necessary characteristics and thus are present on the surface zones of titanium oxide.

When the complete chemical analysis of the weld metal is well balanced in manganese, and possibly nickel (so that its hardenability is optimal for the thermal cycle undergone by the weld), the proeutectoid ferrite network is reduced to a fine edging, and the remainder of austenite is transformed into acicular ferrite. If it is

moreover possible to incorporate an addition of molybdenum, a synergistic boron/molybdenum effect is achieved which makes it possible to remove the proeutectoid ferrite network completely and to obtain a structure made up only of acicular ferrite, which possesses remarkable toughness properties.

C%	Mn%	Si%	S%	P%	Ni%	Nb%	V%	Ti%	B ppm	O ppm	N ppm
0.070	1.39	0.35	0.006	0.007	0.65	0.006	0.008	0.046	40	400	39

State	As welded		Stress relieved (580°C/3hr)	
Position of the notch	As-welded zones	Annealed zones	As-welded zones	Annealed zones
Kv – 40°C (J): av.; (min.)	145 (136)	139 (137)	118 (106)	115 (91)
Kv – 60°C (J): av.; (min.)	109 (85)	121 (118)	98 (88)	94 (82)

Table 5.3. *Characteristics of welds achieved with an optimized Ti-B effect rutile wire*

5.5. Choice of welding products

From the preceding considerations, it is clear that the choice of a wire/flux combination, whether it is solid or gaseous, will have to take into account:

– the supplier data concerning the chemical and mechanical characteristics respectively determined on a weld pad and an all weld metal deposit,

– the joint shape, the thickness and the chemical nature of the base metal.

The supplier catalog indicates the chemical and mechanical characteristics of deposits carried out under standardized conditions with great precision.

These standards (EN, AWS, etc.) indicate in a more or less precise way the welding parameters (U, I, Ws), the temperatures between passes and possibly even the pre-heating temperature, the pass distribution (generally two passes per layer) and the position of the various specimens necessary for characterization in the all weld metal deposit.

This type of information is absolutely essential to check product consistency but, taking into account all that has been said before, it is clear that these data are not necessarily representative of what will be obtained during the execution of a real joint for which the thermal welding cycle and/or the dilution rate of the base metal can bear no relation to the standardized conditions.

This is why welding product suppliers generally publish data sheets relative to their products which, in addition to the characteristics obtained under the standardized conditions, give results on joints produced under various conditions (heat input, dilution rates, etc.) and with various steels. They also provide additional details specific to each product, such as:

– the field of usable parameters,

– the deposit rate according to the current,

– the chemical transfer graphs,

– the behavior with respect to moisture pick-up,

– the granulometric distribution (for fluxes in submerged arc).

It is by starting from these data sheets and by applying metallurgical reasoning that we will be able to choose the products appropriate to achieving the goals imposed by the construction specifications.

When high thicknesses are welded, the dilution ratio is low except in the root zone, but that is frequently gouged before welding the second side of the joint. In this case, we can use the catalog data to choose the products best adapted to the mechanical properties desired or, if the welding conditions considered are very different from the standardized conditions in terms of the thermal welding cycles, we can resort to the data sheets. Moreover, as this type of joint frequently undergoes a stress relieving treatment after welding, the choice of welding products will have to take account of this eventuality, as the weld metal characteristics can be significantly modified during this treatment[1].

---

1 The aim of a stress relieving treatment is to lower the internal stresses which arise due to multiple and non-uniform heatings which is a characteristic of welding. Its principle lies in reducing the yield strength of materials while raising the temperature: in a given structure, there cannot be internal stresses higher than the yield strength because if that were the case, it would lead to deformations which would continue until the stresses had been lowered to their yield strength. The stress relieving treatment then consists of heating to a temperature for which the yield strength of the metal under consideration is sufficiently low (580/600°C for most steels) such that the deformations occur and relieve the stresses.

However, in addition to this stress relief phenomenon, the treatment can cause some useful metallurgical reactions (tempering of out of balance structures, softening of hardened zones, etc.) but sometimes very damaging ones from the point of view of toughness (carbide, nitride or carbonitride hardening precipitations; temper-embrittlement developing during cooling after the relieving stage, etc.). The scale of these harmful secondary phenomena greatly depends on the nature of the products used and so it is essential when choosing products for a given structure to take into account the existence or on the contrary the absence of such a treatment during manufacture.

For welds involving only a small number of passes, the mechanical properties indicated in the supplier catalog are not of any use, since the analysis of the weld metal can be very different from that of the metal deposited by the products. In this case, the choice of welding products can only come from metallurgical reasoning based on the thermal cycle evaluated using the IRSID graph, the estimated dilution rate and the real analysis of the base metal (and not of the standard, which is far too vague from this perspective). On the basis of the thermal cycle, we can deduce the chemical analysis of the weld metal to aim for, depending on the properties desired, then calculate the analysis of the metal to be deposited. We also take into consideration the actual analysis of the plates to be welded and the rate of dilution so as to choose the wire/flux combination which will make it possible to achieve the desired result.

5.6. Welding products and the welder's environment

Welding is at the origin of many harmful effects (UV radiation, noise, fumes, spatters, etc.) which of necessity entail the use of individual and collective protective gear in order to preserve the health of the welders or other personnel working in the vicinity. However, it is not always easy to guarantee the absolute effectiveness of this equipment whatever the localization of the welding, so any reduction in these harmful effects at the source can only have a positive impact on working conditions. This objective has become a major concern in the development of welding consumables and welding procedures and even if there is still a lot of progress to be made, it is now possible to considerably reduce some of these harmful effects.

5.6.1. *Coated electrodes*

The quantity of fumes emitted during welding with a coated electrode depends on the nature of the coating and the electric output employed. This is what Figure 5.20 illustrates for various diameters of two rutile and two basic electrodes of different grades. These results were obtained by using, for each electrode, the average current recommended by the manufacturer for the diameter considered. However, it should be borne in mind that fume emission can be doubled when the welding intensity is varied from the minimum to the maximum application field for a particular diameter. All in all, it can be seen that rutile electrodes have a fume emission rate ranging between 0.8% and 1% of the deposited metal, while for basic electrodes this rate is between 1.5% and 2%.
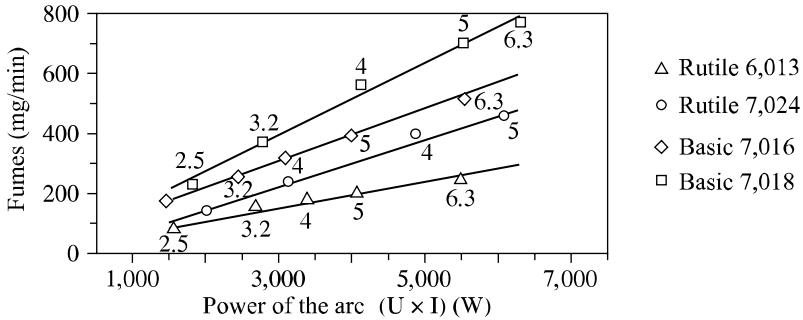
Figure 5.20. *Fume emission rate of various electrode types and diameters depending on the arc power: rutile 6,013 and 7,024; basic 7,016 and 7,018*

In the case of electrodes baked at low temperature (rutile electrodes), the fume emission rate increases with the potential hydrogen content, i.e. hydrogen coming from residual humidity after baking but also from all the organic materials of the coating. On the other hand, for electrodes baked at high temperature (basic and stainless), the fume emission rate is an increasing function of the sodium and potassium content of the coating. Thus, by removing all the components containing these elements from the coating, and by replacing them with lithium compounds, it is possible to halve the quantity of fumes emitted. Applying this formulation to stainless electrodes has the additional advantage of considerably decreasing fume toxicity. Indeed, fumes from traditional stainless electrodes contain approximately 4% of hexavalent chromium, which has a toxicity index 100 times higher than standard fumes and 10 times higher than chromium in a trivalent state (Oel CrVI: 0.05 mg/m^3; Oel CrIII: 0.50 mg/m^3; standard fumes Oel: 5 mg/m^3). However, it proves that the replacement of sodium and potassium compounds by lithium compounds makes it possible to lower the content of CrVI in fumes to less than 1% so that fumes from these electrodes for stainless steels are no longer toxic than those of non-alloyed electrodes (see Figure 5.21).
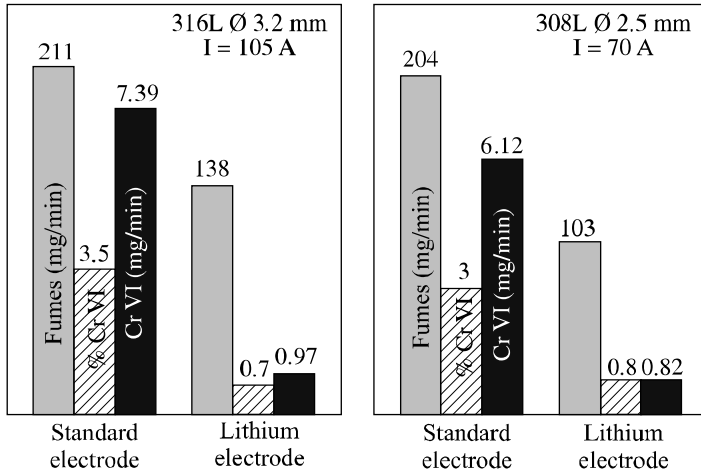
Figure 5.21. *Comparison of fume emission rates and hexavalent chromium between standard stainless electrodes and electrodes with lithium*

Today, the cost premiums associated with these formulation developments is considered to be prohibitive in the case of the traditional basic electrodes. However, it is acceptable for the stainless steels because of the much higher price of the cores of these electrodes. They are now on the market.

5.6.2. Gas mixtures for TIG welding

In TIG welding, fumes and spatters are non-existent but there is the problem of ozone formation during the welding of stainless steels and still more in welding light alloys.

Ozone results from the action of ultraviolet radiation, which "breaks" the surrounding oxygen molecules. The single oxygen atoms thus formed (O) will be able to react with other oxygen molecules (O_2) and form ozone molecules (O_3) whose toxicity is recognized. In fact, in UV radiation, emissions in the spectral band 130 to 180 nm are particularly liable to form these single atoms.
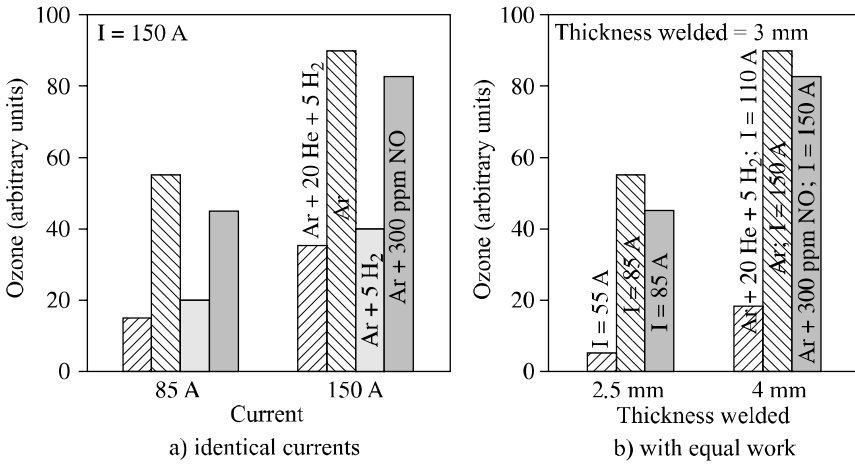
Figure 5.22. *Influence of shielding gas type on the quantity of ozone formed in austenitic stainless steel TIG welding*
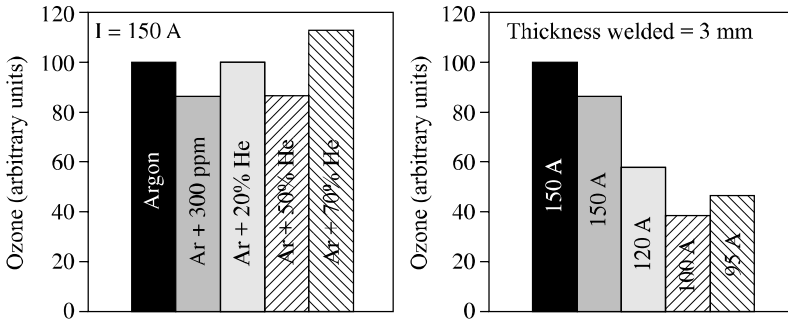
Figure 5.23. *Influence of shielding gas type on the quantity of ozone formed in light alloy (alloy 5086) AC TIG welding*

The radiation spectrum emitted by the arc depends on the energy employed and the chemical elements present. This is why the quantity of ozone formed increases with arc power (U × I) and, with identical power and shielding gases, more ozone is formed when we weld light alloys than stainless steels.

If the aim is to reduce the quantity of ozone which will diffuse into the atmosphere surrounding the welder, several solutions exist:

– minimize the radiation in the spectral band 130 to 180 nm. This can be achieved by replacing argon with helium as far as possible in the shielding gas;

– minimize the energy employed to produce any given joint. This can be achieved by modifying the process: TIG double flux or plasma lead to a deeper penetration than a TIG process with identical energy and thus make it possible to reduce the welding energy required to produce a given joint. It can also be achieved by using a shielding gas containing helium and/or hydrogen which, by modifying the arc morphology and by increasing the voltage with identical arc length, significantly improves the performance of the TIG process;

– introduce gas molecules into the shielding gas which are very reactive with respect to ozone and will cause its destruction (hydrogen or nitrous oxide NO).

Figures 5.22 and 5.23 illustrate the advantages to be gained from these various actions. They show that wherever possible it is found to be beneficial to use argon-helium-hydrogen ternary mixtures which combine the various effects. However, the mixture must be designed to take into account on one hand operational aspects (too high a content of helium and/or of hydrogen can pose problems for out of position welding) and on the other hand, of the metallurgy which leads us to reject, for example, the use of hydrogen for welding light alloys to preserve weld compactness. Finally, we should also note that certain welding equipment does not allow good arc stability with very high helium content. This explains the increase of the ozone content with the argon mixture + 70% helium in Figure 5.23.

5.6.3. *Gas mixtures for GMAW*

Apart from UV radiation, the emission of fumes is the principal harmful effect associated with GMA welding. As a first approximation, this increases in line with the oxidation power of the shielding gas (see Figure 5.24) but fumes and spatters are also closely linked to the metal transfer mode.
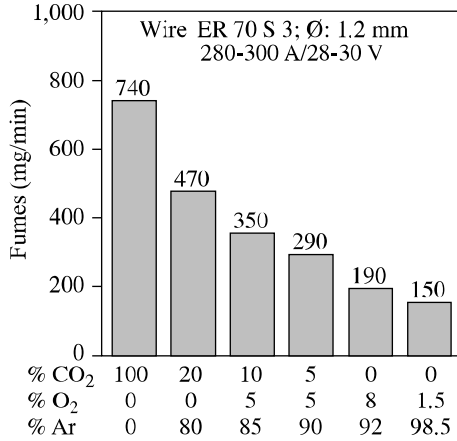
Figure 5.24. *Influence of the shielding gas on the fume emission rate in MAG welding*

When welds are made with a current which produces transfer by axial pulverization for the wire/gas combination used, the fume emission rate and projections decrease when we increase the voltage until a stable transfer by axial pulverization is achieved. Beyond this value, an increase in voltage will not modify the metal transfer but does cause a simple lengthening of the arc, which in turn causes an increase in the volatilization of the metallic elements and, consequently, in the fume emission rate (see Figure 5.25).

This is a very general process, as shown in Figure 5.26 where fume emission rates relative to three gas mixtures in various welding conditions are compared. In this same figure, we can also see that the minimal emission values decrease when the oxidation power of the shielding gas decreases. It is also seen that specific comparisons with constant electric parameters can lead to inverse classifications of shielding gases, as identical electrical parameters do not correspond to similar operational point locations compared to the transfer curves characteristic of each gas.
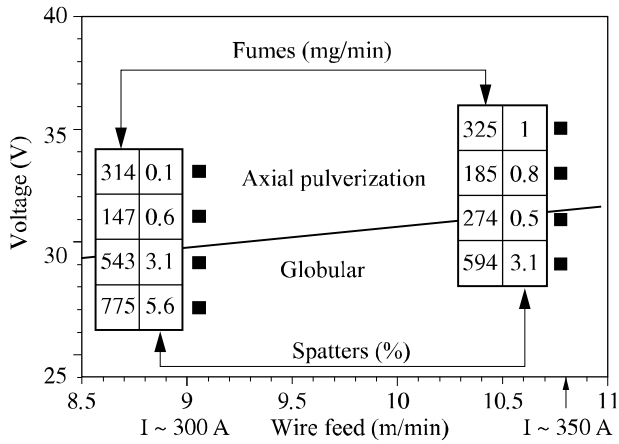
Figure 5.25. *Relations between fume emission rate, spatters and transfer graph. Wire: ER70S6 1.2 mm; gas mixture: Ar + 3% CO$_2$ + 1% O$_2$; distance of contact tube to part: 20 mm*
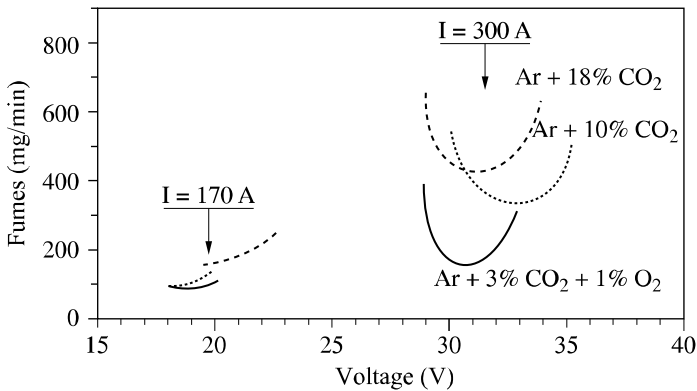
Figure 5.26. *Comparison of the fume emission rate of three gas mixtures according to the voltage for two welding currents. Wire: ER70S6 ϕ 1.2 mm*

In practice, if we wish to reduce the fume emission rate, it will always be beneficial to use the least oxidizing shielding gas compatible with operating requirements. From this perspective, a mixture Ar + 3% CO$_2$ + 1% O$_2$ seems to us an excellent compromise for the welding of ferritic steels, and even more so as this mixture is perfectly adapted to pulsed welding. This will enable us to regularize the metal transfer but also to considerably reduce spatters and fume emissions when we

are obliged to use parameters which correspond to globular transfer if a DC current is used (see Figure 5.27).
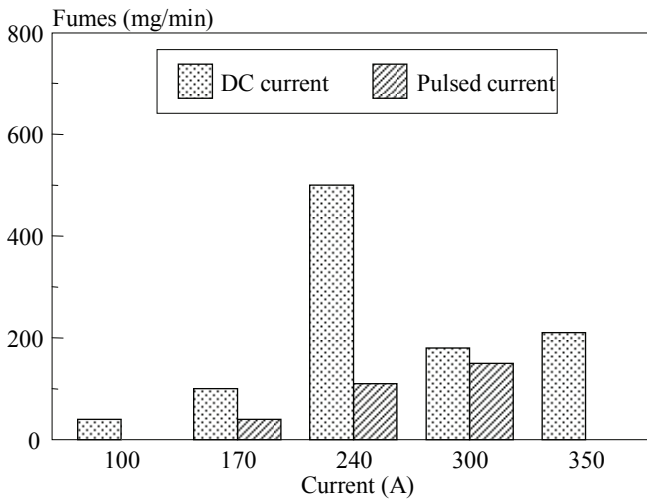
Figure 5.27. *Comparison of fume emission rate between DC current and pulsed current. Wire: ER70S3 ϕ 1.2 mm; gas: Ar + 3% CO$_2$ + 1% O$_2$*

5.6.4. *Cored wires*

The use of cored wire seems to be developing to the detriment of coated electrodes. However, although these products do not generate significantly longer fume emissions than electrodes when we view the results of the quantity of deposited metal, their greater productivity leads to an emission rate per unit of time which sometimes can constitute an impediment to their use.

The operational qualities of a cored wire are partly related to the shielding gas used but also to the nature of the "ingredients" which constitute the filling. Compared to solid wires, there thus exists an additional degree of freedom which makes it possible to consider the development of cored wire/gas combinations whose use would not generate CO. The quantity of CO formed being in direct relationship with the CO$_2$ content of the shielding gas, it is necessary to adapt the wire formulations so that they have the necessary operational qualities with a gas containing no CO$_2$. In addition, to minimize fume emissions, the gas must be the least oxidizing possible.

Today, it is not only metal cored wires that exist but also rutile wires designed to function with an Ar + 3.5% O$_2$ mixture. Furthermore, as a means of minimizing CO

emission, they can reduce fume emissions by about 50% compared to a standard wire used with an Ar + 18% or 25% CO_2 mixture.

5.7. Bibliography

[BOU 83] BOURDIN E., FAUCHAIS P., BOULOS M., "Transient heat conduction under plasma conduction", *Int. J. Heat Mass Transfer*, vol. 26, no. 4, p. 567-582, 1983.

[DIC 88] DICKEHUT G., RUGE J., "Method for predicting the content of diffusible hydrogen in the weld metal under the influence of atmospheric moisture", *Schweissen und Schneiden* 40, no. 5, p. 238-241, May 1988.

[EAG 78] EAGAR T.W., "Sources of weld metal oxygen contamination during submerged arc welding", *Welding Journal*, p. 76s-80s, March 1978.

[GAS 86] GASPARD-ANGÉLI A., BONNET C., "How to optimize the properties of the longitudinal welds of pipes using a fused flux", *Proceedings of the 3rd Intern. Conf., Welding and Performance of Pipelines*, London, 18-21 November 1986.

[JON 95] JÖNSSON P.G., MURPHY A.B., SZEKELY J., "The influence of oxygen additions on argon-shielded gas metal arc welding processes", *Welding Journal*, p. 48-58, February 1995.

[LED 92] LEDUEY B., BONNET C., DAMAGNEZ P., "Principes d'évolution des électrodes enrobées pour réduire l'hydrogène diffusible", *Soudage et Techniques Connexes*, p. 15-19, July-August 1992.

[LES 58] LESNEWICH A., "Effect of shielding gas composition on metal transfer phenomena in high current GMA Welding. Part II – Control of metal transfer", *Welding Journal*, p. 418s-425s, September 1958.

[TAY 75] TAYLOR L.G., FARRAR R.A., "Metallurgical aspects of the mechanical properties of submerged-arc weld metal", *Welding and Metal Fabrication*, p. 305-310, May 1975.

[TUL 69] TULIANI S., BONISZEWSKI T., EATON N.F., "Notch toughness of commercial submerged-arc weld metal", *Welding and Metal Fabrication*, p. 327-339, August 1969.

[USH 93] USHIO M., IKEUCHI K., TANAKA M., SETO T., "Effect of shielding gas composition on metal transfer phenomena in high current GMA welding", *Trans JWRI*, vol. 22, no. 1, p. 7, 1993.

Chapter 6

Fatigue Strength of Welded Joints

6.1. Fatigue strength

6.1.1. *Introduction*

The observation of many failures in welded structures generally points the finger at fatigue as the main cause. Moreover, it has become apparent that for welded structures, admissible service stresses were very low in respect of the static stresses (yield strength, breaking strength) and that it was not enough to apply a safety coefficient based, for example, on a fraction of the yield strength to be certain of avoiding failure. Indeed, welds can introduce severe stress concentrations and which differ from one structural element to another.

For example, Figure 6.1 compares the fatigue performances of an E36 steel plate, and the same plate with a hole or two stiffeners welded longitudinally. Fatigue strength, which is conventionally given as 2×10^6 cycles, passes respectively from 260 (plain plate) and 180 (bored plate) to 70 MPa for the welded joint.

On the other hand, if we apply a sufficiently large safety coefficient to eliminate the possibility of rupture, the welded structure then becomes too large and is not competitive.

In fact, when designing a structure, every aspect of it must satisfy the three following conditions:

– fulfill its function as effectively as possible,

Chapter written by Henri-Paul LIEURADE.

– be manufactured economically,

– ensure a defined in-service lifespan.
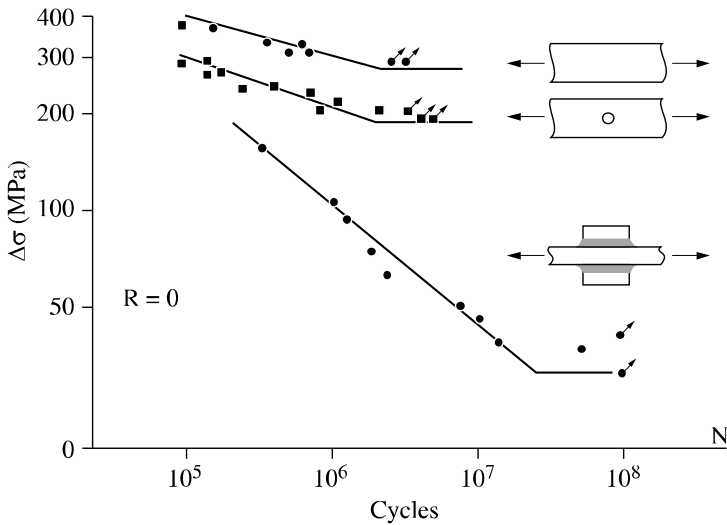
Figure 6.1. *Comparison between the fatigue strengths of a holed or plain steel sheet and of a fillet weld*

The consequences of the first two conditions lead, at the design stage, to a reduction in the safety coefficients, in order to decrease weight and costs. Unfortunately, this tendency conflicts with the need for an adequate lifespan and hence the safety of the structure where fatigue damage can occur. Moreover, the fatigue strength of actual structures cannot be defined uniquely in a theoretical way. This is why the only realistic approach to designing a structure that is subject to fatigue stresses is to relate the load levels applied to the fatigue strength data that correspond with each joint configuration used. To this end, each country has its own standards or recommendations. However, these codes are only applicable to certain types of metal structures.

The aim of this chapter is to present the principal parameters which influence the fatigue behavior of welded joints in both an analytical and diagrammatic way.

6.1.2. *Fatigue failure of the principal welded joints*

Welding operations result in the existence of stress concentrated areas where a fatigue crack may originate and expand from. These zones correspond, either with a

geometric anomaly in the weld bead, an internal defect (lack of penetration, porosities) or external defects (undercuts, slag inclusions); their relative importance depends on the type of assembly and the type of loading applied in service.

6.1.2.1. *Butt welded joints*

Transverse butt welds

Figure 6.2 presents this type of assembly, which makes it possible to join two plates via a transverse welding perpendicular to the load axis.
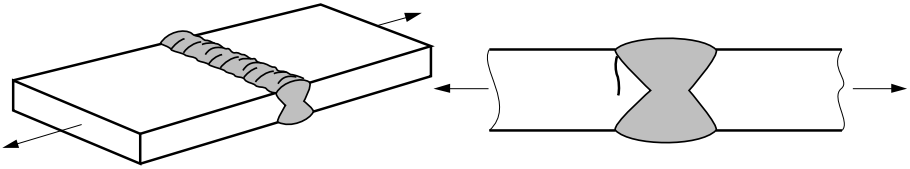
Figure 6.2. *Fatigue cracking of a transverse butt weld*

For this type of joint, the fatigue crack starts at the weld toe and propagates through the thickness of sheet, perpendicular to the load direction. The crack is thus not the result of a defective welding or bad properties of the deposit metal, but the consequence of stress concentrations at the weld toe.

In this type of butt welded joint, the influence of the shape of the weld bead is important for determining the endurance characteristics of the joint. This depends greatly on the welding conditions.

Longitudinal butt welds

For longitudinal joints, the change of section due to a metal excess is now parallel with the direction of the applied load and it could be thought that the fatigue performance of these welds are better than those of transverse joints. However, this is not always the case.

The crack in this type of joint generally starts (see Figure 6.3) at the level of a welding stop and restart, for example, while changing an electrode, or starting from a deformation on the weld bead surface.
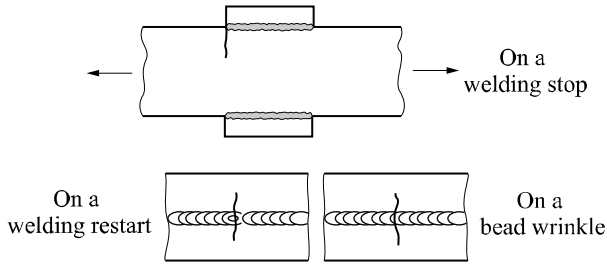
Figure 6.3. *Fatigue cracking of a longitudinal butt weld*

A good fatigue strength of longitudinal joints can only be obtained if they are continuous, and therefore if welding interruptions are avoided.

6.1.2.2. *Fillet welded assemblies*

a) Cruciform joints

There exist two types of cruciform joints, according to whether the weld beads transmit the load or not.

Non-load carrying fillet weld

In the first type (see Figures 6.4a and 6.4b), the fillet weld does not transmit the load in the solid metal sheet. In this case, the crack starts at the weld toe and propagates through the thickness of the plate in a plane perpendicular to that of the stress.
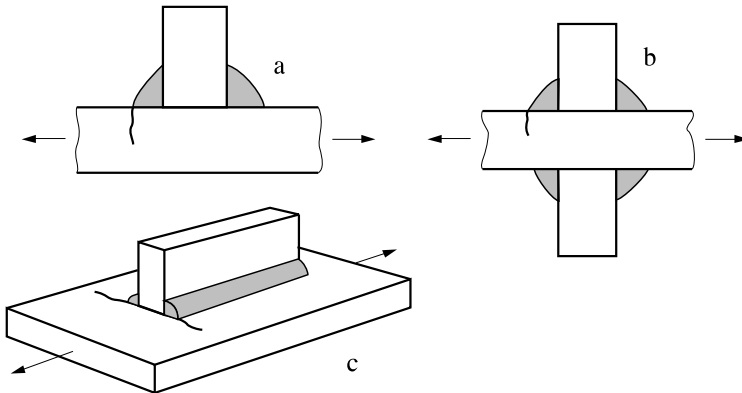
Figure 6.4. *Fatigue cracking of a non-load carrying fillet weld*

There is no advantage in making assemblies with fillet welds parallel to the stress direction (see Figure 6.4c). The crack then starts at the bead end and leads to a low fatigue strength. On the other hand, continuous longitudinal fillet welds present significant improvements in endurance over intermittent fillet welds.

Load-carrying fillet weld

In this type of joint, the entire load is transmitted by the weld (see Figure 6.5a).

In this case, in addition to the stress concentration zones located at the weld toe there are zones of acutely angled internal notches at the weld root. In general, the crack starts here then propagates in the deposited metal in an oblique direction compared to the load direction. This type of failure means that the assembly has relatively low endurance characteristics compared to the preceding welded joints. This is why the aim is to avoid starting a crack at the weld root; however the fact of increasing the throat thickness, by a thicker weld or a better penetration, is not always enough to ensure that the fatigue crack starts, this time, at the weld toe. In general, completely interpenetrating beads (see Figure 6.5b) notably improve the endurance properties.
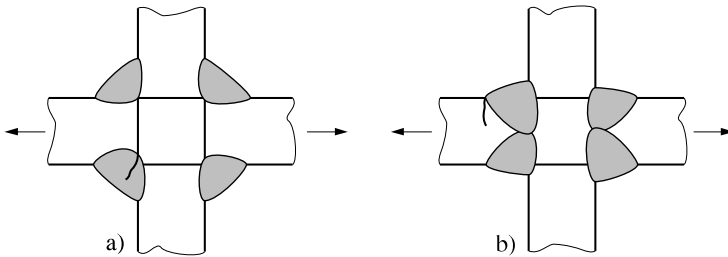
Figure 6.5. *Fatigue cracking of a load-carrying fillet weld*

In general, bead interpenetration is not always necessary to transfer crack initiation at the weld root to the weld toe. Figure 6.6 presents the geometric bead conditions necessary to pass from one type of failure to the other.

b) T-shaped joints

At first sight, this joint resembles half of a cruciform joint (see Figure 6.7) and should show a similar fatigue behavior. However, in this case, a third rupture mode is possible. If the bending stresses applied to the transverse element are in the same order of magnitude as the constraints applied directly to the T, the crack will be able to start on the other weld toes and propagate through the transverse element.
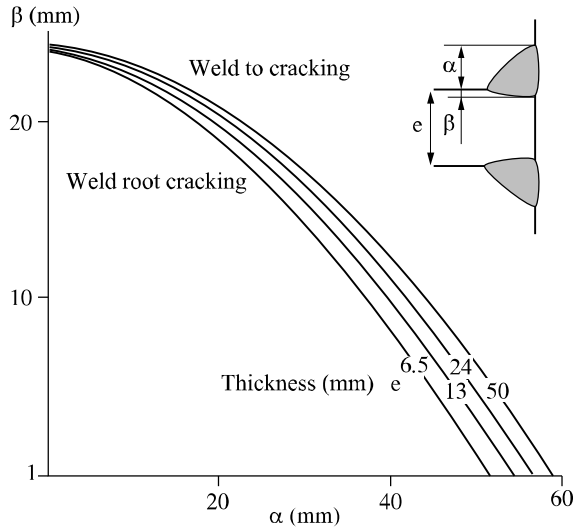
Figure 6.6. *Cracking conditions of a cruciform joint. Influence of lack of penetration; from [LIE 73]*
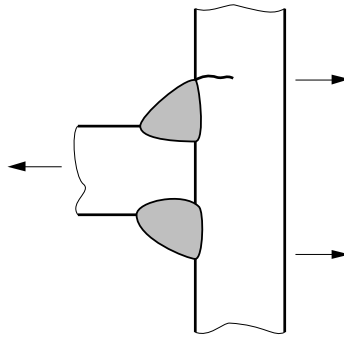
Figure 6.7. *Fatigue cracking of a T-shaped weld when the transverse element undergoes a bending stress*

6.1.3. *Concept of nominal stress*

An elementary weld joint can be regarded as an element with a notched structure, the weld bead constituting the notch. Just as for a notched part, the *extent of the nominal stress range* $\Delta\sigma_N$ is considered to have been extrapolated to the level of the crack initiation point.

Figure 6.8 represents $\Delta\sigma_N$ in the case of an assembly with a transverse stiffener submitted either to tension, or bending. The nominal stress is the distant stress, within the terms of material strength, i.e. without taking account of the local effect due to the weld or to the geometric effect, for example, in the presence of a stiffener for a T-shaped assembly. In tension, this stress is expressed by $\sigma_n = F/S$ (F: force, S: section), and in bending, by $\sigma_n = M.v/I$ (M: bending moment, I: inertia and v distance to neutral fiber).
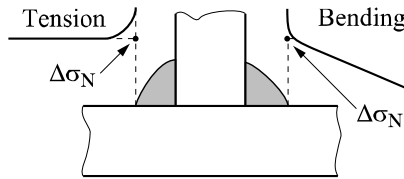
Figure 6.8. *Definition of the varying nominal stress range, $\Delta\sigma_N$, in the case of a fillet weld*

Generally $\Delta\sigma_N$ is used on Wöhler diagrams ($\Delta\sigma$ - N_R), in order to plot the S-N curves (see Figure 6.9).

As will be seen later, the conventional endurance limit 2×10^6 cycles is often taken as a reference. For example, Figure 6.9 presents, for some types of assembly, the admissible stress levels suggested by the International Institute of Welding [CTI 00]. We should notice the relatively low values with respect to the yield strength of the base plate ($R_e \geq 240$ MPa). In fact, these admissible stress values simultaneously express the effect of the numerous parameters involved and the great disparity of test results on assemblies in their as-welded state.

6.1.4. *Factors in welded joint endurance*

The static resistance of a butt welded joint is in general equal to that of the base metal, the rupture occurring away from the weld bead (unless the weld itself is very poor). On the other hand, the fatigue strength is always lower for the welded joint. This varies according to many parameters, primarily relating to the assembly (base metal, added metal, HAZ) and the forces it undergoes (see Figure 6.10).
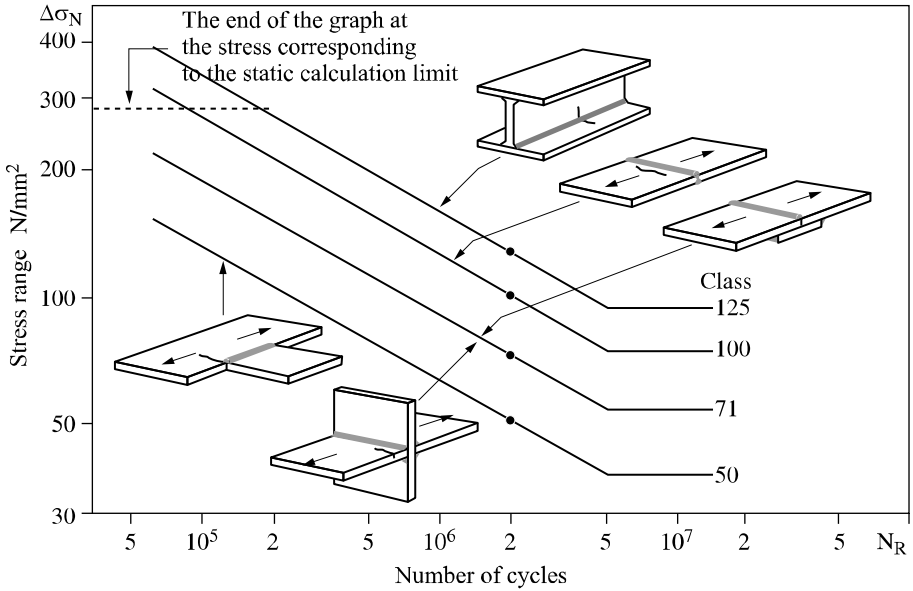
Figure 6.9. *Typical S-N design curves of the IIS and corresponding construction details, showing the fatigue cracking site and the load direction under consideration*
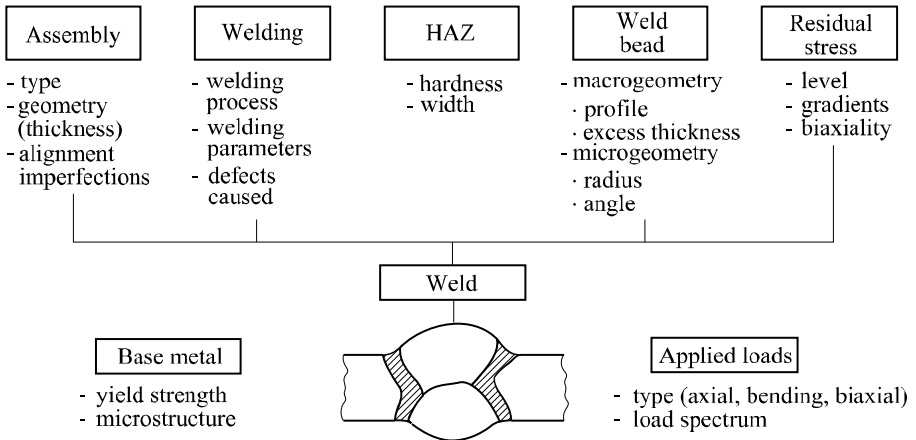
Figure 6.10. *Parameters influencing the fatigue strength of welded joints*

These various parameters which influence the fatigue behavior of welded joints can be put in three categories:

– geometric factors: bead shape, poor sheet alignment, welded element bending, assembly dimensions (sheet thickness, bead geometry);

– metallurgical factors: nature of the base metal, welding process (energy, metal filler product), welding defects, residual stress levels;

– factors related to the load: load pattern (constant or variable amplitude, stress ratio), stress gradient, stress biaxiality, environment.

Each of these many factors generally does not act on its own. Synergetic effects must often be taken into account, thus leading to various in-service stress levels.

6.1.4.1. *Geometric factors*

a) Weld bead shape

We can highlight the total influence of the weld bead by comparing the endurance limits obtained, for butt joints in their as-welded state, to the same welded joints when ground flush [LIE 73].

For flush joints, a slightly lower endurance limit is found (5 to 10%) than that of the base metal, while the endurance limit observed on as welded joints is definitely weaker (30 to 45%) than that of the base metal.

Actually, several authors have shown that it is necessary to consider, on the one hand, the macrogeometric effect due to the general bead profile and, on the other hand, the geometric effect induced by the welding defects located at the connection zone of the bead surface and the base metal skin.

Macrogeometric effect

As a consequence of the nature of welded joints, weld beads involve changes of section leading to stress concentration areas (see Figure 6.11).

If a welded joint is considered as a notched component, we can evaluate the corresponding stress concentration coefficient $K_t = \sigma_{max}/\sigma_{nom}$ (σ_{max}: maximum stress at the notch tip, σ_{nom}: average stress in the section under a component load).
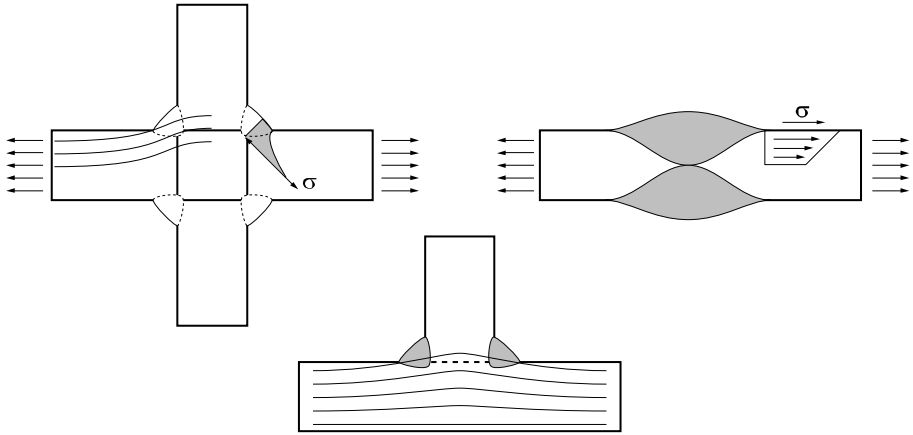
Figure 6.11. *Stress concentration zone in welded joints*

In the case of fillet welded joints, at the point between connection of the base metal and weld bead, values of the stress concentration coefficient ranging between 1.5 and 4.5 have been measured. This coefficient is about 3 for butt welds. These measurements do not take account for defects, which can exist at the point considered, and which can increase this stress concentration locally.

A better weld bead quality leads to an appreciable improvement in fatigue strength.
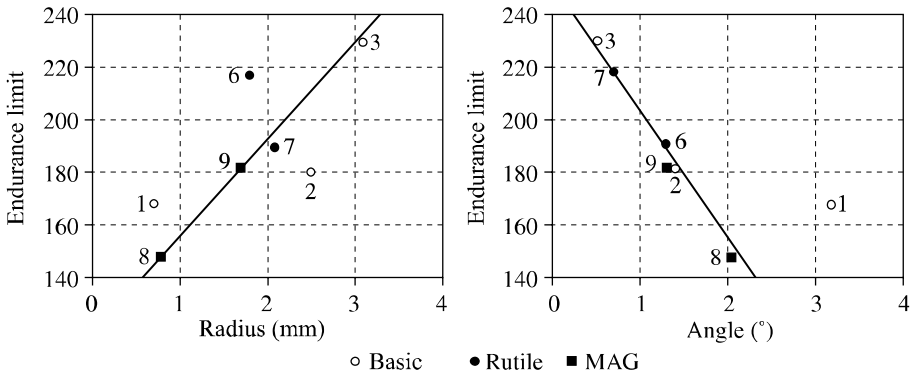
Figure 6.12. *Correlations between the endurance limit of T-shaped assemblies subjected to bending (R = 1) and the weld toe radius or the flank angle [HUT 94]*

For example, in the case of T assemblies submitted to bending loads, Figure 6.12 shows the correlations between the conventional endurance limit, $\Delta\sigma_{2x10^6}$ cycles and the radius $\overline{\rho}$ (at the weld toe radius) or the flank angle $\overline{\theta}$. $\overline{\rho}$ and $\overline{\theta}$ represent the average measurements recorded in each series of assemblies produced by all welding processes in a flat position [HUT 94].

Microgeometric effect

In addition to the stress concentrations caused by section changes, surface defects such as splits, undercuts, unevenness and edge faults, etc. are as just as likely engender failures.

For example, Figure 6.13 shows the role of undercuts on fatigue strength.
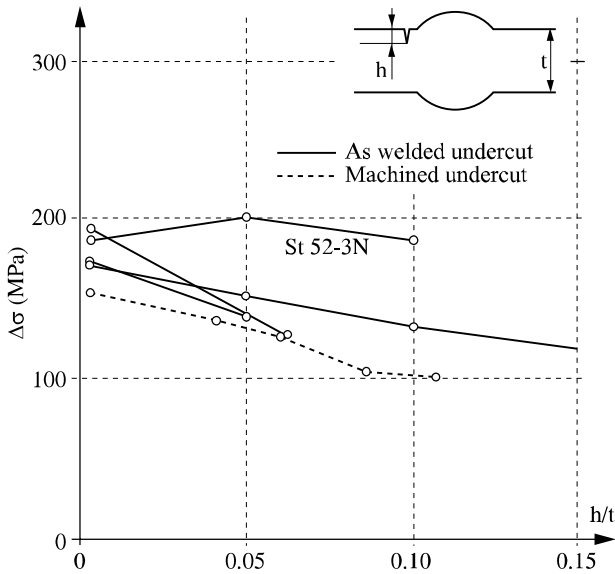
Figure 6.13. *Influence of undercut depth on the endurance limit*

b) Plate thickness

For geometrically similar joints, the fatigue strength tends to decrease as the plate thickness increases [GUR 79]. Figure 6.14 presents the pattern of fatigue lives according to thickness for T assemblies, subjected to bending forces.
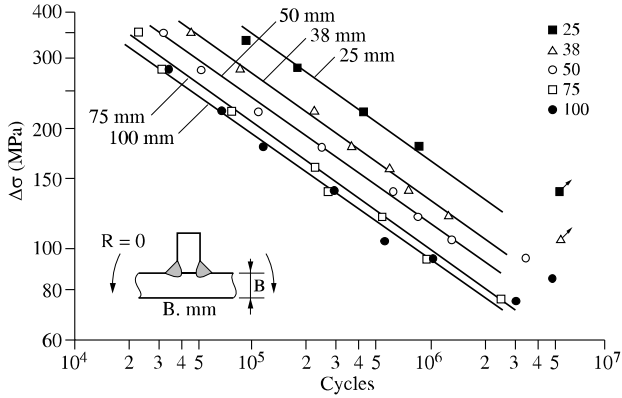
Figure 6.14. *Role of plate thickness on fatigue resistance of T assemblies; from [GUR 79]*

However, it is difficult to separate the effect of the flank angle θ, weld length, s, and plate thickness, t, through experiments; for a given configuration, when s/t decreases, $\Delta\sigma_N$ increases, as Figure 6.15 indicates [GUR 79].

Rather than s, it would undoubtedly be advisable to take into account the embedded plate length, conferred by the assembly [MAD 98] (2 s + thickness of the stiffener).

c) Misalignments

Figure 6.16 presents various axial or angular misalignments which can be found in welded joints. These defects lead to secondary bending moments which are added to the nominal stress.
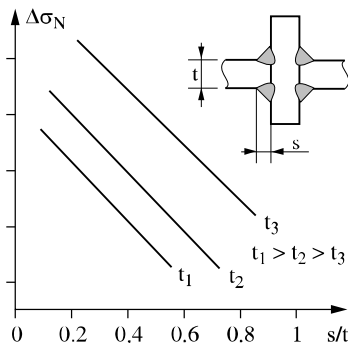
Figure 6.15. *Diagrammatic role of s/t (s: weld length; t: plate thickness) on fatigue strength; from [GUR 79]*
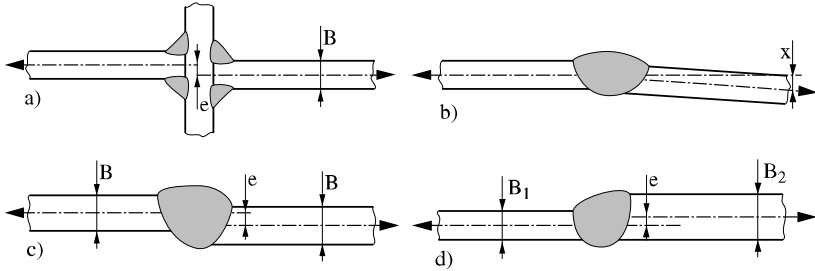
Figure 6.16. *Misalignments: a) axial, in a cruciform assembly; b) angular or c) in a butt welded joint; d) axial, due to a change of thickness in a butt welded joint; from [MAD 80]*

The increase in nominal constraints due to a misalignment can be evaluated by various analytical expressions [MAD 80].

6.1.4.2. *Metallurgical factors*

a) *Internal defects*

Various internal defects can appear in the weld bead: slag inclusions, porosities or lack of penetration. A lack of penetration generally represents a high risk of fatigue crack initiation at the root.

Concerning slag inclusions and porosities, Figures 6.17 and 6.18 show, in the case of a butt welded assembly, that the reduction of fatigue strength must be taken into account.
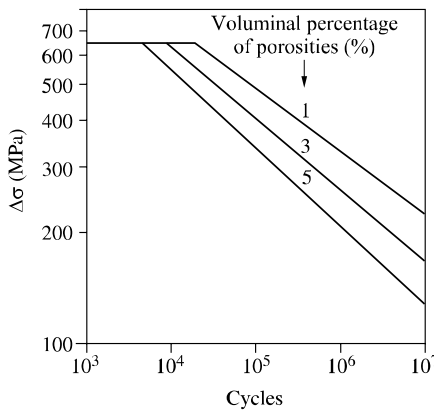
Figure 6.17. *Influence of the voluminal porosity percentage on the endurance of butt welded joints (testing in tension, R = 0); from [GUR 79]*
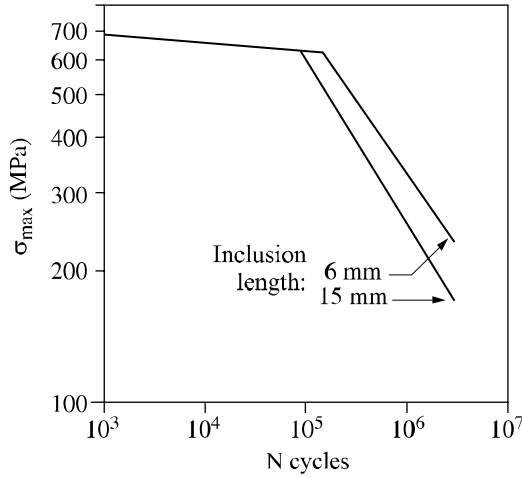
Figure 6.18. *Inclusion lengths influence on the endurance limit of butt welded joints (testing in tension); from [GUR 79]*

b) *Residual stresses*

By definition, residual stresses form a system of internal stresses, in equilibrium, which exist in the absence of an external load. These stresses are generally the result of permanent plastic strains which are produced locally [LIE 97].

In a welded structure, these strains are the result of local heating and cooling cycles associated with welding. When the welded metal cools from the melting point, it tends to contract, but it is restrained by the adjacent base metal. The contraction must then be accommodated by the plastic strain of the filler metal.

This situation is further complicated by technological factors, such as joint type and size, the welding process used and the manner of depositing the filler metal. Nonetheless, the principle of considerable residual stresses existing in the filler metal remains the same.
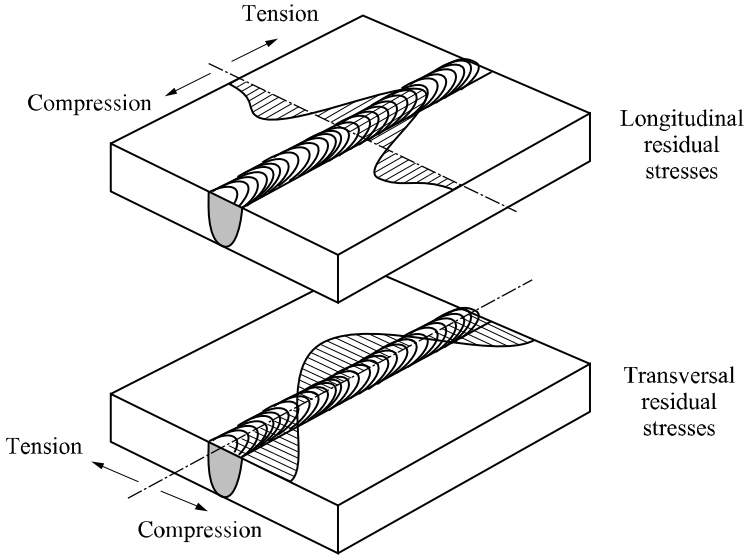
Figure 6.19. *Residual stresses due to welding operation*

In the case of multipass welding, these residual stresses can reach a yield strength close to a sheet's crack initiation point.

Figure 6.19 gives an example of these stresses for a butt welded joint. When the weld is subjected to a load, this residual stress field is added to the cyclic stresses and, if it is under tension, the structure's endurance decreases.

c) *Welding processes*

Generally, a welding process will lead to an optimized assembly endurance provided it gives rise to:

− small defects which are also low in number (TIG welding, welding under a solid flux),

− low residual stresses,

− a favorable weld bead with a low flank angle (automatic welding).

Figure 6.20 shows the test results achieved on specimens of E36 steel, welded manually, resulting in a convex bead, and specimens of the same steel, obtained by automatic welding under a solid flux, producing a concave bead. The fatigue strength of the samples produced by automatic welding is higher than that of the manually welded test pieces by approximately 40%.
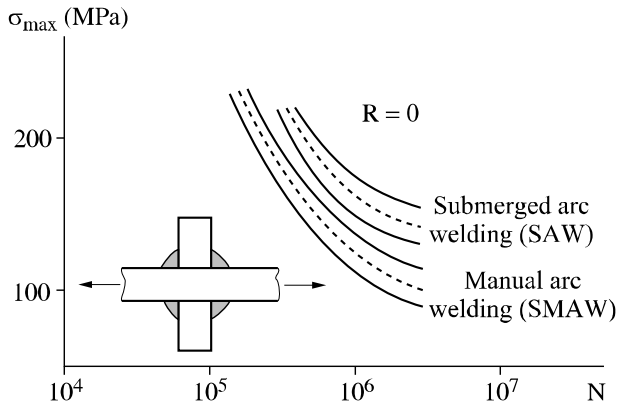
Figure 6.20. *Influence of the welding process on the fatigue strength of a welded joint in E36 steel; from [LIE 73]*

In fact, more than the process, it is the setup of the welding operation which will exert a determining role on the fatigue behavior of assemblies. In particular, for an automatic welding process, the choice of the optimal welding parameters in respect to fatigue performance is a crucial factor.

d) *Nature of the filler metal*

It is obvious that the choice of filler metal depends on the nature of the base metal to be welded. For this choice, it is necessary to take the following points into account.

The filler metal (electrodes, wire) must assure mechanical characteristics of the molten metal compatible with those of the base metal, thus guaranteeing good continuity properties.

Ideally a filler containing little or no hydrogen will be chosen (for example, basic stoved electrodes).

For cruciform assemblies, achieving complete penetration of the filler in the base metal, perfect continuity in the center, and concave beads, leads to a fatigue strength close to that of butt welds. These conditions can be obtained by choosing electrodes with great penetration for the first passes and "shaped" electrodes, with good flow, for the final passes.

e) *Nature of the base metal*

Some joints, in their as-welded state, and formed from mild steel or high strength steels lead to similar $\Delta\sigma$ values, for average low stresses. In this case, the relative insignificance of the yield strength is due mainly to the existence of high tensile residual stresses caused by welding (see Figure 6.21).
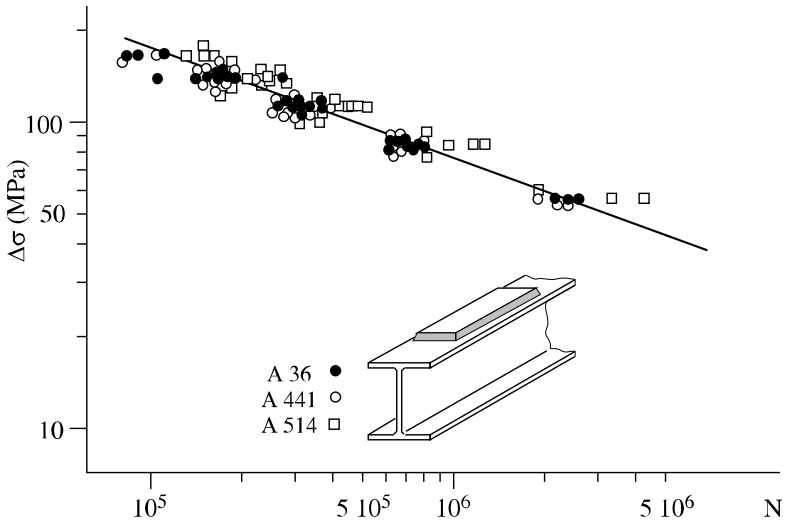
Figure 6.21. *Fatigue strength of welded beams subjected to bending (R>0)*
(A36: YS = 240 MPa; A44: YS = 220 MPa; A 514: YS = 360 MPa)

The advantage of using steels with a higher yield strength is apparent, however, in various situations encountered in reality.

Case of high loads

We observe an improvement in the fatigue behavior of assemblies with an increase in yield strength, either in high stress ranges (medium cycles regime) as shown in Figure 6.22, or in the case of high mean stresses. Figure 6.23 schematizes this latter effect: on a Goodman-Smith diagram, the test results are placed on lines as a function of the mean stress, σ_m; when σ_m is low or zero, the results are comparable. Conversely, the effect of the plate yield strength is apparent when σ_m increases [COL 82]; in the two preceding cases of loading, it is the relation between σ_{max} and YS that we should consider, (with σ_{max}: maximum stress of the load cycle, YS: yield strength of the base metal).
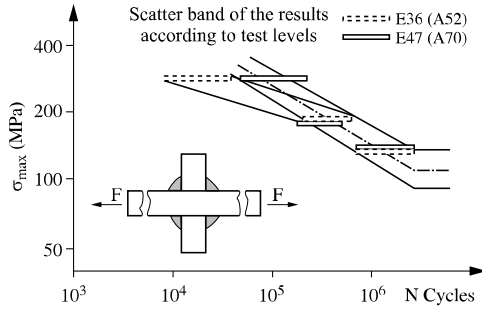
Figure 6.22. *Comparison of the fatigue behavior of E36 and E46 welded joints (tensile-compression test); from [LIE 73]*

Case of variable amplitude loading

Such loading encountered on an in-service structure generally comprises a small number of high stress range cycles. In this very general case, it is often advantageous to use steels with a high yield strength.

Case of low K_t assemblies

Figure 6.24 illustrates the favorable effect achieved by an increase in the yield strength of the base plate steel on the conventional endurance limit $\Delta\sigma_{2x10^6}$ for an as-welded butt assembly with low excess thickness [RAB 79].
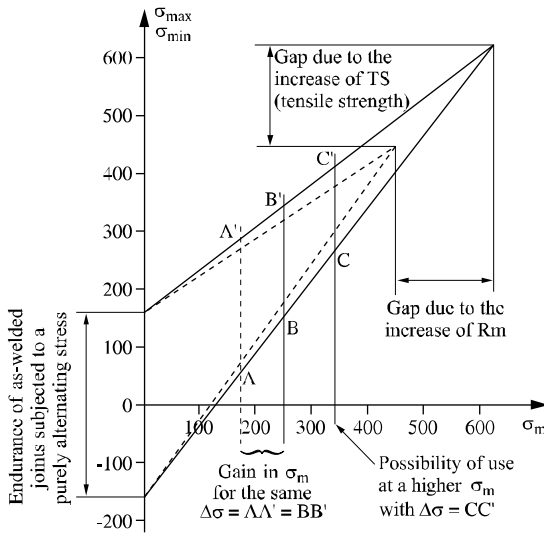
Figure 6.23. *Increase in the fatigue strength subjected to undulating stress by use of a higher performance steel; from [COL 82]*
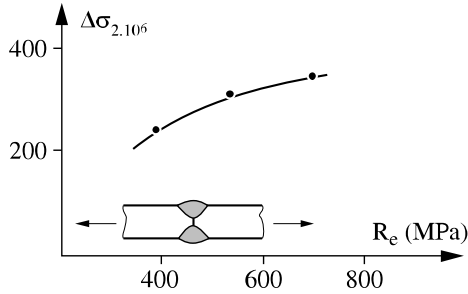
Figure 6.24. *Effect of the yield strength of plate steel on the endurance limit of butt welded joints (R = 0); from [RAB 79]*

f) *Finishing treatments*

The effect of finishing treatments (grinding, hammering or re-melting of the weld bead toe, shotpeening of pre-stressed welding, etc.) highlights substantial improvements (as much as doubling fatigue limits) in the fatigue behavior of welded joints, increasing with the yield strength of the base metal [LIE 91].

6.1.4.3. *Nature of applied loads*

Load pattern

In the case of interpenetrated beads, the comparison of results obtained, either in tension or in bending, reveals different stress gradients in the vicinity of the weld toe. The influence of these gradients leads to a reduction in the fatigue strength, for example by a thickness of a given plate, when the load passes from bending to tension.

For example, in the case of a butt welded steel assembly in E490 (thickness 8 mm), the fatigue strength $\Delta\sigma_{2\times10}{}^6$, determined by bending (R = 0.1), is 30% higher than that found in repeated tension.

In addition, an assembly subjected to bending is much less sensitive to a lack of penetration than the same assembly subjected to tension. This behavioral difference is explained by a different distribution of local stresses, either at the weld toe or at the weld root [LIE 92].

Stress ratio (R = $\sigma_{min}/\sigma_{max}$)

The stress ratio value (or the mean stress of the load cycle) has a certain influence on the endurance characteristics.
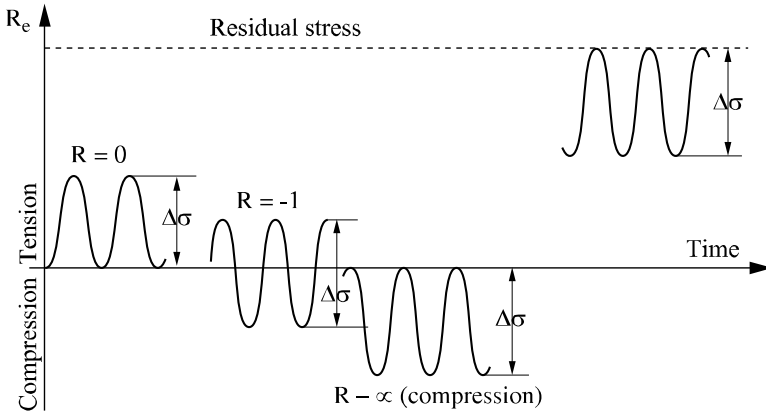
Figure 6.25. *Effective stress level resulting from the superposition of the residual and external stresses*

If $\Delta\sigma$ is the fatigue strength for 2×10^6 cycles corresponding to a given level of R, the following expression can be written:

$$\Delta\sigma_{-1}/\Delta\sigma_0 = 1.25 \text{ and } \Delta\sigma_{-0.5}/\Delta\sigma_o = 0.85$$

These relationships were obtained using tests carried out on small scale samples, taken from real structures. Consequently, the residual stress level in the samples was relatively low (even nil) with respect to that corresponding to a real structure.

In practice, when high residual stresses (close to YS) are expected to be present and that it is not possible to measure them, or to carry out a thermal relief treatment, it is accepted (see Figure 6.25) that, whatever the level of R, the maximum stress is equal to the elastic limit.

In a Goodman diagram (σ_{max} or σ_{min} as a function of σ_m), this practice amounts to considering the extent of admissible stress corresponding to a maximum stress equal to YS (see Figure 6.26).
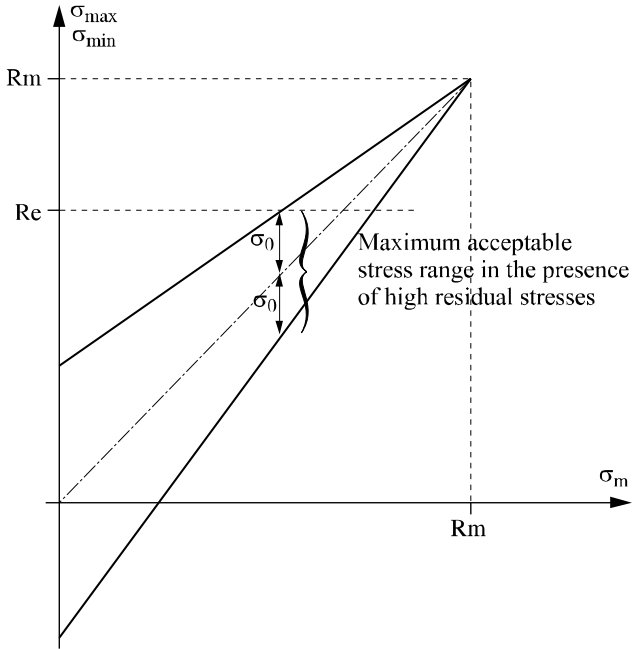
Figure 6.26. *Determination, on the Goodman diagram relative to the welded joint, of the maximum acceptable stress range in the presence of high residual stresses [COL 82]*

Complex loading cases

Few results in the literature relate to examples of complex loading. Such cases are however envisaged in certain calculation methods. Generally, we consider the maximum principal stress applied perpendicular to the bead [CTI 00].

6.2. Dimensioning of joints in mechanized welding

Fatigue behavior is a major concern to designers of mechanized welded structures. Several design methods are proposed in the literature [LIE 00a]. The advantages and disadvantages of each method are presented here. Taking into account the current context, two methods are described in more detail: a method based on the extent of nominal stress and a method based on geometric stress [LIE 00b].

6.2.1. *Position of the problem*

The service lifespan of welded structures is indeed largely governed by the cyclic loading to which it is subjected. This must be evaluated for each assembly, starting from an understanding of the load applied. In fact, several design methods have been proposed (see Table 6.1) which offer many advantages and disadvantages.

The more general method based on the concept of nominal stress range, $\Delta\sigma_n$ is that currently recommended in procedures. It is based on a network of S-N curves (or $S = \Delta\sigma_n$ and N: the number of cycles to failure) corresponding to the principal construction details used.

The geometric structural stress method aims to reduce the number of S-N curves, by taking into account the effects of stiffness achieved by the geometry of a given assembly. It requires finite elements calculations or extensometric measurements, in order to define, on each assembly of a structure, the corresponding geometric structural stress. This method is mentioned in the recent regulations.

The use of stress or strain at the notch tip requires a precise definition, not only of the assembly's geometry, but also of the local geometry right at the potential starting point of a fatigue crack, such as the weld toe. This local geometry varies along the weld toe depending on the welding process and renders such a definition problematic.

METHODS				
Extent of nominal stress	Hot spot methods		Fracture mechanics	Local strain range
	Geometric structural stress	Stress at notch base		
Advantages				
Validated S-N curves taking account of the geometric effects of: *the assembly the weld*.	Just one curve for all the assemblies. The variations in weld quality are included.	Clear definition of the stress. The S-N curve takes account of the effects of the geometry of: *the assembly the weld*.	Just one crack curve is enough for all the assemblies. Usable only on cracked structures.	Only one curve Δε - N is enough for all the assemblies.
Disadvantages				
Difficulty of application for new types of assemblies. Difficulties of defining the nominal stress in the case of: *complex structures combined loads.*	The geometric stress largely depends on the extrapolation method used: *measurements by gauges finite element calculations*.	Difficulty in evaluating the maximum stress due to the local variations in the welding geometry: *either by gauge or by finite element calculation.*	Inaccurate method because it does not take into account the effects of the local geometry of the weld: ($N_{initiation} = 0$).	Difficulty in evaluating the local strain range of the weld geometry.

Table 6.1. *Various design methods*

Fracture mechanics considers the structure once it is cracked and thus does not take into account the crack initiation phase, which is largely influenced by the quality of welding. The fatigue lives obtained are thus by default.

In light of their current importance, we will use this chapter to deal with the first two methods.
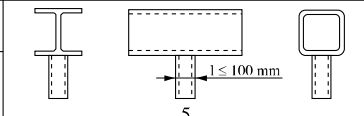
6.2.2. *General method (current regulations)*

In the contemporary fatigue regulations (for example, Eurocode 3, the procedure for civil engineering), S-N curves are used to dimension a welded joint [EURO 92]. The equation for these curves is $N = C.S^{-m}$, where N is the number of cycles, S the nominal stress range and C, m the coefficients dependent on the welded joint. A detailed catalog of the curves is provided, making it possible to determine which class the assembly under consideration belongs and which S-N curve is applicable. The class generally corresponds with the characteristic value (acceptable) of the nominal stress range at 2×10^6 cycles (see Figure 6.27).

The S-N curves giving the number of acceptable cycles for *constant amplitude loading* have the following equation: $N = C.\Delta\sigma^{-m}$, with $m = 3$ and a conventional stress limit defined at 5×10^6 cycles.

For *variable amplitude* loading (in service), the S-N curves to be selected, applying the cumulated damage method (Miner's rule), are expressed by $N = C.\Delta\sigma^{-m}$ with $m = 3$ for $N < 5 \times 10^6$ cycles, $m = 5$ for $N > 5 \times 10^6$ cycles and a truncation limit for $N > 10^8$ cycles.
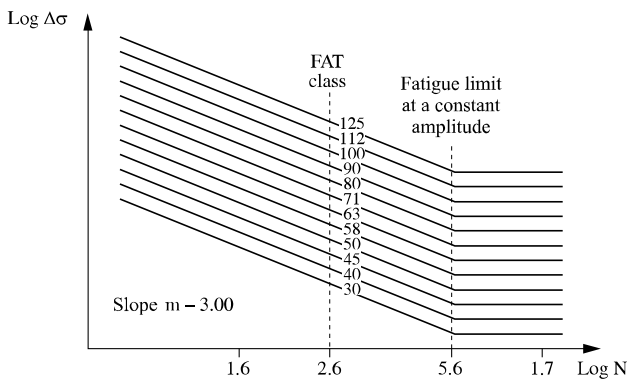
Figure 6.27. *Catalog extract and S-N design curve*

The quality of the weld must conform to that required by the current welding regulations.

6.2.3. *Verification methods*

In the case of constant amplitude loading, checking or dimensioning a fatigue welded structure amounts to checking the following expression:

(for a given number of cycles , *n*) knowing that: $\Delta\sigma_{S,k}.\gamma_F \leq \dfrac{\Delta\sigma_{R,k}}{\gamma_M}$

$\begin{cases} \Delta\sigma_{S,k} & \text{stress range applied to the structure (loadings), } \gamma_F \text{ safety factor} \\ \Delta\sigma_{R,k} & \text{design stress range, } \gamma_M \text{ safety factor} \end{cases}$

or to check $n \leq N$ with *n* the number of cycles applied and *N* the number of cycles to failure for stress $\Delta\sigma_s$.
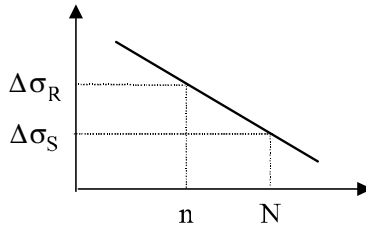
Figure 6.28. *Checking welded structure under fatigue conditions in the case of constant amplitude loading*

The general methodology of fatigue verification is described in Figure 6.29.

Advantages and disadvantages

This method is relatively simple to use if the nominal stress is clearly defined and the type of assembly indexed in the catalog. On the other hand, in the general case (complex structure/loading), the nominal stress cannot always be defined in terms of the resistance of materials and the reference frame is unknown.

Moreover, nominal stress does not take account of the assembly's geometry. For example, it does not consider the presence of a welded fastener, or of that of the corresponding weld bead, and therefore of the stiffness imparted by them. This is why an S-N curve exists for each type of assembly and that, for the same assembly, there can be several curves, depending on the dimension of the assembly and the type of loading.
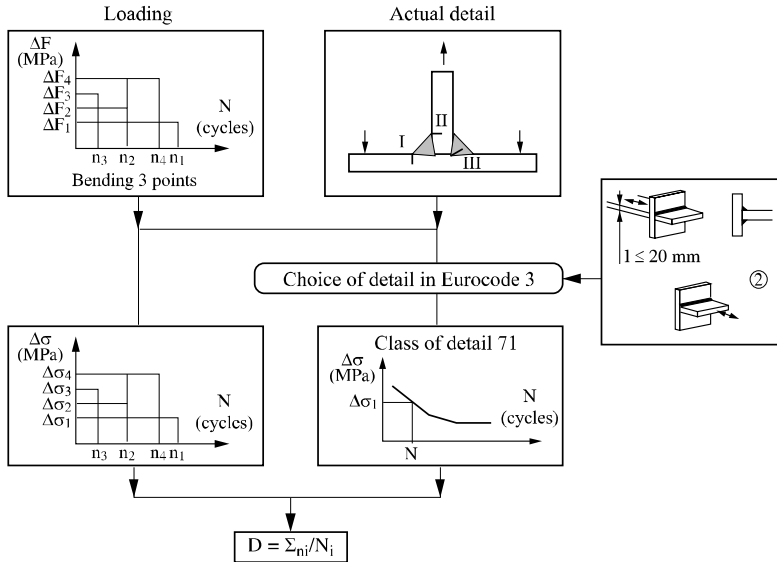
Figure 6.29. *Logigram of the general method*

6.2.4. *Geometric structural stress method*

6.2.4.1. *Principle of the method*

It thus seems sensible to use another stress definition that takes account of the geometric effects of the welded connection, which includes not only the total geometry of the assembly but also the shape of the weld bead, the profile of connection between this bead and the base sheet metal, and, possibly of very local notch effects (see Figure 6.30).

Nevertheless, the definition of local stress is fraught with difficulty, both experimentally and in calculation; moreover, such a stress is random in value because of local geometric variations caused by welding operations. It is however obvious that the value of this local stress governs the fatigue life of the assembly to a certain extent. This stress particularly influences the duration of fatigue crack initiation.

Consequently, an intermediate step consists of adopting as a dimensioning stress the geometric stress, σ_G, which depends only on the assembly's geometry and loading.

This method applies only for initiation at the weld toe, where the concept of geometric welding quality has some relevance.

The advantage of establishing S-N curves in geometric structural stress, as compared to existing curves which are established in nominal stress, is that we are then able to use only one S-N curve whatever the loading and whatever the geometry, for the same group of assemblies (for example fillet welds). Moreover, for real structures, where the nominal stress (distant stress) is often difficult to define, in particular because of the proximity of other connections, the geometric structural stress can be evaluated starting from finite element calculations on the whole of the structure and the assembly under consideration.

Moreover, starting from these S-N curves, certain assembly configurations not currently in the codes can be dimensioned. Thereafter, the use of the geometric structural stress makes it possible for S-N curves to be determined according to the welding quality, and thereby account for the local geometry of the weld bead.

However, there is not, at present, any general method to determine the geometric structural stress nor an associated S-N curve to cover every type assembly group for welded plates. On the other hand, such a method is clearly defined and used in the case of tubular assemblies in offshore oil rig construction, and in the case of assemblies of thin sheet steel in the automotive field [FAY 95].
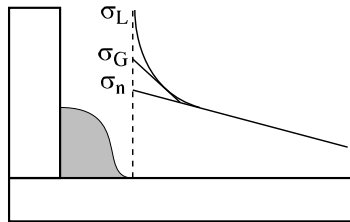
Figure 6.30. *Definition of local (σ_L), geometric (σ_G) and nominal (σ_n) stresses (example: assembly subjected to bending stress)*
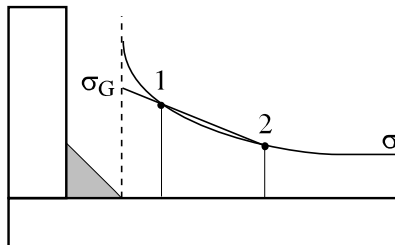
Figure 6.31. *Stress gradient, extrapolation*

6.2.4.2. *Definition of geometric stress*

In Eurocode 3, the geometric stress is defined as: "the maximum principal stress in the parent metal, at the weld toe, taking into account the effects of stress concentration, due to the overall geometry of a particular detail of construction, but excluding the effects of local stress concentration, due to the geometry of the welding and discontinuities in the bead and the adjacent parent metal".

Geometric structural stress is thus an aspect of design or dimensioning which takes account of the total geometry of the assemblies and the loadings; it thus does not have a physical meaning since it does not take account of the actual weld geometry of the bead. It is determined right from the weld toe, as representative of the stresses at the intersection (see Figure 6.31).

It can be obtained numerically by using the finite element method. The advantage of the finite elements method lies in it allowing the definition, not only of the maximum stress value, but also the point of greatest loading (hot spot) as well as the the stress field configuration throughout the structure.

Possible fields of application

In the case of structural analyzes, where the nominal stress is easy to determine and where the object to be calculated exists in procedural catalogs, the traditional method (S-N curve in nominal stress) can be used.

In the other cases, the geometric structural stress must be determined starting from a finite elements calculation, and this must be associated with S-N curves determined with the same definition of the geometric structural stress.

Determination of structural geometric stress

The finite elements method used must satisfy two criteria:

– evaluate a stress field, in the vicinity of the weld toe, as near to reality as possible,

– lead to a fast and inexpensive application.

For this, the type of element selected must be as simple as possible. All the elements located along the intersecting line of a surface must have the same dimension, or at least be in the direction perpendicular to the intersection; it is thus possible to the results being undesirably affected by the mesh size. In addition, it is important that the points where the stresses are calculated (Gaussion points) are correctly placed, i.e. outside the zone which has a 3D behavior, and if possible directly associated with the weld toe.

6.2.4.3. *Practical use of the method*

The method of geometric constraint applies to the points described hereafter.

Definition of the S-N design curve in structural geometric stress

The S-N design curve, in structural geometric stress, can be determined starting from tests carried out on assemblies for which the extent of calculated or measured stress is expressed in geometric stress and the number of cycles is that defined for this level of stress range according to the failure criterion [HUT 92].

Figure 6.32 presents the steps followed to determine the S-N curve, *in structural geometric stress.*
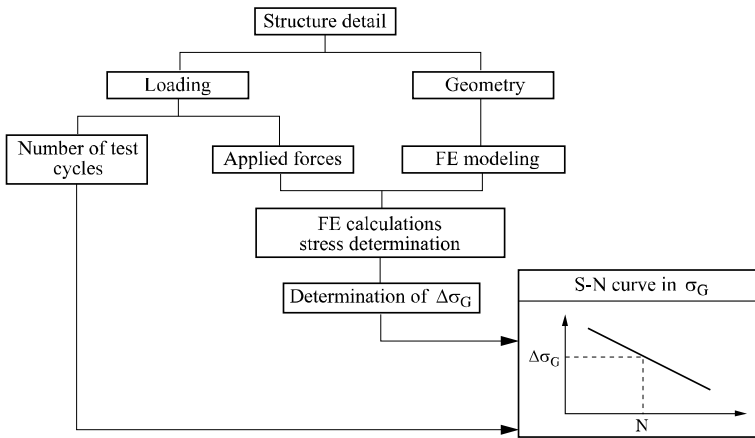
Figure 6.32. *Procedure followed to determine the S-N curve in geometric stress*
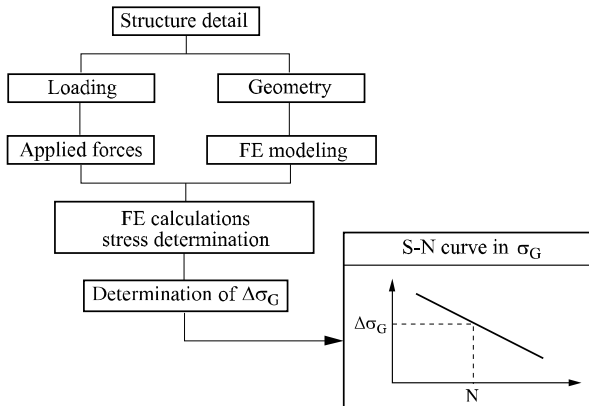
Figure 6.33. *Procedure followed to determine the fatigue life of the assembly*
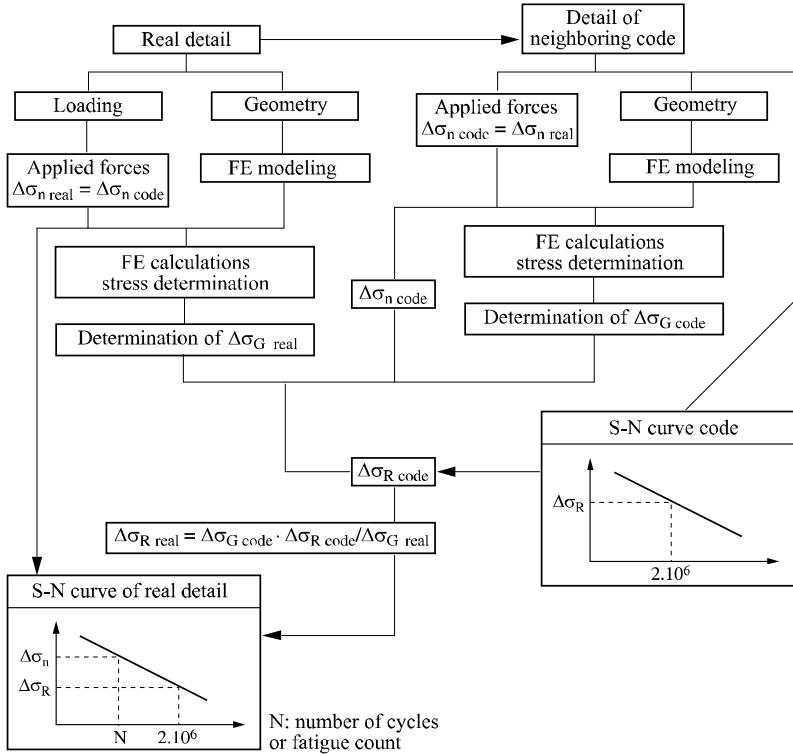
Figure 6.34. *Procedure followed to deduce the new S-N curve of the subject considered*

Calculation of the fatigue life of an assembly

Knowing the S-N curve in geometric (structural) stress for the type of assembly to be checked, the geometric stress method makes it possible to determine the fatigue life of the assembly, N (see Figure 6.33).

Determination of the S-N design curve in nominal stress, of a new construction detail

In the absence of experimental results, the geometric (structural) stress method can be applied to the determination of the S-N design curve, in nominal stress, of a construction object close to a case of the standard catalog or of the regulations [HUT 92].

In this case, we initially proceed with numerical modeling, both of the assembly considered and that of the catalog, before deducing the new S-N curve of the subject under consideration (see Figure 6.34).

6.3. Bibliography

[COL 82] COLLECTIF, *La résistance à la fatigue des assemblages soudés à l'arc en acier de construction métallique*, Collection ATS-OTUA, 1982.

[COL 85] COLLECTIF, *Guides pratiques sur les ouvrages en mer*, *Assemblages tubulaires soudés*, Editions Technip, 1985.

[CTI 00] CTICM, Recommandations pour la conception en fatigue des assemblages et des composants soudés, IIS – Document XIII – 1539-96, CTICM, 2000.

[EUR 92] EUROCODE, Design of Steel Structures – Chapter 9: Fatigue EUROCODE 3 (1992).

[FAY 95] FAYARD J.L., BIGNONNET A., DANG VAN K., "Fatigue design of welded thin sheet structures", *Fatigue Design 95*, vol. II, September 1995.

[GUR 79] GURNEY T.R., *Fatigue of Welded Structures*, Cambridge University Press, 1979.

[HUT 92] HUTHER M., PARMENTIER G., HENRY J., Hot spot stress in cyclic fatigue for linear welded joints, IIS – Document XIII – 1466-92, 1992.

[HUT 94] HUTHER I., PRIMOT L., LIEURADE H.P., JANOSCH J.J., COLCHEN D., DEBIEZ S., "Influence de la qualité de la soudure sur la résistance à la fatigue d'un acier HLE du type E460", *Tôle en acier HLE, choix et mise en volume*, Publications CETIM, 1994.

[HUT 99] HUTHER I., GORSKI S., LIEURADE H.P., LABORDE S., RECHO N., "Longitudinal non-loaded welded joints, geometric stress approach", *Welding in the World*, vol. 43, no. 3, p. 20-26, 1999.

[LIE 73] LIEURADE H.P., "La résistance à la fatigue des assemblages soudés", *Journées "Métallurgie du soudage"* (Société Française Métallurgie), Marseille, 8-9 November 1973.

[LIE 91] LIEURADE H.P., BIGNONNET A., "Les techniques d'amélioration de la tenue en fatigue des composants soudés", *Traitements de surface et composants mécaniques*, Editions CETIM, p. 79-112, December 1991.

[LIE 92] LIEURADE H.P., WYSEUR M., TOURRADE J.C., "Effet de traitements de parachèvement sur le comportement en traction ondulée ou en flexion ondulée d'assemblages bout à bout en acier E 490", *La fatigue des composants et des structures soudés*, Publication CETIM, 1992.

[LIE 97] LIEURADE H.P., "Rôle des contraintes résiduelles dans le comportement en fatigue des composants soudés", *Revue Française de Mécanique*, no. 1997-3, p. 191-205, 1997.

[LIE 00a] LIEURADE H.P., HUTHER I., "Introduction aux méthodes de dimensionnement à la fatigue des composants soudés", *Mécanique et Industrie*, vol. 1, no. 5, p. 465-477, 2000.

[LIE 00b] LIEURADE H.P., HUTHER I., "Dimensionnement des assemblages soudés en mécano-soudage, Calcul à la fatigue", *Soudage et Techniques convexes*, p. 3-8, May-June 2000.

[MAD 80] MADDOX S.J., Effect of misalignment on fatigue strength of transverse butt welded joints, IIS – Document XIII – 972-80, 1980.

[MAD 98] MADDOX A., Private comm., 1998.

[RAB 79] RABBE P., BLONDEAU R., CADIOU L., "Emploi des tôles à haute limite d'élasticité dans les constructions soudées sollicitées en fatigue", *Actes du Congrès sur les aciers à haute limite d'élasticité*, Versailles, January 1979.

Chapter 7

Fracture Toughness of Welded Joints

7.1. Ductile fracture and brittle fracture

In general, manufacturers dimension structures to avoid the risks of failure in service, by avoiding in particular any going beyond, even local, of the yield strength of the material. In spite of that, failures do occur, for various reasons:

– exceptional load conditions;

– progressive cracking related to fatigue, stress corrosion, hydrogen embrittlement;

– behavioral change related to a transition of the ductile-brittle type, which originates in a temperature fall.

Brittle fracture, due to the loss of plasticity, was first studied as early as the second half of the 19th century.

With the development of welding and its application to the construction of large-scale structures, a certain number of spectacular, often catastrophic, failures have occurred. Among the most famous examples we might recall bridge failures (at Berlin Zoo in 1936, in Rudesdorf and Hasselt in 1938) and storage tank failures. Of nearly 5,000 ships built by mechanized welding during World War II, a quarter of them presented important failures and more than 200 suffered catastrophic failure.

The Schenectady oil tanker at anchor, without any particular excess loading, one night in winter 1942 is the classic example (see Figure 7.1).

Chapter written by Marc BOUSSEAU.

From immediately after the War, considerable work was undertaken in order to understand the phenomenon and to reduce the risks. The teams of the *Naval Research Laboratory* in Washington have been at the center of a great deal of work, particularly with W.S. Pellini and G.R. Irwin, which are still valid points of reference today. They concentrated on the study of the ductile-brittle transition temperature and the development of fracture mechanics concepts, taking into account weld defects.

In parallel with the studies of mechanical engineers, metallurgists have devoted much energy to:

– the development of steel types that are easier to weld (by lowering the carbon equivalent), offering higher levels of yield strength while having an increasingly lower ductile-brittle transition temperature;

– the development of welding processes to reduce brittleness and the presence of defects.
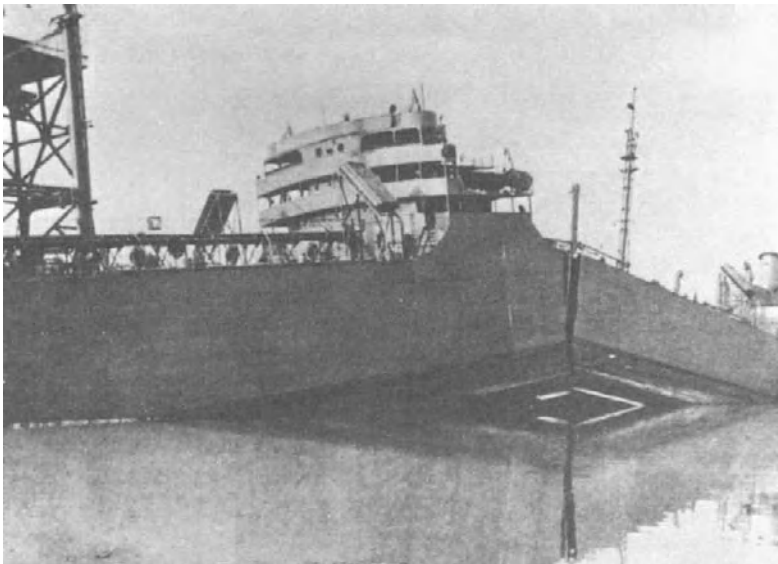
Figure 7.1. *Failure at anchor of the Schenectady tanker*

Despite all these efforts, other failures continued to occur (bridges, pipelines, pressure vessels, ships, etc.). As Toyoda has demonstrated [TOY 00], a considerable amount of the damage noted at the time of the Kobe and Northbridge earthquakes was attributed to concomitant circumstances:

– raised stress load levels, to which residual stresses can be added;

– presence of stress concentrations due to the geometry of the assemblies, possibly with the presence of defects in the form of cracks;

– materials with a low resistance to in-service temperature.

Within the International Institute of Welding (IIW), which meets annually, there is commission X whose work is devoted to the study of the failure of welded structures. The main themes tackled relate to operational suitability, taking account of heterogenities between the base metal and molten metal (characterized by *mismatching*) and the role of residual stresses. A working group was created with the aim, amongst other things, of analyzing the causes of failure in mechanized welded structures.

The work of the IIW is relayed to France within the framework of the advisory committee of research into welding rupture, a mirror image of commission X. This advisory body (CCRS) receives the support of l'Institut de Soudure (French Institute of Welding) and la Société des Ingénieurs Soudeurs (SIS).

7.2. Evaluation of fracture risks in metallic materials

The evaluation of the fracture risks of structural steels was initially tackled by means of the ductile-brittle transition temperature. Later, the introduction of the concept of toughness made it possible to judge the influence of a plane defect according to the load conditions. In all cases, tests have been developed in order to characterize the base materials.

7.2.1. *Determination of the ductile-brittle transition temperature*

Initially, research was concerned with understanding the ductile-brittle transition of base materials, using the Charpy test with toughness test specimens and the Pellini, Batelle, Schnadt tests [SAN 74].

The impact bending test, which replaced the impact test or Charpy test, continues to be widely used to evaluate the ductile-brittle transition temperature. In general, the test-specimens are parallelepipedic bars ($55 \times 10 \times 10$ mm^3) with a 45° V-shaped notch 2 mm deep. The fracture is obtained using a Charpy pendulum (see Figure 7.2).

Some specimens are tested at various temperatures in order to plot the curves:

– impact bending energy (expressed in J) according to the temperature (see Figure 7.3),

– level of crystallinity according to the temperature,

– lateral expansion (related to plastification) according to the temperature.

From these curves, we can in particular determine the bending energy corresponding to the ductile stage as well as the temperatures corresponding to:

– the ductile-brittle transition (Tt),

– 50% of crystallinity,

– the fracture energy at 28 J.

In fact the transition temperature is not an intrinsic property of the material. It is established that this increases with:

– increase in part thickness,

– increase in the loading speed,

– the increase in sharpness/angle at the notch bottom.

K. Kalna [KAL 00] gives a formula making it possible to evaluate the influence of the transition temperature TT_h for a structural element of thickness h:

$$TT_h = T_{50\%} + 30\ln\left(\frac{h}{10}\right)$$

where $T_{50\%}$ corresponds to the transition temperature for an impact bend test specimen 10 mm in thickness.

Between the deformation speed $\dot{\varepsilon}$ and the transition temperature there exists an expression of the type:

$$\dot{\varepsilon} = A\exp\left(-\frac{Q_A}{RT}\right)$$

where A is a constant, Q_A is the activation energy of the phenomenon, R is the constant of perfect gases and T is the absolute transition temperature.
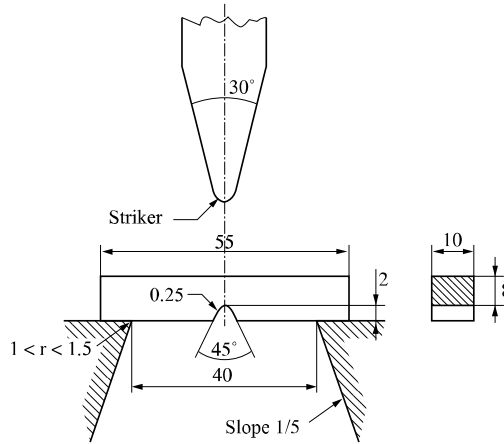
Figure 7.2. *Impact bend test specimen; from [NF 90]*
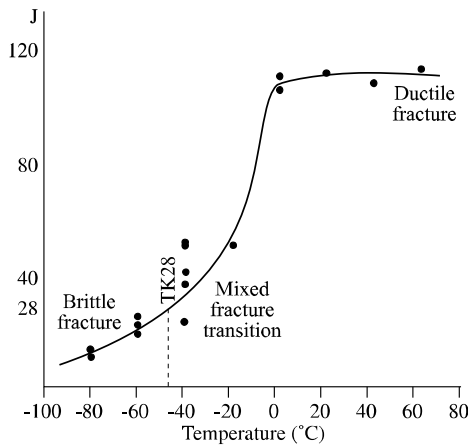
Figure 7.3. *Ductile-brittle transition curve; from [BAL 97]*

Moderate in cost, the Charpy test continues to be widely used and is still, after 100 years in existence, the object of many studies – as the congress organized in 2001 on this topic testifies.

At the beginning of the 1970s, work relating to the apparatus for impact bending testing was undertaken in order to highlight the various phases of fracture propagation by analysis of force-time graphs [SAN 69]. Since 1995, the working group "Instrumented Charpy" of the SF2M have led a study intended to numerically

simulate the impact test by a finite element calculation in the brittle field. From these results, by using the local approach of the mechanic fracture, it is possible to evaluate the material's toughness. The work of Rossol on pressure vessel steel 16MnNiMo5 constitutes an interesting contribution in this field [ROS 98].

Among the various fracture tests developed by Pellini [PEL 71], we will consider the *drop weight test*, which consists of dropping a mass from a given height on a specimen comprising a notched brittle weld deposit (see Figure 7.4). The specimen is subjected to bending and its deformation is limited. Under the effect of the shock the bead breaks, which creates a fine crack crossing the *heat affected zone (HAZ)*. Depending on the temperature at which the test is carried out, the crack spreads to a greater or lesser extent in the base metal. We can, by a framework, determine the highest temperature leading to the fracture of the test specimen (see Figure 7.5). This temperature is called the NDT (*nil ductility transition*). With the original aim of forming steel for ship hulls and submarines, it was then applied to steels for vessels in nuclear installations. The standard defining the Pellini test underwent modifications with regard to the method of bead deposit [AST 95].
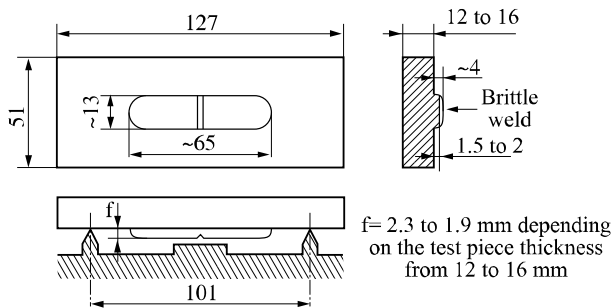
Figure 7.4. *Dimensions of the Pellini test-piece; from [LEI 71]*
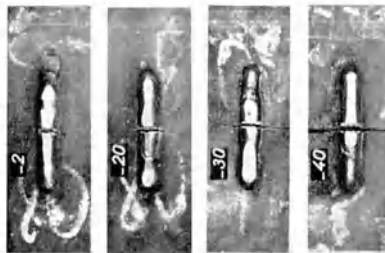
Figure 7.5. *The NDT lies between -20 and -30°C; from [LEI 71]*

As for the Charpy test, studies have been carried out in order to record the load evolution during the impact [SAN 69], thereby to allow a finer analysis of the different fracture phases [FRO 82, WIE 99].

By the early 1970s IRSID had undertaken a systematic comparison between the results obtained from the various tests, considering a wide range of steel types. Correlations were established, showing that the classification of steels is modified little by the choice of tests [SAN 70, SAN 74]. Thus, between temperature NDT obtained by the Pellini test and the temperature giving an energy of 35 J/cm^2 (TK 35), starting from 67 data, the following expression:

(NDT) = -16 + 0.5l(TK35)

is proposed, albeit with a rather low correlation coefficient (0.80).

7.2.2. Determination of a fracture criterion in the elastic linear field

The development of the concepts of fracture mechanics at the beginning of the 1960s in the USA made it possible to take defect dimensions into account in the evaluation of the fracture risks. This was achieved by introducing the concept of stress intensity factor K_I through the formula:

$$K_I = \alpha\sigma\sqrt{\pi a}$$

where α is the coefficient dependant on the geometry of the part and the crack, σ the nominal stress and a the dimension of the crack.

The break occurs when K_I reaches the critical value K_{IC}.

The La-Colle-sur-Loup Summer School of September 1970, which was devoted to the fracture process, marked the nascent interest of various sectors of French industry in this new branch of mechanics. The texts of the conferences gathered by D. François [FRA 72] are still used today as a reference in this field.

The determination of the critical stress intensity factor K_{IC} [AST 97] has been applied in various industrial sectors using high elastic limit steels. In France standard NFA 03-180 [NF 81], intended for iron and steel products, defines the test-specimens, the conditions under which they are taken, the conduct of tests and the analysis of results. To obtain a valid value K_{IC}, various conditions must be fulfilled. In particular, when we are concerned with the extent of the plastic zone, this must be small compared to the dimensions of the test-specimen. As a result, in the case of

ductile materials, it necessitates the use of large-sized specimens. Indeed, it is necessary that the thickness B is such that:

$$B \geq 2.5 \left(\frac{K_{IC}}{R_{p0.2}} \right)^2$$

$R_{p0.2}$ being the yield strength of the material.

Strictly speaking, this standard applies only to homogenous steels. However, in the absence of specific documents, it has also been applied to other materials as well as to welded joints.

Among the standardized test-pieces most commonly used, the bend test specimen and the compact tensile (CT) specimen should be mentioned and are illustrated in Figure 7.6. The mechanical notch is prolonged by a fatigue crack in order to obtain as low a radius as possible at the extremity. It is important that the crack has the same length on the two faces of the specimen and is of similar internal configuration.
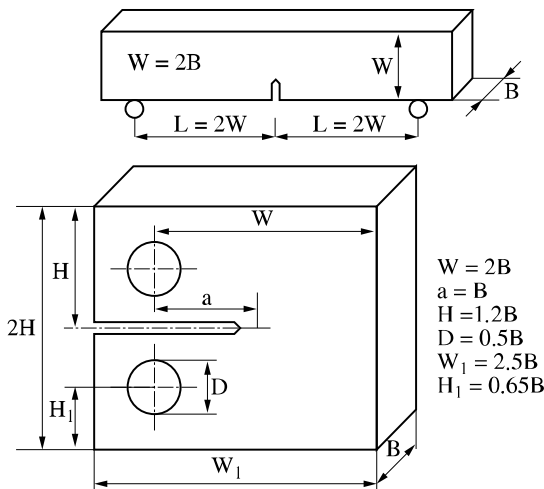
Figure 7.6. *Three point bend test and CT specimens; from [SAN 78]*

The critical stress intensity factor K_{IC} applies in the case where the plastic zone at the crack's extremity is small compared to the structural dimensions and thus applies mainly in the case of materials with low ductility or ductile materials of significant thickness.

Like the impact bending energy, the toughness of materials with a centered cubic structure varies according to temperature. It decreases with a fall in temperature; consequently, for a given defect failure can occur at a lower level of loading.

Much work demonstrates that the load speed of application influences toughness. The curve $K_{IC} = f$ *(temperature)* is shifted towards the right when the load speed increases, as illustrated in Figure 7.7 (taken from a study of Sanz and Marandet) relating to pressure vessel steel 16 MnNiMo5 [SAN 78].
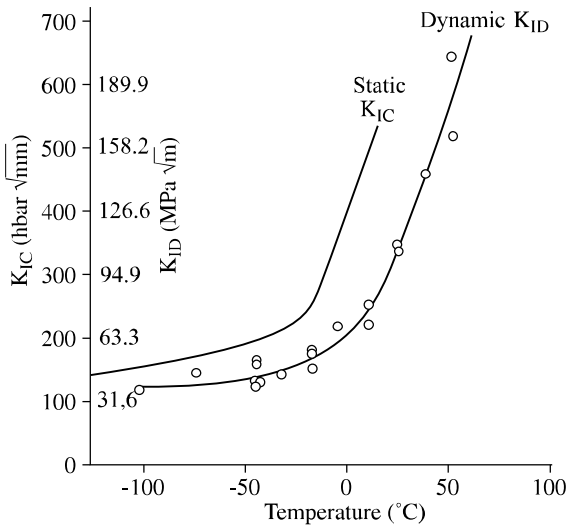
Figure 7.7. *Influence of load speed and temperature on toughness; from [SAN 78]*

Finding equivalence between the toughness and impact strength tests

Right from the first tests to determine toughness using the concept of fracture mechanics, correlations have been sought, in particular between the values of K_{IC} and those obtained by means of much less costly impact tests. Many expressions are presented and analyzed in [COL 97, MEE 88, SAN 78].

As example, in the ductile field we can quote the expression of Rolfe and Novak, verified by IRSID on a wide range of steels, up to a yield strength of 1,720 MPa. It takes the form:

$$\left(\frac{K_{Ic}}{R_e}\right)^2 = 6.4\left[100\left(\frac{KV}{R_e}\right) - 1\right]$$

with $\left(\dfrac{K_{Ic}}{R_e}\right)^2$ in mm, KV in J and R_e in N/mm^2.

Correlations also exist between K_{IC} and impact strength at the lower shelf of the transition zone.

IRSID established two additional types of correlation:

– between the transition temperature defined by the tests of K_{IC} and impact strength,

– between the values of K_{IC} and KV.

By regarding the following temperatures as transition temperatures:

– TK_{IC} = temperature for which K_{IC} = 100 MPa.m$^{1/2}$,

– $TK28$ = temperature for which KV = 28 J (KCV = 35 J/cm^2),

the following correlation can be established, for steels whose crystallinity at temperature $TK28$ is always higher than 80-85%:

TK_{IC} = 1.40$TK28$ in °C

The relation between K_{IC} and KV obtained for values of KV lower than 80 J is expressed for steel as follows:

$$K_{IC} = 19\,(KV)^{\frac{1}{2}}$$

with K_{IC} in MPa.m$^{1/2}$ and KV in J.

From the impact strength curve according to temperature, it is possible to plot curve K_{IC} according to the temperature.

7.2.3. *Fracture criteria in the elasto-plastic field*

In order to evaluate the fracture risks related to the presence of defects in ductile materials, other criteria have been introduced. Among the most used we can quote: J_{IC}, *COD*, *CTOD*, whose definitions are recalled in [FRA 96]. For metallic materials, standards have been established by ASTM and employed by AFNOR in order to define the conditions of taking and dimensioning specimens, the conditions of fatigue pre-cracking, the conduct of tests and the analysis of results. The specimens used are more or less comparable with those used for the determination of the critical stress intensity factor K_{IC}.

Rice's J-integral

The *J*-integral, still called *Rice's integral*, is a contour integral which makes it possible to extend the concepts of elastic linear fracture mechanics to materials presenting a significant plastic deformation at the crack point. This fracture criterion is widely used in the nuclear field to evaluate the risks of ductile tearing. The test conditions are described in [AST 96, NF 87].

The specimens comprise lateral notches facilitating pre-cracking and possibly a chevron notch to facilitate crack initiation. In the case of CT specimens, the notch opening is measured straight along the loading line. During loading, carried out at constant opening speed, the force corresponding to the opening is recorded. The area under the F-d curve, up to the displacement corresponding to the interruption of the test, corresponds to an energy (see Figure 7.8) and is used to calculate *J*. At the end of the test, the test-piece is turned blue, by hot oxidation, before being broken. Examining the fracture topography makes it possible to evaluate the stable propagation amplitude $\Delta\alpha$. The points *J-Δa* are transferred to a reference frame (see Figure 7.9). After checking the validity conditions, the line *dJ/da* is determined by linear regression and the values of J_0 and J_{02} corresponding to the start of ductile fracture.

The method of partial unloadings makes it possible to determine, in theory with only one specimen, the critical displacement J_{IC} which corresponds to the beginning of stable cracking.

Between J_{IC} and K_{IC} a relation exists in the form:

$$J_{IC} = \frac{(1 - v^2)K_{IC}^2}{E}$$

where v is the Poisson coefficient and E the material's elasticity modulus.

J_{IC} is expressed in J/m² when K_{IC} is expressed in MPa.m$^{1/2}$.
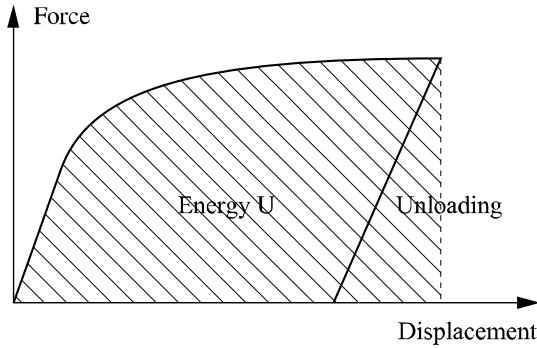
Figure 7.8. *Loading curve and determination of energy U; from [NF 87]*

COD

The concept of COD (*crack opening displacement*) was developed in Great Britain to answer the in-service security issues of the offshore oil rigs built in the North Sea. The specimens used are comparable with those used in elastic linear fracture mechanics and a fatigue crack is developed.
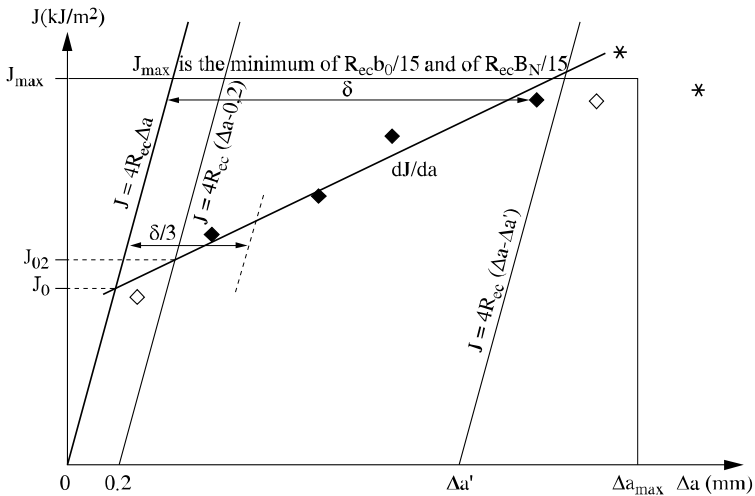
Figure 7.9. *Determination of the conventional values $J_{0,2}$ and dJ/da; from [NF 87]*

In the beginning, the test consisted of measuring the opening at the notch bottom, δ, according to the load applied. Bearing in mind the difficulty of taking this measurement, a method consisting of calculating δ, beginning by measuring the

crack mouth opening by means of a knife edge extensometer, was proposed. This method is based on the assumption that a rotation center exists and will be difficult to determine. It results in uncertainty as to the value of δ [SAN 78].

Assuming we have the COD, the dimension of the critical defect in a structure can be calculated starting from the expression suggested by F.M. Burdekin:

$$a = C\left(\frac{\delta}{e_Y}\right)$$

where $C = \dfrac{1}{2\pi\left(\dfrac{e}{e_Y}\right)^2}$ if $\dfrac{e}{e_Y} < 0.5$

e is the real deformation undergone by the structure in the vicinity of the defect and e_y the deformation at the yield strength.

IRSID has shown that this method resulted in adopting excessive safety margins.

CTOD

Further development has continued, particularly in Anglo-Saxon countries and Japan, leading to CTOD (*crack tip opening displacement*) testing. The experimental conditions are defined in [AST 93, JWE 97, NF 87].

The force-opening curve is plotted until the test-specimen fractures or, failing this, it is stopped when beyond the load curve maximum. The curve is exploited in accordance with standard BS 7448 Part 1 [AST 93, NF 87].

According to the nature of the material, various types of curves can be obtained (see Figure 7.10). The plastic component V_p of the total opening V is obtained by tracing a straight line parallel with the linear part of the load curve. This component V_p is signified by V_C, V_I, V_U or V_m according to the characteristic point considered.
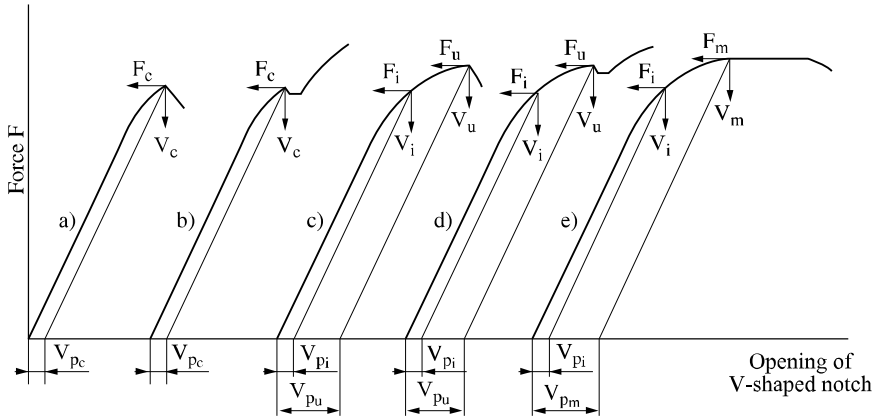
Figure 7.10. *Various types of recordings variations in force applied according to the notch opening; from [NF 87]*

For curves a and b, the force applied increases in a steady way with the opening of the notch mouth, until initiating an abrupt unstable crack propagation, which is not preceded by a stable propagation. The value of δ_C is given starting from the point of coordinates (F_C, V_C).

In the three other cases, where the unstable propagation or the maximum force of plastic instability, is preceded by a certain stable propagation, the critical values δ_U or δ_m of the CTOD are obtained, respectively starting from the points (F_U, V_U) or (V_m, F_m).

The existence of a stable crack propagation preceding a possible brutal rupture can be highlighted *a posteriori* by examining the fracture topography.

In all cases the critical values are calculated by means of the formula:

$$\delta = \frac{K^2(1-v^2)}{2E\,R_{p0.2}} + \frac{0.4(W-a_0)}{(0.4W+0.6a_0+z)}V_p$$

with:

$$K = \frac{F}{BW^{\frac{1}{2}}}Y$$

Y being a function of a/W, a_0 the useful overall length of the initial defect, and *z* the distance between the knife blades and the loading axis in the case of a CT specimen. *E*, $R_{p0.2}$ and *v* are respectively the elasticity modulus, yield strength and the Poisson coefficient of the material.

7.3. Evaluation of fracture risks in welded joints

The evaluation methods used to characterize welded joints are comparable with those implemented to characterize basic materials, except for the added difficulty taking a sample involved with heterogenities of the weld bead.

7.3.1. *Heterogenities of the weld bead*

To assemble one or two materials by welding with or without filler (electron beam or laser beam welding for example) is a complex metallurgical operation which engenders many heterogenities:

– *chemical*, the filler product is often different in composition from that of the materials to be assembled. The dilution effects in the bond zones are an additional factor;
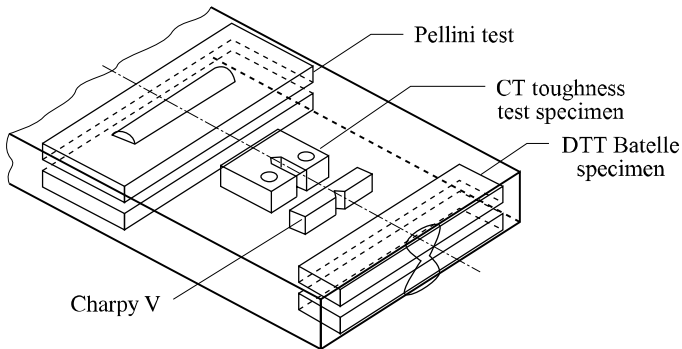
Figure 7.11. *Taking of test-specimens in a welded joint; from [ANS 92]*
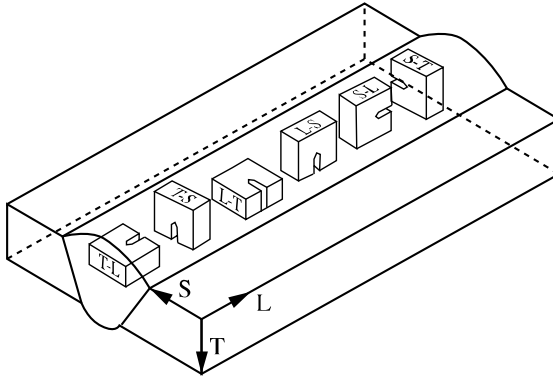
Figure 7.12. *Various possible notch orientations with regard to the weld bead; from [ANS 92]*
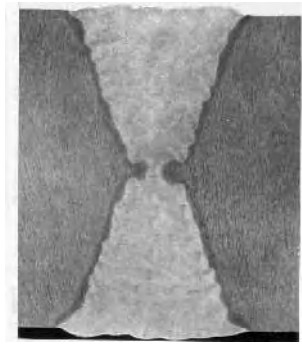
Figure 7.13. *X-shaped bead*

– *metallurgical*, related to the number of heating and cooling phases depending on the number of passes;

– *mechanical*, the behavior of the bead being different from that of the base materials. This type of heterogenity is referred to by Anglo-Saxons as *mismatching*. It is characterized by the relationship *M* between the yield strength of the fusion zone and the yield strength of the base material:

$$M = \frac{\sigma_{YZ}}{\sigma_{YB}}$$

where σ_{YZ} is the yield strength of the HAZ and σ_{YB} that of the base metal.

If $M > 1$ the term used is *overmatching* and, in the contrary case, *undermatching*:

– geometric; taking into account the joint preparations and the shape of the beads (stress concentrations);

– possible defects; planar or volumetric, internal or emerging surfaces which reduce the effective cross section.

To these heterogenities we can add residual stresses, which are a consequence of the juxtaposition of zones brought up to very different temperatures, metallurgical transformations and restrictions of various significance due to clamping.

7.3.2. *Conditions of specimen taking*

The transposition of the preceding tests to the welded joints must take account of the zones to characterize: fusion zone or HAZ. Figure 7.11 illustrates the most commonly used conditions of specimen removal to evaluate the fracture sensitivity of the fusion zone. In general, the notch is positioned in the middle of the cord with various possible orientations (see Figure 7.12).

The determination of HAZ toughness is much more problematic, taking into account the geometry of the weld bead. A crack machined parallel to the bead axis encompasses more or less significant proportions of the HAZ, the remainder being made up of the base metal (see Figure 7.13). To mitigate this disadvantage, at least for the laboratories, K or half K-shaped specimens can be taken (see Figure 7.14), which makes it possible to have a crack located entirely in the HAZ.
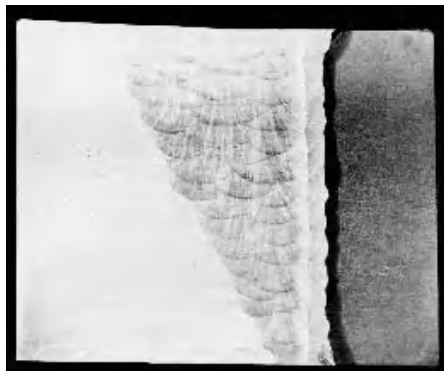
Figure 7.14. *Half K-shaped bead*

However, in spite of this method, the HAZ is far from being homogenous, as can be seen for example in the work of Toyoda [TOY 91]. It is made up of more or less brittle microstructures which are formed at the time of the various thermal cycles (see Figure 7.15) as will be observed later on (see section 7.4.4).
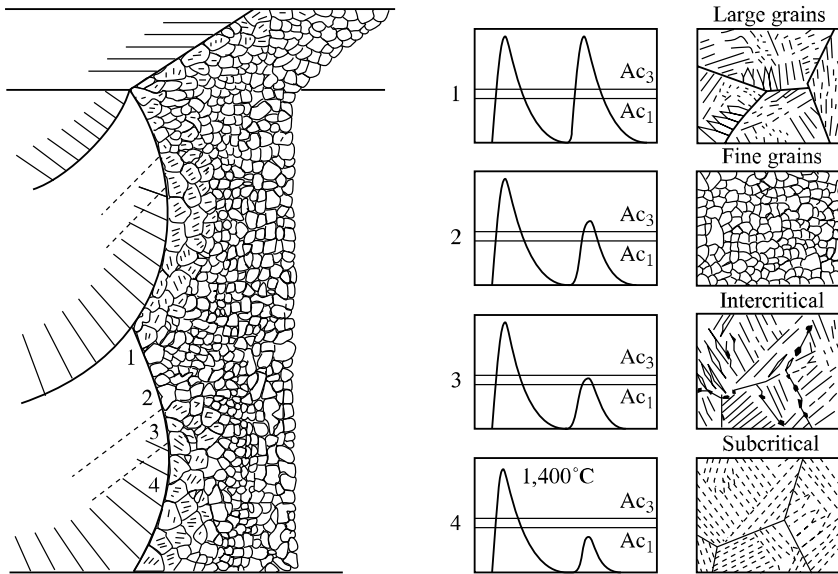
Figure 7.15. *Various types of microstructures found in the HAZ according to the thermal cycles; from [TOY 89]*

In certain cases, the test is carried out on a welded sheet 200 mm wide or more, a fatigue crack being developed either in the bead or in the HAZ [KOC 00]. Such test-specimens are in particular used within the framework of the Brite-Euram project *ASsessment of quality off POwer beam Welded joints* (ASPOW). This project aims at establishing recommendations for the characterization of the joints welded by the processes with high density of energy (electron beam and laser beam) which present a narrow bead with significant property gradients: *overmatching* for structural steels and *undermatching* for aluminum alloys.

7.3.3. *Determination of the ductile-brittle transition temperature*

Concerning the determination of the energy in impact bend tests, standard NF IN 10045-1 [NF 90] defines dimensions and the conditions of sample taking (notch position compared to the FZ or the HAZ). In general, as for the characterization of

basic material, the impact bend-test specimen is a parallelepipedic bar ($55 \times 10 \times 10$ mm^3) with a 45° V-shaped notch 2 mm in depth. The standard envisages the possibility of using test specimens of reduced thickness (7.5 mm or 5 mm).

Following the failures which have occurred during the Kobe and Northbridge earthquakes, impact bend test results showed fracture energies of approximately 10 J at room temperature, for the base metal and the fusion zone, which is very low [TOY 00]. Of the rare plates from Liberty ships which have been examined, energies from 8 to 9 J for the temperature at the time of the accident have been found, whereas energy reached 21 J in the *remoter* zones [SAN 74].

In general, it is necessary that the ductile-brittle transition temperature is lower than the minimum service temperature. Following the work of a group of experts, made up from members of Commission X of the IIW, chaired by H.H. Campbell, recommendations were made for the mechanized welded constructions erected in zones where seismic risks exist [CAM 00]. The simplest procedure gives, for various risk levels, the impact bend energy values to be reached at a temperature corresponding to the minimum temperature of use (see Table 7.1).

According to the specimen taking conditions and the position of the notch bottom in relation to the FZ or the HAZ, the results can vary significantly, as some of the impact bend test results obtained at various temperatures by N. Gubeljak [GUB 99] show.

KV (J) Test temperature = Min. service temperature	Risk of brittle fracture
KV>100	Breakage improbable
47 <*KV* <100	Low risk until rotation factors
27 <*KV* <47	High risk
10 <*KV*<27	High risk. Need for rigorous countermeasures
KV <10	Extremely high risk. Structural insulation essential

Table 7.1. *Risk evaluation as a function of the impact strength level; from [CAM 00]*

In his study, Gubeljak used a high yield strength of low alloyed steel for the base metal, of the HT80 type, at the quenched-tempered state, 40 mm in thickness. Three welded joints, of X-shaped preparation, presenting *overmatching* were evaluated. One of them had a homogenous structure (MF1). The two other welds were carried

out with the less resistant filler products at the root. The results of the impact bend tests are given in Figure 7.16.
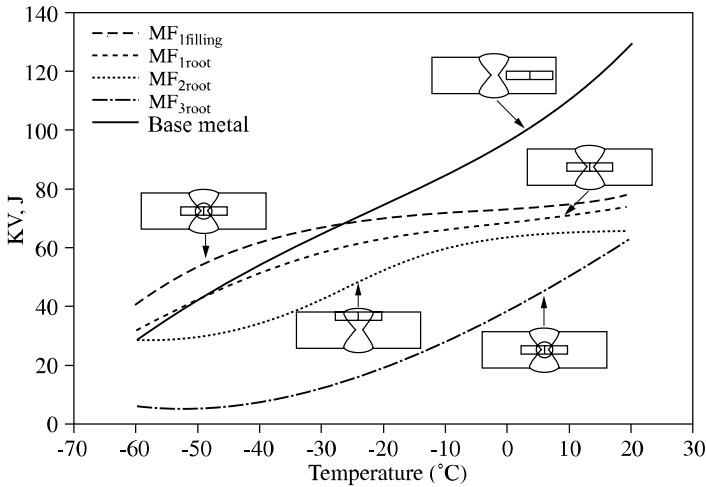
Figure 7.16. *KV = f (T) according to the specimen removal zones; from [GUB 99]*

7.3.4. *Various methods of toughness evaluation*

The concepts of fracture mechanics also apply to mechanized welded constructions, making it possible to evaluate the risks related to the presence of a defect and to judge fitness for use. For that, it is necessary to know the loading conditions, toughness at the crack point as well as the geometry and dimensions of the defect.

The methods determining fracture criteria used for homogenous materials and described in section 7.2 have been transposed to welded joints, in most cases without modification.

Problems involved in pre-cracking

Whatever the method used, it is necessary, initially, to make a fatigue pre-crack. The presence of residual stresses, due to welding, can cause an asymmetric crack front. To mitigate this disadvantage, some studies carry out a stress relief treatment, which modifies the microstructure of the HAZ and the FZ. Dawes, for his part, used a ligament compression procedure in order to redistribute the residual stresses, thus making it possible to obtain a straight crack front [DAW 76].

Critical stress intensity factor K_{IC}

As seen previously, the critical stress intensity factor K_{IC} applies to brittle materials. In the case of welded assemblies, ductile steels are generally used. This criterion can thus only be validated at low temperatures, when the material is in a brittle state.

Fracture in the elasto-plastic field

Under normal service conditions, materials must have, in theory, a ductile behavior. In order to evaluate the rupture risks, related to the presence of a defect, under conditions of a given loading, we use the elasto-plastic rupture criteria (J_{IC}, *COD*, *CTOD*).

P. Hornet observed that the J-force curve of a specimen, or structure, with a defect located in the middle of a welded joint, lies between that of an identical base metal specimen and an identical filler metal specimen.

The relative position of the J-force curve depends on the bead width. If it is wide, plastification at the crack point remains confined to the fusion zone and the curve is similar to that of the homogenous filler metal specimen. In the case of a narrow bead, the behavior is dominated by that of the base metal [HOR 00].

This plasticity extension, in heterogenous structures, has consequences for the analysis of the results determining toughness. Various solutions are currently proposed, consisting of measuring toughness on test-specimens with deep cracks (a/W = 0.5) by using the crack mouth opening rather than the displacement of the crack point by applying force. This makes it possible to estimate the quantity of energy applied in the crack zone by not taking account of that dissipated in the base metal.

Any calculation aiming to evaluate the severity of a defect on the fracture risk implies the ability to determine its dimensions.

Taking defects into account

In the case of welded joints, even planar defects have complex geometries. It is also necessary to take the interaction between adjacent defects into account. Methods have been developed to transform these defects into an equivalent 2D geometrical defect (*a, b*). From this, it is even possible to pass to a 1D parameter of effective size $\bar{a}$. Such a step is proposed both for emerging and internal defects [COL 97, HOB 96].

The use of non-destructive testing techniques adapted to the types of defect sought is fundamental. This need for testing should be taken into account right from

the design stage, which would prevent many problems once the construction is completed.

Analysis of defect severity

When a defect has been detected in a structural element, three reactions can be considered:

– keep it as it is while continuing to use the material;

– repair it, knowing that a repair can be the origin of another even more severe defect;

– replace the defective part.

Various methods of analyzing defect severity exist to help our decision making, based on existing methods for homogenous structures and adapted in the last few years to welded joints. Amongst the most well known are:

– the modified R6 method (method of two criteria),

– the ETM-MM (*Engineering Treatment Model for Mismatched Welds*) method,

– the EM (*Equivalent Material Method*) method,

– the recommendation PD 6493 of the British Standard, entitled: *Guidance on methods for assessing the acceptability of flaws in fusion welded structures*.

These various methods are presented, for the majority, in [BLA 97].

Recommendation PD 6493 of the British Standard

Recommendation PD 6493, in its last version (June 1991), applies:

– to welded assemblies in aluminum alloys, ferritic and austenitic steels,

– to planar or volumical defects,

– to different modes of failure.

A synthesis of this recommendation, with its advantages and its limitations, as well as an application to fluid conduits, was carried out by R. Batisse [BAT 00].

This recommendation is used for pressure vessels, pipelines, bridges, constructions, storage tanks, naval construction and offshore work, etc.

According to this recommendation, the treatment of acceptability of a defect, in terms of risk of rupture, rests on the FAD (*failure assessment diagram*) and requires

the calculation of two parameters corresponding respectively to the brittle risk of fracture *Kr* (y-axis) and that of plastic collapse *Sr* (x-axis).

Various levels of investigation are proposed. Figure 7.17 sets out levels 1 and 2.

Level 1 is the most restrictive. It allows a fast analysis with a minimum of data. It does not require the taking into account of safety factors, those being integrated by an increase of the stresses and dimensions of the defects and a decrease of mechanical properties.

Level 2 admits the possibility of initiation of ductile tearing before failure and takes into account the stresses at the level of the defect. Safety coefficients are applied to the stresses, dimensions of the defect and the mechanical properties.

Level 3 (see Figure 7.18) can be used when the collapse is preceded by a significant plastic deformation.

The point can be placed in the FAD diagram with its position depending on the type of defect (its position and its dimensions) and conditions in use (loading, temperature, etc.). According to its position, inside or outside the diagram, the defect is either acceptable or not.
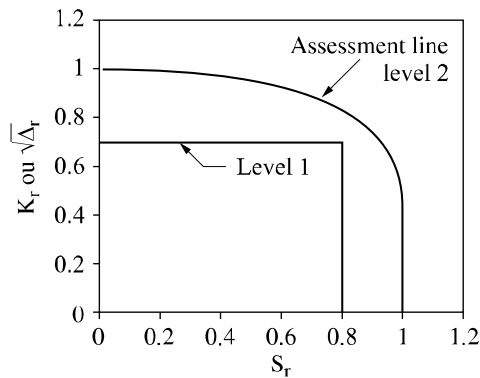
Figure 7.17. *FAD. Levels 1 and 2; from [KON 94]*
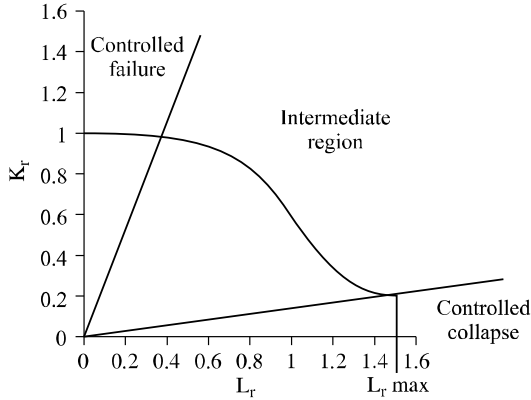
Figure 7.18. *FAD. Level 3*

This recommendation is designed to be simple, capable of meeting industrial needs. However it leads, in a certain number of cases, to results with limited accuracy in relation to certain assumptions such as:

– taking account of residual stresses equal to the elastic limit,

– a K approach, based on linear fracture mechanics, poorly adapted for a crack whose plastification is not confined,

– use of approximate mechanical properties.

The European project SINTAP (*Structures INTegrity Assessment Procedures*) turned its attention to recommendation PD 6493 with the intention of limiting such results by proposing a certain number of simplified solutions.

7.4. Consequences of heterogenities on the evaluation of fracture risks

The evaluation of fracture risks in welded joints will be a major issue in years to come, as much for new buildings as for those in service. The frequency of maintenance, where cost gains are to be hoped for, and the increase in the lifespan of an installation, are ongoing problems that demand a better knowledge of welded structures.

Welded joints are by nature heterogenous and the probability aspects must be taken into account.

7.4.1. *Mismatching effects*

In 1993, at the annual meeting of the IIW, it was decided to establish Sub-Commission X F within Commission X, specifically instructed to take *mismatching* effects into account. Bearing in mind the multi-disciplinary nature of the problem, this group involved specialists working in several different areas. In seven years, nearly 100 documents, whose list appears in the President's Report [KOC 00], were presented and made the subject of debate. Among the topics discussed were:

– taking *mismatching* into account in processes with high energy density,

– *mismatching* occurring during friction welding (*stir friction*),

– consequences of *mismatching* during seismic loadings,

– *mismatching* related to a coating or a recoating.

Currently, the codes do not take *mismatching* into account. They consider a homogenous material, which has the most disadvantageous characteristics among those involved in welding. Generally, this leads to conservative results.

Two programs of the European Community particularly take the effects of *mismatching* into account. In addition to the now deceased SINTAP program, the ASPOW program (*ASsessment of quality of POwer beam Welded joints*) deals with the characterization of joints welded by beams with high density of energy. The applications relate in particular to the use of laser welding of aluminum alloys in aeronautics, within the framework of the Airbus 380 program.

The laboratory tests carried out on welded test-specimens with a defect located in the fusion zone highlight the influence of:

– mismatching,

– dimensions of the HAZ in relation to those of the test-specimen,

– load pattern (tension or bending),

– position of the crack point's extremity compared to the bead,

– evolution of plasticity in the ligament.

In France, many studies have been undertaken to counter the problems presented in the nuclear field. Hornet [HOR 00] showed that in the case of *overmatching*, plasticity develops mainly in the softest metal, except if the FZ is rather wide, in which case plasticity is confined there (see Figure 7.19).

On the other hand, for narrow beads, the overall behavior of the heterogenous structure seems little influenced by the existence of the FZ, whatever the crack

length. Behavior in the vicinity of the crack, like that of the structure as a whole, seems controlled by the base metal. The plasticization, originating at the crack point in the melted zone, joins the bond zone to develop then in the base metal (see Figure 7.19). The mushroom shaped plastic zone, characteristic of *overmatching*, extends in the base metal which governs the crack loading.

Hornet also shows that if the ratio *h/(W-a)* is high, the mechanical strength of the structure is controlled by the molten metal, whereas if it is close to 0, it is controlled by the base material.

The loading conditions (tension or bending) also influence the development of plasticity and the possibility of the plastified zone leaving the added metal. According to Hornet, a bending load favors the containment of plasticity in the molten metal (see Figure 7.20) more than a tensile load.

Similar results are found in the part of the ASPOW project devoted to the characterization of welded joints, made by laser or electron beam, for steels of various strength levels, where the degree of overmatching is important. It was shown that a crack, started in the bead, quickly changes orientation to develop in the more ductile base metal, this phenomenon holding good both for test-specimens comprising wide plates or traditional fracture test pieces, CT type or thin bending specimens. If the thickness *B* of the test-specimens increases, the crack remains in the melted zone, which results in a reduction of CTOD [KOC 99]. The fact that the crack moves towards the most ductile zone is reassuring for those processes with high energy density.
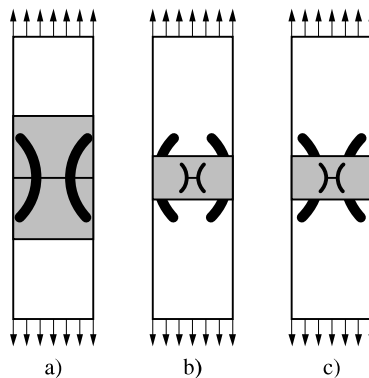
Figure 7.19. *Extension of the plasticized zone in relation to the HAZ width; from [HOR 00]*
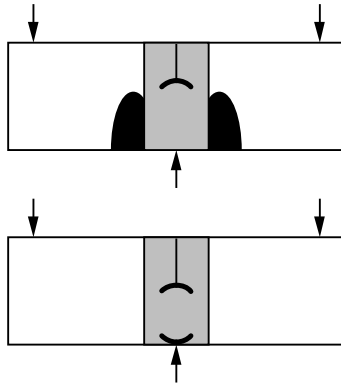
Figure 7.20. *Containment of the plasticized zone during
a bending loading; from [HOR 00]*

The consequences of mismatching on the CTOD were studied for various materials: aluminum alloys presenting undermatching, austenitic stainless steels, Inconel 625 nickel alloys, and titanium alloys.

For the latter, we cite the work of M. Koçak who, while during diffusion welding of titanium and a TA6V titanium alloy, produced either an undermatching equal to 0.36 (TA6V/Ti/TA6V) or an overmatching of 2.5 (Ti/TA6V/Ti) with variable widths and perfectly straight bond zones. In the first case, the crack remains in the most ductile zone and the plastified zone remains confined; in the second case, the crack deviates towards the most ductile material or propagates to the level of the interface.

N. Gubeljak studied, in the case of an X-shaped preparation, the influence of the crack tip's position on the toughness expressed in terms of CTOD (see Figure 7.21). When the a/W ratio increases, the width of the molten zone decreases and reaches a minimum at the level of the root. Constriction effects the development of the plastified zone at the crack tip and thus on the results, which present dispersions. To mitigate this weakness, corrective formulae are proposed [GUB 99].
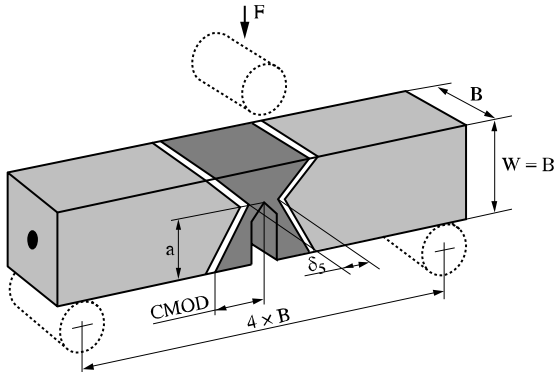
Figure 7.21. *Influence of geometry of the molten zone and position of the bottom of the fatigue crack on the determination of the CTOD; from [GUB 99]*

7.4.2. *Influence of the base material*

Manufacturing conditions

The base material, used for the realization of mechanized welded constructions, must have a ductile-brittle transition temperature lower than the minimum temperature of in-service use. At the beginning of the 1970s, French standard NF A 36-201 defined three levels of quality (R, C and FP) for non-alloyed sheet steels or low alloyed weldable steels (E 355, E 375, E 420 and E 460) guaranteeing minimal impact strength values in more or less low temperatures according to the conditions of use.

In order to provide users with steels that were easier to weld, while being more resistant and tougher, steel manufacturers lowered the percentage of carbon (reduction in equivalent carbon (C_{eq}), which leads to a lowering of TK 28 (see Figure 7.22). Further developments also made it possible to improve the product quality by reducing the impurity content (sulfur, phosphorus) or trace elements (arsenic, antimony, tin). These reductions have made it possible to lower the transition temperature in the affected zone of Cr-Mo steels sensitive to the phenomenon of reversible embrittlement.

Vacuum processes, such as dehydrogenation, made it possible to reduce the hydrogen content to less than 2 ppm, in particular in steels for heavy plates. In addition, it was possible to obtain a low nitrogen content by calling upon techniques that avoid molten steel and ambient air during casting.

For the same sulfur content, the morphology of sulfides plays a big role in impact strength through the thickness. The addition of cerium or calcium

appreciably improves impact strength by the formation of globulized sulfides (see Figure 7.23).

Thermomechanical treatments

Thermomechanical rolling, followed by an accelerated cooling, led to the development of high yield strength (HYS) steels. The decreased percentage of carbon was compensated for by a refinement of the grain size and by the precipitation of dispersoid elements which allow hardening the ferritic phase [DEF 94]. This generates an increase in strength and yield strength while lowering the transition temperature.
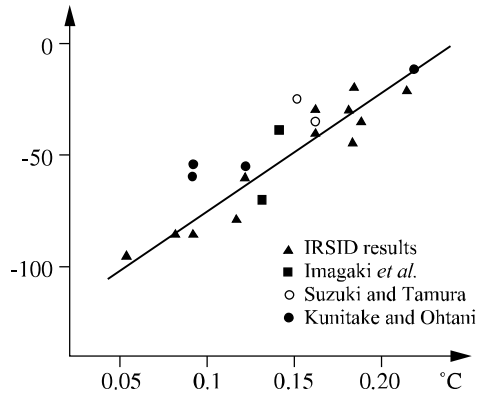
Figure 7.22. *Influence of carbon percentage on optimal TK of the HAZ; from [DEV 88]*
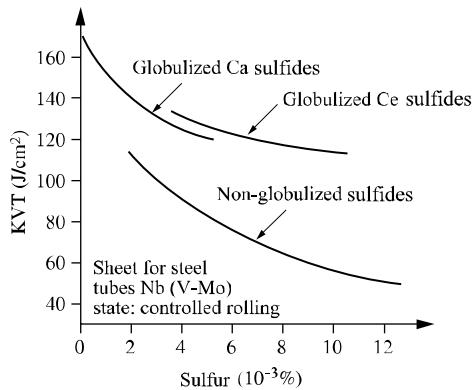
Figure 7.23. *Impact strength through the thickness. Influence of sulfur content and sulfide morphology; from [DEV 88]*

In a paper, Bourges *et al.* [BOU 97] showed that for a steel supplied according to the same designation, the manufacturing conditions can have an important role on the condition of use. Thus steel-killing with aluminum, without silicon, had a beneficial effect, making it possible to limit the sensitivity to ageing after work hardening by bending (see Figure 7.24).

In steels with 0.080% C, 1.5% Mn and 0.5% Ni, the influence of silicon content also occurs on the temperature TK28 in the HAZ, in a way all the more marked when the cooling speed during welding is slower, which is the case for the processes with high density of energy (see Figure 7.25). The reduction of silicon content makes it possible to decrease the fraction of residual austenite in the HAZ, which improves toughness in this zone.
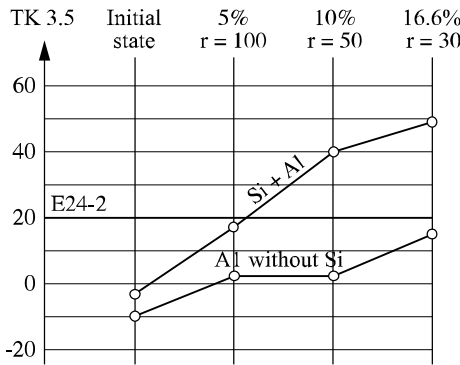
Figure 7.24. *Evolution of the TK35 level in relation to deformation and steel-killing; from [BOU 97]*
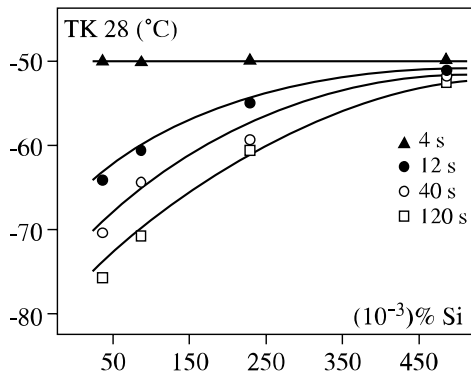
Figure 7.25. *Influence of the Si content and cooling speed in the HAZ on impact strength; from [BOU 97]*

7.4.3. *Influence of filler metals*

An assessment of progress made, in terms of filler materials, was presented by Bourges *et al.* [BOU 98]. A comparison is made between basic and rutile filled wires. The basic wires have the greatest potential because of their chemical composition, and make it possible to obtain a high ductile level in impact strength as well as a good toughness at low temperature. However, the basic wires have inferior operational characteristics to those of rutile wires.

Significant improvements have been made to rutile wire, which uses the titanium/boron effect by selecting the raw materials in a rigorous way, in order to limit the impurities and carbide-forming elements responsible for a decrease in toughness after stress relief treatments. It should also be added that some wires have a diffusible hydrogen rate sufficiently low to be classified in the H5 category (lower than 5 ml/100 g of added metal). These various aspects are detailed by Bonnet (see Chapters 4 and 5 of this book).

7.4.4. *Importance of welding conditions*

In the case of multipass welding, each pass is at the origin of microstructural transformations which vary according to the maximum temperature reached. Thus, the HAZ comprises local brittle zones (LBZ) as stated by [DEF 94]. The complexity of the HAZ is schematized in Figure 7.15.

The research undertaken during recent years has underlined the role of certain microstructural components, composed of martensite and residual austenite (M-A compounds), on toughness. The morphology of these compounds acts on impact strength. It was shown that it is especially large M-A compounds (higher than 2 μm) and/or solid masses (shape factor less than 4) which involve a decrease in impact strength. These compounds constitute the local embrittlement zones.

Figure 7.26 makes it qualitatively possible to judge the influence of the total local brittle zone on the COD. The LBZ is the sum of:

– the reheated coarse grain zone in the subcritical field,

– the reheated coarse grain zone in the intercritical field,

– the non-transformed coarse grain zone.

At the beginning of the 1990s, Kaplan developed a software simulation, called Multipasses, which makes it possible to evaluate, in the case of C-Mn steels, depending on the composition of the base steel, the filler and the welding parameters (voltage, intensity, speed, efficiency coefficient, pre-heating temperature and

interpass temperature), the proportions of LBZ which directly influence toughness. Such predictive tools are an aid for both steelmakers and welders [DEV 94].
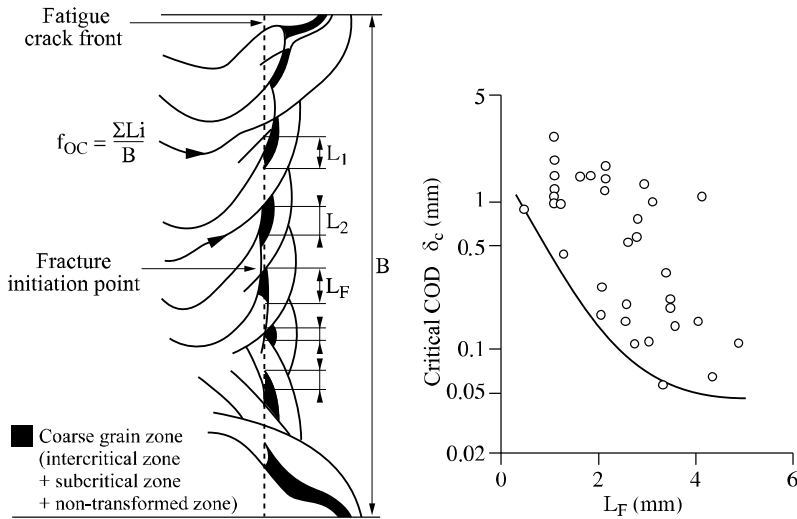
Figure 7.26. *Relation between the COD and the proportion of LBZ intercepted by the fatigue crack; from [AIH 88]*

7.4.5. *Evaluation and taking account of residual stresses*

The welding operations and its related techniques comprise rapid phases of heating and cooling which entail deformations and the creation of residual stresses. In the absence of precise data, it is useful to consider that their level is equal to the elastic limit of the material, which in the majority of the cases is disadvantageous if we refer to the results obtained by simulation.

Modeling and simulation in this field began in France in the 1980s with the development of the software SYSWELD, by Devaux and Leblond. They based their ideas, with regard to the metallurgical transformations, on the work of R. Blondeau [BLO 75] and that of A. Simon's team, a short summary of which is given in [SIM 93].

This software makes it possible to simulate welding while taking thermal, metallurgical and mechanical aspects into account and working by sequential analysis. Starting from the welding parameters, thermo-metallurgical calculation makes it possible to obtain the temperatures and phases formed at any point according to time. This stage takes into account the variations of thermal conductivity, specific heat and volumic mass according to the temperature.

There follows the mechanical calculation, thermo-elastoplastic in nature and requiring us to take into account various phenomena related to metallurgical transformations. The mechanical characteristics depend on the phase proportions. It is necessary to take the variations of volume and the plasticity transformation into account. Digital simulation requires that we have a great deal of data relative to the materials, which is available for only a few steel types.

Figure 7.27 gives an example evaluation of longitudinal and circumferential residual stresses obtained by an EB capacitive pressure weld in 10CrMo9-10 steel. We should note the presence of compressive stresses on the surface in the vicinity of the bead toe and internal tensile stresses. On both sides of the bead, there are on the surface tensile stresses. Qualitatively the stress distribution had been confirmed by X-ray diffraction and the hole drilling method (see Figure 7.28). Quantitatively, the differences between calculation and experimental methods were considerable and were explained by a 2D analysis [DEV 89].

Simulation makes it possible to obtain information otherwise inaccessible by traditional experimental techniques.
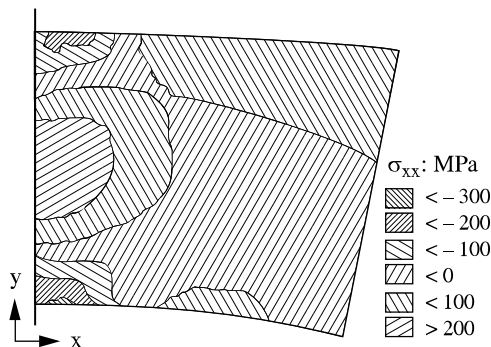
Figure 7.27. *Distribution of transverse stresses; from [DEV 89]*

This data, and in particular the transverse residual stresses in thickness, were taken into account by A. Carmet to evaluate dimensions of the allowable defects by using various fracture criteria. This step made it possible to decrease, in the majority of cases, the severity of the various rules of acceptance [CAR 90].
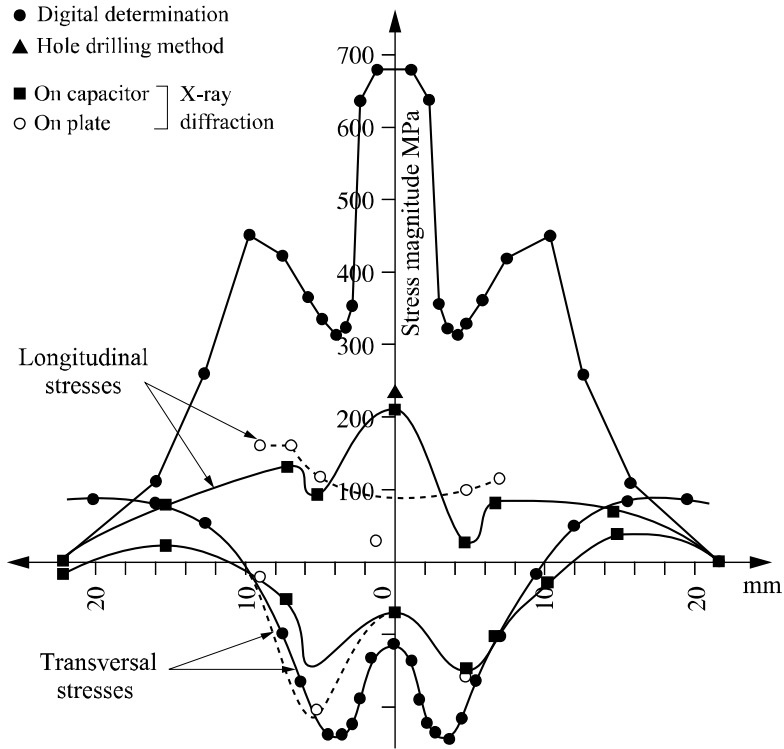
Figure 7.28. *Residual stresses. Calculation/experiment comparison; from [DEV 89]*

Burdekin gathered together exercises dealing with fracture risk evaluation of welded joints by taking account of residual stresses [BUR 96].

Examples of residual stress distribution, for various joint types, exist in the literature. Since 1996, under the initiative of Janosch, a working group has been constituted from members of Commissions X and XV of the IIW, facilitating a considerable exchange of ideas. The titles of the documents presented since 1997 are gathered in [JAN 00].

A round-robin gathering together ten teams undertook the simulation of a circumferential joint for tube welding. The first results show that, according to the methods used, important variations can be observed even in thermal analysis at a given point. The aim of this work is to make recommendations on implementation methods in order to obtain more coherent results [KOP 00].

Within the framework of a co-operative study, teams of the ECA, EDF and Framatome employed different codes (Castem 2000, Aster and Sysweld), to obtain homogenous results with regard to the stress distribution for the multipass welding of a cylinder in austenitic 316L steel. For that purpose, experiments were carried out, with particular regard to thermal cycle analyzing during the various welding passes. Micrographic examination allowed some readjustments. The calculations fit in well with stresses determined by experimental methods [KIC 00].

7.5. Bibliography

[AIH 88] HAZE T., AIHARA S., "Influence of toughness and size of local brittle zone on HAZ toughness of HSLA steels", *Proceedings of the 7th International Conference on Offshore Mechanics and Arctic Engineering*, *OMAE 1988*, ASME, Houston, USA, 1988.

[ANS 92] American National Standards Institute and American Welding Society, Standard methods for mechanical testing of welds, ANSI/AWS B4.0-92, 29 June 1992.

[AST 93] ASTM, Standard test method for crack tip opening displacement (CTOD) fracture toughness measurement, ASTM E 1290-93, 1993.

[AST 95] ASTM, Standard test method for conducting drop-weight test to determine nil-ductility-transition temperature of ferritic steels, ASTM E208-95a, 1995.

[AST 96] ASTM, Standard test method for J-integral characterization of fracture toughness, ASTM E 1737-96, 1996.

[AST 97] ASTM, Standard test method for plane strain fracture toughness of metallic materials, ASTM E 399-90 (reapproved 1997), 1997.

[BAL 97] BALLADON P., DI FANT M., PONSOT A., "Dureté, résistance et ténacité", *Les aciers spéciaux*, Lavoisier, pp. 452-473, Paris, 1997.

[BAT 00] BATISSE R., "Présentation de la recommandation PD 6493. Application aux conduites de transport de fluides", *Séminaire sur la prévention de la rupture dans des joints soudés*, Institut de Soudure, 9 March 2000.

[BLA 96] BLAUEL J.G., BURDEKIN F.M., "Case study collection on the assessment of the significance of weld imperfections", *Welding in the World*, 37, no. 4, pp. 194-216, 1996.

[BLA 97] BLAUEL J.G., Failure assessment concepts and applications, Doc. IIS – IIW X-1407-97, 1997.

[BLO 75] BLONDEAU R., MAYNIER PH., DOLLET J., VIEILLARD-BARON B. "Prévision de la dureté, de la résistance et de la limite d'élasticité des aciers au carbone et faiblement alliés d'après leur composition et leur traitement thermique", *Mém. Scient. Rev. Métall*. pp. 759-769, November 1975.

[BON 97] BONNEFOIS B., BOURGES P., MABELLY P., DEBIEZ S., BONNET C., ROUAULT P., MAGOARIEC A., TAILLARD R., KAPLAN. D. *et al.,* Quelques développements récents permettant une amélioration supplémentaire de la qualité des structures d'aciers soudées, Doc. IIS/IIW IX-1886-97, 1997.

[BON 98] BONNEFOIS B., BOURGES P., MABELLY P., DEBIEZ S., BONNET C., ROUAULT P., MAGOARIEC A., TAILLARD R., KAPLAN. D. *et al.*, "Une amélioration supplémentaire de la qualité des structures soudées en acier", *Soudage et Techniques Connexes*, vol. 52, no. 1/2, January/February 1998.

[BUR 92] BURDEKIN F.M., "Choix des aciers pour les constructions soudées", *Soudage et Techniques Connexes*, vol. 46, no. 11/12, November/December 1992.

[BUR 96] BLAUEL J.G., BURDEKIN F.M., "Case study collection on the assessment of the significance of weld imperfections", *Welding in the World*, 37, no. 4, pp. 194-216, 1996.

[CAM 00] CAMPBELL H.H., Status of the IIW recommendations on fracture control in seismically affected steel structures, Doc. IIS/IIW X-1456-00, 2000.

[CAR 90] CARMET A., SOCQUET J., "Influence des contraintes résiduelles de soudage sur les conditions de rupture d'appareils à pression", *Soudage et Techniques Connexes*, vol. 4, no. 11/12, November/December 1990.

[CHE 70] CHEVIET A., GRUMBACH M., PRUDHOMME M., SANZ G., "Comparaison des résultats de divers essais de rupture fragile", *Revue de Métallurgie*, pp. 217-236, March 1970.

[COL 97] COLLECTIF, Method of assessment for flaws in fusion welded joints with respect of brittle fracture and fatigue crack growth, Doc. IIS/IIW X-1428-98, 1997.

[DAW 76] DAWES M.G., "Contemporary measurements of weld metal fracture toughness", *Welding Journal*, pp. 1052-1057, December 1976.

[DEF 94] DEFOURNY J., "Soudabilité des aciers produits par laminage thermomécanique ou par refroidissement accéléré", *Soudage et Techniques Connexes*, vol. 48, no. 7/8. July/August 1994.

[DEV 89] DEVAUX J.C., CARMET A., LEBLOND J.B., "Détermination numérique des contraintes et des déformations résiduelles dans un joint soudé par faisceau d'électrons", *Soudage et Techniques Connexes*, vol. 48, no. 9/10, September/October 1989.

[DEV 94] DEVILLERS L., KAPLAN D., TESTARD P., "Prévision des microstructures et de la ténacité des ZAT de soudures", *Soudage et Techniques Connexes*, vol. 48, no. 7/8, July/August 1994.

[FOR 00] FORGET P., "Modélisation de la rupture des liaisons soudées bimétalliques", *Séminaire sur la prévention de la rupture dans des joints soudés*, Institut de Soudure, 9 March 2000.

[FRA 72] FRANÇOIS D., JOLY.L., *La Rupture des Métaux. Ecole d'été de la Colle sur Loup, September 1970*, Masson, 1972.

[FRA 92] FRANÇOIS D., Provisional definitive statement of significance of local brittle zones, Doc IIS-IIW X-1246-92, 1992.

[FRA 96] FRANÇOIS D., "Guidelines for terminology and nomenclature in the field of structural integrity", *Fatigue & Fracture of Engineering Materials & Structures*, vol. 19, no. 12, pp. 1515-1533, 1996.

[FRA 00] FRANÇOIS D., "Aspects probabilistes de la rupture des joints soudés", *Séminaire sur la prévention de la rupture dans des joints soudés*, Institut de Soudure, 9 March 2000.

[FRO 82] FROMM K., SCHULZE H.D., Pellini's theory of brittle fracture and the limits of its applicability, Doc IIS – IIW 1011 – 82, 1982.

[GRU 69] GRUMBACH M., PRUDHOMME M., SANZ G., "Essais dynamiques de rupture fragile avec enregistrement", *Revue de Métallurgie*, pp. 271-281, April 1969.

[GUB 99] GUBELJAK N., "Estimation de la ténacité minimale s'assemblages soudés affectés d'une hétérogénéité mécanique (mismatch)", *Soudage et Techniques Connexes*, vol. 53-no. 7/8, July/August 1999.

[HOB 96] HOBBACHER A., Recommandations pour la conception en fatigue des assemblages et composants soudés, Document IIS-IIW XIII-1539-96/ XV-845-96, 1996 (version française, publication CTICM, October 2000).

[HOR 00] HORNET P., "Prise en compte de l'effet mismatch dans le comportement mécanique des structures soudées fissurées", *Séminaire sur la prévention de la rupture dans des joints soudés*, Institut de Soudure, 9 March 2000.

[JAN 00] JANOSCH J.-J., GORDON R., Residual stress and distortion prediction in welded structures, 4th annual report, Doc. IIS – IIW X-1455-00, 2000.

[KAL 00] KALNA K., Design of steels structures against brittle failure in different European standards, Doc. IIS/IIW X-1465-00, 2000.

[KIC 00] KIHENIN J., RAZAKANAIVO A., DESROCHES X., BOIS C., LEJEAIL Y., Tubular welding numerical simulation: Experimental validation, Doc. IIS/IIW X/XV-RSDP-56-00, 2000.

[KIM 98] KIM Y.J., "Effets d'une hétérogénéité mécanique (mismatch) sur les contraintes locales", *Soudage et Techniques Connexes*, vol. 52, no. 3/4, March/April 1998.

[KOC 99a] KOÇAK M. *et al*., "Recommendations on tensile and fracture toughness testing procedures for power beam welds", *European Symposium on Assessment of Power Beam Welds, 4-5 February 1999*, Doc IIS – IIW X-1445-99, 1999.

[KOC 99b] KOÇAK M., THAULOW C., "Special issue on strength of mismatched welded joints", *Engineering Fracture Mechanics*, vol. 64, no. 4, November 1999.

[KOC 00] KOÇAK M., DOS SANTOS J.F., "Le soudage et l'assemblage au XXIe siècle: Soudage laser: tendances dans les applications industrielles et dans l'évaluation de la qualité", *Soudage et Techniques Connexes*, vol. 54, no. 5/6, May/June 2000.

[KOC 00] KOÇAK M., 7th Annual Report of Sub-Commission X-F Weld Mis-Match Effect, Doc. IIS/IIW X-1457-00, 2000.

[KOL 00] KOPPENHOEFER K., GORDON R., IIW Round Robin on residual stress and distortion prediction. Phase 1 results, Doc IIW X/XV-RDSP-55-00, 2000.

[KON 94] KONECZNY H., "De l'utilité des calculs de mécanique de la rupture", *Soudage et Techniques Connexes*, vol. 48, no. 7/8, July/August 1994.

[KON 00] KONECZNY H., JANOSCH J-J., DEBIEZ S., "Définition d'une base de données matériaux pour les constructions soudées lourdes par caractérisation expérimentale de ténacité/résilience", *Revue Française de Mécanique*, no. 1997-1, pp. 17-25, 2000.

[LAF 88] LAFRANCE M., POUPON M., DEVILLERS L., "Les outils et technologies modernes de production des aciers", *Soudage et Techniques Connexes*, vol. 47, no. 11/12, November/December 1988.

[LEI 62] DE LEIRIS H., BONIZEC R., "L'essai au mouton Pellini et les assemblages soudés", *ATMA 1961*, pp. 669-684, 1962.

[LEI 71] DE LEIRIS H., *Métaux et alliages*, Tome I, Cours ENSTA, Masson & Cie, 1971.

[LEI 96] LEI W., YAO M., "The physical nature of drop weight test NDT", *Engineering Fracture Mechanics*, vol. 53, no. 4, pp. 645-652, 1996.

[MEE 88] MEESTER DE B., "Choix des aciers selon leurs propriétés Charpy V en vue d'éviter la rupture fragile", *Le Soudage dans le Monde*, vol. 26, no. 11/12, 1988.

[MUH 98] MUHAMMED A., The effect of prior overload and its application in structural integrity assessments, SINTAP/TWI/014, TWI Report no. 88269/1/98, March 1998.

[NF 81] NORME FRANÇAISE, Produits sidérurgiques. Détermination du facteur d'intensité de contrainte critique des aciers, NFA 03 180, June 1981.

[NF 84] NORME FRANÇAISE, Assemblages plans et tubulaires soudés bout à bout – Essai de flexion par choc sur éprouvette bi-appuyée (entaille en V), NF A 89-202, July 1984.

[NF 87a] NORME FRANÇAISE, Produits sidérurgiques – Mécanique de la rupture – Détermination de l'écartement à fond de fissure (CTOD), NF A 03 182, June 1987.

[NF 87b] NORME FRANÇAISE, Produits sidérurgiques – Mécanique de la rupture – Détermination à partir de la courbe J-δa des valeurs conventionnelles J_0 et DJ/DA-Caractéristique de la résistance à la déchirure ductile, NF A 03 183, June 1987.

[NF 90] NORME FRANÇAISE, Matériaux métalliques – Essai de flexion par choc sur éprouvettes Charpy – Partie 1: Méthode d'essai, NF EN 10045-1, October 1990.

[PEL 71a] PELLINI W.S., "Principles of fracture safe design – part I", *Welding Research Supplement*, pp. 91-109, March 1971.

[PEL 71b] PELLINI W.S., "Principles of fracture safe design – part II", *Welding Research Supplement*, pp. 147-162, April 1971.

[ROS 98] ROSSOL A., Détermination de la ténacité d'un acier faiblement allié à partir de l'essai Charpy instrumenté, PhD Thesis, ECP 98-43, 1998.

[SAN 74] SANZ G., *La rupture des aciers. La rupture fragile 1*, Collection IRSID OTUA, 1974.

[SAN 78] SANZ G., *La rupture des aciers. La mécanique de la rupture 2*, Collection IRSID OTUA, 1978.

[SIM 93] SIMON A., DENIS S., "Modélisation et calcul des transformations de phases et des contraintes internes en traitement thermique des aciers", *Les Entretiens de la Technologie, 11 May 1993, Nantes, Atelier Matériaux 6: Transformations microstructurales*, 1993.

[SOU 97] SOULIGNAC P., BERANGER G., HENRY G., LABBE G., *Les aciers spéciaux*, Lavoisier, Paris, 1997.

[TOY 89] TOYODA M., "Fracture toughness evaluation of steel welds", *Review Part II*, University of Osaka, 1989.

[TOY 91] TOYODA M., Recommendation for understanding the significance of CTOD test, results for steel weld HAZ, IIS – IIW Commission X, 1991.

[TOY 00] TOYODA M. *et al*., Fracture mechanics approach for fracture performance evaluation of steel structures under seismic loading, Doc IIS – IIW X-1462-00, 2000.

[WIE 99] WIESNER C.S., SMITH S.D., Pellini drop-weight testing to charaterise structural crack arrest behaviour, Doc IIS – IIW X-1438-99, 1999.

[WIL 99] WILSIUS J., IMAD A., NAIT ABDELAZIZ M., MESMACQUE G., ERIPRET C., "Analyse des modèles basés sur l'approche locale en mécanique de la rupture", *Soudage et Techniques Connexes*, vol. 53, no. 11/12, November/December 1999.

[WIL 99] WILSIUS J., Etude expérimentale et numérique de la déchirure ductile basée sur des approches locales en mécanique de la rupture, PhD Thesis, Université des Sciences et Technologies de Lille, December 1999.

[XU 97] XU W.G., "Diagrammes d'évaluation de la rupture en présence de contraintes résiduelles", *Soudage et Techniques Connexes*, vol. 51, no. 11/12, November/December 1997.

Chapter 8

Welding of Steel Sheets, With
and Without Surface Treatments

The automotive market is the principal consumer of bare and coated thin steel sheets. It is accepted that a thin sheet has a thickness of less than 5 mm.

The permanent drive to conform to pollution requirements by reducing the weight of motor vehicles has led to the increasing use of ever thinner high-strength sheet steels. For several years now, very high specification sheet steels whose tensile strength exceeds 600 MPa and reaches 1,500 MPa have been entering the market. Among these new products, we find *dual phase* steels (Usiphase D 600), TRIP steels (Usiphase T 800), multiphase structure steels (Usiphase M 1000) as well as steels of a martensitic structure that have been thermally treated during the stamping process (Usibor 1500).

The need to improve the longevity of motor vehicles is also at the origin of developments in coated sheet steels, designed to significantly improve corrosion resistance. The coatings are metallic, sometimes supplemented by a thin organic coating. Hot-dip galvanized steel (pure zinc) is the best known product (Extragal), which can undergo an alliation treatment (Galvallia) in order to improve its suitability for spot welding. To increase corrosion resistance, a steel galvanized with a zinc-aluminum alloy is used (Galfan).

An electro-zinc coating is also used (Usicar) with the possibility of adding a thin organic coating (Usiplex). In Europe, the ten years from 1990 to 2000 saw the

Chapter written by Gilles RIGAUT, Olivier DIERAERT, Pascal VERRIER and Joël CLAEYS.

percentage of coated sheet steel employed in the automotive industry rise from 39% to 84%.

Sheet steel is a product in constant development. As some indication of this, it is enough to know that 50% of steels sold today did not exist five years ago.

These developments have important consequences on the functions of steel and in particular its assembly by welding.

These aspects will be dealt with in the following sections, which will cover the principal welding modes used for thin sheets:

– spot welding,

– seam welding

– laser welding,

– MIG/MAG welding.

8.1. Spot welding

8.1.1. *Principle*

Spot welding belongs to the family of resistance welding, along with seam welding, projection welding or butt joint. It is used to assemble two sheets (or more) whose thicknesses typically range from 0.5 to 10 mm. Note that these two sheets can have different characteristics (composition, coating) and do not necessarily have the same thickness.

Historically, it was Thomson who, in 1877, had the idea of assembling two steel sheets by using, as a heating agent, the effect of a high electric current passing through the assembly. Figure 8.1 shows the principle of spot welding: the two sheets are clamped between two electrodes in order to maintain contact. A strong current is then passed through this assembly which will create a molten nugget at the sheet to sheet point of contact. On cooling, this molten nugget will locally fix the two sheets together.
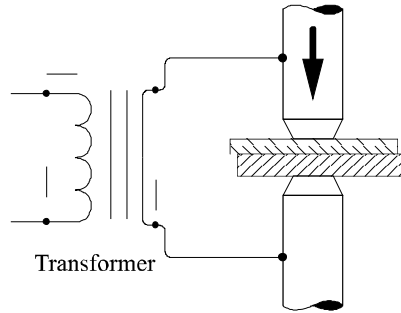
Figure 8.1. *Principle of spot welding*

To have a clear idea of welding conditions, it is important to consider the following parameters:

– welding current: kA, qq. V,

– clamping force: kN,

– cycle duration: one second.

8.1.2. *Tests of spot weldability*

By the concept of sheet weldability, we understand here the study of its suitability for spot welding. In France, when considering the homologation of sheet steels for automobile manufacture, these studies are generally carried out according to the method recommended by standard NF A 87-001 [NOR 94]. It is a question of determining, for a given sheet, its *field of weldability* and the *electrode life* used for its welding.

In both cases, the quality criterion of a spot weld, in terms of mechanical strength, is the *nugget diameter*. The definition of the term *nugget* given in standard NF A 87-001, is the following: "*The rivet remaining on one or other of the sheets after destructive testing of the spot weld*".

According to the study, this destructive test is carried out in different ways. In all cases, it is, however, important to note that the destructive test does not inevitably call into question the spot weld (rupture in mating plane, *tearing* of spot, etc.).

The minimum and maximum diameters of the weld are then measured using slide calipers. The acceptability criterion relates then both to the minimal diameter (greater than 3 mm for sheet thickness less than 1.5 mm and greater than 5 mm for

thicker sheets) and to the average of both (greater than 4 mm for sheet thicknesses under 1.5 mm and greater than 6 mm for thicker sheets).

8.1.2.1. *The field of weldability*

The test-specimens used for this type of study are tensile cruciform samples (see following section).

Standard NF A 87-001 defines the field of weldability as the "*range of effective welding current strength making it possible to achieve a spot weld of yield strength satisfying the criteria defined before*".

It should be borne in mind that the spot diameter and thus the mechanical strength vary with the effective current strength. If it is too weak, the spot is too small; if it is too high, there is molten metal expulsion. This is schematized in Figure 8.2.

By field of weldability we mean the interval $\{I_{min}, I_{max}]$ where I_{min} is the lowest current giving an acceptable diameter and I_{max} the highest current not causing expulsion.
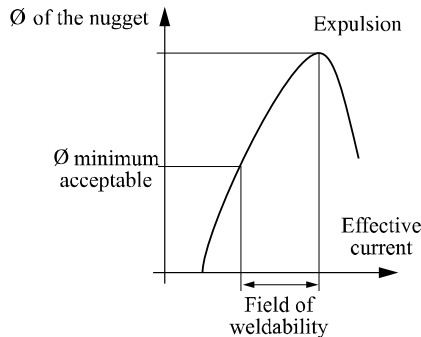
Figure 8.2. *Qualitative variation of weld diameter according to the effective current strength*

Unbuttoning

To measure the spot weld diameter corresponding to a given current, two test-pieces are welded together in the configuration given in Figure 8.3. These are maintained in this position before and in the course of welding by a jig. After welding, unbuttoning is performed by applying two opposing forces whose purpose is to separate the two parts (see Figure 8.3).

The traction force applied increases over time until weld rupture. The operator then notes, insofar as a button appears on one of the two sheets, the minimum and maximum diameters as well as the force – in daN – at which the assembly failed [NOR 94].
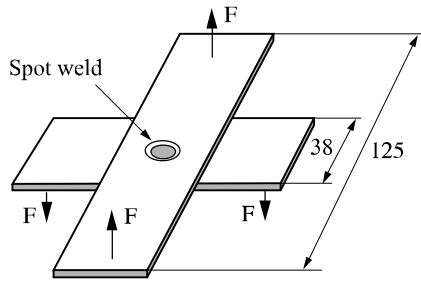
Figure 8.3. *Cruciform tensile specimens*

8.1.2.2. *Electrode life*

This test is designed to estimate the number of good quality spot welds which can be carried out with a set of electrodes while maintaining the same welding conditions.

For that, new but broken in electrodes are used and sheets called *wear strips* are welded at the higher end of the field of weldability According to the electrode life estimated *a priori*, every 200, 100 or 50 spots a control strip of 10 spots is made for mechanical tests. According to the spot diameter obtained on this control band, the operator decides either to continue the test by keeping the same effective current, or to carry out a *resetting* of this current. Indeed, if the spot welds no longer conform to the quality standard, that is due to electrode wear, wear which generally occurs with an increase in their active surface area (electrode wear directly influences a product's field of weldability: it shifts to the top and tends to diminish). One of the ways of curing this current reduction is to increase the effective current. This operation is called *resetting*.

When resetting is undertaken, the new effective current corresponds to the new upper limit of field of weldability. It is thus necessary to again determine the maximum current without expulsion with the worn electrodes.

The test is stopped on the initiative of the operator, when he estimates that the percentage increase in the current is too high, that the number of welds per increment is too low or that the visual quality of the spot is unacceptable.

Measuring the spot diameter

To monitor the weld quality of the control strip, a device which simultaneously peels off the 10 spot welds is used [NOR 94]. This device, commonly called "jaws", is schematized in Figure 8.4.

For reasons of symmetry, the diameters of the two weld ends are not deemed significant.
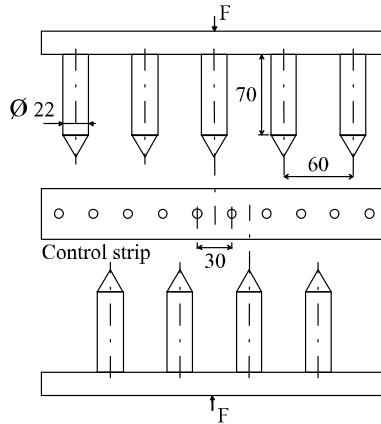
Figure 8.4. *Device to simultaneously unbutton ten spot welds*

8.1.3. *Spot weldability of thin steel sheets*

In this section, we will review the weldability of various families of thin steel sheets:

– steel sheet with a metal coating,

– steel sheet with an organic coating,

– high strength steel sheet.

Concerning the part devoted to the weldability of sheet steel with a metal coating, new light is shed on the advantage of welding these products using an intermediate frequency DC supply.

Standard NF A 87-001 takes into account only two sheet parameters to recommend the welding conditions: thickness and tensile strength. Moreover, the number of coated faces at the sheet interface as well as the thickness of the coating (higher than, lower than or equal to 10 μm) are also taken into account, independent of their composition.

8.1.3.1. *Sheets with a metal coating*

We will find in the sections which follow indications on the results of welding characteristics for several metal coated products currently available on the market. It should be noted that the great majority of these coatings are zinc coated, galvanized, electro-zinc coated or Galvallia.

What occurs when a bare product is changed for a zinc coated product? Concerning the welding parameters, if the force remains unchanged, it is necessary to increase the welding time by a period per layer of zinc coating present. This increase is necessary because it allows the evacuation of zinc. The field of weldability on zinc coated sheet is shifted towards higher currents and it is reduced. The electrode lifespan is decreased. Indeed, the lifespan is reduced from several thousand spot welds with the same set of electrodes to a few hundred welds. The mechanisms of electrode degradation change, whereas on bare sheet there is only mechanical degradation, on coated sheets chemical interactions occur which rapidly curtail electrode life.

Concerning zinc, galvanized or electro-zinc coatings, the results of laboratory analyses and the experience conveyed regularly by industrialists (in particular car manufacturers who have representative samples) indicate that electro-zinc sheet offers longer electrode life than galvanized. That can appear surprising, but the explanation is probably found in the structure of the galvanized coating: this has a very fine layer of interfacial alloy Fe_2Al_5 at the interface sheet/coating. This alloy inhibits the iron/zinc diffusion and thus prevents the iron substrate from diffusing in the zinc coating, which keeps liquid zinc available longer than in the case of electro-zinc, which does not have this inhibiting layer. Interaction times between liquid zinc and the copper of the electrode being longer in the case of galvanized sheet, the electrode degradation is increased, which leads to greater electrode life on electro-zinc than on galvanized zinc.

Figure 8.5. *Fields of weldability on metal coated sheets*
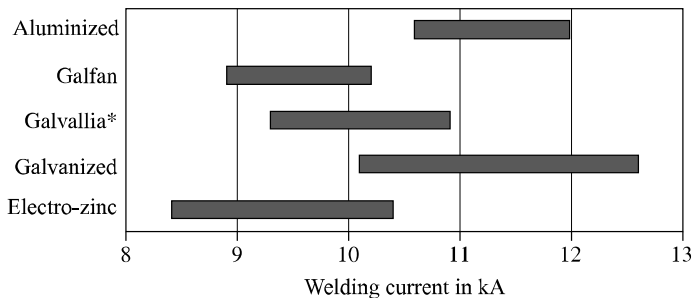
* Galvallia: Galvannealed

Figure 8.5 shows examples of fields of weldability applicable to the principal metal coated products. It should be noted that the values in the graph correspond to a single test and cannot be regarded as definitive results.

It should be noted that the presence of a metal coating does not have an influence on the mechanical resistance of the welded point.

The results for electrode life are indicated in Figure 8.6. Just as for Figure 8.5, the results presented below are single test results.
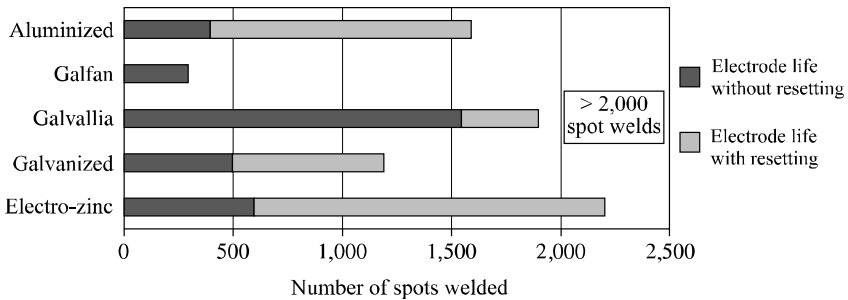
Figure 8.6. *Electrode life on metal coated sheets*

8.1.3.2. *Spot welding using direct current (DC)*

A DC generator has an *efficiency* advantage, insofar as, to obtain the same effective current, an AC generator must be able to provide higher instantaneous currents.

Traditional DC generators (like rectified hexaphase) being rather expensive, an alternative technology has been developed. These generators, known under the term *medium frequency* because they chop the signal at frequencies of about 1,000 Hz, have a price somewhere between that of the traditional AC generators and that of DC generators.
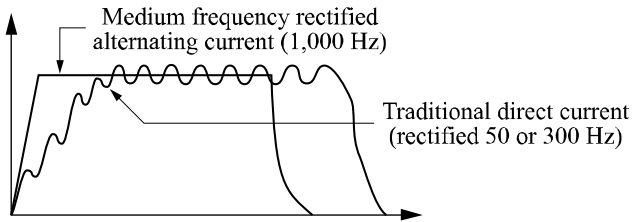
Figure 8.7. *Wave patterns of traditional DC and medium frequency rectified AC*

The following advantages in terms of weldability are advanced.

The electrical energy provided by DC is greater than that provided by AC, which would make it possible to weld more quickly or at lower current levels, which is obviously advantageous [WES 93].

The greater regularity in the application of electrical energy is beneficial to the development of the molten weld nugget, for example by avoiding premature expulsion due to current peaks, characteristic of AC signals [BOS 92].

The Peltier effect between sheet and electrode (generation or absorption of heat in addition to the Joule effect due to the passing of an electric current at the interface), the total effect of which is cancelled in AC, becomes significant again in DC and could make it possible to weld with greater ease dissymmetric assemblies on the condition of polarizing the current in the right direction. The same effect can be the source of dissymmetrical electrode wear [DRO 93].

The changeover to DC for spot welding zinc coated sheet seems advantageous, and is achieved via a widening of the fields of weldability and a clear improvement of the electrode life (see Figures 8.8 and 8.9).

However, these effects are very variable according to the nature of the coating. Moreover, a certain number of mechanisms remain to be understood before we completely master spot welding using DC [DUP 00].
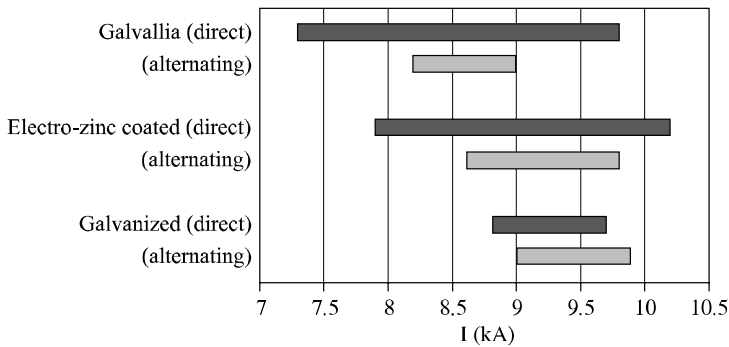
Figure 8.8. *Position of the fields of weldability*
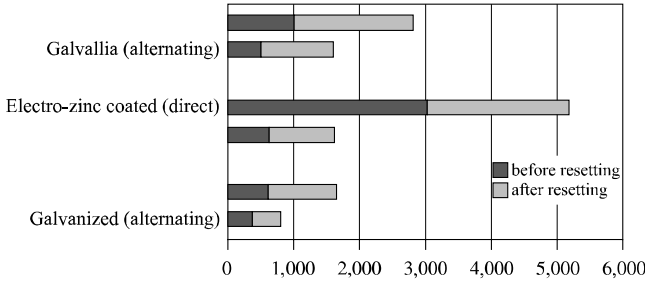
Figure 8.9. *Electrode life*

8.1.3.3. *Sheets with organic coating*

The presence of an organic coating brings with it specific phenomena. The destruction of the coating will generally be accompanied by the release of fumes and, in certain cases, the occurrence of a sharp snapping sound sometimes coupled with a spark (breakdown). A disturbance of the welding signals at the beginning of the current passage is observed. This is due to voltage surge and current drop compared to the normal operating figures.

The mechanical strength of spot welds is not affected by the presence of the organic coating. On the other hand, it brings about an increase in the *total static resistance* by a factor of 10,000.

In general, concerning double-sided products, the presence of an organic coating led to a shift (from 2 to 3 kA) towards the lower current limits in the field of weldability. The addition of a TOC (*thin organic coating*) has a neutral or negative effect on the width of the field of weldability (see Figure 8.10).

A: TOC sheet for household appliances (Solready)
B: Prepainted weldable sheet for the automotive market (Usiprime W)
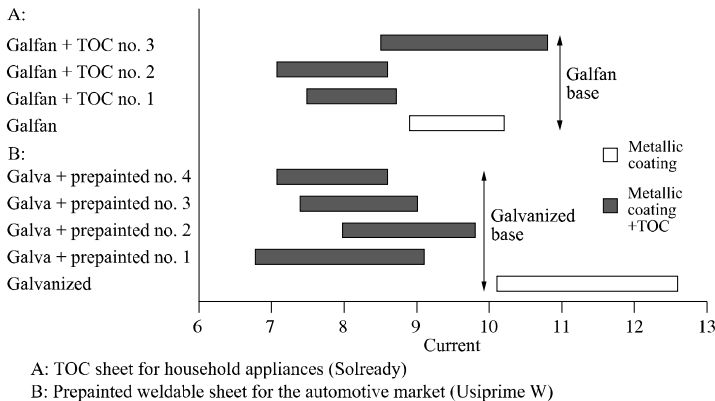
Figure 8.10. *Comparison of the fields of weldability for products with an organic coating*

The optimization of the coating makes it possible to obtain a notable improvement in electrode life, compared to that obtained with metal coatings. However, with a non-optimized coating, electrode life can be severely reduced.

8.1.3.4. *Ultra-high strength steels*

New ultra-high strength steels have been developed quickly to meet the needs of the automobile industry in terms of safety, formability and weight saving. Moreover, it must be possible for these steels to be assembled by the techniques commonly used in the production of bare bodyshells.

Because of its robustness, its simplicity of use and its low costs, resistance welding remains the favored method for assembling ultra-high strength sheet steel, for structural and support applications.

Several metallurgical methods exist simultaneously to fulfill the common requirements of very high strength and improved stampability, calling upon analytical adaptations and a thermomechanical *process*.

Alongside traditional metallurgical methods, such as steels with dispersoids and bainitic steels for hot sheets, one of the most interesting developments has been in Dual-Phase steels: obtaining martensitic islands in a ferritic matrix (from 5% to 20% in proportion) making it possible to reach an excellent compromise between very high mechanical strength and improved formability.

A typical representative of the Dual-Phase range is Usiphase D 600: for this grade the aim is to achieve a minimum tensile strength of 600 MPa, for a minimum elongation of 20%. It is possible to refer to [BAB 99] to find complementary information on Dual-Phase steels.

Spot weldability of Usiphase D 600 was studied on bare and galvanized sheet, and galvanized sheet with alliation treatment (or Galvallia). Its suitability for spot welding was considered on a homogenous assembly according to the welding parameters described in standard NFA 87-001.

Table 8.1 should be referred to for a summary of protocols and test results for welding in several formats, thicknesses and coatings that are representative of the range.

State	Thick. (mm)	Force (daN)	Welding time (per.)	Clamp time (per.)	Cur. min (kA)	Cur. max (kA)	Field of weld-ability (kA)	Electrode life (before/ after resetting)
bare	1.2	400	14	14	7.1	8.6	1.5	nd
Gz*	1.45	450	3* (9+2)	20	8.8	11.2	2.4	600/1,200
Ga**	1.5	450	3* (9+2)	20	8.4	11	2.6	1,800 (nd)

* Gz: galvanized ** Ga: Galvallia = galvanized with alliation treatment (galvannealed) nd: not determined

Table 8.1. *Spot weldability characteristics of Usiphase D 600*

The results show a good weldability of homogenous assemblies with the standard parameters, regardless of the coatings (galvanized and Galvallia). The fields of weldability are, in all cases, higher than 1.5 kA, which constitutes the generally accepted minimum value.

The electrode life on assemblies using Usiphase D 600 coated sheet is satisfactory and does not differ in orders of magnitude from the typical values recorded for coatings applied to substrates other than Usiphase D 600. A broader analysis of all the formats showed that electrode life before resetting, for galvanized and Galvallia Usiphase D 600 sheets, ranged from 600 to 1,000, and from 1,800 to 2,400 welds respectively.

A characteristic phenomenon which can occur during spot welding of high strength steels is weld rupture via partial unbuttoning, or on the mating plane when subjected to purely tensile forces.

These specific rupture modes are different from those obtained on softer steels (rupture by unbuttoning). They can obstruct the application of reference testing based on complete unbuttoning to ascertain the weldability of products. In a more general way, these particular rupture modes are the source of much confusion regarding their origins and their possible consequences on the mechanical strength of the spot weld.

The origin of these particular ruptures results from welded nuggets with a very high content of hard phases: for example, because of its sensitivity to heat treatments, the spot welded nuggets of Dual-Phase steels are mainly composed of martensite. The proximity of these hard nuggets and the notch bottom to the

sheet/sheet interface involves a strong stress concentration in a core with very low ductility, and tensile rupture along the mating plane.

It has been established that it is possible to avoid the problems of interfacial and partial ruptures and to return to a normal unbuttoning by increasing the welding time and force. Obtaining more concentrated nuggets then distances the notch bottom and the martensitic core and thus lowers the stress concentrations in the nugget [FER 97].

The simultaneous increase in welding effort and time leads to the absence of ruptures in the mating plane by increasing the distance between the notch bottom and the weld nugget.

In addition, analysis of the rupture load values of joints welded in Usiphase D 600 Galvallia 2 mm thick and welded according to the two conditions (the standard and time parameters) demonstrate that the occurrence of interfacial or partial fractures does not have a notable influence on the mechanical strength of the spot weld. The increase in the welding load and time prevents interfacial rupture (welds with zero spot diameter) and limits dispersion of tear strength at the lower level (see Figure 8.11).
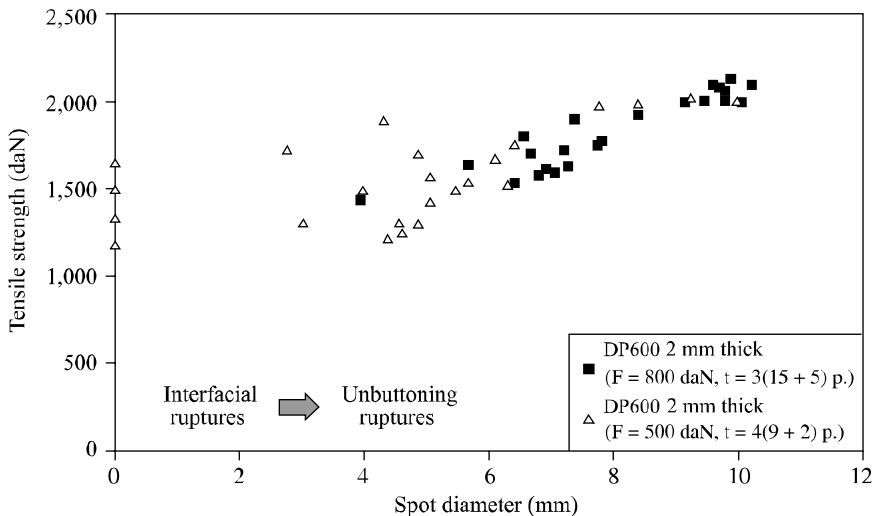
Figure 8.11. *Evolution of tensile strength according to the spot diameter for Usiphase D 600 Galvallia 2 mm in thickness*

8.2. Seam welding

Seam welding is a resistance welding process producing a continuous welded bond between two steel sheets. This welded connection is obtained, after superposition of the sheets, by rolling with friction, on their external faces, two copper electrodes connected to a voltage generator. The Joule effect produced at the sheet interface, combined with their displacement relative to the electrodes, makes it possible to achieve a continuous weld.

This process, according to the applications, presents some variations which are types of roller seam welding.

8.2.1. *Mash seam welding*

When a continuous welded bond between two sheets is required in order to crush their surfaces together, mash welding is the technique employed. This operation is constantly used by the iron and steel industry at the start of continuous annealing processes, electro-zinc coating, galvanization, tinning or inspection. It allows the butting together of reels, a need imposed by the continuity of production. In the automotive industry, this welding mode is employed to produce composite blanks intended to be pressed in one operation. The car manufacturer aims, by using this process, to achieve the twin objectives of reducing his production costs, by the suppression of superfluous stages, and maintaining the constant drive towards vehicle weight reduction (the right thickness at the right place).

To assemble two flanges by mash welding is, for the moment, only a rectilinear welding operation. It is thus necessary to prepare the bond edges by shearing them. A simple workshop shear suffices for this operation. The edges thus prepared are then slightly overlapping throughout their length. Maintaining a constant overlap is the principal requirement at this stage. Figure 8.12 schematizes this welding mode.
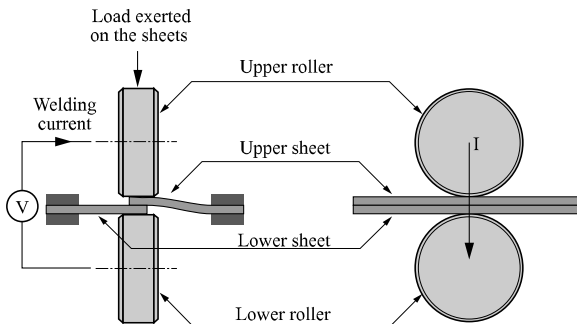
Figure 8.12. *Mash seam welding*

Once the sheets are fixed in this position, they are firmly clamped together. The welding operation then consists of rolling a pair of electrodes (rollers) on the overlapping surfaces. The potential difference between these electrodes generates a strong current (several kiloamps) which creates a Joule effect between the sheets in contact. The compressive force which is applied between the electrodes crushes the volume of steel between them.

Thus a welded strip is formed a few millimeters wide and lower in thickness than the sum of the two sheets (see Figure 8.13).
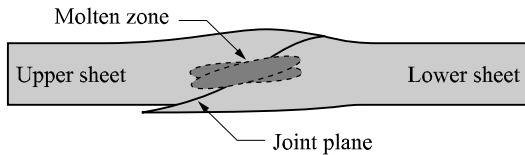
Figure 8.13. *Cross-section of a mash welded joint*

8.2.2. Overlapping seam welding

An overlapping welded bond between two sheets is achieved by resistance seam welding. This welding process is employed in the automotive industry during the assembly of fuel tanks. Two variations of this process are usually employed today:

– wide lapped seam welding;

– narrow lapped seam welding.

These two modes of seam welding differ only in the profile of the rollers used. Figure 8.14 schematizes the mode of wide lapped seam welding.
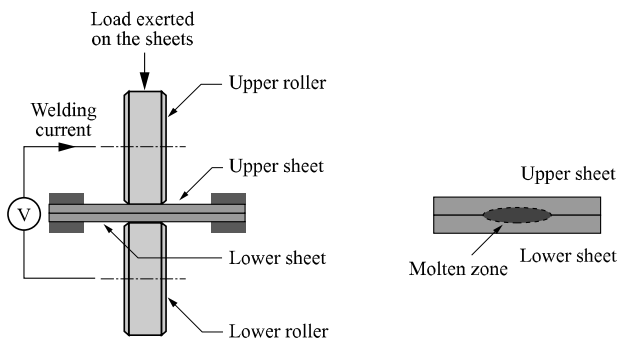
Figure 8.14. *Wide lapped seam welding*

The profile of the roller is flat so that the distribution of the welding effort is uniform. Narrow lap welding brings rollers with a particular cambered profile into play (see Figure 8.15).
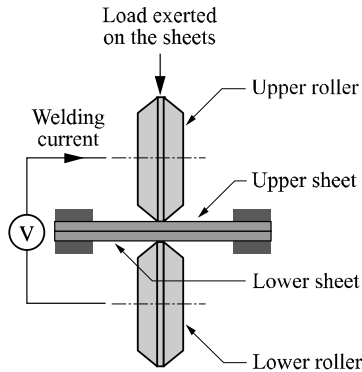
Figure 8.15. *Narrow lapped seam welding*

The parameters which define these two welding modes are:

– welding current,

– welding effort,

– welding speed.

As opposed to mash welding, it is possible to achieve curvilinear welded seams using this overlapping technique.

8.2.3. *Example applications studied or handled with customers*

For applications such as barrels, radiators, boilers and tanks, the air- or water-tightness of the weld is dependent on the continuity of the molten cores. This can be easily assessed in the laboratory by means of micrographic observations (longitudinal sections) and by visual observation of weld surface regularity. Lastly, in an industrial environment, pressure tests (helium for barrels, water under pressure – 8 to 10 bars – for radiators and boilers, vacuum for tanks) are carried out on the production line.

For the particular application known as *longitudinal barrel welding*, two welding modes are encountered: mash welding and narrow lapped welding.

In the case of mash welding, the welding current is in general single-phase unmodulated current. The welding speed often ranges between 10 and 15 m/min. The consistent overlapping of sheets is in the majority of cases ensured by a device called *Z-iron*. Its value generally lies between 1.5 and 2 mm.

In addition to the problems of mechanical adjustments (overlap control), the problems generally encountered for this application relate to changes in steel type and its effect on the quality at the beginning and the end of welding (zones under high loads during crimping), along with controlling the wear of the active surfaces of the rollers.

In the case of lapped welding, the overlap can reach 4 to 6 mm according to the thicknesses to be welded, and welding speeds range between 1 to 3 m/min.

For *tanks made out of aluminized sheets*, the problem we encounter mainly relates to the presence of porosities in the molten zone. Their size can be such that the weld is no longer perfectly sealed. A fast degradation of the active faces of the electrodes frequently necessitates machining of the active surfaces. An optimization of the welding parameters (effort, speed, current and modulation) is sometimes necessary. For this application, water cooling of the weld surface (at the two interfaces of electrode and sheet) makes it possible to minimize the degradation of the active surfaces of the rollers.

For *radiator and boiler* applications, the welding of the products used, generally bare, can be affected by changes in steel types or processes followed (batch annealed, continuous annealed). Thus, the seam welds produced for the closing of radiator panels can be an area of compactness defects. In this case, the welding parameters must then be adapted. The increase in the welding effort and the application of rising or falling current slopes (*slope up* or *slope down*) are generally enough to guarantee a satisfactory weld and the absence of porosities.

8.3. Laser welding of thin sheets

Laser welding is well adapted to the welding of bare and coated sheets; it enables the production of weld beads with particularly interesting characteristics:

– limited vaporization of the coating thus better galvanic protection against corrosion;

– narrow and penetrating beads (up to 10 mm penetration with a 5 kW CO_2 source, bead widths in the order of 0.8 to 2.5 mm for sheets of thickness up to 3 mm);

– very little deformation and clean welding (allowing, for example, to weld finished parts, without any finishing process);

– excellent mechanical characteristics allowing excellent stamping and fatigue characteristics;

– a high degree of welding accuracy and very high speeds.

An increasingly used tool in the automotive sector, laser welding is now accepted as a reliable industrial tool. In certain cases, it tends to replace certain so called *traditional* welding modes. Welding is thus one of the major manufacturing processes in which the laser has found an active application field. Several types of assembly are employed, as indicated in Figure 8.16.
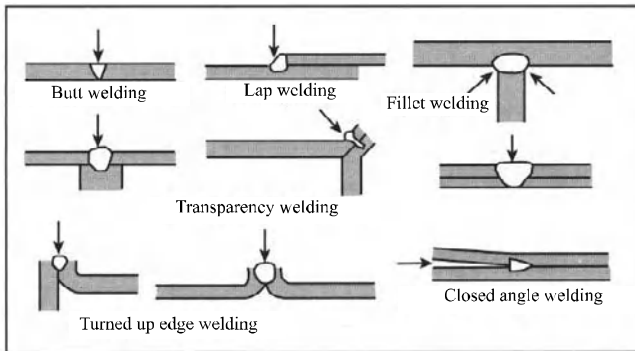
Figure 8.16. *Various types of assembly in laser welding*

In the following sections, only two applications, butt welding and transparency welding (or lapped welding), will be dealt with.

8.3.1. *Principle of keyhole laser welding [BOI 92]*

Initiation: interaction between beam and material

Keyhole laser welding requires high energy densities obtained while working at the focal position of the optical system. Sufficiently high power densities, from approximately $10^6 W/cm^2$ to $10^8 W/cm^2$, can be attained to melt the metal.

The laser beam reacts optically with the material, and the degree to which it interacts thermally with it depends on multiple reflections which are linked to the nature and surface state of the material. At room temperature and a wavelength of

10.6 μm, the reflectivity of materials reaches at least 90%. At its melting point, the material absorbs up to 95% of incidental energy.

Keyhole welding

The beam directed by the optics is thus focused on the workpiece to be welded. Right from the beginning, the laser beam interacts with the material and heats it with the aim of creating a molten pool, followed by its vaporization. Progressively, the molten volume increases and the laser beam penetrates gradually in the material, as is illustrated in Figure 8.17, by forming a capillary or *keyhole*.

After welding, three areas characterizing the weld can be seen:

– the *molten zone* bordered by the bond zone,

– the *heat affected zone*,

– the *base metal* (not affected thermally).

Figure 8.17 shows the cross and longitudinal section of a weld bead. The three zones quoted previously can be distinguished very clearly. The bead aspect is known as the *nailhead* and all the zones that play a part in the weld can be seen: weld pool, vapor capillary in the case of *keyhole* welding and the HAZ.
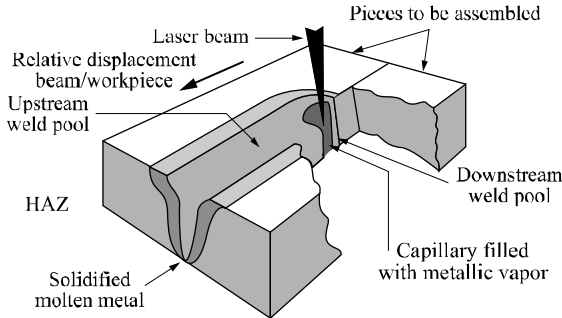
Figure 8.17. *Cross and longitudinal section of a weld bead*

With multikilowatt continuous CO_2 lasers, narrow and deep welds are achieved, without distortion, on steel parts several centimeters thick. These penetration welds are similar to those carried out with electron beams. The advantage of the laser lies primarily in high welding speeds in an open atmosphere. It can be shown that the initial penetration processes depend on the beam, its power and the surface of the material to be welded.

Appearance and blowing away of plasma

Plasma formation occurs during *keyhole* welding which is undesirable, since it interacts with the beam, and significant, since it heats the sheet intensely. It is formed by the ionization of metal vapors and the assistant gas. Plasma can absorb a large part of photon energy (up to 70% in certain cases). It thus constitutes an obstacle to achieving good penetration and its fluctuating character limits speed and causes defects. It is thus necessary to blow or deviate the plasma to avoid beam absorption. This blowing away of plasma must be optimized because it is a source of defects, for example, porosities. The tube diameter, the blowing direction and the flow along with the blowing height must all be carefully controlled.

8.3.2. *Butt welding*

Figure 8.18 shows the various phenomena observed during the formation of a laser weld bead.
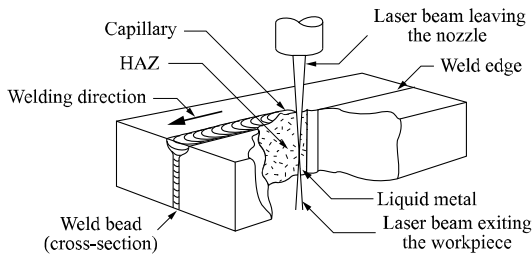
Figure 8.18. *Formation of a weld bead*

The sheets to be assembled are placed edge to edge. Under the focused laser beam the capillary is formed which contains the gas plasma and which is lined by a molten metal layer in dynamic balance. The geometry of the beam at the exit of the part is important because it partly determines the profile of the weld bead.

By moving the part (or the laser beam) in the direction indicated, the molten metal moves from the front to the back under the effect of surface tensions and the variations in temperature. The solidification of metal gives rise to the weld bead and leads to the appearance of chevrons on the surface which point towards the beginning of the weld.

With the laser process, high cooling speeds are achieved (about 100 to 400°C/s). At the metallographic level, the brevity of the interactions generates microstructures with extremely fine, homogenous grains containing few impurities and hardened

microstructures for steels containing alloying elements. The quality of the weld depends enormously on the balance of all the mechanisms involved in the *process*. Any disturbance of this balance can cause a weld defect.

8.3.2.1. *Influence of operational welding parameters*

Obtaining a good quality weld requires the adjustment of several parameters which ensure its quality. The principal parameters are:

– laser power,

– welding speed,

– focusing optics,

– position of the focal point/surface of sheet,

– nature and pressure of the assistant gas,

– beam polarization.

8.3.2.2. *Constraints in laser beam butt welding [VER 99]*

The laser welding of two sheets placed edge to edge must take into account the narrowness of the energy beam just a few hundred microns in diameter. It is essential that the edges to be welded are as close as possible. This condition imposes a very strict limit on the gap between two sheets. Typically, for sheets of thickness below 3 mm, the gap between the sheet lengths to be welded should not exceed 10% of the thickness, using the 6 kw CO_2 lasers currently available on the market.

To this initial gap, which is purely mechanical in nature, we must add sheet displacement in the course of welding due to the welding operation itself. Upstream of the impact point of the laser, the fast cooling of the molten metal leads to a compression stress field which closes the joint on itself. Downstream from the impact point, i.e. in the part yet to be assembled, this stress field pulls apart the edges to be welded. Beyond 500 mm of welded length, the scale of this *thermal opening* of the joint makes the welding operation impossible without the sheet being powerfully clamped, even granting an excellent preparation of the edges.
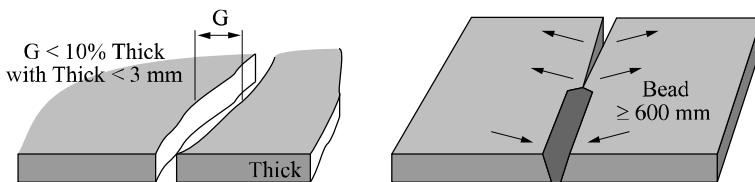
Figure 8.19. *Gap between the sheets: a) mechanical, b) thermal*

Other constraints are related to the positioning of the sheets to be welded on a horizontal plane so that the laser beam reaches the joint line, and does not deviate away from the joint. As a general rule, the tolerance regarding the position of the focal spot, with respect to the weld line, corresponds to 25% of the melted zone width, which is about 0.1 mm. To respect this tolerance in Y positioning, the latest welding machines are equipped with sophisticated systems of joint detection.

Many solutions have been developed to obtain quality welded joints taking account of the narrowness of the laser beam. We mention below the most widely used technical solutions.

This precision between the sheet edges can be obtained by precision cutting with a press or laser cutting before welding. These solutions are generally rather expensive.

The principle of the technical solution patented and developed by Usinor is to hold the sheet edges against each other by pressure exerted laterally in the plane of the blank perpendicular to the joint plane. These laterally applied forces hold the sheet edges against each other, and exert a pressure on the edges of the sheets which results in a local reduction of the apparent gap between sheets. The operation of laser beam welding is thus facilitated when starting from sheets obtained by traditional shearing.

The use of a bifocal welding head, double laser YAG or mixed welding laser plus plasma makes it possible to increase the acceptable tolerances between sheets to be welded. This last solution can be complementary to the two others quoted above.

8.3.2.3. *Laser welding of steels with very high mechanical properties*

Steel types with very high mechanical characteristics are of great research interest for the car manufacturer seeking the best compromise between safety and vehicle weight. However, the weldability of these steels is compromised by the elevated chemical composition of these steels.

The cooling kinetics inherent in laser welding will lead to the formation of hard martensitic structure in the welded zone of HS steels (high strength). This will limit the stampability of these laser welded joints. Figure 8.20 has as an example the martensitic microstructure and the results of the hardness filiation through the weld observed on a laser joint welded in 0.2% carbon steel.
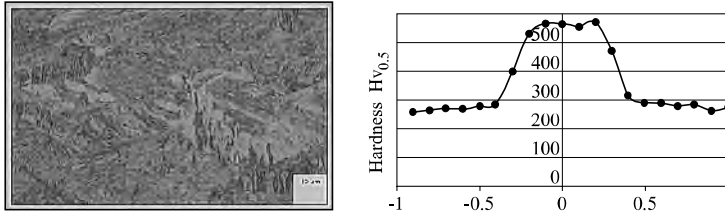
Figure 8.20. *Molten metal microstructure and hardness filiation, steel with 0.2% C*

As shown in Figure 8.21, the mechanical strength (the stamping height to weld rupture joint is related to the stamping height of the sheet at its thinnest part: the percentage thus calculated is called the *Erichsen stamping value*) of laser welded joints is dependent on the average carbon content of the two assembled sheets. For average carbon content higher than 0.17%, the minimum of 70% Erichsen stampability is not achieved. However, in heterogenous welding (the most frequent case in creating laser butt welded blanks), the addition of a stampable low carbon steel type to HS steel types will result in a drop in the average carbon content of the welded zone and thus will very markedly increase the stamping characteristics of the welded joint (Erichsen stamping value for Usiphase T800/XES: 85%).
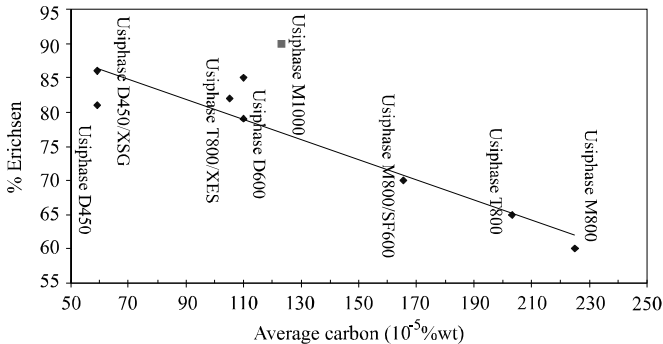
Figure 8.21. *Evolution of Erichsen stampability with average carbon content of the molten zone*

8.3.2.4. *The welding of coated steels*

The properties of the material used (reflectivity, density, thermal conductivity, vaporization temperature, ionization energy) influence the energy absorption of the laser. Monochromatic light, such as that produced by the laser, is more or less absorbed by materials. The absorption level is also a function of the specific wavelength of the laser (CO_2 = 10.6 µm and Nd: YAG = 1.06 µm). In particular, the

nature of the coating can modify the surface absorption of the laser beam's energy. It is generally said that there is a modification of the laser/material interaction. This can lead to important variations in laser output from 5% to 20% at room temperature.

This will effect a modification in acceptable maximum welding speeds or a modification of the tolerances in positioning the sheet under the laser (a more or less penetrated and wide joint according to the laser output).

As an example, a more matt aspect of the coating Usiplex Zn 3000 (organic coating) ensures a very broad field of weldability in comparison to the same electrozinc coated steel assembly. Figure 8.22 compares the fields of weldability between the galvanized assembly (10/10)/Usiplex Zn and the (10/10) electrozinc galvanized assembly.

Welding parameters

Power (kw)	Flow He (l.min-1)	Focal distance (mm)	V (m.min-1)
3.6	24	150	4.5

End to end assemblies

| XES G 10/10 1.5 mm | XES EZ 5/5 TOC 3/3 1 mm | XES G 10/10 1.5 mm | XE 280 P EZ 7.5/7.5 1 mm |
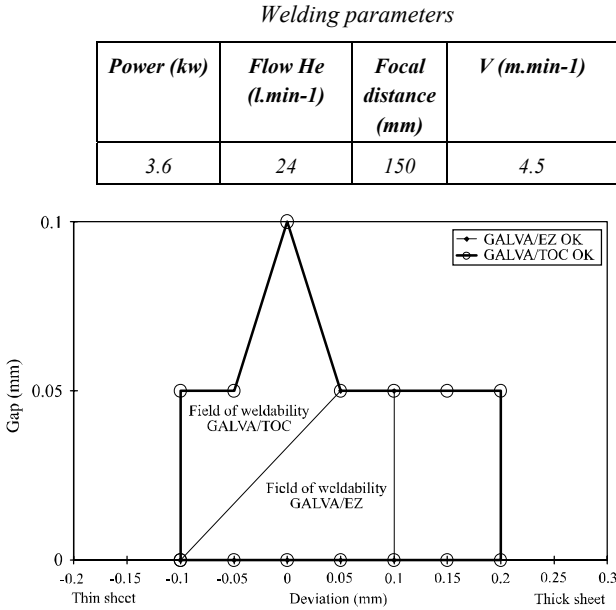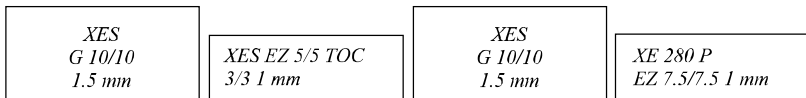
Figure 8.22. *Laser field of weldability (acceptable gap between sheets as a function of laser beam deviation)*

In a more general way, it should be recalled that laser welding is a process of welding without contact. There is thus no change to the welding *process* brought about by the sheet's coating.

Moreover, the low surface vaporization of the coating (0.8 to 2.5 mm) ensures a galvanic protection of the assembly against corrosion. The results of corrosion tests, after a surface treatment (phosphatizing) and painting (cataphoresis), show that laser welds present the same corrosion behavior as the base metal. What is more, a galvanic protection of the bare sheet by the galvanized material in the contact zone can be observed. The width of the protection zone is in the order of 5 mm.

8.3.2.5. *Laser blank welding for the automobile industry [VER 99]*

A laser welded blank is the end to end assembly of two or several single metal parts, of differing thicknesses, characteristics or surfaces, by laser welding. These blanks are intended to be pressed then assembled in automobile manufacture, in particular for bare body shells and doors.

The components produced using welded blanks are, for example, chassis members, floors, inner wings, doors, sills, etc. (see Figure 8.23).
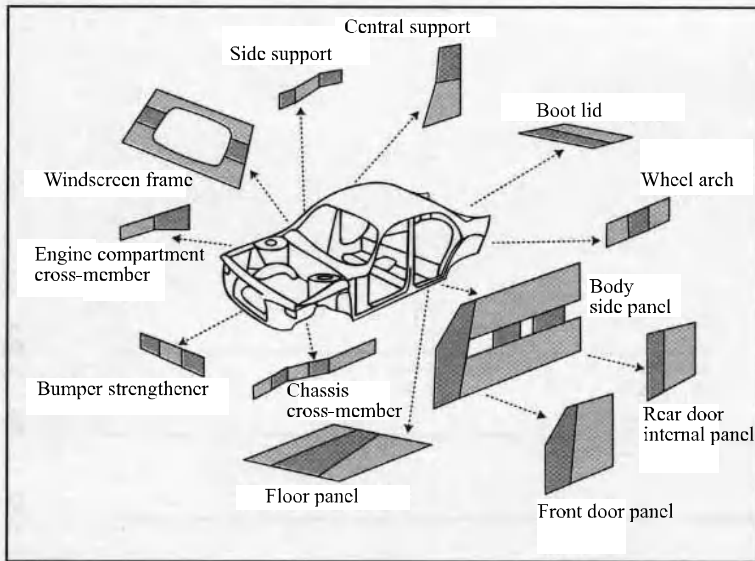
Figure 8.23. *Examples of parts made from welded blanks*

The first industrial blanks were assembled by resistance seam welding. Laser welding, which is better adapted for coated sheets, has been developed in recent years.

The main advantages for manufacturers in using welded blanks are the following:

– weight reduction; the welded blank makes it possible to put thick steel only where it is strictly necessary. Weight savings of 20% to 40% are possible according to the type of component and the technology employed (linear or curvilinear welds);

– improvement in safety thanks to a better impact resistance and a better dynamic behavior of the component weight for weight. The use of laser welded blanks makes it possible to accommodate crumple zones for the absorbtion of energy in the event of an impact;

– improvement in fatigue strength by the replacement of spot welds by continuous welds;

– reduction in the number of components and consequently a reduction in production methods and stages, ensuring an increase in productivity while decreasing the investment and costs with regard to stamping and metal forming;

– improvement in vehicle corrosion performance by local optimization of the coating but also through a reduction of the number of reinforcements, thus avoiding box members susceptible to corrosion.

In practice, it should be noted that when a cost reduction is sought, the profitability of welded blanks comes in general from a reduced investment in stamping tools and metal forming and that it is further increased by thickness savings, coatings and numerous other advantages.

Generally, it is seen that welded blanks make it possible to confer the required properties on a specific part of a component. They make it possible to reduce the component weight by avoiding extra thickness where it is not necessary and they improve safety and longevity thanks to optimized impact strength, fatigue strength and corrosion performance.

8.3.3. *Lapped welding*

Lap welding is under development in the automotive industry. It is used more and more for 3D welding of bare body shells. It allows, in addition to the use of laser welded blanks, to increase vehicle rigidity or to facilitate design which result in an increase in safety and a reduction in vehicle weight. However, the majority of the steels used in car production are zinc coated for the best corrosion resistance.

However, laser lapped welding does throw up certain problems. Indeed, the vaporization temperature of zinc (906°C) is definitely lower than the melting point of steel (1,540°C). The vaporization of zinc at the sheet interface involves expulsion of the molten metal in an explosive way, creating porosities in the molten metal and generate a pollution of the molten metal by zinc.

The well known solution which enables welding technicians to avoid this degasification of zinc in the welded zone is to create a gap between the sheets before welding. An empirical solution suggested by Akhter *et al.* [AKH 88] shows that the necessary gap (*g*) between sheets is linked to the sheet thickness (*ep*) and to the coating thickness (*r*) by the following formula:

$$g = \frac{A\,V\,r}{\sqrt{ep}}$$

with *V* the welding speed and *A,* the constant function of the beam characteristics.

Typically, for sheets of thickness varying between 0.8 mm and 3 mm, the gap between sheets is in the order of 0.1 mm to 0.2 mm.

However, this solution is not always easy to implement on pressed sheets in 3D welding. The gap between sheets must be rigorously controlled. It is important to add that an excessive spacing between sheets will lead to a collapse of the weld pool and to a bad quality weld. Moreover, spacing between sheets will lead to a reduction in the fatigue strength of the assembly. As an example, a gap of 0.2 mm between sheets 1 mm thick leads to a fall of approximately 20% in fatigue strength.

With this in mind, new *process* solutions [BON 00, HON 00, XIE 99] are being worked on for lap weld coated sheets without a gap. Various authors propose welding solutions: bifocal welding, tilted welding or mixed welding (laser + diode, laser + plasma, etc.). All these solutions aim to:

– pre-heat sheets to eliminate all or part of the coating between sheets before welding;

– limit the interaction of the laser beam with the welding plasma;

– extend the molten metal surface to facilitate the evacuation of zinc fumes;

– reduce the cooling speed to leave time for the diffusion of zinc fumes.

It is necessary to adapt the process parameters from one product to another.

8.4. Arc welding

In welding assembly procedures, arc processes have a significant role, in particular TIG (*tungsten inert gas*) welding, plasma and MAG (*metal active gas*), the process most commonly found in industry. As the description and the procedure of these processes were detailed in Chapter 1 we will outline here only a few rules essential to achieving successful welds on thin sheets.

The application fields of thin products are mainly in general industry, where we find manufacturers of radiators, domestic water systems, air-conditioning and then obviously the motor industry.

Product development relates to high yield strength (HYS) steels, with high resistance (HR) and zinc coated products.

8.4.1. *TIG welding*

This welding process is perfectly adapted to very thin products, making it possible to obtain high quality welds, with a low output. Welding speed is generally about 15 to 50 cm/mn; in automated welding, higher speeds are possible [COL 94].

For steel welding, direct polarity (negative electrode) is always used with argon as the shielding gas. The joints recommended are indicated in Table 8.2.

Thickness	Preparation for TIG welding
0.5 to 2 mm	No preparation and without gap; no filler
<5 mm	60° V chamfer or no preparation with gap equal to half its thickness
>5 mm	70° V chamfer – gap = 2.5 mm

Table 8.2. *Types of preparation in TIG*

The edges to be welded must be clean and degreased. A copper support can be employed to facilitate penetration for thicknesses greater than 2 mm.

The welding parameters are determined by the nature and composition of the base metal, the thicknesses to be assembled and fastening method. The parameters set out in Table 8.3 can be adopted as starting values for the adjustment of machines.

Thickness (mm)	Electrode (mm)	Rod (mm)	Speed of welding (cm/mn)	Current (A)
0.5	1.6	None	15 to 25	15 to 30
1.0	1.6	0.8	30 to 50	45 to 60
1.5	1.6	1.2	50 to 60	70 to 100

Table 8.3. *TIG welding parameters*

In the case of welding without filler metal, it is important to give careful consideration to the base metal. Indeed, in this type of welding, only the base metal takes part in the joint construction. Convection movements, which affect the molten metal, are influenced by residual and killing elements contained in steels in particular sulfur and aluminum. To ensure a correct damping and penetration of the molten metal, it is necessary to limit the sulfur content to 0.015% and aluminum to between 0.015 and 0.035%.

8.4.2. *MAG welding*

For thin steel products, MAG welding is the process most universally employed. For thicknesses higher than or equal to 2 mm, it is ideally suited. For thinner materials, the conventional MAG process is more difficult to use; in this case, the pulsed mode makes it possible to obtain satisfactory operational weldability. The wire is of carbon-manganese type according to standard NF EN 440 for solid wire, with the possible addition of alloying elements: molybdenum, nickel and chromium, principally, in order to obtain the properties of mechanical strength in the molten metal. The wire is chosen according to the base metal and mainly the mechanical properties that the weld must guarantee.

The shield gas is primarily a mixture of argon and CO_2 with variable contents from 2.5 to 20% to improve the transfer of metal in the arc. Other possibilities of binary mixtures $Ar + O_2$ or ternary $Ar + CO_2 + O_2$ exist for specific applications such as vertical down welding $(Ar + O_2)$, MAG welding in pulsed mode (ternary) or to suit the nature of the wire. Indeed, pure CO_2 does not allow the transfer of metal in the arc by axial pulverization (or *spray arc*); on the other hand, it enables welds of excellent compactness (without porosity) to be achieved. Generator developments and the introduction of pulsed currents have today made it possible to use only gas mixtures and to lower the weldable thicknesses to some tenths of a mm, e.g. for body work panels.

8.4.2.1. *Types of transfer*

In MAG welding, the type of metal transfer in the arc is a function of the voltage, current and gases used. The principal modes of transfer are the following:

– short-circuit (*short arc*),

– globular or large drop (*free fly*),

– axial pulverization (*spray arc*).
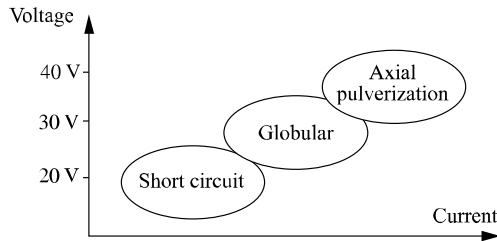
Figure 8.24. *Types of transfer in MAG welding*

Transfer by short-circuit

This method exists with a short arc, low current and a low voltage (lower than 20 V). A drop formed at the wire end comes close to the part. When it touches it, it causes a short-circuit which, by the electromagnetic pinch effect, detaches the drop from the wire. The cycle starts again. The detachment of the drop generates projections. The frequency of the short-circuits lies between 50 and 200 Hz.

This mode is well adapted to the welding of thin sheets, in all positions.

Transfer by axial pulverization

This mode exists with a long arc, a high current (higher than 250 A/mm^2 of wire cross-section) and a high voltage (higher than 20 V). The wire then melts, in the shape of very fine droplets projected towards the part, without creating a short-circuit but with some projections. This mode cannot be used with pure CO_2.

It is generally used on thick sheets (over 6 mm) in a flat position.

Globular transfer

This mode is obtained with intermediate voltage and current values between those of short-circuit and axial pulverization. The formation of large drops, which detach in an erratic way and burst on contact with the part, generates many

projections. This transfer mode is interesting for its high welding speed in applications where projections are not an issue.

The filler transfer modes in the arc are in direct relationship with the electric parameters, the nature of the wire, its chemical composition and the shielding gas. In the case of thin sheet welding, the transfer by axial pulverization is difficult to use while taking required energy into account, except by using copper joint supports which maintain the molten metal bath.

As for globular transfer (or large drop), it is generally advisable to avoid this mode as far as possible, because it generates considerable projections. There thus remains only the short-circuit transfer for thin sheets, as used for body panels.

Recent progress in the electronics of the power source have made it possible to develop generators which provide pulsed currents of great stability which are adjustable in ranges from 30 to 300 Hz and are perfectly suited to thicknesses lower than 2 mm; they make it possible to obtain a stable transfer by axial pulverization in the field of very thin sheets.

8.4.2.2. *Case of coated sheets*

Coated products such as Usicar and Extragal, require an adapted welding process [COL 94]. The difficulty of welding continuous zinc coated products lies in the different vaporization and melting points of Zn compared to steel. Figure 8.25 demonstrates what happens in a weld. The example treats a fillet weld or lapped joint – the most limiting – because zinc in its vaporized state cannot escape.
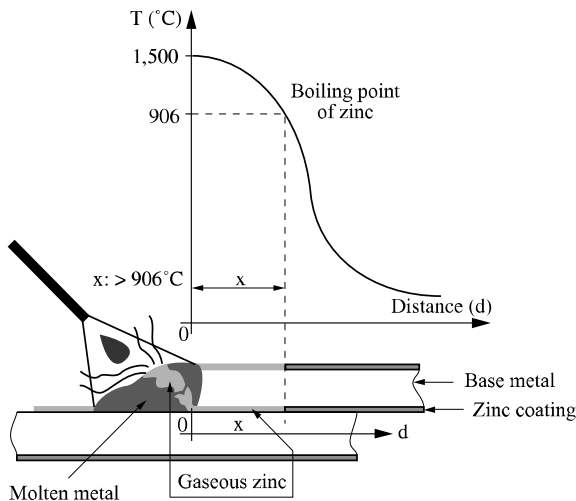
Figure 8.25. *Fillet weld or lapped joint*

Zinc melts at approximately 420°C and vaporizes at 906°C, which means that the arc "is contaminated" by zinc in its vaporous state. This results in an unstable and erratic arc, significant projections and quite a few porosities in the weld beads. The first solution is to maintain a constant gap between the sheets to be assembled, which would make it possible for the zinc to escape. However, such a thing is not easy to guarantee amidst the realities of production.

Another solution consists of limiting the volume of zinc in its vaporous state by acting on the welding parameters; low wire and welding speeds are adapted, that is to say so called *short-circuit* transfer, which generally means a considerable amount of more or less adherent projections.

Filler products specific to coated zinc products have been developed. These generally contain additional elements such as titanium and/or aluminum in the case of solid wire. Another solution has been studied. It consists of using a wire whose fusion is obtained with a very low welding energy. Some cored wires currently correspond to this fusion mode: this is true of Sadual ZN, which makes it possible to weld a 650 g/m^2 galvanized coated product (approximately 50 µm thickness).

A last solution consists of using filler products with a melting point lower than that of steel, in a process called *braze welding*. It is named thus because it associates the technique of brazing (fusion of the filler without fusion of the base metal) with that of welding. The copper based wires, Cu + 8% Al, Cu + 3% Si and Cu + 0.8% Sn are the most frequently used products. The gas used to protect the arc and the molten metal is necessarily ensured by a neutral or inert gas, such as argon or a Ar + He mixture.

8.4.2.3. *Case of HYS and HS steels*

A priori, all non- or low alloyed steels are weldable with the help of a filler wire depositing a bead with mechanical and metallurgical characteristics at least equivalent to those of the base metal. There then arises the problem of products of the type Soldur 355 to 700 (steels with dispersoids), Solform 600 and 800 (ferrite/bainite steels) or UHSS (ultra-high strength steels). The higher the grade, the greater the chemical content of the suitable filler products in order to obtain mechanical characteristics that are at least equivalent to the base metal. The operating conditions become more problematic. Indeed, the risks of cold cracking come from the filler and not from the base metal. According to thicknesses (greater than 5 mm), specific operating conditions such as pre-heating can be implemented according to the fastening degree of the assemblies.

In the example given below, under bead hardness filiations were carried out on a Soldur 700 steel, i.e. of 700 MPa yield strength, with various welding energies. This test makes it possible to define the maximum limit of welding energy applicable to

this steel without fearing too great a softening of the HAZ. Indeed, too long a thermal cycle at high temperature is likely to destroy the mechanical properties obtained by thermomechanical rolling.

8.4.2.4. *Under bead hardness*

Bead deposits (on a solid sheet using MAG with a solid wire) made at various energies makes it possible to define the maximum limit of energy able to be used with Soldur 700.
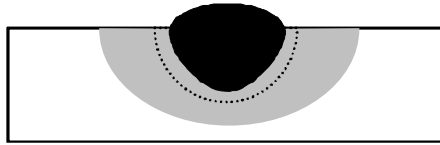
Figure 8.26. *Under bead hardness filiations on Soldur 700 steel*

Measurements of hardness HV10, at 6 points in the HAZ, are carried out on the line of fusion + 1 mm. Table 8.4 presents the results of measurements.

Energy of welding (kJ/cm)	HAZ 6	HAZ 11	HAZ 14	Base metal
Minimal hardness HV10	262	257	244	275
Maximum hardness HV10	278	267	250	283
Average hardness HV10	270	262	248	280

Table 8.4. *Under bead hardness of Soldur 700*

Hardness decreases quickly with the increase in welding energy. The maximum permitted energy is quickly reached, ranging between 5 and 10 kJ/cm. It is necessary to avoid excessive contributions of heat. This recommendation can be defined by a maximum of 2 kJ/cm per millimeter of thickness for the product obtained by thermomechanical rolling.

8.5. Bibliography

[AKH 88] AKHTER R. *et al*., "Laser welding of zinc coated steel", *Lasers in Manufacturing*, Cotswold Press Ltd, UK, 1988.

[BAB 99] BABBIT M., CANTINIEAUX P., "Les aciers HR et THR: offre, mise en œuvre et performances", *Symposium auto et carrosserie automobile*, Cannes, 1999.

[BOI 92] BOISSELIER D. *et al.*, *Le soudage laser de faibles et moyennes épaisseurs*, Centre Technique des Industries Mécaniques, 1992.

[BON 00] BONSS S. *et al.*, Innovations in laser hybrid technology: the combination of CO_2-laser and high power diode laser, Section C-ICALEO, 2000.

[BOS 92] BOSCH, Avantage du soudage en courant continu, Documentation commerciale, 1992.

[COL 94] COLLECTIF, *Le livre de l'acier*, Techniques et documentation, Lavoisier, Paris, 1994.

[DRO 93] DROUART C., *Soudage par résistance,* Publication du soudage et de ses applications (IS), 1993.

[DUP 00] DUPUY T., FARDOUX D., "Spot welding zinc coated steels with medium frequency direct current", *Sheet Metal Welding Conference IX*, Detroit, October 2000.

[ELI 89] ELIOT D., *Le soudage par faisceau laser*, Publication de la Soudure Autogène, 1989.

[FER 97] FERRASSE S., VERRIER P., MEESEMAECKER F., "Resistance spot weldability of high strength steels for use in automotive industry", *The IIW 50th Annual Assembly*, San Francisco, Doc. no. III-1076-97, 1997.

[GEY 93] GEYSEN M. *et al.*, *Tolérances en soudage laser de forte puissance*, Institut de Soudure, 1993.

[GRE 78] GREGORY E.N., *Welding zinc-coated steels*, Welding Institute Publication, 1978.

[HON 00] HONGPING G., A New Method of Laser Lap Welding of Zinc-coated Sheet, Section C-ICALEO, 2000.

[NOR 94] NORME FRANÇAISE A 87-001, Caractérisation de la soudabilité par résistance par points de produits plats revêtus ou non, December 1994.

[PRA 88] PRANGE W. *et al.*, "Utilisation de la soudure par laser des tôles fines", *Revue de Métallurgie*, 1988.

[VER 99] VERRIER P., "Fabrication et utilisation des flans raboutés pour l'industrie automobile", *Revue de Métallurgie*, 1999.

[WES 93] WESTGATE S., LEWIS C., "Current voltage waveform developed in typical AC/DC resistance welding power sources", *Int. Inst. Weld.*, Doc. no. III-1022-93, 1993.

[WES 93] WESTGATE S., LEWIS C., "Comparison between electrical efficiency of AC and DC power sources for spot welding zinc coated steels", *Int. Inst. Weld.*, Doc. no. III-1020-93, 1993.

[XIE 99] XIE J. *et al.*, "Laser lap welding of galvanized steel with no gap", *International Body Engineering Conference*, September 1999.

[XIE 99] XIE J. *et al.*, Single-sided Laser Welding of Galvanized Steel, Cooperative Research Program EWI, 1999.

Chapter 9

Welding of Steel Mechanical Components

9.1. Introduction

This chapter presents the main techniques of welding steel mechanical components using examples from the automotive industry – apart from body panels – and discusses the specific weldability limits due to functional needs and mass production.

To determine these needs, they may be helpfully compared with those of steel construction (see Chapter 10). The latter relates especially to a single construction or to a limited set, and requires easy assembly and relatively crude joints in terms of positioning and finished aspect. It is in this context that welding has, for example, replaced the riveting of railway station beams or plates for ship-building, etc. Moreover, elastic strain limits (a beam's sag limit for example) need specific geometries (moments of inertia) and generally these limits come into play before the strength limitations at the critical bond zones.

For mechanical components, the fatigue performance to weight ratio is often of paramount importance and requires demanding mechanical characteristics which are possible only with alloyed steels and are therefore not easily weldable.

Moreover, mechanical components generally have specific service requirements:

– geometric precision: as an example, many parameters which characterize gear teeth are measured in micrometers,

---

Chapter written by Yves DESALOS and Gérard PRADERE.

– wear resistance and tribology of friction surfaces justifies a very exacting surface condition: roughness, Hertzian pressures, coatings, physico-chemical endurance,

– pitting resistance in certain contact zones,

– various types of fatigue performance: contact, notch, corrosion, etc.

For all these reasons, the steels used for mechanical parts are often treated to strength levels higher than 1,000 MPa, and the corresponding assemblies generally must:

– be welded with a high degree of accuracy in their relative positioning,

– have their mechanical properties lightly down graded especially in restricted loading areas,

– be able to undergo heat treatments or complementary finishing processes.

These stipulations must obviously be modulated according to the type of component concerned. In the automotive industry, for example, the welding requirements are different for suspension components and mechanical parts.

External components, like subframes and suspension assemblies, are generally manufactured in low alloyed steels, with rather low carbon-manganese contents (less than 0.2% C, 1% Mn), often without any finishing treatment. These parts are spot welded (for thin sheets) or with a weld bead, without significant metallurgical problems.

Mechanical parts, as in the power unit or transmission, on the other hand, are manufactured in steels whose composition and heat treatments are especially adjusted to the properties required by use. In automatic gear box manufacture, for example, mild steels locally nitrided in the friction areas are often used for housings, but also mid-carbon steels (i.e. XC 42 grade) subject to local induction hardening, as well as more alloyed nitriding steels for the most severely frictioned parts. As for bending and spalling performances at the tooth root, they can be satisfied by fairly shallow carbo-nitriding and steel alloys such as 27 Mn Cr 5 or 30 Cr Mo 4 for current automotive requirements, although deeper thermochemical treatments and higher alloyed steels are obviously needed for truck pinions. At the very extreme, bearing components are generally manufactured in the emblematic 100 Cr 6 grade without any possibility of welding!

The criteria to evaluate operational weldability depends on the components under consideration, in particular the possible extent of the joint's remolten zone. As long as the latter requires a filler or several passes and remains relatively large (in the order of what was presented for steel construction), the majority of the quite

restrictive metallurgical and mechanical considerations (carbon equivalent, clamping constraints, hydrogen, etc.) which have been set out in the previous chapters remain applicable. On the other hand, more severe tolerances are required the narrower the remolten zone is (high energy beams), and these tolerances may be completely reduced in some contact joining (friction welding, electrical resistance welding, or diffusion welding in the solid phase).

In this presentation, the adaptation of arc welding conditions to alloyed steels [CAZ] and the metallurgy of the welded joint [AWS, GRA] will only be outlined briefly. We will concentrate on the possibilities of limited fusion processes used in welding operations for the mass production of mechanical components. We will show that the mass production requirements for mechanical construction need robotized welding processes, compatible with cycle times and control procedures on the assembly line.

This chapter will proceed via the following technical items:

– bond specificity requirements, operational standards and the weldability of alloyed steels used in mechanical components;

– main types of welding processes used for mechanical components and examples of these processes in automotive engineering;

– specifications and quality control of the welds for these parts;

– developments and tendencies with regards to mechanical component welding.

9.2. Specificities of welded bonds in mechanical components

9.2.1. *Standard welding processes and general recommendations*

Spot welding is the rule for the assembly of thin mild steel sheets in body panels because the sheet clamping and the robotization of spot welding have for some time now operated with a widely recognized productivity and ease of use.

For mechanical components, previous manufacturing practises, which used to aggregate the functional surfaces into fewer sub-parts more or less easy to assembly, seldom encouraged welding.

However, the development range of these parts results from many feasibility and cost factors (ease of machining, assembly, treatment, etc.) in which the opportunity of welding compared to other modes of joining is not always decisive.

Initially, some thermal or mechanical fretting can prove sufficient, either alone or with complementary safety adjuvants like adhesive bonding, keying, pinning or extra spot welding. For the components which need a complementary thermochemical treatment, it is necessary to grind or hone surfaces and delayed failures may be expected in areas with residual stresses.

In some other cases, a traditional assembly by screwing or bolting offers an accurate enough connection without altering the properties of the finished components. An additional "disassembly capability" is thus ensured with limited extra machining and assembly costs.

Without any need for future disassembly, maintenance or exchange, the welding operation may be attractive from the perspective of the assembled parts. As for the process, it allows savings in cycle time, space or assembly personnel and manufacturing cost, especially if it is carried out on robotized multipost machines combining positioning, welding and possibly a stress relief process in less than one minute. This technology is used widely in the assembly of components such as automatic gear boxes, where steel shafts or low alloyed flanges must be solidly connected – with minimal dimensional obstruction – to clutch housings made of extra soft steel.

On the other hand, the risks of initial damage by cold cracking remain significant for the various forms of arc welding as soon as the *carbon equivalent* of the molten metal (dependent on the component parts' composition and that of a possible filler) exceeds 0.47% [AWS, GRA 95] and that the choice of the base metal cannot be modified. An adapted pre-heating, or even a post-heating treatment, may then become essential, according to geometric and thermal parameters of the assembled parts. Brazing can also be a viable option if the assembly is not subjected to excessive loads or if the surface area to be brazed is large enough (with the possible addition of grooves) to spread the static and dynamic loading.

Good part design can contribute to limiting the load a weld is subjected to, or to reducing the functional consequences of a particular assembly configuration. Consequently, a laser beam welding with a precise positioning may be satisfactory, for example because otherwise the assembled part would involve an overly complex or badly stressed geometry.

For some axisymmetric parts like bimetallic valves, high speed friction welding, with subsequent work on the bead, but often without any post treatment, fully justifies the material cost benefit on the component part.

Lastly, for most highly loaded parts, the alteration of mechanical properties after the welding operation is not a problem insofar as the heat treatments required to

achieve the properties demanded by future use are generally carried out after the welding operation. Nevertheless, it is necessary to avoid unacceptable bead defects: porosities and notch factors at weld root for fatigue or shock problems [LIE 82, DER 81].

Some technological recommendations are essential, as for any welding operation:

– in the joint design, it is essential to balance the masses on both sides, and to avoid any weak zones (small section, sharp angle) close to the weld;

– an axial weld has the tendency, unless clamped, to splay out the lightest part, while a radial welding involves a skewed setting. The insertion of one part in another instead of a gap between parts reduces these defects;

– a radial weld is preferable to an axial weld in cases of a difficult material or deformation;

– the permissible gap in the mating plane, established according to the machining tolerances, the positioning gap and the perpendicularity of the faces to be joined compared to their axis must be limited to 0.10 mm;

– the surface finish of the mating edges is limited to 10 μm, and burrs are generally prohibited on these faces;

– it is essential to remove any trace of rust and grease, and to dry the parts after washing.

These inexhaustive recommendations concerning the connection, are derived from experience and are fairly independent of the metallurgical factors affecting joint strength.

9.2.2. *Metallurgical defects in the molten zone and the HAZ*

The various possible defects in the welds may be classified into two main categories:

– technological defects such as those operating upon geometric matching, or the lack of fusion,

– metallurgical defects such as inclusions, porosities, cracks.

In fact, the metallurgical health of the welded joint depends firstly on a good choice of technological parameters: geometry and joint preparation, welding mode, linear energy input and welding speed, parameters of pre- and post-heating. The

molten zone and HAZ are critical areas because of their sensitivity to internal defects, inappropriate metallurgical structures and unfavorable residual stresses.

Furthermore, defects can reduce the cross section of the joint and give rise to stress concentrations which can lead to local failure at unexpected loads.

9.2.2.1. *Defects in the molten zone*

The most common defects in the molten zone after welding are:

– porosities due to dissolved gases either trapped during solidification or coming from chemical reactions in the molten metal;

– lack of penetration at the connection or between two successive beads;

– hot or cold cracking, in the sensitive structures, in areas with high tensile (transitory or permanent) stresses.

The superposition of a residual stress field to the applied stresses can reduce the service load of a defective welded joint still further.

Steelmaking conditions (deoxidation, sulfides, residual nitrogen content) may affect the risk of porosity and the bead shape (wetting capacity of the molten metal), but the main issues are related to the risk of cracking because of an unsuitable choice of operational parameters.

Arc welding, with rather high filler metal content and remelting, can lead to geometric defects (acute angled connections, lack of penetration), metallurgical defects (cracks) or enhanced latent defects (tearing on large inclusions).

Geometric defects mainly concern the positioning of surfaces to be welded and the operational practise. The weld depth may be a problem, in particular for weldings by high density energy beams – of the laser type – for which it is difficult to exceed 10 mm of steel with nominal outputs up to 10 kW.

However, mass produced mechanical components generally have limited dimensions, are the subject of careful ranges of preparation, with automated welding processes, which are therefore very reproducible.

9.2.2.2. *Various types of cracking*

Among the metallurgical risks of cracking, hot cracking may arise, related to the particular compositions of the molten metal (for example, sulfur or lead content higher than 0.025% to improve workability), and worsened by a poor weld bead configuration. Cracking by lamellar tearing because of poor ductility levels in the

through direction remains unusual in mechanical components judiciously welded in series after a whole range of validation tests.

Obviously, cold cracking in the HAZ associated with coarse hardened structures, residual tensile stresses and hydrogen traces remains the most significant obstacle to welding with large remelting zones in structural steels.

As for alloyed steels, cracks are the most frequent metallurgical defects: hot cracking in the melted zone, cold cracking in the HAZ, cracking on reheating:

– *Hot cracking*: this especially affects steels presenting an austenitic solidification. It results from the rejection of sulfur and phosphorus with a corresponding lowering of the solidus. The stresses at the end of bead solidification can then occasion tears at the location of the last liquid zones. This justifies content limitations for critical elements in fusion welded metals, of the type S + P <0.04%.

– *Cold cracking*: the conditions of hydrogen embrittlement (residual tensile stresses) are found in the HAZ as well as in the molten metal, because the latter is richer in hydrogen even with a more dilute composition than the HAZ. A sensitivity estimate of welded steels can be established from the various traditional formulae for carbon equivalent percentage, of the type $Ce = C + Mn/6 + (Cr + Mo + V)/5 + (Cu + Ni)/15$, etc. [DEB 84]. The significant influence of cleanliness, not taken into account in this type of formula, involves a recommendation of low impurity contents (S, P, Sn, As, Sb) in the case of difficult weldings. For sulfur, there are also risks of lamellar tearing which require the simultaneous control of sulfide content and morphology (necking through fibers); for example, sulfur is limited to 0.025% for automotive mechanical components.

– *Reheat cracking*: this is sometimes reported in the case of low alloyed steels for pressure vessels and poorly stabilized stainless steels. This is a case of intergranular crackings which can appear during post-heating, because of intergranular carbide precipitations and impurities.

In addition to the cracking risks, the required service properties of welded steels may impose particular demands on the welded zone: creep resistance for pressure apparatus in hot working conditions, fatigue strength in particular conditions, resistance to the various types of stress corrosion, etc. The intergranular chromium carbide precipitation in the HAZ during a welding cycle can compromise, for example, the tensile corrosion behavior of a stainless steel.

Lastly, welding on an already treated zone can involve cracking, because of the localization of strong residual stresses (for example, on an induction hardened part) or of dangerous alloying (thermo-chemically treated parts). In the latter case, it is

better to spare the zone which will be welded from thermochemical treatment or subsequent machining (grinding).

9.2.3. *Weldability limits for welding with and without remelting*

The metallurgical difficulties for welding result from the structural reactions of welded metals to the particular thermal cycles of the operation.

9.2.3.1. *Principal consequences of a significant remelting*

In case of remelting, solidification shrinking initially occurs in the melted zone, a function of the solidification interval of the metal, and in fact a mixture of the welded metal and the filler. The size of the molten zone, the shrinkage rate and the rheological behavior of metal during cooling governs the distribution of the residual stresses in the welded zone.

In general, the thermomechanical welding effects (solidification shrinkage in the melted zone, dilatations and strains during allotropic transformations, residual stress extensions) depend on the welding mode, the geometry of the joint and the metallurgical behavior of metal.

This behavior is obviously varied for alloyed steels, due to many various heat treatments: solution heat treatment, transformation and precipitation kinetics on cooling, precipitations during post-heating.

The prediction of this behavior requires the assimilation of the phase diagrams (for example, the Schaeffler diagram for stainless steels) and the continuous cooling transformation diagrams after special austenitization conditions prevalent in the HAZ (with particular carbide solubility and grain size). These effects, which have a great influence on the internal integrity and the service properties of the welds, have been the subject of quite complex software simulations (a well known example is SYSWELD). Often it is only necessary, for each type of welding and joint geometry, to refer to thermal data charts, which make it possible to visualize the cycles at the most critical points of the HAZ (see Chapter 3). Having considered the appropriate steel transformation diagrams, the evolution of the structures and their properties can be easily forecast.

It is very useful to reduce the extension of the melted zone as far as possible, in order to reduce the probability of bead defects, hydrogen embrittlement, the extent and danger of coarse grain martensite in the HAZ, damaging residual stresses, etc. From this point of view, raising the power of the thermal source is advantageous since it increases the thermal gradients (Fourier's law). In an extreme case, friction welding without remelting allows the joining, without any complementary

tempering, of bimetallic exhaust valves, a part of which is made of martensitic stainless steel of grade Z 45 Cr Si 9.

Even if it is difficult to avoid remelting and the concomitant risks of hydrogen embrittlement (only one ppm is already too much...), the brittleness of the out of equilibrium structures resulting from the reaustenitized coarse grain areas remains a problem.

Taking into account the relatively high hardenability of the steels used in mechanical parts, it is often difficult to slow down cooling at the end of welding and thus avoid martensitic structures whose hardness, brittleness and sensitivity to hydrogen traces increase with the localized carbon content. The brittleness of some higher carbon bainites or of some austeno-martensitic aggregates can be also a problem (see the example of steel grade 15 Cr Mo V6).

9.2.3.2. *De-embrittlement of the HAZ*

Tempering treatments after welding have two specific functions, often optimized in an independent way: relieving residual stresses and/or reducing brittleness from quenched metallurgical structures.

As soon as the steel composition precludes any possibility of achieving microstructures less sensitive to hydrogen while exploiting welding parameters, it is necessary either to reduce the harmfulness of hydrogen by pre-heating or to promote the diffusion of this gas out of the welded zone by post-heating (generally with a higher temperature than that of pre-heating).

Pre-heating has the main effect of reducing the cooling speed after welding and incidentally lengthening the time of hydrogen desorption on cooling, while post-heating performs only the latter function. The temperature-time cycle of post-heating is defined by a crack curve established from implant tests and leads to the concept of *critical post-heating temperature* for given welding conditions and material compositions.

In multipass welding, the critical post-heating temperature obviously also corresponds to the minimal temperature to be maintained between passes and after the last pass.

To avoid cold cracking on welded parts particularly high in carbon, it is sometimes possible to use an austenitic filler (often an austenitic stainless steel): if dilution makes it possible to preserve an austenitic structure after cooling to room temperature, it is not prone to brittle fracture, therefore to cold cracking. Moreover, hydrogen is relatively soluble in austenite, which contributes to trapping it in the molten zone and to avoid cracking in the HAZ. However, it is necessary to accept

the brittleness of the martensitic HAZ and the low mechanical characteristics of the molten metal.

In the case of stainless steel components, some grades to be welded (for example: exhaust pipes) require care in their composition such as stabilization of titanium or niobium: the trapping of carbon, from the very manufacture of the raw material in very stable carbides, avoids the precipitation of chromium and the loss of the stainless character – while contributing to the control of the grain size – in the HAZ. The welding of heterogenous assemblies such as stainless + low alloyed steels requires some precautions [FAB 83]: precautions in respect of the molten metal, the heterogenity of the molten zone after dilution and microstructural instability in service. For austenitic steels, a hyper-quench under conditions close to delivery treatment makes it possible to simultaneously achieve a stress relieved, fine grained, and stainless metal.

9.2.3.3. *Welding without remelting*

The following characteristics can be expected from this process:

– the absence of porosity defects, shrinkage pipes or gaseous desorptions related to the difference in solubility of the gases (H, N, O) between liquid and solid phase,

– less shrinkage stresses,

– less coarse and brittle structures.

On the other hand, the problems of geometric matching and putting the surfaces to be welded into close contact are more critical, and require better surface preparation, as well as a minimum interfacial work hardening [HOU 91].

During the minute long formation of diffusion welded joints, the mechanisms of recrystallization after interfacial work hardening contribute to eliminate the initial interface, but at a micrometric scale. In fact, the mean free diffusion path during one second in iron austenitic state is only about one micrometer at 1,400°C, so the micrographic observations of grain boundaries crossing the prior interface are related to heterogenous austenite recrystallization with pinned grain boundaries on inclusions.

As no reflection echo can be detected on the interface, when an ultrasonic survey is carried out at wavelengths in the steel around 10 micrometers, it is possible in theory to guarantee the absence of micrometric defects on this surface. On such a scale the echoes corresponding to inclusions also appear.

9.3. Principal types of welding for mechanical components

Various thermal sources offer realistic means to obtain strong joints in less than one minute on decimetric components.

Most traditional is the *electric fusion arc*. Melting allows the connection and filling of the machined joint. The volume of the molten metal can be increased by an external contribution: arc welding with coated electrodes, MIG (*metal inert gas*) or TIG (*tungsten inert gas*) shielded welding. This molten base metal contribution is sometimes impossible, as in electron beam welding. However, it can be carried out using a coating metal whose melting point is lower than that of the base metal which is not melted.

In the case of *brazing*, it is the wetting process which ensures the connection and the continuity of very close surfaces, whereas there is the filling of a wide joint by the filler metal in the case of braze welding. We shall deal with these two last techniques very briefly in this chapter.

The very close solid-solid contact of two clean metallic surfaces can also ensure connection and continuity: this intimate matching can be the result of a plastic deformation under mechanical pressure and of a rise in temperature supporting interdiffusion and interfacial recrystallization (*friction welding*, *resistance welding*).

Sometimes, a fugitive melted phase appears, but it is quickly expelled (as in the case for *spark welding*).

Lastly, friction welding relies upon fusion, just like *explosion welding* or *ultrasound welding*.

The most frequent classifications of these various processes are based on the nature of the energy supply and the protection mode of metal brought to high temperatures (slag, inert gas, or vacuum). However, our presentation will adopt the decreasing order of the lineic powers used, or better still the relative size of the molten zone. For a specific introduction to welding of various mechanical components, the following order will be used:

– electric arc welding and its derivatives,

– welding with narrow high energy beams (laser, electron beam, plasma),

– friction welding (in solid phase with limited intrusion of molten areas),

– butt welding by the Joule effect (with creep and no significant remelting),

– diffusion welding in solid phase (not yet on industrial scale).

9.3.1. *Electric arc welding and alternatives [CAZ 95, COL 83]*

9.3.1.1. *Various categories*

One of the oldest forms of welding is manual welding with a coated electrode, employed for prototypes or small runs with parts of limited size. The filler material consists of a fusible powder coated metallic rod which, upon melting, contributes to the extent of the molten metal and protective slag. Obviously, this technique is not compatible with mass produced automated welds in the automobile industry.

The submerged arc process under a powdered flux is especially used in automated procedures for welding of significant thicknesses in boiler manufacturing or some other mechanized weldings.

The MIG/MAG processes, with a consumable wire electrode from a spool and gas protection, are useful in terms of flexibility and productivity [BOU 89]. The TIG process, with a refractory tungsten electrode and inert gas protection, is primarily used for stainless steels with a particularly good final purity of the molten zone.

As for the welding of structural steels, the welding parameters (equivalent energy, speed, temperature of possible pre-heating) are adjusted from data charts of the type presented in Chapter 3.

For safety components like suspension parts or those transmitting engine torque towards the wheels, the weld beads are always ground to avoid notch effects. Some stress relief tempering is carried out to eliminate the risk of delayed failure, and each series of parts is metallurgically checked by sampling. Various non-destructive testings on the production line are systematic for that kind of part: magnetoscopy for emerging defects, and also radiographic or ultrasonic checks to detect major porosities. For mass production runs in the car sector, controls are especially implemented at the validation stage for that component range (see section 9.4).

To complement bead finishing, a pre-stress shot-blasting is frequently carried out on the welds in order to subject the zones in which fatigue cracks could occur to compression. Operations of scouring-passivation on stainless welds make it possible to standardize corrosion performance of the parts.

Figure 9.1. *View of driveshaft and CV housing (front wheel) with its arc weld*

9.3.1.2. *An example: arc welding of the drive shaft and housing*

The drive spindle and housing (see Figure 9.1) is the outer component of the CV joint taking the role of a stub axle, driven by the half shaft.
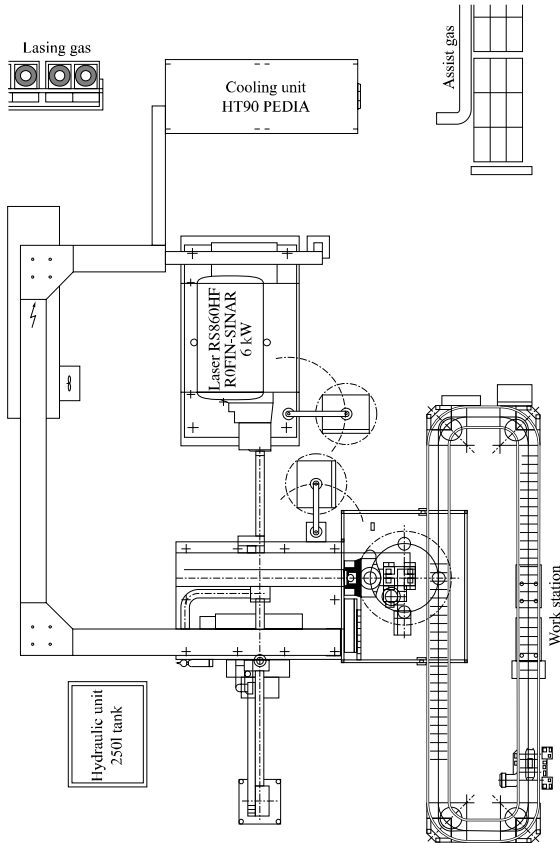

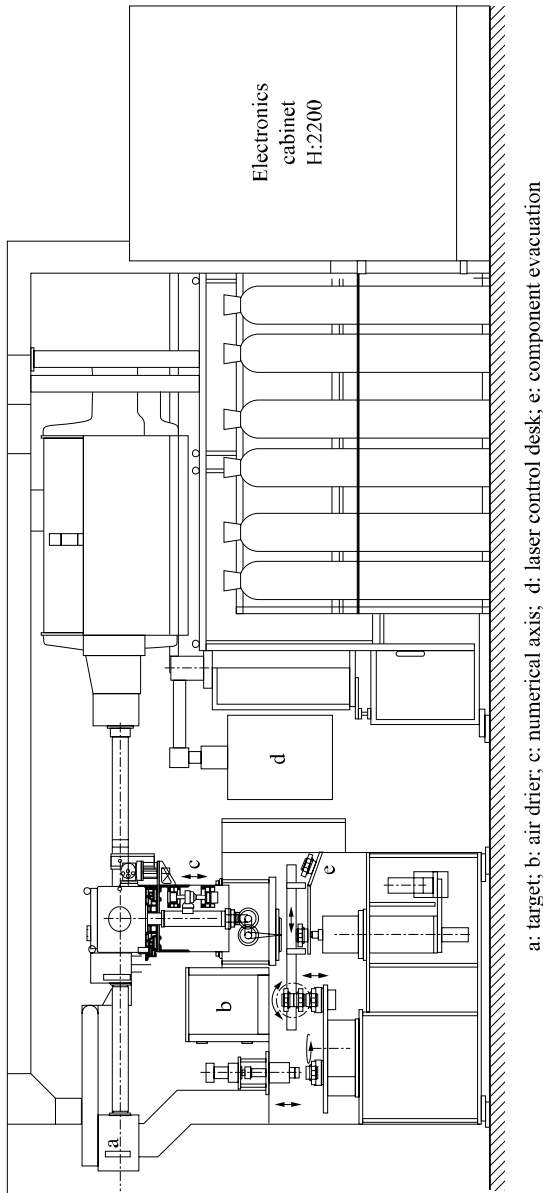**Figure 9.2a.** *Plan of a laser installation for a manufacturing facility in the automotive sector*

Figure 9.2b. *Plan of a laser installation for a manufacturing facility in the automotive sector*

The CV housing is made from low carbon steel hardened by precipitation (HES 400), the splined shaft in XC 42 allowing a later induction hardening of the splines and the bearing surfaces.

The arc welding of the shaft to the CV housing is carried out on a machine with a rotary table and automatic loading of the housings and shafts. The operation is carried out in two stations: vertically, in a turning chuck, with filler wire delivered from a coil; and under a protective gas (92% argon + 8% CO) delivered at a pressure of 3 bars.

After welding, an interior brushing of the housing is carried out to eliminate burrs, then the parts are removed to cool down naturally. The filler wire (GS2) 1 mm in diameter and with a coating of 2 μm is uncoiled at 15 m/mn during welding, while the circumferential chuck speed is 0.8 m/mn. The electric welding parameters are the following: 295 A, 31 V. The time cycle is 0.26 mn, which corresponds to a daily production of 12,000 units. The "fresh" welding, as well as the base of the housing treated by induction, are subjected on line to a tempering process with a peak temperature of 275-300°C controlled by IR pyrometers. A 100% check of the housing to shaft connection is carried out by ultrasonic checks.

9.3.2. *Welds with reduced HAZ using high density energy sources: laser beam, EB, plasma*

9.3.2.1. *Various categories*

To decrease the volume affected by residual stresses, it is helpful to reduce the melted thickness by the use of concentrated high density energy beams as the thermal gradients from the surface are proportional to the incident flux.

The fast developing process is a *laser beam* [BOU 92, CAZ 94, COL 83, MAZ 82] taking into account its convenience in use and the availability of ever more economic sources in terms of capital investment and maintenance costs.

For example, an automatic gear box manufacturing facility in the north of France achieves, for a recent gearbox, ten laser welds on a torque converter and mechanisms thanks to five 6 kW sources (high frequency excitation lasers), each one operating at rates of 200 parts per hour.

In Figures 9.2a and 9.2b a horizontal and side elevation of this installation are presented.

In the latest flat laser source configurations (*slab*), the optical resonator is positioned between the two mirrors and the two parallel radio frequency electrodes: as the heat of the excited gas is dissipated in these two water-cooled electrodes, the traditional systems of gas circulation are no longer necessary, which leads to lower overall dimensions, low gas consumption and improved performance with lower energy and maintenance costs.

Typically, a CO_2 laser with an effective 6 kW power output costs around €4.10^5. To put a coarse price on such laser weldings, we can imagine an automated installation of two transverse flux lasers of this type, consuming 120 kW, and a weld rate of 200 parts per hour (the size of automatic gearbox components, for example): the total cost price (technical costs + indirect costs + depreciation) of the integrated operation is less than €0.5 per component

CO_2 lasers operating at a 10.6 µm wavelength remain the most widely used for their high power output (up to several kW), although YAG or laser diode batteries with a wavelength close to one micrometer have better absorption characteristics and can use fiber optics as a waveguide. Laser diodes are becoming increasingly popular, with output powers close to one kW, and welding robots to weld small runs of various components (see section 9.5).

Laser has limitations in the thicknesses it can weld and the depth penetration of the beam is typically less than 10 mm. Its field of use is still very broad for mechanized welded construction where subsidiary binding parts have to be welded to the main structure (for example: pins, lugs, drive forks, etc.). These weldings can undergo dangerous notch factors at the surface of the molten zone, especially for low toughness special steels (K_{1c} <50 MPa $\sqrt{m}$), and these risks can be avoided by pre or post-passage of a defocalized beam.

Electron beam welding is widely used industrially in boiler operations for the petrochemical industry or for nuclear power plants. In that context, welding concerns specific alloyed steel grades and thick plates. The advantages inherent in the process are the following [BOU 95, GRA 81, VAL 83]:

– better productivity than for the traditional welding processes on the same thicknesses,

– limited deformation of the assemblies,

– no atmospheric pollution.

Figure 9.3. *Picture of a dog clutch welded onto a pinion with teeth cut or not*

Handicaps, mainly porosity and low toughness of the melted zone, relate only to rather thick parts.

The electron beam with power modulation can be easily used for pre or post-heating, and thus high quality multipass weldings can be obtained. The constraints of vacuum techniques (preparation, washing, and degasification of surfaces to be welded, frequent vacuum breakdowns, etc.), the need for component demagnetization before each welding and the rather high investment costs limit the mass welding of small parts. It is still used in the car industry for transmission components.

Plasma torch welding with blown arc (more rarely with transferred arc) takes advantage of the high temperatures of the plasma source, appreciated in particular for welding or coating with stainless steel; these transferred plasma processes can cope with significant welding depths, using relatively inexpensive torches (less than €5.10^4 for a few kW) which are space saving and versatile. This type of torch is quite frequently used in specialized welding installations for small runs of relatively large mechanical components.

9.3.2.2. *Metallurgical quality*

We have seen that electron beam welding allows the creation of very narrow and relatively deep beads, which leads to overall low deformations and clamping effects, a small shrinkage of the molten zone, reduced residual stresses and a narrow HAZ with impaired metallurgical characteristics.

Although inevitable, porosities can easily be brought back to reasonable sizes and densities. They are generally large and round at the bottom and side of the melted well, but small elsewhere (see Figure 9.5). These defects can be minimized by decreasing the welding speed or by oscillating the beam (turbulence). Cold cracking, which can appear a long time after welding, can be avoided by pre-heating and reducing the welding speed.
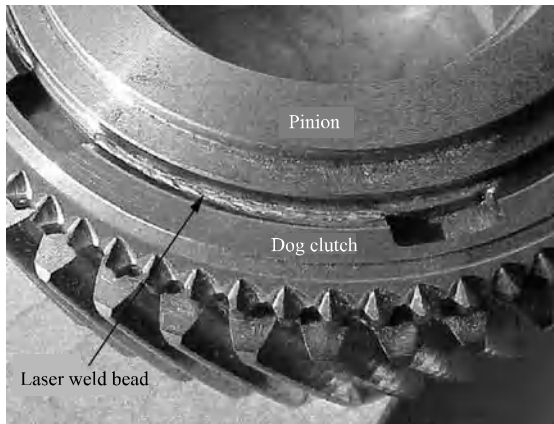

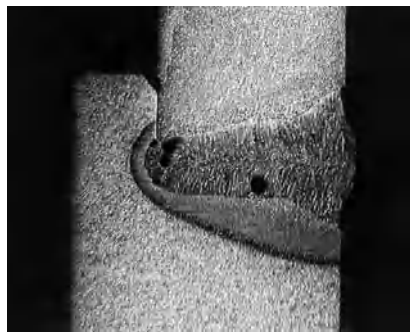**Figure 9.4.** *View of the laser weld bead, dog clutch to pinion*

Figure 9.5. *Micrographic section of a laser welded housing (in 3 mm mild steel) onto a clutch (in 16 Mn Cr 5) for an automatic gear box*

In the automotive industry, the mechanical components concerned by high energy beam welding are often circular, small in size and composite (different steel grades compromises): dog clutch ring for manual gear box pinions (see Figure 9.4), transmissions, forks, etc. In general, laser welds concern complex bead geometries and penetrations lower than 10 mm. The beam's energy density is about 1 to 10 kW/cm² (10 times that of an electric arc).

For the CO_2 lasers, a significant part of the beam is reflected, at least before the beginning of fusion (95%, then 20%) and it is necessary to improve absorption by use of black paint or phosphatizing. It is also necessary to avoid chamfers for the preparation of butt joined assemblies because they cause, by reflection, a considerable loss of penetrative power.

9.3.2.3. *Examples of welded components*

Tulip assemblies designate sliding transmission joints acting as a CV joint on the outside of the gear box. As shown in Figure 9.6, they consist of a casing, a spacer and a sleeve carrying the three bearing surfaces on which rest the transmission needle bearings (sliding motion). Often, the casing and sleeve are in XC 42 (for local induction hardening), while the spacer is formed from a low alloyed steel of the type 10 Mn Cr 5.
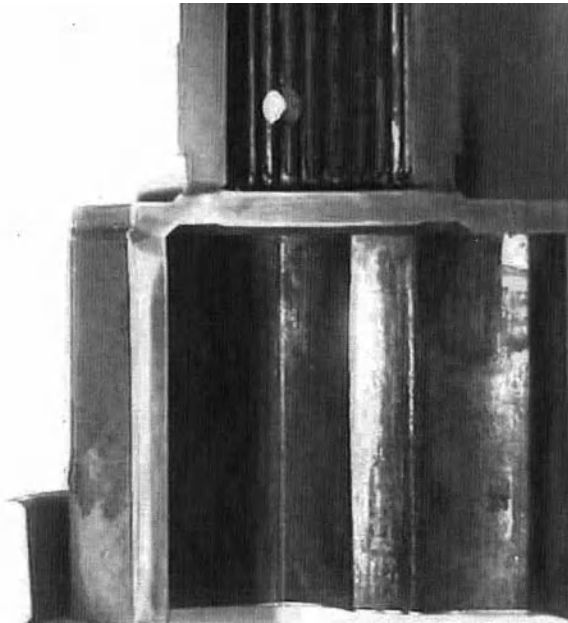

Figure 9.6. *Example of a mass produced laser welded sliding transmission joint*

 The casing can be welded onto the spacer and the sleeve onto the spacer by electron beam or laser. For example, at the Le Mans Renault factory, the two welds of the same type of tulip are welded by a 5.5 kW CO_2 laser at rates of several thousands per day.

The final local hardening by induction of the bearing surfaces must be stopped 7 mm from the area to be welded to avoid cracking. The welding is carried out by chuck rotation, for the casing initially, then for the sleeve, with a welding overlap of about 10 mm. The time cycle is 1.3 minutes while the depth of the melted zone is about 5 mm on the casing and 2.5 mm on the sleeve. Weld quality is controlled at a rate of two or three destructive micrographic tests per shift.

Another example of laser welding consists of the *shielding of tulips* in geometries close to that considered above. This shielding is obtained by welding a thin 18/10 stainless steel sheet on the upper part of the sleeve made from XC 42. A 1 mm through-weld, on the opposite side of the laser beam impact, requires only one 800 W source, and obviously no absorption coating, for welding speeds of about 1 cm a second.

Comparative welding tests, with either laser or electron beam, for the same industrial investment of €5.10^5 and a rate per hour of 400 parts, frankly could not give the advantage to one or other of these techniques. Hourly rates were in both cases around €2 for operational costs, and €8 for maintenance.
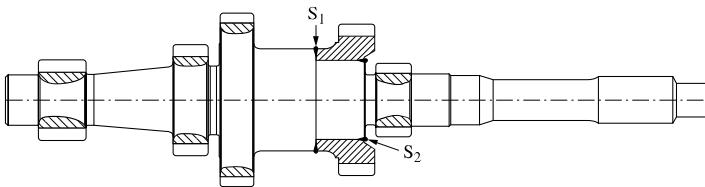
Figure 9.7. *Fitting of a pinion onto a gear box shaft using axial and radial welds*

The third example of laser welding: that of a *pinion* in 27 Mn Cr 5 *on a gear box input shaft* in resulfurized 27 Mn Cr 5 (see Figure 9.7). Taking into account problems of teeth distortions during the carbonitriding treatment at the end of the range, it was necessary to carry out an axial and radial welding of the two parts. In the melted zone, carbon content ranged from 0.23 to 0.39%, and that of sulfur from 0.040 to 0.060%. Weldability depends on the operational configuration. Consequently, the radial welding at 2 cm/sec did not pose any problem, whereas the axial welding, performed with the same halved beam, had to be carried out afterwards (less distortion of pinion teeth) and at half the welding speed to avoid unacceptable cracking.

9.3.3. *Friction welding*

9.3.3.1. *Principle*

The process consists of assembling two parts by mutual forging in a solid or semi solid state, the heat for the forging-diffusion bond coming from preliminary friction between the faces to be welded obtained by putting one part into fast rotation and then pressing it against the other. Generated heat increases the temperature of interface without reaching the melting point of the metal [CAZ 96, COL 83].
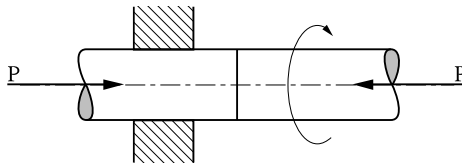
Rotation of one component held against a second fixed component
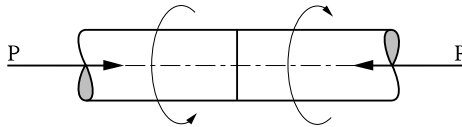
Rotation in opposite directions of both components held against each other
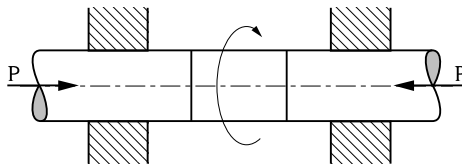
Welding of two fixed components to a third held between them and set in rotation
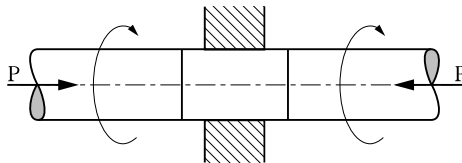
Welding of two components rotating against a third fixed component

Figure 9.8. *Various friction welding methods*

In fact, various friction welding methods exist, as schematized in Figure 9.8. In the elementary lay-out of two components end to end, one being fixed, four phases in the welding operation can be observed:

– setting the moving component into rotation at a constant speed: typically a few hundred revolutions per minute, to reach approximately 2 m/s at the outer edge of the component;

– putting the two components into axial contact: there is heating upon contact, a rise in the resistive torque, but no measurable shortening of the parts;

– maintenance of the axial force until the mating plane reaches the forging temperature. The metal expelled in extreme instances of a semi-liquid state forms a bead, while the parts shorten by plastification of the heated zones. The loss of material begins at the metal solidus: this semi-liquid metal runs out, as a lubricant, towards the outside, under the influence of the compressive force. The duration of this plastic friction is adapted, on the one hand, to the mechanical characteristics of the metals welded and, on the other hand, to the shortening tolerances of the assembly;

– after an abrupt stop of the rotating part, a complementary axial load is applied during a judiciously selected time to carry out the connection through component interdiffusion. The bead increases in volume, the assembly is shortened, and the temperature decreases more or less quickly according to the conduction losses.

Typically, welding of low alloyed steels requires power in the order of 5 CV per cm^2 of section at the beginning of friction and half of this during steady rotation. For a bar of medium carbon steel, 20 mm in diameter, the exerted pressures are about 60 MPa for 5 seconds of heating-friction and 100 MPa during the forging-flow stage.

The geometries adapted to this type of welding are generally cylindrical parts of the same diameter at the weld join, tubes, cylindrical faces onto flat surfaces, faces located in a groove, etc.

Metallurgical continuity is obtained by creep interdiffusion and may involve quite different steel grades. The moving component is pressed immediately against the stationary component at the end of the rotation heating stage. The resulting structure depends on the size of the parts and the hardenability of the steels involved, but they are mainly quenched structures due to the high temperatures reached. Almost always, the welded parts need a final heat treatment.

The *advantages of the process* can be summarized as follows:

– possibility of welding components of different metals and shapes,

– no filler or gas protection,

– reproducible tolerances,

– circumferentially uniform heating, within the solidus of the most fusible metal,

– possibility of automation and on line operation,

– no careful surface preparation (turning + degreasing),

– limited power and low machine maintenance.

The *limitations of the process* are the following:

– it must be possible for one of the assembly parts must be able to be put in rotation,

– difficulty in heating metals with a low friction coefficient (cast iron, brass, etc.),

– maximum weldable diameters: 150 mm for bars, 250 mm for tubular sections.

It should be noted that many metallic couples can be welded by friction, in particular: steel-aluminum, steel-copper, steel-nickel, etc.

This welding mode is largely used for mechanical components in cars:

– gear box shafts, before machining and carburizing (16 Mn Cr 5) or carbonitriding,

– driveshafts in XC 42 for final hardening by induction,

– bimetallic valves, with a stem made out of martensitic stainless steel and a head from heat resisting austenitic stainless.

9.3.3.2. *Some manufacturing examples*

Bonding of forged blanks

Some forged blanks may be easier or less expensive to be machined in two parts, with two different steel grades, or through joining parts manufactured by different techniques (hot, warm, cold forging, etc.).

If these parts are axisymmetric, friction welding is required to achieve a robust bond between the parts, in particular when they have different and complex compositions.

Typically, this process is used to weld gear box input shafts, such as that presented in Figure 9.7 (weight 1.5 kg). In this case, the friction welding machine (of the SCIAKY type presented in Figure 9.9) works at rates of 180 parts per hour with an axial thrust of 250 kN (maximum forging force).
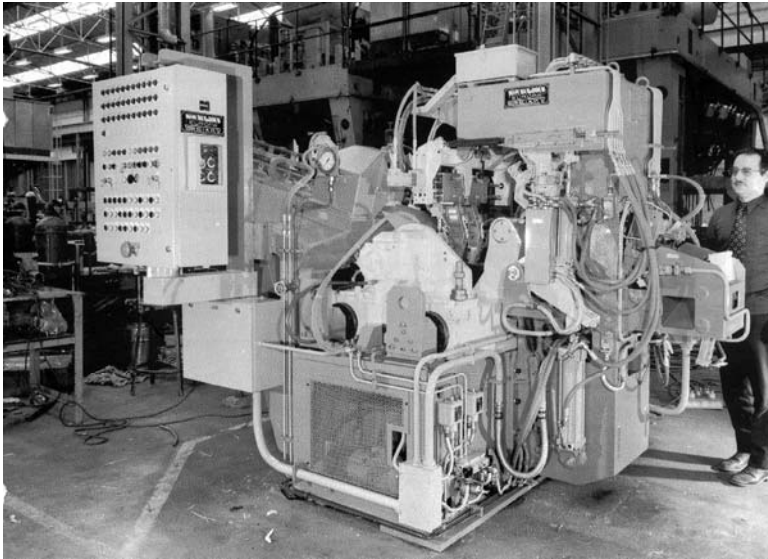
Figure 9.9. *View of a friction welding installation*

The sub-part whose geometry is more complex (pinion teeth) is hot worked and machined, whereas the other is directly cold forged. The shortening of the welded shaft during the operation is 3 mm, for a component length of 135 mm.

Tulip shaft

Another example of friction welding is the assembly of a transmission halfshaft onto a tulip head at the rate of 12,000 parts per day: the central part of a FWD CV joint should adjoin the driven wheel (see Figure 9.10).

Figure 9.10. *Shaft friction welded to tulip*

After automatic loading and checking the assembled length, the shaft head is inserted in a chuck and the tubular shaft blocked in a vice. The head is put into rotation at 2,400 rpm, and the friction of the two components is then ensured by a regulation of the axial load. After braking in 0.7 seconds, forging force is maintained until the desired final length is obtained, with constant control of the power consumption. The machine orders the machining of the weld bead only if both of the two preceding parameters are within tolerance; if not, the part is automatically deposited on the conveyer of rejected parts. Periodic visual monitorings of the circumferential regularity of the bead are also carried out. Apart from these controls, the quality of the end product is ensured by respecting the machine's parameters.

9.3.4. *Butt welding by the Joule effect*

9.3.4.1. *Principle*

Flash resistance welding (FRW) or butt welding consists of assembling two parts end to end without a metal filler, using an electric current for heating the interface, then applying a forging force between them [CAZ 93, COL 83, NEG 95].

The mechanical part of a butt welding machine (see Figure 9.11) is composed primarily of two chucks enclosing the components to be assembled. The mobile chuck is guided by a carriage driven by an automatically controlled displacement system managing the approach and pressure contact stages.

A step-down transformer is able to provide a current output of several thousand amps at 5 to 15 volts. Once the current is applied, the parts are slowly brought closer so as to maintain an electrical resistance at the interface. The contact asperities are volatilized and as the parts are brought together at a controlled speed, it causes new asperities to melt and be expelled in the form of showers of sparks.

The interface is thus covered in a molten metal film, so that the flash phase plays a triple role:

– heating of the parts, more or less controlled by the flashing duration,

– matching of joint surfaces without too much metal loss over their length,

– limitation of the oxidation risk by interfacial vaporizations.

Welding ends in a rapid high pressure contact with the power off. In addition to the intimate contact of the surfaces to be welded, forging expels the molten metal film containing impurities and oxidized elements from the interface. Speed is as important as pressure, in particular on the thickness of the bead which will have to be machined.
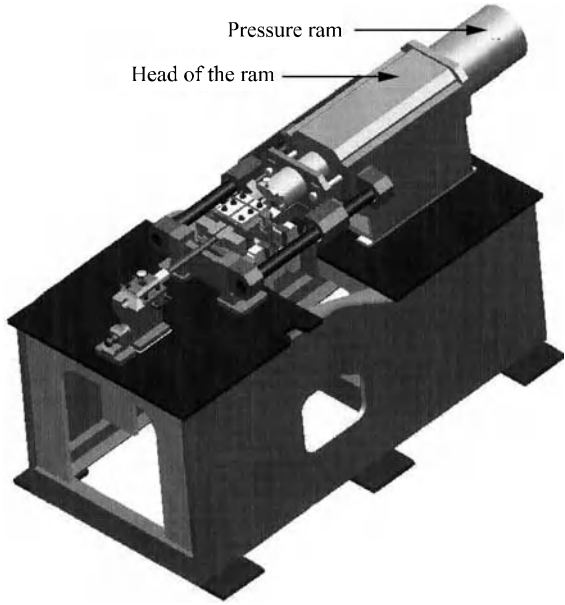
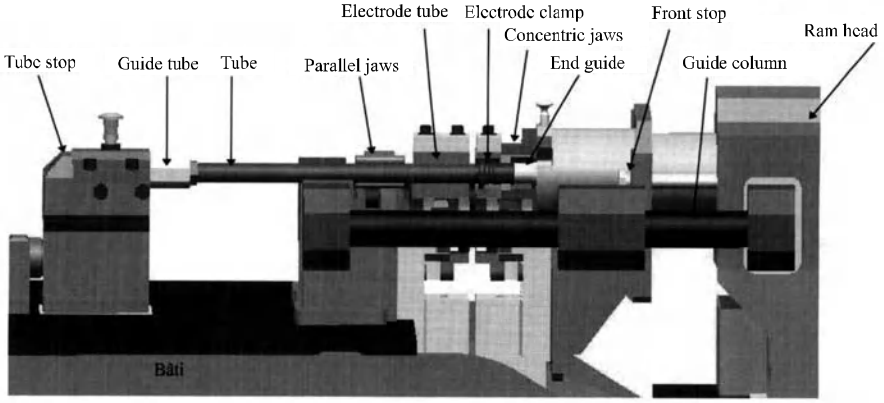General view of the machine

Figure 9.11. *Overall view of a butt welding machine*

This kind of welding may be preceded by a pre-heating stage so as to reduce the power supply (typically: 0.05 kVA per mm^2) and the contact pressure (around 5 hbar).

In FRW processes, a poor matching of the surfaces to be welded during a preliminary stage allows them to be heated to the fusion threshold, while a later pressurized contact makes it possible to laterally expel the interfacial molten metal and oxides, then to create the bond by diffusion in the solid phase. It is not always easy to estimate the flashing duration and to eliminate all trace of oxides or decarburization at the interface.

The majority of alloyed steels, including austenitic stainless types, can thus be welded without post-heating, although this operation is possible for relatively small components heated over small lengths.

In the case of butt welding by the Joule effect without the flash phase, the initial heating is localized by adapting the geometry of the contact surfaces. It is then the speed at which the welding pressures are applied which allows a progressive distribution of the plastic deformations and temperatures compatible with the final geometries and desired joint qualities. A certain number of alternatives to this process can be imagined according to: the speed of pressure application on the parts, the rate of plastification and the evolution of the recrystallization close to the weld, albeit with the main processes occuring in solid phase. The thickness of metal concerned with the plastification-recrystallization and hence the dimensional change in the part can be reduced to a minimum, as well as the size of the martensitic layer and the harmful residual stress zones. It is generally necessary to eliminate the beads by machining, but the moderate brittleness of the martensitic zones in the absence of hydrogen does not necessarily impose complementary treatment if the carbon equivalent content at the interface is reasonable.

9.3.4.2. *Example: welding of an end piece on a camshaft*

A new generation of camshafts consists of steel cams assembled on a drawn tube, with a steel end envisaged for the drive. Although the tube (26 Mn 5) and the end (forged C25 or turned C35) are made from steel grades that are relatively easy to weld by laser beam, butt welding by the Joule effect may be preferred for the sake of productivity.

In the machine presented in Figure 9.12, two conducting copper jaws enclose at a distance of a few centimeters from the mating plane, one the flange of the end piece, the other the tube. The latter has a cone shaped machining which, when in contact with the annular face of the tube, localizes the initial electrical resistance of contact. A thrust load of about 1,500 daN is applied constantly to the mobile chuck holding the tube, whereas the jaws holding the end are fixed.
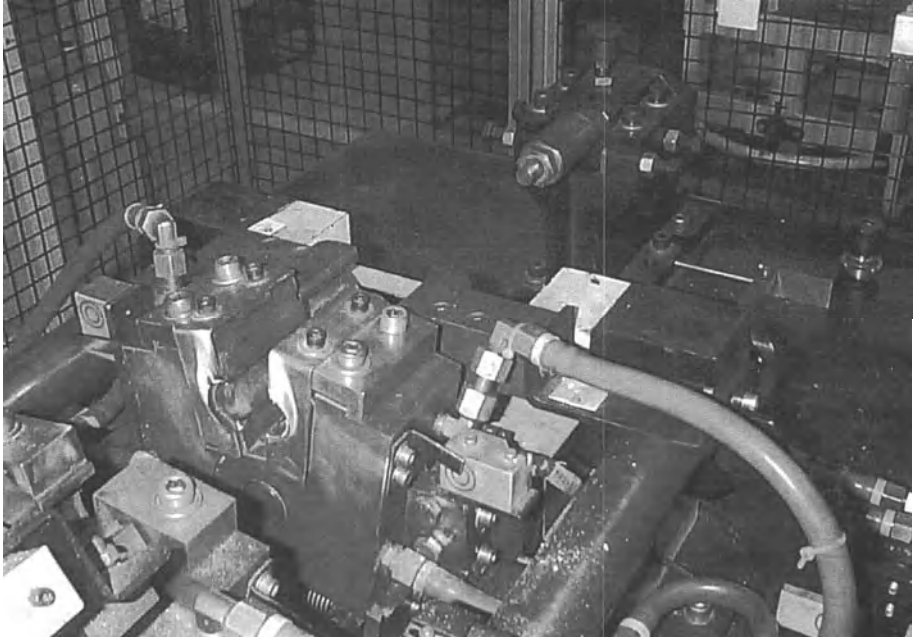
Figure 9.12. *Detail of the machine jaws presented in Figure 9.11*

The multistage program of electric inputs can be very diverse, with currents of several thousand amps being delivered in multiple periods.

A typical cycle comprises the following phases during 12 seconds:

– putting the two parts in contact under a 1,500 daN load,

– pre-heating for 0.25 seconds at 15,000 A, up to 500°C at the interface,

– a first flash of 0.5 seconds at 28,500 A,

– thermal rehomogenization over 1 second while interfacial creep increases the current passage to the nominal value of the tube,

– a second flash of 1 second at 13,500 A at the end of which the interfacial temperature reaches 1,200°C, the pressure remaining around few Mpa,

– a 2 second diffusion time when the joint at the interface is completed,

– six heating cycles of 0.5 seconds at 11,500 A with a gap between each 0.5 second cycle. This phase is intended to slow down the cooling of the austenitized areas, reduce the martensite extent and improve joint toughness.

At the end of welding, a turning operation is carried out on the bead in order to eliminate the risks of early fatigue crack initiation. The length of the assembled shaft, after cooling, must be precise within a hundredth of a millimeter.

The welding quality is also controlled by the absence of molten metal droplets, which could remain stuck inside the tube and be detached in-service with the risk of obstructing the component's lubrication.

This type of welding has been proved to offer great flexibility with respect to the various end pieces (depending on engine type) for production line assembly, and good reproducibility with respect to the geometric precision of the assembly and the bending-torsion fatigue strength. Bending strength evaluated by Baldwin tests confirmed the metallurgical health observed in micrographic samples: continuity with ultrasound, absence of oxidation at the initial interface, and a martensitic thickness of several millimeters. The absence of static embrittlement and the good fatigue strength of these areas, even for ends in resulfurized C35 steel, confirm that untempered martensites at 650 HV do not present the cracking risks encountered upon remelting (hydrogen, residual stresses).

9.3.5. *Diffusion welding in the solid phase*

The various assembly techniques in solid phase [COL 83] all call upon the same operational parameters: temperature, pressure, time of action, and we can visualize the areas of variation in these parameters on the same graph (see Figure 9.13), for the most commonly used techniques.

We should particularly note that the graph demonstrates how diffusion welding can be the least deforming and the least disruptive process with respect to the initial structure (volume concerned and extent of damage).

This development is too recent to have reached a level of industrialization comparable with the preceding processes [HOU 91]. However, it is being used more and more in advanced technological industries: nuclear power, armament, aeronautics, electronics, biomedical, etc. This process also has potential benefits with a future for difficult connections like steel-cast iron, high alloyed steels and carburized steels. The more productive version, dynamic diffusion welding, would give this process a place in the manufacturing ranges of traditional industry.
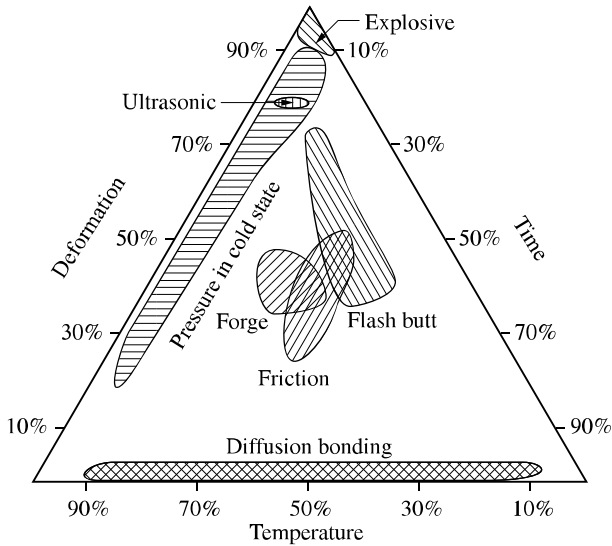
Figure 9.13. *Positioning on a temperature-pressure-time action graph for various techniques of solid phase welding*

9.3.5.1. *Description and characteristics*

Such welding requires a careful preparation of the surfaces to be welded in terms of superior interfacial matching, microgeometry, roughness and physico-chemical state (elimination of surface oxides). These are then assembled in a vacuum vessel or in a suitable protective atmosphere, possibly equipped with means of complementary cleaning via ionic *sputtering*, radiation heating, as well as the clamp making it possible to maintain the compressive pressure (a few tens of MPa) just below the flow limit of the involved metals at the selected temperature. This temperature is always lower than the solidus of the alloys being welded, usually significantly lower to avoid excessive creep affecting the dimensional accuracy of the welded part. The welding time depends on the alloys used. If D is the interdiffusion coefficient and τ duration of interaction under constraint, care is taken that the mean free path of diffusion $\lambda = (D\,\tau)^{\frac{1}{2}}$ exceeds a few micrometers. In fact, the creation of the metallic connection depends not only on interdiffusion and hot recrystallization but also on the resorption of contact defects by a mechanism similar to that of sintering.

Dynamic diffusion welding consists of heating the components to the welding temperature as quickly as possible (induction heating) by modulating the contact pressure at a level just lower than the *flow limit* of the least resistant material.

Thus, intimate surface contact is very quickly obtained and a strong metallic bond can be established in a few minutes. In this way connections between gray cast-iron and steel have become industrially possible, with an overall strength higher than that of the cast iron [CAL 86].

The macroscopic deformation of the parts can be limited to 2% of the heated length and a subsequent machining can often be avoided, all the more so as the parts assembled under a protective atmosphere are not oxidized.

The localized thermal evolution of the structures during welding does not always demand a complementary heat treatment of the welded joint.

The quality of the welded joint is primarily related to the cleanliness and the intimacy of the surface contacts. A light rubbing together (relative micro-sliding) makes it possible to improve this contact.

9.3.5.2. *Potential uses*

This type of connection should especially develop in micro-mechanics and for connections of steel-cast iron or high alloyed steels that are difficult to weld by other techniques. So, for example, it is possible to weld carburized or nitrided parts, removing the treatment only from the joint surfaces, either by masking them or by machining. It is also possible to interpose a thin nickel sheet before putting steel surfaces in contact.

Diffusion welding could be used on parts already subjected to thermochemical treatment. The advantage could be a simplification of the ranges and production line flexibility. It was thus employed for carbonitrided tulip drive shafts in 27 Cr Mo 4 [LEP 92], as friction welding does not give good results on these structures.

The welding conditions adopted could be as follows:

– careful mechanical polishing (Rmax = 1 μm) followed by degreasing,

– joining pressure: 300 MPa, cycled during the application time,

– welding in five seconds at around 1,050°C *in vacuo*.

However, it should be noted that:

– a good interfacial roughness is necessary, whether or not we preserve a carbonitrided layer at the interface;

– the hardness of the carbonitrided layer is lost on the height thermally affected by the inductor;

– it is better to work on grades with less than 0.020% sulfur so as not to affect the interfacial toughness;

– the interfacial properties can be further improved by recrystallization, resulting for example from work hardening due to relative angular oscillations or vibrations of the samples during the temperature rise;

– there would remain microporosities of about 20 nanometers at the interface, stabilized by the diffusion of base metal elements (S, P, N) towards the interface during welding.

Under nearly the same operating conditions, good mechanical joint characteristics can be obtained in diffusion welding for the combinations: SG cast iron/perlitic cast iron and cast iron/steel with interposition of a 10 μm nickel strip.

9.4. Specifications and quality control of the weldings for these components

The various welding modes are obviously the object of operational specifications and quality controls [NOR 83], as is the norm for any mass production of mechanical components.

These specifications, and the corresponding traceability process, are based primarily on former experience, from systematic recordings of the thermal cycles or the thermal source parameters making it possible to control these cycles.

In small-scale machine shops producing low volumes, welds can be individually checked by the various non-destructive testing techniques: penetrant dye testing and magnetoscopy for emerging defects, radiography and ultrasound for internal porosities.

In the high volume automotive and the mechanical engineering industries, the quality control of the production must be both rigorous, flexible and simple, as we will briefly show as an example of safety in the welding operation.

The preliminary study (at the prototype stage) must initially define methods and a range of controls that are easy to implement on the production line; it is one of the keys to successful quality assurance of the manufactured parts. The specifications of the various defects which can affect the weld must be established very accurately with the aim of being both practical and effective. The *quality assurance plan*, applying and checking these specifications, must be simple and in particular must allow development, without risks, of the frequency of controls, in order to space

them out during production. This plan must also make it possible to minimize storage in the body of parts between two controls.

As these two documents have legal authority, it is important to note that all the operations which are mentioned must be verifiable. That justifies the rigorous simplicity which they must have in order to be applied in a realistic way.

9.4.1. *Weld quality specifications*

9.4.1.1. *Contents*

This document must list all the possible weld defects (macro and micro) and give their level of acceptance; it also defines the means to be used to carry out controls.

The acceptable defect levels must be defined precisely and take into account:

– metallurgical risks: appearance of micro-defects such as cracks, blisters, shrinkages, etc.,

– static mechanical behavior of the assembly: traction, shearing, tearing, torsion, etc.,

– dynamic behavior: shock, fatigue.

The metallurgical risks are minimized by the preliminary choice of material (the specifications must mention the acceptable content level of carbon, sulfur, phosphorus, etc.) and, if difficult steel grades cannot be avoided, by the range and the welding parameters (pre-heating, post-heating, reheating *in situ*, etc.); specifications will detail the means of controlling this operation's performance, in particular by a printed trace of the machine's welding parameters.

The mechanical strength of the assembly is ensured by the limitation of macro defects and a correct weld geometry: a good general rule is to mention in the specifications that, in all directions of the weld section, the size of the joint must be greater than the thickness of the thinnest part.

The dynamic behavior of the assembly is minimized, with regard to shock, by a metallurgy or welding conditions preventing excessive weld brittleness; in fatigue strength, it is optimized by limiting all the inherent geometric singularities which could lead to crack initiation.

For example, the recommendations of Figures 9.14 to 9.16 show how static and dynamic weld behavior can be better controlled by geometric bead constraints.
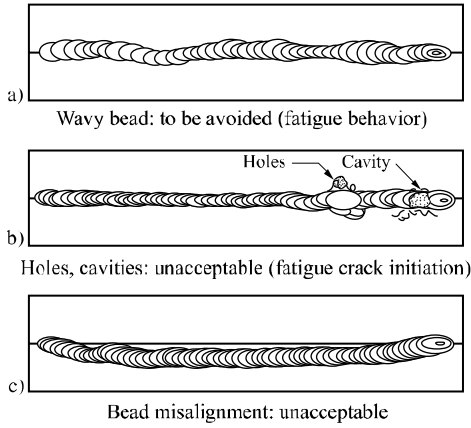
Figure 9.14. *Fatigue crack initiation*
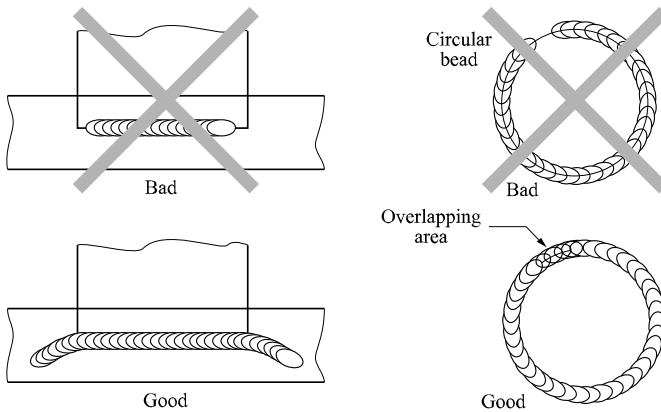
Figure 9.15. *Example of the development of a monitoring plan*

Static behavior:
- Le > e_1 (bead width)
- h > 0 (total penetration)

Dynamic behavior:
- c < 0.1e_1 (groove)
- h > 0 (total penetration)

Figure 9.16. *Laser weld bead*

Figure 9.17. *Arc weld bead*

Internal micro-defects: their occurrence is mainly linked to the various metallurgical risks already explained.

An example of acceptance for laser or EB welding is shown below.

Figure 9.18. *Porosities*

Figure 9.19. *Cracks*

The control methods for these defects (statistics on a certain number of micrographic sections, ultrasounds, etc.) are difficult to implement in mass production.

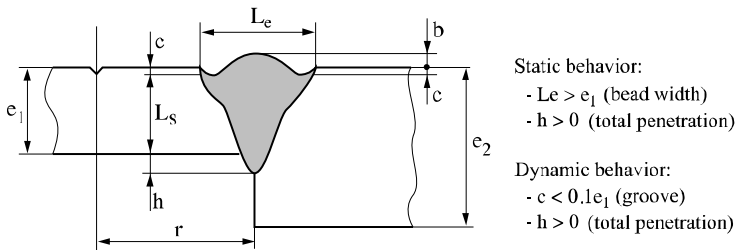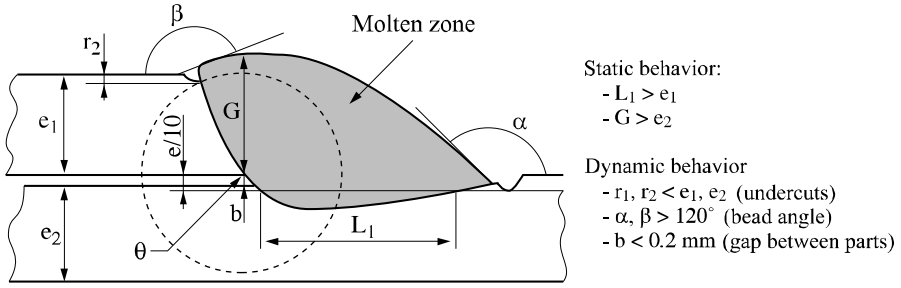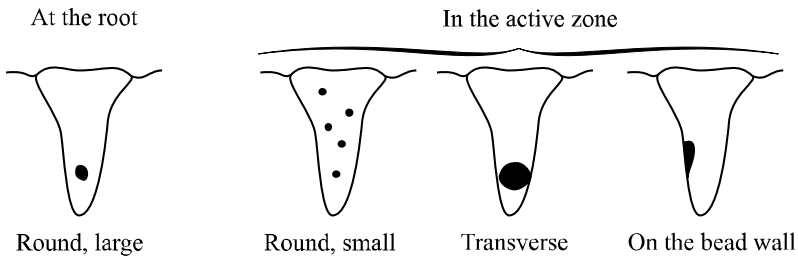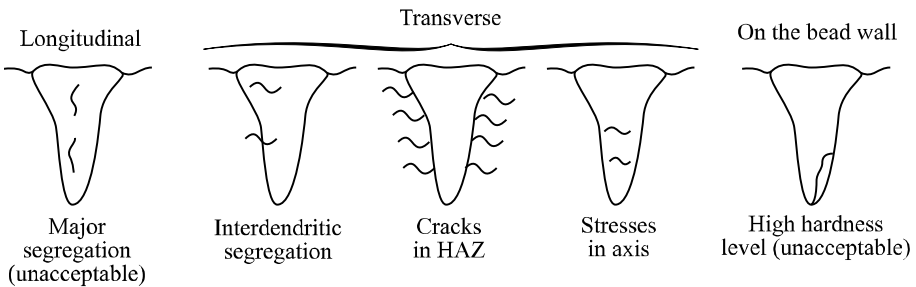It is often agreed that with the precise matching of components, the harmfulness of non-emergent defects remains within acceptable limits. On the other hand, when they are visible on the surface as in the examples attached, their occurrence is no longer tolerable.
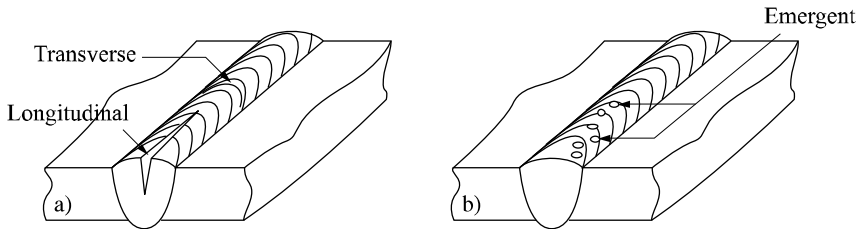
Figure 9.20. *(a) Cracks and (b) emergent porosities*

A way of reducing and simplifying production control is to tolerate all micro-defects if they cannot be detected in visual monitoring of the bead (with the naked eye or with a reasonable magnification method). This acceptance of internal defects must obviously be justified by preliminary validation testing of the parts.

9.4.1.2. *The basic specification schedule*

A provisional specification schedule, taking all the above principles into account, is determined for the production of prototype components. This document is important; it enables parts of well-known characteristics to be manufactured serving as reference and facilitating possible future improvements.

In most cases, the recommendations of this provisional schedule make it possible to obtain a welding quality that satisfies the performance requirements of the component during the validation tests.

However, it is possible that, during these tests, loads higher than those envisaged lead to weld failure. A detailed evaluation of the break makes it possible to refine the tolerance levels in order to establish the final specification schedule.

Generally, modifications relate to the joint geometry or a stricter tolerance for defects leading to the start of fatigue cracking.

9.4.1.3. *The final specification schedule*

This is the document which will be applied when the components are in mass production. Incorporating the modifications resulting from prototype validation evaluations, this document will comprise:

– a list and description of the defects,

– the level of defect acceptance,

– a description of the means to evaluate this level of acceptance.

The method of defect control is not imposed but it must be selected among those mentioned and validated in the specification schedule. The choice of these means and their frequency of application is the subject of the quality assurance plan of the weld.

9.4.2. *The quality assurance plan of the weld*

This applies and checks the specification methods for each weld of the assembled component.

9.4.2.1. *Contents*

For each defect indexed on the specification schedule, it will indicate:

– the method of control used to check this defect (precise check of the welding parameters, visual, macrographic, others, etc.);

– the frequency for each one of these controls (100%, every n^{th} part, etc.),

– the decision taken in the event of non-conformity (alarm, rejection of the part or the batch, rectification, etc.); in this last case, a rectification procedure will have to be described and validated,

– actions taken for the filing of control results (logs, graphs, etc.) and to facilitate checks (standard parts, good and bad examples of the components are on hand at the work station, etc.).

An archive table, such as that presented in Figure 9.21, can be used.

A good quality assurance plan takes into account that the selected control methods must be the simplest possible. The checking of the machine's welding parameters must be encouraged and the consequences of any deviation on the appearance of well-known weld defects. Systems for directly observing the bead after welding (camera, etc.) are to be encouraged, as the following controls are often greatly reduced. Methods of non-destructive testing must be favored in order to

minimize the total control costs. With each control, a precise filing of the measured parameters is advised. The storage of batches on standby awaiting control results must, for reasons of product flow, be reduced to the minimum; the follow-up of the parameters, previously quoted, is a good means of ensuring a good quality flow by a system of alert thresholds with immediate corrective action on the welding parameters, without blocking the batch. The frequency of each control must be flexible: close together in development, frequent at the beginning of production, the aim being to space these controls out in the course of production in order to reduce costs. This decision must only be taken on the basis of good record keeping,
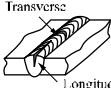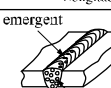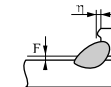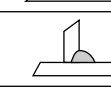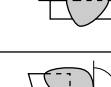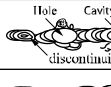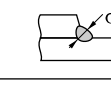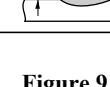
Defect description		Control method	Bead Acceptance	Decision	Action work station
Cracks/ emerging cracks					
Blow holes, emergent porosities					
Undercuts					
Lack of penetration					
Hollow bead Collapse Excessive penetration					
Join defect Rolled bead					
Positional defect Bead deviation					
Wavy bead					
Hole Bead discontinuity					
Poor overlap					
Bead section too low Throat G insufficient					
Gap between parts J too large					

Figure 9.21. *Record sheet for archiving*

This demonstrates the importance of follow-up and filing the control results. A frequency modification procedure will then be written ("after *n* controls giving satisfactory quality, the frequency control will be..."). As an efficient frequency interval can only be defined by taking the reliability of the material into account, only the users of this material are capable of establishing this.
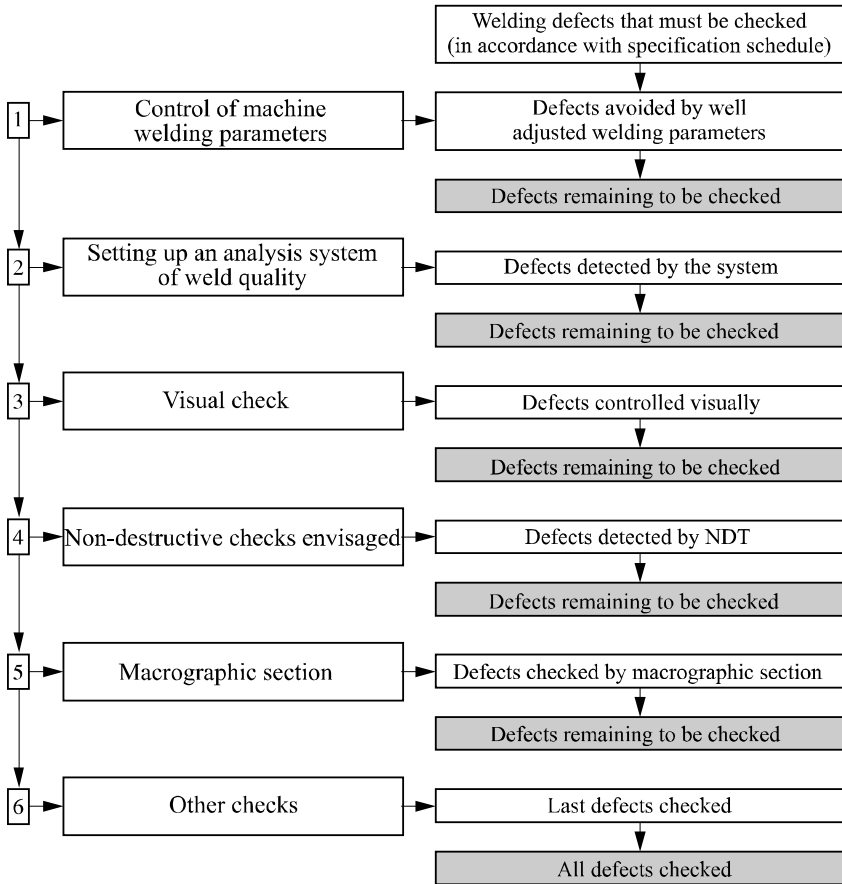
Figure 9.22. *Control methods*
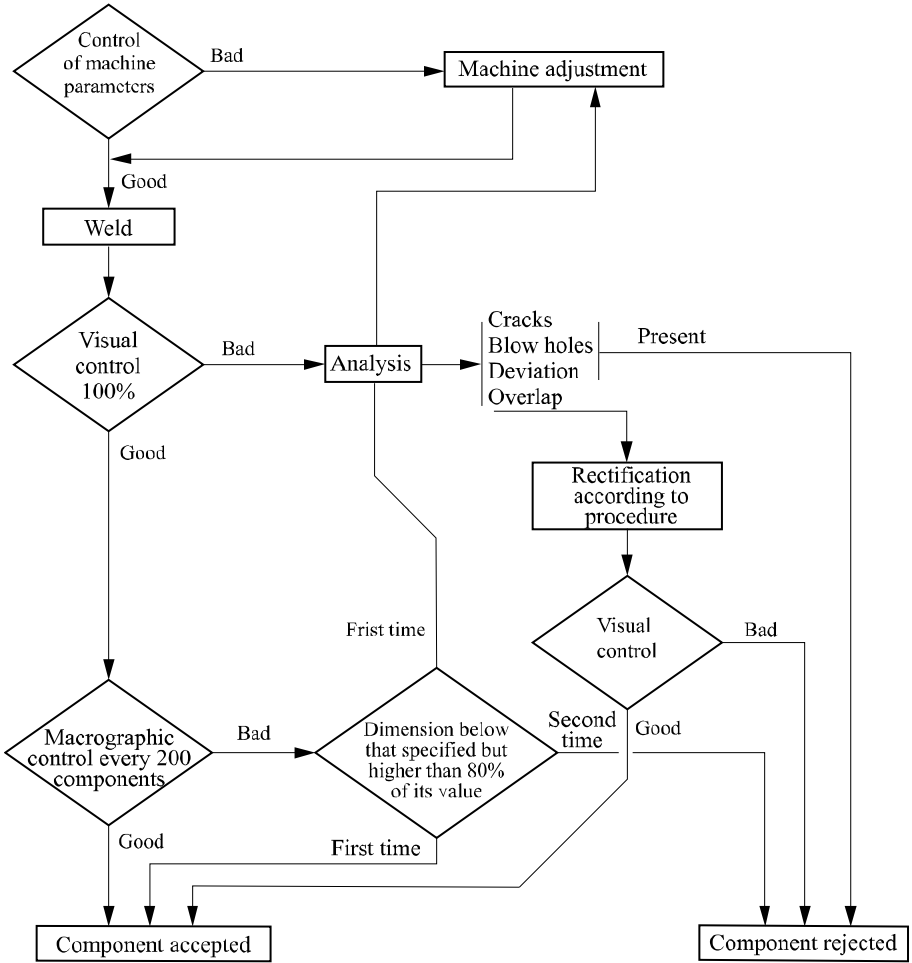
Figure 9.23. *Example of a quality assurance plan*

The development of the quality assurance plan: having listed all the defects to be controlled according to the weld specification schedule, the control methods are to be employed in the order given in Figure 9.22. The control plan stops when there are no more defects to detect.

9.4.2.2. *An example of a quality assurance plan*

Figure 9.23 gives an example of a quality assurance plan set up for the laser welding of dog teeth onto a gear box pinion.

9.5. Developments and trends

9.5.1. *Evolution of the context*

We can foresee that increased intervals between disassembly periods for maintenance, the trend towards interchangeable modules and reductions of costs and assembly times will lead to the rise of automated welding. For mass produced mechanical components, we have to be increasingly concerned with:

– installation flexibility: the same machine must be able to weld all the variants of the same or sister component, and will therefore have robotized transfers and sources with a real margin of trajectory training;

– cycle time, which must be adapted to that of machining times;

– delays of tool changes and preventative maintenance which does not inhibit the operational efficiency of the installation;

– on line control requirements.

These *process* constraints eliminate some small-scale welding or brazing processes employed in mechanized welding for steel construction, as well as some techniques for which suitable industrial machines do not yet exist.

9.5.2. *Favored processes*

For non-axisymmetric parts unsuited for friction or resistance welding, welding with high density thermal flow seems most promising because the affected structures apply to only a small part of the component, and this in a relatively reproducible way. The example of bimetallic valves, friction welded with a band of some tenths of millimeters of untempered martensite at 650 HV, shows the advantage of drastically reducing the thickness of the remelted layer. The reduced affected zone must, however, be accompanied by a more precise interfacial matching and adequate plastification to allow an intimate contact between the surfaces to be welded. A good compromise between contact precision, localization of the temperatures close to the fusion of the base metal and plastification-recrystallization of the interface are key to automated welding installations for alloyed (or unalloyed) steel components.

Much is expected of compact lasers in terms of production developments (YAG or diode batteries), because they do not imply expensive maintenance.

Let us recall that the heart of a powerful laser diode consists of a row of diodes $(0.1 \times 0.6 \times 10 \text{ mm})$ which emits a very divergent beam $(90° \times 20°)$. Typically, such

a row emits 30 W for a wavelength around 900 nm. To increase the overall output power, the rows are piled up and the beam divergence corrected by adequate micro-optics directly linked to the rows. It is thus possible to build up very powerful and compact devices, the size of a lighter, supplying some 300 W.

Currently, continuous powers up to 4 kW can deliver power densities of 3.10^4 W/cm^2 at the focal point. The total electrical efficiency is 30%, with lifespans from 10 to 20,000 hours. Work in progress at the Institut fûr Laser Technik in Aix-la-Chapelle are achieving power densities of 10^6 W/cm^2 for powers of a few kW and lifespans higher than 25,000 hours.

The market potential is thus considerable. These thermal sources are coupled with robotized devices carrying out the contact stage and the interface plastification with precision, for a broad range of component geometries and with a controlled dispersion process. Such a transfer machine is often more expensive than the laser source.

The compactness and the reduced investment and maintenance costs also militate in favor of plasma torches with transferred arcs, whose precision of arc positioning is definitely superior to that of blown arc torches.

On the other hand, the extension of diffusion welding technology, beyond micro-mechanics and alloys that are difficult to weld by other means, remains improbable in the near future.

Butt welding by Joule effect will remain limited to the welding of accessories on tubes, but should lead to a better knowledge of exactly what is necessary for the creation of a welded bridge, with or without recrystallization, by taking advantage of transformation plasticity and good ductility in TRIP martensites.

Finally, the developmental perspectives of multipurpose robotized installations could make us reconsider certain metallurgical choices for mechanical components or call into question traditional assemblies.

First example: machine welded front triangular suspension arm out of a sheet steel

The suspension arm connects the wheel pivot to the car body by allowing vertical displacements via a ball joint. It is involved in the rigidity of the suspension with respect to longitudinal forces (acceleration, braking) and lateral forces in bends. To design an economic suspension arm, sheet steel solutions are preferred to hardened forged steels, but it is difficult to take advantage of the higher mechanical strengths of the newest steel grades (high-strength sheets or stainless) because the fatigue failures start systematically at the toe of the weld beads. For the design, it is necessary to move the beads away from the highly stressed zones, which is often

difficult for heavily loaded components. An installation linking very localized welding and hardening would be particularly advantageous.

Second example: welding or brazing of pinions on shafts

The possibility of replacing a *machined shaft with pinions*, which are difficult to harden without excessive distortions, by an assembly of pre-manufactured and hardened pinions which could be welded or brazed on a tubular shaft, would be interesting in terms of weight saving and economy. For helicoidal gear train, the axial and bending loadings in operation justify special attention to weld or braze toe toughness. To avoid softening during brazing, this operation must obviously precede carburizing hardening and occur at a slightly higher temperature.

Finally, in all cases of welding, we are confronted with two alternatives. On the one hand we have a difficult interfacial matching because of shortcomings (for technical or economic reasons) in the geometric precision or preparation of surfaces to be welded. On the other hand, a significant metal and energy supply to the joints resulting in risks of embrittlement because of defects and structures arising in them. Improved precision machining of mechanical components leads us to think that solid phase welding will gain in importance.

9.6. Conclusions

We have pointed out the distinctions, in terms of welding needs, between machine welding of structural steels as studied in previous chapters, and the assembly of mechanical components, often from alloyed steel unsuited to traditional welding with extensive remelted zones. We also evoked the requirements of mass production in terms of cycle time length, automation and quality control.

In this context, welding processes involving a minimum of molten metal are compatible with precision interfacial matching and mechanical finishing. They often seem best placed, from a metallurgical perspective (reproducibility, low levels of shrinkage and porosities, better control of residual stresses, etc.), from the *process* perspective (automation), and in facilitating quality checks. In these categories of parts, a final heat treatment often reduces the risks of cold cracking related to rather highly alloyed compositions.

Friction welding is the archetypal process for all cylindrical components in relatively high alloyed steels or difficult alloys. It has standardized industrial machines at its disposal capable of handling large runs. The example of friction welded bimetallic valves, with a thin layer of untempered very hard martensite, shows the metallurgical benefit of drastically reducing the thickness of the remolten layer.

More recently, butt welding by the Joule effect is now made possible on automated industrial machines, which can also combine other operations on tubular parts.

Diffusion welding is too recent a development to be suggested for use in standardized industrial machines. However, it may be considered as a last resort for particularly difficult cases of welding where a high degree of accuracy in interfacial matching and cleaning allows enough recrystallization, interdiffusion and microscopic indenting by creep. It seems to be a potentially interesting solution for assembling otherwise unweldable iron alloys.

Between the specific methods that we have just presented and traditional arc welding poorly adapted to high alloyed steels, we find welding processes based on high energy beams: they can limit the "metallurgical damage" of the affected zone to so narrow a layer that it does not have any consequences on the overall behavior. The new lasers working at shorter wavelengths (for good absorption of the radiation) – which are compact, not particularly expensive, easy to set up and inexpensive in maintenance – are commonly seen as the most promising. In this context, electron beam welding should be reserved for thicker parts, long welded lengths or coating of pressure vessels. Moreover, the plasma gun with transferred arc will find its place for mechanical components and welded joints of intermediate size.

9.7. Bibliography

[AWS] American Welding Society, *Welding Handbook*, 8th edition, Section 1.

[BON 87] BONNET C., "Traitements thermiques associés au soudage des aciers", *Techniques de l'ingénieur*, B 7810, 1987.

[BOU 82] BOURGEOIS P., *Soudage à l'Arc Tome 3, Procédés avec fil électrode fusible, procédés avec électrode réfractaire*, Publication de la Soudure Autogène, Paris, 1989.

[BOU 92] BOURGES P., BERNIOLLES J., "Laser beam welding of high hardness steels: applications to armoured vehicles", *ICALEO' 92,* Laser Institute of America, p. 574-583, 1992.

[BOU 95] BOURGES P., CHEVIET A., "Soudage par faisceau d'électrons d'aciers au chrome-molybdène de forte épaisseur pour application en pétrochimie", *Colloque AFIAP 1995*, Paris, 17 October 1995.

[CAL 86] CALVO F.A., "Soldadura por diffusion de materiales ferreas", *Soldadura*, 16, 3, p. 125, 1986.

[CAZ 93] CAZES R., "Soudage par résistance", *Techniques de l'ingénieur*, B 7720, 1993.

[CAZ 94] CAZES R., "Soudage par faisceaux à haute énergie: faisceau d'électrons et laser", *Techniques de l'ingénieur*, B 7740, 1994.

[CAZ 95] CAZES R., "Soudage à l'arc", *Techniques de l'ingénieur*, B 7730, 1995.

[CAZ 96] CAZES R., "Soudage par fiction", *Techniques de l'ingénieur*, 7745, 1996.

[CAZ 97] CAZES R., "Soudage automatique", *Techniques de l'ingénieur*, BM 7750, 1997.

[COL 83] COLLECTIF, Welding, Brazing and Soldering Arc Welding of Low-alloy Steels and Ferrous Metals, *Metals Handbook* no. 6, ASM, 1983.

[DEB 84] DEBIEZ S., "Détermination des conditions de soudage des aciers faiblement alliés pour prévenir le risque de fissuration à froid", *Soudage et Techniques Connexes*, May-June 1984.

[DER 81] DE ROO P., DEVILLERS L., MARANDET B., "Conditions d'amorçage et de propagation d'un défaut localisé dans le métal fondu d'un joint soudé", *Quatrième réunion SFM-SIS*, May 1981.

[FAB 83] FABER G., GOOCH T., "Assemblages soudés entre aciers inoxydables et aciers faiblement alliés", *Soudage et Techniques Connexes*, March-April 1983.

[FEN 84] FENN J., "Solid phase welding: an old answer to new problems", *Metallic Materials Technologies*, vol. 16, no. 7, p. 341, 1984.

[GRA 81] GRANJON H., "Travaux sur le soudage par faisceau d'électrons", *Soudage et Techniques Connexes*, January-February 1976, May-June 1981.

[GRA 95] GRANJON H., *Bases métallurgiques du soudage*, Publications de la Soudure Autogène, Eyrolles, 1995.

[HOU 91] HOURCADE M., "Le soudage-diffusion à l'état solide", *Traitement Thermique* – 250-1991, p. 21-29, 1991.

[LEP 92] LE PAGE G., Soudage-diffusion de l'acier 27 Cr Mo 4 et de l'acier 100 Cr 6, PhD Thesis, CNAM, 1992.

[LIE] LIEURADE H.P., "Application de la Mécanique de la Rupture à la fatigue des joints soudés", *Communication IIS*, Ljubljana, September 1982.

[MAZ 82] MAZUMDER J., "Laser welding, state of the art review", *Journal of Metals*, p. 16- 24, July 1982.

[NEG 95] NEGRE J., *Le Soudage Electrique par Resistance*, Publication de la Soudure Autogène, Paris, 1995.

[NOE 84] NOEL L., "Brasage", *Techniques de l'ingénieur*, B 5195, 1984.

[NOR] NORME FRANÇAISE NF E 83-100: "Construction d'ensembles mécanosoudés – Techniques de soudage", – Partie 1: "Généralités – terminologie – classe de qualité de soudure – étendue des contrôles", – Partie 4: "Fabrication – Contrôle".

[VAL 83] VALETTE G., CHEVIET A., "Soudage F.E. de l'acier à 2,25%Cr-1% Mo en forte épaisseur", *3e CISFFEL*, Lyon, 5-9 September 1983.

Chapter 10

Welding Steel Structures

10.1. Introduction

10.1.1. *History*

Although electric welding dates from the end of the 19th century, it is a relatively recent technique in steel construction. The shipbuilding, automobile, aeronautical and boiler making industries quickly adopted it, because it presented considerable advantages in weight saving or it solved the problems of water or air tightness. The Titanic was launched in 1911 and the first instance of welded car bodies dates from 1912.

In the construction industry, the first entirely welded metal constructions were a building erected in the USA in 1924, followed by two railway bridges, one spanning 19 m, over Turtle Creek in Pittsburgh in 1928, and the other 27 m over the Sludwia in Lowicz in Poland, in 1929.

In France, the first welded civil engineering projects date from 1936: a 40 m road-bridge at Ourscamp in the Oise, and an 80 m railway bridge of in three spans (two outer spans of 22.5 m and a central span of 35 m) in Paris, Porte de la Chapelle. It should be noted that it was not in the French tradition to construct entirely welded steel buildings.

Chapter written by Jean-Pierre PESCATORE and Jean-Henri BORGEOT.

Figure 10.1. *Footbridge in Bilbao – Santiago Calatrava Architect – photograph from CTICM*
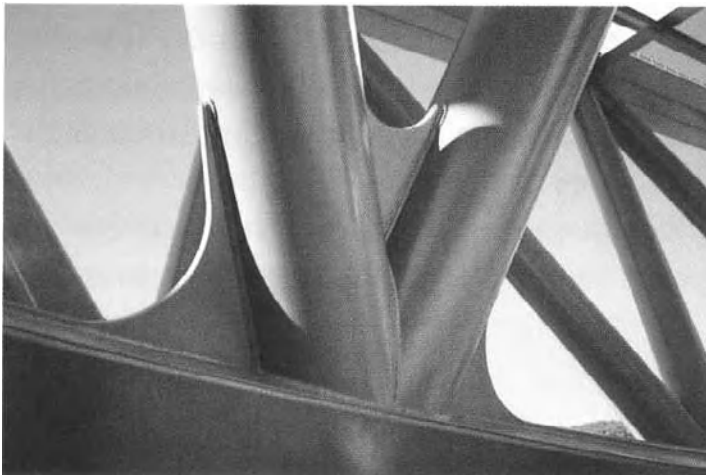

Figure 10.2. *Viaduc de l'Arc, TGV Méditerranée – detail of a node*
Designers: SNCF & GAUDIN Architects – photograph from OTUA

These early large scale welded constructions soon suffered problems, due in particular to brittle fracture phenomenon (see section 10.5.2).

The American Welding Society (AWS) published the first *Guide on welding* in 1922, then the *Code for fusion welding and gas cutting in building construction* in 1928 and the *Specifications for design, construction, alteration and repair of highway and railway bridges by fusion welding* in 1936.

For the French construction industry, the first circular giving *Provisional instructions for the execution of electric arc welded steel structures and bridges* was published in July 1934. One year later, in the light of the conclusive experimental results, a modified circular removed the term *Provisional* and increased the acceptable loadings for welded joints, effectively marking the first development of this technique.

10.1.2. *Applications*

Before dealing with welded steel structures, it is necessary to expand on the fields where they are employed.

It is difficult to give a precise and exhaustive definition, because of the great diversity of constructions.

As examples, we can consider:

– frameworks of agricultural buildings, greenhouses and silos;

– industrial facilities;

– frameworks of buildings used as offices or dwellings;

– road or railway bridge structures, and pedestrian footbridges;

– offshore platforms such as oil rigs;

– electricity pylons, telecommunication pylons, ski lifts and chimneys.

These constructions, of varying complexity, subjected to very different actions (permanent and imposed loads, static or dynamic loads, climatic and thermal forces, possibly seismic phenomena and the effects of fire), as well as to very different requirements as regards personal safety, which further extends this diversity, can also be characterized by inherent construction particularities on-site.

Lastly, it is necessary to take into account the specificity according to use in the same structure of hot rolled long products (mainly I, H and U- shaped beams) tubes, sheets or wide flats (parts of assemblies and welded I-sections or box sections).

This highlights the virtual impossibility of stating general rules that are valid for the structure as a whole; only specific regulations make it possible to deal with various aspects.

It must be noted that the current rules are in booklet 61, title V (Design and calculation of steel bridges and structures) and in booklet 66 (Execution of civil engineering structures in steel) for steel bridges, and in CM 66 (Rules for calculation of steel constructions) and the construction standards series NF P22-XXX for buildings and other works. These documents will undoubtedly be replaced by European standards, respectively Eurocode 3 (steel structures) and 4 (composite steel and concrete structures) for design and calculation, and the standard EN 1090, relating to the execution of the structures, including general rules and specific instructions for buildings, bridges, hollow sections and stainless steels.

10.2. Steels for steel structures

10.2.1. *Grades and qualities*

The *grade* of a structural steel in steel construction is primarily defined by the three basic mechanical characteristics: yield strength (the main criterion used to check an element's strength), tensile strength and elongation strength to fracture. These characteristics refer to uniaxial loads.

A state of multiaxial stresses can, under certain conditions, create a risk of brittle fracture for values significantly lower than the constraint considered acceptable by a traditional calculation of material strength. Also, in addition to stability, it is necessary, according to the construction in question and its technological provisions, and the foreseeable operating conditions (like temperatures down to 30°C in cold stores or for bridges), to ensure safety by controlling this risk.

Within the same grade, and with almost identical basic mechanical characteristics, *qualities* are defined which offer complementary guarantees against the risks that can be caused by particular conditions of use and service.

The principal criterion for resisting brittleness – i.e. toughness – is sensitivity to the notch effect. This is evaluated starting from the greater or lesser susceptibility of a material to deformation by energy absorption under the effect of a load or a shock. This is determined in experiments by the shock deflection test, known as the *Charpy test*.

10.2.2. *Steels used*

In the great majority of structures, non-alloyed steels are used, complying with the standard NF EN 10025-2, whose mechanical characteristics are the following:

– yield strength in a range between 235 and 355 N/mm^2,

– tensile strength between 340 and 630 N/mm^2,

– elongation to fracture higher than 20% for the current thicknesses,

– KV failure energy of 27 J at +20°C or -20°C.

We also use steels with improved corrosion performance for special applications, according to standard NF EN 10155; their mechanical characteristics are equivalent.

In addition, fine-grained steels are used particularly for civil engineering projects, in accordance with standard NF EN 10025-3, characterized as follows:

– yield strength between 275 and 460 N/mm^2,

– tensile strength between 350 and 720 N/mm^2,

– elongation between 17 and 24%,

– KV failure energy of 40 J at -20, even 27 J at -50°C.

For specific applications (see section 10.5.1.1), all these steels can be obtained with improved deformation properties perpendicular to the surface of the product, in accordance with standard NF EN 10025-5.

The steels used have a yield strength of 235 N/mm^2; they are mainly used in building structures, as girders, bars and flats.

High yield strength steels (HSS) have a limit higher than or equal to 355 N/mm^2. They are primarily sheets.

The fine-grain steels obtained by thermomechanical rolling, according to standard NF EN 10025-4, are increasingly used in civil engineering and offshore oil rigs, in the highest grades and in significant thicknesses (greater than 80 mm) due to the following:

– a better aptitude for welding compared to that of non-alloyed steels and for all the processes (except the MAG process with a solid wire) used in steel construction, and without pre-heating. Limiting the presence of hydrogen (see section 10.5.1.2 on the prevention of cold cracking) is achieved by pre-heating (see section 10.5.3.1);

– improved ductility (raised impact failure energy at very low temperatures).

10.3. Steel construction welding processes and techniques

There are a great number of welding processes and each one has an application. The table below recapitulates the various processes usually used and their characteristics, while technical details can be found in Chapter 1 of this book.

10.3.1. *Table of the usual processes*

Welding processes according to ISO 4063	Construction		Procedure				Product -ivity	Observations
	work-shop	on-site	man-ual	semi -auto	auto	robot	output	
111: Metal-arc welding with covered electrode	X	X	X				+	Rutile coating (current use) or basic coating (HSS)
135: MAG-welding	X			X	X	X	++	Sensitivity to draughts Risk of lack of fusion
136: Tubular-cored arc welding with active gas shield	X			X	X		+++	Sensitivity to draughts Use in all positions
114: Self-shielded tubular cored arc welding		X		X			+++	Use with narrow preparations Copious fumes
121: Submerged arc welding with onewire electrode	X	X			X		++++	Good penetration Horizontal only

Other welding processes, such as spot, TIG or laser are generally not used, the thicknesses of the elements being too great.

10.3.2. *Preliminary operation: tack weld*

This operation consists of joining the parts to be assembled by short discontinuous beads before forming the weld itself. Apparently simple, it is actually a delicate operation which requires a great deal of care. Indeed, it must be carried out with the same precautions given to the first pass (filler product, checks, pre-heating or post-weld heat treatment, etc. (see section 10.5.3).

A specific difficulty of tack welds in steel construction is due to the fact that the parts can be very long (a few meters to several tens of meters) or very stiff.

10.3.3. *Particular welding techniques*

10.3.3.1. *Horizontal bench assembly*

An assembly for the manufacture of I-shaped girders of uniform or slightly variable height, composed of a bench, receiving a flat plate as web and the two vertical flanges placed vertically against its edges, is equipped with two welding heads to create two beads on the same side of the web (process 121). The two other beads are welded after turning over the assembly. This equipment requires a lot of floor space, limits joist dimensions to that of the bench and does not allow the manufacture of curved parts.

Figure 10.3. *Construction of an I section on a horizontal bench – photograph from Baudin-Châteauneuf*

10.3.3.2. *Vertical bench assembly*

This is a machine for manufacturing a straight or curved (in plan) I section of constant or variable height: a flange is laid down on the bench upstream with the web held vertically by arms; this assembly passes under a gantry equipped with a hydraulic jack and two welding heads to create the web to flange weld (process 121). The T-shaped assembly thus formed is turned over, laid out on the second flange and welded as in the first operation.

Figure 10.4. *Construction of an I section on a vertical bench –*
photograph from Baudin-Châteauneuf

10.3.3.3. *Stud welding*

This technique is used in the workshop or on-site in composite steel-concrete construction for the welding of connectors (diameters from 6 to 22 mm) on steel beams destined to be an integral part of a solid concrete floor. It is carried out using a *welding gun* in which a stud is pushed into the weld pool, after conducting an electric current, forming an arc.

Figure 10.5. *Stud welding: welding of connectors – photograph from Baudin-Châteauneuf*

10.3.3.4. *Aluminothermy*

This technique is used on-site to join lengths of rails for overhead traveling cranes.

The filler, resulting from the reduction of iron oxide by aluminum, is released in liquid form in a mould of suitable shape to form the joint.

10.3.4. *Usual welding positions*

According to the joint to be welded, various types of welds are encountered.

In the workshop, fillet and butt welds are most commonly used (see Figure 10.6), the most frequently found positions being:

– flat bead (joint on roughly horizontal surface, with filler metal deposited from above);

– angled horizontal bead (roughly vertical surface placed on a roughly horizontal surface).

Flat bead   Angled horizontal bead

Figure 10.6. *Commonly used welds*

On-site (see Figure 10.7), we will also encounter:

– vertical bead (roughly vertical axis);

– overhead bead (roughly horizontal surface and filler deposited from below).

10.3.5. *Edge preparation*

As soon as a certain thickness is reached, and according to the process selected, it is necessary to carry out plate edge preparation by creating chamfers to ensure good weld penetration.

Vertical bead   Overhead bead

Figure 10.7. *Commonly used on-site welding positions*

With butt welds, two forms of preparation are primarily used depending on the thicknesses to be welded:

– V shaped for low thickness ranges, i.e. from 6 and up to approximately 12 mm,

– double V shaped for mid-range and significant thicknesses, namely from approximately 12 mm to 100 mm and beyond.

The angles of the V or double V shaped preparation vary according to the thickness of the parts and the welding process. These preparations generally include a root face.

The double V preparation can be dissymmetric, to minimize overhead welding, particularly when on-site.

The double bevel preparation (symmetric or not) can be regarded as an alternative to the double V preparation, with the advantage of only needing the preparation of one edge.

For fillet welds, the same type of preparation, V or double V, is found when it is necessary to reconstitute the section or to ensure the full penetration of the weld bead.

These preparations are carried out mainly by grinding for thin parts, or manual or automatic thermal cutting in the other cases.
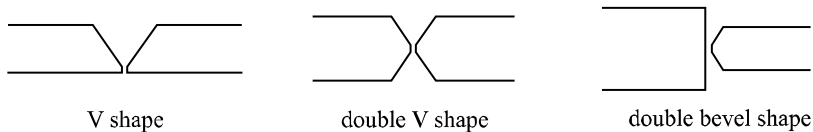

V shape   double V shape   double bevel shape

Figure 10.8. *Edge preparations*

10.4. Welding distortion

As mentioned above, the thicknesses to be welded are relatively significant. As a result there is considerable heat input which, given the good conductivity of metal, entails the parts being heated.

It is necessary to limit the effects of this heat release, because they produce stresses which lead to distortions needing subsequent correction.

The following distortions are distinguished:

– translation, producing a transverse and longitudinal shrinkage,

– rotational, involving a tightening effect and cambering/folding.

It must be remembered that a lack of ductility in the metal absorbing these stresses can lead to failure due to cracking.

10.4.1. *Precautions in execution*

To minimize distortion and its effects, several solutions are available and can be combined if necessary:

– choose a welding process with a low linear heat input, MAG for example preferably with tubular cored metal arc welding;

– limit to a minimum compatible with the calculation rules and good practise, the lengths and sections of welds (which also makes good economic sense);

– seek symmetric weld layouts; opposing shrinkage effects avoids distortion;

– perform opposing welds simultaneously to avoid imbalance;

– optimize the order of weld execution, indicated by the term *welding sequence*, which is governed by the following rules:

    - weld with free transverse shrinkage,

    - weld symmetrically, with several operators functioning simultaneously, or in alternation with only one operator, observing symmetric (or roughly symmetric) layouts,

    - clamp the part in a rigid assembly with opposing preliminary distortion.

Figure 10.9. *Bridge beam with double V shaped preparation –*
photograph from Baudin-Châteauneuf

Figure 10.10. *Butt weld joint – photograph from Baudin-Châteauneuf*

10.4.2. *Straightening*

When it is necessary, in spite of the precautions taken, to correct distortion, this can be carried out by flame straightening or mechanically by hydraulic jacking or with a press.

A local application of heat is often the only means of remedying the defects of a distorted element. It consists of very localized drastic heat application, around 600°C, generating contraction forces during cooling which straighten the element. This operation requires knowledge of the temperature limits when heating which depend on the grades and thicknesses of steel, also bearing in mind that HYS steels require greater precautions when using this technique.

10.5. Defects and their prevention

We recall the usual welding defects such as porosities, cracks, cavities, inclusions, lack of fusion and penetration or defects in shape only as a reminder of a subject dealt with extensively elsewhere in this work.

We will, however, draw attention to the high porosity risk associated with prepainted steels frequently used in steel construction. Its use requires great care, in particular for fillet welds of susceptible assemblies, where paint must be removed beforehand.

We mention primarily metallurgical defects in steel construction and indicate the precautions required to prevent these risks.

10.5.1. *Cracks*

Two types can be distinguished: cracks due to lamellar tearing and cold cracking.

10.5.1.1. *Cracks due to lamellar tearing*

Such cracks occur parallel to the skin of a rolled product, at the part of the weld putting strain on the material in the direction of thickness.

The prevention of this risk is mainly achieved by:

– designing joints to facilitate with free shrinkage, while avoiding stresses perpendicular to the skin of products;

– choosing a filler material with a yield strength close to the base metal and operating conditions likely to decrease the stresses perpendicular to the skin;

– Using plates with a guaranteed improvement in deformation properties perpendicular to the surface knowing that the reduction in thickness does not involve a corresponding reduction of the risk.

10.5.1.2. *Cold cracking*

These are generally located parallel to the fusion line and take various forms according to their position: at the root, at the connection or connection between passes, under the bead. Primarily, there are three causes for this:

– significant compressive and shrinkage stresses at the weld site; the design of the assembly and the choice of the welding sequence generally make it possible to minimize them;

– tempering the metal in the vicinity of the fusion line; limiting the cooling speed in the HAZ is one of the important parameters to decrease this risk;

– presence of hydrogen in the bead; clean and dry parts, baked filler products, electrodes with very low hydrogen and an atmosphere without excessive moisture all serve to reduce the risk.

10.5.2. *Fracture*

10.5.2.1. *Brittle fracture*

Brittle fracturing occurs without plastic deformation, unlike ductile fracturing, and develops slowly after a significant preliminary plastic deformation.

The sensitivity of a joint to this phenomenon depends on:

– steel used: yield strength and intrinsic toughness;

– thickness of the components;

– load application speed and levels and nature of stresses;

– lowest service temperature.

In addition to these considerations, risk limitation involves:

– a limitation of work hardening the edges, because this involves a reduction in ductility;

– a welding operation with notch defects such as undercuts;

– low energy welding;

– if necessary, a reduction of the residual stresses with an adapted mechanical treatment of the weld such as hammering.

10.5.2.2. *Fatigue fracture*

This occurs when a joint subjected to in-service stresses, with cyclic loadings, suddenly cracks and breaks, with very reduced elongation or distortion of the part.

Fatigue behavior depends primarily on the care taken over the weld shape and finishing treatment. This phenomenon is covered in Chapter 6.

10.5.3. *Other thermal and mechanical precautions*

Thermal precautions make it possible to limit certain risks generated by the specific heating at the time of welding operations.

10.5.3.1. *Low pre-heating*

This consists of maintaining the temperature of the component between 40 and 80°C during welding, in order to limit the risk of brittle fracture.

10.5.3.2. *Pre-heating*

This helps to limit the cooling speed by heating the component to between 100 and 200°C, in order to reduce the risks of hardening under the bead and cold cracking in steels sensitive to hardening. It can contribute to a decrease in the level of residual stresses and prevents shrinkage fractures.

10.5.3.3. *Post-heating*

Post-heating must take place immediately after welding, without the component cooling. This reinforces the effects of preheating with an identical temperature maintained long enough to obtain the equalization of the temperature of the various parts.

Holding the temperature steady also allows the evacuation of hydrogen and aids its diffusion in the mass, which reduces the risk of cold cracking.

10.5.3.4. *Heat treatment*

This technique is very little used in steel construction because of the dimensions of the components. However, stress relief treatments are commonly carried out on prefabricated tubular nodes in offshore rig structures.

Lastly, post-weld mechanical treatments such as hammering or shot-blasting are sometimes used to improve fatigue strength of welded joints.

10.6. Specificities of non-destructive testing of steel structures

The principal methods of non-destructive weld testing, that is, visual examination, penetrant testing, magnetic particle testing, radiography, gammagraphy or ultrasonic testing, are obviously applicable to steel construction. However, it must be noted that X-ray inspection is unsuited to the examination of fillet welds, and that with ultrasonic tests an uncontrolled zone might remain at the root, understanding that these welds are characteristic in basic metal structures.

10.7. Developmental perspectives

The use of welding in steel construction has developed rapidly and looks to have a promising future because of its many specific qualities. The most important are:

– good structural reliability because welding is carried out using both welding procedure specifications (WPS) and welding procedure qualification records (WPQR);

– simplification of joints, which are otherwise very sensitive to atmospheric corrosion;

– facilitating the continuity of structural elements by using abutment or rigid connections;

– assembly of closed sections;

– optimization of sections, due to simpler joints, and thus economizing significantly on materials;

– possibility of making complicated shapes economically.

Chapter 11

Welding Heavy Components
in the Nuclear Industry

11.1. General presentation of a PWR pressure vessel

The actual nuclear part of pressurized water reactors (PWR), or nuclear pressure vessels, consists of all the systems involved in generating steam, which is then delivered to the turbines and electric generators.

The large components of this boiler are as follows (see also Figure 11.1):

– the reactor vessel where energy derived from nuclear fuel is transmitted to the coolant, known as the primary loop, with water under high pressure (154 bars) and where temperature can reach 350°C. This vessel is a cylinder approximately 12 m in height, 5 m in diameter and 250 mm in thickness, closed by two hemispherical domes. On the vessel a certain number of welded taps of differing dimensions are connected, some of which are the nozzles linking up with the main primary pipes;

– the steam generators where the energy of the primary circuit fluid is converted, through heat exchanger tubes, into steam intended to feed the turbines. The steam generators are approximately 20 m high and have a diameter ranging between 3.5 and 5 m; their thickness is about 100 mm.

NOTE: the water circulation of the steam generators and the system taking the steam to the turbines takes place in C-Mn steel pipes, A42 and A48 grades, similar to the

---

Chapter written by François FAURE and Léon DUNAND-ROUX.

grades used in conventional power generation plants. These materials are not discussed in this chapter.

A pressurizer allows the primary circuit to reach its operating pressure during start-up phases. It is a component approximately 13 m in height, 2.5 m in diameter and 120 mm in thickness. This component also has various connecting nozzles.

Motor-driven pumps ensure the circulation of fluid in the primary circuit.

Pipes, 900 mm in external diameter and approximately 80 mm in thickness, connect the different components listed above.
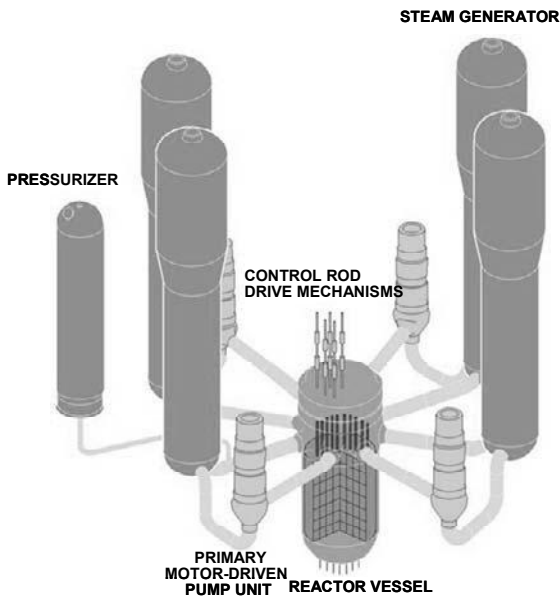

Figure 11.1. *Components of the PWR*

11.2. Main materials used for manufacturing

11.2.1. *Principle of material choice – construction code*

The large pressurized components of a nuclear installation must be designed in order to cope with high pressure, at a temperature as high as 350°C, in contact with the primary circuit fluid. Moreover, the reactor vessel is subjected to neutron radiation.

In addition to the safety aspect, the difficulty and the cost of possible repair or replacement operations, associated with an envisaged working life of 40 years, mean that ageing must be taken into account right from the design stage, both for the base materials and for the welds used to assemble the various elements.

Very precise legal requirements appeared in France in the ministerial decree of 26 February 1974 regarding "application of the regulations concerning nuclear PWRs". This decree puts a legal obligation on the manufacturer to constitute a *material file* for all the parts subjected to pressure in the principal primary circuit, including the welds of these parts.

Technical and statutory constraints are at the origin of material selection criteria and assembly modes. These choices result from a permanent and ongoing optimization of steel alloys and perfectly controlled processes. The regulations appear in the code of design and construction code (RCC-M) jointly elaborated by EDF and Framatome within the framework of the AFCEN (the French association for construction regulations relating to PWRs).

11.2.2. *Low alloyed steels for pressure vessels*

The first vessels with pressurized water reactors, brought into service in 1960s USA, were manufactured from 175 mm thick plates in carbon-manganese steel. However, as soon as it was a question of manufacturing high output reactors (initially 300 MWe and now up to 1,450 MWe), the C-Mn steels could no longer guarantee adequate toughness for the pressure vessel thicknesses under consideration. Successive developments have led to manganese-molybdenum steel plates or forgings (ASME SA 302 B), then to Mn-Ni-Mo steel (ASME SA 533 grade B cl 1 plates or SA 508 cl 3) forgings. This last grade has been used for all French PWRs with the additional requirements detailed below. It is designated 16 MND 5 in the RCC-M and is covered by referenced technical specifications.

16 MND 5 is a manganese-nickel-molybdenum low alloy steel, with a bainitic structure, hardened and tempered. It represents an excellent compromise between relatively high mechanical characteristics, making it possible to limit the thickness of the pressure vessels, and a good toughness. Compared to the ASME code requirements, the materials used in France are characterized by a more limited carbon, sulfur, phosphorus and copper content. The lower carbon content makes it possible to improve weldability. Toughness is improved by the reduction of carbon, sulfur and phosphorus. For core shells exposed to radiation, additional requirements relate to the content of copper and phosphorus, the chemicals responsible for hardening and embrittlement by neutron radiation.

Material	C%	Mn%	Si%	P%	S%
16 MND 5	≤0.22	1.15/1.60	0.10/0.30	≤0.020	≤0.012
	Ni%	**Cr%**	**Mo%**	**Fe%**	**B%**
	0.50/0.80	≤0.25	0.43/0.57	balance.	-
16 MND 5 (core shells)	**C%**	**Mn%**	**Si%**	**P%**	**S%**
	≤0.22	1.15/1.60	0.10/0.30	≤0.008	≤0.008
	Ni%	**Cr%**	**Mo%**	**Fe%**	**B%**
	0.50/0.80	≤0.25	0.43/0.57	balance.	-
Z2 CN 19-10 (N-strengthened)	**C%**	**Mn%**	**Si%**	**P%**	**S%**
	≤0.035	<2.00	<1.00	<0.040	<0.030
	Ni%	**Cr%**	**Mo%**	**Fe%**	**B%**
	9.0/10.0	18.5/20.0	-	balance.	≤0.0018
Z2 CND 18-12 (N-strengthened)	**C%**	**Mn%**	**Si%**	**P%**	**S%**
	≤0.038	<2.00	<1.00	<0.040	<0.030
	Ni%	**Cr%**	**Mo%**	**Fe%**	**B%**
	11.5/12.5	17/18.2	2.25/2.75	balance.	≤ 0.0018
NC 15 Fe (Alloy 600)	**C%**	**Mn%**	**Si%**	**P%**	**S%**
	<0.10	<1.00	<0.50	<0.015	<0.015
	Ni%	**Cr%**	**Mo%**	**Fe%**	**B%**
	≥72.0	14.0/17.0	-	6.0/10.0	-
NC 30 Fe (Alloy 690)	**C%**	**Mn%**	**Si%**	**P%**	**S%**
	0.01/0.04	<0.50	<0.50	<0.015	<0.010
	Ni%	**Cr%**	**Mo%**	**Fe%**	**B%**
	≥58.0	28.0/31.0	-	7.9/11.0	-

Table 11.1. *Chemical composition of the main materials of PWR plants*

The specified characteristics of 16 MND 5 steel are presented in Tables 11.1 and 11.2.

Material	RP 0.2 (20°C) (MPa)	Rm (20°C) (MPa)	To%	Charpy energy	RP 0.2 (350°C) (MPa)
16 MND 5	≥400	550/670	≥20	Transverse direct.: KU at 0°C ≥40 J Longitudinal direct.: KU at 0°C ≥56 J	≥300
16 MND 5 (core shells)	≥400	550/670	≥20	Transverse direct.: KU at 0°C ≥40 J Longitudinal direct.: KU at 0°C ≥60 J	≥300
Z2 CN 19-10 (N-strengthened)	≥210	≥510	≥35	KU at 20°C ≥60 J	≥130
Z2 CND 18-12 (N-strengthened)	≥210	≥510	≥35	KU at 20°C ≥60 J	≥130
NC 15 Fe (Alloy 600)	≥240	≥550	≥30	-	≥190
NC 30 Fe (Alloy 690)	275/ 375	≥ 630	≥30	-	≥215

Table 11.2. *Specified mechanical properties of the main materials of PWR plants*

16 MND 5 steel is used for all the reactor vessel parts (shells, flanges, domes, nozzles). A very close steel grade is used for the pressurizer plates, and the steam generator plates, forged head and tubesheet.

11.2.3. *Austenitic stainless steel circuits*

Because of their general corrosion resistance and their simplicity, austenitic stainless steels have been used from the outset in solid part manufacturing (pipes, pump and tap casings, reactor vessel internals), or to coat low alloyed steels of large components in the areas in contact with the cooling fluid. The major advantage is to reduce corrosion products liable to be activated when they pass into the reactor core. The first American designers chose grades of the type AISI 304 (18% Cr – 10% Ni) and AISI 316 (17% Cr – 12% Ni – 2.5% Mo) and derived cast grades (CF8 and CF8M).

In France, from the beginning of the nuclear program, low carbon austenitic grades were selected, in spite of the problems encountered when obtaining such

grades at that time. The intention was to reduce, even to remove, the risk of sensitivity to intergranular corrosion caused by the dechromization of the grain boundaries during welding operations or stress relief. For this reason, in collaboration with EDF, Framatome and Creusot-Loire, two specific grades were created (see Tables 11.1 and 11.2):

– the nitrogen-hardened Z2 CN 19/10 grade, with a very low carbon content, but with mechanical properties equivalent to those of the high carbon grade of the AISI 304 type,

– the nitrogen-hardened Z2 CND 18/10 grade, equivalent to AISI 316.

The austeno-ferritic alternatives of these two austenitic grades, intended for castings (pump casings, primary circuit pipe elbows), are Z4 CN 20-09 M (CF8) and Z4 CND 19-10 M (CF8M).

The austenic and austeno-ferritic stainless steels undergo an annealing treatment at high temperature followed by water quenching (*hyper-hardening*). This confers a homogenous structure upon them, free from carbides and optimal from the perspective of corrosion resistance. The ductility and sudden breaking strengths of these materials are extremely high. Their tensile characteristics are weak (see Table 11.2), which excludes their use for large pressurized components.

These steels are easily weldable with appropriate austeno-ferritic fillers. Contrary to the case of low alloy steels, they require neither pre-heating, post-heating, or relief treatment and as such constitute ideal materials for on-site assembly. For this reason, low alloyed large steel components have safety connectors made from austenitic stainless steel in order to facilitate their connection with on-site pipework.

Forged or rolled stainless steels are used for primary pipework. Molded austeno-ferritic steels are used for pump casings and certain primary circuit pipe components.

11.2.4. *Nickel alloy parts*

Nickel based alloys of nickel-chromium-iron type have an excellent corrosion resistance including chloride mediums, contrary to stainless steels. If we add their good heat transfer characteristics, the reasons for choosing these materials in steam generator piping are easily understood.

Alloy 600 (NC 15 Fe) is chosen, an alloy with 75% Ni, 15% Cr and 8% Fe, whose corrosion behavior was regarded as exemplary. Ni-Cr-Fe alloys have another interesting property: a dilation coefficient relatively close to that of low alloyed

steels. For this reason, alloy 600 was also used for cross-sections, pipe take-offs and the internal supports of the large pressure vessel components. Moreover, the procedures and filler products (alloy 82 and 182) for the welding of alloy 600 were well established.

Alloy 600's sensitivity to stress corrosion in water from the primary loop has gradually come to light. From the end of the 1970s, French and international work programs were devoted to the characterization of a replacement alloy, alloy 690 (NC 30 Fe), comprising approximately 30% Cr, as well as corresponding welding products (alloys 52 and 152). About 15 years of tests in many laboratories, including those of the CEA (the French atomic energy commission), EDF and Framatome, made it possible to confirm the corrosion resistance of this material in the primary loop water medium. This material is now systematically used in France to replace alloy 600 on a purely preventative basis in the majority of its applications. The respective chemical compositions of these two alloys are presented in Table 11.1.

As for austenitic stainless steels, the heat treatment consists of an annealing at high temperature followed by a hardening. Hardening is not quite as fast to avoid a certain sensitizing of the grain boundaries. To produce an unsensitized material, a complementary treatment is carried out at 715°C, for a sufficient time to recharge in chrome the grain boundaries.

Ductility and the breaking strength of Ni-Cr-Fe alloys are extremely high. Their tensile characteristics when hot are appreciably higher than those of austenitic stainless steels (see Table 11.2).

These materials are not as easy to weld as austenitic stainless steels. They present a marked tendency to hot micro-cracking, either during the solidification of the metal added by welding, or in the HAZ. A very careful optimization of the chemical composition is necessary to combat this tendency, with particular attention given to low impurity contents and high Nb/Si ratios.

Ni-based alloys are used for steam generator tubes and partition plates, along with the CRDMs and instrumentation tubes and the core support pads.

11.3. Welding of large low alloy steel components

Large components are made up of forgings or rolled components assembled by welding.

The major parts of these components are:

– for the pressure vessel: the upper dome, closure head flange, vessel flange, nozzle shell, both core shells, transition ring and lower dome;

– for the steam generator: the upper head, two shells of the upper part, feedwater nozzle, manways, conical shell, three shells of the lower part, tubesheet, head with nozzles and manways;

– for the pressurizer: the upper head with its nozzles, three shells, lower had with its nozzle.

11.3.1. *Properties aimed for*

The requirements regarding mechanical properties of the large component welds, as specified in RCC-M code, are identical to those of the base materials, set out in Table 11.2. With regard to chemical requirements, particular values depend on weldability constraints, for example resistance to hot cracking for austenitic alloys such as stainless steels or nickel alloys. These chemical compositions are indicated in Table 11.3.

11.3.2. *Procedural description*

Welding of the parts that make up large components (pressure vessel, steam generator, pressurizer) is carried out by an automatic electric welding process under a powder flux with a wire electrode in a narrow chamfer (approximately 22 mm wide) with the deposit of two beads per layer.

Material	C %	Mn %	Si %	P %
Low alloyed Mn-Ni-Mo steel	≤0.100	0.80/1.80	0.15/0.60	≤0.015
	S %	**Ni %**	**Cr %**	**Mo %**
	≤0.025	≤1.50	≤0.30	0.35/0.65
	Co %	**Cu %**	**Fe %**	**B**
		≤ 0.25		
	V	**Nb + Ta**	**Ti**	
	≤0.04			
Austeno-ferritic stainless steel	**C %**	**Mn %**	**Si %**	**P %**
	≤0.030	1.00/2.50	≤1.0	≤0.030
	S %	**Ni %**	**Cr %**	**Mo %**
	≤0.030	9.00/11.00	18.00/22.00	≤0.50
	Co %	**Cu %**	**Fe %**	**B**
	≤0.20			
	V	**Nb + Ta**	**Ti**	**Ferrite δ %**
				5/15
Nickel alloy with 15% Cr	**C %**	**Mn %**	**Si %**	**P %**
	≤0.100	5.00/9.50	≤1.00	≤0.020
	S %	**Ni %**	**Cr %**	**Mo %**
	≤0.015	≥59.00	13.00/17.00	
	Co %	**Cu %**	**Fe %**	**B**
	≤0.10	≤0.50	6.00/10.00	
	V	**Nb + Ta**	**Ti**	
		1.00/2.50	≤1.00	
Nickel alloy with 30% Cr	**C %**	**Mn %**	**Si %**	**P %**
	≤0.045	≤5.00	≤0.65	≤0.020
	S %	**Ni %**	**Cr %**	**Mo %**
	≤0.010	Balance	28.00/31.50	≤0.50
	Co %	**Cu %**	**Fe %**	**B**
	≤0.10	≤0.50	8.00/12.00	
	V	**Nb + Ta**	**Ti**	
		1.20/2.20	≤0.50	

Table 11.3. *Chemical composition of welds for large components*

Two types of welds are used:

– welding on only one side (external side) with overthickness located towards the inside to eliminate root passes (see Figure 11.2),

– welding on both sides (outside and inside) with elimination of root passes by grinding or machining (see Figures 11.3 and 11.4).
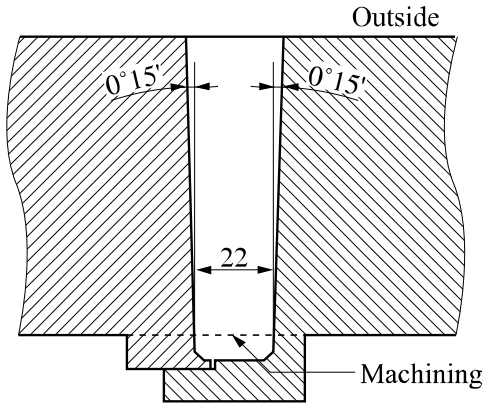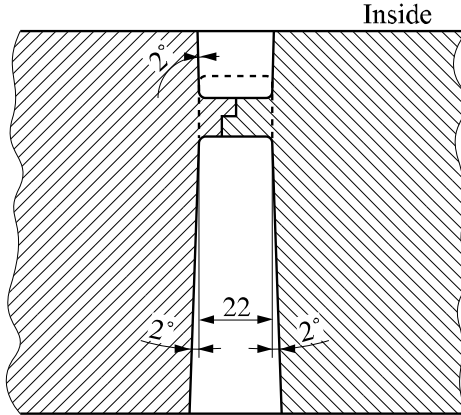
Figure 11.2. *Joint welded on only one side*

Figure 11.3. *Welding from both sides with fit-up*
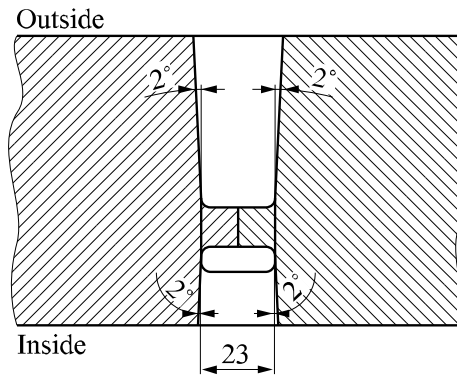
Outside

Inside

Figure 11.4. *Welding from both sides without fit-up*

Throughout the welding operation, the welding speed is controlled and a guidance system also ensures correct positioning of the head with regard to the weld pool as well as to the chamfered edges.

This highly productive process, while giving excellent mechanical characteristics, particularly in terms of impact strength, makes it possible to achieve a weld of *zero defects* thanks to its complete automation and by the regular and symmetrical laying down of passes in the chamfer (see Figure 11.5).
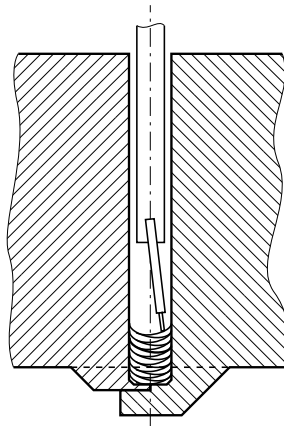
Figure 11.5. *Sketch of a narrow gap weld*
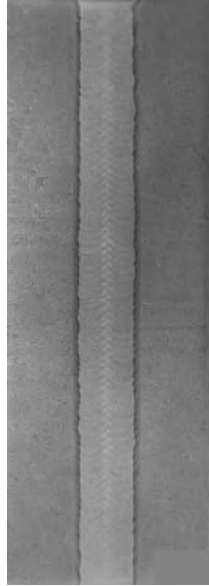
Figure 11.6. *Macrographic section of a weld carried out by the wire/flux process*

Figure 11.6 demonstrates the regular build up of passes which is made possible by the narrow chamfer wire/flux process.

To contribute to guaranteeing very high weld quality, the construction codes (RCC-M, ASME, etc.) oblige compliance with a precise process which involves:

– checking the chemical composition and the mechanical characteristics of the filler products,

– a legitimate welding procedure,

– a qualified welder or operator,

– production of test weld samples,

– non-destructive testing of the welded joints.

Welding procedures are legitimized before implementation. The validity of the procedure depends on:

– grade of the base metal,

– shape and dimension of the base metal,

– welding process,

– filler products,

– type of welded joint,

– welding position,

– welding parameters,

– heat treatments.

The legitimacy is checked and test samples are taken to verify the chemical composition under macrographic and micrographic examinations.

Each welding is carried out according to a procedure described on a welding data card and by welders who have passed the qualification tests.

All the welds are monitored by radiography and/or ultrasound. Any defective welds are repaired and undergo a second control procedure.

Pilot coupons are produced with the same filler products and the same welders as the joints that they represent and then monitored by radiography and/or ultrasound. From these coupons, test samples are taken for macrographic examinations, verifying the chemical composition and mechanical characteristics.

Precautions are taken to avoid *cold cracking*:

– powder fluxes are subject to baking at controlled temperatures,

– the welding of low alloy Mn-Ni-Mo steel requires pre-heating to a temperature higher than 150°C and a post-heating thermal treatment.

After welding, the welded joints undergo a stress relieving heat treatment at 610°C, which aims to decrease the level of residual stresses.

11.3.3. *Welding with coated electrodes*

Electric arc welding with fusible coated electrodes is used for local repairs like the assemblies of small pipes or accessories.

The process, the criteria concerning the mechanical characteristics, controls and more generally the requisite joint quality are the same as those for joints welded by the automated wire/flux process.

11.4. Cladding

The technology of reactor pressure vessels (RPVs) with pressurized water attaches a particular importance to the prevention of the corrosion phenomena. This importance is due initially to the fact that the whole of the primary circuit contains water at high temperature in which boric acid and lithine are put in solution. The materials which constitute the internal surfaces of the primary loop's equipment are

placed in a medium which allows their generalized corrosion. Limiting generalized corrosion requires the use of stainless steels or alloys with high nickel content for surfaces in contact with the primary fluid. Bare low alloy steels have, in fact, a generalized corrosion rate in the primary loop medium which remains low (about 30 microns per year), but is considered unacceptable because of the products it releases.

The concerns about generalized corrosion of steels are thus not due to the slow destruction of metal surfaces but to the formation of chemical compositions which, put in solution or suspension in the primary fluid, would be likely to stop the vessel from being used, because of the following phenomena:

– reduction in the heat transfer coefficients due to the corrosive products deposited on the heat-exchanger surfaces (SG tubes, fuel sleeves),

– increase in pressure losses,

– increase in the activity induced in the whole of the primary loop by activation in the reactor core of corrosive products in solution or suspension in the medium of the primary circuit,

– acceleration of localized corrosion,

– deterioration of valve parts and fittings,

– malfunction of instrumentation devices,

– disruption of monitoring checks due to the presence of corrosive products on surfaces.

Obtaining a low emission level of corrosive products was thus the top priority in the selection of materials used for surfaces in contact with the primary loop fluid.

Consequently, the search for materials with a low emission level quite naturally led towards materials with a very low generalized corrosion rate in the primary loop fluid, hence the choice of stainless steels and nickel based alloys.

For large-sized vessels – RPVs, steam generators, pressurizers – taking into account the thicknesses in question prevents the use of intrinsically corrosion resistant materials, and so low alloyed steel is the material of choice. To obtain a low emission level, surfaces are lined with stainless steel (308 L or Z 2 CN 20-10) or with nickel-based alloys by the arc welding process. In the case of the material used for the tube banks of steam generators, it was necessary to employ a nickel based alloy with a very good generalized corrosion resistance in both the primary and secondary circuit medium and also possessing an excellent localized corrosion resistance in these mediums. This is why stainless steel is replaced by a nickel-chromium-iron alloy on the surface of the tube plate. The welding of the nickel-chromium-iron alloy tubes can thus be carried out under better conditions, between compatible materials, and avoiding the risk of hot cracking.

11.4.1. *Cladding method*

Cladding is applied using the automatic welding process with powder flux and strip or electric arc welding with fusible coated electrodes.

Two major procedures are used for automatic strip welding:

– welding under solid flux,

– welding under an electroconducting flux.

The strip is 30 to 60 mm wide for welding with a solid flux and from 50 to 75 mm wide for welding with an electroconducting flux. The strip width can be adapted for example to match a conical component (connecting parts of different thicknesses).

The electroconducting flux process is used for cylindrical shells. In heads, the electroconducting flux process cannot be used in connection areas, and it is replaced by the solid flux process.

Stainless steel cladding comprises two or three layers depending on the expected thickness, the first layer carried out using a strip with 24% Cr and 12% Ni results in a deposit, taking into account dilution, with a chemical composition in the order of 20% Cr and 10% Ni. The second layer and possibly the subsequent layers are produced with a strip of the 20% Cr and 10% Ni type.

Special precautions are taken concerning thermal welding conditions, the welding parameters and the relative bead positions to avoid cold cracking and cracking on reheating.

Coatings using electrodes are used in the case of repair and on small surface areas, or to connect coatings carried out by automatic welding. The use of a 24% Cr and 12% Ni electrode is required for the deposit of the first layer, whereas for the following layers a 20% Cr and 10% Ni electrode is used.

As for automatic strip/flux welding, precautions are taken concerning thermal welding conditions and the welding parameters required to avoid cold cracking.

11.4.2. *Cladding inspection*

Ni-Cr-Fe alloy and stainless steel coatings are inspected by ultrasonic testing to check the absence of defects in the interface. Chemical analyses are carried out on the stainless steel cladding surface to check that the carbon percentage is lower than 0.035%.

11.5. Welding of stainless steel circuits

The circuits made from austenitic stainless steel are used to connect the various pressure components described above. The main primary pipes have dimensions up to 900 mm in diameter and 80 mm in thickness; taps and pipes with a smaller diameter are connected to these primary pipes; they are called auxiliary pipes.

Since Chapter 12 is dedicated to the welding of stainless steels, it is sufficient here to mention the peculiarities of nuclear installations. A certain number of *prefabricated* welds are carried out in the workshop transporting the sections to the site: the traditional electric arc processes with fusible coated electrodes or automatic electric welding with powder flux and wire electrode (wire/flux) are most often used. On-site, for welding small pipes or taps, coated electrode processes or manual TIG welding are used (with the electric arc in inert atmosphere and tungsten electrodes).

For on-site assembly of the largest pipes, the process initially used was manual welding with coated electrodes, but the demand for quality and productivity has led to a progressive evolution. Moreover, these manual processes cannot be easily employed when operating in irradiated zones while repairing or replacing of components. For these reasons, automatic welding processes, such orbital TIG welding in various positions, have been developed, initially with traditional chamfers, similar to those used in the manual process with coated electrodes (see Figure 11.7), then with a narrow chamfer (see Figure 11.8).
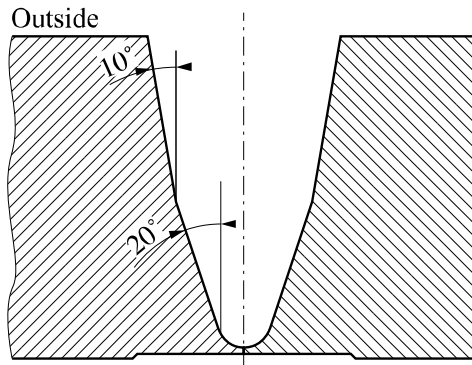
Figure 11.7. *Traditional chamfer for orbital TIG welding*

The principle of narrow chamfer orbital TIG welding is presented in Figure 11.9. It is a single pass layered welding process, with string passes, using a 1 mm diameter cold wire of 316L grade, in a narrow gap from 7 to 10.5 mm in width. This process makes it possible to weld in various positions, including on a vertical axis (2GT), horizontal axis (5GT) and tilted at 45° (6GT).
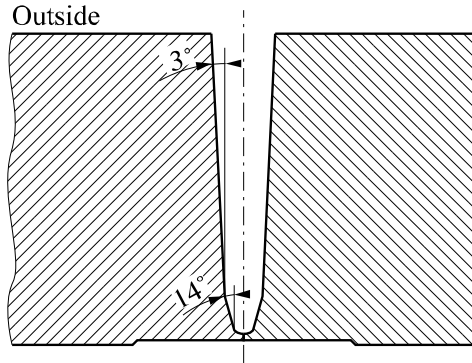
Outside
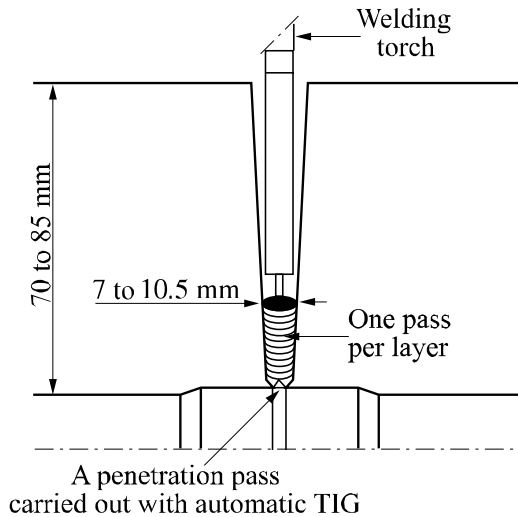
Figure 11.8. *Narrow chamfer for orbital TIG welding*

Figure 11.9. *Principle of narrow chamfer orbital TIG process*

The advantage of the narrow chamfer orbital TIG process lies primarily in the simplification of operation, and results in improved productivity. The gains in time

and filler metal is 1 to 4 when the narrow chamfer process is compared with the other wide chamfer processes, such as can be noted in Table 11.4. It is clear that these gains are the direct consequences of the narrowness of the chamfer.

This process also improves reliability and metallurgical quality. Thanks to the simplicity of the process and the guarantee of stable parameters from the root to the final filling, a homogenous welding is obtained, made up of completely identical passes, as can be seen in Figure 11.10. Moreover, this type of welding shows excellent mechanical characteristics.

Process	Metal weight to be deposited	Number of passes	Time taken
Coated electrode	50 kg		250 h. machine
Coated electrode (root) + TIG	Coated electrode 6 kg + TIG 44 kg	180 TIG	70 h. machine + 150 h. machine
Narrow chamfer TIG	14 kg	43	50 h. machine

Table 11.4. *Performance of narrow chamfer compared with other processes*

Figure 11.10. *Macrographic section of a narrow chamfer*
TIG weld carried out in the 5GT position

11.6. Dissimilar metal interfaces

Heavy components (RPV, steam generator, pressurizer) are made of low alloyed steel clad entirely with stainless steel, whereas the primary pipes are actually made from stainless steel. This type of design requires welding of the low alloy steel nozzles to austenitic or austeno-ferritic stainless steel pipes. Such an assembly necessarily requires on-site welding operations.

In order to carry out this welding operation when using a cold austeno-ferritic material, a stainless steel buttering is carried out in the factory at the end of the pipes, onto which is almost always welded a stainless steel safety end fitting.

Because of this the connection between the pipe and piping comprises the following materials (see Figure 11.11):

– pipe base metal in low alloy steel,

– interior lining of the pipe in stainless steel,

– buttering of the pipe end in Ni-Cr-Fe alloy or stainless steel,

– junction weld with the safety end fitting in stainless steel or Ni-Cr-Fe alloy,

– buttering of the safety end piece with Ni-Cr-Fe alloy. This buttering is not necessary if the weld is carried out in stainless steel,

– base metal of the stainless steel end fitting,

– welding of junction between the end fitting and stainless steel piping,

– base metal of stainless steel piping.

The buttering of the stainless steel nozzle end makes up the dissimilar metal interface. When the weld material is stainless steel, welding is carried out either by hot wire TIG process or manually with coated electrodes, the first layer being in 24% Cr and 12% Ni and the subsequent layers in 20% Cr and 10% Ni. When the welding is in Ni-Cr-Fe alloy, it is carried out by the hot wire TIG process. All the layers of added metal which can affect the base metal thermally are carried out with pre-heating and post-heating. This precaution offers the maximum guarantee against the risk of cold cracking.

These dissimilar metal interfaces mandatorily undergo a stress relieving heat treatment. They are inspected by radiographic and ultrasonic testing.

A narrow gap TIG process with a Ni-Cr-Fe filler – without buttering the pipe and end fitting – should replace the existing process in the future.
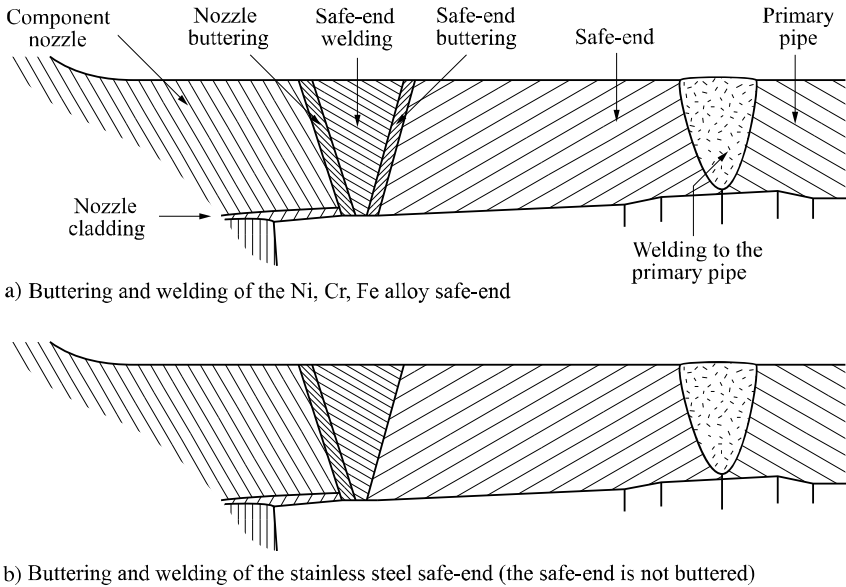
a) Buttering and welding of the Ni, Cr, Fe alloy safe-end

b) Buttering and welding of the stainless steel safe-end (the safe-end is not buttered)

Figure 11.11. *Sketch of the nozzle/pipe connection*

11.7. Welding of steam generator pipes

The tubes of the tube bundle through which the primary loop fluid flows are welded to the tubesheet coated beforehand with a Ni-Cr-Fe alloy.

The tubes, whose diameter is close to 20 mm with a thickness around 1 mm composed of a Ni-Cr-Fe alloy with 30% Cr, are welded by an automatic TIG process without filler in two consecutive turns and using a *pulsed* welding current. This current contributes to the maintenance of the weld pool during the operation and makes it possible to obtain a good compactness and sound weld surface (absence of oxide layers).

Test coupons are carried out regularly, with the welds being examined by macrography and micrography (see Figure 11.12). The criteria of acceptance particularly take the throat value and size of microporosity pits into account.
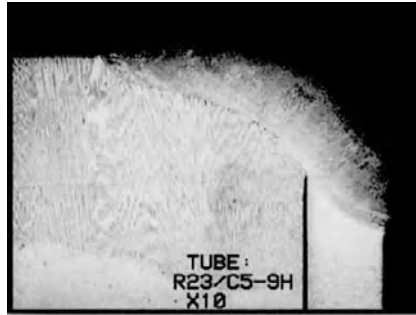
Figure 11.12. *Macrographic section of a tube/tubesheet weld*

These welds undergo many non-destructive tests, with the following being particularly prominent: visual checks, dimensional, penetrant dye, radiography and water tightness (helium test).

Before welding, the tubes are brought together by mechanical expansion over a short length (<25 mm), the aim of which is to ensure correct location of the tube for the welding operation. A correctly carried out positioning prevents a decohesion forming at root level that does not conform to the criteria in the construction code. Moreover, this positioning should not be too forceful in order to avoid a failure in water tightness in the helium test carried out after the welding of the tubes. Figure 11.13 gives a representation of the assembly immediately after welding.
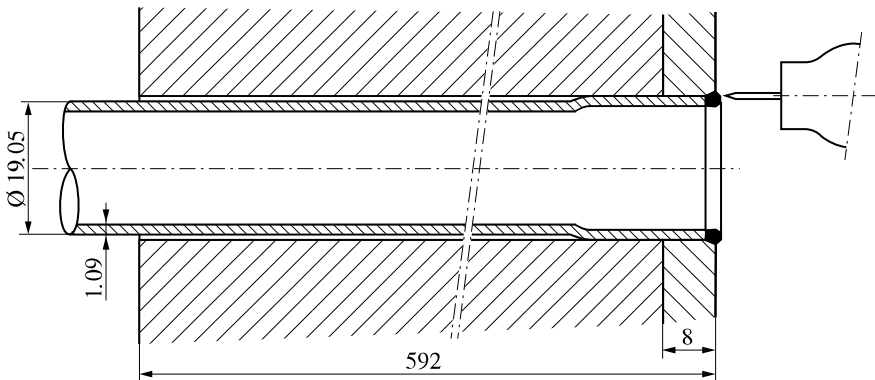
Figure 11.13. *Sketch of a tube/tubesheet assembly*

After welding and non-destructive tests, full depth expansion of the tube in the plate guarantees the following functions:

– protection of the tube weld with respect to the forces exerted on the tube bundle in operation,

– mechanical resistance,

– closing the tube/hole gap on the secondary side limits the penetration of the secondary fluid into the tube/hole interstice.

Expansion consists of increasing the tube diameter in the hole to obtain a residual interface pressure between the tube and hole surfaces, after spring back.

The expansion can be obtained:

– either by a hydraulic process of fluid pressurization in the tube; a very high pressure is necessary ($\geq$2,000 bars),

– or by expansion, which is a mechanical process with revolving rollers.

11.8. Conclusions

Because of the high stakes both in terms of safety and industry, the manufacture of components for PWR nuclear plants uses tested and proven materials and assembly processes.

Since the first choices made by designers have proved largely judicious, subsequent developments have been minor with regard to materials: the chemical composition ranges have been narrowed down and the impurity contents decreased; knowledge of their properties has progressed significantly and a substantial database has been established starting from the tests carried out to qualify materials used for the manufacture of 70 nuclear plants during the past 25 years.

With regard to the assembly processes, there have been continuous improvements in efficiency and quality by adopting, whenever possible, well controlled automatic processes.

The final objective of all these improvements remains the demonstration of operational aptitude of the components under all operating conditions and for the lifespan of the reactor.

Chapter 12

Welding Stainless Steels

12.1. Definitions

The definition from *The Concise Oxford Dictionary*, "stainless: a kind of chromium-steel alloy immune to rusting and corrosion", is not a particularly apt description for these metals.

A better definition is given by the following:

– a steel is known as *stainless* if, in ambient air, it is covered naturally and quasi-instantaneously with a very fine layer of impermeable chromium oxide due to atmospheric agents in the environment,

– the stainless steel is then known as *passive*;

– a steel is known as stainless if it contains at least 12% chromium (10.5% according to the standards).

12.2. Principal stainless steel families

Stainless steels can be classified in five main groups according to their composition and their metallurgical structure (see Table 12.1).

Transitional structures or analytical particularities give rise to sub groups placed between the main groups or added to them. Specifically these tend to be martenso-ferritic steels and martensitic or austenitic steels with precipitation hardening.

Chapter written by Jean-Louis MOIRON.

Family	Principal elements	Elements of addition	Possible stabilizers
1 - Martensitic steels	Cr 10.5 – 17% C >0.1%	Mo – V	
2 - Ferritic steels	Cr 10.5 – 29%	Mo – Al	Ti – Nb – (Zr)
3 - Austenitic steels	Cr 16 – 18% Ni 8 – 13%	Mo – Cu Mn – N	Ti – Nb
4 - Refractory steels (austenitic)	Cr 20 – 25% Ni 10 – 20%	Si	
5 - Austeno-ferritic steels (duplex)	Cr 20 – 25% Ni 4 – 7% N 0.1 – 0.3%	Mo – Cu	

Table 12.1. *The five principal stainless steel families*
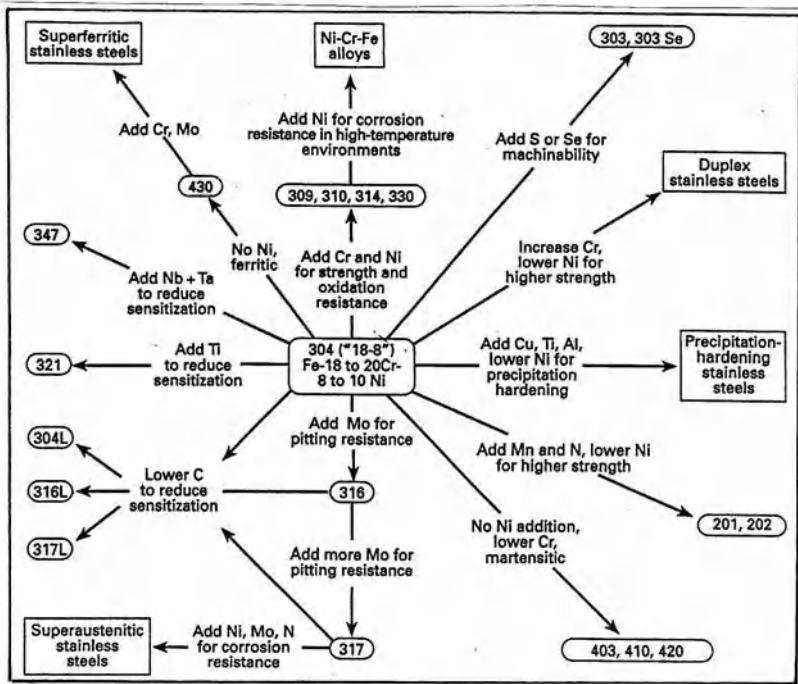
Figure 12.1. *Classification of stainless steels*

All these stainless steels can be derived from the basic austenitic steel AISI 304 (EN 1.4301) by the addition or subtraction of one or more elements to achieve a particular property in preference to another. This is clearly described in Figure 12.1 (an American classification).

12.3. Metallurgical structures

Stainless steels present three principal structures from which they draw their name, as well as a fourth, not very stable but important, in particular for the phenomena of cold hardening.

– *Austenite*:

   – face-centered cubic structure (FCC),

   – non-magnetic,

   – soft but extremely work-hardenable,

   – very malleable and workable.
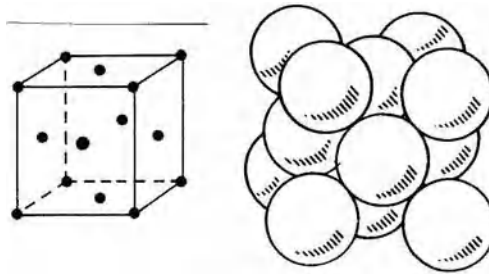
Figure 12.2. *Austenite*

– *Ferrite*:

   – body-centered cubic (BCC) structure,

   – ferromagnetic,

   – soft and not very work-hardenable,

   – malleable and moderately workable.
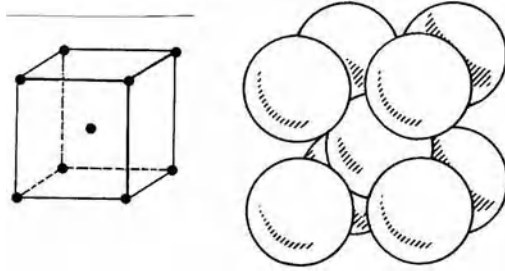
Figure 12.3. *Ferrite*

– *Martensite*:

    – body-centered cubic (BCC) structure,

    – ferromagnetic,

    – hard and brittle,

    – not very malleable and unworkable.

– *The hexagonal compact structure*

    – densest of the structures,

    – transformation during cold work hardening from austenite γ to martensite $\alpha'\gamma \to \in \to \alpha'$.
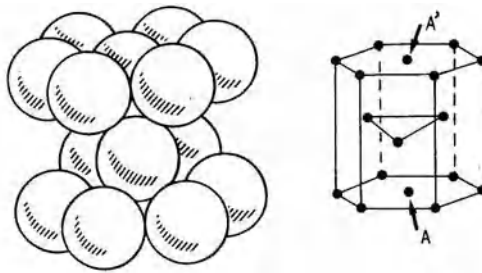
Figure 12.4. *The hexagonal compact structure*

Some micrographical images of the principal structures are presented in Figures 12.5, 12.6 and 12.7.
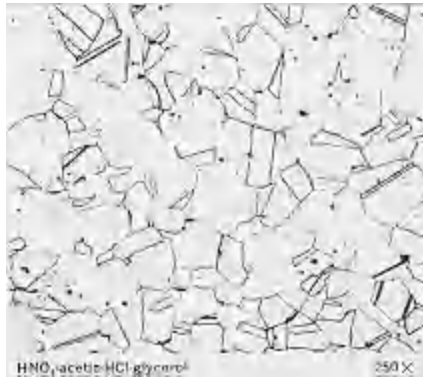
Austenite
AISI 304
EN 1.4301

Figure 12.5. *Structure of austenite A1S1 304 EN 1.4301*
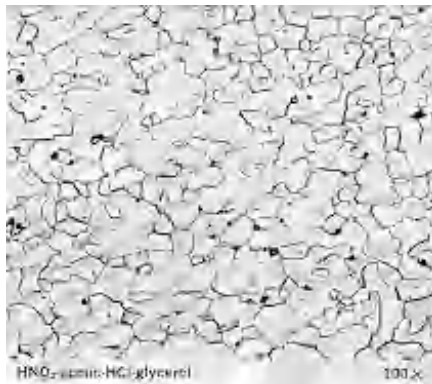
Ferrite
AISI 409
EN 1.4512

Figure 12.6. *Structure of ferrite A1S1 409 EN 1.4542*

Martensite
AISI 409
EN 1.4512

Figure 12.7. *Structure of martensite AISI 630 EN 1.4542*

12.4. Constitution diagrams

12.4.1. *Introduction*

Man has always sought to predict the future. It is not always easy, but industry lends itself relatively well to this idea.

Welders wish in particular to predict the immediate or eventual risks which they (or their customers) will encounter at the time of assembly. They wish to know what is the best procedure to use and, if a filler is necessary, which one, metallurgically speaking, is the best.

On the basis of the *alpha gene* effect (favoring ferrite formation) and *gamma gene* effect (supporting austenite formation), diagrams have been devised with the aim of predicting the metal's structure in its as welded state. These are prediction diagrams.

These diagrams have been established then modified and improved over time by examination of the micrographic structures of the molten zones in their as welded state.

Regression calculations have enabled various authors to define calculation formulas of Cr (chromium) and Ni (nickel) equivalents which are employed as the alpha gene and gamma gene effect coefficients of the various elements taken into account and which are used as coordinates for the diagrams.

12.4.2. *Calculation of the equivalent formulae*

Without prejudice to other formulae which have been and are still used, the principal Cr and Ni equivalent formula are presented in Table 12.2.

The first, Schaeffler, tried to predict the welding of stainless steels.

Thus, he was the first to establish formulas giving Cr_{eq} and Ni_{eq} for the grades of stainless steels existing at that time.

In the 1960s, Delong integrated the gamma gene effect of nitrogen, which he considered as powerful as that of carbon.

In the 1970s, Espy, taking up Schaeffler's calculations and extending their scope of application (grades with nitrogen, manganese and duplex *inter alia*), discovered and introduced:

– the significant alpha gene effect of vanadium and aluminum,

– the gamma gene effect but weighted by its nitrogen content,

– the constant manganese gamma gene effect.

At the end of the 1980s, the *Welding Research Council* established simplified formulae by:

– removing the alpha gene effects of Si (questionable for steels whose Si content can vary from 0.1 to 2%) V, Al, Ti and others;

– removing the constant Mn gamma gene effect, but by integrating it in the diagram,

– fixing the C and N gamma gene effect, while modifying them slightly.

The other formulae quoted in the table give are associated with very particular applications which will be discussed later.

	Cr_{eq}	Ni_{eq}
Schaeffler	Cr + Mo + 1.5 Si + 0.5 Nb	Ni + 30 C + 0.5 Mn + 0.6 Cu
Delong	Cr + Mo + 1.5 Si + 0.5 Nb	Ni + 30 (C + N) + 0.5 Mn
WRC 1992	Cr + Mo + 0.7 Nb	Ni + 35 C + 20 N + 0.25 Cu
Espy	Cr+Mo+1.5 Si+ 0.5 Nb + 5 V + 3 Al	Ni + 30 C + x (N-0.045) + 0.87 + 0.33 Cu x = 30 if N = 0/0.20 x = 22 N = 0.21/0.25 x = 20 N = 0.26/0.35
	Cr + Mo + 1.5 Si + 0.5 (Nb+Ta) + 2Ti + W + V + Al	Ni + 30 C + 0.5 Mn + 0.5 Co
Hammar and Svensson	Cr + 1.37 Mo + 1.5 Si + 2 Nb + 3 Ti	Ni + 22 C +14.2 N + 0.31 Mn + Cu
Eckenrot and Kovach (12% Cr)	Cr + 4 Mo + 6 Si + 8 Ti + 2 Al	4 Ni + 40 (C + N) + 2 Mn

Table 12.2. *Calculation formulae*

12.4.3. *Constitution diagrams*

Various diagrams are presented in the following pages. They are used to predict the structure of the as welded molten metal.

– *Schaeffler diagram*

This is the best known and most widely used diagram by pressure vessels manufacturers, in particular for heterogenous welds.
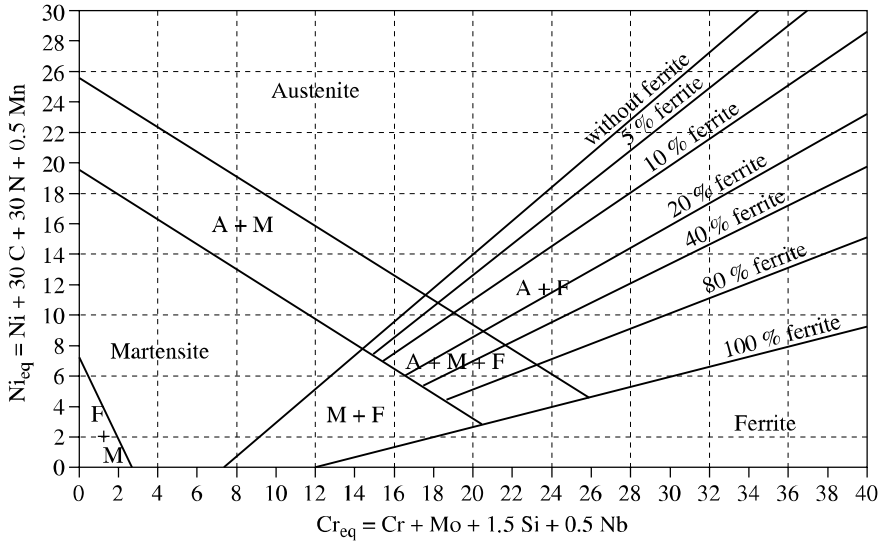

Figure 12.8. *Schaeffler diagram*

This diagram has one major disadvantage in that it is not suited to grades with high manganese and/or high nitrogen content.

In the case of completely homogenous welds in austenitic stainless steel or when the analysis of the molten metal is known, the calculation of the ferrite content in the as welded metal can be made by Séférian's formula, which is derived from the Schaeffler diagram:

$$\% \text{ ferrite} = 3 \ (Cr_{eq} - 0.93 \ Ni_{eq} - 6.7)$$

– *Delong diagram*

Taking account of nitrogen content as a gamma gene effect led W. Delong to construe a different diagram from that of Schaeffler.
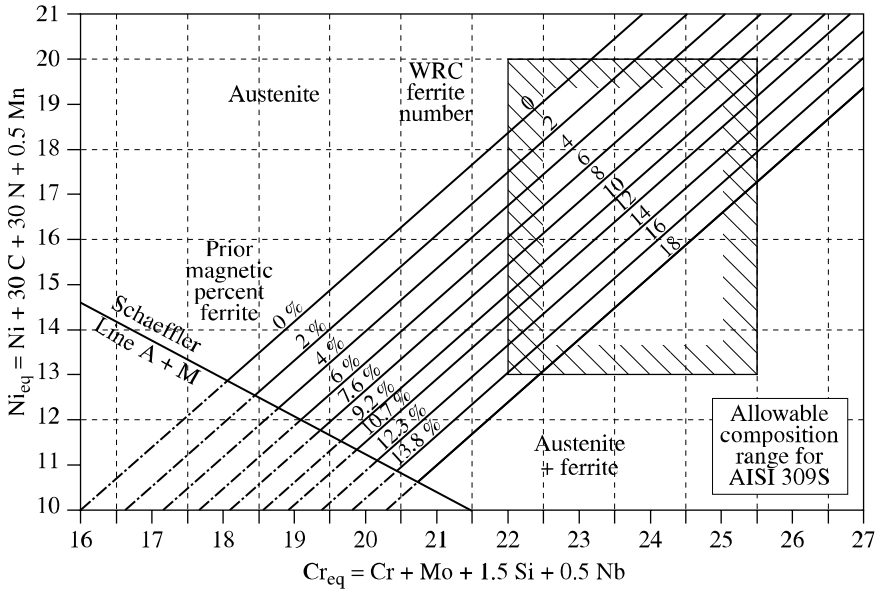
Figure 12.9. *Delong diagram*

Commonly used in nuclear stainless pressure vessel construction, this diagram presents two major disadvantages:

– its limited application field makes it unusable for heterogenous weldings in particular,

– it cannot be applied to grades with high manganese and/or nitrogen content.

– Espy diagram

This is the Schaeffler diagram refined for the equivalent Cr and Ni calculation formulae.

This diagram is particularly well adapted to stainless grades with high manganese and/or nitrogen content and to duplex steels.

– WRC92 diagram

This is the simplest, but unfortunately the least precise diagram:

– a reduced number of elements for the Cr_{eq} and Ni_{eq} calculation,

– a limited application field, making it impractical for heterogenous welds.

1) X = 30 if N = 0/0.2; X = 22 if N = 0.21/0.25; X = 20 if N = 0.26/0.35
2) Constant for Mn between 0 and 10%
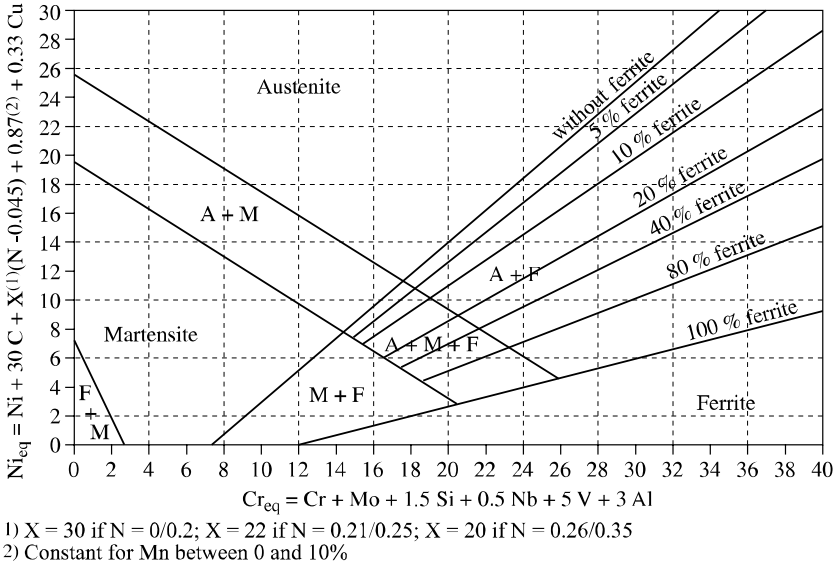
Figure 12.10. *Espy diagram*
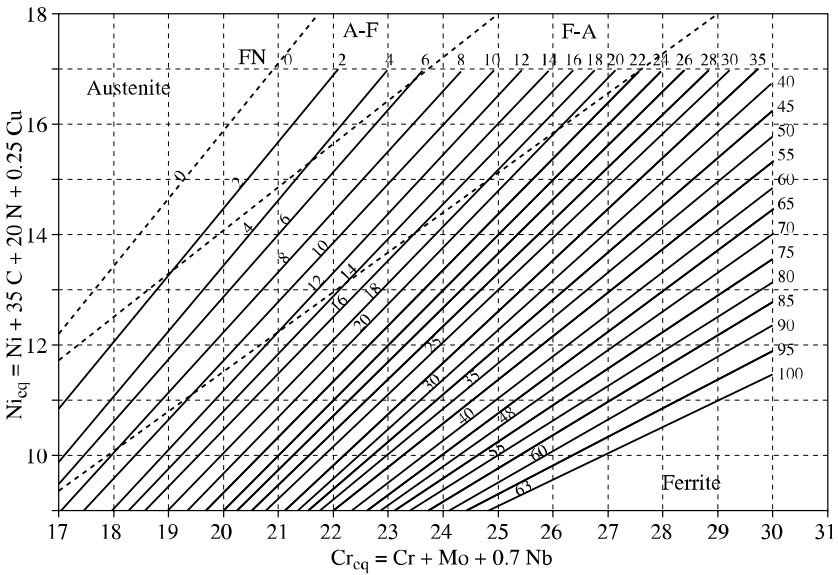
Figure 12.11. *WRC 92 diagram*

Originally, this diagram was graduated only in FN *(ferrite number* or ferrite index) which was not transposable linearly to % ferrite content, which made it rather

impractical. This defect was corrected and the graduation is now made both in FN and ferrite %.

– *Comparison of the various diagrams*

The advantages and disadvantages of the various diagrams are summarized in Table 12.3.

Diagram	Advantages	Disadvantages
Schaeffler	- heterogenous welding - scope of application	- not for high Mn (>2%) - not for high N (>0.10%) - not very precise (ferrite >20%)
Delong	- approved by ASME - ferrite % and FN	- limited field Cr_{eq} >16 Ni_{eq} >10 ferrite <20% - not for high Mn (>2%) - not for high N (>0.10%)
Espy	- heterogenous welding - scope of application - many elements - high Mn and/or N	- not very precise (ferrite >20%)
WRC 92	- standardized in Europe (EN standard…) - simplified calculation	- few elements - limited field Cr_{eq}>17 Ni_{eq} >9

Table 12.3. *Comparison of the various diagrams*

– *Bystram diagrams*

Brystram diagrams are not constitution diagrams, but, when superimposed on them, they allow the identification of four major risk zones:

  – risk of hot cracking,

  – risk of sigma phase formation,

  – risk of cold cracking,

  – risk of grain growth.

The complete diagram represented in Figure 12.12 shows that the zero risk field is relatively reduced and that various stainless steels are susceptible to one or other of the above risks (even two at the same time).
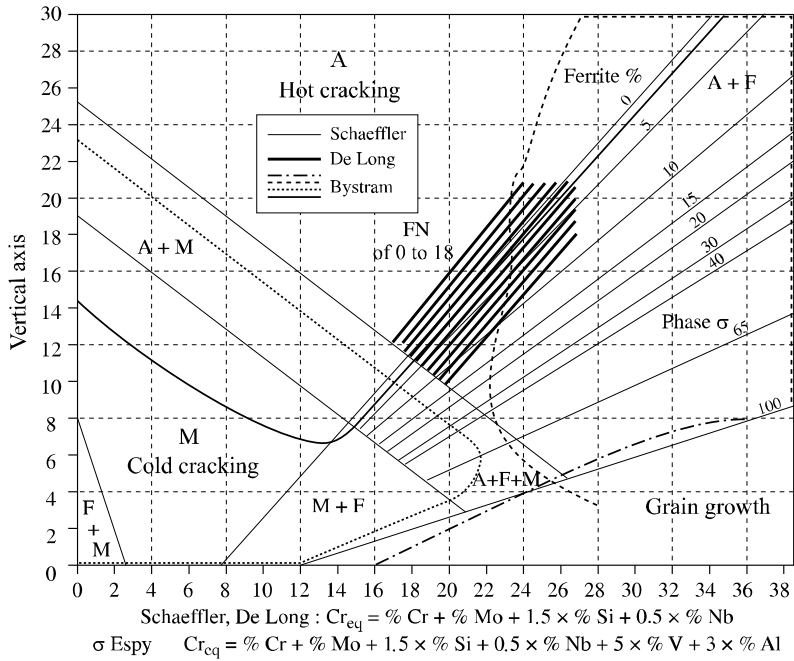
Vertical axis: Schaeffler : Ni_{eq} = % Ni + 30 % C + 0.5 × % Mn
               De Long   : Ni_{eq} = % Ni + 30 % C + 30 % N + 0.5 × % Mn

     σ Espy Ni_{eq} = % Ni + 30 % C + X* × (% N − 0.045) + 0.87** + 0.33 × % Cu

* X = 30 if N = 0/0.2; X = 22 if N = 0.21/0.25; X = 20 if N = 0.26/0.35; ** constant for Mn between 0 and 10%

Figure 12.12. *Complete diagram*

12.5. Welding ferritic stainless steels

12.5.1. *Introduction*

The family of ferritic stainless steels covers an important range of chemical compositions, based in general on the ternary diagram Fe-Cr-C. These steels contain a minimum of 11.5% chromium and a maximum of 0.1% carbon.

The properties of these steels are primarily based on the chromium content associated with a corrosion resistance.

As far as welding is concerned, ferritic stainless steels are weldable subject to care being taken to mitigate certain critical properties.

Critical properties		Precautions
C carbides		
$\approx$ insoluble $\Rightarrow$ $\Rightarrow$ corrosion		stabilization
N_2 nitrides		
Risk of grain growth		
Insoluble $H_2 \Rightarrow$ embrittlement		H_2 and N_2 forbidden

Table 12.4. *Critical properties and precautions related to ferritic stainless steels*

12.5.2. *Risks incurred in welding*

Ferritic stainless steels contain in practise from 11.5 to 29% of chromium, a generally low carbon content and other different alloying elements (Mo for corrosion performance, Al for temperature behavior, Ti and/or Nb for stabilization).
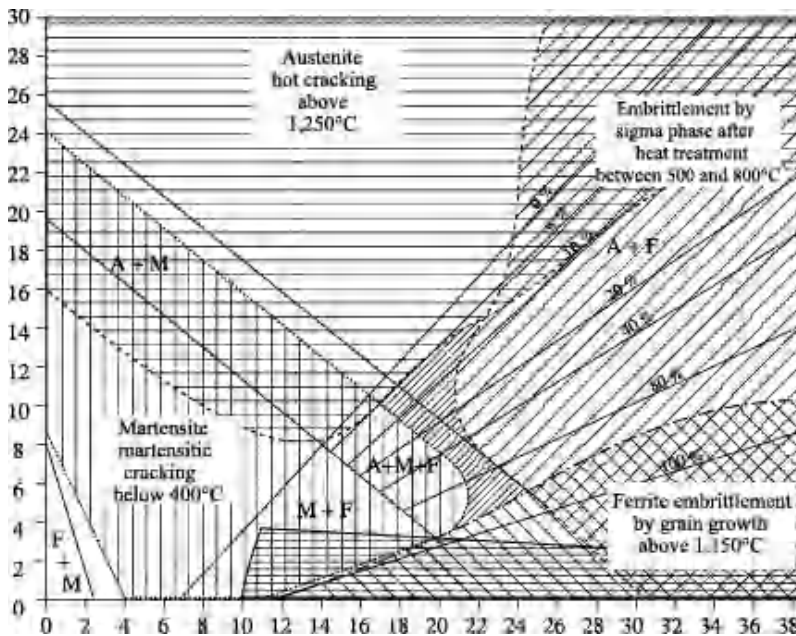
Figure 12.13. *Position of ferritic stainless steels on a Schaeffler-Bystram diagram*

The position of stainless steels on a Schaeffler-Bystram diagram reveals the risks incurred in welding these steels:

– risk of cold cracking for semi-ferritic steels, particularly with a strong hydrogen sensitivity,

– risk of forming intermetallic compounds (phase σ), at least for steels with very high chromium equivalent. Taking into account the speed of the thermal cycles, the formation of phase σ is not normally expected during the welding operation itself,

– risk of grain growth, which is all the more likely the higher the welding energy is.

Lastly, it is important to emphasize a very important point about the metallurgy of ferritic stainless steels: the very low solubility of carbon and nitrogen, imposing for many welding applications in particular, stabilization by titanium and/or niobium, whose mechanism and other effects are presented hereafter.

12.5.3. *Stabilization*

The majority of these risks are removed or significantly decreased by the use of stabilized steel types.

The stabilizing elements (Ti, Nb) are elements whose carbides and nitrides are formed in preference to those of chromium during heat treatments. They are used to trap carbon and nitrogen.

Stabilization plays several roles. Indeed, we know that: carbon and nitrogen are practically insoluble in ferrite; precipitated chromium carbides and nitrides are instigators of intergranular corrosion by chromium impoverishment of the surrounding matrix; post-operative heat treatments are not always easy or feasible; grain growth of the ferritic structure is not recoverable by heat treatment; the use of stabilized Ti or Nb grades, or even *bistabilized* Ti + Nb types is strongly advised as soon as a welding operation is envisaged.

The effects of stabilization are numerous and can be summarized as follows:

– stabilization by titanium is characterized by titanium nitride precipitation in the liquid state, (solidification occurs around these TiN germs, creating favorable conditions in the molten zone for obtaining an equiaxial structure giving rise to a good impact strength), and by the precipitation of titanium carbides in the solid state around 1,050°C, around titanium nitrides;

– stabilization by niobium is characterized by niobium carbo-nitride precipitation in the solid state around 1,150/1,200°C, and possible precipitation between 600 and 950°C of intermetallic Fe_2Nb with the effect of blocking grains favorable to creep behavior at high temperature;

– niobium or titanium carbo-nitrides decrease sensitivity to ferrite grain growth;

– titanium and niobium, by "trapping" the strong gamma gene elements, carbon and nitrogen, tend to stabilize ferrite, therefore avoiding the formation of martensite.

The stabilization formulas most generally selected are:

– Ti% >0.2 + 4 (C% + N%),

– Nb% >0.15 + 7 (C% + N%).

12.5.4. *Risks of embrittlement*

There are four risks of ferritic stainless steel embrittlement:

– embrittlement at 475°C,

– sigma phase,

– embrittlement at high temperature,

– sensitivity to the notch effect.

Embrittlement at 475°C

Ferritic stainless steels are sensitive to embrittlement at 475°C (between 400 and 600°C) due to poor chromium miscibility (and also molybdenum) in a Fe-Cr alloy involving the formation of a phase α' rich in chromium (30%) and in molybdenum, a hard and brittle phase.

This phase is formed after very long periods in its field of stability. It is very seldom observed. Embrittlement at 475°C is not to be feared after a welding operation.

Sigma phase

The sigma phase is an intermetallic compound appearing in the iron-chromium system. This is why we mention it in this chapter, although it does not play a significant role in the welding of ferritic and semi-ferritic steels. The sigma phase is hard and brittle, and its appearance in welds can cause a true brittleness appearing even in the absence of a notch and which does not disappear with a moderate rise in temperature.

However, welds of ferritic and semi-ferritic steels having a low impact strength at room temperature, the importance of the formation of the sigma phase in these welds remains secondary.

The sigma phase has a composition based on a chromium content of 45%, and it can occur by prolonged treatment above 550°C in iron-chromium type alloys containing more than around 22% chromium.

Embrittlement at high temperature

Embrittlement due to maintaining a high temperature for a prolonged period is influenced by many factors, analytical as well as structural: chromium content and interstitial compounds, grain size, nature and distribution of precipitates. The welding operation does not generate embrittlement at high temperature.

Sensitivity to the notch effect

Semi-ferritic stainless steels low in chromium (Cr <15%) are not sensitive to the notch effect.

On the other hand, for steels containing more than 15% chromium, the sensitivity is dependent on interstitial compounds (C + N) content and increases with the chromium content.

The only means of decreasing this sensitivity is to control the C + N content, either by maintaining them at a very low level (be careful of grain growth) or by trapping them with a stabilizing element (Ti, Nb).

12.5.5. *Filler products*

Filler products are generally composed of austenitic stainless steel. However, it is important to note the availability of ferritic filler product grades which enable the formation of homogenous welds which has a significant advantage with regard to their performance in coping with a possible deformation.

The choice of filler product is made according to the base metals: the filler must be more alloyed than the noblest of the base materials to compensate for the losses in welding and in respect to the constitution diagrams.

The filler products are standardized:
– AWS standard:
  – S.F.A. 5.4 – Electrodes,
  – S.F.A. 5.9 – Bare wire,
  – S.F.A. 5.22 – Filled wire;

– European standard:
  – NF EN 1600 – Electrodes,
  – NF EN 12072 – Bare wire,
  – NF EN 12073 – Filled wire.

12.5.6. *Shielding gases*

Knowing that H_2 and N_2 are out of the question and CO_2 not recommended (less than 3%), the shielding gases usable for welding ferritic stainless steels are set out in Table 12.5.

Procedures	TIG	MIG
Primary gas	Ar	Ar + O_2 (<3%)
Doping gas	He (<20%)	He (<20%)

Table 12.5. *Shielding gases*

12.5.7. *Summary: partial conclusion*

Ferritic stainless steels are *weldable* without pre-heating or post-heating by respecting the following advice set out in Table 12.6.

Advice	To combat
Stabilized steel grades	Corrosion Grain growth Embrittlement at high temperature Notch sensitivity
Stability of ferrite	% of martensite in semi-ferritics
Low welding energy	Grain growth Embrittlement
H2 ⎫ N2 ⎭ PROHIBITED	Cold cracking Corrosion
CO_2 inadvisable	C ↗ ⇨ Carbides ↘

Table 12.6. *Advice*

12.6. Welding of martensitic stainless steels

12.6.1. *Introduction*

The family of martensitic stainless steels comprises steels which combine a raised level of hardness with certain level of corrosion behavior (thanks to their chromium content), comparable with that of treated alloyed steels, and which can be produced by martensitic hardening.

This family generally includes certain structural hardening steels, whose low carbon martensite is relatively soft, but whose characteristics can be significantly increased by tempering treatments at average temperatures (from 500 to 750°C) judiciously selected to ensure the precipitation of hardening intermetallic compounds.

The positioning of martensitic stainless steels and those with structural hardening is schematized in the Schaeffler-Bystram diagram in Figure 12.14.
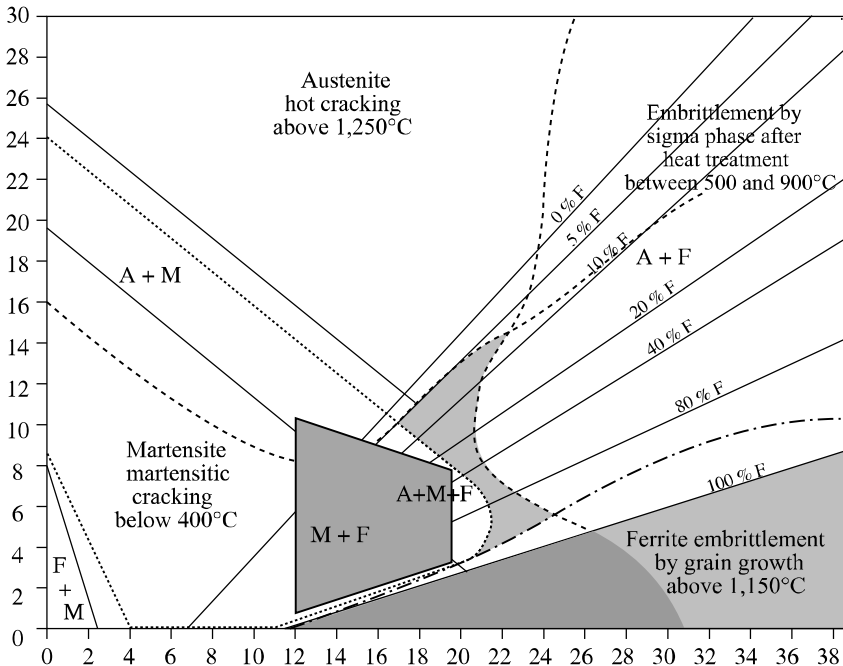
Figure 12.14. *Schaeffer-Bystram diagram of martensitic stainless steels and those with structural hardening*

Martensitic stainless steels have a similar behavior with regard to welding to that of heat treated alloyed steels with an equivalent carbon percentage, and will thus be treated in a similar way.

12.6.2. List of martensitic stainless steels

A non-exhaustive list of the principal martensitic stainless steels and precipitation hardened steels taken from the EN 10.088-2 standard is presented in Table 12.7 below.

X12Cr13	
*X12CrS13	S = 0.15/0.35
X20Cr13	
X30Cr13	
*X29CrS13	S = 0.15/0.35
X39Cr13	
X46Cr13	
X50CrMoV15	V = 0.10/0.20
X70CrMo15	Mo = 0.40/0.80
*X14CrMoS17	S = 0.15/0.35; Mo = 0.20/0.60
X39CrMo17-1	
X105CrMo17	Mo = 0.40/0.80
X90CrMoV18	Mo = 0.90/1.30; V = 0.07/0.12
X17CrNi16-2	
X3CrNiMo13-4	Mo = 0.30/0.70
X4CrNiMo16-5-1	
X5CrNiCuNb16-4	Cu = 3.00/5.00; Nb = 5xC/0.45
X7CrNiAl17-7	Al = 0.70/1.50
X8CrNiMoAl15-7-2	Al = 0.70/1.50
X5CrNiMoCuNb14-5	Mo 1.20/2.00; Cu = 1.20/2.00; Nb = 0.15/0.60

Table 12.7. *Extract from the EN 10.088-2 standard*

12.6.3. Effect of the elements C, Cr and Ni on the γ loop

Martensitic stainless steels are characterized by the $\gamma \rightarrow \alpha'$ transformation which occurs without diffusion at low temperature ($\leq 400°C$), between M_S and M_F.

The grades concerned can be richer in Cr because the greater the extent of gamma gene elements such as C and Ni, the more stable the γ field at high temperature.
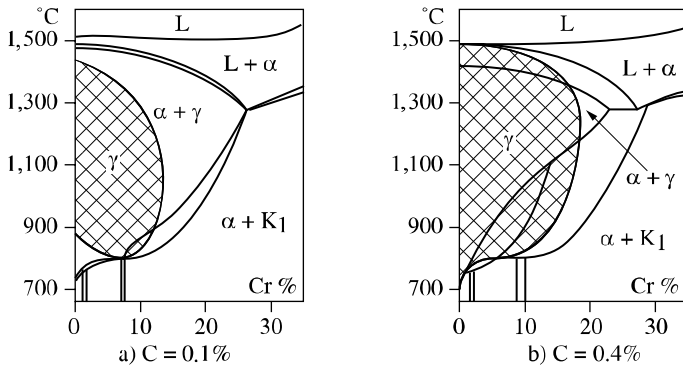
Figure 12.15. *Extension of the γ loop by carbon*
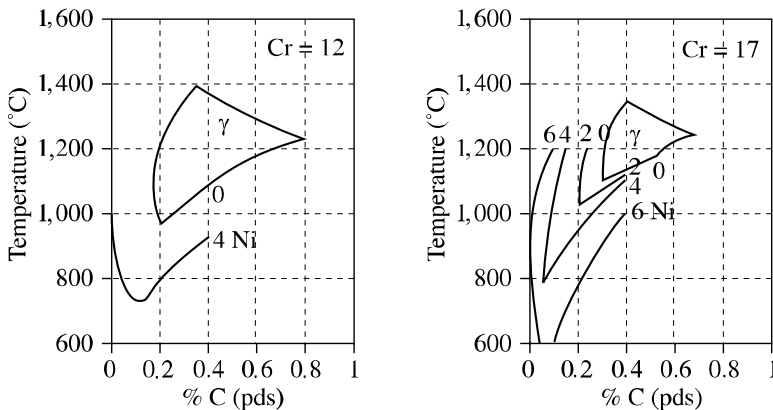
Figure 12.16. *Widening of the γ field by Ni*

12.6.4. *Metallurgical weldability of martensitic stainless steels*

In the Schaeffler-Bystram diagram, these steel types are situated to the right of the martensite range, i.e. with sufficiently high Cr content (equal to or higher than 12%) to ensure a good corrosion resistance in relatively unaggressive environments. In the welds (MZ and HAZ in the immediate vicinity of the MZ), the rapid cooling starting from temperatures above the monophase γ field can favor the presence of δ ferrite at room temperature. In these zones, the structure will be made up of "fresh" martensite (as quenched state), and possibly of δ ferrite and also of residual austenite for the most alloyed grades. Some as hardened martensite will also be present in the HAZ of welds with austenitic filler. This martensite can be sensitive to cold cracking

(hydrogen embrittlement with possibly differed rupture) and all the more so the higher the carbon percentage is (hard martensite), the more hydrogen is present, and the higher the thermal stresses. It is thus, in general, essential to pre-heat and post-heat the materials with $T < M_S$, but close to M_F to limit the stresses due to the phase change, to carry out a slight stress relief of the martensite immediately after its formation and to operate in a temperature range where hydrogen does not have a tendency to segregate in the former γ joints. Then it is necessary to relieve the weld stress in a temperature range equivalent to that used for the tempering of these grades (approximately 550 to 750°C according to the grades and the desired level of hardness). The stress level must also be limited by slow cooling and heating rates, especially for heavy parts, and also by a component design which avoids the concentration of stresses around the weld.

In the case of a weld with austenitic filler (308L, 309L, etc), the stress relief treatment of α' is not possible because it would cause diffusion of the carbon of α' towards γ and a reduction in corrosion resistance of γ by chromium intergranular carbide precipitation (sensitizing). Stress relief at around 250°C of the martensitic HAZ is possible.

The welding of high carbon or resulfurized grades is not advisable, whereas that of low carbon steel types (C <0.05%) can be practiced without pre-heating and post-heating, in particular for low carbon, highly alloyed (Ni, Mo, etc.) grades, which have a M_F close to room temperature. For products which allow it, it is possible to carry out after welding, an austenitization followed by a hardening, which, in the particular case of grades with precipitation hardening in heavy products, makes it possible to obtain mechanical characteristics in the molten zone and corrosion resistance comparable with those of the forged product. The welding process can have a significant influence on ductility/impact strength properties, in particular by introducing elements which affect these properties, such as oxygen brought in by the welding operation on the coated electrode. Whereas nitrogen and especially hydrogen are harmful, H_2 and N_2 are formally prohibited in the welding processes which require a gas protection. For thin products, these steels are weldable by spot resistance, roller and flash welding processes.

12.6.5. *Conclusion: partial summary*

In short, the weldability of martensitic stainless steels is as follows. The martensitic structure is sensitive to the phenomenon of cold cracking: rupture (differed) due to hydrogen embrittlement. The phenomenon is less marked the lower the carbon percentage, the lower the hydrogen content and the lower the stress level. The welding of high carbon (>0.30%) or resulfurized steel types is ill-advised. Welding low carbon (<0.05%) grades is possible without pre-heating or post-

heating, but a *stress relief/tempering treatment* is necessary. When it is possible, an *austenitization + hardening* ensures the best compromise between *mechanical resistance/ductility/corrosion resistance,* in particular for the grades hardened by precipitation.

12.7. Welding of austenitic stainless steels

12.7.1. *Introduction*

Austenitic stainless steels have remarkable properties which clearly differentiate them from all the other categories of steel. For this reason, it appears useful to point out a certain number of concepts concerning the constitution, the structure and the uses of these alloys, essential concepts for understanding the phenomena occurring during welding operations.

The austenitic structure and the presence of nickel improve the corrosion resistance of chrome steels, particularly in slightly oxidizing or reducing environments. Austenitic stainless steels are characterized moreover by the following properties: a raised ductility and impact strength, a significant work hardenability without embrittlement including at low temperature, no real yield strength, an elevated mechanical resistance at high temperature, and a unique weldability.

12.7.2. *Risks incurred during welding*

The family of austenitic stainless steels is also extremely vast, as the positioning shows on the Schaeffler-Bystram diagram (see Figure 12.17).

As this diagram also shows, austenitic stainless steels are faced with, according to the grade, two types of risks:

– embrittlement by phase σ for the most alloyed steels; this risk, real in use, remains very limited during welding operations, the heating and cooling speeds being in general too fast for the start of precipitation;

– hot cracking, which is a real risk in welding and which we will study in more detail.
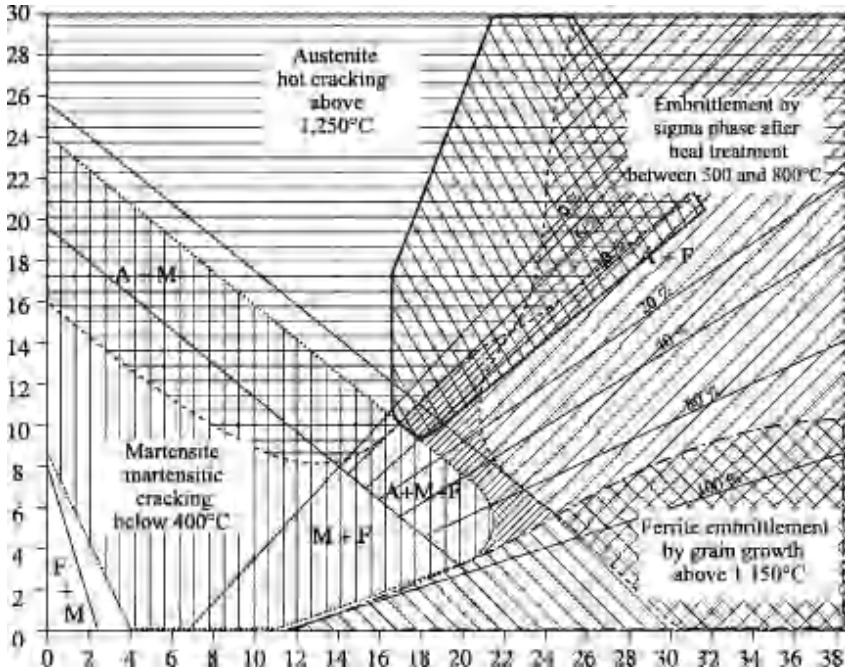
Figure 12.17. *Schaeffer-Bystram diagram of austenitic stainless steels*

Another risk not described in this diagram lies in the precipitation of chromium carbides ($Cr_{23}C_6$), synonymous with the risk of intergranular corrosion.

12.7.3. *Carbide precipitation*

The presence of carbon in austenitic stainless steels can be responsible for a deterioration in their corrosion resistance when they are subjected to temperatures maintained for a long period and ranging between around 500 and 850°C.

For grades with average carbon content (0.04% or more), carbide precipitation in the affected zone is perfectly possible.

However, the steelmaker has two means to reduce or eliminate the risk of such a precipitation: to decrease the percentage of carbon, which reduces the quantity of carbon which can precipitate and modifies the precipitation speed (the temperature range is lowered and the duration very slightly increased), or to add elements with a greater affinity for carbon than chromium; the elements thus added are generally titanium and niobium. The precipitation of Ti (TiC) and niobium (NbC) carbides

occurs in a temperature range higher than that in which $M_{23}C_6$ would precipitate and the carbon thus trapped cannot take part in this last precipitation.

12.7.4. *Hot cracking*

Although it is very commonly used, the term *hot cracking* is not well suited to describing the multiplicity of phenomena which the word covers. Indeed, under this umbrella term we find cracks in the HAZ as well as in the molten metal zone, but also different cracking mechanisms.

Various types of hot cracking

First of all we should note the characteristics of hot cracking. Such cracks are very often small in size, in the affected zone or molten metal. They are often quite numerous, perpendicular to the fusion line (HAZ), parallel to the direction of solidification or in the weld pool axis. In addition, they most often occur in austenitic steels where they are practically the only type of cracking that results from welding.

Two mechanisms can cause cracking: liquation and lack of ductility in the material.

Cracking due to liquation is explained by the presence of liquid phases in the grain boundaries at high temperature (approximately 1,250°C), when the metal is already solid. Any stress then allows the opening of liquid films by shearing. This can occur with solidification of the molten metal (local delay in solidification) or in the HAZ and molten metal during a reheating (premature fusion of segregated phases), for example during a second pass.

Cracking due to the lack of ductility occurs at temperatures lower than the preceding one (approximately 1,000°C). It is primarily due to the precipitation of certain phases (carbides for example) which decrease the ductility of the material. There too, cracking can occur in the molten metal during solidification or in the HAZ and molten metal during a heating at sufficient temperature during a welding cycle (reactivation of a bead by a later pass).

NOTE: very often, the cracks are initiated by liquation and propagate due to lack of ductility, the liquation crack being the initial defect leading to subsequent failure.

Mechanism of hot cracking

An austenitic steel welded joint (including MZ, HAZ and a previously reheated bead) can be at the center of a cracking generated by shrinkage stresses and developing at high temperature (more than 1,200°C) in interdendritic spaces of the

molten metal or HAZ. This is caused by localized enrichment at grain joints in elements with low melting points forming a liquid film with a low level of cohesion. The presence of certain elements like sulfur, phosphorus and boron encourage this cracking.

The mechanism arises from the primary mode of solidification. If the first solidification occurs in austenite (γ solidification on the left of eutectic), growth will be of the *basalt* type with aligned low melting point phases. If the first solidification occurs in ferrite (δ solidification on the right of eutectic), growth will be of the dendritic type with disseminated low melting point inclusions, and is therefore less brittle.

The position of the eutectic which delineates the two modes of solidification is defined by the ratio:

$$\frac{\text{Cr equivalent}}{\text{Ni equivalent}} = 1.5$$

according to the principal diagrams. Thus the susceptibility of austenitic stainless steels to hot cracking can easily be predicted.

Solutions

To decrease or avoid the risks of hot cracking in austenitic stainless steels, the principal advice is to limit clamping so as to decrease the stresses as far as possible, and to choose a basic material and/or a filler which guarantee a Cr_{eq}/Ni_{eq} ratio greater than 1.5 in the molten zone. If this ratio cannot be met, it is necessary to adjust the welding conditions by limiting the welding energy and ensuring a very effective protection (neither too much nor too little).

12.7.5. *The sigma phase*

Metal alloys containing a B transition element (Fe, Ni, Mn, Co, etc.) and an A transition element (Cr, Ti, V, etc.) can form intermetallic phases whose formula can vary from B_4A to BA_4.

The σ phase is the best known among the intermetallic compounds. Excepting multipass welding of significant thicknesses, the formation of the σ phase is rare when welding traditional austenitic stainless steels because the process is relatively slow, which will not be the case for steels high in transition elements, such as austenitic steels with high chrome and molybdenum content. This risk is avoided by decreasing welding energies and accelerating cooling speeds in order to shorten the

time spent in the risk temperature zone. This is valid for the molten zone and the affected zones.

12.7.6. *Filler products*

Welding of stainless steels will generally be homogenous, with a filler metal close in composition to the base material, while taking care to obtain a molten zone free from the risks of hot cracking if possible.

In all cases, the filler metal will be slightly over-alloyed compared to the base metal: for chromium, to compensate for the losses in the course of welding and for other elements this may be necessary to improve the corrosion resistance of the welded joint or its resistance to hot cracking when the welding must remain purely austenitic. The filler products are standardized.

12.7.7. *Shielding gas*

All argon based shielding gases can be used without risk when welding austenitic stainless steels, including:

– gases doped with hydrogen to increase welding speeds because the content of δ ferrite remains weak ($\leq$10% in the molten zone);

– gases doped with nitrogen because the solubility of nitrogen is high in austenite;

– gases used for the welding of steels which contain nitrogen themselves.

	TIG	MIG
Protective gas	Argon (1 1)	Ar + O_2 (M 13) Ar + CO_2 (M 12)
Shielding gases	He (<20%) (L 3) H_2 (<10%) (R 1) N_2 (<10%)	He (<20%) He (<15%) M 11) N_2 (<10%)
Root gas	Ar (I 1) Ar + H_2 (R 1)	Ar (I 1) Ar + H_2 (R 1)

Table 12.8. *Shielding gases*

12.8. The welding of austeno-ferritic stainless steels (duplex)

12.8.1. *Introduction*

For an austeno-ferritic steel, the microstructure of the base metal with approximately 50% ferrite and 50% austenite is obtained after temperature maintenance at between 1,050°C and 1,100°C followed by a hardening, generally in water.

The so called *duplex* austeno-ferritic steel has 22.5% Cr and a PREN (pitting resistance equivalence number) equal to or higher than 36. Its guaranteed yield strength is higher than 500 MPa.

The so called *super-duplex* austeno-ferritic steel has 25% Cr and a PREN higher than 40. Its guaranteed yield strength is higher than 550 MPa. The high mechanical properties of duplex steels allow reductions in thickness when designing equipment.

The molybdenum and nitrogen content is optimized to obtain the best corrosion resistance properties, including for the thickest sheets. The high levels of nitrogen in austeno-ferritic steels confer a good microstructural stability, particularly in the HAZ.

12.8.2. *Risks incurred in welding*

The positioning of duplex steels on a Schaeffler-Bystram diagram shows that the main risk incurred during welding lies in the precipitation of intermetallic phases, in particular the σ phase.
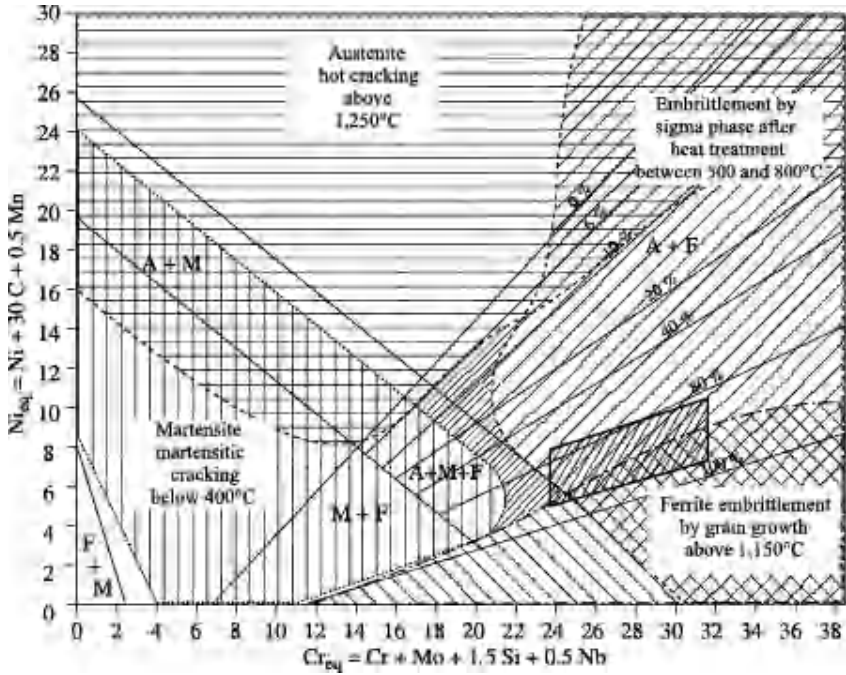
Figure 12.18. *Schaeffler-Bystram diagram of austeno-ferritic stainless steels*

12.8.3. *Principal austeno-ferritic stainless steels*

The following non-exhaustive list is taken from the EN10 088-2 standard.

Designation	N (%)	Others
X2CrNiN23-4	0.05/0.20	
X3CrNiMoN27-5-2	0.05/0.20	
X2CrNiMoN22-5-3	0.10/0.22	
X2CrNiMoCuN25-6-3	0.15/0.30	Cu = 1%
X2CrNiMoN25-7-4	0.20/0.35	
		Cu = 0.7%
X2CrNiMoCuWN25-7-4	0.20/0.30	W = 0.7%

Table 12.9. *Principal austeno-ferritic stainless steels*

12.8.4. *Weldability of austeno-ferritic steels*

The steels taken into account in the new European standard contain approximately 0.2 to 0.28% nitrogen, low percentages of carbon (lower than or equal to 0.05%), and amounts of Cr, Ni, Mo and, possibly, Cu and W which ensure a ferrite solidification, then a partial transformation (approximately 50%) of δ ferrite into γ austenite if the cooling speed is sufficiently slow to reach a phase balance (see Figure 12.19).
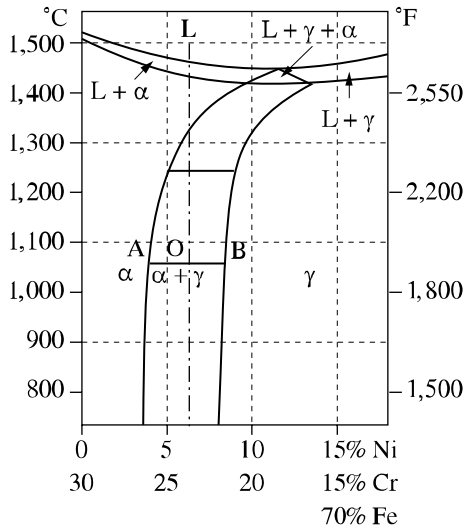
Figure 12.19. *Phase diagram*

In a weld (the HAZ and MZ are homogenous), rapid cooling speeds prevent the balance being reached and the content of ferrite increases with the cooling speed. This effect is less marked when the nitrogen content increases and in particular for the super-duplex grade where $N = 0.25\%$. As the weld properties are dependent on the δ/γ phase ratio, it is important to be able to predict this ratio. Among the diagrams available, the Schaeffler-Espy diagram seems the most suitable. However, more precise formulae do exist, based on the composition of the weld and taking the cooling speed into account.

To reduce the ferrite content, in particular in the HAZ and MZ without filler where the composition cannot be adjusted, it is necessary to use high welding energies, and possibly to pre-heat the products to be welded and limit the cooling speed.

For this, it is necessary to take account of the degree of sensitivity of the grade to structural changes of the ferrite which can occur in two temperature ranges centered at approximately 800°C (in particular formation of the σ phase) and 475°C (precipitation of the α' – Cr and possibly ε – Cu phase). On the one hand, this will limit the cooling speed (high temperature field) and on the other hand, the reheating temperature (low temperature field).

12.8.5. *Filler products*

In the case of welding with filler, it must be adapted to achieve on the one hand an ideal dual phase structure in the as welded state and on the other hand to obtain a weld corrosion resistance comparable with that of the forged product. The first aim is achieved by increasing the nickel content of the filler and thereby intensifying the concentration of gamma gene in the melted zone. Ni is preferred to N, which reduces impact strength at low temperature. However, during welding, part of the nitrogen tends to evaporate, which produces a more alpha gene composition with less corrosion resistance (PREN). To combat this effect in gas shielded welding, a gas containing 2 to 3% nitrogen must be used, as this element will be partly transferred in the added metal.

In multipass welding, the amount of ferrite in the reaffected passes can then be considerably lower than 50%, reheating producing a significant amount of secondary austenite, which can be less corrosion resistant than primary austenite. However, this effect is largely minimized by the increase in nitrogen content.

The corrosion resistance of the welded joint is lower than that of the base metal with the same composition. As these steels are especially used for their very good compromise between mechanical resistance and corrosion resistance in severely corrosive media, it is important that the weld is not a weak point. This condition being met, it is then possible to adapt the composition of the filler equivalent to the grade to be welded by slightly increasing Cr and Mo, which, given the discussion above, leads to an optimal added metal deposit. For the most corrosive environments, it is preferable to "over" alloy the weld, either by using a more alloyed austeno-ferritic grade filler, or by using a Ni based filler with a high content of Cr and Mo to weld super-duplex steels.

12.8.6. *Shielding gases*

The wire/flux or wire/gas combinations proposed by product manufacturers cannot be dissociated without risking serious problems for the weld properties, while the coated electrodes and welding fluxes will be carefully baked according to manufacturers' instructions.

Gas protection is very important in plasma, TIG, MIG or pulsed MIG welding of duplex or super-duplex steels. As well as protecting the molten metal from oxidation, the welding gas must also avoid any nitrogen loss from the molten metal.

Many gas combinations are now available, including binary gases $Ar + N_2$ for TIG or plasma welding, and ternary $Ar + CO_2 + N_2$ or quaternary $Ar + CO_2 + He + N_2$ for MIG and pulsed MIG welding.

Welding gases with the addition of hydrogen are not authorized for the welding of austeno-ferritic steel.

12.9. Heterogenous welding

12.9.1. *Reminder of definitions*

A welding is known as *homogenous* when the two basic materials and the filler are of a comparable composition. For example: MIG welding of two steels AISI 316 L (EN 1.4404) with a filler 316 LSi (EN 12.072 – 19.12.3 L).

A welding is known as *autogenous* when two base materials of the same composition are assembled without a filler product. For example: resistance welding of two stainless steels AISI 304 (EN 1.4301).

A welding is known as *heterogenous* when at least one of the three materials (base or filler) is different from the others. For example: a MIG welding between a metal AISI 409 (EN 1.4512) and a metal AISI 304 (EN 1.4301) with a filler ER 308 LSi (EN 12.072 – 19.9 L).

12.9.2. *Treatment and forecast of heterogenous welds*

This treatment is carried out thanks to the use of constitution diagrams.

The mechanism is simple and is represented in Figure 12.20.

Y-axis label: $Ni_{eq} = Ni + 30\,C + X^{(1)}(N-0.045) + 0.87^{(2)} + 0.33\,Cu$

Figure labels: Austenite; A + M; Martensite; without ferrite; 5 % ferrite; 10 % ferrite; 20 % ferrite; 40 % ferrite; 80 % ferrite; 100 % ferrite; A + F; MIG welding with filler metal; Welding without filler metal; M; A + M + F; M + F; F + M; Ferrite; X; Y; Z

X-axis label: $Cr_{eq} = Cr + Mo + 1.5\,Si + 0.5\,Nb + 5\,V + 3\,Al$
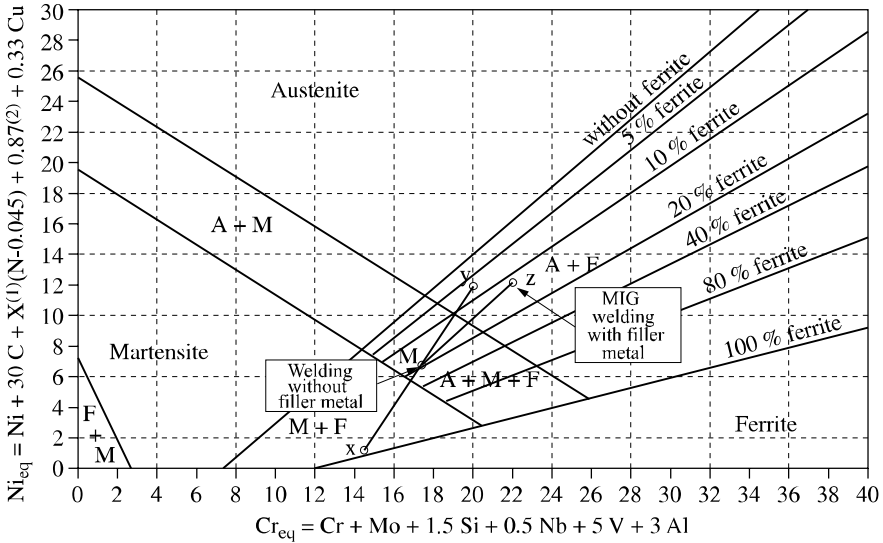
1) X = 30 if N = 0/0.2; X = 22 if N = 0.21/0.25; X = 20 if N = 0.26/0.35
2) Constant for Mn between 0 and 10%

Figure 12.20. *Espy diagram*

If two materials X and Y are welded without filler, the respective analyses of the materials make it possible to locate their representative points on the diagram. The representative point of the molten metal is located at the barycenter of the two items X and Y, namely the middle of line XY if the two materials are molten in equal quantities (point M).

If two materials X and Y are welded with a MIG process and filler Z, the analyses make it possible to locate items X, Y and Z on the diagram, the point representative of the mixture XY is as previously (point M), the representative point of mixture XYZ is at the barycenter of the points M and Z, taking account of 25% dilution in this example (point B).

It would be possible to carry out the calculation using the weighted content of each element in the molten metal, but that is generally longer and moreover less visible.

The addition of Bystram diagrams makes it possible, by positioning the representative point of the melted zone, to forecast if a welding without filler is possible, risky or unadvisable; if a filler is necessary; and, in this case, which filler is best adapted to obtaining a risk free melted zone.

12.10. Finishing of welds

Finishing concerns the cleaning of beads after the welding operation. Indeed, the corrosion resistance of stainless steel welded joints can be strongly affected by their surface quality. In all cases, this cleaning will be all the easier the better the protection in the course of welding (protection on both sides, use of a sufficiently long training shields, etc.). Cleaning of welded stainless steels joints can be carried out by various processes (as described in the procedure EN 1011-3: 1997 classification index 89-101-3), employed singly or in combination.

For brushing, special brushes made of stainless steel wire or another compatible material are recommended. In general, this technique is not appropriate for eliminating very adherent impurities. It is recommended that special attention is given to the use of rotary brushes because these are likely to deform the surface and to cause microcrevasses which will reduce corrosion resistance. It is sometimes necessary to follow brushing with a chemical cleaning.

Shot-blasting or sand-blasting products must be free from pollution by iron or non-alloyed steel. This technique is used to eliminate the adherent impurities and also to create residual compression stresses on the surface of the parts. Among the products recommended for shot-blasting are glass and stainless steel.

For grinding, it is recommended we use special disks, bands or grinding stones, free from iron. It is advisable to avoid excessive grinding, which damages the surface and thins the base metal. This technique is also used to eliminate the vast majority surface pollutants and to obtain a regular transition between the welding and the base metal. A light chemical clean can be carried out after grinding.

Scouring eliminates surface oxides or surface layers by chemical reaction. An acid medium is used, whose composition depends on the steel type, the temperature and the cleaning duration. It is necessary to carefully eliminate all the scouring products after the operation.

The weld cleaning operations quoted above, mechanical or chemical, not only removes oxides but also the passive layer of the stainless steel. To accelerate the reconstitution of the passive layer, it is recommended we carry out a passivation operation after chemical or mechanical cleaning.

In general, electrolytic polishing is applied to unstabilized steels in order to obtain a smooth surface, and thereby optimal corrosion resistance.

For optimal corrosion resistance, the most effective processes are chemical scouring and electrolytic polishing.

Lastly, and although it is not a question of a finishing operation *per se*, a decontamination operation is advisable, especially in workshops not solely dedicated to handling stainless steels. The purpose of this decontamination, similar to passivation in its process, is to avoid any traces of foreign matter, especially ferrous particles, from reaching the surface of the part.

12.11. Glossary

Austenitic stainless steel: stainless steel whose structure is austenitic in all temperature ranges. Austenitic stainless steels are of the iron-chromium-nickel type (molybdenum).

Austeno-ferritic stainless steel: stainless steel whose structure at room temperature is made up of approximately 50% austenite and 50% ferrite. Austeno-ferritic stainless steels are also called "duplex".

Ferritic stainless steel: stainless steel whose structure is mainly or only ferritic in all temperature ranges. Ferritic stainless steels are of the iron-chromium type (molybdenum).

Martensitic stainless steel: stainless steel with an austenitic structure at high temperature, liable to undergo phase transformations on cooling:

– austenite: martensite by hardening,

– austenite: ferrite + carbides by slow cooling.

Chromium equivalent Cr_q: calculated value in which all the alpha gene elements are translated in the form of chromium by the means of coefficients.

Scouring: scouring is a chemical surface treatment of steels which makes it possible to remove oxides which are formed on the metal surface.

Decontamination: chemical operation which dissolves non stainless metal particles, primarily ferrous, deposited on the metal's surface at the time of cold transformation or completion – finishing of the metal.

Dilution: quantity of base metal remelted at the time of a welding operation, brought back into the total volume of the molten pool.

Alpha gene element: element supporting the formation and stabilizing of the ferric structure. The principal alpha gene elements are Cr, Mo, Si, Al, Ti, Nb, V.

Gamma gene element: element supporting the formation and stabilizing of the austenitic structure. The principal gamma gene elements are Ni, C, N, Cu.

Nickel equivalent Ni_{eq}: calculated value in which all the gamma gene elements are translated in the form of nickel by the means of coefficients.

Passivation: chemical surface treatment of the metal which makes it possible to remove from it the polluting elements which could be deposited there and to accelerate the formation of the passive layer.

PREN: *pitting resistance equivalent number*, corrosion resistance index by puncture.

γ austenitic structure: austenite is a face-centered cubic structure which presents in the softened state the following properties:

  – soft but supremely work-hardenable,

  – very malleable and workable,

  – non-magnetic.

α ferritic structure: ferrite is a body-centered cubic structure which presents in the softened state the following properties:

  – soft but not very work-hardenable,

  – malleable and fairly workable,

  – magnetic.

α′ martensitic structure: martensite is a body-centered cubic structure deformed and hardened by the presence of elements in supersaturation. It presents the following properties:

  – hard and fragile,

  – not very malleable and unworkable,

  – magnetic.

HAZ: heat affected zone.

MZ: molten zone.

12.12. Bibliography

[CAS 68] CASTRO R., DE CADENET J.J., *Métallurgie du soudage des aciers inoxydables et résistant à chaud*, Dunod, Paris, 1968.

[COZ 98] COZAR R., MOIRON J.L., *Ecole Inox Ugine S.A.*, presentation 1998.

[MOI 96] MOIRON J.L., BONNEFOIS B., *Soudabilité des aciers inoxydables*, Institut de Soudure 1996.

[MOI 00] MOIRON J.L., BONNEFOIS D., CUNAT P.J., *Souder les aciers inoxydables*, OTUA 2000.

Chapter 13

Welding Aluminum Alloys

13.1. Metallurgy of welding

13.1.1. *Weldability of aluminum alloys (steels/aluminum comparison)*

The weldability of aluminum alloys is, unlike carbon steels, not linked, as with carbon steels, to the problem of transformation phases which, coupled with dissolved hydrogen and the mechanical constraints, can lead to weld brittleness. Their weldability criteria[1] depend, like austenitic stainless steels, on the susceptibility to hot cracking (solidification cracking). The compatibility of metals to be welded and the choice of the filler metal are also important points, because they can cause a lack of bead ductility.

Equally, hydrogen does not have the same effect on aluminum alloys as it does on carbon steels (cold cracking). With aluminum alloys, it causes gaseous porosities because of the great difference in solubility between the liquid and the solid (0.036 against 0.69 cm^3/100 g at a melting point of 660°C). This gas is eliminated in practice during the production of semi-finished products but it is sometimes present in castings. It can be produced during welding (see section 13.3.1).

Chapter written by Michel COURBIÈRE.
1 The classification of weldable alloys [FD 96] and their metallurgy concern conventional arc welding processes.

a)   b)
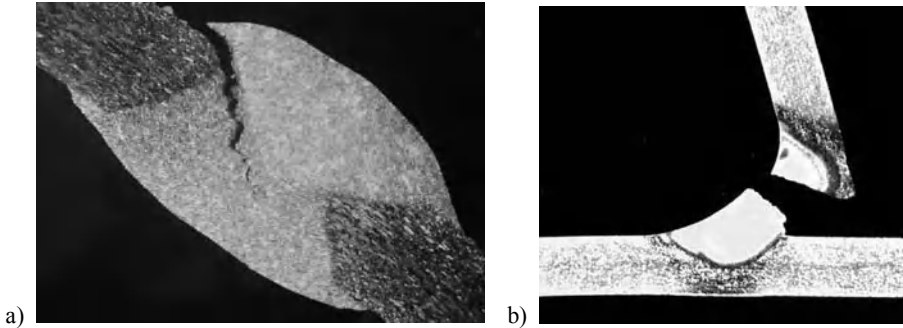
Figure 13.1. *a) Hot cracking: 2024 filler 5356 (TIG);*
b) brittleness of the molten zone: 5083 filler 4043A (TIG)

Pressure die cast components are not weldable because the gas dissolved during their manufacture is expelled during welding.

In practice, the calculation codes and the standards recommend the properties of use and, in particular, draw up the list of alloys that are weldable or non-weldable by arc processes, which does not necessarily mean they perform in the same way with different techniques (resistance, electron beam welding, etc.).

Generally the metallurgical state does not affect the weldability of aluminum alloys. Thus, it is possible to weld an alloy whatever the work hardened state (H1x and H2x) or the thermal state. On the other hand, the assembly properties depend on the welded metal and this state. Indeed, with aluminum alloys, the heating of the material by the arc or the molten metal leads most of the time to a softening of the base metal (see section 13.6), unlike carbon steels which it tends to harden. This heat affected zone (HAZ) is not visible by macroscopic or microscopic observation; its extent depends on the welding process.

Work hardened alloys (the 1000, 3000, 5000 series) in the H states (wrought and restored) lose their properties by excessive heating of the metal, which entails a partial recrystallization of the HAZ, except for the O states (annealed) and H111 which corresponds to an annealed state subjected to subsequent planishing. The strength of the joint is equal to that of the base metal, in an annealed state, whatever the original state: annealed or work-hardened (see section 13.5.1).
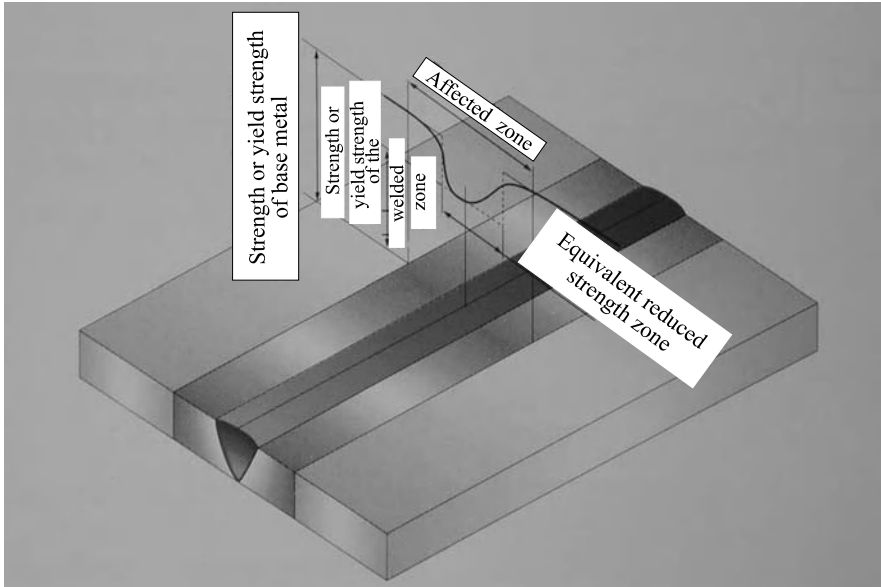
Figure 13.2. *Changes in mechanical characteristics in the HAZ*

Structural hardened alloys (the 6000, 40000 series) generally used either in a quenched and artificially aged state (T5, T6) or more rarely in a quenched and naturally aged state (T1, T4), undergo a complex treatment. The joint strength is equal to an intermediate value between that of the thermally treated base metal and that of quenched, naturally aged, metal. Cast and thermally treatable Al-Si-Mg alloys such as 42100 (Al-Si7Mg03) in the T6 state follow the same rules. Weldable 7000 alloys delivered in the T4 state have the effect of regaining their original properties after a maturation period lasting several weeks after welding.

The loss of mechanical properties following welding is irremediable with work-hardened alloys but the softened zone can be partly regenerated with heat treatable alloys[2]. If the complete heat treatment (setting in solution, quenching and tempering) is not possible on large deformable structures, a post-welding tempering treatment is sometimes feasible. It is very interesting when welding is practiced between the quench and temper with 6000, 7000 alloys and on 40000 castings. In the case of a post-weld process, care must be taken to use a filler susceptible to hardening (see section 13.2.2).

---

2 The problem is economic but especially due to the size of structures which for the most part renders the operation impossible.

Unlike carbon steels (but like certain stainless steels), all aluminum alloys, but more particularly alloys of the 6000 and 7000 families, are sensitive to welding energy. This must be reduced as far as possible in order to minimize the remelting of the intergranular phases (over burn phenomenon). This phenomenon, called *liquation* and associated with shrinkage stresses, can generate microscopic cracks in the HAZ. To a lesser extent, welding with a controlled energy reduces recrystallization of 1000, 3000 and 5000 alloys. An excessive arc height encourages these defects and impairs the mechanical properties of the weld.

In terms of welding temperature (temperature between passes, pre-heating), we will endeavor not to exceed 80°C for heat treatable alloys and 120°C for wrought alloys. Stress relief processes using heating are seldom used with aluminum alloys because it is necessary to reach temperatures and times corresponding to the softening of the majority of the alloys (250°C for 12 hours). In certain cases, temperatures ranging between 100 and 200°C affect their properties during use (mechanical characteristics of the 6000 and 7000 types, and corrosion performance of the 5000 types, etc.).

13.1.2. *Filler metals*

Although the majority of alloys are weldable without a filler metal, it is practically always required to have a sufficient welded section, to be able to fill the shrinkages, sags and gaps and to prevent hot cracking.

Additionally, the filler wire forms an integral part of the process of MIG welding.

Generally, the welding of all aluminum alloys is possible with an Al-Si filler and particularly 4043A. Indeed, as the maximum sensitivity to hot cracking ranges between 0.5 and 1% of silicon, the risks are avoided by dilution ratios[3], usually obtained in welding.

This advantage is coupled with low solidification shrinkage, which limits the stresses in the bead and reduces deformations. However, if it serves as an "all purpose" alloy, it does not constitute the best choice in the following cases:

---

3 The dilution ratio is defined as the volume of filler metal deposited over the total volume of the MZ (melting zone).

– with 1000 series alloys for which good corrosion resistance or an optimal electric conductibility is required and thus demands a filler of comparable nature (in decreasing order of purity: 1080A, 1050A, 1100);

– for the welding of 5000 alloys with more than 2% magnesium, where magnesium alloys are exclusively used[4] (in ascending % order Mg 5154, 5554, 5754, 5654, 5087, 5183, 5356, 5056, 5556A);

– with 6000 and 7000 alloys when a good static strength is required, especially when the molten zone and not the HAZ (see section 13.5.1) is the weak link, the use of 5356 or 5183 is preferred;

– when a uniform color is required, after anodization, between bead and base metal, a composite filler is employed when possible (1000, 3000, 5000).

Lastly, some wires are imposed by certified organizations for specific applications (5183 for the welding of marine plate alloy 5083 for example).

4043A, even those higher silicon loaded alloys (4045, 4047A), are the basic fillers for the welding and the repair of castings.

Other filler grades are used in very specific operations:

– 3103 to obtain a uniform color during the anodization of 3000 alloys;

– silicon alloys for recharging of castings of particular grades (4009, 4043A, 4045, 4047A, 4145);

– 2319 for the welding of 2000 weldable alloys in particular 2219;

– 4009 and 4145 for the welding of 2000 weldable ones and the recharging of the castings of the series 45xxx and 46xxx;

– 5180 with weldable 7000 alloys, in particular with 7020 in significant thicknesses, and/or if a post-treatment is carried out;

– 4010 and 4643 with the 6000 series and for castings of the 42xxx and 43xxx family in the case of a thermal post-treatment to increase mechanical properties.

The filler metal recommended to weld in TIG and MIG for the various alloy combinations is given in Table 13.1 [EN 99]. In each box, at the intersection of the lines and the columns corresponding to basic materials, the best filler metal is indicated. This is selected according to three criteria:

---

4 Magnesium filler products are divided into two categories: alloys with more than 3.5% Mg and those with less than 3.5% Mg.

Base metal A									
Al	4 1 4								
AlMn	4 or 5 1 4	3 or 4 3 4							
AlMg Mg <1.5% 1)	4 or 5 1 4	4 4 4	4 4 4						
AlMg 1.5≤Mg ≤3.5%	4 or 5 5 4) 4 or 5	5 5 4) or 3 4	5 5 4) 4	5 5 4) 5					
AlMg Mg >3.5% 2)	5 5 5	5 5 5	5 5 5	5 5 5	5 5 5				
AlMgSi 3)	4 or 5 5 4	4 or 5 5 4	4 or 5 5 4	5 5 4	5 5 4	5 or 4 5 4			
AlZnMg3)	5 5 5	5 5 5	5 5 5	5 5 5	5 5 5	5 5 5	5 5 5		
AlSiCu Cu ≤ 1% 5) 6)	4 4 4	4 4 4	4 4 4	4 4 4	4 4 4	4 4 4	4 4 4	4 4 4	
AlSiMg 5)	4 4 4	4 4 4	4 4 4	4 4 4	4 4 4	4 4 4	4 4 4	4 4 4	4 4 4

	Al	Al Mn	AlMg Mg$\leq$1.5%	AlMg 1.5$\leq$Mg $\leq$3.5%	AlMg Mg >3.5%	Al MgSi	AlZn Mg	AlSi Cu Cu $\leq$1%	AlSi Mg[5]	AlSi Cu[5][6]	AlCu[3]
AlSiCu [5][6]	4	4	4	4	4	4	4	4	4	4	
	4	4	4	4	4	4	4	4	4	4	
	4	4	4	4	4	4	4	4	4	4	
AlCu[3]						4	4	4	4	4	2
	NR	NR	NR	NR	NR	4	4	4	4	4	2
						4	4	4	4	4	4
Base metal B	Al	Al Mn	AlMg Mg$\leq$1.5%	AlMg 1.5$\leq$Mg $\leq$3.5%	AlMg Mg >3.5%	Al MgSi	AlZn Mg	AlSi Cu Cu $\leq$1%	AlSi Mg[5]	AlSi Cu[5][6]	AlCu[3]
CR TR 15608	21	22.1	22.2	22.3	22.4	23.1	23.2	24.1	24.2	25	26
EN573-3 & EN 1706	1000	3000	5000	5000 or 51000	5000 or 51000	6000	7000 or 70000	44000 or 47000	42000 or 43000 or 44000	45000 or 46000 or 48000	2000 or 20000

Note: when the base metal containing more than approximately 2% Mg is welded with a 4000 filler (or when the base metal containing more than 2% of silicon is welded with a 5000 filler), a sufficient quantity of Mg_2Si can be formed in the molten zone to weaken it. These combinations are not recommended in structures liable to shock or fatigue.

1) When they are welded autogenously (without filler or the same filler composition as the base metal), these alloys are sensitive to hot cracking. This problem can be avoided by increasing the magnesium content of the weld pool to 3% or by compressive fastening.
2) In certain conditions of use (employment at a temperature >65°C and in a corrosive environment), the alloys containing more than approximately 3% magnesium can be subjected to intergranular corrosion and/or to stress. Susceptibility increases with the percentage of Mg and/or work hardening. The dilution of the filler in the molten zone must take account of it.
3) These alloys should not be welded without filler because they are susceptible to hot cracking.
4) Intergranular corrosion and/or stress corrosion of wrought 5000 alloys can appear (use at a temperature >65°C and in a corrosive environment) when the magnesium content exceeds approximately 3%. In the case of use in such an environment, the Mg content of the molten zone should not exceed that of the base metal. It is preferable to use a filler of composition similar to that of the base metal.
5) The silicon composition of the filler must be as near as possible to that of the base material.
6) When these alloys are pressure die cast, they are not weldable because of the gas contained in the metal.

Table 13.1. *Compatibility of alloys and choice of filler metals*

– maximum mechanical properties of the molten zone (top line);

– corrosion strength (middle line). As for corrosion, the best color uniformity after anodization is obtained using the filler wire grade closest to the metal to be welded. When welding alloys of the 6000 series, 4xxx fillers, which give a dull gray color, should not be used;

– operational weldability (bottom line) including hot cracking and wetting. This property induces a bead shape favorable to fatigue strength.

The choice of metal is often a compromise between these considerations.

Welding generally does not pose corrosivity problems with a suitable filler[5]. However, the case of wrought weldable 7000 alloys must be noted, as they have a poor corrosion behavior in a quenched naturally hardened T4 state (exfoliant corrosion). The HAZ of these alloys (in the T6 and T4 state) must for that reason be protected. Post-tempering improves the problem appreciably.

13.2. Welding techniques

13.2.1. *Introduction*

Welding techniques for aluminum alloys are numerous, the majority derive more or less from those used with other metals, steels in particular (resistance welding, arc welding, etc.). However their physical, physico-chemical and mechanical properties have necessitated the adaptation of existing processes but also allowed the development of new welding techniques. Thus, the presence of a very stable oxide, high electric and thermal conductivity precluded welding using coated rods; the weak hot properties led to the development of friction stir welding (see section 13.2.5).

We will cite the most current techniques here, without going into detail about the principles but specifying the adaptations and the characteristics that aluminum alloys impose. The choice of technique depends on many criteria, such as the shape of the parts, the thickness of the products to be welded, the productivity aimed for, the level of weld quality, capital investment, the degree of automation, etc. It will be sufficient to give background information knowing that comparison is not always possible.

---

5 Aluminum alloys considered unweldable by the arc process generally do not have good corrosion resistance properties.

13.2.2. *Arc welding processes (TIG-MIG)*

Two processes of arc welding, TIG (*tungsten inert gas*) and MIG (*metal inert gas*), are employed with weldable aluminum alloys. They use a plasma to transfer the heat obtained by ionization of an inert gas (argon, helium or their mixtures) in the passage of an electric current between the part to be welded and an electrode, which can be refractory (TIG) or formed by the filler (MIG). The gas is also used to protect the fused metal against oxidation.

In theory, argon is used because it offers a better protection (higher density than air), although a plasma arc that is easier to generate (weaker ionization energy) and lower cost. Helium is generally used to obtain a greater penetration (better heat transfer) in MIG and continuous or pulsed TIG. The use of a mixture can also be useful but with a proportion of He at least equal to 50%. The addition of other gases (NR_2, O_2) has never revealed substantial advantages.

The selection criteria of the process is based mainly on the productivity (automation, welding speed), on the thickness of the products to be assembled and on the weld quality required.

The MIG process incorporating filler metal delivery, comprises only one torch and as a result of this is easily automated, and *a fortiori* capable of robotization. The TIG process, on the other hand, often remains a manual process, because automatically it is necessary to separately manage the supply of the wire in the weld pool, a delicate operation, especially at its outset. Consequently, such a process is not easily robotizable with filler. In manual TIG, the degree of intervention in the course of welding is total whereas in MIG all the adjustments must be made on test pieces.

The MIG process allows faster welding speeds than TIG (generally between 0.4 and 1.5 m/mn against 0.2 to 0.4 m/mn according to the thicknesses to be welded). From the perspective of its use, the TIG process requires, compared to MIG, more careful surface preparation (see section 13.2). On the other hand, it gives better bead quality. In MIG, this quality (penetration, bead form, etc.) is often dependent on edge preparation of the products to be welded.

It should be noted that MIG welding, a higher energy process than TIG, involves more localized heating, thus the deformations generated by welding are less. These two techniques make it possible to obtain welds of virtually identical mechanical characteristics. However, on structural hardening alloys, MIG produces welds that are tougher overall (see section 13.5).

Welding is always carried out by "pushing" the torch towards the unwelded zone; it is tilted at approximately 80° to the surface of the part, in the direction of displacement so as to achieve a better gas protection.

The welding is preferentially flat and in a half-risen position, although cornice and overhead welding do not present a particular problem. On the other hand, a descending welding position is to be avoided so as not to weld onto the molten metal bath (a common cause of lack of penetration).

With MIG, butt welding on a support slat is highly recommended to remove the risks of burning-through and to guarantee total penetration. The slats can be integrated to good effect right from the design stage of castings and profiles (see Figure 13.21). No protection on the reverse is necessary, unlike with stainless steels.

Care should be taken to ensure a good electrical contact of the earth clamp; the failure to do so being a common cause of bad starts to the welding or an impairment to arc stability due to the presence of alumina on the surface of the parts (see section 13.3.1).

13.2.2.1. *TIG alternating current*

The electric arc is formed between a tungsten refractory electrode and the part to be welded. Unlike with stainless steels, an alternating current is used. During the negative phase on the piece, there is a scouring of the alumina layer present on the aluminum surface and penetration during the positive phase at the electrode. For this reason the end of the electrode is rounded. The diameter of the electrode is in direct relationship to the welding current: 35 to 50 A/mm of thickness to be welded. Generally, a diameter equal to this thickness is recommended.

The sources are now of chopped type and make it possible to reduce the scouring effect by shifting the polarity towards the positive at the electrode. The filler is introduced into the molten metal weld pool in the form of a rod (manual welding) or wire (automatic welding). As the welding energy is independent of the filler, the process is very flexible; it makes it possible to weld manually with significant gaps (several times the thickness for products under 3 mm) and is well adapted to repair.

Generally, it is a manual process used frequently for the production of individual parts, and demanding great dexterity. It is used in all cases where high quality is required, in particular to carry out water-tight weld beads. The welding speed is controlled by the operator, who can control the energy and the filler quantity as he observes the molten weld pool.

The thickness of products to be welded ranges from some tenths of a mm and is in practice limited to 5 or 6 mm. Above this, there is difficulty in melting the metal,

while the distortions due to overheating become significant. For thick materials, a process with a DC (or pulsed) current is used but more usually the choice favors the MIG process.

13.2.2.2. *DC and pulsed current TIG*

The TIG process is also used with a smooth or pulsed DC current. The process uses helium exclusively as a protective gas, but activation of the arc is carried out using argon, which is more easily ionized. The current is direct, i.e. the electronic transfer, is made from the cathode (electrode) towards the part. In this case, there is no scouring phase applied to the oxide coating (nor of erosion of the electrode). On the other hand, the current is easily controllable, making it possible to weld products ranging from 0.01 mm to 10 mm in thickness. The refractory electrode is made of tungsten containing oxide particles (generally 2% ThO_2, but also 2% CeO_2 or 5% (ZrO_2) to maintain the grinding angle[6]. It is sharpened at an angle between 15° and 120° according to the thickness of the part to channel the electron emission. As the arc height is low (some tenths of a millimeter), this process is almost exclusively used for automatic welding. However, its use in the repair of thick parts (castings, molds for the plastics industry, etc.) should be noted.

An alternative process uses a pulsed current (frequency of a few Hz) which offers the advantage of better control of the heat transfer thus better control of penetration depths and bead width. This pulsed mode results in hot phases and cold phases, which generates a layered solidification that refines the structure and reduces the segregations.

13.2.2.3. *Metal inert gas*

MIG is a process derived from MAG (*metal active gas*) and applied to steels which use a filler wire (generally 1.2 but also 1.6 even 2.5 mm for thick products) as a consumable electrode and a neutral gas (generally argon) to form the plasma. The latter is maintained by controlling the arc height, which depends on the wire feed speed and the welding voltage. The electrical contact of the wire in the torch is ensured via a copper contact tube. The low rigidity of the filler wire necessitates the use of spools, with appropriate drive rollers which push the wire to the torch through a PTFE sheath and thus facilitate unwinding (there is a risk of seizing with a steel sheath). The torch can benefit from being equipped with a traction system (push-pull system) which allows better regulation of wire speed and arc height by also avoiding

---

6 Thorium is a slightly radioactive element, so it is important to take precautions when sharpening and storing electrodes.

the phenomenon of wire buckling on initiation. Its use is essential in robotized welding.

The process is less flexible than TIG because the welding energy is proportional to the quantity of wire applied. To optimize the bead, the welder can generally regulate three parameters:

– the wire speed, proportional to the welding current (and, indirectly, to the thickness of the products to be welded),

– the welding speed,

– the arc height, proportional to the welding voltage.

With aluminum alloys, the pulverization (*spray arc*) mode of metal deposit is maintained by a high arc voltage (the short-circuit or globular modes used with steel are not suitable). This problem has for a long time limited the minimum thicknesses for welding to 3-4 mm. A reduction in energy can be obtained by changing the arc mode (pulsed current) thus causing a regular detachment of the metal drops. The voltage and average current reduction makes it possible to weld thicknesses from 1.2 to 1.5 mm.

Certain so-called synergic welding equipment integrate, for each wire/gas combination (diameter, nature), presettings of the numerous parameters (high low currents and voltages, frequency, etc.). These synergic curves, a function of wire speed, are time-saving when setting up. Welding programs already used are stored in memory and this facilitates the manufacturing process (there is the possibility of working in program recall mode for robotized production).

From a practical perspective, it remains necessary to adjust the arc voltage[7], because depending on the products to be welded and of the position of welding, *inter alia*, penetration problems, porosities or lack of sidewall fusion can appear.

Such electronically regulated equipment also uses the programming of a welding cycle[8] (see Figure 13.3), which allows a pre-heating and thus avoids lack of penetration (lack of fusion) at the beginning of the bead as well as the appearance of a final crater (shrinkage pipe with risk of hot cracking) when the arc is extinguished. It should be noted that the displacement of the torch is carried out at the end of the pre-heating slope. Certain welding equipment also has a high current pulse (700 A) which optimizes initiation and thus avoids wire entanglement when beginning without an arc. The process is thus well suited to the production of small beads (<50 mm) and to robotized manufacture.

---

7 Some manufacturers also offer modifications to other parameters.

8 This cycle must be adjustable for each programme as it depends on the weld's environment.
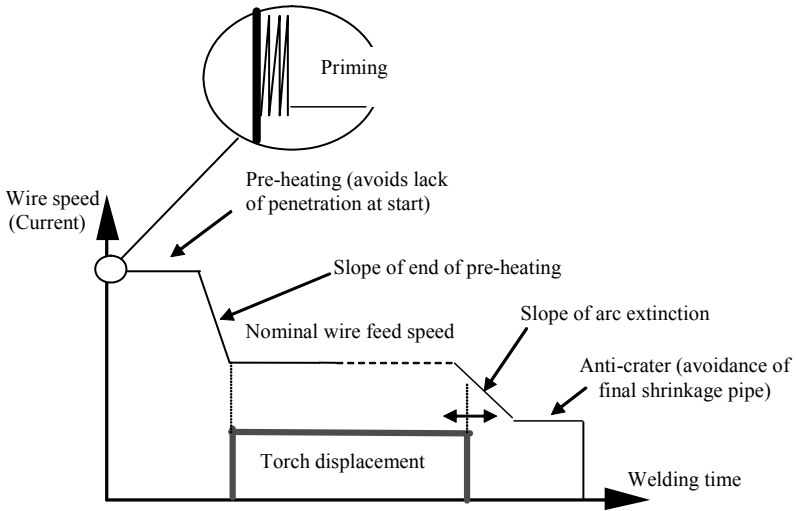
Figure 13.3. *Synergic MIG welding cycle*

The development of a twin wire technique should be noted, which allows an increase in the metal deposited but especially a considerable gain in welding speed (up to several m/mn).

Some manufacturers also offer equipment for robotized welding which optimizes the relation between power and metal deposited. The welding of thin materials (below 1.5 mm) becomes less sensitive to whether parts are in contact or there is a gap, if they are of dissimilar thicknesses, etc.

Problem	Cause	Remedies
Insufficient penetration	Insufficient welding energy	Increase the wire feed speed Carry out edge preparation on products >6 mm Use a gas other than argon[9]
	Inadequate preparation	Open the chamfer to decrease the heel on thick products
	Torch displacement too rapid	Decrease the welding speed[10]
	Excessive arc height	Decrease the welding voltage
Excessive penetration	Excessive energy	Decrease the wire feed speed
	Inadequate preparation	Optimize edge preparation on thick products
Excessive bead convexity	Excessive wire volume	If the penetration is correct, optimize the edge preparation of the products and consequently adapt the wire feed speed
	Torch displacement too slow	Increase the welding speed
	Excessive arc height	Decrease the arc voltage
Bead too wide	Torch displacement too slow	Increase the welding speed
	Excessive arc height	Decrease the arc voltage
Finely distributed porosity	Excessive arc height	Decrease the arc voltage

Table 13.2. *Summary of bead quality problems in MIG*

---

9 In the case of welding thick sheets (e >8 mm), penetration is improved by using helium or a He/Ar mixture (70/30) in place of pure helium.

10 Check that the wire does not strike the weld pool vertically, in which case it would be necessary to increase welding speed (never weld "on the weld pool").

13.2.3. *Electric resistance welding*

This is a technique derived from that used on steel but, because of the high electric and thermal conductivity of aluminum alloys, lower hardness and the sensitivity to hot cracking, the equipment has been significantly adapted.

The principal differences are the following:

– use of more powerful machines, in particular using tri-phase currents, even intermediate frequency, rectified for thicknesses >3 mm;

– use of large radius electrodes, typically 100 mm, to limit the hertzian pressure under the electrode;

– use of a welding cycle (current/pressure) adapted to remove projections and to reduce internal defects (cracks and porosities).
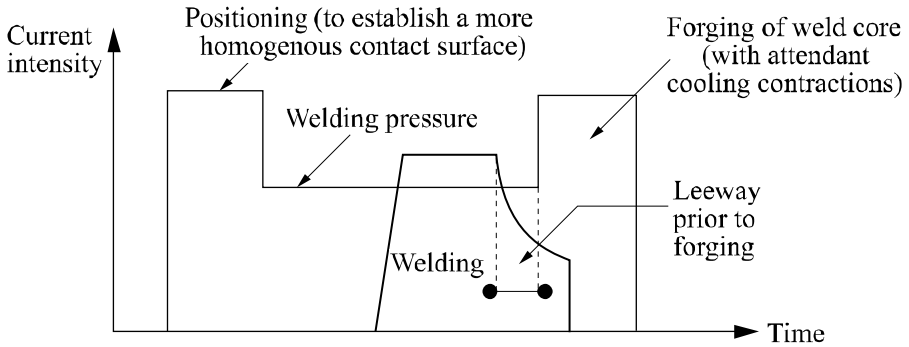
Figure 13.4. *Resistance welding cycle*

The thermal properties of aluminum alloys (see Table 13.3, section 13.4.1) necessitate very short welding times. For this, it is necessary to use high current intensities. In the same way, a highly resistant oxide coating must be obliterated by significant deformations. It should be noted that the high contact resistance is favorable to the formation of the molten zone (nugget) at the interface, thus facilitating the welding of thin products on thick products.
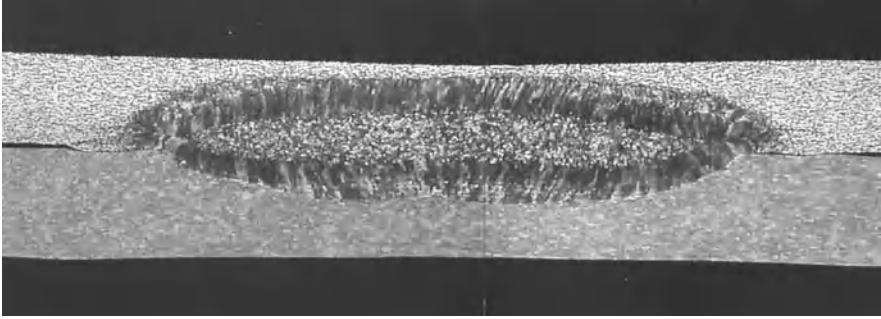
Figure 13.5. *Weld of 5182-O 1 mm thick
on 6016-T4 1.2 mm thick (automotive application)*[11]

The majority of alloys, those of the 2000 and 7000 families (2024, 7075, etc.), are weldable using this process because the compressive character eliminates any risk of hot cracking.

Continuous seam welding is not suitable for aluminum alloys because it induces too much deformation in the same way, while resistance butt welding is not used because of the very high currents necessary, thus flash welding is preferred.

13.2.4. *Flash welding*

Flash welding relies on the initiation, between two parts to be welded, of an electric arc which melts the materials superficially. It is followed by a forging operation which expels the molten metal and creates a very limited HAZ.

The process is generally used in discontinuous butt welding (connections in metal joinery, wheel rims, etc.) or uninterrupted in tube manufacture (welded tubes starting from a roll of sheet metal).

All the alloy families are weldable by this process, and in particular 7000 alloys (7075).

---

11 It should be noted that the MZ is offset towards the metal with the lowest thermal conductivity. This general welding phenomenon is also observed in other techniques (MIG, TIG).
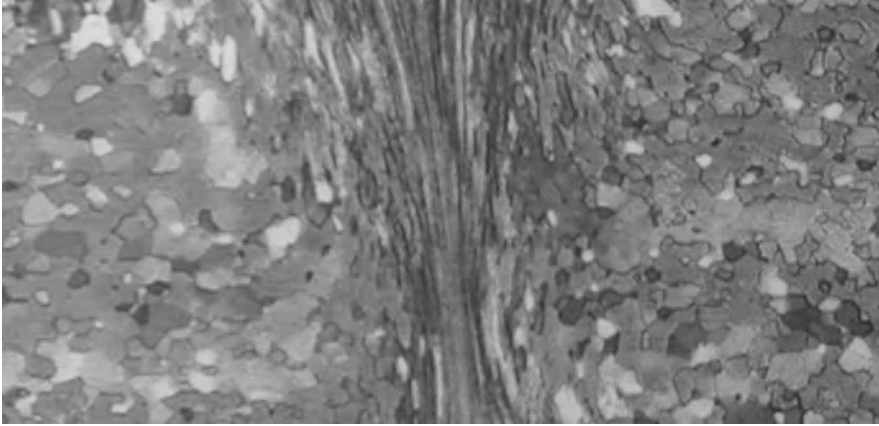
Figure 13.6. *A 6005A-T5 flash weld*

13.2.5. *Friction welding and friction stir welding*

The friction welding technique is limited by the need to put at least one of the parts to be assembled in rotation[12]. Its application remains marginal and is limited to cylindrical parts and mainly to aluminum/copper assemblies for electric connectors.

The process of friction stir welding (FSW in the literature) is recent and relies on welding without fusion, obtained by a strong shearing of the matter by means of a pin/rotating tool which mixes the metal of the materials to be assembled without melting them. The reduction of the material flow stress is achieved first of all by a heating of metal by friction with a plate on the surface of the metal before the displacement of the tool, which leads to gradual creation of the weld. The plate also makes it possible to contain metal and to maintain a pressure thus avoiding the ejection of metal away from the welded zone.

The process offers the following advantages:

– all alloys are weldable,

– no porosities, which means reduced surface preparation,

– no filler metal or shielding gas,

– no fumes or metal spatter and no UV emission,

---

12 The tests of so-called linear friction welding have not demonstrated the feasibility for welding aluminum alloys.

– reduced deformations compared to arc welding.

The process is mainly used with 6000 alloys (6060, 6082) because of high welding speeds, but also with the 2000 (2024, 2219, etc.) and 7000 series (7075, 7049, etc.), the majority of which are not weldable by the arc processes.
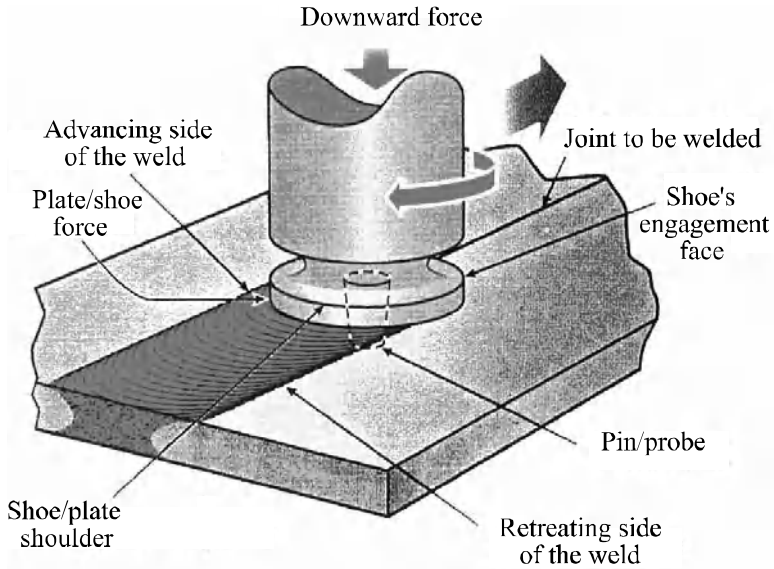
Figure 13.7. *General diagram of friction stir welding*
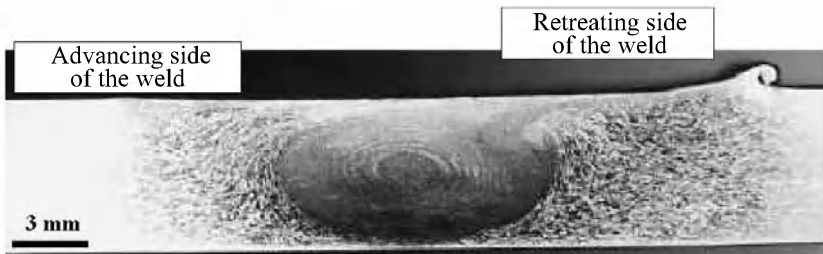
Figure 13.8. *Microstructure of a 2024 T3 weld*

13.2.6. *Electron beam welding*

Welding depends on the material fusion under the impact of an electron beam accelerated by a magnetic field and focused on the part in a vacuum chamber[13]. The process is very flexible, and enables the welding of parts a few hundredths of a mm to 250 mm (limit of the machines available on the market).

The power required depends on the thickness of the products to be welded; generally, it is considered that 1 kW is necessary to penetrate a thickness of 3 mm.

Practically all alloys are weldable (1050A, 5083, 7075, 2024, 6061, 42100, 48000, etc.). The problems of hot cracking are very much reduced if low welding speeds are used. However, these speeds are much higher than with traditional arc welding techniques, since 5 m/mn can easily be attained. The reduced sensitivity to hot cracking is also due to low heating of the products to be welded; this also results in reduced deformations which are limited to the shrinkage of the molten metal. Welding is carried out without a filler, but alloy foils can sometimes be used to mitigate cracking.

The HAZ is quasi-non-existent and the molten zone generally constitutes the weak point of the weld.

The favored method is butt configuration. Fusion is carried out gradually with a keyhole effect; the welding is generally carried out throughout the parts to avoid the defect of beam extinction (shrinkage pipe). The strong energy density often produces metal vaporization; also, certain elements with weak vapor tension have a lowered concentration in the molten zone. This is particularly true for zinc and magnesium.

The process offers useful advantages with hollow products such as tubular sections and hollow castings because welding can be completely carried out through the walls. The most appropriate configuration is butt welding; no chamfering or preparation needs to be made on the parts to be welded.

---

13 On steel, the process functions with a "partial vacuum" which cuts down on pumping time. It is not used on aluminum alloys due to their highly oxidizing characteristics. Some installations allow welding at atmospheric pressure provided the beam can be focused at a few mm from the gun.
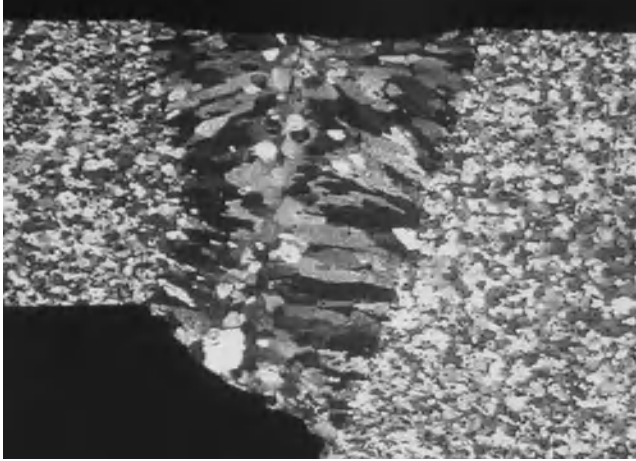
Figure 13.9. *A 2 mm thick 6061T6 electron beam weld*

On thin products it is also possible to carry out welding by transparency (lap weld).

It is imperative to have clean surfaces, chemically cleaned if possible, to prevent the appearance of porosities. Welding is usually carried out on machined parts in order to remove gaps as far as possible.

13.2.7. *Laser welding*

The fusion of metal is obtained by monochoromatic coherent radiation focused on the part to be welded so as to obtain a high energy density ranging between 10 and 100 kW/mm^2. Two types of laser sources are available:

– CO$_2$ gas laser (wavelength 10.6 μm) which enables the use of high power levels, but which permits beam transport solely by mirrors. The process is thus limited to plane welding (extremely difficult for robotization);

– solid YAG laser (wavelength 1.06 μm), which uses lower power levels (5 kw maximum), but which allows beam transport by fiber-optics and thus relatively easy robotization.

The strong reflection of this beam due to the brightness of the aluminum alloy surfaces prevents the absorption required to melt the parts to be welded. It is thus necessary to initiate metal vaporization to form the bead. The presence of elements with low vapor tension (magnesium in particular) thus makes it possible to weld with reduced energy levels. Power levels higher than 100 kW/mm^2 are of no use, as the metallic vapors form a plasma which blocks the laser, especially CO$_2$ sources.
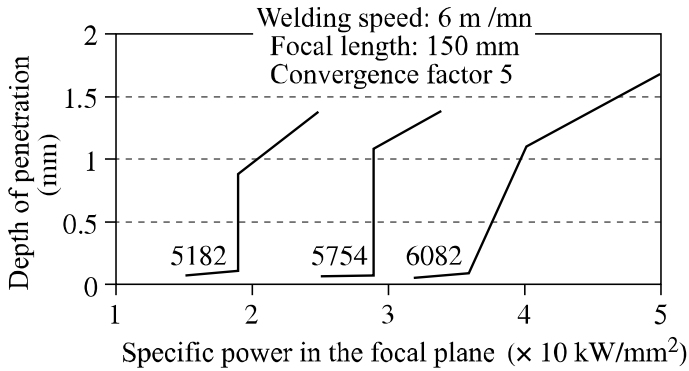
Figure 13.10. *Threshold of laser interaction with various aluminum alloys*

Laser welding, along with EB, is one of the rare techniques which allow continuous welding by transparency while working in keyhole mode. The resolution of this problem (due to the oxide coating which prevents interpenetration) allows the production of continuous welds which can sometimes replace spot fastened assemblies (resistance welding, riveting, clinching, etc.) but especially resistance seam welding, which is used infrequently because of deformations. However, bead section limits the weld's behavior when the thickness of the products to be welded exceeds 2 or 3 mm. As in arc welding, but to a lesser extent, laser welding may induce hot cracking, a problem which can be eliminated by using a filler metal.

The high energy density allows welding speeds of several m/mn (typically 5 m/mn to join 3 mm thick sheets).

The major disadvantage of the laser remains the capital cost and the thicknesses to be welded which remain low (lower than 5 mm).

13.2.8. *Other techniques*

Other, more marginal techniques can be used with aluminum alloys. Very often, these techniques have been developed to assemble very dissimilar materials and produce heterogenous assemblies.

Explosive welding makes it possible to plate sheets and thus achieve bimetallic combinations, often steel/aluminum, used in arc welding for mixed steel/aluminum structures (a naval construction application).

A technique derived from this is magnetic induction welding, where energy is delivered from an electromagnetic coil. It is especially used to carry out hafted joints (external or internal).

Ultrasonic welding makes it possible to weld small surfaces using a sonotrode. The principal application is the welding of thermocouples to measure the temperature on the surface of a part.

Further techniques include stud welding by condenser-discharge, etc.

13.3. Preparation and use of semi-finished aluminum welding products

13.3.1. *Particularities of aluminum alloy surfaces*

Aluminum alloys are naturally covered with a very stable oxide film, alumina, whose melting point exceeds that of aluminum (2,030°C). The thickness of this film depends on the manufacturing process of the semi-finished products; it is greater on foundry blanks and hot rolled sheets.

This oxide is susceptible to hydration during manufacture (hardening of 6000 alloys for example) or storage. The hydrates are of two types:

– those formed at high temperature, during hot rolling in particular; they are very stable and can only be eliminated by mechanical or chemical scouring;

– those formed at low temperature (T <90°C), during storage in particular, which are likely to be broken down by a simple heating.

All these hydrates can be to an extent magnesium enriched in the case of 5000 and 6000 alloys.

Finally, the product surfaces can contain grease, adsorbed or condensed water, which, like hydrates, break down under the electric arc (or simply by the heat of fused metal), to give hydrogen. This gas is harmful and generates porosities as soon as it is present in liquid aluminum, which is the case with fusion welding techniques.

The preparation and employment of semi-finished products require special attention to obtain good quality welds. It goes without saying these points could be specific to a technique, but the quality aimed for will always have to conform to the specification schedule requirements.

13.3.2. *Storage*

In spite of their good corrosion resistance, semi-finished products and aluminum alloy castings must be stored in a dry, ventilated environment because the protective oxide coating can deteriorate.
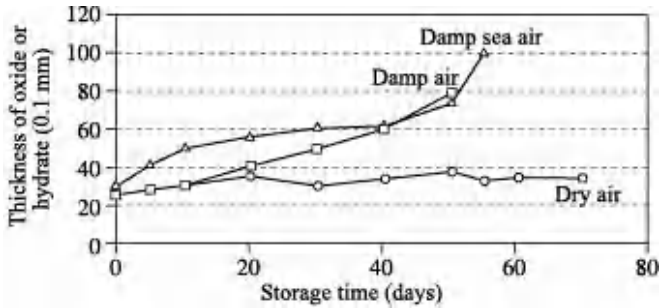
Figure 13.11. *Change in oxide layer thickness according to storage conditions*

To avoid condensation, care should be taken that there is no difference in temperature between the storage area and that of welding. It is advisable that the temperature of the products to be welded and the fillers is equal to or higher than that of the dewpoint.

The fillers must be stored in their original packing. Apart from periods of use, it is sensible to store them in heated dust-free cupboards (40°C).

For MIG stations, it is possible to install heated and/or spools with inert gas.

13.3.3. *Surface preparation*

These stages aim at helping weldability (TIG wettability, fume emissions) but also ensuring good internal bead health (porosities, oxide films). The basic operation is a degreasing with an unchlorinated solvent of the propylene glycol ester type, aliphatic hydrocarbons, hydrofluoroalcanes, etc.

This degreasing can be followed by scouring to obtain very a good bead quality with maximum compactness. Scouring can be carried out, either mechanically using a rotary brush with stainless steel wire or chemically (using soda, passivation with nitric acid and rinsing with water). In certain cases, degreasing and scouring can be carried out together using alkaline detergents or sulfochromic acid scouring agents.

Whereas degreasing is often essential, brushing can be omitted if the products are stored in dry environments and if a very high compactness is not required (class D of standard NF EN 10042). On the other hand, degreasing must always be carried out before brushing to avoid recontamination.

In the case of castings, a sand or shot-blasting is recommended to eliminate the refractory wash. Degreasing is not advised because the volatility of solvents is not always sufficient for them to be eliminated without heating, resulting in grease residues being trapped in surface porosities. Machining of castings should preferably be carried out dry.

In TIG, a degreased surface, a brushing or a chemical scouring of the oxide coating are obligatory to obtain a stable arc and a sufficient wetting of the molten metal. If a great compactness is required, scraping the products, including the filler rods, may be resorted to.

With MIG, for undemanding applications in terms of bead quality (blow holes), it is not necessary to carry out a brushing or a scouring if the semi-finished products were stored in a moisture free environment; a local degreasing is enough. On the other hand, if a low level of porosity is required, degreasing must be followed by a brushing.

In resistance welding, degreasing and scouring are optional if some porosities in the weld core are admissible.

In electron beam welding, degreasing is obligatory and scouring recommended.

For friction stir welding, degreasing is recommended.

13.3.4. *Cleaning of the weld beads*

In MIG welding, Al-Mg filler wires (5356, 5754, etc.) leave non-adherent black soot on the surface and bead edge. Welds carried out with Al-Si filler wires (4043A, 4047A, etc.) do not leave traces, except at the beginning of the bead, if they are carried out under good conditions (correct adjustment of the equipment, sufficient gas protection of weld pool). Soot can be eliminated by an alkaline washing under pressure. Scouring by immersion is not recommended for hollow products without an effective rinsing (risk of subsequent corrosion).

13.4. Deformations

13.4.1. *Introduction*

All fusion welding processes, and in particular arc welding, induce deformations and stresses in the welded parts. Deformation and stresses are closely linked, the elimination of the latter often resulting in distortion.

These phenomena, which relate to all materials, are amplified by the physical properties of aluminum alloys (see Table 13.3), mainly their high thermal conductibility which causes significant heating of the parts. This rise in generalized temperature, coupled with the high dilation coefficient of aluminum alloys, causes expansion which it is necessary to allow it to occur as freely as possible, to prevent the overheated parts being plasticized in compression, with residual deformation after cooling. Contrary to generally accepted beliefs, it is more often the heating, and not the shrinkage during bead solidification, which is the source of the problems encountered during the welding of aluminum alloys.

Properties	Al 1050A	S235 steel	Aluminum/ steel
Elasticity modulus (Young) (MPa)	70,000	210,000	0.33
Density (kg/m^3)	2,700	78,000	0.34
Melting point (°C)	658	1,535	
Mass heat capacity (J/kg°K)	897	420	2.1
Mass internal energy (kJ kg^{-1})	385	210	1.8
Thermal conductivity (W/m°K)	237	46	5.1
Coeff. linear expansion (10^{-6} K^{-1}) between 20 and 100°C	23	12	2

(*) The shrinkage depends on the nature of the filler. The filler metals of the 4000 family reduce it considerably, it is very low with 4047 (Al-Si12).

Table 13.3. *Comparison of the physical properties of aluminum and mild steel*

Maintaining parts in position, along with the sequences and the direction of bead execution, are major factors in the reduction of deformations. Deformation caused during heating by clamping used to reduce distortion can be distinguished from that due to the welding itself.

13.4.2. *Steel/aluminum comparison (deformation due to heating)*

In the case of welding clamped structures[14], the mechanism which causes the deformations of aluminum alloys is the same as that of steel alloys but the effects are very different. On a steel part, the total temperature reached remains significantly lower than 100°C; with aluminum alloys, it is often higher, hence a more significant dilation. No stress appears (see Figure 13.12) as long as the parts are free to dilate.
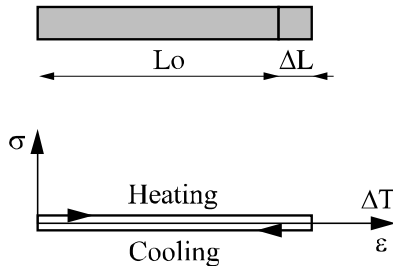
Figure 13.12. *Strain/stress diagram during the welding of unclamped structures*

On the assumption of welding a part 1 m in length, heating leads to a thermal expansion (1) $\Delta l = E.\alpha.\Delta T.l$ of 1.8 mm for an aluminum alloy such as 5083-O, compared to 0.2 mm for a steel of the S235 type, on the basis of the assumption that after welding the average temperature of the steel part is 40°C and 100°C for the aluminum part.

On the other hand, if the assembly is clamped, the part will be compressed in the assembly with an equal compressive stress (2) $\sigma = \varepsilon. E = \alpha.\Delta T. E$. This stress can reach such levels that the material's yield strength is exceeded, especially in the HAZ[15], giving rise to a reduction in the length of the part. It should be noted in addition that the yield strength drops under the influence of temperature more quickly with aluminum alloys than with steel (see Table 13.4).

---

14 In welding, the term clamping is taken to mean the prevention of expansion along its longest length.

15 The zone close to the bead (20 mm) reaches more than 300°C whatever the alloy.

Material	Rp$_{0.2}$ (MPa)			
	20°C	100°C	200°C	300°C
S235 steel	220	220	210	200
6061-T6	275	260	220	90
5083-O	145	145	140	50

Table 13.4. *Evolution of the yield strength of various materials according to temperature (duration <5 mn)*
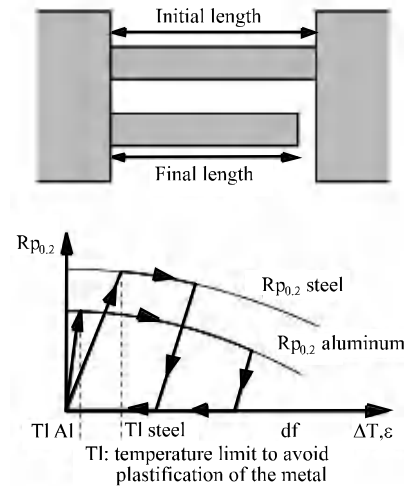
Figure 13.13. *Stain/stress diagram during the welding of clamped parts*

As a first approximation, according to formula (2) in the case of a mild steel with a yield strength of 220 MPa, the temperature limit for the metal not to be entirely plasticized is about 100°C, against 90°C for 5083-O. More significant stresses and deformations are inevitable with aluminum alloys compared to steels.

The total shrinkage after welding is translated in a simplified way either by considerable residual stresses in rigid structures or thick products, or by deformations in flexible structures (see Figure 13.14).
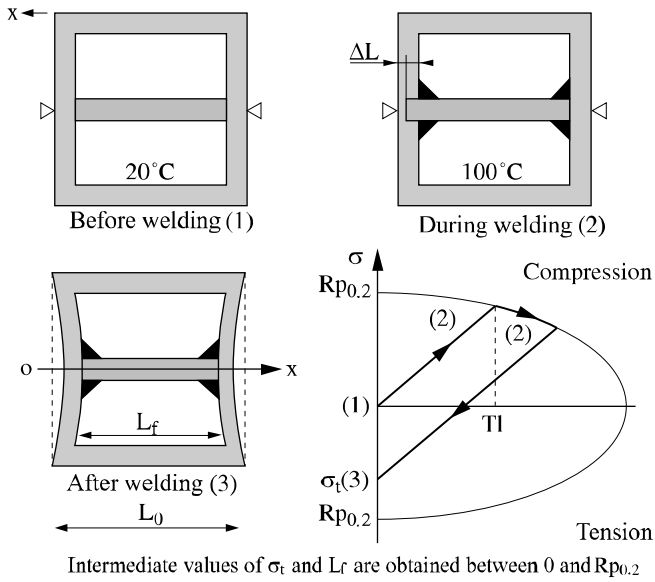
Figure 13.14. *Strain/stress diagram in the welding of flexible structures*

To eliminate these deformations or these internal stresses that affect all the parts, the adapted welding process imposes a specific positioning and an order of bead execution (see Figure 13.15). The overall level of the residual stress in the parts thus depends primarily on the edge positioning and clamping.
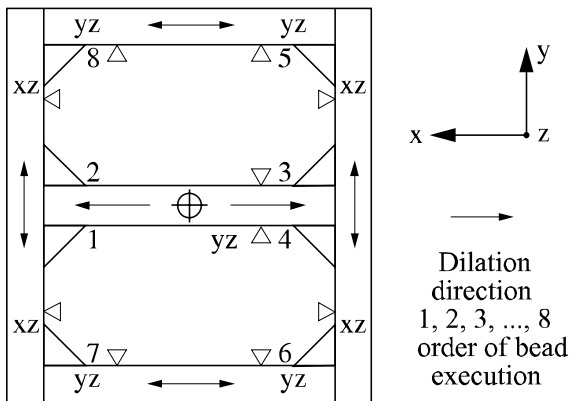
Figure 13.15. *Welding sequence for non-clamped structures*

Holding parts in position will always be achieved by clamping in a direction minimizing the dilation effect during the welding cycle; according to product thickness in the case of sheets, and in a direction parallel to the weld beads for profiles.

13.4.3. *Shrinkage*

The shrinkage phenomena, which accompanies the formation of a melted zone, are complex because they depend on the chemical composition of the weld pool, and the quantity of molten metal. It is reduced by employing fillers of the 4000 series (4043A and especially 4047A). This shrinkage is in fact the combination of two phenomena:

– a very localized heating of a compressed zone (as described in section 13.5.1), the liquid zone being free from any stress;

– the solidification of the molten zone, which is then subject to tension (with risk of hot cracking if the alloy is susceptible), and thus ends in generalized tensile forces being exerted on the bead zone.

We must keep in mind that a bead is always shorter than the parts at the outset. The deformations can sometimes be reduced by pre-deformations or a positioning that anticipates them. At this stage it is necessary to distinguish transverse bead shrinkage from longitudinal bead shrinkage.

In basic terms, transverse bead shrinkage can be estimated as varying between 0.3 and 1 mm according to the bead shape (fillet or butt weld) and according to its volume (a function of product thickness). In the case of deformable products, it is not uncommon that it results in angular deformations of the welded parts.

Longitudinal shrinkage, always self-restrained, is often transformed on thick products into internal stresses and it is difficult to eliminate it on thin and/or long products without pre-deformation of the parts to be welded (local lengthening of the zone to be welded).

The welding of discontinuous beads (short runs) is used to decrease the amplitude of the deformation from these shrinkages.

13.4.4. *Basic rules*

To minimize these deformations, there are two rules to respect:

– to allow dilation to take place readily by designing so-called *sliding* assemblies. These are very often in the form of lap welds in the dilation direction.

This type of assembly ensures the parts are held in position and also avoids welding with a gap between products, but it can have repercussions on mechanical strength, particularly on fatigue strength (lapped weld). We may also have recourse to free assemblies to accompany expansion of the component parts. The most exacerbated deformations are noted when fastening is carried out by compressive equipment, the screw clamp being the best example;

– to optimize the bead execution order to compensate for their shrinkage. Thus, the beads will be initially placed in the middle of the parts while moving towards the free edges to limit their self-restraint. In the case of discontinuous (short run) welds, the beads must begin from the middle of the parts to be welded and alternated in order (see Figure 13.16).
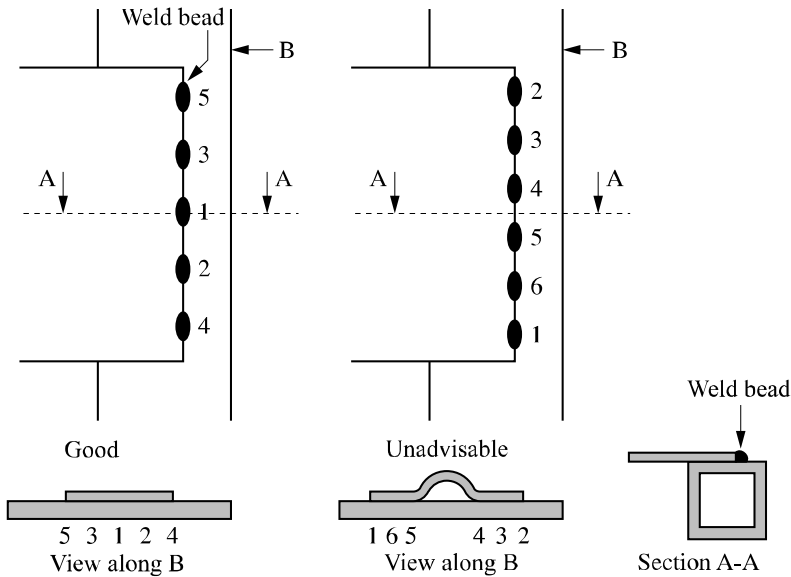
Figure 13.16. *Short run welding of a floor sheet on a rigid framework*

As mentioned, shrinkage during solidification can be more significant with aluminum alloys than with steels. This phenomenon can be all the more serious when the welding is performed with a gap. Although the new MIG equipment accommodates welding thin aluminum alloy products, this initial gap is canceled after the first few millimeters of welding under the cumulated effects of dilation and shrinkage. The butt welding of a bead with a gap will result in parasitic deformations or internal stresses.

In the same way, for a unit welded in a rigid assembly, the cumulative shrinkage effects can result in deformations accentuated by a local reduction in the flow stress in the HAZ during the welding of the last beads (see Figure 13.17). As far as possible, the positioning points will be placed at the maximum distance from the welded zones.

◁ Fixing positioners
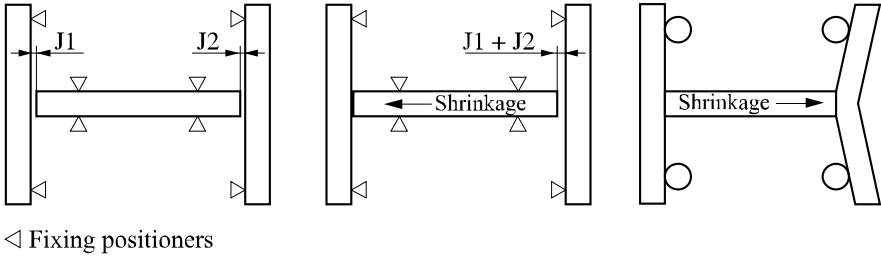
Figure 13.17. *Distribution of gaps and associated angular deformation*

The use of spring-loaded or retractable contacts is a means of avoiding these parasitic deformations. It is necessary to bear in mind that transverse bead shrinkage is invariably more significant at the end of a weld than at the beginning. This principle is applied in the example of Figure 13.18, knowing that the deformation of a bead is seldom compensated by a subsequent weld.
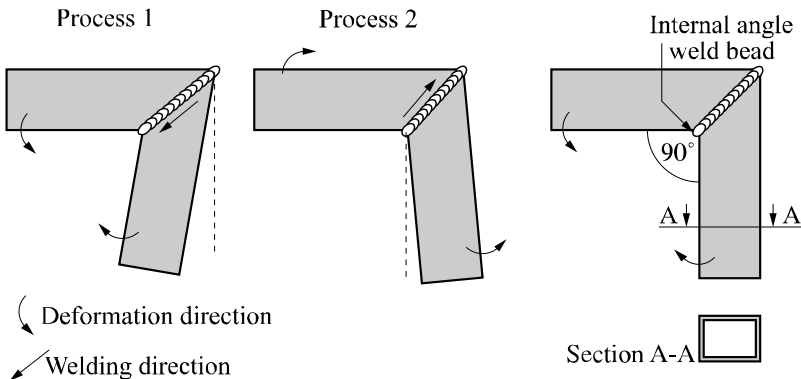
Figure 13.18. *Accentuation of the deformations at the end of the weld bead (the angular deformation could be compensated by a bead in the lower angle)*

It is important:

– to weld two parallel cords in the same direction to mitigate any warping,

– to weld towards the self restrained or low restrained zones, which are often the part edges, that is, the zones with little material and/or less rigid.

13.5. Dimensioning of the welded structures

13.5.1. *Static*

The presence of welds decreases the mechanical properties of aluminum alloys: it is necessary to take the dimensioning calculations of structures into account. We present below the broad outlines for checking calculations in Eurocode 9 [ENV 99a] for welds carried out by the traditional arc welding processes (TIG and MIG)[16].

Calculations of component strength must take into account the behavior of the zone close to the bead, as well as the HAZ and the molten zone (MZ) itself. Generally the calculation of the HAZ is enough, but checks must be made on both the zones for fillet welds of thick products in particular.

For dimensioning, it is accepted that material strength is reduced in the vicinity of the welds in a uniform way. This softening is expressed using a coefficient ρHAZ[17] which, multiplied by the allowable stress in tension (*fo* for tension, *fu* = *fo*/√3 for shearing), gives an operational limit value f_{ZAT} (MPa) that should not be exceeded in the HAZ.

The width of the HAZ depends on the thickness of the products, the geometric configuration, the temperature between passes as well as the welding process. With TIG or MIG processes, the half-width can thus vary between 20 and 40 mm.

Generally, it is considered that the HAZ extends to all thicknesses of the part to be welded.

---

16 With other welding processes, preliminary tests and measurements of microhardness can be referred to, in order to estimate the extent and the loss of mechanical characteristics in the HAZ.

17 This so-called metallurgical efficiency factor is referred to as β in the DTU aluminum or in the ECCS rules; this is not to be confused with the β of the formula of the same name.

Thickness of the products	Width of HAZ (mm)
0 <thick. ≤ 6 mm	20
6 ≤ thick. ≤ 12 mm	30
12 ≤ thick. ≤ 25 mm	35
thick. > 25	40

Table 13.5. *Width of the HAZ taken into account in calculations*

These values are generally lower than those of unassembled materials because of the presence of a softened HAZ or a molten zone which does not have the same metallurgical structure.

The softening factor ρ_{HAZ} depends on the initial state of the products and the process used. It is tabulated according to the alloy, its thermal state (H or T) and the welding process for 6000 alloys (TIG or MIG).

Family of alloys	Thermal state	ρHAZ(MIG)	ρHAZ(TIG)
1000	H14	0.6	0.6
3000	H14, H16, H18	0.6	0.6
5000	H22	0.86	0.86
	H24	0.8	0.8
6000	T4	1	
	T5	0.65	0.6
	T6	0.65	0.5
7000	T6	0.8 to 1	0.6 to 0.8

The value of 1 is taken with alloys in the state F, O or H111

Table 13.6. *Coefficient of ρHAZ modification; from [ENV 99b]*

Allowable stress value f_{MZ} (MPa)	Filler	Alloy							
		5052	5454	5083	6060	6005A	6061	6082	7020
	5356	170	220	240	160	180	190	210	260
	4043A				150	160	170	190	210

Table 13.7. *Allowable stress value in the molten zone f_{MZ} of some alloys; from [ENV 99b]*

The bead stress limit f_W depends on the metals to be assembled and the filler used (5356 and 4043A).

In the case of a heterogenous weld, the lowest stress limit is used.

The checking of the weld is carried out, by applying the traditional Von Mises criterion to the HAZ, thereby taking account of the reduction of allowable stress fHAZ in the HAZ and fMZ in the MZ.

In the case of fillet welds, the *Beta formula*, which is also applicable to steel, is used to take into account parallel and perpendicular shearing of the cord. With aluminum alloys, β is taken as equal to 1.

$$\sigma_c = \beta \sqrt{\sigma_\perp{}^2 + 3\left(\tau_\perp{}^2 + \tau_{//}{}^2\right)}$$

The normal stresses, parallel to the fillet weld beads, are not taken into account in the calculation of the beads.

Moreover, the stability conditions of the parts to buckling take into account the influence of the HAZ by means of an asymmetry coefficient s which is increased in the presence of welds.

The factors of welding dispersion and execution quality are taken into account by using a safety coefficient γ_{MS} which reduces the stress limit. For beads carried out with a normal welding quality, this coefficient has the value $\gamma_{MS} = 1.25$. For beads welded at a lower quality level, the value is $\gamma_{MS} = 1.60$.

In the case of a fillet weld or lapped joint, the dimensioning calculations of two particular cases that are frequently dealt with are presented below (see Figures 13.19 and 13.20).

$$a > 0.7 \frac{\sigma \cdot e}{fZF/\gamma MS} \text{ where } \sigma = \frac{F \cdot e}{1} \text{ with: } \begin{array}{l} F : \text{Force applied} \\ L : \text{Length welded} \\ e : \text{Thickness of the part} \end{array}$$
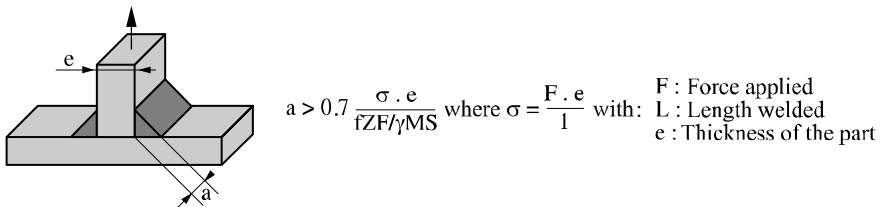
Figure 13.19. *Double fillet weld, subject to a load perpendicular to the welding axis*
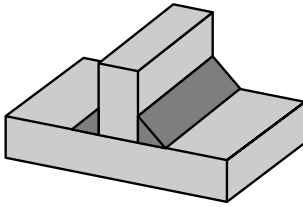
$$a > 0.85 \ \frac{\tau \cdot e}{fZF/\gamma MS} \ \text{where } \tau = \frac{F \cdot e}{1}$$

Figure 13.20. *Double fillet weld, subjected to a load parallel to the welding axis*

13.5.2. *Fatigue dimensioning*

The fatigue strength of welded structures is governed, as with steel, by the design (configuration of assembly); see Chapter 6.

The broad welding compatibility of alloys allows optimal use of profiles (mainly 6000) and castings (40000) jointly with flat products (5000). Spun and cast semi-finished aluminum products offer the advantage of being able to integrate, by their design, end to end configurations capable of improving performance. All these products have the same intrinsic fatigue characteristics once welded, the behavior being dependent on the local geometric stress level (hot spot) and secondly on bead quality [ENV 99b]. Often, the best performance is obtained by strong configurations which will, on the other hand, allow an average quality bead, but a good quality bead execution does not compensate for bad design. It should be noted that given that unacceptable defects are situated more at the beginning of the bead (risk of sticking, insufficient penetration), placing bead ends on free edges is often less harmful for fatigue behavior.

13.5.3. *Rules governing the optimal use of welded structures*

The first rule consists of placing the welds in zones subjected to little or no loads, the second of using butt welds in preference to fillet welds, because they offer better static and fatigue behavior. Moreover, in the case of butt welding of profiles or castings, it is judicious to place a weld pool support slat on castings or spun half-finished products, possibly including an edge preparation to guarantee consistent penetration (see Figure 6.21).

Certain measures concerning deformations during welding must be taken into account from the design stage. It is necessary to respect the compatible thicknesses between the parts to be assembled.

It should be noted that if a ratio of two is a sufficient safety factor in arc welding, significant variations can be tolerated in transparency welding (laser,

electron beam) or in resistance welding (weldability governed by the lowest value thickness). Provision should be made to minimize deformations during welding, by designing sliding joints for example.
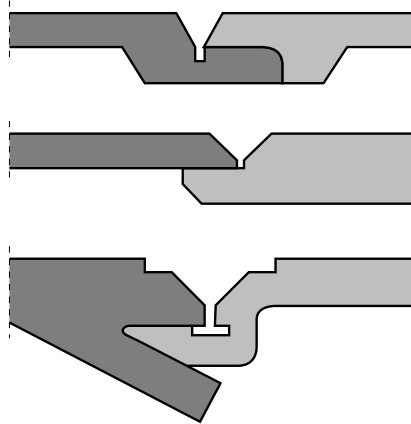
Figure 13.21. *Layout of edge preparations for profiles or castings*

13.6. Welding defects

We will mention here the defects most usually encountered during the welding of aluminum alloys, especially with arc welding techniques.

Static behavior is related to the effective bead cross-section whereas fatigue strength is highly dependent on the level of local stresses. As far as static performance is concerned, it is the defects affecting the effective cross-section of the bead which are more harmful. Thus, non-emergent porosities produced during arc welding have little influence on fatigue strength, but can quite seriously affect the static properties of the weld beads.

On thin products less than 2 mm, the risk of pipe shrinkage on the back of the bead can reduce this section, especially in fillet welds.

Misalignment defects and all leverage effects (weldings on only one side on hollow products) are very damaging compared to the intrinsic bead defects, in particular with regard to fatigue.

The most harmful bead defects are lack of penetration, because of the weakening of the section which this involves, and lack of fusion or sticking at the bead edges, which is often caused by too high an arc voltage, particularly with fillers of the 5000 family.

Joint angles and bead convexity must also be mentioned. They can be reduced by using edge preparations in the case of butt weldings[18]. Non-emergent gas porosities have little effect on the lifespan (see Figure 13.22).

Assembly in 5083 O subjected to undulating loading; $\Delta\sigma = 90$ MPa ; R = 0.1
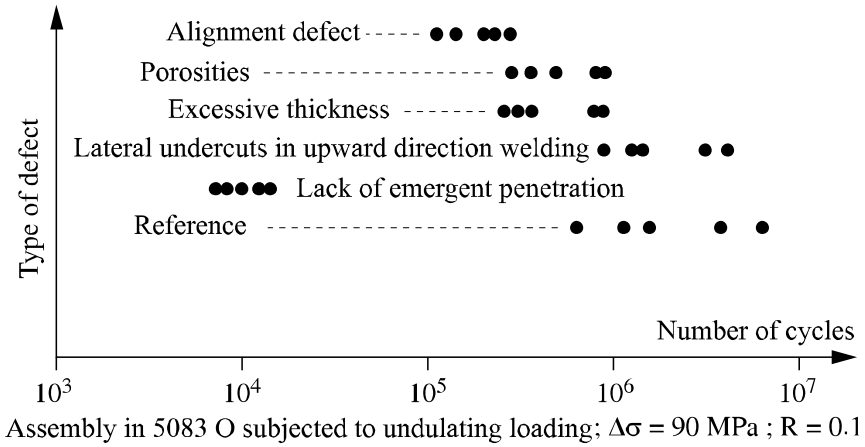
Figure 13.22. *Harmfulness of butt weld defects.*
Fatigue behavior on tensile specimens

In Table 13.8, the origin of the most current defects is shown with their IIW identification number, and in accordance with standard NF EN 26520.

---

18 It must be remembered that such preparations can be supplied directly and at no extra cost for spun or cast products.

IIW Nº	Defects	Probable origins
104	Fissure crater	Bead end with abrupt arc extinction
200	Blow holes	Presence of chemical compounds which are likely to break up on the surface (without forgetting the filler which can be dirty or badly levelled) Poor stabilization of the liquid bath Metal "gassed" (castings particularly) Excessive arc height (arc processes)
402	Lack of penetration	Insufficient wire speed, in particular at the beginning of the bead (lack of current on MIG start-up) Excessive welding speed (or welding on the weld pool) Incorrect chamfer preparation (too narrow, excessive heel) on thick products in MIG Excessive arc height
4011	Lack of fusion (sticking)	Excessive arc height Insufficient wire feed speed, in particular at the beginning of the bead (MIG) Component too cold (difference in thickness between materials to be welded)
506	Overflow	Solidification interval different between filler wire and base material (often encountered in TIG with 4000 filler metal) Excessive arc height
5013	Root undercuts or back shrinkage cavity (only on thin products thick. <2 mm)	Excessive welding energy Excessive gap between the parts Poor torch angle
509	Collapse	Excessive welding energy Torch speed too slow Poor torch angle

Table 13.8. *Principal defects*

13.7. Health and safety

The risks related to the welding of aluminum alloys are those generally encountered with other materials (dazzle in arc techniques, thermal burns, fumes and ozone emissions with arc welding processes, etc.). The physical and chemical properties specific to aluminum alloys must, however, be taken into account.

The great reflectivity of surfaces requires particular vigilance concerning dazzling, face protection (integral mask) and protection of all exposed skin parts is essential (in welding of tanks or enclosed vessels); protective filters of class 10 to 13 according to S 77-104 must be used (which are more opaque than when welding steel).

Aluminum alloys are good conductors of heat, so burn risks are increased (protective clothing essential).

The production of ozone is important in arc welding; it should be noted that the emission level is higher with a Al-Si filler (0.15 ppm on average) than with an Al-Mg filler (0.05 ppm on average). This value increases significantly above a welding voltage of 22 volts.

Certain alloys contain small quantities of beryllium (in particular 5000 alloys). Arc welding processes impose the use of fillers with low levels (lower than 0.0008%). Certain alloys are exceptions to this rule (4011). The user must specify this requirement when ordering half-finished products.

13.8. Bibliography

[EN 99] EN.1011-4, Soudage – Recommandations pour le soudage des métaux – Partie 4: Soudage à l'arc de l'aluminium et des alliages d'aluminium, 1999.

[ENV 99a] ENV1999-1, Eurocode 9 part 1: general rules, 1999.

[ENV 99b] ENV1999-2, Eurocode 9 part 2: fatigue, 1999.

[FD 96] FD.CR.12187, Lignes directrices pour un groupement des matériaux pour le soudage, 1996.

Chapter 14

Standardization: Organization and Quality Control in Welding

14.1. Introduction

The manufacture of assemblies or welded constructions has for many years been the object of statutory texts or standardization. The field of pressure vessels has been covered by a code for about 30 years, while the French standards of the P 22 series, relating to steel construction, were established from 1975 onwards. Similarly, assemblies fabricated by welding are dealt with in the five parts of the French standard NF E 83-100 "Construction of fabricated assemblies – welding processes" published at the end of the 1980s and revised in 1995.

Coming into effect in 1987, the European Directive "Simple pressure vessels", followed by the more recent "unfired pressure vessels", involved the drafting and adoption of standards developed by the Technical Committee CEN/TC 121 "Welding", standards which aimed to replace the existing national standardization corpora.

It is not an easy matter to analyze these European standards in so far as they are not completely stabilized and, for various reasons, are subject to revision which will result in a significant modification of their structure. However, the work is sufficiently advanced for general themes to be discussed and the main thread concerning their application to be explained.

Chapter written by Jean-Paul GOURMELON.

Three subjects are thus developed hereafter:

– standards for general organization of quality;

– standards for qualification of procedures or personnel;

– standards relating to non-destructive testing.

14.2. Standards of general organization of quality

14.2.1. *Presentation*

The general organization of quality requirements for welding was first of all the subject of the European standard NF EN 729 "Quality requirements for welding – fusion welding of metallic materials" in four parts, published in November 1994, as well as a technical report CEN (CR 13576) "Welding – application of the EN 729 quality requirements for the fusion welding of metallic materials" aiming to clarify its proscribed objectives and implementation methods.

This European standard was taken up at an international level under the reference ISO 3834 and its revision in order to ensure a perfect coherence with the new version of the ISO 9000 standards, carried out within the framework of the Vienna agreement, led in April 2006 to the publication of EN ISO 3834 "Quality requirements for fusion welding of metallic materials" in five parts:

– Part 1: Criteria for the selection of the appropriate level of quality requirements.

– Part 2: Comprehensive quality requirements.

– Part 3: Standard quality requirements.

– Part 4: Elementary quality requirements.

– Part 5: Documents with which it is necessary to conform with to meet the quality requirements of ISO 3834-2, ISO 3834-3 or ISO 3834-4.

These five parts were accompanied, as was the case for EN 729, by a technical report ISO/TR 3834-6 "Guidelines on implementing ISO 3834".

14.2.2. *Principles*

The key to interpreting this series of standards relating to quality in welding is found in the introduction of ISO 3834-1 "Criteria for the selection of the appropriate level of quality requirements" which specifies: "*The specification of quality requirements for welding processes is important because the quality of these processes cannot be readily verified. For this reason they are considered to be special processes as noted by ISO 9000: 2000. Quality cannot be inspected into a product, it has to be built-in. Even the most extensive and sophisticated non-destructive testing does not improve the quality of the product.*" This appears self-evident and does not only concern welding, but there are obvious points which it is a good idea to bear in mind sometimes.

On this basis, ISO 3834 covers, in Parts 2, 3 and 4 decreasing in strictness, the quality requirements applicable to welding, both in the workshop and on-site, Part 1 giving the elements of choice according to the contractual requirements using a brief comparison of the requirements. These indications are supplemented in the ISO 3834-6 technical report by Figure 14.1 which follows.

As Parts 3 and 4 only represent restrictions of Part 2, "Comprehensive requirements of quality", we will restrict ourselves to analyzing the latter by highlighting particular points.

14.2.3. *Analysis*

The clause giving an overview of ISO 3834 defines the objectives of the standard as follows:

– to be independent of the type of construction manufactured;

– to define welding quality requirements for welding in workshops and/or on-site;

– to provide guidance describing a manufacturer's capability to produce constructions to meet specified requirements;

– to provide a basis for assessing a manufacturer's welding capacity.

It is clearly seen that this standard can be used for several purposes. It can be used as a reference in a contract, but also as a tool for the organization of welding quality, as the synopsis of the clauses taken from the ISO 9000 requirements attests by applying them to the particular welding field:
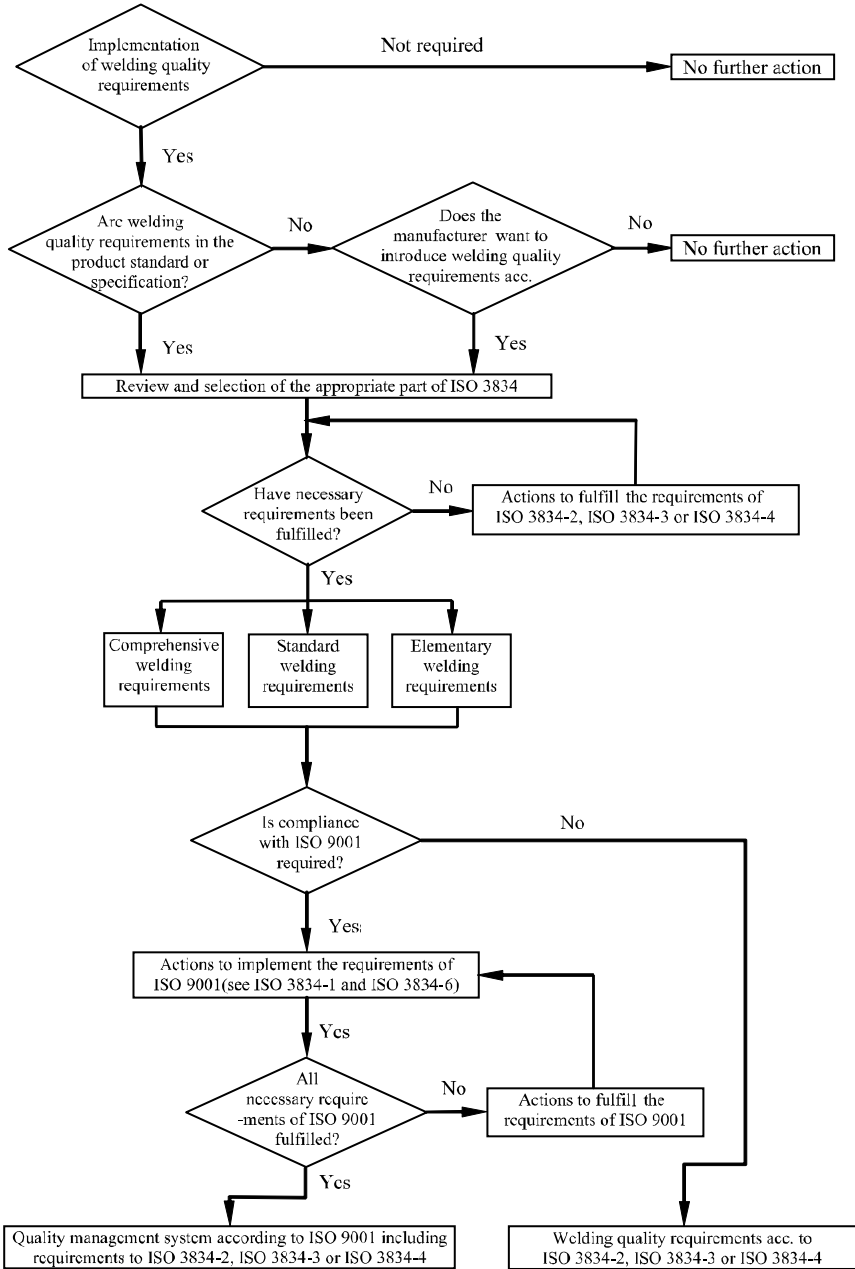
Figure 14.1. *Flow diagram for the choice of welding requirements*

– review of requirements and technical review,

– subcontracting,

– welding personnel,

– inspection and testing personnel,

– equipment,

– welding and related activities,

– welding consumables,

– storage of parent materials,

– post-weld heat treatment,

– inspection and testing,

– non-conformance and corrective actions,

– calibration and validation of measuring, inspection and testing equipment,

– identification and traceability,

– quality records.

Some of these clauses do not need to be commented on because they are traditional and only contain technical elements specifying the application modes of welding operations. Such are the demands relating to the review of requirements and technical review (review of contract), to subcontracting, to the equipment, to welding consumables, to the storage of parent materials, to post-welding heat treatment, to non-conformance and corrective actions, to calibration, to identification and traceability and to quality records.

In all these fields, welding is hardly distinguished from other industrial operations for which it is advisable to have sufficient documentation for the characteristics of equipment and materials, the provisions taken in the event of non-conformance, as well as all information relative to the traceability of the operations.

Three points, however, deserve a much closer examination. They concern the welding itself and related activities, the personnel in charge of welding, and finally inspection and testing and the inspection and tests themselves. Indeed, in these three fields the particular technical requirements concerned with the application of the general quality principles are supplemented by references to a whole body of

specific standards representing a more or less complex architecture, which it seems advisable to expand on in detail.

14.2.3.1. *Welding and related activities*

Welding and the activities linked with welding must, like all the other activities, have under the heading of quality organization, a program of production comprising a list of and identification of the operations to be undertaken, of the inspection and tests to be carried out as well as references to the applicable processes. This last point is of particular importance and is the object of a series of standards dealing with the specifications and qualifications of welding procedures which we shall come back to.

14.2.3.2. *Personnel in charge of welding and inspection*

The expression "personnel in charge of welding" traditionally applies to welders involved in manual welding and operators in automatic or semi-automatic processes. For each of these categories it is specified that they must be qualified by a suitable test defined in the series of the standards EN 287 concerning welders or of EN 1418 concerning operators. There is nothing new here except that only one qualification level is used compared to the three levels that appear in the former French standard NF A 88-110. One of the arguments put forward to justify this position was that the qualifying tests generally take place under optimal conditions, making it possible to obtain the best quality levels; furthermore, for the other levels, the need for a qualification remains an issue.

In addition to personnel categories defined above, clause 7.3 of ISO 3834-part 2 introduces the concept of "welding coordination personnel" defined according to three levels of technical knowledge in the ISO 14731 standard "Coordination in welding – tasks and responsibilities". This function has been developed in detail in the report referred to above (ISO/TR 3834-6) insofar as it is infinitely variable and can be undertaken by various people: welding engineer, welding technologist, production manager, foreman, etc. Before the transcription of EN 719 into the ISO standard, this concept met with a certain amount of difficulty because of the ambiguity of the standard which could imply that a certification by third party was necessary. This is incorrect and we refer readers to the above-mentioned report which contains all the explanations necessary.

It is altogether a different matter for personnel in charge of carrying out non-destructive testing for whom a certification complying with EN 473 "Qualification and certification of NDT personnel – general principles" is necessary. Let us recall that this certification comprises three levels and that it is awarded according to the examination technique employed: ultrasonic, radiographic, magnetic particles, or penetrant testing. The French certification organization is COFREND, the French confederation for non-destructive testing; bilateral agreements of mutual recognition already exist for such bodies and a European organization has been set up.

14.2.3.3. *Inspection, examinations and tests*

The requirements for quality relating to inspection, examinations and tests depend mostly on good operational welding practice. Before welding it is advisable to identify the products used, parent materials and welding consumables, to check the validity of the qualifications, joint preparations, etc. During welding, it is the welding parameters, the temperatures, etc., which are of most concern; after welding, dimensional checks and non-destructive testing should be carried out.

The series of standards concerning the latter is particularly important, while their structure has been the object of thorough reflection and deserves particular explanation.

14.3. Standards for welding procedure qualification

The standards for welding procedures qualification are among the oldest published by CEN/TC 121, particularly concerning manual arc welding of steels and aluminum alloys. Four parts inaugurated the series of the standards EN 288 "Specification and qualification of welding procedures for metallic materials":

– Part 1: General rules for fusion welding.

– Part 2: Welding procedure specification for arc welding.

– Part 3: Welding procedure tests for arc welding of steels.

– Part 4: Welding procedure tests for arc welding of aluminum and its alloys.

Their publication was not revolutionary compared to the practices of the time; thus Part 3 did not differ greatly from the French standard NF A 89-010 except in some particular points, for example, the definition of the validity fields or the methods for indentation rows. The general rule remained a choice between "no qualification" or "qualification by test".

Over the course of time and as the standardization works advanced, complementary parts describing new methods of qualification appeared: use of consumable products subjected to tests, reference to experience, reference to a standard welding procedure, execution of a particular welded joint prior to production, etc.; the general philosophy, based on an honourable intention, is of offering a range of possibilities enabling the choice of the most economical and technically suitable solution.

To this aspect of the problem, which can be considered surmountable, was added the question of extending standards to other welding processes (gas welding, electron beam welding, laser welding, resistance welding, etc.), as well as with other metals (steel or aluminum castings, nickel, titanium, zirconium, copper, etc.). The application of each one of these variables to the various possibilities offered by arc welding on steel or aluminum led, not only to EN 288 comprising some 50 parts, but also completely independent standards, which are diverse in number. Needless to say that the user would have been completely lost.

The search for a practical solution, combined with the fact that a revision made it possible to envisage the publication of these standards internationally, led to a complete recasting of the system, with a general structure, defined in Table 14.1. The main aim was to reduce the number of documents as far as possible by extending the common parts. To complement this, a technical report was drawn up establishing a metallic material grouping system usable for all welding operations; the practical aim has been to obtain validity fields common to all the qualifications, thereby avoiding the existing discrepancies, for example, between welders and welding procedures.

Process	Arc welding	Gas welding	Electron beam	Laser welding	Resistance welding	Stud welding	Friction welding
General rules	EN ISO 15607						
Grouping of materials	CR 15608					EN ISO 14555	EN ISO 15620
Welding Procedure Specification (WPS)	EN ISO 15609-1	EN ISO 15609-2	EN ISO 15609-3	EN ISO 15609-4	EN ISO 15609-5		
Tested welding consumables	EN ISO 15610						
Previous welding experience	EN ISO 15611						
Standard welding procedure	EN ISO 15612						
Pre-production welding test	EN ISO 15613						
Welding procedure test	EN ISO 15614 - 1: Steel/Nickel - 2: Al/Mg - 3: Cast steel - 4: Cast Al - 5: Ti/Zr - 6: Copper - 7: Overlay welding - 8: Tube to tube-plate joints - 9: Arc underwater hyperbaric wet welding - 10: Hyperbaric dry welding		EN ISO 15614 - 11 Electron and laser beam welding		EN ISO 15614 - 12 Resistance welding		

Table 14.1. *Organization of the standards relating to the qualification of welding procedures*

The analysis of the table above emphasizes the following data:

– general rules apply to all processes,

– only stud welding and friction welding do not conform to the general outline, and this takes their specificity into account,

– metallic material grouping systems are common to all the other processes (arc welding, gas welding, electron beam welding, laser welding, resistance welding),

– qualification methods for use of tested welding consumable; by reference to previous welding experience, by adoption of a standard welding procedure, by execution of a particular welded joint prior to production are also common to these same processes. This means that the same type of procedure can be applied,

– concerning the welding procedure test, regroupings were made comprising arc welding and gas welding on the one hand, and EB and laser welding on the other hand. This means that the same types of tests are used and interpreted according to the same methods,

– however, and this is quite normal, the requirements relating to the welding procedure specifications (WPS) are specific to each process.

Despite all these efforts at simplification, the end result still appears to be inaccessible and rather cumbersome to use. This need not be the case in practice, provided precise details are made available as to the potential application fields of the various qualification methods for welding procedures, as well as their limits.

Questions remain, in particular regarding qualifications for procedures based on tested welding consumables. These can be answered by making it clear that the methods of approval of welding consumables are now covered by the European standard EN 13479 "Welding consumables – general product standard for filler metals and fluxes for fusion welding of metallic materials" drawn up in accordance with the European "Construction Product Directive". In addition, these methods can be agreed between the customer and the supplier.
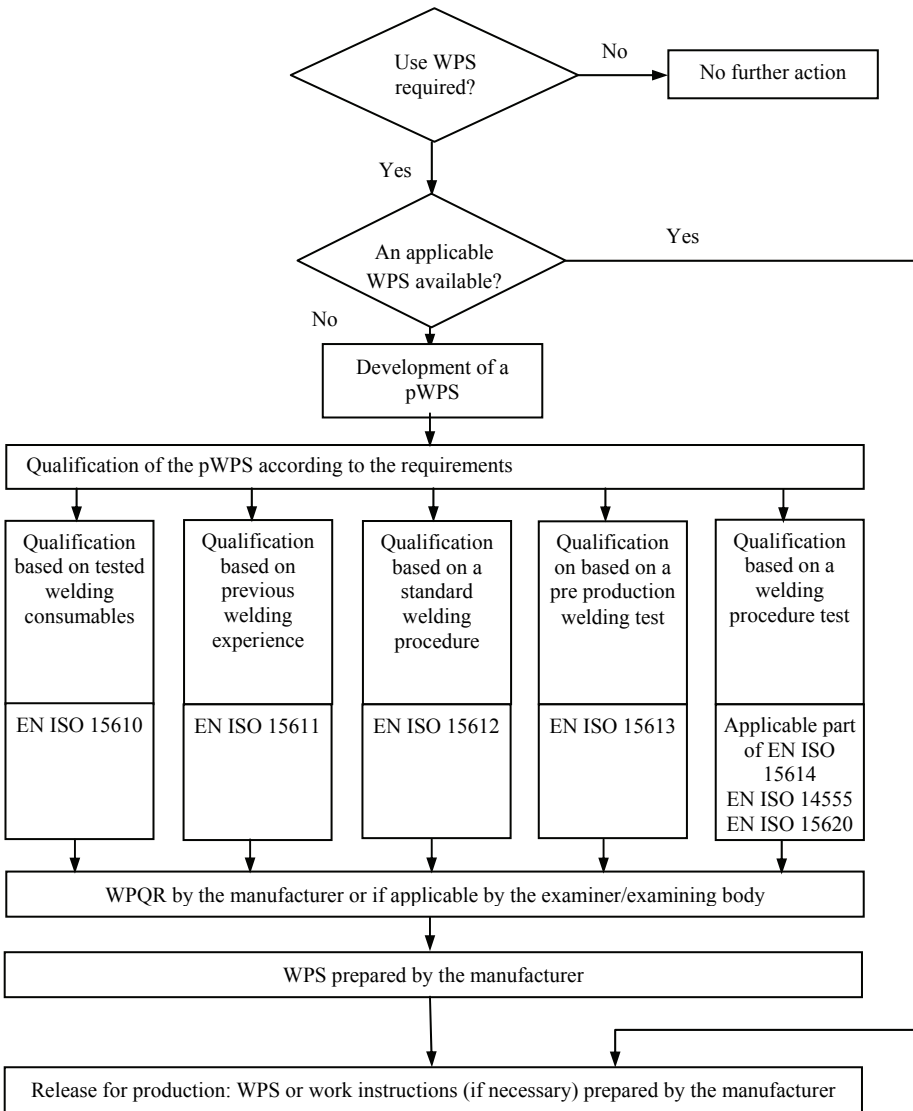
Figure 14.2. *Flow diagram of the process of qualification*
of a welding procedure

– *WPS: Welding procedure specification*

– *WP: Welding procedure*

– *pWPS: Preliminary welding procedure specification*

– *WPQR: Welding procedure qualification record*

It will undoubtedly take some time for each party – client and supplier – to fully take in the possibilities offered by the range of solutions suggested, the advantages afforded by this opening (which takes account of industrial practice), and then choose the most suitable solution from a full knowledge of the facts.

The standard EN ISO 15607 relating to the general rules contains appendices making the precise details necessary available. Equally it describes the course of the procedure, in particular using a diagram such as that in Figure 14.2, thus making it possible to pose the appropriate questions at the appropriate time.

14.4. Non-destructive testing standards

For non-destructive testing, which is the last aspect of quality assurance organization, even if it does not suffice to guarantee a determined level of quality, although this is nevertheless a determining factor for the acceptance of a welded structure or apparatus. Over the last few years it has also been the object of a significant amount of standardization work, the general concept of which has evolved considerably.

The standards relating to the quality requirements for fusion welding (EN ISO 3834 series) only make reference to the applicable EN or ISO standards. It is thus convenient to develop here the principles which governed their development.

Let us point out the current practice first of all. For steel construction, for example, French standard NF P 22-471 "Metal construction – execution of welded joints" describes and defines three classes of defects liable to be encountered in welds. In addition, it specifies the limits of non-destructive testing: up to 40 mm in depth for radiography, starting from 20 mm for ultrasonic. Finally, it presents for each method, in terms of indication levels, the permissible defects according to the degree of quality required.

This presentation offers an undeniable advantage, namely that it gathers in only one document all the information necessary for the user. It does have, on the other hand, some disadvantages:

– the classes of defects are likely to be defined in a different way according to the applications (steel construction, pressure vessels, etc.) whereas the manufacturing technique is similar,

– the operational limits of the various methods are fixed (unless there is a revision of the standard) whereas in reality progress is made or various factors tend to favor a particular method,

– the methods for interpreting the indications evolve, often becoming more complex.

Such a practice could be allowed at a national level, where several texts comprising identical or similar specifications (CODAP for pressure vessels, metal construction standards, etc.) have coexisted for many years. This is less helpful at the European level insofar as the objective is freedom of movement for goods and people by removal of the technico-economic barriers to exchanges.

This takes place by a harmonization of technical specifications and, concerning welding, a "horizontal" approach independent of the applications, which occurs as follows:

– development of a single reference frame for the description and the definition of the defect classes,

– definition of the enforcement modes for each method as well as their validity limits, while also specifying at what moment an indication can be regarded as significant or not,

– interpretation, for each method, of the indication levels it provides by it with reference to the basic defect class.

Such a structure constitutes a tool at the disposal of users, particularly of technical committee members, in charge of the drafting of the European execution standards (CEN/TC 54 for pressure vessels, CEN/TC 135 for steel structures).

Overseeing all of this standardization work is the standard EN ISO 5817 "Welding – fusion welded joints in steel, nickel, titanium and their alloys – quality levels for imperfections", which describes and defines in order of decreasing severity three classes of defects: B, C and D. It constitutes a reference frame to which specialists in non-destructive testing and end users can refer, the quality level adapted to each case being defined in the application standard or by the designer responsible in liaison with the manufacturer, the user and/or other parties concerned. An equivalent standard exists for aluminum alloy assemblies, EN ISO 10042.

Thus we find then the standard EN 12062 "Non-destructive examination of welds – general rules for metallic materials". The analysis appearing on the first page states that this standard "*gives guidance for the choice of non-destructive testing methods for the examination of welds and evaluation of the results for quality control. It also specifies general rules and standards to be applied to the different types of examination, for either the methodology or the acceptance levels for metallic materials*". It can be considered regrettable that the term "acceptance levels" is employed as it implies a certain ambiguity by mixing two concepts: that of

classification and that of qualitative appreciation, the second point being debatable insofar as the criteria of acceptance could not be uniform for all the applications and must remain the responsibility of the users; it can only be a question in fact of "transference", in terms of indications and according to the method used, of the classes defined in ISO 5817: this could be called the transfer function method. The details are then given, both with regard to the technique and its validity limits as well as the "acceptance levels", in the standards specific to each method.

Six different examination methods are thus covered: visual, penetrant, magnetic particle, eddy current, radiographic and ultrasonic. The structure of the system can be schematized as in Figure 14.3.

Reference frame	EN ISO 5817 - EN ISO 10042					
General rules	EN 12062					
	Visual	Penetrant	Magnetic particle	Eddy current	Radiographic	Ultrasonic
Technique and validity limits	EN 970	EN 571-1	EN 1290	EN 1711	EN 1435	EN 1714 EN 1713
Acceptance levels	EN ISO 5817 EN ISO 10042	EN 1289	EN 1291	To be agreed	EN 12517	EN 1712
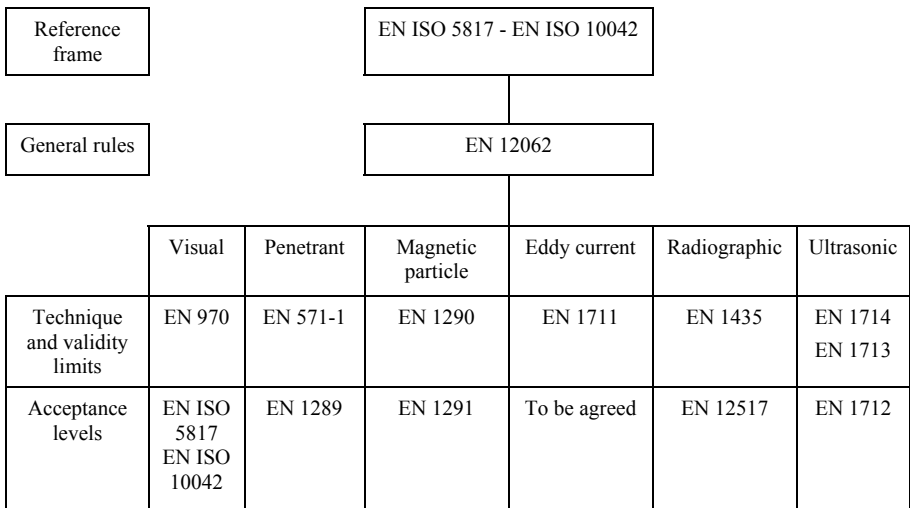
Figure 14.3. *Structure of NDT standards*

As for the standards dealing with the welding procedure qualification, the unit may appear complex, but it answers a certain logic which corresponds to the reality on the ground.

A designer or manufacturer responsible for a project or a construction must know the nature and the size of permissible defects during its construction and, in general, cannot prejudge the methods of non-destructive testing which will be used. In the system suggested, his only concern will be to choose the defect class tolerated with reference to the basic reference frame, EN ISO 5817 or ISO 10042.

In addition, the independence of the standards with respect to defect classes and the nature of structures or equipment to be produced allows them to develop according to progress in the techniques, without impacting on the basic reference frame or the procedural standards. We thus have a coherent and progressive system.

However, this field still demands a certain adaptation period. Certainly, the scattering of clauses in different documents and the loss of a conclusive overall picture, such as is experienced today in the codes or specific standards, is a matter of regret. The task of the European technical committees in charge of procedural standards is now to take this whole group of concepts into account and as far as possible guide the user in their application.

14.5. Conclusion

The presentation and analysis of documents such as standards, particularly those which cover complex subjects both from a technical and organizational perspective, is never an easy matter. The situation is complicated by the fact that it is evolving. Many standards worked out at the European level have been taken up again at an international level, with technical modifications as well as changes in presentation. Others will follow suit in the near future and this requires vigilance at every moment.

What should be remembered is that welding is a horizontal technique with a plethora of applications, that the processes and methods are in continuous development and are also becoming more complex, and finally that international competition can only proceed normally if it has reference texts, constituted with the consensus of the majority and used as a basis for contracts.

In this context, industrialists involved in welded construction, in co-operation with clients and partners concerned are equipped, by the means of the standardization committees, with the tools allowing them to achieve outcomes that are satisfactory, both in terms of economics and quality levels. For some this represents a change of practice, even of culture, but in the long term everyone will benefit from this.

List of Authors

Régis BLONDEAU
Ecole nationale supérieure des mines
de Saint-Etienne
France

Christian BONNET
Air Liquide/CTAS
Saint-Ouen-l'Aumône
France

Jean-Henri BORGEOT
CTICM
St-Rémy-lès-Chevreuse
France

Marc BOUSSEAU
DCN-Indret
Nantes
France

Abdelkrim CHEHAÏBOU
Institut de soudure
Metz
France

Joël CLAEYS
Arcelor Mittal
Dunkirk
France

Michel COURBIÈRE
Pechiney Alcan
Voreppe
France

Yves DESALOS
Renault
Guyancourt
France

Olivier DIERAERT
Arcelor Mittal
Dunkirk
France

Léon DUNAND-ROUX
Areva NP
Chalon-sur-Saône
France

François FAURE
Areva NP
Paris
France

Jean-Paul GOURMELON
Honorary "Ponts et chaussées"
civil engineer general
Nantes
France

Jean-Claude GOUSSAIN
Institut de soudure
Metz
France

Dominique KAPLAN
Arcelor Mittal
Paris
France

Henri-Paul LIEURADE
CETIM
Senlis
France

Guy MURRY
Ingénieur conseil
Clermont-Ferrand
France

Jean-Louis MOIRON
Ugine SA
Gueugnon
France

Jean-Pierre PESCATORE
CTICM
St-Rémy-lès-Chevreuse
France

Gérard PRADERE
Renault
Guyancourt
France

Gilles RIGAUT
Arcelor Mittal
Dunkirk
France

Pascal VERRIER
Arcelor Mittal
Dunkirk
France

Index